MOLECULAR MECHANISMS UNDERLYING TOURETTE'S DISORDER AND OBSESSIVE-COMPULSIVE DISORDER
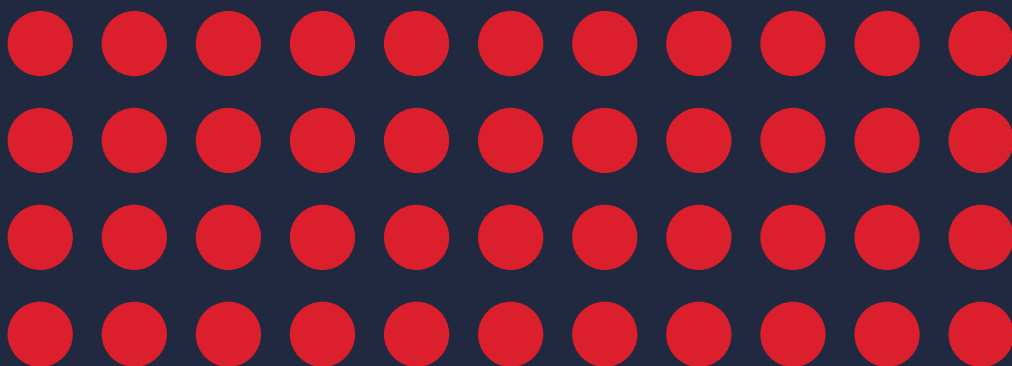
Insights from animal and human studies

Joanna Widomska

MOLECULAR MECHANISMS UNDERLYING TOURETTE'S DISORDER AND OBSESSIVE-COMPULSIVE DISORDER:
insights from animal and human studies

Joanna Widomska

MOLECULAR MECHANISMS UNDERLYING TOURETTE'S DISORDER AND OBSESSIVE-COMPULSIVE DISORDER: INSIGHTS FROM ANIMAL AND HUMAN STUDIES

Proefschrift ter verkrijging van de graad van doctor

aan de Radboud Universiteit Nijmegen

op gezag van de rector magnificus prof. dr. J.H.J.M. van Krieken,

volgens besluit van het college voor promoties

in het openbaar te verdedigen op

maandag 12 juni 2023

om 16.30 uur precies

door

Joanna Maria Widomska

geboren op 22 april 1988

te Kielce, Polen

MOLECULAR MECHANISMS UNDERLYING TOURETTE'S DISORDER AND OBSESSIVE-COMPULSIVE DISORDER: INSIGHTS FROM ANIMAL AND HUMAN STUDIES

Dissertation to obtain the degree of doctor

from Radboud University Nijmegen

on the authority of the Rector Magnificus prof. dr. J.H.J.M. van Krieken,

according to the decision of the Doctorate Board

to be defended in public on

Monday, June 12, 2023

at 4.30 pm

by

Joanna Maria Widomska

born on April 22, 1988

in Kielce, Poland

TABLE OF CONTENTS

CHAPTER 1

INTRODUCTION AND OUTLINE OF THE THESIS

INTRODUCTION

The main focus of this thesis is the identification of the (altered) molecular mechanisms and biological processes that are involved in the etiology and treatment of Tourette's disorder and obsessive-compulsive disorder. In the following section, a summary of the main epidemiological, genetic, and animal model-derived findings for these disorders will be presented. Subsequently, we will provide an overview of the aims and outline of the thesis.

Historical context

Gilles de la Tourette Syndrome (often shortened as Tourette syndrome (TS) or Tourette's disorder (TD), which is currently the used term) was first described in 1825 by the French physician Jean-Marc Gaspard Itard [1]. However, the disorder was later named after Georges Gilles de la Tourette, who in 1885 described nine patients suffering from what he called 'maladie des tics' at the time [2]. The word 'tic' has probably an onomatopoeic origin and was used to convey the idea of repetition, as in 'ticktack'. Its derivatives are present in many languages, e.g., German: zucken, ziehen, zugen, tucken, ticken, tick; English: tug, tick; Italian: ticchio; Spanish: tico, French: tique, ticq, tic. Tics are not exclusive to the human species. In fact, the term was initially applied to animals and appears to come from veterinary medicine, where it was used to describe horses' sudden movements and eructated sounds, as reported by Jean Jourdin in 1655 [3].

The first description of obsessive-compulsive disorder (OCD) in the psychiatric literature dates to 1838, when Jean-Étienne Esquirol described OCD symptoms as a monomania that could be attributed to a disordered intellect or will. Several concepts have been later proposed to understand obsessions and compulsions, describing OCD as, e.g., impulsive insanity ('folie impulsive'), madness of doubt ('folie du doute'), or disease of the emotions ('delire emotif'). In 1877, Carl Westphal described OCD with the term 'Zwangsvorstellun', which gave rise to the currently used terminology. In the twentieth century, Pierre Janet and Sigmund Freud further conceptualized OCD. Freud described obsessional neurosis, in which OCD symptoms derive from a patient's maladaptive response to unresolved conflicts between unacceptable unconscious impulses and the requirements of conscience and reality [4-6].

Current definitions and classifications of TD and OCD

Since the original descriptions, the phenotypic definitions of TD and OCD have changed. At present, TD and OCD are described and classified by the two major diagnostic classification systems used in clinical practice: the Diagnostic and Statistical Manual of Mental Disorders,

Fifth Edition (DSM-5), published in 2013 by the American Psychiatric Association (APA) [7] and the International Classification of Diseases and Related Health Problems, Eleventh Revision (ICD-11), developed by the World Health Organization (WHO) [8]. Both systems are descriptive in nature and diagnoses are based on patient's behavior and reports of their subjective experiences (observable signs and self-reported symptoms), and there are no definitive biomarkers or diagnostic tests that can aid in this essentially clinical diagnosis. The DSM-5 diagnostic criteria for TD and OCD are presented in Table 1. TD, along with other tic disorders, is classified as a motor disorder in the chapter on neurodevelopmental disorders in the DSM-5 and as a movement disorder in the chapter on diseases of the nervous system in the ICD-11. Until recently, OCD was classified as an anxiety disorder, but it now has its own separate diagnostic category in both the DSM-5 and ICD-11. This new section, 'Obsessive-Compulsive and Related Disorders (OCRDs)' includes OCD as well as body dysmorphic disorder, skin picking disorder, trichotillomania, and hoarding disorder. To address the close relationship between OCD and TD and its clinical implications, the DSM-5 diagnosis of OCD added a 'tic-related' specifier to denote individuals with a current or past tic disorder, and ICD-11 cross-listed TD in the OCRDs.

TABLE 1. The DSM-5 diagnostic criteria for TD and OCD

DSM-5 Diagnostic criteria for Tourette's Disorder
Note: A tic is a sudden, rapid, recurrent, nonrhythmic motor movement or vocalization.
A. Both multiple motor and one or more vocal tics have been present at some time during the illness, although not necessarily concurrently.
B. The tics may wax and wane in frequency but have persisted for more than 1 year since first tic onset.
C. Onset is before age 18 years.
D. The disturbance is not attributable to the physiological effects of a substance (e.g., cocaine) or another medical condition (e.g., Huntington's disease, postviral encephalitis).
DSM-5 Diagnostic criteria for Persistent (Chronic) Motor or Vocal Tic Disorder
A. Single or multiple motor or vocal tics have been present during the illness, but not both motor and vocal.
B. The tics may wax and wane in frequency but have persisted for more than 1 year since first tic onset.
C. Onset is before age 18 years.
D. The disturbance is not attributable to the physiological effects of a substance (e.g., cocaine) or another medical condition (e.g., Huntington's disease, postviral encephalitis).
E. Criteria have never been met for Tourette's disorder.
Specify if:
With motor tics only
With vocal tics only

TABLE 1. Continued

DSM-5 Diagnostic criteria for Provisional Tic Disorder

A. Single or multiple motor and/or vocal tics.

B. The tics have been present for less than 1 year since first tic onset.

C. Onset is before age 18 years.

D. The disturbance is not attributable to the physiological effects of a substance (e.g., cocaine) or another medical condition (e.g., Huntington's disease, postviral encephalitis).

E. Criteria have never been met for Tourette's disorder or persistent (chronic) motor or vocal tic disorder.

DSM-5 Diagnostic criteria for obsessive-compulsive disorder

A. Presence of obsessions, compulsions, or both:

Obsessions are defined by (1) and (2):

1. Recurrent and persistent thoughts, urges, or images that are experienced, at some time during the disturbance, as intrusive and unwanted, and that in most individuals cause marked anxiety or distress.

2. The individual attempts to ignore or suppress such thoughts, urges, or images, or to neutralize them with some other thought or action (i.e., by performing a compulsion).

Compulsions are defined by (1) and (2):

1. Repetitive behaviors (e.g., hand washing, ordering, checking) or mental acts (e.g., praying, counting, repeating words silently) that the individual feels driven to perform in response to an obsession or according to rules that must be applied rigidly.

2. The behaviors or mental acts are aimed at preventing or reducing anxiety or distress, or preventing some dreaded event or situation; however, these behaviors or mental acts are not connected in a realistic way with what they are designed to neutralize or prevent, or are clearly excessive.
   Note: Young children may not be able to articulate the aims of these behaviors or mental acts.

B. The obsessions or compulsions are time-consuming (e.g., take more than 1 hour per day) or cause clinically significant distress or impairment in social, occupational, or other important areas of functioning.

C. The obsessive-compulsive symptoms are not attributable to the physiological effects of a substance (e.g., a drug of abuse, a medication) or another medical condition.

D. The disturbance is not better explained by the symptoms of another mental disorder (e.g., excessive worries, as in generalized anxiety disorder; preoccupation with appearance, as in body dysmorphic disorder; difficulty discarding or parting with possessions, as in hoarding disorder; hair pulling, as in trichotillomania [hair-pulling disorder]; skin picking, as in excoriation [skin-picking] disorder; stereotypies, as in stereotypic movement disorder; ritualized eating behavior, as in eating disorders; preoccupation with substances or gambling, as in substance-related and addictive disorders; preoccupation with having an illness, as in illness anxiety disorder; sexual urges or fantasies, as in paraphilic disorders; impulses, as in disruptive, impulse-control, and conduct disorders; guilty ruminations, as in major depressive disorder; thought insertion or delusional preoccupations, as in schizophrenia spectrum and other psychotic disorders; or repetitive patterns of behavior, as in autism spectrum disorder).

TABLE 1. Continued

Specify if:
With good or fair insight: The individual recognizes that obsessive-compulsive disorder beliefs are definitely or probably not true or that they may or may not be true.
With poor insight: The individual thinks obsessive-compulsive disorder beliefs are probably true.
With absent insight/delusional beliefs: The individual is completely convinced that obsessive-compulsive disorder beliefs are true.
Specify if:
Tic-related: The individual has a current or past history of a tic disorder

Epidemiology and clinical characteristics

TD

Once regarded as a rare and bizarre curiosity, TD is now recognized to be a relatively common disorder, affecting 0.3% to 1% of the pediatric population and up to 0.05% of the adult population [9-12]. Although tics can occasionally occur in every individual, their persistent and pervasive manifestations are classified as tic disorders, with TD representing the most severe end of the spectrum (Table 1). The broader group of 'tic disorders' – including persistent (chronic) motor or vocal tic disorders and provisional tic disorder – has an estimated prevalence of 5% [13], and these broadly defined tic disorders are found across most ethnic groups worldwide and are more common in males than females (3-4:1) [14].

Tics, the cardinal feature of TD, are sudden, rapid, recurrent, nonrhythmic motor movements (motor tics) or vocalizations (vocal tics) that typically mimic fragments of normal behavior [7,14]. They usually begin around the age of 4-6 as simple motor movements (e.g., eye blinking, nose twitching) and progress with time in a rostro-caudal direction. Motor tics generally precede vocal tics, which typically begin as simple vocalizations (e.g., throat clearing, sniffing). With increasing age, both motor and vocal tics become more complex (e.g., gestures, words, or phrases) and reach their peak severity around 10-12 years of age [15]. Tics occur in bouts and wax and wane in severity, intensity, and frequency, with a substantial reduction in severity during adolescence and early adulthood, although a small percentage of adult individuals will have persistently severe or worsening symptoms [14,16]. Although the most publicly recognized features of TD are coprophenomena, i.e., expression of socially inappropriate verbal words (coprolalia) or gestures (copropraxia), coprophenomena are present in only about 20% of TD patients [17].

Tics are typically preceded by 'sensory phenomena', which include premonitory urges (PUs), 'just right' phenomena and somatic hypersensitivity. Although they are not diagnostic criteria for TD, these symptoms help to distinguish tics and TD from other movement

disorders, such as stereotypies, dystonia, and tremor, in which they do not occur. PUs can be described as uncomfortable feelings of tightness, itching or tickling (similar to the need to sneeze or scratch) experienced at the site where a tic is about to be executed or as a generalized inner tension. They can be viewed as the driving force of tics, building up before and subsiding after the execution of tics [18]. Thus, although previously described as involuntary or unvoluntary, tics are often experienced as voluntary and intentional responses to uncontrollable/unwanted PUs [19-21]. PUs are more often proceeding complex tics than simple tics and the awareness of PUs increases over time and is present in the majority of adolescents with TD [22]. Moreover, TD patients may also feel the need to perform a tic in a specific way or repeat it until they look, feel or sound 'just right' [23]. Tics are also temporarily suppressible, i.e., they can be delayed and camouflaged, but often with rebound afterwards. The ability to suppress/control tics increases with age, and PUs are not a prerequisite for the ability to suppress tics [24,25].

OCD

OCD is estimated to affect approximately 1-3% of the general population [26-28]. The age at onset of OCD is bimodal, peaking in late childhood or early adolescence and again in early adulthood [29,30]. OCD is more common among males in childhood, whereas an equal or a greater proportion of females are affected by OCD in adolescence and adulthood. The majority of patients experience a gradual onset and a chronic and waxing and waning course, with fluctuations often related to the occurrence of stressful life events [31]. OCD is responsible for a diminished quality of life and a substantial socio-economic burden for affected individuals, their relatives, and caregivers [32]. Despite this severe impairment and burden of OCD, it often goes unrecognized and undertreated or even untreated.

Defining features of OCD include the presence of obsessions or compulsions that are associated with clinically significant distress or functional impairment (Table 1). This is important given that intrusive thoughts and repetitive behaviors are experienced by nearly everyone (in the population), and these rituals are a part of normal development [33]. In this respect, obsessive-compulsive symptoms (OCS) in the population occur along a severity continuum, ranging from nonclinical through subclinical and clinical symptoms [34]. Subclinical OCS are much more prevalent (up to 28.2%) and may be a precursor to the development of the disorder [31,35,36]. Moreover, up to 60% of individuals with OCD experience sensory phenomena, which are defined as subjective experiences that precede compulsions and can include physical sensations, 'just right' sensations, and feelings of incompleteness [37,38].

Although considered as a unitary entity by the diagnostic system, OCD is very heterogeneous, in that two patients with this diagnosis may have distinct, nonoverlapping

symptom profiles. As the identification of more homogeneous subtypes of OCD patients is essential for the search of etiological factors and more effective treatment strategies, various potentially (more) homogeneous subtypes of OCD have been proposed, including, amongst others, those based on symptom dimensions [39,40], comorbidities, such as tic-related OCD [41,42], age of onset (e.g., early onset OCD) [43,44], and Pediatric Autoimmune Neuropsychiatric Disorders Associated with Streptococcal infections (PANDAS) (see below).

OCD symptom dimensions

Obsessive-compulsive symptoms (OCS) are thematically heterogeneous and reflect an individual's idiosyncratic concerns. Nonetheless, as shown by numerous structural (factor-analytic) studies, particular obsessions and compulsions often co-occur in OCD patients and can be summarized by using a few consistent and temporally stable symptom dimensions, including cleaning (contamination obsessions and washing/cleaning compulsions), symmetry (symmetry obsessions and repeating, ordering, and counting compulsions), forbidden or taboo thoughts (e.g., aggressive, sexual, or religious obsessions and related compulsions), and harm (e.g., fears of harm to oneself or others and checking compulsions) [39]. These symptom dimensions occur across different cultures [45] and are associated with different patterns of comorbidity and various genetic, neuroimaging and treatment response-related variables. Importantly, symptom dimensions may coexist in a patient, are continuous with 'normal' OCS observed in the general population and extend beyond traditional nosological boundaries of OCD [39]. As suggested for psychiatric nosology in general [46], a dimensional approach allows for reconciliation between a 'lumping' perspective – in which all symptom dimensions are manifestations of a single broad disorder (i.e., OCD) – and a 'splitting' perspective – where each symptom dimension is a separate entity. These views are not incompatible, as both common and distinct etiologic factors may exist within the broad OCD phenotype [39]. Preliminary evidence supporting the validity of these dimensions comes from genetic, neuroimaging, and treatment response studies, as described further below.

TD and OCD: phenomenological similarities and distinctions

Although classified as separate disorders, TD and OCD share common characteristics [47]. Both TD and OCD have a childhood onset, a chronic waxing and waning course, and share similar clinical presentations, including sensory phenomena, repetitive behaviors, and impairment in behavioral inhibition [47-50]. Both disorders are also responsive to similar aggravating (e.g., stress, fatigue, physical illness) and attenuating factors (e.g., focusing attention on specific physical or mental activities) [14]. Similar environmental risk factors, such as pre- and perinatal complications/factors (e.g., infections, gestational smoking) or acute or chronic stress, may contribute to the development of OCD and TD, but most of

the studies assessing this subject are based on retrospective self-reports, limiting causal inference. Moreover, these associations may reflect specific maternal environmental and/or genetic influences [51-53].

PANDAS

Unusually abrupt, dramatic onset of OCD and tics in children has been associated with (repeated) infections with group A beta-hemolytic Streptococcus (GAS) bacteria and postinfectious autoimmune mechanisms. This condition was initially termed 'Pediatric Autoimmune Neuropsychiatric Disorders Associated with Streptococcal infections (PANDAS) [54], and recently has been broadened to 'Pediatric Autoimmune Neuropsychiatric Syndrome' (PANS), emphasizing that the illness may start with infectious triggers other than streptococcal bacteria [55,56]. The proposed definition criteria for PANDAS are: (1) prepubertal onset, (2) the presence of chronic tic disorders and/or OCD, (3) a relapsing-remitting time course, (4) clinical evidence of GAS infection associated with onset or exacerbation of tics, (5) association with neurological abnormalities such as a reduced motor coordination or motor hyperactivity (but not chorea). Despite the potential role attributed to streptococcal infections in modulating OCD and TD symptoms, the precise relationship between such infections, antineuronal antibodies, and TD and OCD remains elusive. In this respect, a very recent study suggested a role of familial factors (e.g., genetic pleiotropy) in susceptibility to both infections (prenatal maternal infections and early-childhood infections in the offspring) and OCD and/or TD/tic disorders, in that compromised (innate and adaptive) immunity could result in increased susceptibility to infections and autoimmune diseases, which in turn may compromise the host protection to pathogens (e.g., in PANDAS) and result in physiological conditions [53].

TD and OCD comorbidity

Most patients with TD do not have 'pure TD' (tics only) but present with additional psychiatric comorbidities, colloquially referred to as 'TD-plus', with OCD and attention-deficit/hyperactivity disorder (ADHD) being the most common. These comorbidities are often more distressing than the tics themselves, they contribute substantially to the reduction in quality of life and are often the primary reason for seeking treatment. The rates of OCD in TD subjects vary from 40% to 60%, whereas OCS may also be present in up to 90% of TD subjects, adding significantly to the clinical burden of TD. Conversely, the rates range from 7% of TD in OCD patients to 53% of tics in OCD patients [14,57]. In DSM-5, a 'tic-related' specifier is added to the OCD diagnosis to denote these individuals (Table 1). When comorbidity does occur, the clinical presentation may be somewhat different from either OCD or TD symptoms alone. Patients with OCD with tics tend to differ from those without a history of tic disorders:

they have earlier age of OCD onset [58-60], are more likely males [44,61-63], have higher rates of symmetry and sexual/aggressive obsessions [41,63,64] and sensory phenomena preceding the compulsions [61,65], have a higher number of psychiatric comorbidities [66] – in particular ADHD and autism spectrum disorders (ASDs) [64] – and a greater likelihood of family members also having OCD. Conversely, compared with individuals with tic-related OCD, individuals with non-tic-related OCD had higher rates of comorbid anxiety disorders and mood disorders [50,64]. As for preceding sensory phenomena, a 'just right' perception is an important feature of tic-related OCD and then relates to a mental phenomenon (e.g., a want), whereas a typical PU involves a bodily sensation (e.g., an itch). In addition, TD symptoms may resemble OCD rituals and it may be often challenging to differentiate compulsions from complex motor tics (especially 'tic-like' compulsions such as touching, tapping, or rubbing), as the goal of both TD symptoms and OCD rituals is the same, i.e., to produce relief. However, the nature of the subjective experience that precedes them is typically different, i.e., compulsions are triggered by obsessions, whereas tics function as the physical response to reduce sensory urges and somatic tension [49,50]. Given the abovementioned similarities and differences between TD and OCD and the fact that the diagnosis of these disorders is based solely on behavioral features, the boundaries between the disorders and the boundaries between TD/OCD and normal variation are often arbitrary.

Etiology

TD and OCD are recognized as complex multifactorial disorders, i.e., influenced by the combination of multiple genetic and environmental factors. As with most complex (neuropsychiatric) disorders, the causes and pathophysiological mechanisms that lead to TD and OCD are not well understood. That being said, the frequently observed comorbidity of TD and OCD suggests that these disorders may share some etiological factors. In addition, characterizing the relationship between genetic variation and susceptibility to TD/OCD helps in identifying the biological processes that, when altered contribute to disease pathogenesis and providing clues towards novel strategies for prevention and treatment.

Genetics

Family and twin studies clearly demonstrate that there is a considerable genetic component to both TD/tic disorders and OCD/OCS. Traditional genetic studies have utilized a hypothesis-driven candidate gene approach, i.e., specific genes were chosen to study further based on the putative biological mechanisms involved in and drug targets of existing medications. However, with advances in genomic technology and bioinformatics, the use of genome-wide association studies (GWASs) has significantly increased in the past decade, enabling

the detailed and unbiased investigation of previously unexplored genetic regions that may be of great importance in the etiology of TD and OCD.

TD

Twin studies have shown substantially higher concordance rates of TD in monozygotic twins (MZ, 53-56% for TD and 77-94% for tics) as compared to dizygotic twins (DZ, 8% for TD and 23% for tics), implying that there is a strong genetic component to TD [67,68]. In addition, family studies have shown that TD aggregates (or clusters) in families and the risk of TD/tic disorders increases proportionally to the degree of genetic relatedness to the affected individual and is significantly higher among biological relatives of individuals with tic disorders than in relatives of unaffected controls [69-71]. There is a TD recurrence risk of about 30% in first-degree relatives, and this is higher for males than females [72]. Moreover, a polygenic risk score (PRS) derived from a TD GWAS predicted the presence of tics in a population-based cohort, explaining 0.48% of the phenotypic population variance in tics [73]. All these findings support the hypothesis that chronic tics and TD are genetically related and fall along a continuum and not into the distinct categories that are implied by the current diagnostic criteria [69].

With a population-based heritability estimate of 77 % [71] and SNP-based heritability estimates ranging from 21 to 58 % [74,75], TD is one of the most heritable neuropsychiatric conditions. Because of the high heritability of TD, many studies have been conducted to identify the genetic factors contributing to the disorder. However, so far, the identification of definitive TD risk genes with major effects has been hindered by small genetic study cohorts and associated limited statistical power. In short, candidate gene studies have focused on genes encoding proteins of the neurotranmitter pathways that were thought to be implicated in the pathology and treatment of TD, especially genes/proteins from the dopaminergic (*DRD2*, *MAOA*, *SLC6A3*) and serotonergic systems (*HTR2C*, *SLC6A4*, *TPH2*) (reviewed in [76]). Moreover, hypothesis-free studies implicated potential susceptibility genes, including a gene from the SLIT and NTRK family of proteins (*SLITRK1*) [77] and the gene encoding l-histidine decarboxylase (*HDC*), the rate-limiting enzyme in histamine biosynthesis [78], although defects/variants in these genes may only account for a small fraction of TD cases. Subsequent genetic analyses have also implicated disruption of *HDC* [79] or of histaminergic signaling in general [80] in TD beyond the index family. In this respect, TD seems to be highly polygenic, with a contribution from both multiple common risk variants, each with small individual effect, and a few rare variants with moderate or large effects to disease etiology. Regarding common variation, two genome-wide association studies (GWASs) have been published to date [74,81]. Although no genome-wide significant hits that survive replication analyses were found, further analyses have indicated an enriched expression of TD GWAS-implicated genes in tissues within the cortico-

striatal circuits, and particularly, the dorsolateral prefrontal cortex, as well as an enrichment of proteins encoded by TD GWAS genes in processes such as ligand-gated ion channel signaling, lymphocytic processes, and cell adhesion and trans-synaptic signaling processes. A recent study in a large, densely affected British pedigree found that contribution to TD risk in this family comes from multiple common risk variants rather than one or a few variants of strong effect, highlighting the importance of common genetic variation in TD etiology [82].

As for rare genetic variants contributing to TD, there is now evidence for likely gene-disrupting mutations or copy number variants (CNVs) in several genes. Two rare CNVs (deletions in *NRXN1*, which encodes neurexin 1, and duplications in *CNTN6*, which encodes contactin 6) have been identified as significant genetic risk factors for TD [83]. The implication of NRXN1 deletions confirmed two earlier studies [84,85]. In addition, one of these studies also identified recurrent exon-affecting microdeletions in the gene encoding arylacetamide deacetylase (AADAC) [85], which was later confirmed in a large meta-analysis of TD patients and controls from six European countries [86]. In studies of de novo coding (and rare) single nucleotide variants (SNVs) and indels, Wang et al. [87] observed an overrepresentation of de novo damaging variants in simplex families (i.e., without a family history of a tic disorder), but not in multiplex families, and they identified six probable risk genes, including *CELSR3* and *WWC1*, which have roles in establishing cell polarity.

OCD

Family and twin studies provided strong evidence for a substantial genetic contribution to OCD and OCS risk. Higher rates of OCD and OCS (4-20-fold increased risk) were observed in family members of individuals with OCD compared to family members of unaffected controls [88,89]. Much higher concordance rates of OCD symptoms were also observed among monozygotic twins compared to dizygotic twins. Heritability estimates for OCD from twin studies are somewhat lower than for TD (0.29 to 0.58), [90,91], with the childhood-onset form of OCD consistently being reported to have a higher heritability than the adult-onset form [92].

Numerous candidate gene studies have been reported for OCD but failed to provide reproducible results [93]. Most of these studies have examined genes related to serotoninergic, dopaminergic, and glutamatergic pathways, which represent neurotransmitters that are thought to be most involved in the pathophysiology and treatment of OCD [94,95]. A potential role for variants in genes from the serotonergic (*HTTLPR* and *HTR2A*) and catecholaminergic (*COMT*, in males only) systems have been reported [96,97]. Further, several variants influencing expression of *SLC1A1* – which encodes for neuronal glutamate transporter EAAT3 – have been associated with OCD [93,98]. Other putative OCD genes, such as *SAPAP3* and *SLITRK5*, have been identified through studies in animal models of OCD-like behaviors (e.g., excessive self-grooming) [99].

Furthermore, evidence suggests that OCD is influenced by several genes of small effect, which collectively affect the risk for developing obsessions and compulsions. So far, two GWASs have been performed [100,101]. These studies did not identify single nucleotide polymorphisms (SNPs) associated with OCD at genome-wide significance level, nor did a meta-analysis of the two studies [102], although top SNPs were found near or within glutamatergic signaling-related genes (*GRID2* and *DLGAP1*). In addition, studies of CNVs found a 3.3-fold increased burden of large deletions at 16p13.11 that were (also) associated with other neurodevelopmental disorders in patients with OCD [103]. Lastly, in 2016, the then available genetic data for OCD were integrated into a so-called 'molecular landscape' that implicated central nervous system (CNS) insulin signaling modulating synaptic functions as one of the core biological mechanisms underlying the disorder [104].

OCS symptoms and dimensions

Similar to OCD, twin studies indicate that OCS in the general population are heritable, with genetic factors accounting for 36-42% of its phenotypic variance [105,106]. Similarly, SNP-based heritability estimates of OCS in population-based samples were found to be lower than the estimates derived from twin and family studies as well as SNP-based heritability estimates for OCD and ranged from 6.8 to 14% [105,107]. Furthermore, OCD and OCS share some genetic risk factors, although the proportion of phenotypic variance explained between OCD and OCS is small, with PRS analyses reporting that PRS derived from OCD case/control GWASs explained between 0.2% and 0.57% of the phenotypic variance in population-based OCS [105,107].

Shared genetic basis of TD and OCD

High rates of comorbidity between TD and OCD lend support to the hypothesis of a (partially) shared genetic susceptibility between the disorders. Indeed, multiple studies have indicated that TD/tic disorders and OCD are genetically related [108-110], with both shared and distinct genetic risk factors for each disorder. Two studies used GWAS data to examine the unique and shared components of heritability for TD and OCD [75,111]. Davis et al. [75] observed a significant proportion of shared heritability between the two disorders (r = 0.41), although the overall genetic architecture was different. Yu et al. [111] used PRS to identify differences between the polygenic risk burden for OCD with or without co-occurring TD and chronic tic disorder. While OCD polygenic risk scores predicted OCD case status when examined in cases without co-occurring TD or chronic tic disorder, these risk scores were less strongly associated with case status among individuals with OCD plus co-occurring tic disorders. Similarly, individuals with 'pure TD' were shown to have no family history of OCD, altogether indicating the presence of distinct genetic components to TD and OCD [112]. That being said,

a large-scale cross-disorder study using GWAS data from different neurological and psychiatric disorders demonstrated that a significant proportion of TD polygenic heritability is shared with OCD (0.7) and that TD and OCD have also distinct correlations with other psychiatric disorders, e.g., OCD was found to have a considerable shared genetic risk with anorexia nervosa, bipolar disorder, and schizophrenia, and TD showed genetic overlap with ADHD, major depressive disorder, and migraine with aura [113,114]. The most recent cross-disorder study reported 11 previously unidentified regions that are likely associated with TD, ADHD, and ASDs, as well as two separate pleiotropic regions that are associated with both TD and OCD, indicating that the genetic etiology that is shared between TD and OCD may differ from that shared between TD, ADHD and ASDs [115]. Furthermore, tic-related OCD was found to be a particularly familial subtype of OCD: the risk of OCD in relatives of individuals with tic-related OCD is considerably greater than the risk of OCD in relatives of individuals with non-tic-related OCD [60]. In addition, a family study reported that certain OCS – aggressive/ sexual/religious obsessions and checking compulsions and symmetry/ordering symptoms – were significantly correlated in sibling pairs concordant for TD [116]. A more recent study identified two OCD factors (symmetry/exactness and fear-of-harm) that were clinically and genetically related to TD [117]. The symmetry/exactness factor replicates and expands on earlier work in this sample that also found a relationship between symmetry symptoms and tics [118,119] and is in line with the DSM-5 classification system that recognizes a specific tic-related subtype of OCD. Aggressive urges were also found to be associated with TD, OCD, and ADHD. Furthermore, Wang et al. observed a significant overlap between TD and OCD for de novo damaging sequence variants, even when restricting their analysis to TD probands without comorbid OCD, (again) suggesting that TD and OCD share a subset of genetic risk loci [87]. Lastly, a genome-wide study of large, rare genomic duplications and deletions in TD and OCD identified recurrent 16p13.11 deletions in individuals with TD, TD plus OCD, and OCD alone, suggesting that this locus could contribute to both phenotypes [103].

In summary, TD and OCD have a highly complex and heterogenous genetic architecture, with both common and rare variants contributing to their etiologies. In addition, there are both overlapping and distinct susceptibility genes for TD and OCD – which to some extent also reflects the clinical similarities and differences between both disorders/population traits – but further research is needed to elucidate the shared and distinct genes (and hence molecular mechanisms) for the disorders.

Pathophysiology and neurobiology of TD and OCD

The considerable overlap between TD and OCD in terms of clinical phenomenology, epidemiology and genetics points towards possible common neurobiological mechanisms associated with both disorders. At this point, we have limited understanding of the

pathophysiology underlying TD and OCD. Nevertheless, converging evidence (from neurophysiological, brain imaging, and postmortem studies) suggests that dysregulation of the cortico-striatal-thalamo-cortical (CSTC) circuitry and its integrated neurotransmitter systems is central to the pathogenesis of TD and OCD [120,121]. CSTC circuits are involved in emotional processing, cognitive control, and motor functioning and consist of multiple parallel, interconnected loops that project information from cortical areas to the striatum (caudate, putamen, nucleus accumbens), and back to the cortex via the thalamus. Specifically, glutamatergic pyramidal cortical neurons project onto striatal subnuclei, from where GABAergic neurons project to basal ganglia and the thalamus throughout both direct and indirect pathways. In turn, the thalamus sends recurrent projections back to cortical areas [122].

Currently, the complex phenotype of both disorders is thought to be associated with structural and functional abnormalities in all three major CSTC circuits: (i) the sensorimotor/ habitual behavioral circuit (from the supplemental motor area/primary motor cortex to the putamen) involved in motor control and habit learning, (ii) the associative/goal-directed circuit (from the ventromedial prefrontal cortex to the caudate), and (iii) the limbic/ emotion-related circuit (from the anterior cingulate cortex (ACC), medial orbitofrontal cortex (OFC), as well as hippocampus and amygdala to the ventral striatum) [123,124]. In each disorder, different loops seem to be primarily involved, e.g., TD was found to be associated with an imbalance in the sensorimotor circuits [125,126] and OCD with changes/hyperactivity in the OFC/ACC limbic loops [127,128]. However, the complex phenotype in both disorders is more likely to be associated with an interplay between disturbed sensorimotor, associative, and limbic circuits [129,130]. For instance, in TD, structural changes in the motor cortex were related to simple motor tics, while changes in associative loops to complex tics and disturbances in limbic loops were associated with OCS [47]. As for the neuroanatomical areas that are most affected, OCD patients with symmetry/ordering symptoms were more similar to TD and have more sensorimotor involvement whereas in OCD patients with contamination/cleaning symptoms, limbic pathways were more prominent [131]. In addition, recent studies have implicated regions outside the CSTC circuitry, e.g., an involvement of the insula and somatosensory cortices in PUs present in TD [132] and an involvement of the cerebellum in OCD [133,134]. Lastly, numerous neurotransmitters, including acetylcholine, dopamine, gamma-aminobutyric acid (GABA), glutamate, norepinephrine, serotonin, and opiates, are involved in the transmission of messages through CSTC circuits, and each of these has been proposed to be involved in the pathophysiology of TD and OCD [14,135].

Two studies focused on postmortem brain tissue from TD patients have investigated alterations in neuronal cell populations in the disorder and reported a decrease in GABAergic

and cholinergic interneurons in the striatum [136,137]. In line with this, a transcriptome study of postmortem brain tissue from TD patients found reduced expression of multiple genes, including those that are preferentially expressed in striatal interneurons [138]. Few postmortem studies of patients with OCD have been published. A recent study found evidence of molecular abnormalities in brain regions consistently implicated in OCD human imaging studies (e.g., OFC and striatum) [139]. The authors of this study also found lower excitatory synaptic gene expression in the OFC of OCD patients compared with unaffected controls.

In summary, the precise anatomical site(s) and primary underlying neurotransmitter abnormalities for TD and OCD remain undetermined. Some hypotheses favour a specific abnormality of the cortex or striatum, while others recognize influences from the thalamus or cerebellum or prefer alterations in the interactions within and between the CSTC circuits [140] as the main pathophysiological mechanisms involved. Moreover, the observed neurobiological alternations could indicate either a pathological state (i.e., a consequence of having symptoms and/or efforts to suppress these symptoms) or could be related to an intrinsic genetic vulnerability to the disorders.

Treatment of TD and OCD

TD and OCD may be managed behaviorally, pharmacologically, or surgically, all of which aim at ameliorating symptoms. Behavioral therapies are recommended first-line treatments for both OCD/OCS and TD/tics.

TD

The treatment of TD begins with an assessment of tic frequency and severity (often with the Yale Global Tic Severity Scale (YGTSS) [141]) and the presence of comorbid conditions. Psychoeducation of patients, parents, and teachers is important, especially for children, to improve acceptance and reduce stigma, and is usually sufficient for patients with mild tics. When treatment is needed, the first-line options are (cognitive) behavioral therapies directed at improving the ability to voluntarily suppress tics, including exposure and response prevention (ERP), habit reversal therapy (HRT), or comprehensive behavioral interventions for tics (CBIT) [142,143]. Pharmacological treatment is the second-line option and involves use of alpha-2 adrenergic agonists (clonidine and guanfacine), dopamine receptor blockers (typical and atypical neuroleptics, such as pimozide and aripiprazole), benzamides (sulpiride and tiapride), and GABAergic medications (baclofen, topiramate). When tics affect few muscles or muscle groups, botulinum toxin injections may be considered [144]. In case of refractory, severe, or injurious tics, deep brain stimulation is an emerging option,

most frequently targeting the centromedian thalamus, the globus pallidus (internus and externus), the subthalamic nucleus, and the ventral striatum/ventral capsule of the nucleus accumbens [142]. There is also some promising evidence regarding the use of cannabis-based medication and Chinese herbal medicines to treat TD [145,146].

OCD

First-line treatments for OCD include cognitive–behavioral therapy (CBT) that involves exposure and response prevention (ERP), and pharmacotherapy with selective serotonin reuptake inhibitors (SSRIs), and both were shown to bring at least partial symptom reduction and improve the quality of life [147]. Insufficient response to CBT or SSRI monotherapy (observed in about 30 - 50% of OCD patients) can be further addressed by combinatorial/adjunctive therapy with different agents, e.g., pharmacological SSRI augmentation with the use of neuroleptics (either typical or atypical), clomipramine (a serotonin-selective tricyclic antidepressant), and glutamatergic agents, e.g., riluzole [148,149], memantine [150], ketamine [33,151]. Neuromodulation treatments, including both noninvasive (e.g., transcranial direct current stimulation (tDCS) and repetitive transcranial magnetic stimulation (rTMS)) and invasive procedures (neurosurgical interventions – either ablative approaches or deep brain stimulation (DBS)) are (only) considered in highly refractory and severe cases. The main DBS targets include the anterior limb of the internal capsule, nucleus accumbens and/or the subthalamic nucleus [152].

While some studies suggest that patients with OCD and comorbid tics may not respond optimally to SSRIs [153,154], it has been consistently shown that patients with OCD, with and without comorbid tics, respond equally well to cognitive behavioral therapy [153,155]. Another treatment option for OCD patients with comorbid tics is neuroleptic augmentation. Lastly, treatment strategies for PANDAS include antibiotics and immunomodulatory therapies, such as intravenous immunoglobulin (IVIG), as well as standard therapies (i.e., ERP, SSRIs) [156].

Animal models of TD and OCD

Modeling of human neuropsychiatric disorders in animals is challenging, given the complex and subjective nature of the (human) symptoms as well as the lack of biomarkers and objective diagnostic tests for these disorders [157]. Nevertheless, animal models play an important role in increasing our understanding of disease pathophysiology, identifying novel therapeutic targets, as well as testing experimental treatments and characterizing the mechanism by which these treatments exert their beneficial influences [158-160]. In general, animal models are constructed to fulfill at least one of the following criteria:

construct validity (the model is developed according to a rationale matching the etiological hypothesis), face validity (the model presents symptoms similar to those of human patients), and predictive validity (the treatment response in the animal model is very similar to the treatment response in patients) [157,161]. Because of the genetic relationships between TD and OCD and the overlapping phenomenology of the disorders, both clinically and (even more so) in the evaluation of animal models, we describe a number of animal models below.

TD

The abovementioned and other findings from genetic studies in TD led to the development of genetic animal models, e.g., knockout (KO) mice of *Slitrk1* [162], *Hdc* [163], the dopamine transporter gene (*Slc6a3*) [164], and the dopamine receptor 3 gene (*Drd3*) [165], although all these models lack the spontaneous 'ticking' phenotype that is characteristic for TD, as in these models, tics are induced by stress and/or amphetamine injections. Meeting the face validity criterion in TD animal models is challenging due to the complexity of the TD phenotype, positioning TD at the crossroads of movement disorders (based on the existence of motor tics) and psychiatric disorders (based on PUs and comorbid symptoms). In addition, animal models of tics (described in the literature as tic-like movements, repetitive movements, stereotypies, abnormal involuntary movements such as dyskinesia and dystonia) include those obtained through the systemic or focal administration of active substances, e.g., striatal injections of the GABAergic antagonist bicuculline [166] or systemic administration of hallucinogens acting on serotonin receptors (e.g., DOI (1-)2,5-dimethoxy-4-iodophenyl-2-aminopropane) [167], or through a genetic approach, e.g., the D1CT-7 transgenic mouse [168]. The D1CT-7 transgenic mouse is the first model to show face validity for tics and feature also common TD-related phenotypes such as OCD-like behaviors and PPI deficits [169]. The above being said, addressing the psychiatric component of TD is more complicated, as PUs cannot be directly assessed in animals. However, some associated deficits can be tested and may serve as useful proxies. PUs are hypothesized to reflect deficits in sensorimotor gating that can be measured in both rodents and humans with the experimental paradigm of pre-pulse inhibition (PPI) of the startle response [170]. PPI describes the phenomenon in which a weak initial stimulus (the prepulse) reduces the startle response that is elicited by a subsequent stronger stimulus (the pulse). A deficient PPI has been documented in TD, OCD, and in other neuropsychiatric disorders [171,172]. Animal models of PPI abnormalities include rats treated with dopaminergic agonists [173] or hallucinogens (PPI in mice and rats is impaired by direct or indirect DA agonists, which can exacerbate tics). In this thesis, we used the well-established unilaterally lesioned 6-hydroxydopamine (6-OHDA) adult rat model used in Levodopa-induced dyskinesia research in juvenile rats to generate insights into the molecular mechanisms underlying tics during development.

In addition to genetic factors, environmental factors play a role in the onset and severity of TD and its comorbidities, including infections and stress, and these have been addressed through immune-mediated rodent models, including exposure to autoantibodies, e.g., induced by injection of TD sera in rat striatum [174] or immunogenic microbial components, such as group A beta-hemolytic streptococcus (GAS) bacteria, i.e., the PANDAS mouse model [175,176]. This PANDAS model is aimed at recapitulating three features of the human disease: the presence of serum IgGs directed against S. pyogenes (i.e., humoral response to immunization), regions of the CNS where IgGs (autoantibodies) cross the blood brain barrier and recognize cognate antigens such as dopamine receptors, and behavioral anomalies such as motor coordination deficits, tics and compulsive/stereotypical/exploratory/aggressive behaviors, and social deficits.

Considerable debate continues regarding the (face) validity of most existing animal models of tics, given the inability to assess animals for premonitory sensations and tic suppression, which are crucial for distinguishing tics from other repetitive movements, such as stereotypies or myoclonus [14].

OCD

Modeling OCD presents with even more difficulties with face, predictive, and construct validity than modeling TD [159]. Nevertheless, several genetic, pharmacological, and behavioral models have emerged. Animal models of OCD are focused on the presence of behavioral compulsivity, intended as the performance of repetitive, and perseverating actions and stereotypies [177]. The glutamatergic hypothesis of OCD finds a strong support in animal models. In mice lacking the AMPA receptor trafficking protein Sapap3, glutamatergic signaling dysfunction is accompanied by compulsive grooming behavior [178,179]. In addition, astrocyte-specific glutamate transporter (Slc1a2) KO mice exhibit a range of OCD/TD-like behaviors, with marked increased self-injurious grooming behavior [180]. Lastly, transmembrane protein Slitrk5 KO mice [181] and Slc1a1 overexpressing mice [182] show OCD-like behavioral abnormalities that seem to be associated with a deficient cortico-striatal neurotransmission.

AIMS AND OUTLINE OF THE THESIS

Although considerable progress has been made in understanding the etiology, pathophysiology and treatment of TD and OCD since their first descriptions, much remains to be learned. Therefore, in this thesis, we conducted human and animal model studies to increase our knowledge on the biological processes and molecular mechanisms implicated in both

disorders and their treatments. Specifically, we used self-generated and publicly available high-throughput data at different molecular, omics levels, such as genomic, transcriptomic and metabolomic data, and deployed several methods to analyze these data, including gene enrichment analyses and shared genetic etiology analyses based on polygenic risk scores (PRS).

The two specific aims of the thesis are:

(i) to identify molecular mechanisms underlying TD- and OCD-related behaviors and the beneficial effects of their treatments using brain transcriptomics data from two intervention-based rodent models of these disorders; (ii) to provide insights into molecular processes underlying TD and OCD and/or related symptoms through analyses and integration of results from multiple types of omics data from human studies.

In **Chapter 2**, we investigated the molecular mechanisms underlying the PANDAS-like behaviors in mice elicited by repeated Group A streptococcus (GAS) infections from late infancy to adulthood and the modulatory role of neonatal corticosterone administration – mimicking chronic stress – through enrichment analyses of transcriptomic data from striatal brain tissue.

In **Chapter 3**, we used a similar approach to investigate the molecular mechanisms underlying Levodopa-induced abnormal involuntary movements (dyskinesia) in unilaterally lesioned 6-hydroxydopamine juvenile rats and the modulatory, beneficial role of Riluzole through enrichment analyses of transcriptomic data from the striatal brain tissue.

In **Chapter 4**, based on the available human omics data, we compiled a list of TD candidate genes, and we subsequently conducted enrichment analyses of this list. Using genomic data, we also investigated genetic sharing between TD and blood and cerebrospinal fluid metabolite levels using PRS-based analyses. Lastly, we integrated the results from our analyses with literature data on the interactions between the TD candidate genes and metabolites to build a molecular landscape of TD that also suggests potential drug targets.

In **Chapter 5**, we built on previous studies that identified genetic sharing between clinical OCD and obsessive-compulsive symptoms (OCS) in the population and implicated altered central nervous system (CNS) insulin signaling as a molecular mechanism involved in OCD etiology. To this end, we conducted PRS-based analyses to assess the extent of genetic overlap between OCD, OCS in the population and (peripheral) insulin-related traits, and we assessed the enrichment of CNS insulin signaling-related genes in genetic data for OCS.

In **Chapter 6**, I summarized and discussed the main findings from this thesis and provided suggestions for future research.

REFERENCES

1. Itard, J.M. Mémoire sur quelques fonctions involontaires des appareils de la locomotion, de la préhension et de la voix. *Arch Gen Med* **1825**, *8*, 385-407.

2. Gilles de la Tourette, G. *tude sur une affection nerveuse caractĔrisÈe par de l'incoordination motrice accompagnÈe d'Ècholalie et de coprolalie (jumping, latah, myriachit)*; Aux bureaux du ProgrËs mÈdical : V.-A. Delahaye et Lecrosnier: Paris, 1885.

3. Walusinski, O. *Georges Gilles de la Tourette: Beyond the Eponym, a Biography*; Oxford University Press: 2018.

4. Penzel, F. 11Clinical Presentation of OCD. In *Obsessive-compulsive Disorder: Phenomenology, Pathophysiology, and Treatment*, Pittenger, C., Pittenger, C., Eds.; Oxford University Press: 2017; p. 0.

5. Medicine, S. Obsessive-Compulsive and Related Disorders. History. Available online: https://med.stanford.edu/ocd/treatment/history.html

6. Boileau, B. A review of obsessive-compulsive disorder in children and adolescents. *Dialogues Clin Neurosci* **2011**, *13*, 401-411, doi:10.31887/DCNS.2011.13.4/bboileau.

7. American Psychiatric Association, A.P.A.D.S.M.T.F. *Diagnostic and statistical manual of mental disorders : DSM-5*; American Psychiatric Association: Arlington, VA, 2013.

8. World Health Organization, W.H.O. International classification of diseases for mortality and morbidity statistics (11th Revision). **2019**.

9. Scharf, J.M.; Miller, L.L.; Gauvin, C.A.; Alabiso, J.; Mathews, C.A.; Ben-Shlomo, Y. Population prevalence of Tourette syndrome: a systematic review and meta-analysis. *Mov Disord* **2015**, *30*, 221-228, doi:10.1002/mds.26089.

10. Knight, T.; Steeves, T.; Day, L.; Lowerison, M.; Jette, N.; Pringsheim, T. Prevalence of tic disorders: a systematic review and meta-analysis. *Pediatr Neurol* **2012**, *47*, 77-90, doi:10.1016/j.pediatrneurol.2012.05.002.

11. Yang, C.; Zhang, L.; Zhu, P.; Zhu, C.; Guo, Q. The prevalence of tic disorders for children in China: A systematic review and meta-analysis. *Medicine* **2016**, *95*, e4354, doi:10.1097/md.0000000000004354.

12. Levine, J.L.S.; Szejko, N.; Bloch, M.H. Meta-analysis: Adulthood prevalence of Tourette syndrome. *Prog Neuropsychopharmacol Biol Psychiatry* **2019**, *95*, 109675, doi:10.1016/j.pnpbp.2019.109675.

13. Dooley, J.M. Tic Disorders in Childhood. *Seminars in Pediatric Neurology* **2006**, *13*, 231-242, doi:https://doi.org/10.1016/j.spen.2006.09.004.

14. Robertson, M.M.; Eapen, V.; Singer, H.S.; Martino, D.; Scharf, J.M.; Paschou, P.; Roessner, V.; Woods, D.W.; Hariz, M.; Mathews, C.A.; et al. Gilles de la Tourette syndrome. *Nat Rev Dis Primers* **2017**, *3*, 16097, doi:10.1038/nrdp.2016.97.

15. Leckman, J.F.; Zhang, H.; Vitale, A.; Lahnin, F.; Lynch, K.; Bondi, C.; Kim, Y.S.; Peterson, B.S. Course of tic severity in Tourette syndrome: the first two decades. *Pediatrics* **1998**, *102*, 14-19, doi:10.1542/peds.102.1.14.

16. Bloch, M.H.; Leckman, J.F. Clinical course of Tourette syndrome. *J Psychosom Res* **2009**, *67*, 497-501, doi:10.1016/j.jpsychores.2009.09.002.

17. Freeman, R.D.; Zinner, S.H.; Müller-Vahl, K.R.; Fast, D.K.; Burd, L.J.; Kano, Y.; Rothenberger, A.; Roessner, V.; Kerbeshian, J.; Stern, J.S.; et al. Coprophenomena in Tourette syndrome. *Dev Med Child Neurol* **2009**, *51*, 218-227, doi:10.1111/j.1469-8749.2008.03135.x.

18. Brandt, V.C.; Beck, C.; Sajin, V.; Baaske, M.K.; Bäumer, T.; Beste, C.; Anders, S.; Münchau, A. Temporal relationship between premonitory urges and tics in Gilles de la Tourette syndrome. *Cortex* **2016**, *77*, 24-37, doi:https://doi.org/10.1016/j.cortex.2016.01.008.

19. Crossley, E.; Seri, S.; Stern, J.S.; Robertson, M.M.; Cavanna, A.E. Premonitory urges for tics in adult patients with Tourette syndrome. *Brain and Development* **2014**, *36*, 45-50, doi:10.1016/j.braindev.2012.12.010.

20. Leckman, J.F.; Walker, D.E.; Cohen, D.J. Premonitory urges in Tourette's syndrome. *Am J Psychiatry* **1993**, *150*, 98-102, doi:10.1176/ajp.150.1.98.

21. Kwak, C.; Dat Vuong, K.; Jankovic, J. Premonitory sensory phenomenon in Tourette's syndrome. *Movement Disorders* **2003**, *18*, 1530-1533, doi:https://doi.org/10.1002/mds.10618.

22. Eapen, V.; Crncec, R. Tourette syndrome in children and adolescents: special considerations. *J Psychosom Res* **2009**, *67*, 525-532, doi:10.1016/j.jpsychores.2009.08.003.

23. Leckman, J.F.; Walker, D.E.; Goodman, W.K.; Pauls, D.L.; Cohen, D.J. "Just right" perceptions associated with compulsive behavior in Tourette's syndrome. *Am J Psychiatry* **1994**, *151*, 675-680, doi:10.1176/ajp.151.5.675.

24. Banaschewski, T.; Woerner, W.; Rothenberger, A. Premonitory sensory phenomena and suppressibility of tics in Tourette syndrome: developmental aspects in children and adolescents. *Dev Med Child Neurol* **2003**, *45*, 700-703, doi:10.1017/s0012162203001294.

25. Ganos, C.; Kahl, U.; Schunke, O.; Kühn, S.; Haggard, P.; Gerloff, C.; Roessner, V.; Thomalla, G.; Münchau, A. Are premonitory urges a prerequisite of tic inhibition in Gilles de la Tourette syndrome? *J Neurol Neurosurg Psychiatry* **2012**, *83*, 975-978, doi:10.1136/jnnp-2012-303033.

26. Dell'Osso, B.; Benatti, B.; Hollander, E.; Fineberg, N.; Stein, D.J.; Lochner, C.; Nicolini, H.; Lanzagorta, N.; Palazzo, C.; Altamura, A.C.; et al. Childhood, adolescent and adult age at onset and related clinical correlates in obsessive-compulsive disorder: a report from the International College of Obsessive-Compulsive Spectrum Disorders (ICOCS). *Int J Psychiatry Clin Pract* **2016**, *20*, 210-217, doi:10.1080/13651501.2016.1207087.

27. Fawcett, E.J.; Power, H.; Fawcett, J.M. Women Are at Greater Risk of OCD Than Men: A Meta-Analytic Review of OCD Prevalence Worldwide. *J Clin Psychiatry* **2020**, *81*, doi:10.4088/JCP.19r13085.

28. Ruscio, A.M.; Stein, D.J.; Chiu, W.T.; Kessler, R.C. The epidemiology of obsessive-compulsive disorder in the National Comorbidity Survey Replication. *Mol Psychiatry* **2010**, *15*, 53-63, doi:10.1038/mp.2008.94.

29. Albert, U.; Manchia, M.; Tortorella, A.; Volpe, U.; Rosso, G.; Carpiniello, B.; Maina, G. Admixture analysis of age at symptom onset and age at disorder onset in a large sample of patients with obsessive-compulsive disorder. *J Affect Disord* **2015**, *187*, 188-196, doi:10.1016/j.jad.2015.07.045.

30. Anholt, G.E.; Aderka, I.M.; van Balkom, A.J.; Smit, J.H.; Schruers, K.; van der Wee, N.J.; Eikelenboom, M.; De Luca, V.; van Oppen, P. Age of onset in obsessive-compulsive disorder: admixture analysis with a large sample. *Psychol Med* **2014**, *44*, 185-194, doi:10.1017/s0033291713000470.

31. Mathes, B.M.; Morabito, D.M.; Schmidt, N.B. Epidemiological and Clinical Gender Differences in OCD. *Curr Psychiatry Rep* **2019**, *21*, 36, doi:10.1007/s11920-019-1015-2.

32. Macy, A.S.; Theo, J.N.; Kaufmann, S.C.; Ghazzaoui, R.B.; Pawlowski, P.A.; Fakhry, H.I.; Cassmassi, B.J.; IsHak, W.W. Quality of life in obsessive compulsive disorder. *CNS Spectr* **2013**, *18*, 21-33, doi:10.1017/s1092852912000697.

33. Stein, D.J.; Costa, D.L.C.; Lochner, C.; Miguel, E.C.; Reddy, Y.C.J.; Shavitt, R.G.; van den Heuvel, O.A.; Simpson, H.B. Obsessive-compulsive disorder. *Nat Rev Dis Primers* **2019**, *5*, 52, doi:10.1038/s41572-019-0102-3.

34. Abramowitz, J.S.; Deacon, B.J.; Olatunji, B.O.; Wheaton, M.G.; Berman, N.C.; Losardo, D.; Timpano, K.R.; McGrath, P.B.; Riemann, B.C.; Adams, T.; et al. Assessment of obsessive-compulsive symptom dimensions: development and evaluation of the Dimensional Obsessive-Compulsive Scale. *Psychol Assess* **2010**, *22*, 180-198, doi:10.1037/a0018260.

35. Rachman, S.; de Silva, P. Abnormal and normal obsessions. *Behav Res Ther* **1978**, *16*, 233-248, doi:10.1016/0005-7967(78)90022-0.

36. Fullana, M.A.; Mataix-Cols, D.; Caspi, A.; Harrington, H.; Grisham, J.R.; Moffitt, T.E.; Poulton, R. Obsessions and compulsions in the community: prevalence, interference, help-seeking, developmental stability, and co-occurring psychiatric conditions. *Am J Psychiatry* **2009**, *166*, 329-336, doi:10.1176/appi.ajp.2008.08071006.

37. Ferrão, Y.A.; Shavitt, R.G.; Prado, H.; Fontenelle, L.F.; Malavazzi, D.M.; de Mathis, M.A.; Hounie, A.G.; Miguel, E.C.; do Rosário, M.C. Sensory phenomena associated with repetitive behaviors in obsessive-compulsive disorder: an exploratory study of 1001 patients. *Psychiatry Res* **2012**, *197*, 253-258, doi:10.1016/j.psychres.2011.09.017.

38. Shavitt, R.G.; de Mathis, M.A.; Oki, F.; Ferrao, Y.A.; Fontenelle, L.F.; Torres, A.R.; Diniz, J.B.; Costa, D.L.; do Rosário, M.C.; Hoexter, M.Q.; et al. Phenomenology of OCD: lessons from a large multicenter study and implications for ICD-11. *J Psychiatr Res* **2014**, *57*, 141-148, doi:10.1016/j.jpsychires.2014.06.010.

39. Mataix-Cols, D.; Rosario-Campos, M.C.; Leckman, J.F. A multidimensional model of obsessive-compulsive disorder. *Am J Psychiatry* **2005**, *162*, 228-238, doi:10.1176/appi.ajp.162.2.228.

40. Leckman, J.F.; Bloch, M.H.; King, R.A. Symptom dimensions and subtypes of obsessive-compulsive disorder: a developmental perspective. *Dialogues Clin Neurosci* **2009**, *11*, 21-33, doi:10.31887/DCNS.2009.11.1/jfleckman.

41. Leckman, J.F.; Grice, D.E.; Barr, L.C.; de Vries, A.L.; Martin, C.; Cohen, D.J.; McDougle, C.J.; Goodman, W.K.; Rasmussen, S.A. Tic-related vs. non-tic-related obsessive compulsive disorder. *Anxiety* **1994**, *1*, 208-215.

42. Leckman, J.F.; Denys, D.; Simpson, H.B.; Mataix-Cols, D.; Hollander, E.; Saxena, S.; Miguel, E.C.; Rauch, S.L.; Goodman, W.K.; Phillips, K.A.; et al. Obsessive-compulsive disorder: a review of the diagnostic criteria and possible subtypes and dimensional specifiers for DSM-V. *Depress Anxiety* **2010**, *27*, 507-527, doi:10.1002/da.20669.

43. Chabane, N.; Delorme, R.; Millet, B.; Mouren, M.C.; Leboyer, M.; Pauls, D. Early-onset obsessive-compulsive disorder: a subgroup with a specific clinical and familial pattern? *J Child Psychol Psychiatry* **2005**, *46*, 881-887, doi:10.1111/j.1469-7610.2004.00382.x.

44. do Rosario-Campos, M.C.; Leckman, J.F.; Curi, M.; Quatrano, S.; Katsovitch, L.; Miguel, E.C.; Pauls, D.L. A family study of early-onset obsessive-compulsive disorder. *Am J Med Genet B Neuropsychiatr Genet* **2005**, *136b*, 92-97, doi:10.1002/ajmg.b.30149.

45. Mataix-Cols, D.; Rauch, S.L.; Baer, L.; Eisen, J.L.; Shera, D.M.; Goodman, W.K.; Rasmussen, S.A.; Jenike, M.A. Symptom stability in adult obsessive-compulsive disorder: data from a naturalistic two-year follow-up study. *Am J Psychiatry* **2002**, *159*, 263-268, doi:10.1176/appi.ajp.159.2.263.

46. Krueger, R.F.; Piasecki, T.M. Toward a dimensional and psychometrically-informed approach to conceptualizing psychopathology. *Behav Res Ther* **2002**, *40*, 485-499, doi:10.1016/s0005-7967(02)00016-5.

47. Worbe, Y.; Mallet, L.; Golmard, J.L.; Béhar, C.; Durif, F.; Jalenques, I.; Damier, P.; Derkinderen, P.; Pollak, P.; Anheim, M.; et al. Repetitive behaviours in patients with Gilles de la Tourette syndrome: tics, compulsions, or both? *PLoS One* **2010**, *5*, e12959, doi:10.1371/journal.pone.0012959.

48. Ferrão, Y.A.; Miguel, E.; Stein, D.J. Tourette's syndrome, trichotillomania, and obsessive-compulsive disorder: how closely are they related? *Psychiatry Res* **2009**, *170*, 32-42, doi:10.1016/j.psychres.2008.06.008.

49. Franklin, M.E.; Harrison, J.P.; Benavides, K.L. Obsessive-compulsive and tic-related disorders. *Child Adolesc Psychiatr Clin N Am* **2012**, *21*, 555-571, doi:10.1016/j.chc.2012.05.008.

50. Lewin, A.B.; Chang, S.; McCracken, J.; McQueen, M.; Piacentini, J. Comparison of clinical features among youth with tic disorders, obsessive-compulsive disorder (OCD), and both conditions. *Psychiatry Res* **2010**, *178*, 317-322, doi:10.1016/j.psychres.2009.11.013.

51. Han, V.X.; Patel, S.; Jones, H.F.; Dale, R.C. Maternal immune activation and neuroinflammation in human neurodevelopmental disorders. *Nature Reviews Neurology* **2021**, *17*, 564-579, doi:10.1038/s41582-021-00530-8.

52. Mahjani, B.; Klei, L.; Hultman, C.M.; Larsson, H.; Devlin, B.; Buxbaum, J.D.; Sandin, S.; Grice, D.E. Maternal effects as causes of risk for obsessive-compulsive disorder. *Biological psychiatry* **2020**, *87*, 1045-1051.

53. Zhang, T.; Brander, G.; Isung, J.; Isomura, K.; Sidorchuk, A.; Larsson, H.; Chang, Z.; Mataix-Cols, D.; Fernández de la Cruz, L. Prenatal and Early Childhood Infections and Subsequent Risk of Obsessive-Compulsive Disorder and Tic Disorders: A Nationwide, Sibling-Controlled Study. *Biological Psychiatry* **2022**, doi:https://doi.org/10.1016/j.biopsych.2022.07.004.

54. Swedo, S.E.; Leonard, H.L.; Garvey, M.; Mittleman, B.; Allen, A.J.; Perlmutter, S.; Lougee, L.; Dow, S.; Zamkoff, J.; Dubbert, B.K. Pediatric autoimmune neuropsychiatric disorders associated with streptococcal infections: clinical description of the first 50 cases. *Am J Psychiatry* **1998**, *155*, 264-271, doi:10.1176/ajp.155.2.264.

55. Chiarello, F.; Spitoni, S.; Hollander, E.; Matucci Cerinic, M.; Pallanti, S. An expert opinion on PANDAS/PANS: highlights and controversies. *Int J Psychiatry Clin Pract* **2017**, *21*, 91-98, doi:10.1080/13651501.2017.1285941.

56. E. Swedo, S. From Research Subgroup to Clinical Syndrome: Modifying the PANDAS Criteria to Describe PANS (Pediatric Acute-onset Neuropsychiatric Syndrome). *Pediatrics & Therapeutics* **2012**, *02*, doi:10.4172/2161-0665.1000113.

57. Rothenberger, A.; Roessner, V. Psychopharmacotherapy of Obsessive-Compulsive Symptoms within the Framework of Tourette Syndrome. *Curr Neuropharmacol* **2019**, *17*, 703-709, doi:10.2174/1570159x16666180828095131.

58. Kloft, L.; Steinel, T.; Kathmann, N. Systematic review of co-occurring OCD and TD: Evidence for a tic-related OCD subtype? *Neurosci Biobehav Rev* **2018**, *95*, 280-314, doi:10.1016/j.neubiorev.2018.09.021.

59. Grados, M.A.; Riddle, M.A.; Samuels, J.F.; Liang, K.Y.; Hoehn-Saric, R.; Bienvenu, O.J.; Walkup, J.T.; Song, D.; Nestadt, G. The familial phenotype of obsessive-compulsive disorder in relation to tic disorders: the Hopkins OCD family study. *Biol Psychiatry* **2001**, *50*, 559-565, doi:10.1016/s0006-3223(01)01074-5.

60. Brander, G.; Kuja-Halkola, R.; Rosenqvist, M.A.; Ruck, C.; Serlachius, E.; Fernandez de la Cruz, L.; Lichtenstein, P.; Crowley, J.J.; Larsson, H.; Mataix-Cols, D. A population-based family clustering study of tic-related obsessive-compulsive disorder. *Mol Psychiatry* **2021**, *26*, 1224-1233, doi:10.1038/s41380-019-0532-z.

61. Gomes de Alvarenga, P.; de Mathis, M.A.; Dominguez Alves, A.C.; do Rosário, M.C.; Fossaluza, V.; Hounie, A.G.; Miguel, E.C.; Rodrigues Torres, A. Clinical features of tic-related obsessive-compulsive disorder: results from a large multicenter study. *CNS Spectr* **2012**, *17*, 87-93, doi:10.1017/s1092852912000491.

62. Nestadt, G.; Addington, A.; Samuels, J.; Liang, K.Y.; Bienvenu, O.J.; Riddle, M.; Grados, M.; Hoehn-Saric, R.; Cullen, B. The identification of OCD-related subgroups based on comorbidity. *Biol Psychiatry* **2003**, *53*, 914-920, doi:10.1016/s0006-3223(02)01677-3.

63. Zohar, A.H.; Pauls, D.L.; Ratzoni, G.; Apter, A.; Dycian, A.; Binder, M.; King, R.; Leckman, J.F.; Kron, S.; Cohen, D.J. Obsessive-compulsive disorder with and without tics in an epidemiological sample of adolescents. *Am J Psychiatry* **1997**, *154*, 274-276, doi:10.1176/ajp.154.2.274.

64. de Vries, F.E.; Cath, D.C.; Hoogendoorn, A.W.; van Oppen, P.; Glas, G.; Veltman, D.J.; van den Heuvel, O.A.; van Balkom, A.J. Tic-Related Versus Tic-Free Obsessive-Compulsive Disorder: Clinical Picture and 2-Year Natural Course. *J Clin Psychiatry* **2016**, *77*, e1240-e1247, doi:10.4088/JCP.14m09736.

65. Miguel, E.C.; Baer, L.; Coffey, B.J.; Rauch, S.L.; Savage, C.R.; O'Sullivan, R.L.; Phillips, K.; Moretti, C.; Leckman, J.F.; Jenike, M.A. Phenomenological differences appearing with repetitive behaviours in obsessive-compulsive disorder and Gilles de la Tourette's syndrome. *Br J Psychiatry* **1997**, *170*, 140-145, doi:10.1192/bjp.170.2.140.

66. Diniz, J.B.; Rosario-Campos, M.C.; Hounie, A.G.; Curi, M.; Shavitt, R.G.; Lopes, A.C.; Miguel, E.C. Chronic tics and Tourette syndrome in patients with obsessive-compulsive disorder. *J Psychiatr Res* **2006**, *40*, 487-493, doi:10.1016/j.jpsychires.2005.09.002.

67. Hyde, T.M.; Aaronson, B.A.; Randolph, C.; Rickler, K.C.; Weinberger, D.R. Relationship of birth weight to the phenotypic expression of Gilles de la Tourette's syndrome in monozygotic twins. *Neurology* **1992**, *42*, 652-658, doi:10.1212/wnl.42.3.652.

68. Price, R.A.; Kidd, K.K.; Cohen, D.J.; Pauls, D.L.; Leckman, J.F. A twin study of Tourette syndrome. *Arch Gen Psychiatry* **1985**, *42*, 815-820, doi:10.1001/archpsyc.1985.01790310077011.

69. O'Rourke, J.A.; Scharf, J.M.; Yu, D.; Pauls, D.L. The genetics of Tourette syndrome: a review. *J Psychosom Res* **2009**, *67*, 533-545, doi:10.1016/j.jpsychores.2009.06.006.

70. Browne, H.A.; Hansen, S.N.; Buxbaum, J.D.; Gair, S.L.; Nissen, J.B.; Nikolajsen, K.H.; Schendel, D.E.; Reichenberg, A.; Parner, E.T.; Grice, D.E. Familial clustering of tic disorders and obsessive-compulsive disorder. *JAMA Psychiatry* **2015**, *72*, 359-366, doi:10.1001/jamapsychiatry.2014.2656.

71. Mataix-Cols, D.; Isomura, K.; Pérez-Vigil, A.; Chang, Z.; Rück, C.; Larsson, K.J.; Leckman, J.F.; Serlachius, E.; Larsson, H.; Lichtenstein, P. Familial Risks of Tourette Syndrome and Chronic Tic Disorders. A Population-Based Cohort Study. *JAMA Psychiatry* **2015**, *72*, 787-793, doi:10.1001/jamapsychiatry.2015.0627.

72. Heiman, G.A.; Rispoli, J.; Seymour, C.; Leckman, J.F.; King, R.A.; Fernandez, T.V. Empiric Recurrence Risk Estimates for Chronic Tic Disorders: Implications for Genetic Counseling. *Front Neurol* **2020**, *11*, 770, doi:10.3389/fneur.2020.00770.

73. Abdulkadir, M.; Mathews, C.A.; Scharf, J.M.; Yu, D.; Tischfield, J.A.; Heiman, G.A.; Hoekstra, P.J.; Dietrich, A. Polygenic Risk Scores Derived From a Tourette Syndrome Genome-wide Association Study Predict Presence of Tics in the Avon Longitudinal Study of Parents and Children Cohort. *Biol Psychiatry* **2019**, *85*, 298-304, doi:10.1016/j.biopsych.2018.09.011.

74. Yu, D.; Sul, J.H.; Tsetsos, F.; Nawaz, M.S.; Huang, A.Y.; Zelaya, I.; Illmann, C.; Osiecki, L.; Darrow, S.M.; Hirschtritt, M.E.; et al. Interrogating the Genetic Determinants of Tourette's Syndrome and Other Tic Disorders Through Genome-Wide Association Studies. *Am J Psychiatry* **2019**, *176*, 217-227, doi:10.1176/appi.ajp.2018.18070857.

75. Davis, L.K.; Yu, D.; Keenan, C.L.; Gamazon, E.R.; Konkashbaev, A.I.; Derks, E.M.; Neale, B.M.; Yang, J.; Lee, S.H.; Evans, P.; et al. Partitioning the heritability of Tourette syndrome and obsessive compulsive disorder reveals differences in genetic architecture. *PLoS Genet* **2013**, *9*, e1003864, doi:10.1371/journal.pgen.1003864.

76. Levy, A.M.; Paschou, P.; Tumer, Z. Candidate Genes and Pathways Associated with Gilles de la Tourette Syndrome-Where Are We? *Genes (Basel)* **2021**, *12*, doi:10.3390/genes12091321.

77. Abelson, J.F.; Kwan, K.Y.; O'Roak, B.J.; Baek, D.Y.; Stillman, A.A.; Morgan, T.M.; Mathews, C.A.; Pauls, D.L.; Rasin, M.R.; Gunel, M.; et al. Sequence variants in SLITRK1 are associated with Tourette's syndrome. *Science* **2005**, *310*, 317-320, doi:10.1126/science.1116502.

78. Ercan-Sencicek, A.G.; Stillman, A.A.; Ghosh, A.K.; Bilguvar, K.; O'Roak, B.J.; Mason, C.E.; Abbott, T.; Gupta, A.; King, R.A.; Pauls, D.L.; et al. L-histidine decarboxylase and Tourette's syndrome. *N Engl J Med* **2010**, *362*, 1901-1908, doi:10.1056/NEJMoa0907006.

79. Karagiannidis, I.; Dehning, S.; Sandor, P.; Tarnok, Z.; Rizzo, R.; Wolanczyk, T.; Madruga-Garrido, M.; Hebebrand, J.; Nothen, M.M.; Lehmkuhl, G.; et al. Support of the histaminergic hypothesis in Tourette syndrome: association of the histamine decarboxylase gene in a large sample of families. *J Med Genet* **2013**, *50*, 760-764, doi:10.1136/jmedgenet-2013-101637.

80. Fernandez, T.V.; Sanders, S.J.; Yurkiewicz, I.R.; Ercan-Sencicek, A.G.; Kim, Y.S.; Fishman, D.O.; Raubeson, M.J.; Song, Y.; Yasuno, K.; Ho, W.S.; et al. Rare copy number variants in tourette syndrome disrupt genes in histaminergic pathways and overlap with autism. *Biol Psychiatry* **2012**, *71*, 392-402, doi:10.1016/j.biopsych.2011.09.034.

81. Scharf, J.M.; Yu, D.; Mathews, C.A.; Neale, B.M.; Stewart, S.E.; Fagerness, J.A.; Evans, P.; Gamazon, E.; Edlund, C.K.; Service, S.K.; et al. Genome-wide association study of Tourette's syndrome. *Mol Psychiatry* **2013**, *18*, 721-728, doi:10.1038/mp.2012.69.

82. Halvorsen, M.; Szatkiewicz, J.; Mudgal, P.; Yu, D.; Psychiatric Genomics Consortium, T.S.O.C.D.W.G.; Nordsletten, A.E.; Mataix-Cols, D.; Mathews, C.A.; Scharf, J.M.; Mattheisen, M.; et al. Elevated common variant genetic risk for tourette syndrome in a densely-affected pedigree. *Mol Psychiatry* **2021**, doi:10.1038/s41380-021-01277-w.

83. Huang, A.Y.; Yu, D.; Davis, L.K.; Sul, J.H.; Tsetsos, F.; Ramensky, V.; Zelaya, I.; Ramos, E.M.; Osiecki, L.; Chen, J.A.; et al. Rare Copy Number Variants in NRXN1 and CNTN6 Increase Risk for Tourette Syndrome. *Neuron* **2017**, *94*, 1101-1111 e1107, doi:10.1016/j.neuron.2017.06.010.

84. Nag, A.; Bochukova, E.G.; Kremeyer, B.; Campbell, D.D.; Muller, H.; Valencia-Duarte, A.V.; Cardona, J.; Rivas, I.C.; Mesa, S.C.; Cuartas, M.; et al. CNV analysis in Tourette syndrome implicates large genomic rearrangements in COL8A1 and NRXN1. *PLoS One* **2013**, *8*, e59061, doi:10.1371/journal.pone.0059061.

85. Sundaram, S.K.; Huq, A.M.; Wilson, B.J.; Chugani, H.T. Tourette syndrome is associated with recurrent exonic copy number variants. *Neurology* **2010**, *74*, 1583-1590, doi:10.1212/WNL.0b013e3181e0f147.

86. Bertelsen, B.; Stefansson, H.; Riff Jensen, L.; Melchior, L.; Mol Debes, N.; Groth, C.; Skov, L.; Werge, T.; Karagiannidis, I.; Tarnok, Z.; et al. Association of AADAC Deletion and Gilles de la Tourette Syndrome in a Large European Cohort. *Biol Psychiatry* **2016**, *79*, 383-391, doi:10.1016/j.biopsych.2015.08.027.

87. Wang, S.; Mandell, J.D.; Kumar, Y.; Sun, N.; Morris, M.T.; Arbelaez, J.; Nasello, C.; Dong, S.; Duhn, C.; Zhao, X.; et al. De Novo Sequence and Copy Number Variants Are Strongly Associated with Tourette Disorder and Implicate Cell Polarity in Pathogenesis. *Cell Rep* **2018**, *24*, 3441-3454 e3412, doi:10.1016/j.celrep.2018.08.082.

88. Nestadt, G.; Samuels, J.; Riddle, M.; Bienvenu, O.J., 3rd; Liang, K.Y.; LaBuda, M.; Walkup, J.; Grados, M.; Hoehn-Saric, R. A family study of obsessive-compulsive disorder. *Arch Gen Psychiatry* **2000**, *57*, 358-363, doi:10.1001/archpsyc.57.4.358.

89. Hanna, G.L.; Veenstra-VanderWeele, J.; Cox, N.J.; Boehnke, M.; Himle, J.A.; Curtis, G.C.; Leventhal, B.L.; Cook, E.H., Jr. Genome-wide linkage analysis of families with obsessive-compulsive disorder ascertained through pediatric probands. *Am J Med Genet* **2002**, *114*, 541-552, doi:10.1002/ajmg.10519.

90. van Grootheest, D.S.; Cath, D.C.; Beekman, A.T.; Boomsma, D.I. Twin studies on obsessive-compulsive disorder: a review. *Twin Res Hum Genet* **2005**, *8*, 450-458, doi:10.1375/183242705774310060.

91. Van Grootheest, D.S.; Cath, D.C.; Beekman, A.T.; Boomsma, D.I. Genetic and environmental influences on obsessive-compulsive symptoms in adults: a population-based twin-family study. *Psychol Med* **2007**, *37*, 1635-1644, doi:10.1017/S0033291707000980.

92. Pauls, D.L. The genetics of obsessive compulsive disorder: a review of the evidence. *Am J Med Genet C Semin Med Genet* **2008**, *148c*, 133-139, doi:10.1002/ajmg.c.30168.

93. Fernandez, T.V.; Leckman, J.F.; Pittenger, C. Genetic susceptibility in obsessive-compulsive disorder. *Handb Clin Neurol* **2018**, *148*, 767-781, doi:10.1016/B978-0-444-64076-5.00049-1.

94. Goodman, W.K.; McDougle, C.J.; Price, L.H.; Riddle, M.A.; Pauls, D.L.; Leckman, J.F. Beyond the serotonin hypothesis: a role for dopamine in some forms of obsessive compulsive disorder? *J Clin Psychiatry* **1990**, *51 Suppl*, 36-43; discussion 55-38.

95. Pittenger, C.; Bloch, M.H.; Williams, K. Glutamate abnormalities in obsessive compulsive disorder: neurobiology, pathophysiology, and treatment. *Pharmacol Ther* **2011**, *132*, 314-332, doi:10.1016/j.pharmthera.2011.09.006.

96. Taylor, S. Molecular genetics of obsessive-compulsive disorder: a comprehensive meta-analysis of genetic association studies. *Mol Psychiatry* **2013**, *18*, 799-805, doi:10.1038/mp.2012.76.

97. Taylor, S. Disorder-specific genetic factors in obsessive-compulsive disorder: A comprehensive meta-analysis. *Am J Med Genet B Neuropsychiatr Genet* **2016**, *171b*, 325-332, doi:10.1002/ajmg.b.32407.

98. Escobar, A.P.; Wendland, J.R.; Chávez, A.E.; Moya, P.R. The Neuronal Glutamate Transporter EAAT3 in Obsessive-Compulsive Disorder. *Front Pharmacol* **2019**, *10*, 1362, doi:10.3389/fphar.2019.01362.

99. Zai, G.; Barta, C.; Cath, D.; Eapen, V.; Geller, D.; Grünblatt, E. New insights and perspectives on the genetics of obsessive-compulsive disorder. *Psychiatr Genet* **2019**, *29*, 142-151, doi:10.1097/ypg.0000000000000230.

100. Stewart, S.E.; Yu, D.; Scharf, J.M.; Neale, B.M.; Fagerness, J.A.; Mathews, C.A.; Arnold, P.D.; Evans, P.D.; Gamazon, E.R.; Davis, L.K.; et al. Genome-wide association study of obsessive-compulsive disorder. *Mol Psychiatry* **2013**, *18*, 788-798, doi:10.1038/mp.2012.85.

101. Mattheisen, M.; Samuels, J.F.; Wang, Y.; Greenberg, B.D.; Fyer, A.J.; McCracken, J.T.; Geller, D.A.; Murphy, D.L.; Knowles, J.A.; Grados, M.A.; et al. Genome-wide association study in obsessive-compulsive disorder: results from the OCGAS. *Mol Psychiatry* **2015**, *20*, 337-344, doi:10.1038/mp.2014.43.

102. International Obsessive Compulsive Disorder Foundation Genetics, C.; Studies, O.C.D.C.G.A. Revealing the complex genetic architecture of obsessive-compulsive disorder using meta-analysis. *Mol Psychiatry* **2018**, *23*, 1181-1188, doi:10.1038/mp.2017.154.

103. McGrath, L.M.; Yu, D.; Marshall, C.; Davis, L.K.; Thiruvahindrapuram, B.; Li, B.; Cappi, C.; Gerber, G.; Wolf, A.; Schroeder, F.A.; et al. Copy number variation in obsessive-compulsive disorder and tourette syndrome: a cross-disorder study. *J Am Acad Child Adolesc Psychiatry* **2014**, *53*, 910-919, doi:10.1016/j.jaac.2014.04.022.

104. van de Vondervoort, I.; Poelmans, G.; Aschrafi, A.; Pauls, D.L.; Buitelaar, J.K.; Glennon, J.C.; Franke, B. An integrated molecular landscape implicates the regulation of dendritic spine formation through insulin-related signalling in obsessive-compulsive disorder. *J Psychiatry Neurosci* **2016**, *41*, 280-285, doi:10.1503/jpn.140327.

105. den Braber, A.; Zilhão, N.R.; Fedko, I.O.; Hottenga, J.J.; Pool, R.; Smit, D.J.; Cath, D.C.; Boomsma, D.I. Obsessive-compulsive symptoms in a large population-based twin-family sample are predicted by clinically based polygenic scores and by genome-wide SNPs. *Transl Psychiatry* **2016**, *6*, e731, doi:10.1038/tp.2015.223.

106. Mathews, C.A.; Delucchi, K.; Cath, D.C.; Willemsen, G.; Boomsma, D.I. Partitioning the etiology of hoarding and obsessive-compulsive symptoms. *Psychol Med* **2014**, *44*, 2867-2876, doi:10.1017/s0033291714000269.

107. Burton, C.L.; Lemire, M.; Xiao, B.; Corfield, E.C.; Erdman, L.; Bralten, J.; Poelmans, G.; Yu, D.; Shaheen, S.M.; Goodale, T.; et al. Genome-wide association study of pediatric obsessive-compulsive traits: shared genetic risk between traits and disorder. *Transl Psychiatry* **2021**, *11*, 91, doi:10.1038/s41398-020-01121-9.

108. Pinto, R.; Monzani, B.; Leckman, J.F.; Rück, C.; Serlachius, E.; Lichtenstein, P.; Mataix-Cols, D. Understanding the covariation of tics, attention-deficit/hyperactivity, and obsessive-compulsive symptoms: A population-based adult twin study. *Am J Med Genet B Neuropsychiatr Genet* **2016**, *171*, 938-947, doi:10.1002/ajmg.b.32436.

109. O'Rourke, J.A.; Scharf, J.M.; Platko, J.; Stewart, S.E.; Illmann, C.; Geller, D.A.; King, R.A.; Leckman, J.F.; Pauls, D.L. The familial association of tourette's disorder and ADHD: the impact of OCD symptoms. *Am J Med Genet B Neuropsychiatr Genet* **2011**, *156b*, 553-560, doi:10.1002/ajmg.b.31195.

110. Bienvenu, O.J.; Samuels, J.F.; Wuyek, L.A.; Liang, K.Y.; Wang, Y.; Grados, M.A.; Cullen, B.A.; Riddle, M.A.; Greenberg, B.D.; Rasmussen, S.A.; et al. Is obsessive-compulsive disorder an anxiety disorder, and what, if any, are spectrum conditions? A family study perspective. *Psychol Med* **2012**, *42*, 1-13, doi:10.1017/s0033291711000742.

111. Yu, D.; Mathews, C.A.; Scharf, J.M.; Neale, B.M.; Davis, L.K.; Gamazon, E.R.; Derks, E.M.; Evans, P.; Edlund, C.K.; Crane, J.; et al. Cross-disorder genome-wide analyses suggest a complex genetic relationship between Tourette's syndrome and OCD. *Am J Psychiatry* **2015**, *172*, 82-93, doi:10.1176/appi.ajp.2014.13101306.

112. Eapen, V.; Robertson, M.M. Are there distinct subtypes in Tourette syndrome? Pure-Tourette syndrome versus Tourette syndrome-plus, and simple versus complex tics. *Neuropsychiatr Dis Treat* **2015**, *11*, 1431-1436, doi:10.2147/ndt.S72284.

113. Brainstorm, C.; Anttila, V.; Bulik-Sullivan, B.; Finucane, H.K.; Walters, R.K.; Bras, J.; Duncan, L.; Escott-Price, V.; Falcone, G.J.; Gormley, P.; et al. Analysis of shared heritability in common disorders of the brain. *Science* **2018**, *360*, doi:10.1126/science.aap8757.

114. Cross-Disorder Group of the Psychiatric Genomics Consortium. Electronic address, p.m.h.e.; Cross-Disorder Group of the Psychiatric Genomics, C. Genomic Relationships, Novel Loci, and Pleiotropic Mechanisms across Eight Psychiatric Disorders. *Cell* **2019**, *179*, 1469-1482 e1411, doi:10.1016/j.cell.2019.11.020.

115. Yang, Z.; Wu, H.; Lee, P.H.; Tsetsos, F.; Davis, L.K.; Yu, D.; Lee, S.H.; Dalsgaard, S.; Haavik, J.; Barta, C.; et al. Investigating Shared Genetic Basis Across Tourette Syndrome and Comorbid Neurodevelopmental Disorders Along the Impulsivity-Compulsivity Spectrum. *Biol Psychiatry* **2021**, *90*, 317-327, doi:10.1016/j.biopsych.2020.12.028.

116. Leckman, J.F.; Pauls, D.L.; Zhang, H.; Rosario-Campos, M.C.; Katsovich, L.; Kidd, K.K.; Pakstis, A.J.; Alsobrook, J.P.; Robertson, M.M.; McMahon, W.M.; et al. Obsessive-compulsive symptom dimensions in affected sibling pairs diagnosed with Gilles de la Tourette syndrome. *Am J Med Genet B Neuropsychiatr Genet* **2003**, *116B*, 60-68, doi:10.1002/ajmg.b.10001.
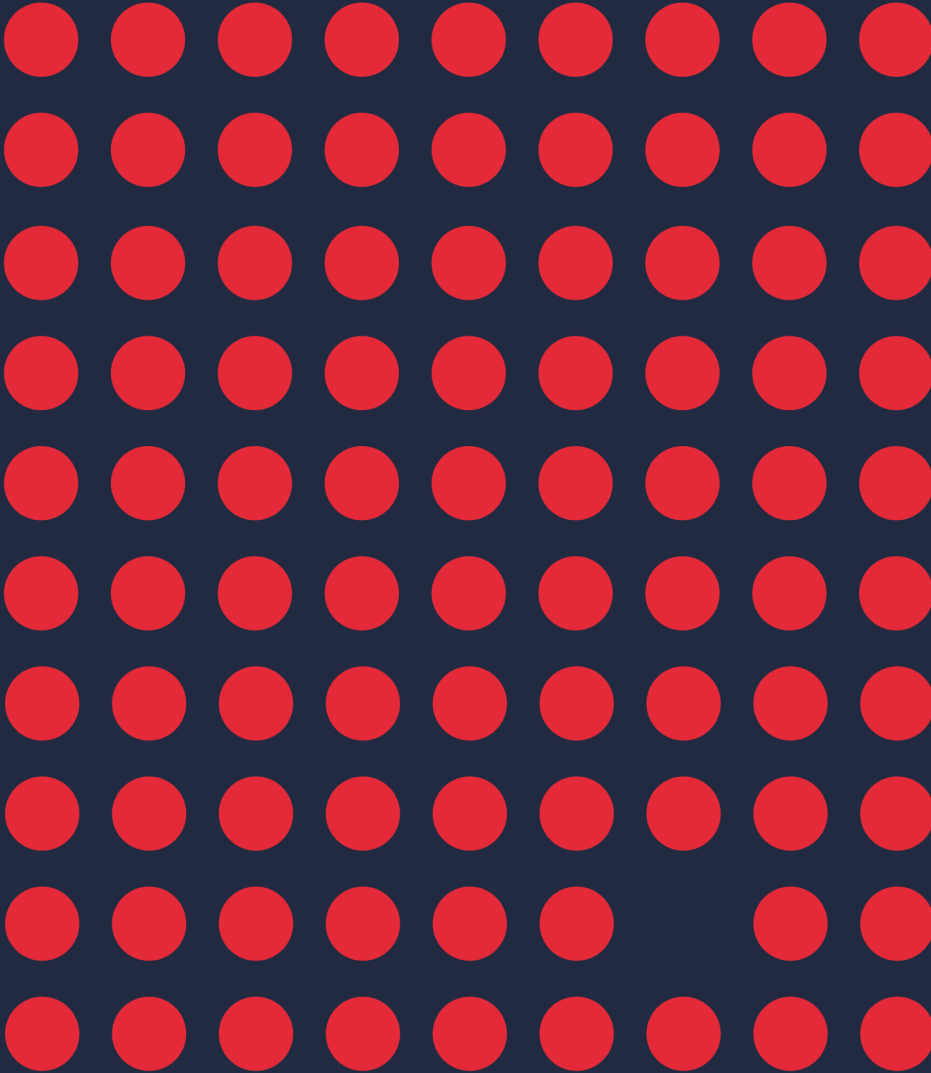
117. Hirschtritt, M.E.; Darrow, S.M.; Illmann, C.; Osiecki, L.; Grados, M.; Sandor, P.; Dion, Y.; King, R.A.; Pauls, D.; Budman, C.L.; et al. Genetic and phenotypic overlap of specific obsessive-compulsive and attention-deficit/hyperactive subtypes with Tourette syndrome. *Psychol Med* **2018**, *48*, 279-293, doi:10.1017/s0033291717001672.

118. Darrow, S.M.; Hirschtritt, M.E.; Davis, L.K.; Illmann, C.; Osiecki, L.; Grados, M.; Sandor, P.; Dion, Y.; King, R.; Pauls, D.; et al. Identification of Two Heritable Cross-Disorder Endophenotypes for Tourette Syndrome. *Am J Psychiatry* **2017**, *174*, 387-396, doi:10.1176/appi.ajp.2016.16020240.

119. Hirschtritt, M.E.; Darrow, S.M.; Illmann, C.; Osiecki, L.; Grados, M.; Sandor, P.; Dion, Y.; King, R.A.; Pauls, D.L.; Budman, C.L.; et al. Social disinhibition is a heritable subphenotype of tics in Tourette syndrome. *Neurology* **2016**, *87*, 497-504, doi:10.1212/wnl.0000000000002910.

120. Marsh, R.; Maia, T.V.; Peterson, B.S. Functional disturbances within frontostriatal circuits across multiple childhood psychopathologies. *Am J Psychiatry* **2009**, *166*, 664-674, doi:10.1176/appi.ajp.2009.08091354.

121. Pauls, D.L.; Abramovitch, A.; Rauch, S.L.; Geller, D.A. Obsessive-compulsive disorder: an integrative genetic and neurobiological perspective. *Nat Rev Neurosci* **2014**, *15*, 410-424, doi:10.1038/nrn3746.

122. Alexander, G.E.; Crutcher, M.D. Functional architecture of basal ganglia circuits: neural substrates of parallel processing. *Trends Neurosci* **1990**, *13*, 266-271, doi:10.1016/0166-2236(90)90107-l.

123. Singer, H.S. Habitual and goal-directed behaviours and Tourette syndrome. *Brain* **2016**, *139*, 312-316, doi:10.1093/brain/awv378.

124. Jahanshahi, M.; Obeso, I.; Rothwell, J.C.; Obeso, J.A. A fronto-striato-subthalamic-pallidal network for goal-directed and habitual inhibition. *Nat Rev Neurosci* **2015**, *16*, 719-732, doi:10.1038/nrn4038.

125. Sowell, E.R.; Kan, E.; Yoshii, J.; Thompson, P.M.; Bansal, R.; Xu, D.; Toga, A.W.; Peterson, B.S. Thinning of sensorimotor cortices in children with Tourette syndrome. *Nat Neurosci* **2008**, *11*, 637-639, doi:10.1038/nn.2121.

126. Neuner, I.; Werner, C.J.; Arrubla, J.; Stöcker, T.; Ehlen, C.; Wegener, H.P.; Schneider, F.; Shah, N.J. Imaging the where and when of tic generation and resting state networks in adult Tourette patients. *Front Hum Neurosci* **2014**, *8*, 362, doi:10.3389/fnhum.2014.00362.

127. Chamberlain, S.R.; Menzies, L.; Hampshire, A.; Suckling, J.; Fineberg, N.A.; del Campo, N.; Aitken, M.; Craig, K.; Owen, A.M.; Bullmore, E.T.; et al. Orbitofrontal dysfunction in patients with obsessive-compulsive disorder and their unaffected relatives. *Science* **2008**, *321*, 421-422, doi:10.1126/science.1154433.

128. Burguière, E.; Monteiro, P.; Mallet, L.; Feng, G.; Graybiel, A.M. Striatal circuits, habits, and implications for obsessive-compulsive disorder. *Curr Opin Neurobiol* **2015**, *30*, 59-65, doi:10.1016/j.conb.2014.08.008.

129. Worbe, Y.; Marrakchi-Kacem, L.; Lecomte, S.; Valabregue, R.; Poupon, F.; Guevara, P.; Tucholka, A.; Mangin, J.F.; Vidailhet, M.; Lehericy, S.; et al. Altered structural connectivity of cortico-striato-pallido-thalamic networks in Gilles de la Tourette syndrome. *Brain* **2015**, *138*, 472-482, doi:10.1093/brain/awu311.

130. van den Heuvel, O.A.; van Wingen, G.; Soriano-Mas, C.; Alonso, P.; Chamberlain, S.R.; Nakamae, T.; Denys, D.; Goudriaan, A.E.; Veltman, D.J. Brain circuitry of compulsivity. *Eur Neuropsychopharmacol* **2016**, *26*, 810-827, doi:10.1016/j.euroneuro.2015.12.005.

131. Mataix-Cols, D.; van den Heuvel, O.A. Common and distinct neural correlates of obsessive-compulsive and related disorders. *Psychiatr Clin North Am* **2006**, *29*, 391-410, viii, doi:10.1016/j.psc.2006.02.006.

132. Conceição, V.A.; Dias, Â.; Farinha, A.C.; Maia, T.V. Premonitory urges and tics in Tourette syndrome: computational mechanisms and neural correlates. *Current Opinion in Neurobiology* **2017**, *46*, 187-199, doi:https://doi.org/10.1016/j.conb.2017.08.009.

133. Narayanaswamy, J.C.; Jose, D.; Kalmady, S.V.; Agarwal, S.M.; Venkatasubramanian, G.; Janardhan Reddy, Y.C. Cerebellar volume deficits in medication-naïve obsessive compulsive disorder. *Psychiatry Res Neuroimaging* **2016**, *254*, 164-168, doi:10.1016/j.pscychresns.2016.07.005.

134. Subirà, M.; Cano, M.; de Wit, S.J.; Alonso, P.; Cardoner, N.; Hoexter, M.Q.; Kwon, J.S.; Nakamae, T.; Lochner, C.; Sato, J.R.; et al. Structural covariance of neostriatal and limbic regions in patients with obsessive-compulsive disorder. *J Psychiatry Neurosci* **2016**, *41*, 115-123, doi:10.1503/jpn.150012.

135. Singer, H.S.; Minzer, K. Neurobiology of Tourette's syndrome: concepts of neuroanatomic localization and neurochemical abnormalities. *Brain and Development* **2003**, *25*, S70-S84, doi:10.1016/S0387-7604(03)90012-X.

136. Kalanithi, P.S.A.; Zheng, W.; Kataoka, Y.; DiFiglia, M.; Grantz, H.; Saper, C.B.; Schwartz, M.L.; Leckman, J.F.; Vaccarino, F.M. Altered parvalbumin-positive neuron distribution in basal ganglia of individuals with Tourette syndrome. *Proceedings of the National Academy of Sciences of the United States of America* **2005**, *102*, 13307, doi:10.1073/pnas.0502624102.

137. Kataoka, Y.; Kalanithi, P.S.A.; Grantz, H.; Schwartz, M.L.; Saper, C.; Leckman, J.F.; Vaccarino, F.M. Decreased number of parvalbumin and cholinergic interneurons in the striatum of individuals with Tourette syndrome. *Journal of Comparative Neurology* **2010**, *518*, 277-291, doi: https://doi.org/10.1002/cne.22206.

138. Lennington, J.B.; Coppola, G.; Kataoka-Sasaki, Y.; Fernandez, T.V.; Palejev, D.; Li, Y.; Huttner, A.; Pletikos, M.; Sestan, N.; Leckman, J.F.; et al. Transcriptome Analysis of the Human Striatum in Tourette Syndrome. *Biol Psychiatry* **2016**, *79*, 372-382, doi:10.1016/j.biopsych.2014.07.018.

139. Piantadosi, S.C.; Chamberlain, B.L.; Glausier, J.R.; Lewis, D.A.; Ahmari, S.E. Lower excitatory synaptic gene expression in orbitofrontal cortex and striatum in an initial study of subjects with obsessive compulsive disorder. *Mol Psychiatry* **2021**, *26*, 986-998, doi:10.1038/s41380-019-0431-3.

140. Augustine, F.; Singer, H.S. Merging the Pathophysiology and Pharmacotherapy of Tics. *Tremor Other Hyperkinet Mov (N Y)* **2018**, *8*, 595, doi:10.7916/d8h14jtx.

141. Leckman, J.F.; Riddle, M.A.; Hardin, M.T.; Ort, S.I.; Swartz, K.L.; Stevenson, J.; Cohen, D.J. The Yale Global Tic Severity Scale: initial testing of a clinician-rated scale of tic severity. *J Am Acad Child Adolesc Psychiatry* **1989**, *28*, 566-573, doi:10.1097/00004583-198907000-00015.

142. Pringsheim, T.; Okun, M.S.; Müller-Vahl, K.; Martino, D.; Jankovic, J.; Cavanna, A.E.; Woods, D.W.; Robinson, M.; Jarvie, E.; Roessner, V.; et al. Practice guideline recommendations summary: Treatment of tics in people with Tourette syndrome and chronic tic disorders. *Neurology* **2019**, *92*, 896-906, doi:10.1212/wnl.0000000000007466.

143. Verdellen, C.; van de Griendt, J.; Hartmann, A.; Murphy, T. European clinical guidelines for Tourette syndrome and other tic disorders. Part III: behavioural and psychosocial interventions. *Eur Child Adolesc Psychiatry* **2011**, *20*, 197-207, doi:10.1007/s00787-011-0167-3.

144. Pringsheim, T.; Holler-Managan, Y.; Okun, M.S.; Jankovic, J.; Piacentini, J.; Cavanna, A.E.; Martino, D.; Müller-Vahl, K.; Woods, D.W.; Robinson, M.; et al. Comprehensive systematic review summary: Treatment of tics in people with Tourette syndrome and chronic tic disorders. *Neurology* **2019**, *92*, 907-915, doi:10.1212/wnl.0000000000007467.

145. Müller-Vahl, K.R. Treatment of Tourette syndrome with cannabinoids. *Behav Neurol* **2013**, *27*, 119-124, doi:10.3233/ben-120276.

146. Zheng, Y.; Zhang, Z.J.; Han, X.M.; Ding, Y.; Chen, Y.Y.; Wang, X.F.; Wei, X.W.; Wang, M.J.; Cheng, Y.; Nie, Z.H.; et al. A proprietary herbal medicine (5-Ling Granule) for Tourette syndrome: a randomized controlled trial. *J Child Psychol Psychiatry* **2016**, *57*, 74-83, doi:10.1111/jcpp.12432.

147. Hirschtritt, M.E.; Bloch, M.H.; Mathews, C.A. Obsessive-Compulsive Disorder: Advances in Diagnosis and Treatment. *JAMA* **2017**, *317*, 1358-1367, doi:10.1001/jama.2017.2200.

148. Pittenger, C.; Bloch, M.H.; Wasylink, S.; Billingslea, E.; Simpson, R.; Jakubovski, E.; Kelmendi, B.; Sanacora, G.; Coric, V. Riluzole augmentation in treatment-refractory obsessive-compulsive disorder: a pilot randomized placebo-controlled trial. *J Clin Psychiatry* **2015**, *76*, 1075-1084, doi:10.4088/JCP.14m09123.

149. Emamzadehfard, S.; Kamaloo, A.; Paydary, K.; Ahmadipour, A.; Zeinoddini, A.; Ghaleiha, A.; Mohammadinejad, P.; Zeinoddini, A.; Akhondzadeh, S. Riluzole in augmentation of fluvoxamine for moderate to severe obsessive-compulsive disorder: Randomized, double-blind, placebo-controlled study. *Psychiatry Clin Neurosci* **2016**, *70*, 332-341, doi:10.1111/pcn.12394.

150. Ghaleiha, A.; Entezari, N.; Modabbernia, A.; Najand, B.; Askari, N.; Tabrizi, M.; Ashrafi, M.; Hajiaghaee, R.; Akhondzadeh, S. Memantine add-on in moderate to severe obsessive-compulsive disorder: randomized double-blind placebo-controlled study. *J Psychiatr Res* **2013**, *47*, 175-180, doi:10.1016/j.jpsychires.2012.09.015.

151. Rodriguez, C.I.; Kegeles, L.S.; Levinson, A.; Feng, T.; Marcus, S.M.; Vermes, D.; Flood, P.; Simpson, H.B. Randomized controlled crossover trial of ketamine in obsessive-compulsive disorder: proof-of-concept. *Neuropsychopharmacology* **2013**, *38*, 2475-2483, doi:10.1038/npp.2013.150.

152. Alonso, P.; Cuadras, D.; Gabriëls, L.; Denys, D.; Goodman, W.; Greenberg, B.D.; Jimenez-Ponce, F.; Kuhn, J.; Lenartz, D.; Mallet, L.; et al. Deep Brain Stimulation for Obsessive-Compulsive Disorder: A Meta-Analysis of Treatment Outcome and Predictors of Response. *PLoS One* **2015**, *10*, e0133591, doi:10.1371/journal.pone.0133591.

153. March, J.S.; Franklin, M.E.; Leonard, H.; Garcia, A.; Moore, P.; Freeman, J.; Foa, E. Tics moderate treatment outcome with sertraline but not cognitive-behavior therapy in pediatric obsessive-compulsive disorder. *Biol Psychiatry* **2007**, *61*, 344-347, doi:10.1016/j.biopsych.2006.09.035.

154. McDougle, C.J.; Goodman, W.K.; Leckman, J.F.; Barr, L.C.; Heninger, G.R.; Price, L.H. The efficacy of fluvoxamine in obsessive-compulsive disorder: effects of comorbid chronic tic disorder. *J Clin Psychopharmacol* **1993**, *13*, 354-358.

155. Conelea, C.A.; Walther, M.R.; Freeman, J.B.; Garcia, A.M.; Sapyta, J.; Khanna, M.; Franklin, M. Tic-related obsessive-compulsive disorder (OCD): phenomenology and treatment outcome in the Pediatric OCD Treatment Study II. *J Am Acad Child Adolesc Psychiatry* **2014**, *53*, 1308-1316, doi:10.1016/j.jaac.2014.09.014.

156. Williams, K.A.; Swedo, S.E.; Farmer, C.A.; Grantz, H.; Grant, P.J.; D'Souza, P.; Hommer, R.; Katsovich, L.; King, R.A.; Leckman, J.F. Randomized, Controlled Trial of Intravenous Immunoglobulin for Pediatric Autoimmune Neuropsychiatric Disorders Associated With Streptococcal Infections. *J Am Acad Child Adolesc Psychiatry* **2016**, *55*, 860-867.e862, doi:10.1016/j.jaac.2016.06.017.

157. Nestler, E.J.; Hyman, S.E. Animal models of neuropsychiatric disorders. *Nat Neurosci* **2010**, *13*, 1161-1169, doi:10.1038/nn.2647.

158. Godar, S.C.; Mosher, L.J.; Di Giovanni, G.; Bortolato, M. Animal models of tic disorders: a translational perspective. *J Neurosci Methods* **2014**, *238*, 54-69, doi:10.1016/j.jneumeth.2014.09.008.

159. Pittenger, C. Animal Models of Tourette Syndrome and Obsessive-Compulsive Disorder. In *Movement Disorders*, LeDoux, M.S., Ed.; Academic Press: Boston, 2015; pp. 747-764.

160. Yael, D.; Israelashvili, M.; Bar-Gad, I. Animal Models of Tourette Syndrome-From Proliferation to Standardization. *Front Neurosci* **2016**, *10*, 132, doi:10.3389/fnins.2016.00132.

161. Willner, P. Validation criteria for animal models of human mental disorders: Learned helplessness as a paradigm case. *Progress in Neuro-Psychopharmacology and Biological Psychiatry* **1986**, *10*, 677-690, doi:10.1016/0278-5846(86)90051-5.

162. Katayama, K.; Yamada, K.; Ornthanalai, V.G.; Inoue, T.; Ota, M.; Murphy, N.P.; Aruga, J. Slitrk1-deficient mice display elevated anxiety-like behavior and noradrenergic abnormalities. *Mol Psychiatry* **2010**, *15*, 177-184, doi:10.1038/mp.2008.97.

163. Baldan, L.C.; Williams, K.A.; Gallezot, J.D.; Pogorelov, V.; Rapanelli, M.; Crowley, M.; Anderson, G.M.; Loring, E.; Gorczyca, R.; Billingslea, E.; et al. Histidine decarboxylase deficiency causes tourette syndrome: parallel findings in humans and mice. *Neuron* **2014**, *81*, 77-90, doi:10.1016/j.neuron.2013.10.052.

164. Berridge, K.C.; Aldridge, J.W.; Houchard, K.R.; Zhuang, X. Sequential super-stereotypy of an instinctive fixed action pattern in hyper-dopaminergic mutant mice: a model of obsessive compulsive disorder and Tourette's. *BMC Biology* **2005**, *3*, 4, doi:10.1186/1741-7007-3-4.

165. Garner, J.P.; Mason, G.J. Evidence for a relationship between cage stereotypies and behavioural disinhibition in laboratory rodents. *Behavioural Brain Research* **2002**, *136*, 83-92, doi: https://doi.org/10.1016/S0166-4328(02)00111-0.

166. Bronfeld, M.; Yael, D.; Belelovsky, K.; Bar-Gad, I. Motor tics evoked by striatal disinhibition in the rat. *Front Syst Neurosci* **2013**, *7*, 50, doi:10.3389/fnsys.2013.00050.

167. Tizabi, Y.; Russell, L.T.; Johnson, M.; Darmani, N.A. Nicotine attenuates DOI-induced head-twitch response in mice: implications for Tourette syndrome. *Prog Neuropsychopharmacol Biol Psychiatry* **2001**, *25*, 1445-1457, doi:10.1016/s0278-5846(01)00194-4.

168. Nordstrom, E.J.; Burton, F.H. A transgenic model of comorbid Tourette's syndrome and obsessive-compulsive disorder circuitry. *Mol Psychiatry* **2002**, *7*, 617-625, 524, doi:10.1038/sj.mp.4001144.

169. Godar, S.C.; Mosher, L.J.; Strathman, H.J.; Gochi, A.M.; Jones, C.M.; Fowler, S.C.; Bortolato, M. The D1CT-7 mouse model of Tourette syndrome displays sensorimotor gating deficits in response to spatial confinement. *Br J Pharmacol* **2016**, *173*, 2111-2121, doi:10.1111/bph.13243.

170. Swerdlow, N.R.; Braff, D.L.; Geyer, M.A. Cross-species studies of sensorimotor gating of the startle reflex. *Ann N Y Acad Sci* **1999**, *877*, 202-216, doi:10.1111/j.1749-6632.1999.tb09269.x.

171. Zebardast, N.; Crowley, M.J.; Bloch, M.H.; Mayes, L.C.; Wyk, B.V.; Leckman, J.F.; Pelphrey, K.A.; Swain, J.E. Brain mechanisms for prepulse inhibition in adults with Tourette syndrome: initial findings. *Psychiatry Res* **2013**, *214*, 33-41, doi:10.1016/j.pscychresns.2013.05.009.

172. Kohl, S.; Heekeren, K.; Klosterkotter, J.; Kuhn, J. Prepulse inhibition in psychiatric disorders--apart from schizophrenia. *J Psychiatr Res* **2013**, *47*, 445-452, doi:10.1016/j.jpsychires.2012.11.018.

173. Mosher, L.J.; Frau, R.; Pardu, A.; Pes, R.; Devoto, P.; Bortolato, M. Selective activation of D1 dopamine receptors impairs sensorimotor gating in Long-Evans rats. *Br J Pharmacol* **2016**, *173*, 2122-2134, doi:10.1111/bph.13232.

174. Taylor, J.R.; Morshed, S.A.; Parveen, S.; Mercadante, M.T.; Scahill, L.; Peterson, B.S.; King, R.A.; Leckman, J.F.; Lombroso, P.J. An animal model of Tourette's syndrome. *Am J Psychiatry* **2002**, *159*, 657-660, doi:10.1176/appi.ajp.159.4.657.

175. Hoffman, K.L.; Hornig, M.; Yaddanapudi, K.; Jabado, O.; Lipkin, W.I. A murine model for neuropsychiatric disorders associated with group A beta-hemolytic streptococcal infection. *J Neurosci* **2004**, *24*, 1780-1791, doi:10.1523/jneurosci.0887-03.2004.

176. Macrì, S.; Ceci, C.; Proietti Onori, M.; Invernizzi, R.W.; Bartolini, E.; Altabella, L.; Canese, R.; Imperi, M.; Orefici, G.; Creti, R.; et al. Mice repeatedly exposed to Group-A β-Haemolytic Streptococcus show perseverative behaviors, impaired sensorimotor gating, and immune activation in rostral diencephalon. *Sci Rep* **2015**, *5*, 13257, doi:10.1038/srep13257.

177. Alonso, P.; López-Solà, C.; Real, E.; Segalàs, C.; Menchón, J.M. Animal models of obsessive-compulsive disorder: utility and limitations. *Neuropsychiatr Dis Treat* **2015**, *11*, 1939-1955, doi:10.2147/ndt.S62785.

178. Welch, J.M.; Lu, J.; Rodriguiz, R.M.; Trotta, N.C.; Peca, J.; Ding, J.-D.; Feliciano, C.; Chen, M.; Adams, J.P.; Luo, J.; et al. Cortico-striatal synaptic defects and OCD-like behaviours in Sapap3-mutant mice. *Nature* **2007**, *448*, 894-900, doi:10.1038/nature06104.

179. Wu, K.; Hanna, G.L.; Rosenberg, D.R.; Arnold, P.D. The role of glutamate signaling in the pathogenesis and treatment of obsessive-compulsive disorder. *Pharmacol Biochem Behav* **2012**, *100*, 726-735, doi:10.1016/j.pbb.2011.10.007.

180. Aida, T.; Yoshida, J.; Nomura, M.; Tanimura, A.; Iino, Y.; Soma, M.; Bai, N.; Ito, Y.; Cui, W.; Aizawa, H.; et al. Astroglial Glutamate Transporter Deficiency Increases Synaptic Excitability and Leads to Pathological Repetitive Behaviors in Mice. *Neuropsychopharmacology* **2015**, *40*, 1569-1579, doi:10.1038/npp.2015.26.

181. Shmelkov, S.V.; Hormigo, A.; Jing, D.; Proenca, C.C.; Bath, K.G.; Milde, T.; Shmelkov, E.; Kushner, J.S.; Baljevic, M.; Dincheva, I.; et al. Slitrk5 deficiency impairs corticostriatal circuitry and leads to obsessive-compulsive-like behaviors in mice. *Nat Med* **2010**, *16*, 598-602, 591p following 602, doi:10.1038/nm.2125.

182. Delgado-Acevedo, C.; Estay, S.F.; Radke, A.K.; Sengupta, A.; Escobar, A.P.; Henríquez-Belmar, F.; Reyes, C.A.; Haro-Acuña, V.; Utreras, E.; Sotomayor-Zárate, R.; et al. Behavioral and synaptic alterations relevant to obsessive-compulsive disorder in mice with increased EAAT3 expression. *Neuropsychopharmacology* **2019**, *44*, 1163-1173, doi:10.1038/s41386-018-0302-7.

CHAPTER 2

NEONATAL CORTICOSTERONE MITIGATES AUTOIMMUNE NEUROPSYCHIATRIC DISORDERS ASSOCIATED WITH STREPTOCOCCUS IN MICE

ABSTRACT

Increased glucocorticoid concentrations have been shown to favor resilience towards autoimmune phenomena. Here, we addressed whether experimentally induced elevations in circulating glucocorticoids mitigate the abnormalities exhibited by an experimental model of Pediatric Autoimmune Neuropsychiatric Disorders Associated with Streptococcus (PANDAS). This is a pathogenic hypothesis linking repeated exposures to Group-A-beta-hemolytic streptococcus (GAS), autoantibodies targeting selected brain nuclei and neurobehavioral abnormalities. To persistently elevate glucocorticoid concentrations, we supplemented lactating SJL/J mice with corticosterone (CORT; 80 mg/L) in the drinking water. Starting in adolescence (postnatal day 28), developing offspring were exposed to four injections – at bi-weekly intervals – of a GAS homogenate and tested for behavioral, immunological, neurochemical and molecular alterations. GAS mice showed increased perseverative behavior, impaired sensorimotor gating, reduced reactivity to a serotonergic agonist and inflammatory infiltrates in the anterior diencephalon. Neonatal CORT persistently increased circulating glucocorticoids concentrations and counteracted these alterations. Additionally, neonatal CORT increased peripheral and CNS concentrations of the anti-inflammatory cytokine IL-9. Further, upstream regulator analysis of differentially expressed genes in the striatum showed that the regulatory effect of estradiol is inhibited in GAS-treated mice and activated in GAS-treated mice exposed to CORT. These data support the hypothesis that elevations in glucocorticoids may promote central immunomodulatory processes.

INTRODUCTION

Neonatal experiences persistently adjust individual adaptation towards future challenges [1]. While adverse events may relate to an increased risk of pathology [2], stimulating neonatal conditions may favor resilience towards future environmental insults [3]. Although these considerations originally pertained to emotional [4] and cognitive [5] domains, they have been recently extended to the immune system. For example, Bakker and collaborators [6] observed that neonatal dexamethasone administration – exerting a long-term reduction of corticosterone reactivity – increased individual susceptibility to an experimental autoimmune disease in rats. Meagher et al. [7] reported that brief (15-min/day) and long (180-min/day) maternal separations during the first two weeks of life increased vulnerability to acute Theiler's virus infection [7]. Importantly, also in this study, exposure to neonatal stressors resulted in a blunted activity of the hypothalamic-pituitary-adrenocortical (HPA) axis. These data support the hypothesis that experimental interventions capable of reducing corticosterone reactivity to stressors may potentiate autoimmune responses [8]. Likewise, experimentally-induced increases in corticosterone reactivity have been reported to favor resilience towards autoimmunity in experimental allergic encephalomyelitis (EAE). Specifically, Levine and collaborators exemplified the bimodal regulatory role of corticosteroids on individual reactivity to autoimmunity by showing that stress suppresses [9] and adrenalectomy potentiates [10] vulnerability to EAE.

Epidemiological, clinical and preclinical data support the notion that autoimmune phenomena constitute a vulnerability factor in the onset of psychiatric disturbances. Swedo and colleagues coined the acronym PANDAS (Pediatric Autoimmune Neuropsychiatric Disorders Associated with Streptococcus) to define a series of motor disturbances in which repeated exposures to bacterial (Group-A β-Hemolytic Streptococcus, GAS) infections are causally linked to symptoms [11]. Besides its pediatric onset, the defining criteria of PANDAS include the temporal proximity of neurological disturbances and GAS infections, recurrent abnormal behaviors, and remitting-relapsing presence of obsessive-compulsive symptoms and/or tics [11]. A proof of principle of these pathological sequelae has been obtained through several independent preclinical studies [12-14]. Hoffman et al. observed that repeated exposures to GAS homogenate resulted in locomotor alterations associated with increased IgG antibody deposits in deep cerebellar nuclei. We recently reported that in the long term, an analogous treatment resulted in increased repetitive behaviors, impaired sensorimotor gating, and inflammatory processes in the rostral diencephalon [14]. Tourette's Syndrome (TS) and obsessive-compulsive disorder (OCD) have been proposed to constitute instances of PANDAS: while several studies reported the presence of elevated concentrations of anti-streptococcal antibody titers in TS patients [15], Orlovska et al. [16] demonstrated that streptococcal infections relate to an increased risk of OCD in a Danish nationwide study. Both TS and OCD have been associated with alterations at the level of the basal ganglia [17].

Here, we addressed through a longitudinal study (see Figure 1 for the study outline) conducted in mice whether neonatal stress may modulate individual susceptibility to PANDAS [14]. We thus tested the prediction that neonatal CORT administration – mimicking sustained chronic stress – mitigates behavioral, immunological and neurochemical abnormalities in SJL mice repeatedly exposed to GAS between late infancy and adulthood. To elucidate the molecular mechanisms underlying the observed phenotypic alterations, we performed RNA sequencing of the striatum, the main component of the basal ganglia that is typically affected in PANDAS [17].
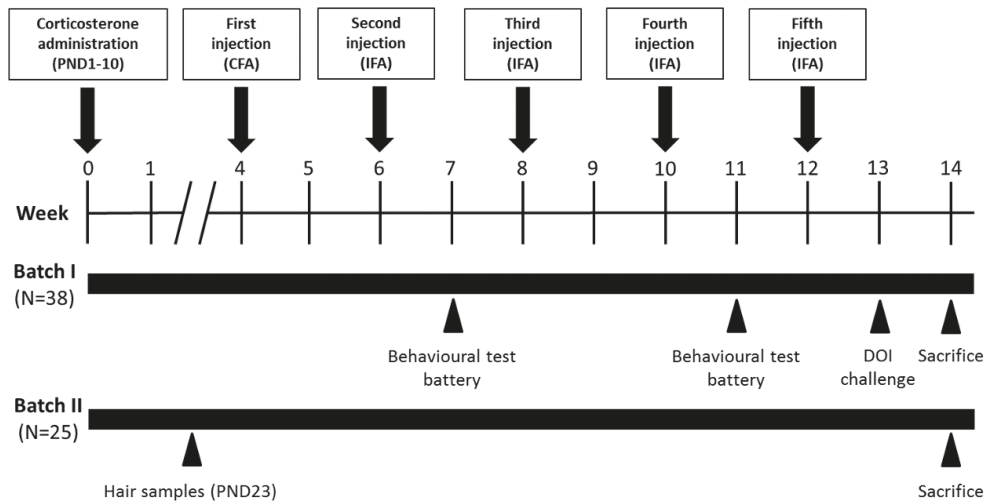
FIGURE 1. Experimental design: Timing of the neonatal treatment and of the injections, expressed in weeks, and the experimental procedures performed with two different and independent batches of mice. After corticosterone administration during the neonatal phase (postnatal days, PND, 1-10), mice received 5 injections of GAS homogenate or Phosphate Buffer Saline (PBS), formulated with the indicated adjuvants (CFA = Complete Freund's adjuvant; IFA = Incomplete Freund's adjuvant). At sacrifice, we collected: in Batch I, plasma samples for antibody and cytokine determination and brain samples for immunohistochemistry; in Batch II, we collected brain areas for monoamine determinations and RNA sequencing.

RESULTS

Physiological indicators of the efficacy of experimental treatments

Neonatal CORT administration increases circulating CORT concentrations in the short- and long-term.

Hair CORT concentrations at weaning were significantly elevated in CORT offspring compared to WATER controls (neonatal treatment: $F(1,21) = 4,839$, $p = 0,0392$, see Figure 2a). An analogous increment in CORT concentrations was also observed in adulthood (see Figure 2b), irrespective of GAS administration, when we evaluated serum basal CORT concentrations (neonatal treatment: $F(1,32) = 4,611$, $p = 0,0394$, see Figure 2b).

Repeated GAS exposures elicit the production of anti-GAS antibodies

Western Blot analyses demonstrate that sera from GAS-treated mice recognized specific GAS proteins and suggest that CORT administration did not influence this response (see Figure 2c).
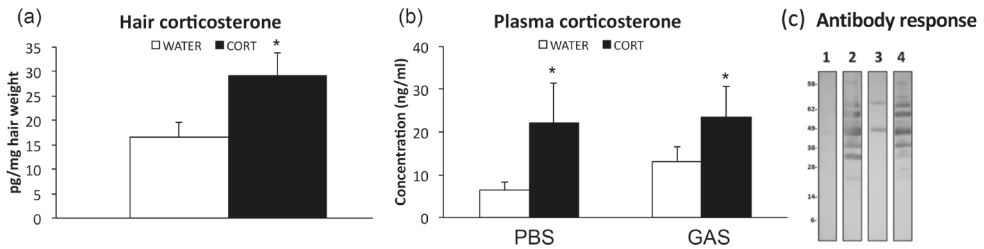
FIGURE 2. (a) Hair corticosterone (CORT) concentrations measured at weaning in control (WATER) and CORT-treated subjects (n=11 per group); (b) Plasma CORT concentrations measured at sacrifice (i.e., two weeks after the fifth GAS injection; n=8-12 per group): log-transformed data were used for the statistical analysis; actual concentration data are reported for the sake of clarity. CORT-treated subjects showed increased concentrations of CORT both in the short- (weaning) and long-term (adulthood). * p < 0,05 compared to respective WATER controls; (c) Western Blot analysis of GAS extracts probed with pooled sera from mice treated with GAS homogenates or adjuvant alone as Control, neonatal CORT and GAS homogenates or neonatal CORT and adjuvant. Lane 1, Western Blot results after probing with sera of control mice injected with four doses of adjuvant alone; lane 2, Western Blot results after probing with sera of mice injected with four doses of GAS homogenates; lane 3, Western Blot results after probing with sera of mice injected with four doses of neonatal CORT and adjuvant; lane 4, Western Blot results after probing with sera of mice injected with four doses of neonatal CORT and GAS homogenates. Lanes have been cropped from different parts of the same gel (see Supplementary Figure 2).

Behavioral testing

Neonatal CORT administration compensates for the PANDAS-like behavioral abnormalities induced by repeated GAS exposures

In the absence of major effects of experimental treatments on anxiety-related behaviors, general locomotion, and motor coordination (see Supplementary Results and Supplementary Table 1 for details), repeated GAS exposures exerted long-term effects in PANDAS-relevant phenotypes. Additionally, precocious exposure to CORT hampered the onset of most of these alterations.

To evaluate the functionality of the serotonergic system, we assessed the behavioral response to a pharmacological challenge with the 5-HT2a agonist DOI after the fifth GAS injection (week 13). As expected, administration of DOI resulted in the appearance of *head twitch* in all experimental subjects. While neither neonatal CORT administration nor GAS exposure *per se* apparently influenced duration (neonatal treatment: $F(1,33) = 0,469$, $p = 0,4981$; PBS/GAS treatment: $F(1,33) = 0,027$, $p = 0,8699$), and frequency (neonatal treatment,

$F(1,30) = 0,606$, $p = 0,4424$; PBS/GAS treatment, $F(1,30) = 1,304$, $p = 0,2626$) of *head twitch*, individual response to DOI varied depending on early CORT administration and PBS/GAS treatment (*head twitch* duration, neonatal treatment x PBS/GAS treatment: $F(1,33) = 5,237$, $p = 0,0287$; *head twitch* frequency, neonatal treatment x PBS/GAS treatment: $F(1,30) = 5,311$, $p = 0,0283$). Specifically, WATER-GAS mice exhibited reduced *head twitch* compared to WATER-PBS. Furthermore, neonatal CORT administration reduced individual reactivity to DOI in PBS mice. Finally, in accordance with our predictions, neonatal CORT administration prevented the effects of GAS administration ($p < 0,05$ in post hoc tests, see Figure 3a).

Sensory integration deficits contribute to the PANDAS phenotype. We thus measured sensorimotor gating through PPI after the second (week 7) and fourth injection (week 11). As expected, all subjects showed intact PPI (reduced startle reflex in reaction to prepulse plus pulse trials than pulse alone trials). In accordance with previous evidence indicating that few GAS exposures are insufficient to induce a pathological phenotype, following the second injection, the percentage of inhibition did not vary among groups (neonatal treatment: $F(1,31) = 2,116$, $p = 0,1559$; PBS/GAS treatment: $F(1,31) = 0,061$, $p = 0,8061$; neonatal treatment x PBS/GAS treatment, $F(1,31) = 0,611$, $p = 0,4405$). Following the fourth injection, while neither neonatal CORT administration nor GAS exposure *per se* apparently influenced PPI (neonatal treatment: $F(1,34) = 0,596$, $p = 0,4454$; PBS/GAS treatment: $F(1,34) = 0,208$, $p = 0,6512$), individual responses varied depending on the interaction between early CORT administration and PBS/GAS treatment (neonatal treatment x PBS/GAS treatment: $F(1,34) = 13,256$, $p = 0,0009$). As expected, GAS administration resulted in impaired PPI in subjects precociously exposed to water. Neonatal CORT administration, which *per se* impaired PPI in PBS mice, prevented the effect of GAS administration ($p < 0,05$ in post-hoc tests, see Figure 3b).

Finally, to test whether GAS exposures and CORT administration influenced the exhibition of perseverative behavior, we conducted the T-Maze test after the fourth injection (week 11). On average, experimental subjects showed spontaneous alternations, a natural tendency to alternate between the two arms of the apparatus (95% CI 57.15 to 80.35). Such natural tendency, considered an inverse index of perseveration, is variable among experimental conditions. In particular, while mice exposed to CORT showed spontaneous alternations (95% CI 63.90 to 76.53) mice exposed to GAS treatment did not show spontaneous alternation since their preference score did not differ from chance level (95% CI 46.27 to 65.95, see Figure 3c). Conversely, neonatal corticosterone administration mitigated the consequences of GAS treatment whereby CORT-GAS subjects showed a percentage of spontaneous alternations higher than chance level (95% CI 50.82 to 71.12, see Figure 3c). Additionally, GAS treatment significantly reduced the percentage of spontaneous alternations compared to WATER-PBS individuals ($F(1,34) = 9,074$, $p = 0,0049$,

see Supplementary Figure 3). With respect to neonatal treatment and its interaction with GAS administration, we did not observe significant differences (neonatal treatment: $F(1,34)$ = 0,003, p = 0,9559; neonatal treatment x PBS/GAS treatment: $F(1,34)$ = 1, 163, p = 0,2884).
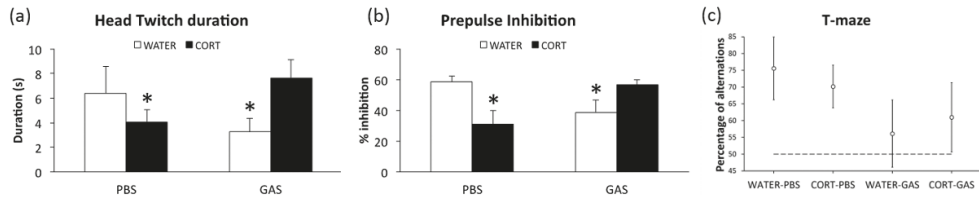
FIGURE 3. (a) Behavioral response (head twitch) to challenge with DOI (5 mg/kg, i.p., week 13, fifth injection) during a single 10-min session. Data are expressed as mean+SEM (n=8-12 per group); (b) Sensorimotor gating measured through PPI (week 11, fourth injection). Average inhibition of the startle reflex to a 120-dB stimulus following the presentation of a pre-pulse of 67, 70, 73, and 76dB. Values are expressed as mean percentage PPI (%PPI)+SEM (n=8-12 per group); (c) Perseverative behavior in a T-maze (week 11, fourth injection) measured as the percentage of spontaneous alternations (circular symbol) with 95% CI (whiskers). The dashed lines represent chance level; a CI intersecting the dashed line indicates that percentage of alternations was not statistically different from chance.

Immune activation in response to experimental treatments

We first analyzed whether GAS exposure resulted in inflammatory processes in the brain and then whether CORT compensated for them. In accordance with our predictions, while GAS injections resulted in visible inflammatory infiltrates in adult subjects, neonatal CORT exposure remarkably mitigated this effect (Figure 4). While CORT-PBS mice and WATER-GAS mice were characterized by the presence of inflammation (Figure 4B and 4C respectively), WATER-PBS mice and CORT-GAS mice did not show inflammatory infiltrates (Figure 4A and 4D respectively). Furthermore, the diffused microglial activity observed in the mesencephalon of WATER-GAS mice (Figure 4G) was remarkably reduced in CORT-GAS mice (Figure 4H), and CORT-PBS mice (Figure 4F), while was absent in CORT-PBS mice (Figure 4E). When we analyzed cytokine activation in the plasma (see Supplementary Table 3 for data on cytokine concentrations), we observed that, in the absence of effects due to GAS exposure, CORT administration resulted in remarkable increases of IL-9, IL-17, MCP-1, and MIP-1beta (see Supplementary Table 3 for details). We therefore evaluated whether inflammatory infiltrates were positive for IL-9, a factor indicative of inflammatory processes. Accordingly, we observed a considerable number of IL-9+ cells in the inflammatory infiltrates of CORT-GAS (Figure 4I,L) but not of CORT-PBS mice.
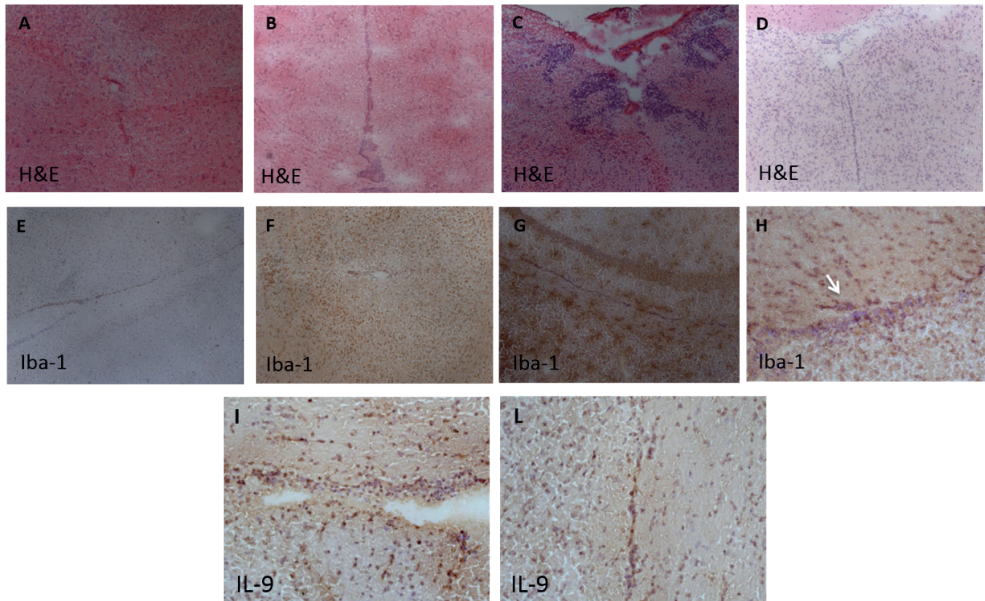
FIGURE 4. Neuropathology assessment of microglia activity in mice brains. H&E staining shows the presence of inflammatory infiltrates in the white matter of the rostral diencephalon of a representative CORT-PBS mouse (B) and a WATER-GAS mouse (C) not detected in WATER-PBS mice (A) and CORT-GAS mice (D). The presence of Iba1+ microglia activity – diffusely present in WATER-GAS mice (G) – was rarely observed in CORT-PBS mice (F) and CORT-GAS mice (H), and was mainly detected associated with small, periventricular inflammatory infiltrates. Iba1+ microglia activity was not detected in WATER-PBS mice (E). A considerable number of IL-9+ cells were observed in the inflammatory infiltrates persisting in different regions of the brains of CORT-GAS mice (I and L). The arrow in H indicates the area Ion serial brain sections where increased density of IL-9+ cells was detected. (Original magnification: 5x (B, D), 10x (A,C,E,F,G,L), 20x (H, I).

Monoamine measurements

Concentrations of serotonin, dopamine, their metabolites and respective turnovers are reported in Supplementary Table 2. In the absence of differences in hippocampus and prefrontal cortex, experimental treatments modulated monoamine concentrations in striatum and hypothalamus. Both CORT and GAS reduced striatal concentrations of DOPAC (neonatal treatment: $F(1,17) = 12,073$, $p = 0,0029$; PBS/GAS treatment: $F(1,17) = 4,456$, $p = 0,0499$) and 5HIAA (neonatal treatment: $F(1,17) = 9,370$, $p = 0,0071$; PBS/GAS treatment: $F(1,17) = 6,068$, $p = 0,0247$). Furthermore, neonatal CORT administration reduced absolute concentrations of 5-HT in striatum, although this effect was limited to PBS subjects (neonatal treatment: $F(1,17) = 7,239$, $p = 0,0155$, $p < 0,05$ in post-hoc tests). With respect to hypothalamus, GAS administration increased dopamine concentrations only in mice precociously exposed to water and not to CORT (neonatal treatment x PBS/GAS treatment:

$F(1,20)$ = 8,394, p = 0,0089; $p < 0,05$ in post-hoc tests). Furthermore, CORT treatment significantly reduced dopamine turnover (neonatal treatment: $F(1,20)$ = 5,184, p = 0,0339; WATER-PBS = 1,03 ± 0,17, WATER-GAS = 0,63 ± 0,04, CORT-PBS = 0,62 ± 0,03, CORT-GAS = 0,69 ± 0,08) and serotonin turnover (neonatal treatment: $F(1,20)$ = 6,399, p = 0,0199; WATER-PBS = 0,85 ± 0,05, WATER-GAS = 0,68 ± 0,06, CORT-PBS = 0,64 ± 0,03, CORT-GAS = 0,69 ± 0,07) in the hypothalamus. Both treatments did not affect dopamine and serotonin turnover in striatum, prefrontal cortex and hippocampus (see Supplementary Table 2 for details).

RNA sequencing and upstream regulator analysis

To unravel the molecular mechanisms potentially involved in GAS-mediated effects and CORT-dependent compensatory influences, we performed RNA sequencing and upstream regulator analysis. All data are reported in Supplementary Table 4 (see Supplementary Results and Supplementary Figure 1 for a Venn diagram illustrating the unique and overlapping differentially expressed genes for all comparisons). In Table 1, for the sake of clarity, we only refer to the genes that were differentially expressed between WATER-GAS vs WATER-PBS and CORT-GAS vs WATER-GAS. In the Supplementary Results, we have provided a detailed and referenced description of our results. Below we give a more succinct overview of the most important findings and how they could be tentatively interpreted.

We observed that the regulatory effect of (beta-)estradiol is predicted to be inhibited in GAS mice and activated in CORT-GAS mice. Thus, while inhibition of estradiol-dependent regulation may be linked to the GAS-dependent impairments, its activation in CORT-GAS subjects may contribute to the mitigating effects of CORT. In this respect, the effects of dihydrotestosterone – a metabolite that is converted from testosterone by 5α-reductase – and fibroblast growth factor 2 (FGF2) – which has a positive effect on motor function and is upregulated by estradiol and CORT – were also predicted to be inhibited in WATER-GAS mice. Further, estradiol activates the HPA-axis, resulting in increased CORT production, reinforcing the observed beneficial effect of CORT on GAS-induced behavior. Estradiol also regulates the immune response through modulating the immunologic potency of IgG antibodies that are formed against bacteria such as GAS. In PANDAS, it is thought that IgG antibodies produced in response to GAS cross the blood brain barrier and are aimed at specific neuronal proteins in the basal ganglia, including receptors for the neurotransmitter dopamine (DA), which is converted from its precursor L-dopa. In this respect, it is interesting that our findings indicate that signaling dependent on both DA and L-dopa is dysregulated in CORT-exposed GAS mice. Furthermore, IgG-dependent regulation is predicted to be inhibited in CORT-exposed GAS mice and both estradiol and CORT increase the striatal release of DA, which

further implies that increased estradiol signaling mediates the beneficial effect of CORT on GAS-induced behavior through both attenuating the IgG response and increasing DA-dependent regulation.

In addition to estradiol, signaling involving two extracellular hormones – i.e., luteinizing hormone (LH) and leptin (LEP) – is modulated by exposing GAS mice to CORT. LH is secreted by the pituitary gland and activates the production of sex hormones, including estradiol and testosterone. Interestingly, estradiol upregulates LH expression while its secretion is decreased by dihydrotestosterone, DA and interleukin-2 (IL-2). IL-2 is a pro-inflammatory cytokine that activates the immune response, is downregulated by beta-estradiol and increased in expression following IgG-mediated GAS infection. As LH-dependent regulation is predicted to be activated in CORT-exposed GAS mice while regulation downstream of IL-2 is presumably inhibited in these animals, it follows that CORT attenuates the immune response by promoting and counteracting signaling downstream of LH and IL-2, respectively. LEP, a hormone with multiple functions including appetite regulation, is predicted to be inhibited in CORT-treated GAS mice, which fits with the finding that CORT downregulates LEP expression. Further, dihydrotestosterone and beta-estradiol upregulate and downregulate LEP expression, respectively. In addition, LEP inhibits the release of DA, which fits with the finding that in CORT-treated GAS mice, the effect of LEP is inhibited while DA-dependent signaling is activated. Interestingly, LEP also plays a pro-inflammatory role through increasing IL-2 production, which suggests that the anti-inflammatory effect of CORT on GAS mice could be mediated at least in part by inhibiting LEP-dependent regulation.

Lastly, our findings point towards two proteins that represent potential targets for developing novel treatments of PANDAS, i.e., IKBKB and TREM1. IKKbeta (IKBKB) is a cytoplasmic kinase that is predicted to be inhibited in CORT-exposed GAS mice and activates NF-kappaB, a pro-inflammatory transcription factor that is an important regulator of innate immunity. Furthermore, both glucocorticoids such as CORT and estradiol negatively regulate the activity of IKBKB. In addition, IKBKB upregulates IL-2 expression. Moreover, the transmembrane protein TREM-1 is a receptor for GAS and positively mediates the GAS-induced inflammatory response, which fits with our finding that CORT exposure leads to an inhibition of TREM-1-dependent regulation in GAS mice. Given the findings for IKBKB and TREM1, we would offer that drugs inhibiting or reducing the function of both proteins could be further developed as novel PANDAS treatments (see below).

TABLE 1. Upstream regulator analysis – using Ingenuity – of the mRNAs that were differentially expressed in GAS-treated mice compared to controls (WATER-GAS vs WATER-PBS) (1) and in GAS-treated mice neonatally exposed to CORT compared to GAS-treated mice (CORT-GAS vs water-GAS) (2). All upstream regulators are listed with a z-score ≤ - 1.50 or ≥ 1.50 or (see Supplementary Methods), indicating that they are inhibited or activated, respectively. The upstream regulators that could be linked to streptococcal/GAS infection, CORT exposure and/or OCD/tic disorders are indicated in bold. For each regulator, the downstream target genes are listed.

Upstream Regulator	WATER-GAS vs WATER-PBS (1)	CORT-GAS vs WATER-GAS (2)	Target genes
Chemicals - endogenous mammalian			
beta-estradiol	-1.97	2.47	(1): *Btg2, Cbl, Cshl1, Enpp2, Fos, Inpp5j, Sdc3, Sema3b, Srd5a1, Tnnt3;* (2): *Adm, Bcat1, Bmp2, Calb1, Ccng1, Cdkn2b, Chgb, Ctps1, Dlg2, Fgf9, Fmo1, Fnbp1, Fzd2, Gab2, Gsk3b, Hsd17b12, Ier2, Insl3, Lhcgr, Lmcd1, Mapt, Mpz, Myh3, Nedd4l, Nkx2-1, Notch3, Pak5, Pdap1, Pitpna, Ptgds, Pttg1, Pxdn, Pycr1, Pygl, Qsox1, Rapgef6, Slc38a2, Smad3, Snap25, Sstr4, Tgfb3, Thrsp, Timp3, Tpo, Trib1, Vav3, Zyx*
butyric acid	–	2.16	*Calb1, Ccng1, Col5a2, Gli3, Ly6e, Myh3, Nfatc4, Oas2, Ptgds, Pygl, Serpine1, Timp3, Uqcrq*
dihydrotestosterone	-1.95	–	*Btg2, Elovl7, Fos, Sdc3, Slc7a7, Srd5a1*
dopamine	–	1.63	*Adra2c, Bcl2l2, Gprc5b, Ncf1, Ppp2r2a, Scn1b, Scn9a*
L-dopa	–	-4.59	*Adra2c, Ajap1, C1qtnf12, C2cd2l, Cbr3, Cdc42ep2, Csmd3, Cyld, Dgki, Dlg2, Grid2, Kcne5, Klf16, Mpp6, Nedd4l, Per2, Plekha2, Ppp2r2a, Ptprd, Rell1, Reln, Slc38a2, Sorcs2, Wdr17, Zfhx3*
oleic acid	–	-2.00	*Ncf1, Npc1l1, Serpine1, Thrsp*
Complexes			
IgG	–	-2.24	*Adm, Cdkn2b, Csnk2b, Ier2, Serpine1*
LH	–	2.00	*Actn1, Btc, Gprc5b, Insl3, Lhcgr, Snap25, Thbs2, Trib1*
IL-2	–	-1.76	*Bmp2, Card9, Ccng1, Ccr6, Cmklr1, Csf2rb, Csrnp1, Ctps1, Dapk2, Gcnt1, Ly6e, Pus1, Tnfrsf4*
Enzymes			
CASZ1	–	-1.96	*Acan, Myh3, Nefl, Tgfb3*
EGLN1	–	-1.98	*Acan, Adm, Cdkn2b, Tgfb3*
TGM2	–	1.91	*Acan, Csrnp1, Dapk2, Ifit2, Ly6e, Mpp6, Oas2*
Growth Factors			
FGF2	-1.93	–	*Btg2, Enpp2, Fos, Prkce, Ptma (Includes Others)*
INHBA	–	-2.34	*Actn1, Bmp2, Calb1, Cdkn2b, Edar, Lhcgr, Nkx2-1, Pcdh9, Serpine1, Vav3*
LEP	–	-2.16	*Cps1, Dffa, Gsk3b, Insl3, Ncf1, Per2, Pln, Rfx1, Serpine1, Snap25, Thrsp, Timp3*

TABLE 1. Continued

Upstream Regulator	WATER-GAS vs WATER-PBS (1)	CORT-GAS vs WATER-GAS (2)	Target genes
Kinases			
IKBKB	–	**-1.98**	*Bmp2, Cdh13, Timp3, Tnfrsf4*
Transcription Regulators			
KMT2A	–	**2.00**	*Gcnt4, Pigz, Trib1, Zmat4*
NKX2-3	–	**-1.61**	*Adm, Bmp2, Cd34, Cerk, Cryab, Csrnp1, Ly6e, Srpx2, Tmem158*
TP53	–	**2.11**	*Actn1, Apbb2, Ccng1, Col5a2, Col9a1, Cryab, Csmd3, Fmo1, Gsk3b, Hs3st1, Kcng1, Kifc1, Me2, Nab1, Ncf1, Otx1, P2rx4, Ptgds, Ptger1, Pttg1, Serpine1, Sirt6, Tgfb3, Thbs2, Timp3, Tmem151a, Zyx*
TP63	–	**-1.78**	*Adm, Bmp7, Ccng1, Cdkn2b, Kcng1, Notch3, Serpine1, Smad3, Smad4, Tgfb3, Timp3*
Transmembrane Receptors			
TREM1	–	**-2.45**	*Cdkn2b, Ifit2, Nedd4l, Nme7, Rhou, Tmem158*

DISCUSSION

In accordance with our previous observations [14], while two streptococcal injections failed to induce substantial abnormalities, four or more exposures altered behavioral, neurochemical, and immuno-histological parameters analogous to those identified in PANDAS patients. Furthermore, as predicted [3], neonatal CORT administration compensated for most of the GAS-induced abnormalities. These effects co-occur with modifications in HPA activity, increased serum protein levels of IL-9 paralleled by IL-9+ microglia in the CNS, and changes in striatal gene expression. These results support the view that the HPA axis contributes to the regulation of immune responses ultimately modulating the severity of the abnormal phenotype. Lastly, the analysis of the differentially expressed genes in the striatum provides information regarding the potential molecular mechanisms associated with the pathogenic effects of repeated GAS exposures and the CORT-mediated compensatory role.

In line with the hypothesis that repeated GAS injections induce PANDAS-like behavioral abnormalities, GAS mice exhibited reduced sensorimotor gating and sensitivity to DOI and increased perseverative behavior. These phenotypes constitute the preclinical analog of two of the core symptoms observed in PANDAS: impaired sensory integration [18] and obsessive-compulsive behaviors [11]. The possibility that a failure of sensory integration relates to OCD traits in children has already been discussed elsewhere [19]. The relevance of PPI within the field of PANDAS has been substantiated by anatomical and pharmacological evidence

indicating that sensorimotor gating requires an intact cortico-striato-thalamo-cortical (CSTC) circuit, generally affected in PANDAS patients [20]. Additionally, while experimental lesions of the striatal circuit impair PPI in laboratory rodents [21], drugs acting on dopaminergic transmission modulate PPI in both rodents [22] and humans [23]. WATER-GAS mice also exhibited increased perseverative responding in a binary-choice test, in which rodents are requested to spontaneously alternate between two choices [24]. This natural tendency requires an intact prefrontal cortex and dorsal striatum [25]. Furthermore, dopaminergic [26] and serotonergic [27] drugs have been shown to modulate this capability. The altered integrity of the serotonergic system in WATER-GAS mice was supported by a reduced reactivity to the pharmacological challenge with DOI and further confirmed by significant reductions in 5-HT and 5HIAA concentrations in the striatum. Moreover, in accordance with the hypothesis that anti-GAS antibodies result in central inflammatory processes [14,28], we detected inflammatory infiltrates and ramified microglia at the level of the rostral diencephalon in GAS mice, thus supporting a role for microglia in autoimmune basal ganglia disorders like TS, OCD and PANDAS in general [29]. One aspect that warrants consideration relates to the fact that our experiments have been conducted under animal facility rearing (AFR) conditions and not under specific pathogen free (SPF) conditions, which by definition guarantee a higher level of sterility. Therefore, since immune responses may vary depending on the pathogens encountered by the organism, we cannot exclude the possibility that our results may have been different had the experiments been conducted under SPF conditions. We speculate, however, that rather than devaluing our study, this factor may confer additional validity to our results. Specifically, the higher variability of pathogens, characteristic of AFR compared to SPF, is hypothesized to introduce an additional source of uncontrolled variation in the study. The observation of remarkable effects of GAS administration, despite the presence of such unavoidable bias, further strengthens our study whereby it indirectly suggests that the long-term consequences of streptococcus administration are stronger than the background noise associated with AFR-related pathogens. Future studies are needed to clarify this aspect.

Predictably, neonatal CORT administration resulted in short- and long-term increases in basal concentrations of CORT in developing subjects [3]. In line with previous studies [30], CORT-PBS mice exhibited remarkably reduced striatal concentrations of DA, 5HT, DOPAC and 5HIAA. Furthermore, neonatal corticosterone administration resulted, in the long-term, in reduced hypothalamic turnover of serotonin and dopamine. Alterations in brain monoamines and their turnover have already been reported in adult rodents exposed to different forms of neonatal stress [30]. Furthermore, several authors suggested that variations in brain monoamines in response to neonatal stressors may relate to deficits in prepulse inhibition [31]. Accordingly, monoamine results were functionally paralleled by behavioral alterations

in PPI and sensitivity to DOI. Lastly, neonatal CORT administration resulted in increased levels of interleukin 9 (IL-9), IL-17, MCP1, MIP-1beta and in the presence of inflammatory infiltrates. IL-9 is produced by activated Th2 lymphocytes and is active on various immune cells [32]. In addition to its effect on the immune system, IL-9 has been shown to regulate cell differentiation of a hippocampal progenitor cell line [33]. Therefore, it could be hypothesized that the increased IL-9 secretion detected in CORT-PBS mice may have a role in immune regulation [34]. Analogous considerations may be proposed for IL-17, produced by Th17 lymphocytes, and for which a role in autoimmune disturbances has been identified [35]. Finally, the CORT dependent elevation in MCP1 and MIP-1beta may have also partly contributed to the compensatory effects of neonatal corticosterone administration whereby these chemokines have been shown to play a role in experimental models of autoimmunity [36].

While both CORT and GAS exerted independent effects, the main finding of the present study resides in the modulatory role exerted by the former over the latter [9], whereby neonatal CORT mitigated the behavioral and immunohistochemical effects of GAS. The autoimmune hypothesis of PANDAS postulates that the behavioral alterations are secondary to inflammatory phenomena at the level of the rostral diencephalon. Accordingly, besides mitigating the behavioral alterations, neonatal CORT reduced the inflammatory infiltrates and ramified microglia observed in WATER-GAS mice. Furthermore, the rare inflammatory infiltrates detected in CORT-GAS subjects contained an elevated number of IL-9+ cells. We propose that the compensatory effects of CORT on CNS inflammatory phenomena are related to the organizational long-term increase in circulating corticosteroids [9]. Such increase may act through different pathways potentially inhibiting immune activation, thereby mitigating the consequences of autoimmune-regulated phenomena. Alternatively, increased corticosteroids may regulate the production of inflammatory cytokines which could, in turn, protect the CNS. Experimental data support the latter as all GAS-treated subjects produced similar anti-GAS antibodies irrespective of glucocorticoid exposure. Therefore, we investigated whether CORT modulated the inflammatory intracerebral processes induced by repeated exposures to streptococcus. Immunological analyses performed in the serum showed that neonatal CORT increased concentrations of IL-9 in adulthood. These peripheral alterations were paralleled by IL-9+ cells with microglial morphology in the CNS. The latter may exert an anti-inflammatory role [34] and potentially hamper the consequences of GAS administration. This finding suggests that the CORT-mediated compensatory effects would be associated with the activation of cerebral innate immunity. While current data seem to suggest that the compensatory influences of CORT occur via the activation of cytokines, the possibility that CORT modulates the production of antibodies cannot be fully excluded based on the available data. Thus, although Western Blot data indicate that the antibody response observed in CORT-GAS mice was indistinguishable from that observed in GAS mice, we note that our measure was qualitative, and not quantitative, in

nature. Thus, we cannot exclude the possibility that a more detailed investigation shall identify minor between-group differences in antibody response to GAS administration. Quantitative investigations are needed to further clarify this aspect.

The upstream regulator analysis of the differentially expressed genes provides insights into the putative molecular mechanisms underlying the phenotypic abnormalities observed in GAS mice and the compensatory role of neonatal CORT. Importantly, while GAS exposures inhibited the female sex hormone (beta)-estradiol-mediated regulation of gene expression, neonatal CORT compensated for this effect. The hypothesis that estradiol exerts a regulatory role is in line with literature showing that estradiol-deficient rodents show decreased PPI [37] and develop OCD-like behavioral abnormalities [38]. Additionally, lower estradiol levels have been shown to correlate with increased OCD symptoms in men and women [39]. Furthermore, estradiol has been reported to regulate the individual response to bacterial infections [40] through a modulation of IgG antibodies [41]. Individuals with tics and/or OCD also have elevated serum IgG against the human dopamine D_1 receptor (D1R) [42]. In addition, while IgG has been shown to induce PANDAS symptoms in humans, its depletion from PANDAS patient sera alleviates the symptoms [13]. Thus, the inhibitory effect exerted by CORT on IgG-regulated gene expression in GAS mice may partly contribute to its compensatory role. Lastly, in males, estradiol is produced through the conversion of the male sex hormone testosterone, which, in turn, is indirectly regulated by CORT [43]. An involvement of testosterone metabolism in regulating the consequences of GAS infection is further suggested by our finding that the effects of the testosterone metabolite dihydrotestosterone on gene expression are inhibited in WATER-GAS mice.

Furthermore, we found that CORT negatively regulates effect on gene expression mediated by Leptin (LEP), a hormone and growth factor that exerts a proinflammatory role through increasing IL-2 production by T-lymphocytes [44]. Hence, the anti-inflammatory effect of CORT could be mediated in part by an inhibition of LEP-dependent regulation. Moreover, the effect of IKKbeta (IKBKB), a kinase activating the proinflammatory transcription factor NF-kappaB (NF-kB), was predicted to be inhibited in CORT-GAS mice. IKBKB has been proposed to mediate GAS infections and the exhibition of OCD-like symptoms. Accordingly, inactivation of *Ikbkb* in mice has been shown to reduce GAS infections [45] and normalize OCD-like behavior [46]. Lastly, CORT-GAS mice were predicted to have a reduced activation of gene expression regulated by TREM1, a receptor for GAS directly involved in inflammatory responses [47]. TREM1 has also been tested and confirmed as a drug target in the treatment of GAS-induced [48] and other immunity-related disorders [49]. Further, it was demonstrated that CORT treatment significantly decreased the plasma expression levels of TREM-1 in febrile patients with autoimmune disease [50]. Thus, IKBKB and TREM1 represent interesting potential targets for future studies aimed at developing novel interventions to treat PANDAS, in that novel drugs could be developed that negatively regulate both targets.

In conclusion, this study provides a proof of principle of the hypothesis that HPA functionality modulates the individual response to autoimmune phenomena (Figure 5). Furthermore, we identified a potential link between neonatal experiences and the underlying molecular mechanisms that are involved in alleviating the PANDAS-related pathological phenotype.
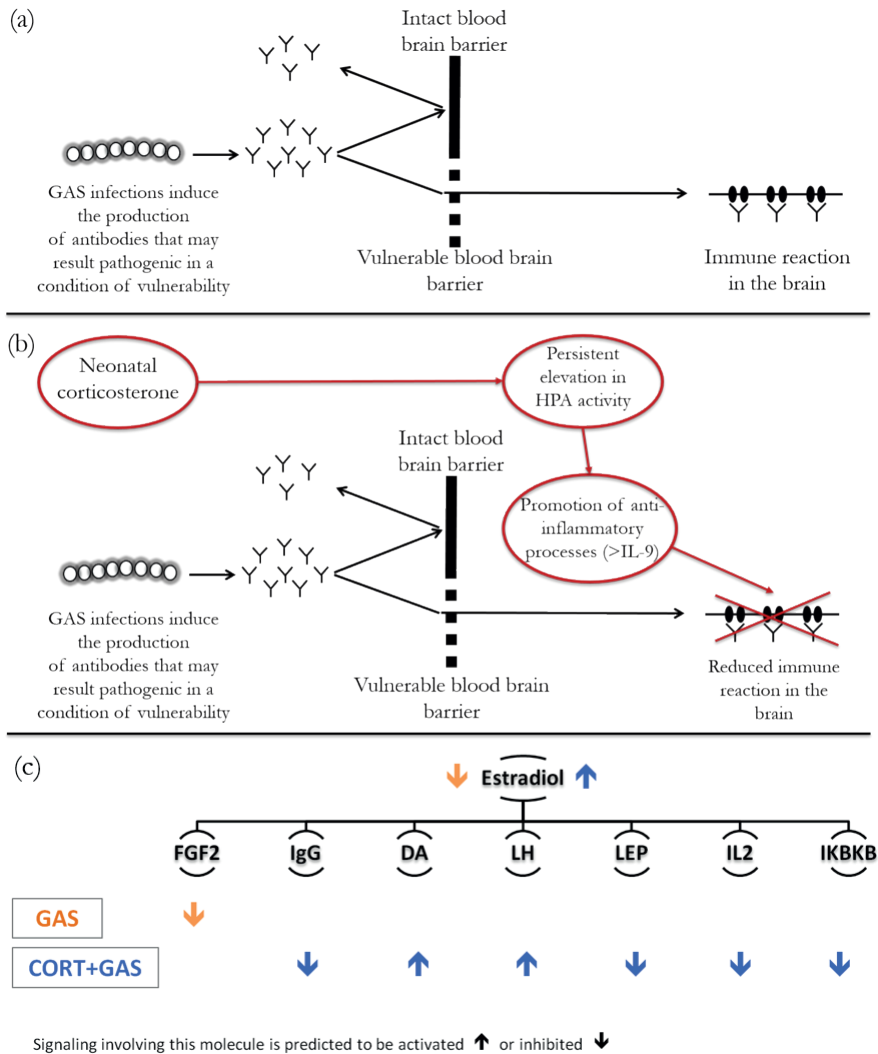
FIGURE 5. Schematic recapitulating the main topics addressed in the current study: etiological hypothesis (a), modulatory role of neonatal corticosterone administration (b), and potential molecular mechanisms involved (c). Specifically, in panel (a) we exemplified the etiological hypothesis linking streptococcal immunizations, antibody response and behavioral abnormalities. In panel (b) we sketched a candidate mechanism through which neonatal corticosterone may mitigate the PANDAS-like neurobehavioral abnormalities. In (c) we visually represented the main findings from the upstream regulator analysis. The predicted effects of GAS and CORT+GAS are shown for signaling involving estradiol and the other signaling molecules from the analyses that are regulated by estradiol.

MATERIALS AND METHODS

Animals and rearing

All animal experiments have been performed at ISS in compliance with the European Directive 2010/63/UE and Italian Legislative Decree 26/14 on laboratory animal protection and experimentation, and authorized by the Italian Ministry of Health (Decree Nr. 217/2010-B). Thirty-six female and 18 male SJL/J young adult mice, postnatal day (PND) 56 on the day of arrival, were purchased from Charles River, Italy (Calco, Lecco, Italy). Four days after arrival, female mice were removed from their cages and housed with a male (two females per cage). After 10 days of mating, male mice were removed, dams for which mating was determined (N=22) were housed individually in standard type-1 polycarbonate cages (33.0×13.0×14.0 cm) and checked daily at 11:00 am for delivery (see Supplementary Methods).

Neonatal treatment

On PND0, dams were divided into two groups: control (WATER) dams (N=11), and corticosterone-treated (CORT) dams (N=11). CORT was supplemented in drinking water between PND1-10 as described elsewhere [30] (see also Supplementary Methods).

Immunization protocol

A GAS homogenate prepared as described elsewhere [12,14] was administered through five injections interspaced by two weeks, starting on PND28 (see Supplementary Methods). To minimize litter effects, we planned not to inject siblings with the same GAS/PBS treatment. However, since litters were not perfectly balanced, out of 22 viable litters, we used littermates five times. The experimental population was composed as follows: control (WATER)-PBS, WATER-GAS, CORT-PBS, and CORT-GAS.

Experimental design

The experimental design (See Figure 1) entailed repeated behavioral testing, blood sampling for the evaluation of the immune response to the injection protocol, blood sampling for CORT level determination in basal conditions, and brain sampling/sectioning for neurochemical and immunohistochemical assays, and RNA sequencing. We conducted the experiments in two batches:

batch 1: WATER-PBS, N=8; WATER-GAS, N=8; CORT-PBS, N=10; CORT-GAS, N=12.

batch 2: WATER-PBS, N=5; WATER-GAS, N=6 mice; CORT-PBS, N=7; and CORT-GAS, N=7.

Physiological indicators of the efficacy of experimental treatments

To determine the efficacy of CORT and GAS treatments, we quantified the short- and long-term effects of CORT administration on corticosterone concentrations and of repeated exposures to GAS on the formation of antibodies. We thus evaluated: CORT concentrations in hair on PND23, and in plasma in adulthood; and anti-GAS antibodies in serum samples following the fourth GAS injection (Supplementary Methods for details).

Behavioral testing

The first test battery, performed one week after the second injection (week 7), entailed: elevated zero-maze (day 1) to evaluate potential effects on anxiety-like behavior; pre-pulse inhibition (PPI, day 2 for habituation and day 3 for testing) to demonstrate that GAS affected sensorimotor integration processes characteristic of PANDAS and OCD; and the evaluation of spontaneous locomotion through an automated scoring system (day 4). While elevated zero-maze and locomotion were assessed in the animal facility, PPI was conducted in a separate testing room.

The same animals were screened one week after the fourth injection (week 11), in a behavioral test battery entailing five tests, performed in the following sequence: elevated plus maze, rotarod (to control for potential effects of treatments on motor coordination), and PPI habituation on day 1; PPI testing on day 2; t-maze, to evaluate repetitive behaviors, (days 3-7); locomotor activity (days 7-8); individual response (exhibition of head twitch) to the serotonergic agonist DOI to evaluate the functionality of the serotonergic system. The behavioral test procedures are detailed in the Supplementary Methods.

Immune activation in response to experimental treatments

We evaluated inflammatory processes in the central nervous system (CNS) through immunohistochemistry and peripheral cytokines in plasma samples. For immunohistochemistry, coronal cryosections (10μm thickness) were cut from whole brains from 5 CORT-PBS and 5 CORT-GAS treated mice and stored at -80°C. As previously described [14], hematoxylin and eosin staining was performed on all the examined brain samples (1 cryosection every 15 cut cryosections) in order to assess the presence of potential inflammatory infiltrates and any evident tissue alteration. Air-dried cryosections were used for immunohistochemistry assessment of the level of microglia activation (Iba1) and for the immunolocalization of TNF and IL-9 cell expression (see Supplementary Methods). Cytokine concentrations in the serum were determined through the Bio-Plex Cytokine Assay (23-Plex, Bio-Rad) following the producer's protocol (see Supplementary Methods for details).

Monoamine measurements

To confirm previous evidence that GAS administration alter brain monoamines, and further confirm the similarity between our model and PANDAS, we evaluated 5-HT, DA and their metabolites, i.e., 5-hydroxyindole acetic acid (5-HIAA), and 3,4-dihydroxyphenylacetic acid (DOPAC) in prefrontal cortex, striatum, hippocampus, hypothalamus and cerebellum. These were quantified by a modified method of HPLC combined with an electrochemical detector as previously described [14]. See Supplementary Methods for further details.

RNA sequencing

Using RNA sequencing, we quantified total RNA levels in 22 mice (5 WATER-PBS, 5 WATER-GAS, 6 CORT-PBS and 6 CORT-GAS). Further details are provided in the Supplementary Methods. Briefly, the final sets of differentially expressed genes comprised those that were identified as such – fold change ≥ 1.2 and P-value < 0.01 – by at least two of the four used methods. The Venn diagram of the final sets of differentially expressed genes for all comparisons was built with Venny (see Supplementary Methods). For genes that showed differential expression, upstream regulator analysis was performed using the Ingenuity Pathway Analysis software (IPA), version 00.06 (Ingenuity Systems Inc., Redwood City, CA). Further details are provided in the Supplementary Methods.

Statistical analyses

Statistical analyses were conducted using the software Statview 5.0 (Abacus Concepts, USA). The experimental design entailed two between-subjects factors (neonatal treatment: WATER vs. CORT; and PBS/GAS treatment, two levels: PBS vs. GAS) and one within-subject factor (repeated measures with a variable number of levels, depending on the specific parameter). Thus, the experimental model consisted of a 2 (neonatal treatment) x 2 (PBS/GAS treatment) x k (repeated measurements) ANOVA for split-plot designs. Tukey's post hoc tests were used for between-group comparisons. Statistical significance was set at $p < 0.05$. Finally, to evaluate whether experimental subjects met the criterion for T-maze paradigm, the observed phenotype has been compared to the threshold through one-sample T- tests.

Author contributions

Conceived and designed the experiments: SM, CS, IM, JG, GL; Performed the experiments: CS, SM, JW, RM, GP, RWI, VR, RC, EB; Analyzed the data: CS, SM, JW, GP, EB; Wrote the paper: SM, CS, GP, JW, RM, JG, GL; Reviewed and approved the final version of the manuscript: All authors

Funding

Acknowledgements

Conflicts of Interest

The authors declare that they have no non-financial interest to disclose. SM, CS, JW, RM, GP, RWI, RC, VR, JG and GL have no financial interest to disclose. EB and IM were employees of Novartis Vaccines at the time of the study; in March 2015 the Novartis non-influenza Vaccines business was acquired by the GSK group of companies. EB and IM are now employees of the GSK group of companies. IM and EB are listed as inventors on patents owned by the GSK group of companies. IM reports ownership of restricted GSK shares.

REFERENCES

1. Bateson, P.; Barker, D.; Clutton-Brock, T.; Deb, D.; D'Udine, B.; Foley, R.A.; Gluckman, P.; Godfrey, K.; Kirkwood, T.; Lahr, M.M.; et al. Developmental plasticity and human health. *Nature* **2004**, *430*, 419-421, doi:10.1038/nature02725.

2. Heim, C.; Plotsky, P.M.; Nemeroff, C.B. Importance of studying the contributions of early adverse experience to neurobiological findings in depression. *Neuropsychopharmacology* **2004**, *29*, 641-648, doi:10.1038/sj.npp.1300397.

3. Macrì, S.; Zoratto, F.; Laviola, G. Early-stress regulates resilience, vulnerability and experimental validity in laboratory rodents through mother-offspring hormonal transfer. *Neurosci Biobehav Rev* **2011**, *35*, 1534-1543, doi:10.1016/j.neubiorev.2010.12.014.

4. Macrì, S.; Wurbel, H. Developmental plasticity of HPA and fear responses in rats: a critical review of the maternal mediation hypothesis. *Horm Behav* **2006**, *50*, 667-680, doi:10.1016/j.yhbeh.2006.06.015.

5. Plamondon, A.; Akbari, E.; Atkinson, L.; Steiner, M.; Meaney, M.J.; Fleming, A.S. Spatial working memory and attention skills are predicted by maternal stress during pregnancy. *Early Hum Dev* **2015**, *91*, 23-29, doi:10.1016/j.earlhumdev.2014.11.004.

6. Bakker, J.M.; Kavelaars, A.; Kamphuis, P.J.; Cobelens, P.M.; van Vugt, H.H.; van Bel, F.; Heijnen, C.J. Neonatal dexamethasone treatment increases susceptibility to experimental autoimmune disease in adult rats. *J Immunol* **2000**, *165*, 5932-5937.

7. Meagher, M.W.; Sieve, A.N.; Johnson, R.R.; Satterlee, D.; Belyavskyi, M.; Mi, W.; Prentice, T.W.; Welsh, T.H., Jr.; Welsh, C.J. Neonatal maternal separation alters immune, endocrine, and behavioral responses to acute Theiler's virus infection in adult mice. *Behav Genet* **2010**, *40*, 233-249, doi:10.1007/s10519-010-9333-5.

8. Wick, G.; Hu, Y.; Schwarz, S.; Kroemer, G. Immunoendocrine communication via the hypothalamo-pituitary-adrenal axis in autoimmune diseases. *Endocr Rev* **1993**, *14*, 539-563, doi:10.1210/edrv-14-5-539.

9. Levine, S.; Strebel, R.; Wenk, E.J.; Harman, P.J. Suppression of experimental allergic encephalomyelitis by stress. *Proc Soc Exp Biol Med* **1962**, *109*, 294-298.

10. Levine, S.; Wenk, E.J.; Muldoon, T.N.; Cohen, S.G. Enhancement of experimental allergic encephalomyelitis by adrenalectomy. *Proc Soc Exp Biol Med* **1962**, *111*, 383-385.

11. Swedo, S.E.; Leonard, H.L.; Garvey, M.; Mittleman, B.; Allen, A.J.; Perlmutter, S.; Lougee, L.; Dow, S.; Zamkoff, J.; Dubbert, B.K. Pediatric autoimmune neuropsychiatric disorders associated with streptococcal infections: clinical description of the first 50 cases. *Am J Psychiatry* **1998**, *155*, 264-271, doi:10.1176/ajp.155.2.264.

12. Hoffman, K.L.; Hornig, M.; Yaddanapudi, K.; Jabado, O.; Lipkin, W.I. A murine model for neuropsychiatric disorders associated with group A beta-hemolytic streptococcal infection. *J Neurosci* **2004**, *24*, 1780-1791, doi:10.1523/jneurosci.0887-03.2004.

13. Yaddanapudi, K.; Hornig, M.; Serge, R.; De Miranda, J.; Baghban, A.; Villar, G.; Lipkin, W.I. Passive transfer of streptococcus-induced antibodies reproduces behavioral disturbances in a mouse model of pediatric autoimmune neuropsychiatric disorders associated with streptococcal infection. *Mol Psychiatry* **2010**, *15*, 712-726, doi:10.1038/mp.2009.77.

14. Macrì, S.; Ceci, C.; Proietti Onori, M.; Invernizzi, R.W.; Bartolini, E.; Altabella, L.; Canese, R.; Imperi, M.; Orefici, G.; Creti, R.; et al. Mice repeatedly exposed to Group-A beta-Haemolytic Streptococcus show perseverative behaviors, impaired sensorimotor gating, and immune activation in rostral diencephalon. *Sci Rep* **2015**, *5*, 13257, doi:10.1038/srep13257.

15. Martino, D.; Dale, R.C.; Gilbert, D.L.; Giovannoni, G.; Leckman, J.F. Immunopathogenic mechanisms in tourette syndrome: A critical review. *Mov Disord* **2009**, *24*, 1267-1279, doi:10.1002/mds.22504.

16. Orlovska, S.; Vestergaard, C.H.; Bech, B.H.; Nordentoft, M.; Vestergaard, M.; Benros, M.E. Association of Streptococcal Throat Infection With Mental Disorders: Testing Key Aspects of the PANDAS Hypothesis in a Nationwide Study. *JAMA Psychiatry* **2017**, doi:10.1001/jamapsychiatry.2017.0995.

17. Dale, R.C.; Brilot, F. Autoimmune basal ganglia disorders. *J Child Neurol* **2012**, *27*, 1470-1481, doi:10.1177/0883073812451327.

18. Swerdlow, N.R. Update: studies of prepulse inhibition of startle, with particular relevance to the pathophysiology or treatment of Tourette Syndrome. *Neurosci Biobehav Rev* **2013**, *37*, 1150-1156, doi:10.1016/j.neubiorev.2012.09.002.

19. Stein, D.J. Advances in the neurobiology of obsessive-compulsive disorder. Implications for conceptualizing putative obsessive-compulsive and spectrum disorders. *Psychiatr Clin North Am* **2000**, *23*, 545-562.

20. Ganos, C.; Roessner, V.; Münchau, A. The functional anatomy of Gilles de la Tourette syndrome. *Neurosci Biobehav Rev* **2013**, *37*, 1050-1062, doi:10.1016/j.neubiorev.2012.11.004.

21. Baldan Ramsey, L.C.; Xu, M.; Wood, N.; Pittenger, C. Lesions of the dorsomedial striatum disrupt prepulse inhibition. *Neuroscience* **2011**, *180*, 222-228, doi:10.1016/j.neuroscience.2011.01.041.

22. Mansbach, R.S.; Geyer, M.A.; Braff, D.L. Dopaminergic stimulation disrupts sensorimotor gating in the rat. *Psychopharmacology (Berl)* **1988**, *94*, 507-514.

23. Csomor, P.A.; Stadler, R.R.; Feldon, J.; Yee, B.K.; Geyer, M.A.; Vollenweider, F.X. Haloperidol differentially modulates prepulse inhibition and p50 suppression in healthy humans stratified for low and high gating levels. *Neuropsychopharmacology* **2008**, *33*, 497-512, doi:10.1038/sj.npp.1301421.

24. Deacon, R.M.; Rawlins, J.N. T-maze alternation in the rodent. *Nat Protoc* **2006**, *1*, 7-12, doi:10.1038/nprot.2006.2.

25. Lalonde, R. The neurobiological basis of spontaneous alternation. *Neurosci Biobehav Rev* **2002**, *26*, 91-104.

26. Irwin, J.; Tombaugh, T.N.; Zacharko, R.M.; Anisman, H. Alteration of exploration and the response to food associated cues after treatment with pimozide. *Pharmacol Biochem Behav* **1983**, *18*, 235-246.

27. Jaffard, R.; Mocaer, E.; Poignant, J.C.; Micheau, J.; Marighetto, A.; Meunier, M.; Beracochea, D. Effects of tianeptine on spontaneous alternation, simple and concurrent spatial discrimination learning and on alcohol-induced alternation deficits in mice. *Behav Pharmacol* **1991**, *2*, 37-46.

28. Spinello, C.; Laviola, G.; Macrì, S. Pediatric Autoimmune Disorders Associated with Streptococcal Infections and Tourette's Syndrome in Preclinical Studies. *Front Neurosci* **2016**, *10*, 310, doi:10.3389/fnins.2016.00310.

29. Frick, L.; Pittenger, C. Microglial Dysregulation in OCD, Tourette Syndrome, and PANDAS. *J Immunol Res* **2016**, *2016*, 8606057, doi:10.1155/2016/8606057.

30. Zoratto, F.; Fiore, M.; Ali, S.F.; Laviola, G.; Macrì, S. Neonatal tryptophan depletion and corticosterone supplementation modify emotional responses in adult male mice. *Psychoneuroendocrinology* **2013**, *38*, 24-39, doi:10.1016/j.psyneuen.2012.04.015.

31. Niwa, M.; Matsumoto, Y.; Mouri, A.; Ozaki, N.; Nabeshima, T. Vulnerability in early life to changes in the rearing environment plays a crucial role in the aetiopathology of psychiatric disorders. *Int J Neuropsychopharmacol* **2011**, *14*, 459-477, doi:10.1017/S1461145710001239.

2

32. Demoulin, J.B.; Renauld, J.C. Interleukin 9 and its receptor: an overview of structure and function. *Int Rev Immunol* **1998**, *16*, 345-364.

33. Mehler, M.F.; Rozental, R.; Dougherty, M.; Spray, D.C.; Kessler, J.A. Cytokine regulation of neuronal differentiation of hippocampal progenitor cells. *Nature* **1993**, *362*, 62-65, doi:10.1038/362062a0.

34. Elyaman, W.; Bradshaw, E.M.; Uyttenhove, C.; Dardalhon, V.; Awasthi, A.; Imitola, J.; Bettelli, E.; Oukka, M.; van Snick, J.; Renauld, J.C.; et al. IL-9 induces differentiation of TH17 cells and enhances function of FoxP3+ natural regulatory T cells. *Proc Natl Acad Sci U S A* **2009**, *106*, 12885-12890, doi:10.1073/pnas.0812530106.

35. Tabarkiewicz, J.; Pogoda, K.; Karczmarczyk, A.; Pozarowski, P.; Giannopoulos, K. The Role of IL-17 and Th17 Lymphocytes in Autoimmune Diseases. *Arch Immunol Ther Exp (Warsz)* **2015**, *63*, 435-449, doi:10.1007/s00005-015-0344-z.

36. Youssef, S.; Wildbaum, G.; Karin, N. Prevention of experimental autoimmune encephalomyelitis by MIP-1alpha and MCP-1 naked DNA vaccines. *J Autoimmun* **1999**, *13*, 21-29, doi:10.1006/jaut.1999.0306.

37. van den Buuse, M.; Simpson, E.R.; Jones, M.E. Prepulse inhibition of acoustic startle in aromatase knock-out mice: effects of age and gender. *Genes Brain Behav* **2003**, *2*, 93-102.

38. Hill, R.A.; McInnes, K.J.; Gong, E.C.; Jones, M.E.; Simpson, E.R.; Boon, W.C. Estrogen deficient male mice develop compulsive behavior. *Biol Psychiatry* **2007**, *61*, 359-366, doi:10.1016/j.biopsych.2006.01.012.

39. Boon, W.C.; Horne, M.K. Aromatase and its inhibition in behaviour, obsessive compulsive disorder and parkinsonism. *Steroids* **2011**, *76*, 816-819, doi:10.1016/j.steroids.2011.02.031.

40. Garcia-Gomez, E.; Gonzalez-Pedrajo, B.; Camacho-Arroyo, I. Role of sex steroid hormones in bacterial-host interactions. *Biomed Res Int* **2013**, *2013*, 928290, doi:10.1155/2013/928290.

41. Ercan, A.; Kohrt, W.M.; Cui, J.; Deane, K.D.; Pezer, M.; Yu, E.W.; Hausmann, J.S.; Campbell, H.; Kaiser, U.B.; Rudd, P.M.; et al. Estrogens regulate glycosylation of IgG in women and men. *JCI Insight* **2017**, *2*, e89703, doi:10.1172/jci.insight.89703.

42. Cox, C.J.; Zuccolo, A.J.; Edwards, E.V.; Mascaro-Blanco, A.; Alvarez, K.; Stoner, J.; Chang, K.; Cunningham, M.W. Antineuronal antibodies in a heterogeneous group of youth and young adults with tics and obsessive-compulsive disorder. *J Child Adolesc Psychopharmacol* **2015**, *25*, 76-85, doi:10.1089/cap.2014.0048.

43. Lescoat, G.; Lescoat, D.; Garnier, D.H. Influence of adrenalectomy on maturation of gonadotrophin function in the male rat. *J Endocrinol* **1982**, *95*, 1-6.

44. Lord, G.M.; Matarese, G.; Howard, J.K.; Baker, R.J.; Bloom, S.R.; Lechler, R.I. Leptin modulates the T-cell immune response and reverses starvation-induced immunosuppression. *Nature* **1998**, *394*, 897-901, doi:10.1038/29795.

45. Hsu, L.C.; Enzler, T.; Seita, J.; Timmer, A.M.; Lee, C.Y.; Lai, T.Y.; Yu, G.Y.; Lai, L.C.; Temkin, V.; Sinzig, U.; et al. IL-1beta-driven neutrophilia preserves antibacterial defense in the absence of the kinase IKKbeta. *Nat Immunol* **2011**, *12*, 144-150, doi:10.1038/ni.1976.

46. Krabbe, G.; Minami, S.S.; Etchegaray, J.I.; Taneja, P.; Djukic, B.; Davalos, D.; Le, D.; Lo, I.; Zhan, L.; Reichert, M.C.; et al. Microglial NFkappaB-TNFalpha hyperactivation induces obsessive-compulsive behavior in mouse models of progranulin-deficient frontotemporal dementia. *Proc Natl Acad Sci U S A* **2017**, *114*, 5029-5034, doi:10.1073/pnas.1700477114.

47. Tsatsaronis, J.A.; Walker, M.J.; Sanderson-Smith, M.L. Host responses to group a streptococcus: cell death and inflammation. *PLoS Pathog* **2014**, *10*, e1004266, doi:10.1371/journal.ppat.1004266.

48. Horst, S.A.; Linner, A.; Beineke, A.; Lehne, S.; Holtje, C.; Hecht, A.; Norrby-Teglund, A.; Medina, E.; Goldmann, O. Prognostic value and therapeutic potential of TREM-1 in Streptococcus pyogenes-induced sepsis. *J Innate Immun* **2013**, *5*, 581-590, doi:10.1159/000348283.

49. Murakami, Y.; Akahoshi, T.; Aoki, N.; Toyomoto, M.; Miyasaka, N.; Kohsaka, H. Intervention of an inflammation amplifier, triggering receptor expressed on myeloid cells 1, for treatment of autoimmune arthritis. *Arthritis Rheum* **2009**, *60*, 1615-1623, doi:10.1002/art.24554.

50. Lin, C.H.; Hsieh, S.C.; Keng, L.T.; Lee, H.S.; Chang, H.T.; Liao, W.Y.; Ho, C.C.; Yu, C.J. Prospective Evaluation of Procalcitonin, Soluble Triggering Receptor Expressed on Myeloid Cells-1 and C-Reactive Protein in Febrile Patients with Autoimmune Diseases. *PLoS One* **2016**, *11*, e0153938, doi:10.1371/journal.pone.0153938.

SUPPLEMENTARY MATERIALS

Supplementary Methods

Animals and rearing

Upon arrival, males were housed individually in type-1 polycarbonate cages (33.0×13.0×14.0 cm), while females were housed in groups of 6 in type-3 polycarbonate cages (42.0×26.0×15.0 cm). All cages were equipped with sawdust bedding, an enrichment bag (Mucedola, Settimo Milanese, Italy), metal top and *ad libitum* water and food pellets (Mucedola, Settimo Milanese, Italy). Mice were maintained on a reversed 12-h-light-dark cycle (light on at 7:00 PM) in an air-conditioned room (temperature 21 ± 1°C and relative humidity 60 ± 10%).

Neonatal treatment

Starting on PND1, were supplemented with corticosterone (80 μg/ml) in their drinking water. CORT administration was maintained until PND10. CORT concentration was selected based on previous literature [1-3]. CORT-exposed mice drank on average 13,9±0,49 ml of CORT solution; this resulted in an average daily intake of 1,11±0,039 mg. Except for the solution in the drinking bottle, neonatal environmental conditions were identical among groups. Subjects were left undisturbed until PND9, when pups were weighed and sexed. In addition, from PND9 onwards, cages were regularly cleaned once a week. On PND23, individuals were weaned and housed in same-sex, same-treatment groups of two or three individuals. On PND27, all mice were marked through ear clipping.

Immunization protocol

After preparation, GAS homogenate was stored at -70°C. A blood agar plate was used to inoculate a sample of homogenate (2.5 μl), to verify that it contained no viable bacteria. The immunization protocol, described by Hoffman et al [4] and adopted in our previous study [5], comprised five injections interspaced by a time interval of two weeks, starting on PND28. During the first injection, PBS mice were injected subcutaneously (s.c.) with 125 μL of an emulsion (1:1), containing PBS and Complete Freund's adjuvant (CFA; Sigma-Aldrich, Milano, Italy). GAS mice were injected with 125 μL of the same emulsion (CFA:PBS), containing 5 μL of GAS homogenate (0.52 mg/ml of total protein as determined by Bradford Assay, Bio-Rad). All mice were then treated four additional times at two-weeks intervals with 125 μL of vehicle - an emulsion containing PBS and Incomplete Freud's Adjuvant (IFA; Sigma-Aldrich, Milano, Italy) - for PBS mice, or 125 μL of vehicle and 5 μL of GAS homogenate for GAS mice. To prepare the PBS/adjuvant emulsions, we used the vortex method described by Flies and Chen [6].

Experimental Design

Experimental tests were distributed among batches as follows: Batch 1 was used for behavioral testing (elevated 0-maze, locomotor activity, elevated plus maze, rotarod, T-maze, pre-pulse inhibition, and observation of DOI-induced behavioral responses), basal CORT concentrations, antibody response, plasma cytokines and immunohistochemistry at sacrifice (fourth injection); Batch 2 was used to evaluate hair CORT concentrations at weaning, brain monoamines at sacrifice, and RNA sequencing. All animals were sacrificed two weeks after the fifth injection.

Physiological indicators of the efficacy of experimental treatments

Hair and blood sampling

To evaluate the effects of neonatal and adult treatment on HPA activity, we evaluated CORT levels both at weaning (through non-invasive CORT analysis of hair samples) and at the end of the study through trunk blood collection. Blood samples were also used for the determination of antibodies. Hair samples were collected through shaving a small portion of hair on the back of the subjects. Trunk blood serum samples (~200 μL) were collected after the fourth boost of immunization, at the moment of the sacrifice. Blood samples were allowed to clot at room temperature for 4 hours, centrifuged at 3000 rpm for 15 minutes. The serum was transferred into Eppendorf tubes and maintained at -80°C until the biochemical assays were performed. CORT concentration was assessed using a commercial radioimmunoassay (RIA) kit (ICN Biomedicals, Costa Mesa, CA). Vials were counted for 2 minutes in a gamma counter (Packard Minaxi Gamma counter, Series 5000). The procedures for washing and steroid extraction followed the protocol described by Gao and colleagues [7], who analyzed hair steroids with liquid chromatography tandem mass spectrometry (LC-MS/MS). One change was made to the protocol: the dry residue was resuspended using 175μL distilled water. Afterward, 100μL of the medium was injected into a Shimadzu HPLC system (Shimadzu, Canby, OR, USA) coupled to an AB Sciex API 5000 Turboion-spray1triple quadrupole tandem mass spectrometer equipped with Atmospheric Pressure Chemical Ionization (APCI) Source (AB Sciex, Foster City, CA, USA). The system was controlled by AB Sciex Analyst1 software (version 1.5.1). The lower limit of detection was ~0.1pg/mg. Intra- and inter-plate coefficients of variance ranged between 3.7–8.8%. All samples were prepared and analyzed within the same time period in order to prevent batch effects.

Analysis of anti-Group A Streptococcal antibodies in serum samples

GAS homogenates obtained as described above were size-separated by SDS-PAGE (4–12% acrylamide) under reducing conditions and electroblotted onto nitrocellulose membranes. Immunostaining was performed by blocking the membrane overnight with 3% (w/v)

skimmed milk in TPBS (0.1% Tween in PBS) and incubating for 2 h with sera from mice of all experimental groups (all sera were diluted 1: 200). After 3 washes with TPBS, the membrane was incubated with HRP-conjugated secondary antibody (1:1000), washed again with TPBS and PBS, and developed with a chromogenic substrate.

Behavioral testing

Elevated 0-maze

Mice were tested for anxiety-related behaviors on the elevated 0-maze, which imposes an approach-avoidance conflict. The apparatus consisted of a 5.5 cm wide circular runway made of black plastic with an outer diameter of 46 cm and placed 40 cm above the floor. Two closed sectors, positioned opposite to each other, were protected by 16 cm high walls made of transparent Plexiglas; the two remaining sectors were unprotected (open sectors). Mice were tested between 10:00 and 12:00 am directly in the housing room, under dim light. At the beginning of the experimental session, the animal was gently positioned into one of the two closed sectors and allowed to explore the apparatus for 5 minutes. Between experimental sessions, the apparatus was cleaned with an alcohol/water solution (50%). Data acquired through a camera (Sony, Handycam, DCR-SX21E) were saved on a personal computer (Dell, Dell Precision T1600) and scored offline using the 'Observer 10.5' (Noldus, Wageningen, The Netherlands). For each animal, we detected spatiotemporal variables (time spent and the number of entries in each sector), and behavioral variables in frequency and duration (*rearing*, *grooming*, *stretched attend posture (SAP)*, and *head dipping*). The total number of entries was considered as an index of general activity, while time spent in the closed sectors was used as a measure of anxiety [2].

Pre-pulse inhibition (PPI)

Apparatus: The apparatus (Med Associates inc. St Albans, VT, United States of America [8]) consisted of an acoustic stimulator (ANL-925, Med Associates inc.) and a platform with a transducer amplifier (PHM-250-60, Med Associates inc.), and was positioned in a foam-lined isolation chamber (ENV-018S, Med Associates inc.), defined as startle chamber. The presence of a red light and a fan, both enclosed in the chamber, guaranteed dimmed lighting and ventilation. The platform was enclosed in a perforated compartment to ensure that the experimental subjects remained on it. Experimental data were acquired through dedicated software (SOF-815, Med Associates inc.).

Procedure: During habituation, each mouse was positioned individually inside the startle chamber, and left undisturbed (without any stimulus) for five minutes. On the following day, mice were placed again inside the startle chamber for testing. At the beginning of the experimental session, mice were exposed to a white noise (62dB) for five minutes. After

acclimation, mice were then exposed to a sequence of ten trials (pulses of 120dB), that were interspaced by an average inter-trial interval of 15 s (block I). Then, an 8-min long session started (block II). This session entailed 28 trials comprising four different types of trials that were presented in a pseudorandomized order. Trials were defined as follows: prepulse alone (one trial for prepulse intensity), prepulse plus pulse (four trials for prepulse intensity), startle alone (four trials) and no stimulation (four trials). The inter-trial interval varied between 10-s and 20-s to avoid habituation. Each trial started with a null period of 50 ms, followed by a prepulse noise. The intensity of the prepulse varied among four different values, represented by 67, 70, 73 or 76 dB. Following the prepulse, a startle stimulus was presented. The startle stimulus, as described previously, was constituted by a white noise of 40ms long and with an intensity of 120 dB. Prepulse and pulse stimuli were interspaced by an inter-stimulus period of 100 ms. The galvanic response was considered as the dependent variable and was measured 65 ms following the onset of the startle. Prepulse inhibition (PPI) was measured as PPI= [(A-B)/A*100], wherein A is the Galvanic reflex registered after the startle stimulus alone, and B is the reflex registered in response to the startle in prepulse plus pulse trials.

Locomotor activity

After the second and the fourth injection, mice were monitored for spontaneous locomotion over a 24-hr period. General locomotion was evaluated in experimental cages identical to the home cages and positioned on a rack within the housing room. Six hours before the beginning of the registration session, mice were housed individually. Locomotor activity was then monitored for 24 consecutive hours through an automated device using small passive infrared sensors positioned on the top of each cage (ACTIVISCOPE system, NewBehavior Inc., Zurich, Switzerland) [9,10]. The movement of the mice was detected with sensors operating at a frequency of 20 events per second (20 Hz). When mice were sleeping or inactive, the sensor did not detect any movement. Average scores measured in 60-min intervals and expressed as count per minute (cpm) were detected for each mouse using dedicated software (NewBehavior Inc., Zurich, Switzerland). At the end of the test, mice were relocated to their original home cages.

Accelerating rotarod test

Accelerating rotarod test was performed to evaluate mouse balance and motor coordination, by measuring the latency to fall from a rotating cylinder (Basile, Comerio, Italy). The apparatus consisted of a rotating rod (3 cm in diameter), on which mouse had to walk to avoid falling. To prevent harm to subjects, the cylinder was positioned 13 cm above the falling surface. A timer connected to a switch was used to record the latency, and the timer stopped when the

mouse fell from the rod. During each trial, the rate of rotation progressively increased from 4 to 40 revolutions per minute (r.p.m.) over 4 minutes. Mice performed three consecutive trials interspaced by a time interval of 10 minutes. The trial stopped when the mouse fell down from the cylinder, or when it reached the cut-off (4 minutes). The test was performed in an experimental room, adjacent to the housing room, between 10:00 and 14:00, where mice were carried to one hour before the beginning of the experimental session.

T-maze

Animals were screened for perseverative behaviors in the T-maze test. The experimental apparatus consisted of an enclosed T-shaped maze, composed of three equally sized arms (50x16 cm). Ten sessions were performed during five consecutive days (2 sessions per day), always in the housing room. The experimental session, consisting of two choice trials, started with the mouse positioned in the starting compartment, facing the wall of the apparatus. Then, the subject was allowed to explore the apparatus for two minutes. As soon as the animal completed the trial (entering one of the two alternative arms), such instance was scored as the first choice and the door of the arm was closed. After a few seconds, the animal was gently removed from the arm, placed again in the starting compartment, and allowed to perform a second choice trial. If the subject entered the arm opposite to the previously chosen one, an instance of alternation was scored. Alternatively, if the mouse re-entered the same arm, an instance of perseveration was scored. The percentage of alternations, measured as the number of alternations divided by the number of completed sessions times 100, was scored for each mouse. In a T-maze, rodents have the natural tendency to alternate their choice of the arm (spontaneous alternation) [11].

Elevated plus maze

The elevated plus maze test was performed after the fourth injection, to evaluate the exploration of an environment imposing on the animal an approach-avoidance conflict. The apparatus, elevated to a height of 40 cm above the floor level, comprised two open arms (27x5x0.25 cm) and two closed arms (27x5x15 cm), extended from a common central platform (5x5 cm). The floor and walls of the apparatus were both made of Plexiglas (black floor, transparent walls). The test was performed in an experimental room between 10:00 and 14:00, where mice were carried to one hour before the beginning of the experimental session. At the beginning of the test, mice were positioned gently in the central platform of the apparatus facing one of the two closed arms, and allowed to explore the maze for 5 minutes. The test was performed under dim illumination, and the apparatus was cleaned with an alcohol solution (50%) after each animal was tested. All sessions were recorded by

a video camera (Sony, Handycam, DCR-SX21E), saved on a personal computer (Dell, Dell Precision T1600), and scored offline using the 'Observer 10.5' (Noldus). For each animal, we detected spatiotemporal variables (time spent and number of entries in each sector), and behavioral variables in frequency and duration. In particular, we scored: *rearing* (head raising standing on hind legs), *grooming* (self-cleaning with mouth or paws), *stretched attend posture (SAP)* (stretched posture with the head and two or three paws on the open arm and retraction to previous position) and *head dipping* (downward movement of the head towards the floor while on the open arms).

Individual reactivity to serotonergic agonist (DOI)

In order to observe the individual reaction to a serotonergic agonist, we evaluated the behavioral response to the administration of the 5-HT2a agonist DOI (2,5-dimethoxy-4-iodoamphetamine, Sigma-Aldrich, St. Louis, MO, USA, 5 mg/kg). DOI was dissolved in saline (NaCl 0,9%) and administered i.p. at a volume of 1 ml/100 g body weight [12], to the animals of batch 1 after the fifth injection (week 13). Starting 5 minutes after the injection, animals were video recorded for the following 10 minutes, using a video camera mounted on the back of the home cages. To prevent the occlusion of the visual space targeted by the video camera, the day before the test all animals were housed individually in cages where only a thin layer of bedding was left. The video-recording apparatus was composed of 32 video cameras (Simon TLC, PRS Italia, Rome, Italy) positioned on the back of the rack and connected to a DVR system (Gifran, 16 Channels Realtime, H.264 Full D1). Each black and white video camera (resolution: 420 lines, illumination: 0.01 Lux, lens: 3.6 mm) was positioned on a panel at a distance of 4.0 cm from the short side of the cages, with the centre of the lens focused on the cage to allow the tracking of animal movements and behaviors (see [10] for details). Behavioral responses were then scored using a computer with a dedicated software (The Observer 10.5, Noldus). Frequency and duration of two behavioral responses were scored: *head twitch*, a rapid and violent head shaking [13], and *skin jerk*, a muscle contraction of the body longer in duration than the twitch [10].

Immunohistochemistry

For immunohistochemistry, air dried cryosections were passed in 70%, 95%, and 100% ethanol, and after rehydration with PBS and 20-min incubation with 0.3% H_2O_2 in PBS to eliminate endogenous peroxidase activity, sections were pre-incubated with 10% of normal sera and incubated at 4°C overnight with rabbit polyclonal IBA1 antibody (Wako-Chem, Japan), or goat polyclonal TNF antibody (R&D System, Minneapolis, Minn) or IL-9 (diluted in PBS containing 5% normal donkey serum, followed by incubation with biotinylated

secondary antibodies (Jackson ImmunoResearch Laboratories, Suffolk, UK) visualized with the avidin-biotin horseradish peroxidase complex (ABC Vectastain Elite kit, Vector Laboratories, Burlingame, CA, USA) and 3,3 diaminobenzidine (Sigma Chemical, St. Louis, MO, USA). All sections were counterstained with haematoxylin, sealed with Canada balsam and viewed and photographed with an Axiophot Zeiss microscope (Germany) equipped with an Axiocam digital camera using the Axiovision 4AC software. Qualitative analysis of the presence and distribution of inflammatory cells was performed by a trained observer who did not perform the cutting (R.M.) and was blind to the treatment across all the different brain areas.

Cytokine concentrations in the serum were determined through the Bio-Plex Cytokine Assay (23-Plex, Bio-Rad). Briefly, differentially stained microbeads, each type of which is coated with antibodies recognizing different cytokines, were incubated with mouse sera, washed, and incubated with biotinylated detection antibodies. Then the beads with the sandwich between antibodies and cytokines were washed, incubated with streptavidin-PE, washed again, and read in the Bio-Rad array. We determined cytokine concentration as an average of two replicates per serum.

Monoamine measurements

In order to collect brain samples, mice were rapidly decapitated. Samples collected for evaluation of brain monoamines by HPLC analyses were immediately sectioned on ice to obtain five sections: prefrontal cortex, striatum, hippocampus, hypothalamus, and cerebellum. All samples were flash frozen and then stored at -80°C until analysis. Brain samples collected for immunohistochemical analyses and RNA sequencing were collected after decapitation, kept intact, flash frozen and stored at -80°C.

Briefly, each brain region was weighed and a measured volume (10% W/V) of 0.1 N perchloric acid containing 0.05% $Na_2S_2O_5$ and 0.1% Na2EDTA was added. The tissue was then disrupted by ultrasonication, centrifuged (10,000 × g; 5 minutes), and 100 µl of the supernatant was removed and filtered through 0.45 µm PVDF syringe filters (Perkin-Elmer, Italy). Aliquots of 20 µl were injected directly onto the HPLC/EC system by a refrigerated (5°C) autosampler (MIDAS, Spark-Holland, The Netherlands) for the separation of 5-HT, DA, 5-HIAA, and DOPAC through a Supelcosil LC-18DB, 3 µm (75 × 3.0 mm) analytical column (Supelchem, Italy), thermostated at 40°C. The mobile phase consisted of sodium acetate anhydrous (5 g/L), citric acid (4.5 g/L), sodium octane sulphonate (100 mg/L), Na2EDTA dihydrate (112 mg/L); CH3OH 7%. Monoamines and metabolites were measured by a Coulochem II electrochemical detector (Dionex, Switzerland) equipped with a 5011 electrochemical cell (E1 and E2 potentials were 0 and +350 mV, respectively). A data system

(Azur 4.6, Datalys, France) was used to calculate the concentration of analytes based on calibration curves prepared daily with appropriate concentrations of pure standards.

RNA sequencing

Total RNA was extracted from striatum tissue using the Qiagen AllPrep Kit (Qiagen, Hamburg, Germany), according to the manufacturer's instructions. RNA was further quantified using the NanoDrop 1000 Spectrophotometer and Qubit Fluorometer (Thermo Fisher Scientific, MA, USA) and RNA integrity was assessed with the 2200 TapeStation Instrument (Agilent Technologies, CA, USA). A total of 500 ng RNA was used for library preparation with the TruSeq Stranded Total RNA with Ribo-Zero Gold sample preparation kit (Illumina, CA, USA). Successfully prepared cDNA libraries were then submitted for sequencing at the Department of Human Genetics, Radboud University Medical Center, Nijmegen, The Netherlands, on the Illumina NextSeq500 platform to obtain 76 bp paired-end reads. FASTQC [14] and MultiQC [15] software was used to assess and summarize the quality of the raw sequence data. Reads were aligned to the Mus musculus genome (primary assembly GRCm38, version 75) using GSNAP with (default) parameters [16]. Alignment was assessed using RSeQC [17], RNA-SeQC [18] and gene expression abundance (read count) was estimated. It was shown that estimation of gene expression is less reliable for genes with low read count [19] and therefore recommended to filter low-count genes prior to differential expression testing [20]. Hence, transcripts with at least 10 reads in 5 samples were retained and further used to identify differentially expressed genes between the four experimental groups: water-GAS vs water-PBS, CORT-GAS vs water-GAS, CORT-PBS vs water-PBS, and CORT-GAS vs CORT-PBS. Statistical analyses were performed using R (www.r-project.org) and Bioconductor packages ([21], www.bioconductor.org), applying four methods: limma voom, limma voomWithQualityWeights [22], EdgeR glm [23], [24] and DESeq2 [25] to test for differences in gene expression between groups. Batch effects (library preparation, sequencing run, striatum hemisphere) were modeled according to the statistical design of each method. Genes were called as differentially expressed if they passed the selection criteria threshold of absolute fold change ≥1.2 and P-value <0.01 for each of the four methods. The final sets of differentially expressed genes comprised those that were identified as differentially expressed by at least two of the four used methods. As suggested by Zhang et al. [26], this approach was taken to account for false positive discoveries.

Venn diagrams (see Supplementary Figure 1) of the final sets of differentially expressed genes were built with Venny [27]. For genes that showed differential expression, upstream regulator analysis was performed using the Ingenuity Pathway Analysis software (IPA) (Ingenuity Systems Inc., Redwood City, CA). Based on the 'Ingenuity Knowledge Base', a repository of data from publicly accessible databases and data that are manually curated by

systematically reviewing published literature, IPA can generate a list of 'upstream regulators', i.e., proteins or compounds that regulate the expression of multiple target mRNAs/genes from an input list. The program also calculates a z-score that is based on the expression changes of the input mRNAs and that is a measure for the directionality of the upstream regulator. In this respect, a z-score <-1.5 or >1.5 (reflecting inhibition or activation of the upstream regulator-dependent effects on target gene expression, respectively) is considered as 'suggestive'.
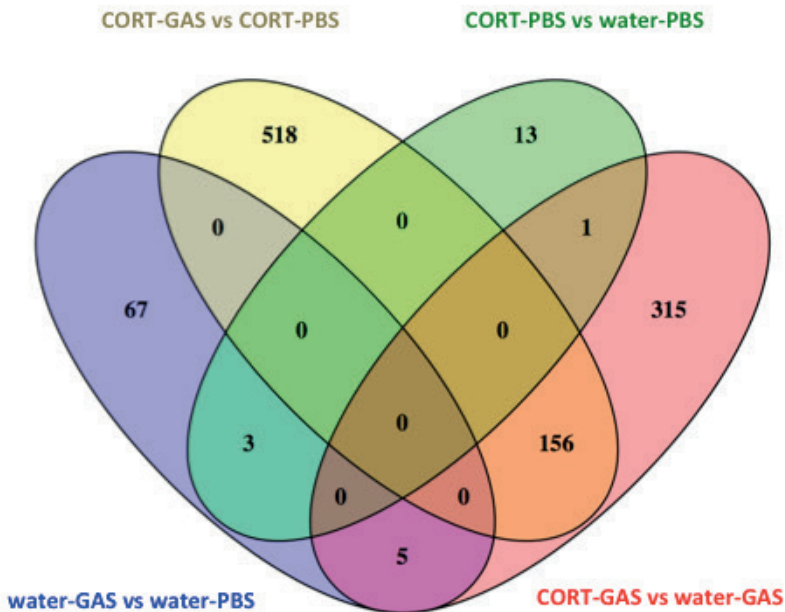
SUPPLEMENTARY FIGURE 1. Venn diagrams showing the unique and overlapping differentially expressed genes between the four comparisons, i.e., WATER-GAS vs WATER-PBS (75 genes), CORT-GAS vs WATER -GAS (477 genes), CORT-PBS vs WATER -PBS (17 genes), and CORT-GAS vs CORT-PBS (674 genes).

Supplementary Results

Antibody response to GAS administration

Predictably, while Western Blot analyses conducted on sera from WATER-GAS and CORT-GAS mice revealed several bands (Supplementary Figure 2, lane 3 and 5 respectively), WATER-PBS and CORT-PBS mice did not reveal any or very few bands (Supplementary Figure 2, lane 2 and 4 respectively).
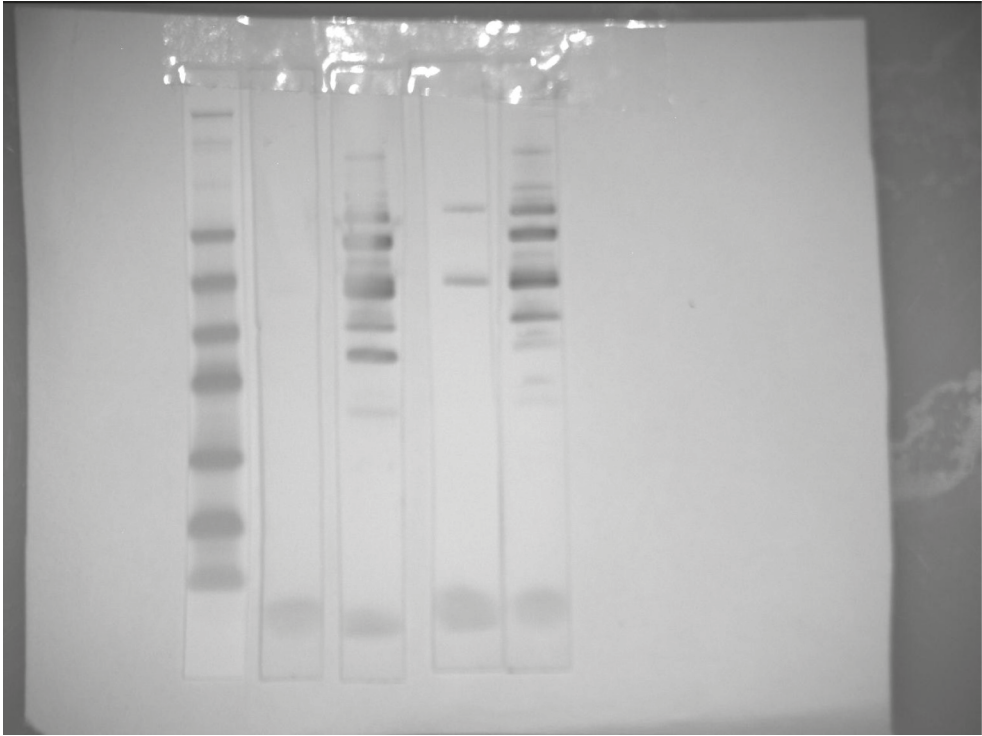
SUPPLEMENTARY FIGURE 2. Western Blot analysis of GAS extracts probed with pooled sera from mice treated with GAS homogenates or adjuvant alone as Control, neonatal CORT and GAS homogenates or neonatal CORT and adjuvant. Lane 1, Coomassie staining of GAS homogenates; Lane 2, Western Blot results after probing with sera of control mice injected with four doses of adjuvant alone; lane 3, Western Blot results after probing with sera of mice injected with four doses of GAS homogenates; lane 4, Western Blot results after probing with sera of mice injected with four doses of neonatal CORT and adjuvant; lane 5, Western Blot results after probing with sera of mice injected with four doses of neonatal CORT and GAS homogenates.

Elevated 0-Maze (E0M) test (week 7, second injection)

As expected, all mice showed a preference for the closed sectors of the maze, wherein they spent on average 68,1% of the time. All experimental groups did not significantly differ in terms of time spent in the open arms (neonatal treatment: $F(1,34) = 1,395$, $p = 0,2457$; PBS/GAS treatment: $F(1,34) = 0,016$, $p = 0,9003$; neonatal treatment x PBS/GAS treatment: $F(1,34) = 0,614$, $p = 0,4388$). The frequency of entries in the open sectors of the maze, considered an index of general locomotion, was significantly reduced in CORT-treated subjects (neonatal treatment: $F(1,33) = 4,410$, $p = 0,0434$) regardless of GAS administration (neonatal treatment x PBS/GAS treatment: $F(1,33) = 0,021$, $p = 0,8866$). Furthermore, GAS administration *per se* did not influence the frequency of open arm entries (PBS/GAS treatment: $F(1,33) = 0,614$, $p = 0,4388$). Finally, CORT-treated animals exhibited increased

2

levels of *SAP* (duration, neonatal treatment: $F(1,34) = 5,391$, $p = 0,0264$) and decreased levels of *head dipping* (frequency, neonatal treatment: $F(1,34) = 5,683$, $p = 0,0229$; duration, neonatal treatment: $F(1,34) = 6,797$, $p = 0,0135$). None of the other behavioral parameters considered differed significantly among experimental groups (see Supplementary Table 1).

Elevated Plus-Maze test (EPM, week 11, fourth injection)

We evaluated the behavioral profile of experimental subjects on the EPM after the fourth injection (week 11). As expected, mice showed an 85.9% preference (calculated as: 100 * time spent in the closed arms / (time in open arms + time in closed arms)) for the closed instead of the open arms of the maze. Experimental groups did not differ in terms of time spent in the open arms of the maze (neonatal treatment: $F(1,34) = 0,076$, $p = 0,9217$; PBS/GAS treatment: $F(1,34) = 0,010$, $p = 0,7851$; neonatal treatment x PBS/GAS treatment: $F(1,34) = 0,492$, $p = 0,4877$). Early CORT administration significantly reduced the time spent in the center of the apparatus (neonatal treatment: $F(1,33) = 4,565$, $p = 0,0401$). General locomotion did not significantly vary among groups (frequency of entries, neonatal treatment: $F(1,34) = 0,711$, $p = 0,4050$; PBS/GAS treatment: $F(1,34) = 0,606$, $p = 0,4417$; neonatal treatment x PBS/GAS treatment: $F(1,34) = 0,092$, $p = 0,7640$). With respect to the ethological parameters considered, we observed that early CORT administration significantly reduced *SAP* (frequency of *SAP*, neonatal treatment: $F(1,33) = 4,621$, $p = 0,0390$; duration of *SAP*, neonatal treatment: $F(1,34) = 10,024$, $p = 0,0033$) and *sniffing* (frequency of *sniffing*, neonatal treatment: $F(1,34) = 6,227$, $p = 0,0176$; duration of *sniffing*, neonatal treatment: $F(1,34) = 4,132$, $p = 0,0499$). We did not observe between-group differences for all the other behavioral parameters considered (see Supplementary Table 1).

Rotarod test (week 11, fourth injection)

We evaluated motor coordination through the Rotarod Test after the fourth injection (week 11). With respect to the latency to fall from the apparatus, all experimental subjects showed a progressive tendency towards an improvement of their performance across trials (trial: $F(2,68) = 7,410$, $p = 0,0012$). Additionally, the progressive improvement was undistinguishable among experimental groups (latency to fall, neonatal treatment: $F(1,34) = 0,806$; PBS/GAS treatment: $F(1,34) = 0,305$, $p = 0,5846$; neonatal treatment x PBS/GAS treatment: $F(1,34) = 0,467$, $p = 4988$).

T-maze (week 11, fourth injection)

Repeated GAS injections significantly reduced the percentage of spontaneous alternations in a T-maze test ($F(1,34) = 9,074$, $p = 0,0049$, see Supplementary Figure 3). Neonatal corticosterone administration neither altered the exhibition of spontaneous alternations (neonatal treatment: $F(1,34) = 0,003$, $p = 0,9559$) nor influenced the consequences of

repeated GAS administrations (neonatal treatment x PBS/GAS treatment: $F(1,34) = 1$, 163, $p = 0,2884$, see Supplementary Figure 3).
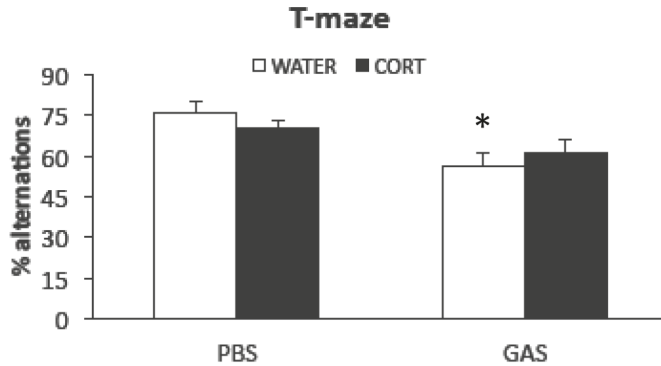
SUPPLEMENTARY FIGURE 3. Perseverative behavior in a T-maze (week 11, fourth injection) measured as the percentage of spontaneous alternations (mean+SEM; n=8-12 per group). *p<0.05 in post-hoc tests versus WATER-PBS subjects.

Monoamine measurements

While striatal dopamine concentrations were apparently reduced in response to both treatments, such reduction was not statistically significant (neonatal treatment: $F(1,17) = 4,017$, $p = 0,0612$; PBS/GAS treatment: $F(1,17) = 4,058$, $p = 0,0601$).

RNA seq data analysis: effects at the molecular level

The upstream regulator analysis of the genes that were found to be differentially expressed in the striatum between the experimental groups (Table 1 and Supplementary Table 4) provides insights into the (putative) molecular mechanisms underlying the observed behavioral changes. More specifically, the analysis in Table 1 gives clues as to which mechanisms convey the effects of neonatal corticosterone treatment on GAS-induced abnormal behavior.

First and foremost, the regulatory effect of **(beta-)estradiol** – the active form of the main female sex hormone estrogen that is converted from testosterone, the main male sex hormone, by the aromatase enzyme [28] – is predicted to be inhibited in GAS mice, while it is activated in GAS mice that have been neonatally exposed to corticosterone (CORT) and that have attenuated GAS-induced behaviors. This is in keeping with literature findings, i.e., **estradiol**-deficient rodents show decreased PPI [29,30] and develop OCD-like behavior [31-33]. In addition, tics have been reported to worsen in women during times of (relatively) lower **estradiol** levels (e.g., during the premenstrual phase) [34,35] and both

2

in women and men – in whom estradiol can only be produced through conversion from testosterone – increased (and earlier) OCD symptoms have been linked to (relatively) lower **estradiol** levels [36,37]. **Estradiol** has been reported to regulate the immune response through e.g., having a protective effect against bacterial infections [38]. Interestingly, this effect is probably achieved through **estradiol** modulating the immunologic potency of **IgG** antibodies for that are formed against bacteria (see below) [39]. Further, **estradiol** activates the HPA-axis, resulting in an increased **CORT** production and associated stress response [40-42], reinforcing the observed attenuating effect of CORT on GAS-induced behavior. Lastly, **estradiol** is involved in upregulating the expression of **luteinizing hormone (LH)** [43] and it increases the striatal release of **dopamine (DA)** [44,45] (see below).

As indicated above, testosterone is converted to beta-estradiol by the aromatase enzyme. Therefore, it is interesting that in GAS-induced mice, the effect of **dihydrotestosterone**, a metabolite that is converted from testosterone by 5α-reductase enzymes [28] of which one family member, SRD5A1, was found to be downregulated in GAS-induced mice (see Supplementary Table 4). **Dihydrotestosterone** also decreases the release of **LH** [46] and upregulates the expression of **LEP** [47] (see below).

The neurotransmitter **DA** is converted from its precursor, **L-dopa**, by the DDC enzyme [28,48]. As already indicated above, the core hypothesis relating streptococcal infections to the onset of PANDAS is that **IgG** antibodies produced in response to GAS cross the blood brain barrier and are aimed at specific neuronal proteins (in the basal ganglia). In this respect, it was shown that **IgG** from GAS-exposed rats reacts with D1 and D2 **DA** receptors (D1R and D2R) in vitro. In vivo, **IgG** deposits in the striatum of infused rats co-localize with these dopamine receptors [49]. Further, **IgG** from human PANDAS patients was found to react with D2R and have a negative effect on signaling downstream of D2R [50]. Individuals with tics and/or OCD also have elevated serum **IgG** against human D1R [51]. In addition, it was demonstrated that **IgG** is sufficient to induce PANDAS symptoms in humans and the depletion of **IgG** from PANDAS patient sera alleviates these symptoms [52]. Therefore, it is interesting that **IgG**-dependent regulation is predicted to be inhibited in CORT-exposed GAS mice, which also fits with the reported negative effect of corticosteroids on **IgG** activity [53,54].

In CORT-exposed GAS mice, the downstream regulatory effects of **DA** are predicted to be activated while those of **L-dopa** are inhibited. This has to be considered against the findings from the literature on **DA/L-dopa** and tic disorders as well as OCD, i.e., both increased and decreased **DA** signaling have been suggested as etiological factors in these disorders. For example, decreased striatal **DA** receptor availability has been demonstrated in both tic disorders and OCD, presumably reflecting higher endogenous **DA** levels in both

disorders [55]. However, another study indicates that **DA** receptor availability is not different between tic disorder patients and controls [56].

Likewise, both **DA** agonists and antagonists – correcting for decreased and increased **DA** levels/signaling, respectively – have been reported to alleviate tics [57]. Moreover, **L-dopa** reduces tics [58,59]. In light of all these findings, it is difficult to correctly interpret the upstream regulator analysis results for **DA** and **L-dopa** in the CORT-exposed GAS mice so we can only conclude that **DA** signaling is dysregulated in GAS-induced mice. That being said, both **estradiol** (see above) and corticosterone [60] increase striatal **DA** release, which is in line with the fact that **DA-**dependent regulation is predicted to be activated in CORT-exposed GAS mice.

LH is secreted by the pituitary gland upon stimulation by hypothalamic gonadotropin-release hormone (GnRH) and activates gonadal production of sex hormones (i.e., **estradiol**, testosterone, and progesterone), which then – as a part of the HPG axis – provide negative feedback to the hypothalamus [37]. As already indicated above, **estradiol** upregulates the expression of **LH** while **dihydrotestosterone** decreases its secretion. In addition, **DA** – which is predicted to have an increased downstream effect in CORT-exposed GAS mice – is a potent *inhibitor* of GnRH-induced **LH** secretion by the pituitary [40,61]. The latter finding seems to be in contradiction with the results of our experiments, i.e., that **LH**-dependent regulation is *activated* in CORT-exposed GAS mice. However, as mentioned before, it is not clear what the exact mechanisms are through which increased and/or decreased **DA** levels and activity alleviate the behavioral changes in CORT-exposed GAS mice.

Oleic acid-dependent regulation is inhibited in CORT-exposed GAS mice. In this respect, it is interesting that **oleic acid** is a fatty acid component of triglycerides [62] and increased triglyceride levels have been found in the serum of OCD patients [63,64]. In addition, **dihydrotestosterone** decreases the production of **oleic acid** [65].

Interleukin-2 (IL2) is a cytokine that is crucial for regulating the T-cell-mediated immune response [28] and that is downregulated by **beta-estradiol** [66]. Further, **IgG**-mediated GAS infection leads to increased **IL2** expression in T cells [67].

IL2 decreases the release of **LH** from the anterior pituitary [68], while high doses of **dopamine (DA)** (see below) reinforce the inhibitory effect of **IL2** on **LH** release [69]. Furthermore, **IL2**-dependent regulation is predicted to be inhibited in CORT-exposed GAS mice which is in line with the fact that an increased **IL2** expression was found postmortem in the basal ganglia of TS patients [70] and serum **IL2** concentrations were found to be positively associated with tic severity [71]. In addition, plasma levels of **IL2** were increased in drug-naive OCD patients [72]. Lastly, chronic **IL2** exposure leads to an overactivation of the HPA axis, which in turn causes a significant increase in CORT plasma levels [73].

Fibroblast growth factor 2 (FGF2) has multiple roles, including the positive regulation of neurite outgrowth and linked to this, motor function in rats [74]. **FGF2**-dependent regulation is predicted to be inhibited in GAS mice and interestingly, the effect of **FGF2** is activated when comparing CORT-GAS with CORT-PBS mice (see Supplementary Table 4). In addition, **estradiol** and **IL2** are involved in (up)regulating the expression of **FGF2** [75]. Further, CORT exposure leads to an upregulation of **FGF2** in various brain regions, which fits with the observed inhibited **FGF2**-dependent regulation in GAS mice and may represent a defense mechanism through which the brain limits the deleterious effect of stress over time [76-79].

Leptin (LEP), a hormone and growth factor with multiple functions including appetite regulation [28], is predicted to be inhibited in the CORT-treated GAS mice, which fits with the finding that CORT downregulates **LEP** expression [80]. Further, **dihydrotestosterone** and **beta-estradiol** are also involved in upregulating [47] and downregulating [81,82] **LEP** expression, respectively. Moreover, **LEP** inhibits the release of **DA**, which fits with the finding that in CORT-treated GAS mice, the effect of **LEP** is inhibited while **DA**-induced regulation is activated [83]. Interestingly, **LEP** also plays a pro-inflammatory role through increasing **IL2** production by T-lymphocytes [84], which implies that the anti-inflammatory effect of CORT on GAS mice could be mediated in part by an inhibition of **LEP**-dependent regulation.

IKKbeta (IKBKB) is a cytoplasmic kinase that is predicted to be inhibited in CORT-exposed GAS mice and activates NF-kappaB (NF-κB), a pro-inflammatory transcription factor that is critical for the regulation of innate immunity [85]. In this respect, it is interesting that an inducible deletion of *Ikbkb* reduces GAS infection in mice [86] and that selective inactivation of *Ikbkb* normalizes OCD-like behavior in mice [87]. Furthermore, both glucocorticoids and **estradiol** negatively regulate the activity of **IKBKB** [88]. In addition, **IKBKB** is involved in upregulating the expression of **IL2** [89] while **FGF2** and **LEP** both regulate the activity of **IKBKB** [90,91].

Lastly, the transmembrane protein **TREM-1** – which is highly expressed in neutrophils and macrophages – is a receptor for GAS and positively mediates the GAS-induced inflammatory response [92]. In this respect, it is interesting that **TREM-1** has been tested and confirmed as a drug target to block in the treatment of GAS-induced [93] and other immunity-related disorders [94,95]. Further, it was demonstrated that **CORT** treatment significantly decreased the plasma expression levels of TREM-1 in febrile patients with autoimmune disease [96]. This all fits very nicely with our findings, i.e., neonatal exposure to **CORT** led to an inhibition of **TREM-1**-dependent regulation in GAS mice.

Supplementary Tables

SUPPLEMENTARY TABLE 1. Synopsis of the results obtained in the elevated zero-maze (A) and elevated plus-maze (B)

	WATER-PBS	WATER-GAS	CORT-PBS	CORT-GAS	Neonatal treatment		PBS/GAS treatment		Neonatal treatment x PBS/GAS treatment	
					F(1,34)	p	F(1,34)	p	F(1,34)	p
(A)										
Closed sectors(d)	201,74±9,40	195,2±11,3	205,7±9,48	214,69±8,96	1,397	0,2454	0,016	0,901	0,615	0,438
Closed sectors (f)	22,75±3,494	21±2,970	17,4±2,267	18,167±1,918	2,472	0,1252	0,036	0,851	0,234	0,632
SAP (d)	10,305±2,004	9,47±2,180	15,607±2,197	15,47±2,659	5,391	0,0264	0,040	0,843	0,021	0,887
Head dipping (f)	55±3,713	56±4,162	43,1±3,662	47,167±4,756	5,683	0,0229	0,339	0,564	0,124	0,727
Rearing (f)	17,5±2,885	14,5±1,427	16,5±2,478	18,417±1,454	0,473	0,4963	0,065	0,799	1,344	0,254
Grooming (d)	13,47±3,673	14,243±4,694	26,139±9,429	20,518±4,459	0,127	0,7241	0,089	0,768	0,018	0,895
Sniffing (f)	5,25±1,916	4±0,897	3,4±0,897	4,667±0,995	0,236	0,6299	0,00005	0,995	1,070	0,308
(B)										
Open arms (d)	36,1±8,999	29,86±9,584	28,5±7,37	33,17±5,69	0,076	0,7851	0,010	0,922	0,492	0,488
Open arms (f)	6,12±1,11	4,875±1,381	4,8±1,42	4,25±0,687	0,711	0,4050	0,606	0,442	0,092	0,764
Closed arms (d)	193±20,998	217,7±19,35	231,56±14,3	223,3±16,28	1,531	0,2244	0,211	0,649	0,855	0,362
Closed arms (f)	11,5±0,845	11±1,389	10±1,183	8,75±0,922	2,857	0,1001	0,622	0,436	0,114	0,737
% Open arms (f)	33,1±4,1	28,8±4,7	25,4±5,4	28,8±4,6	0,599	0,4445	0,008	0,929	0,621	0,436
SAP (d)	16,715±4,560	18,6±7,179	4,986±1,317	5,632±2,074	10,024	0,0033	0,105	0,748	0,025	0,875
Head dipping (f)	8,75±1,971	8,875±2,349	10,7±1,535	9,917±1,612	0,649	0,4259	0,031	0,860	0,060	0,808
Rearing (f)	12,75±1,634	13,625±1,238	14,1±1,574	12,917±1,401	0,045	0,8332	0,010	0,919	0,464	0,501
Grooming (d)	57,823±11,081	59,906±14,806	51,649±8,734	57,088±13,505	0,127	0,7241	0,089	0,768	0,018	0,895
Sniffing (f)	8,125±1,54	8,125±2,191	4,9±0,849	4,75±0,789	6,227	0,0176	0,003	0,955	0,003	0,955

Behavioral phenotypes (mean±SEM; N=38) exhibited by adolescent (A) and adult (B) WATER-PBS (n=8), WATER-GAS (n=8), CORT-PBS (n=10) and CORT-GAS (n=12) mice. The three rightmost columns indicate the F and p values (together with degrees of freedom) of the main effects of neonatal treatment, PBS/GAS treatment, and their interaction.

SUPPLEMENTARY TABLE 2. Monoamine concentrations in selected brain areas.

	WATER-PBS	WATER-GAS	CORT-PBS	CORT-GAS	Neonatal treatment		PBS/GAS treatment		Neonatal treatment x PBS/GAS treatment	
					F(1,21)	p	F(1,21)	p	F(1,21)	p
(A)										
DA	30.200±12.142	24.333±5.064	58.143±21.835	25.286±3.441	1.109	0.163	1.991	0.1729	0.967	0.3365
DOPAC	69.200±30.170	42.333±3.703	57.714±18.855	45.714±10.936	0.055	0.8171	1.261	0.2742	0.184	0.6719
DOPAC/DA	2.940±0.780	2.793±1.103	1.516±0.289	1.832±0.301	3.268	0.0850	0.016	0.8995	0.124	0.7286
5-HT	455±69.804	396±84.367	585±95.201	503±55.012	2.208	0.1521	1.991	0.1729	0.021	0.8867
5-HIAA	261.400±41.086	209.167±19.919	279.857±55.183	232.143±38.420	0.235	0.6331	1.365	0.2557	0.003	0.9584
5-HIAA/5-HT	0.593±0.070	0.615±0.087	0.503±0.060	0.485±0.071	2.263	0.1474	0.001	0.9748	0.074	0.7889
(B)										
DA	13391.5±2077.654	11180.6±1167.124	11192.667±537.17	9150.667±1082.517	4.017	0.0612	4.058	0.0601	0.089	0.7694
DOPAC	2471.75±370.522	1784.167±142.165	1784.167±201.933	1566±160.949	12.073	0.0029	4.456	0.0499	1.155	0.2976
DOPAC/DA	0.200±0.020	0.190±0.021	0.160±0.012	0.177±0.021	1.856	0.1909	0.026	0.8744	0.534	0.4748
5-HT	473.250±62.073	355.800±56.840	328.500±18.938	277±30.670	7.239	0.0155	4.134	0.0579	0.630	0.4383
5-HIAA	338.500±33.977	259.200±28.645	245.333±15.322	210.333±17.718	9.370	0.0071	6.068	0.0247	0.912	0.3531
5-HIAA/5-HT	0.729±0.039	0.753±0.053	0.748±0.028	0.784±0.069	0.231	0.6366	0.323	0.5775	0.014	0.9088
(C)										
DA	43.600±25.789	234.667±202.316	36.857±9.674	28.714±7.846	1.167	0.2923	0.863	0.3634	1.024	0.3231
DOPAC	65±30.158	147±89.506	53.143±12.219	40.714±8.983	1.675	0.2096	0.581	0.4544	1.070	0.3127
DOPAC/DA	1.809±0.166	1.823±0.322	1.614±0.182	1.703±0.233	0.435	0.5165	0.046	0.8319	0.025	0.8763
5-HT	429.8±42.878	422.5±75.996	469.857±65.376	464.429±38.860	0.478	0.4971	0.012	0.9156	0.0003	0.9876
5-HIAA	568.2±57.504	511.500±86.119	592.571±88.826	600.714±45.327	0.588	0.4517	0.107	0.7463	0.192	0.6660
5-HIAA/5-HT	1.327±0.061	1.281±0.174	1.264±0.080	1.329±0.095	0.012	0.9136	0.002	0.9681	0.199	0.6598

SUPPLEMENTARY TABLE 2. Continued

	WATER-PBS	WATER-GAS	CORT-PBS	CORT-GAS	Neonatal treatment		PBS/GAS treatment		Neonatal treatment x PBS/GAS treatment	
					$F_{(1,21)}$	p	$F_{(1,21)}$	p	$F_{(1,21)}$	p
(D)										
DA	128.250±36.346	260.167±29.703	297.286±43.340	221.286±24.610	3.289	0.0848	0.607	0.4450	8.394	0.0089[€]
DOPAC	114.750±29.304	160±13.140	181.857±28.117	157.857±26.934	1.518	0.2322	0.162	0.6912	1.725	0.2040
DOPAC/DA	1.032±0.169	0.633±0.041	0.616±0.035	0.692±0.078	5.184	0.0339	4.225	0.0531	9.180	0.0066[°]
5-HT	593.250±175.001	664.667±72.203	795.429±47.884	810.429±63.982	4.352	0.500	0.268	0.6101	0.114	0.7387
5-HIAA	480.500±132.751	432.500±19.419	501.714±26.225	501.286±62.472	0.555	0.4650	0.161	0.6928	0.155	0.6979
5-HIAA/5-HT	0.848±0.050	0.684±0.065	0.638±0.033	0.618±0.068	6.399	0.0199	2.823	0.1085	1.718	0.2048

Concentrations of: dopamine (DA), its metabolite 3,4-dihydroxyphenylacetic acid (DOPAC) and turnover (DOPAC/DA); and serotonin (5-HT), its metabolite 5-hydroxyindole acetic acid (5-HIAA) and turnover (5-HIAA/5-HT). Data, expressed as mean±SEM (N=25), refer to prefrontal cortex (A), striatum (B), hippocampus (C) and hypothalamus (D) of adult WATER-PBS (n=5), WATER-GAS (n=6), CORT-PBS (n=7) and CORT-GAS (n=7) mice (ng/g tissue weight). The three rightmost columns indicate the F and p values (together with degrees of freedom) of the main effects of Neonatal treatment, PBS/GAS treatment, and their interaction. [€] Post-hoc comparisons conducted based on this significant interaction show that CORT-GAS mice have increased concentrations of DA compared to WATER-PBS subjects. [°] Post-hoc comparisons conducted based on this significant interaction show that CORT-GAS mice have reduced concentrations of dopamine turnover (DOPAC/DA) compared to WATER-PBS subjects.

SUPPLEMENTARY TABLE 3. Cytokines concentrations measured through Bio-Plex assay

	WATER-PBS	WATER-GAS	CORT-PBS	CORT-GAS	Neonatal treatment		PBS/GAS treatment		Neonatal treatment x PBS/GAS treatment	
					F(1,33)	p	F(1,33)	p	F(1,33)	p
IL-1α	22.924±7.551	18.720±5.547	25.987±6.183	28.592±6.169	0.993	0.3264	0.015	0.9027	0.275	0.6033
IL-1β	140.088±74.173	47.265±26.270	160.029±49.587	168.805±44.508	1.838	0.1846	0.649	0.4265	0.948	0.3375
IL-2	4.443±2.683	5.271±3.511	2.893±0.881	5.164±1.946	0.124	0.7272	0.434	0.5156	0.094	0.7614
IL-4	26.643±12.070	10.273±3.707	31.714±8.736	30.882±7.560	2.132	0.1540	0.956	0.3354	0.780	0.3836
IL-5	60.094±23.792	48.368±16.569	73.099±16.834	73.107±14.827	1.112	0.2992	0.107	0.7454	0.108	0.7451
IL-6	16.833±9.181	10.161±6.265	23.711±7.686	21.881±7.003	1.433	0.2382	0.302	0.5866	0.098	0.7564
IL-9	29.964±18.625	20.247±18.572	151.221±51.374	40.778±17.479	4.717	0.0372	3.387	0.0747	2.380	0.1324
IL-10	26.951±13.666	21.156±9.635	22.490±6.961	40.547±11.507	0.437	0.5137	0.295	0.5912	1.114	0.2993
IL-12 (p40)	183.868±16.774	269.915±39.717	256.023±25.159	235.985±18.784	0.686	0.4140	1.168	0.2884	3.294	0.0796
IL-12 (p70)	171.641±92.267	99.930±43.821	133.633±44.496	201.708±74.426	0.213	0.6479	0.001	0.9792	1.022	0.3201
IL-13	300.687±152.826	125.080±50.982	389.125±118.941	405.037±99.229	2.528	0.1217	0.475	0.4957	0.683	0.4146
IL-17	97.993±32.558	78.069±20.155	176.910±43.508	153.938±38.384	5.094	0.0307	0.391	0.5359	0.002	0.9648
IFN-γ	30.026±15.311	17.267±8.608	41.824±13.003	46.605±12.798	2.318	0.1374	0.116	0.7356	0.394	0.5347
KC	35.112±12.111	28.484±6.347	47.963±7.517	49.807±10.556	3.028	0.0912	0.059	0.8091	0.186	0.6690
MCP-1	278.820±128.265	182.994±58.424	496.364±132.571	547.354±130.244	4.778	0.0365	0.028	0.8674	0.304	0.5853
MIP-1β	33.355±16.086	20.819±6.079	69.099±18.159	67.513±17.701	5.320	0.0279	0.156	0.6954	0.094	0.7614
RANTES	8.711±2.270	6.565±1.190	9.134±1.633	12.700±2.260	2.268	0.1141	0.124	0.7270	2.010	0.1666
TNF-α	213.822±128.008	123.126±56.475	377.411±126.426	585.178±176.747	3.949	0.0561	0.138	0.7126	0.899	0.3507

Plasma concentrations (mean±SEM; N=37), in serum of adult WATER-PBS (n=7), WATER-GAS (n=8), CORT-PBS (n=10) and CORT-GAS (n=12) mice (pg/ml) of the following cytokines: interleukin 1α (IL-1α), interleukin 1β (IL-1β), interleukin 2 (IL-2), interleukin 4 (IL-4), interleukin 6 (IL-6), interleukin 9 (IL-9), interleukin 10 (IL-10), interleukin 12 (p40) (IL-12 (p40)), interleukin 12 p70 (IL-12 (p70)), interleukin 13 (IL-13), interleukin17 (IL-17), interferon γ (IFN-γ), keratinocyte chemoattractant (KC), monocyte chemoattractant protein-1 (MCP-1), macrophage inflammatory protein 1β (MIP-1β), Regulated on Activation, Normal T Cell Expressed and Secreted (RANTES), Tumor necrosis factor α (TNF-α). The three rightmost columns indicate the F and p values (together with degrees of freedom) of the main effects of Neonatal treatment, PBS/GAS treatment, and their interaction.

SUPPLEMENTARY TABLE 4. Upstream regulator analysis – using Ingenuity – of the mRNAs that were differentially expressed in GAS-treated mice compared to controls (water-GAS vs water-PBS) (1), GAS-treated mice neonatally exposed to CORT compared to GAS-treated mice (CORT-GAS vs water-GAS) (2), CORT-exposed mice compared to control (CORT-PBS vs water-PBS) and GAS-treated mice neonatally exposed to CORT compared to CORT-exposed mice (CORT-GAS vs CORT-PBS). All upstream regulators are listed with a z-score ≥ 1.50 or ≤ - 1.50 (see Methods), indicating that they are activated or inhibited, respectively. For each regulator, the downstream target genes are listed.

Upstream Regulator	water-GAS vs water-PBS (1)	CORT-GAS vs water-GAS (2)	CORT-PBS vs water-PBS (3)	CORT-GAS vs CORT-PBS (4)	Target genes
Chemicals - endogenous mammalian					
beta-estradiol	-1.97	2.47	-	2.58	(1): Btg2, Cbl, Cshl1, Enpp2, Fos, Inpp5j, Sdc3, Sema3b, Srd5a1, Tnnt3; (2): Adm, Bcat1, Bmp2, Calb1, Ccng1, Cdkn2b, Chgb, Ctps1, Dlg2, Fgf9, Fmo1, Fnbp1, Fzd2, Gab2, Gsk3b, Hsd17b12, Ier2, Insl3, Lhcgr, Lmcd1, Mapt, Mpz, Myh3, Nedd4l, Nkx2-1, Notch3, Pak5, Pdap1, Pitpna, Ptgds, Pttg1, Pxdn, Pycr1, Pygl, Qsox1, Rapgef6, Slc38a2, Smad3, Snap25, Sstr4, Tgfb3, Thrsp, Timp3, Tpo, Trib1, Vav3, Zyx; (4): Ace, Acta2, Adora1, Alcam, Aldh1a2, Blnk, Bmp2, C8orf44-SGK3/SGK3, Calb1, Casp9, Cav1, Ccl2, Ccne1, Cdc25a, Cdkn2b, Chgb, Chrm3, Clstn2, Clybl, Col1a2, Ctps1, Cyth3, Dcn, DyrK2, Etv4, Fhl2, Fmo1, Gadd45a, Grik4, Grin2a, Gucy1b3, Hdac4, Hes1, Hunk, Id4, Ifngr2, Il18, Itgb3, Jag1, Klf10, Klh26, Ldha, Ltbp1, Mapt, Mpz, Myh3, Nell2, Net1, Nptx1, Nrp1, Nucb2, Pak5, Pdgfb, Pdk2, Pik3r2, Pitpna, Plau, Pmm2, Ppp5c, Prss23, Prss35, Ptger2, Rab6a, Rara, Rdh10, Runx2, Sdc2, Serpina3, Sertad4, Snai1, Snap25, Spock1, Sstr4, Stc1, Thrsp, Timp3, Tpd52l1, Trib1, Tspan5, Ttr, Vav3, Ypel3, Ywhah, Zbtb18, Zeb2, Zyx
butyric acid	-	2.16	-	-	Calb1, Ccng1, Col5a2, Gli3, Ly6e, Myh3, Nfatc4, Oas2, Ptgds, Pygl, Serpine1, Timp3, Uqcrq
dihydrotestosterone	-1.95	-	-	-	Btg2, Elovl7, Fos, Sdc3, Slc7a7, Srd5a1
dopamine	-	1.63	-	2.00	(2): Adra2c, Bcl2l2, Gprc5b, Ncf1, Ppp2r2a, Scn1b, Scn9a; (4): Asic2, Bcl2l2, Gpr68, Ppp1r2, Scn1b
L-dopa	-	-4.59	-	-4.62	(2): Adra2c, Ajap1, C1qtnf12, C2cd2l, Cbr3, Cdc42ep2, Csmd3, Cyld, Dgki, Dlg2, Grid2, Kcne5, Klf16, Mpp6, Nedd4l, Per2, Plekha2, Ppp2r2a, Ptprd, Rell1, Reln, Slc38a2, Sorcs2, Wdr17, Zfhx3; (4): Acta2, AI987944 (Includes Others), C14orf37, Clic6, Crtac1, Cyld, Dlgap1, Erlin1, Htr1b, Lrrc1, Ltbp1, Mterf2, Myl4, Nos1ap, Plekha2, Plppr1, Ppm1l, Ppp1r2, Prickle1, Rapgefl1, Rassf5, Rell1, Spock3, Tcf4, Tmem238, Trib3, Vat1l, Wdr1, Zeb2

SUPPLEMENTARY TABLE 4. Continued

Upstream Regulator	water-GAS vs water-PBS (1)	CORT-GAS vs water-GAS (2)	CORT-PBS vs water-PBS (3)	CORT-GAS vs CORT-PBS (4)	Target genes
oleic acid	-	-	-	-	Ncf1, Npc1l1, Serpine1, Thrsp
progesterone	-	-	-	-1.96	Ace, Acta2, Aldh1a2, Bmp2, Cav1, Ccl2, Ccne1, Cdc25a, Cdkn2b, Dnajb4, Dpp4, Hunk, Klf10, Ldha, Mpz, Net1, Npl, Nrp1, P2rx4, Pnkd, Prss23, Prss35, Ptger1, Ptger2, Rbp1, Sfi1, Spsb1, Thrsp, Timp3, Tnfrsf21, Ttr
tretinoin	-	-	-	2.53	Adam11, Aldh1a2, Ap1s2, Bmp2, Calb1, Casp9, Ccl2, Ccne1, Cd34, Cd59a, Cdkn2b, Chgb, Col1a2, Csrnp1, Cyp2s1, Dcn, Dkk3, Dpp4, E2f5, Fgf5, Gtpbp10, Hes1, Hey2, Hgs, Hk1, Hmga1, Ifit1, Ighm, Itgb3, Kctd11, Klf13, Limk1, Ly6e, Mapk8ip3, Mgst3, Nid2, Nrp1, Nth1, P4ha2, Pdgfb, Plau, Plk3, Prtn3, Psmb10, Rara, Rbp1, Runx2, Serpinb8, Slco2a1, Stc1, Wnt2b, Zbtb16, Zeb2
Complexes					
IgG	-	-2.24	-	-	Adm, Cdkn2b, Csnk2b, Ier2, Serpine1
LH	-	2.00	-	-	Actn1, Btc, Gprc5b, Insl3, Lhcgr, Snap25, Thbs2, Trib1
PDGF	-	-	-	1.80	Acta2, Anxa11, Ccl2, Ccne1, Dcn, Fbln5, Fhl2, Fmo1, Gadd45a, Gucy1b3, Hdac4, Hes1, Klf10, Klhl21, Myh11, Plau, Prss35, Rbp1, Serpina3, Snai1, Trib1, Trib3
Cytokines					
IL1A	-	-	-	1.50	Asic2, Ccl2, Ccr6, Dpp4, Ifngr2, Il18, Itgb3, Ldha, Lox, Pdgfb, Plau, Serpina3
IL2	-	-1.76	-	-	Bmp2, Card9, Ccng1, Ccr6, Cmklr1, Csf2rb, Csrnp1, Ctps1, Dapk2, Gcnt1, Ly6e, Pus1, Tnfrsf4
SPP1	-	-	-	1.66	Ccl2, Ccne1, Cd163, Cdc25a, Itgb3, Jag1, Lox, Plau, Runx2, Snai1
TNF	-	-	-	2.26	Acan, Ace, Acta2, Adora1, Alcam, Anxa11, Arhgdib, Bcl2l2, Bmp2, Cav1, Ccl2, Ccne1, Ccr6, Cd163, Col1a2, Cyld, Cyth3, Dcn, Dpp4, Edar, Ext1, Fgf5, Fmo1, Gadd45a, Gast, Hes1, Hid1, Ifit1, Ifngr2, Il18, Itgb3, Jag1, Klf10, Ldha, Lox, Map2k4, Net1, Nrp1, Nucb2, Pdgfb, Plau, Plk3, Ppp2r1b, Ppp5c, Prss23, Prtn3, Psmb10, Rab6a, Rapgefl1, Rara, Rbp1, Runx2, Sdc2, Serpina3, Serpinb8, Sirt3, Snai1, Spock1, Spsb1, St8sia4, Tcfl5, Thrsp, Timp3, Tnfrsf21, Vash1, Vav3, Wisp1, Zyx

SUPPLEMENTARY TABLE 4. Continued

Upstream Regulator	water-GAS vs water-PBS (1)	CORT-GAS vs water-GAS (2)	CORT-PBS vs water-PBS (3)	CORT-GAS vs CORT-PBS (4)	Target genes
WNT1	-	-	-	1.76	Acta2, Etv4, Hes1, Ly6e, Runx2, Wisp1
Enzymes					
CASZ1	-	-1.96	-	-	Acan, Myh3, Nefl, Tgfb3
EGLN1	-	-1.98	-	-	Acan, Adm, Cdkn2b, Tgfb3
TGM2	-	1.91	-	2.28	(2): Acan, Csrnp1, Dapk2, Ifit2, Ly6e, Mpp6, Oas2; (4): Acan, Ccl2, Csrnp1, E2f5, Gtpbp10, Ifit1, Itgb3, Ly6e, Rara, Runx2
G-Protein Coupled Receptors					
ADORA2A	-	-	-	2.24	Dgkz, Ifitm3, Klc1, Rab6a, Tubb4a
Growth factors					
BDNF	-	-	-	2.29	Bcl2l2, Bmp2, Crmp1, Grin2a, Klc1, Klf10, Limk1, Mapk8ip3, Mapt, Myh3, Myl4, Nell2, Snap25, Sorl1
BMP7	-	-	-	1.94	Acta2, Adora1, Aldh1a2, Ccl2, Cd34, Col1a2, Runx2
DKK1	-	-	-	-1.98	Acta2, Dvl3, Runx2, Tcf4
EGF	-	-	-	2.56	Alcam, Cav1, Ccne1, Chgb, Col1a2, Dcn, Dpp4, Gadd45a, Gast, Hes1, Itgb3, Kctd11, Klf10, Ldha, Nrp1, Plau, Runx2, Serpina3, Snai1, Snap25, Timp3
FGF2	-1.93	-	-	1.90	(1): Btg2, Enpp2, Fos, Prkce, Ptma (Includes Others); (4): Ace, Acta2, Calb1, Cav1, Ccl2, Cdc25a, Chrm3, Cnmd, Col1a2, Dcn, Gadd45a, Grik4, Grin2a, Lox, Mapt, Mpz, Pdgfb, Plau, Runx2, Snai1, Timp3
INHBA	-	-2.34	-	-	Actn1, Bmp2, Calb1, Cdkn2b, Edar, Lhcgr, Nkx2-1, Pcdh9, Serpine1, Vav3
LEP	-	-2.16	-	-	Cps1, Dffa, Gsk3b, Insl3, Ncf1, Per2, Pln, Rfx1, Serpine1, Snap25, Thrsp, Timp3
NGF	-	-	-	2.11	Asic2, Cav1, Chgb, Etv4, Gadd45a, Grin2a, Gucy1b3, Kctd11, Mapk8ip3, Snap25
NRG1	-	-	-	2.08	Cav1, Ccne1, Col6a3, Hes1, Hmga1, Itgb3, Plau, Snai1

SUPPLEMENTARY TABLE 4. Continued

Upstream Regulator	water-GAS vs water-PBS (1)	CORT-GAS vs water-GAS (2)	CORT-PBS vs water-PBS (3)	CORT-GAS vs CORT-PBS (4)	Target genes
TGFB1	-	-	-	1.88	Acan, Ace, Acta2, Adam19, Adamts3, Adora1, Anxa11, Bmp2, C1r, Casp9, Cav1, Ccl2, Ccne1, Ccr6, Cd163, Cd34, Cdc25a, Cdkn2b, Col1a2, Col6a3, Crmp1, Ctps1, Dach1, Dcn, Dkk3, Dnajb4, Dyrk2, Ext1, Fbln5, Fgf5, Gabra4, Gadd45a, Gpr146, Grin2a, Hes1, Hmga1, Id4, Ighm, Il18, Itgb3, Jag1, Klf10, Ldha, Lox, Ltbp1, Mapk8ip3, Masp1, Mpz, Myh11, Net1, Nfib, Nrp1, Nucb2, Pdgfb, Pdk2, Pigf, Plau, Pmm1, Prkcg, Ptger2, Rab6a, Rara, Rasl11b, Rbms1, Runx2, Serpina3, Snai1, Spock1, Tcf4, Timp3, Vat1l, Wisp1, Xylt1, Zeb2, Zfpm2, Zyx
VEGFA	-	-	-	1.68	Ace, Cav1, Ccl2, Ccne1, Cd34, Etv4, Hes1, Hk1, Itgb3, Me2, Nrp1, Pdgfb, Plau, Runx2, Stc1, Uqcrb, Vash1
Kinases					
ERBB2	-	-	-	2.00	Abracl, Acta2, Adam19, Ccne1, Cd34, Cdc25a, Cdkn2b, Col6a3, E2f5, Etv4, Hes1, Itgb3, Jag1, Mapk8ip3, Net1, Nfib, Nrp1, Nucb2, P4ha2, Plau, Poldip2, Serpina3, Snai1, Spock1, Timp3, Tpd52l1, Tubb4a
IKBKB	-	-1.98	-		Bmp2, Cdh13, Timp3, Tnfrsf4
MAPK1	-	-	-	-1.60	Cav1, Ccl2, Cetn4, Dxo, Fam20a, Fhl2, Ifit1, Ifitm3, Itgb3, Nrp1, Pdgfb, Plau, Ptger2, Snai1, Spock1, Spsb1, Ube2i
MKNK1	-	-	-	2.65	Crmp1, Klc1, Klf13, Mapk8ip3, Mapt, Nell2, Snap25
PRKAA2	-	-	-	-1.54	Acta2, Arhgdib, Chgb, Ldha, Nfib, Pak5, Snai1, Sorl1, Zyx
Ligand-Dependent Nuclear Receptors					
PGR	-	-	-	2.20	Dnajb4, Hes1, Net1, P2rx4, P4ha2, Plau, Serpinb8, Sfi1, Snap25, Stc1, Tnfrsf21
Transcriptional Regulators					
ASCL1	-	-	-	2.00	Ephb3, Hey2, Nfasc, Snap25
BRCA1	-	-	-	2.35	Atp11c, Ccne1, Dgka, Ensa, Fhl2, Gadd45a, Ifit1, Stc1, Ube2i

SUPPLEMENTARY TABLE 4. Continued

Upstream Regulator	water-GAS vs water-PBS (1)	CORT-GAS vs water-GAS (2)	CORT-PBS vs water-PBS (3)	CORT-GAS vs CORT-PBS (4)	Target genes
CTNNB1	-	-	-	1.58	Acan, Acta2, Alcam, Aldh1a2, Bmp2, C14orf37, Ccne1, Cd34, Cdkn2b, Cnmd, Dnajc6, Ephb3, Etv4, Fgf5, Gast, Hes1, Id4, Ifit1, Ighm, Ly6e, Mpz, Myh3, Myl4, Nptx1, Pcdh9, Plau, Prss35, Rassf5, Rcn1, Runx2, Sdc2, Sema5a, Serpina3, Snai1, Tcf4, Timp3, Wisp1, Ypel3, Zeb2
EHF	-	-	-	2.00	Blnk, Gpr68, Jag1, Serpina3, Tcf4
FOS	-	-	-	2.80	Ccl2, Ccne1, Large1, Lox, Ltbp1, Net1, Nptx1, Plau, Rara, Rbp1, Snai1, Sulf2, Sult2b1, Vav3, Xylt1
GATA4	-	-	-	2.21	Adora1, Cdkn2b, Clstn2, Col1a2, Myl4
HIC1	-	-	-	-2.00	Acta2, Fhl2, Id4, Snap25
JUN	-	-	-	1.85	Cav1, Ccl2, Col1a2, Fbln5, Hes1, Hmga1, Ltbp1, Mpz, Nrap, Plau, Rara, Runx2, Sulf2, Vav3, Xylt1
JUNB	-	-	-	1.73	Cav1, Col1a2, Fbln5, Hes1, Itgb3, Plau, Runx2, Snai1
KDM5B	-	-	-	2.00	Cav1, Ccne1, Cdc14a, Gadd45a, Kif2c, Mapk8ip3
KLF2	-	-	-	-1.77	Ace, Cav1, Ccl2, Fgf5, Gadd45a, Itgb3, Runx2, Slco2a1, Tcf4
KMT2A	-	2.00	-	-	Gcnt4, Pigz, Trib1, Zmat4
MEF2C	-	-	-	1.97	Clstn2, Col1a2, Myl4, Runx2

2

REFERENCES

1. Macrì, S.; Pasquali, P.; Bonsignore, L.T.; Pieretti, S.; Cirulli, F.; Chiarotti, F.; Laviola, G. Moderate neonatal stress decreases within-group variation in behavioral, immune and HPA responses in adult mice. *PLoS One* **2007**, *2*, e1015, doi:10.1371/journal.pone.0001015.

2. Zoratto, F.; Berry, A.; Anzidei, F.; Fiore, M.; Alleva, E.; Laviola, G.; Macrì, S. Effects of maternal L-tryptophan depletion and corticosterone administration on neurobehavioral adjustments in mouse dams and their adolescent and adult daughters. *Prog Neuropsychopharmacol Biol Psychiatry* **2011**, *35*, 1479-1492, doi:10.1016/j.pnpbp.2011.02.016.

3. Zoratto, F.; Fiore, M.; Ali, S.F.; Laviola, G.; Macrì, S. Neonatal tryptophan depletion and corticosterone supplementation modify emotional responses in adult male mice. *Psychoneuroendocrinology* **2013**, *38*, 24-39, doi:10.1016/j.psyneuen.2012.04.015.

4. Hoffman, K.L.; Hornig, M.; Yaddanapudi, K.; Jabado, O.; Lipkin, W.I. A murine model for neuropsychiatric disorders associated with group A beta-hemolytic streptococcal infection. *J Neurosci* **2004**, *24*, 1780-1791, doi:10.1523/jneurosci.0887-03.2004.

5. Macrì, S.; Ceci, C.; Proietti Onori, M.; Invernizzi, R.W.; Bartolini, E.; Altabella, L.; Canese, R.; Imperi, M.; Orefici, G.; Creti, R.; et al. Mice repeatedly exposed to Group-A beta-Haemolytic Streptococcus show perseverative behaviors, impaired sensorimotor gating, and immune activation in rostral diencephalon. *Sci Rep* **2015**, *5*, 13257, doi:10.1038/srep13257.

6. Flies, D.B.; Chen, L. A simple and rapid vortex method for preparing antigen/adjuvant emulsions for immunization. *J Immunol Methods* **2003**, *276*, 239-242.

7. Gao, W.; Stalder, T.; Foley, P.; Rauh, M.; Deng, H.; Kirschbaum, C. Quantitative analysis of steroid hormones in human hair using a column-switching LC-APCI-MS/MS assay. *J Chromatogr B Analyt Technol Biomed Life Sci* **2013**, *928*, 1-8, doi:10.1016/j.jchromb.2013.03.008.

8. Olivier, B.; Leahy, C.; Mullen, T.; Paylor, R.; Groppi, V.E.; Sarnyai, Z.; Brunner, D. The DBA/2J strain and prepulse inhibition of startle: a model system to test antipsychotics? *Psychopharmacology (Berl)* **2001**, *156*, 284-290.

9. Dell'Omo, G.; Vannoni, E.; Vyssotski, A.L.; Di Bari, M.A.; Nonno, R.; Agrimi, U.; Lipp, H.P. Early behavioural changes in mice infected with BSE and scrapie: automated home cage monitoring reveals prion strain differences. *Eur J Neurosci* **2002**, *16*, 735-742.

10. Proietti Onori, M.; Ceci, C.; Laviola, G.; Macrì, S. A behavioural test battery to investigate tic-like symptoms, stereotypies, attentional capabilities, and spontaneous locomotion in different mouse strains. *Behav Brain Res* **2014**, *267*, 95-105, doi:10.1016/j.bbr.2014.03.023.

11. Deacon, R.M.; Rawlins, J.N. T-maze alternation in the rodent. *Nat Protoc* **2006**, *1*, 7-12, doi:10.1038/nprot.2006.2.

12. Egashira, N.; Shirakawa, A.; Okuno, R.; Mishima, K.; Iwasaki, K.; Oishi, R.; Fujiwara, M. Role of endocannabinoid and glutamatergic systems in DOI-induced head-twitch response in mice. *Pharmacol Biochem Behav* **2011**, *99*, 52-58, doi:10.1016/j.pbb.2011.04.003.

13. Canal, C.E.; Morgan, D. Head-twitch response in rodents induced by the hallucinogen 2,5-dimethoxy-4-iodoamphetamine: a comprehensive history, a re-evaluation of mechanisms, and its utility as a model. *Drug Test Anal* **2012**, *4*, 556-576, doi:10.1002/dta.1333.

14. Andrews S. 2015. FastQC: A Quality Control Tool for High Throughput Sequence Data. Available from: http://www.bioinformatics.babraham.ac.uk/projects/fastqc.

15. Ewels, P.; Magnusson, M.; Lundin, S.; Kaller, M. MultiQC: summarize analysis results for multiple tools and samples in a single report. *Bioinformatics* **2016**, *32*, 3047-3048, doi:10.1093/bioinformatics/btw354.

16. Wu, T.D.; Nacu, S. Fast and SNP-tolerant detection of complex variants and splicing in short reads. *Bioinformatics* **2010**, *26*, 873-881, doi:10.1093/bioinformatics/btq057.

17. Wang, L.; Wang, S.; Li, W. RSeQC: quality control of RNA-seq experiments. *Bioinformatics* **2012**, *28*, 2184-2185, doi:10.1093/bioinformatics/bts356.

18. DeLuca, D.S.; Levin, J.Z.; Sivachenko, A.; Fennell, T.; Nazaire, M.D.; Williams, C.; Reich, M.; Winckler, W.; Getz, G. RNA-SeQC: RNA-seq metrics for quality control and process optimization. *Bioinformatics* **2012**, *28*, 1530-1532, doi:10.1093/bioinformatics/bts196.

19. Soneson, C.; Delorenzi, M. A comparison of methods for differential expression analysis of RNA-seq data. *BMC Bioinformatics* **2013**, *14*, 91, doi:10.1186/1471-2105-14-91.

20. Anders, S.; McCarthy, D.J.; Chen, Y.; Okoniewski, M.; Smyth, G.K.; Huber, W.; Robinson, M.D. Count-based differential expression analysis of RNA sequencing data using R and Bioconductor. *Nat Protoc* **2013**, *8*, 1765-1786, doi:10.1038/nprot.2013.099.

21. Huber, W.; Carey, V.J.; Gentleman, R.; Anders, S.; Carlson, M.; Carvalho, B.S.; Bravo, H.C.; Davis, S.; Gatto, L.; Girke, T.; et al. Orchestrating high-throughput genomic analysis with Bioconductor. *Nat Methods* **2015**, *12*, 115-121, doi:10.1038/nmeth.3252.

22. Ritchie, M.E.; Phipson, B.; Wu, D.; Hu, Y.; Law, C.W.; Shi, W.; Smyth, G.K. limma powers differential expression analyses for RNA-sequencing and microarray studies. *Nucleic Acids Res* **2015**, *43*, e47, doi:10.1093/nar/gkv007.

23. Robinson, M.D.; McCarthy, D.J.; Smyth, G.K. edgeR: a Bioconductor package for differential expression analysis of digital gene expression data. *Bioinformatics* **2010**, *26*, 139-140, doi:10.1093/bioinformatics/btp616.

24. McCarthy, D.J.; Chen, Y.; Smyth, G.K. Differential expression analysis of multifactor RNA-Seq experiments with respect to biological variation. *Nucleic Acids Res* **2012**, *40*, 4288-4297, doi:10.1093/nar/gks042.

25. Love, M.I.; Huber, W.; Anders, S. Moderated estimation of fold change and dispersion for RNA-seq data with DESeq2. *Genome Biol* **2014**, *15*, 550, doi:10.1186/s13059-014-0550-8.

26. Zhang, Z.H.; Jhaveri, D.J.; Marshall, V.M.; Bauer, D.C.; Edson, J.; Narayanan, R.K.; Robinson, G.J.; Lundberg, A.E.; Bartlett, P.F.; Wray, N.R.; et al. A comparative study of techniques for differential expression analysis on RNA-Seq data. *PLoS One* **2014**, *9*, e103207, doi:10.1371/journal.pone.0103207.

27. Oliveros, J.C. Venny. An interactive tool for comparing lists with Venn's diagrams. http://bioinfogp.cnb.csic.es/tools/venny/index.html. **2007-2015**.

28. The UniProt, C. UniProt: the universal protein knowledgebase. *Nucleic Acids Res* **2017**, *45*, D158-D169, doi:10.1093/nar/gkw1099.

29. Van den Buuse, M.; Eikelis, N. Estrogen increases prepulse inhibition of acoustic startle in rats. *Eur J Pharmacol* **2001**, *425*, 33-41.

30. van den Buuse, M.; Simpson, E.R.; Jones, M.E. Prepulse inhibition of acoustic startle in aromatase knock-out mice: effects of age and gender. *Genes Brain Behav* **2003**, *2*, 93-102.

31. Hill, R.A.; McInnes, K.J.; Gong, E.C.; Jones, M.E.; Simpson, E.R.; Boon, W.C. Estrogen deficient male mice develop compulsive behavior. *Biol Psychiatry* **2007**, *61*, 359-366, doi:10.1016/j.biopsych.2006.01.012.

32. Flaisher-Grinberg, S.; Albelda, N.; Gitter, L.; Weltman, K.; Arad, M.; Joel, D. Ovarian hormones modulate 'compulsive' lever-pressing in female rats. *Horm Behav* **2009**, *55*, 356-365, doi:10.1016/j.yhbeh.2008.10.002.
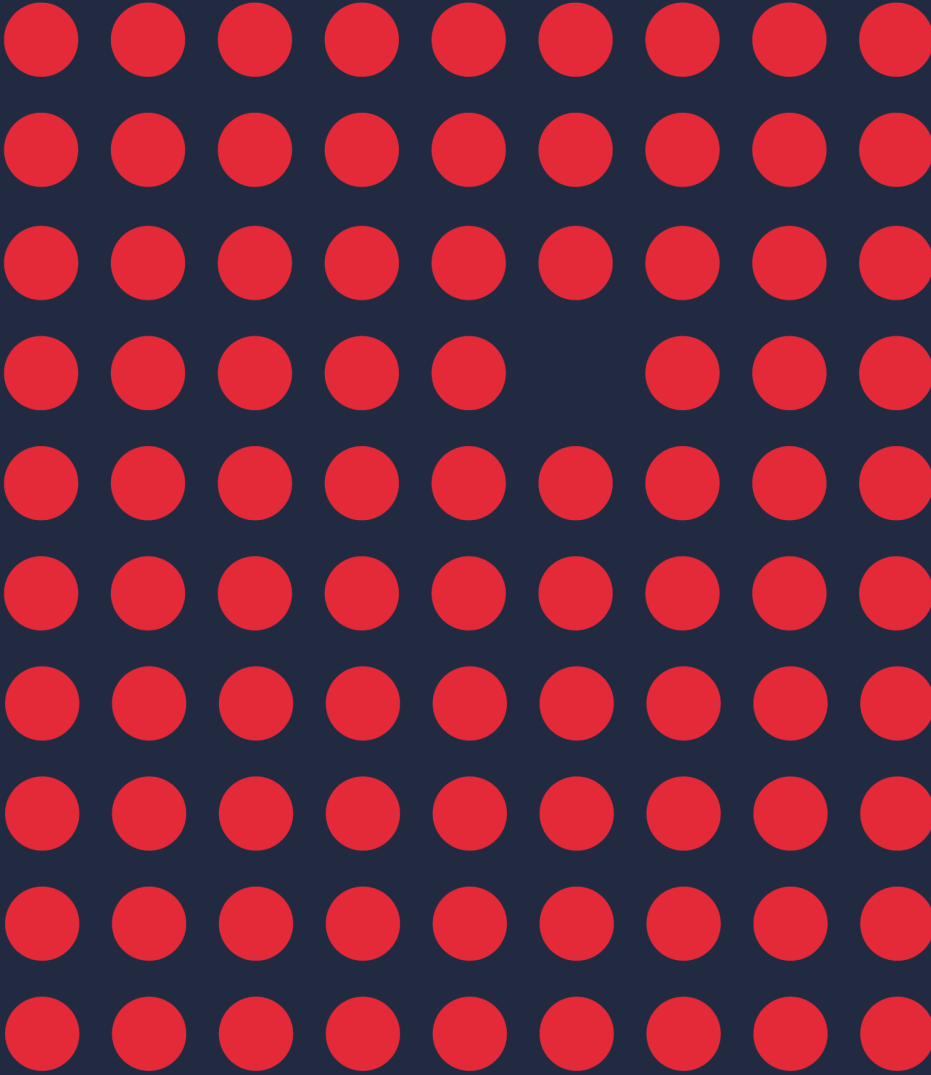
33. Mitra, S.; Bastos, C.P.; Bates, K.; Pereira, G.S.; Bult-Ito, A. Ovarian Sex Hormones Modulate Compulsive, Affective and Cognitive Functions in A Non-Induced Mouse Model of Obsessive-Compulsive Disorder. *Front Behav Neurosci* **2016**, *10*, 215, doi:10.3389/fnbeh.2016.00215.

34. Schwabe, M.J.; Konkol, R.J. Menstrual cycle-related fluctuations of tics in Tourette syndrome. *Pediatr Neurol* **1992**, *8*, 43-46, doi:10.1016/0887-8994(92)90051-y.

35. Kompoliti, K.; Goetz, C.G.; Leurgans, S.; Raman, R.; Comella, C.L. Estrogen, progesterone, and tic severity in women with Gilles de la Tourette syndrome. *Neurology* **2001**, *57*, 1519.

36. Boon, W.C.; Horne, M.K. Aromatase and its inhibition in behaviour, obsessive compulsive disorder and parkinsonism. *Steroids* **2011**, *76*, 816-819, doi:10.1016/j.steroids.2011.02.031.

37. Martino, D.; Macerollo, A.; Leckman, J.F. Neuroendocrine aspects of Tourette syndrome. *Int Rev Neurobiol* **2013**, *112*, 239-279, doi:10.1016/B978-0-12-411546-0.00009-3.

38. Garcia-Gomez, E.; Gonzalez-Pedrajo, B.; Camacho-Arroyo, I. Role of sex steroid hormones in bacterial-host interactions. *Biomed Res Int* **2013**, *2013*, 928290, doi:10.1155/2013/928290.

39. Ercan, A.; Kohrt, W.M.; Cui, J.; Deane, K.D.; Pezer, M.; Yu, E.W.; Hausmann, J.S.; Campbell, H.; Kaiser, U.B.; Rudd, P.M.; et al. Estrogens regulate glycosylation of IgG in women and men. *JCI Insight* **2017**, *2*, e89703, doi:10.1172/jci.insight.89703.

40. Liu, X.; Herbison, A.E. Dopamine regulation of gonadotropin-releasing hormone neuron excitability in male and female mice. *Endocrinology* **2013**, *154*, 340-350, doi:10.1210/en.2012-1602.

41. Bailey, M.; Silver, R. Sex differences in circadian timing systems: implications for disease. *Front Neuroendocrinol* **2014**, *35*, 111-139, doi:10.1016/j.yfrne.2013.11.003.

42. Mitsushima, D.; Takase, K.; Funabashi, T.; Kimura, F. Gonadal steroid hormones maintain the stress-induced acetylcholine release in the hippocampus: simultaneous measurements of the extracellular acetylcholine and serum corticosterone levels in the same subjects. *Endocrinology* **2008**, *149*, 802-811, doi:10.1210/en.2007-0827.

43. Turzillo, A.M.; Nolan, T.E.; Nett, T.M. Regulation of gonadotropin-releasing hormone (GnRH) receptor gene expression in sheep: interaction of GnRH and estradiol. *Endocrinology* **1998**, *139*, 4890-4894, doi:10.1210/endo.139.12.6344.

44. Hussain, D.; Cossette, M.P.; Brake, W.G. High Oestradiol Replacement Reverses Response Memory Bias in Ovariectomised Female Rats Regardless of Dopamine Levels in the Dorsal Striatum. *J Neuroendocrinol* **2016**, *28*, doi:10.1111/jne.12375.

45. Shams, W.M.; Sanio, C.; Quinlan, M.G.; Brake, W.G. 17beta-Estradiol infusions into the dorsal striatum rapidly increase dorsal striatal dopamine release in vivo. *Neuroscience* **2016**, *330*, 162-170, doi:10.1016/j.neuroscience.2016.05.049.

46. Turgeon, J.L.; Waring, D.W. Androgen modulation of luteinizing hormone secretion by female rat gonadotropes. *Endocrinology* **1999**, *140*, 1767-1774, doi:10.1210/endo.140.4.6642.

47. Gui, Y.; Silha, J.V.; Murphy, L.J. Sexual dimorphism and regulation of resistin, adiponectin, and leptin expression in the mouse. *Obes Res* **2004**, *12*, 1481-1491, doi:10.1038/oby.2004.185.

48. Gjedde, A.; Reith, J.; Dyve, S.; Leger, G.; Guttman, M.; Diksic, M.; Evans, A.; Kuwabara, H. Dopa decarboxylase activity of the living human brain. *Proc Natl Acad Sci U S A* **1991**, *88*, 2721-2725.

49. Lotan, D.; Benhar, I.; Alvarez, K.; Mascaro-Blanco, A.; Brimberg, L.; Frenkel, D.; Cunningham, M.W.; Joel, D. Behavioral and neural effects of intra-striatal infusion of anti-streptococcal antibodies in rats. *Brain Behav Immun* **2014**, *38*, 249-262, doi:10.1016/j.bbi.2014.02.009.

50. Cox, C.J.; Sharma, M.; Leckman, J.F.; Zuccolo, J.; Zuccolo, A.; Kovoor, A.; Swedo, S.E.; Cunningham, M.W. Brain human monoclonal autoantibody from sydenham chorea targets dopaminergic neurons in transgenic mice and signals dopamine D2 receptor: implications in human disease. *J Immunol* **2013**, *191*, 5524-5541, doi:10.4049/jimmunol.1102592.

51. Cox, C.J.; Zuccolo, A.J.; Edwards, E.V.; Mascaro-Blanco, A.; Alvarez, K.; Stoner, J.; Chang, K.; Cunningham, M.W. Antineuronal antibodies in a heterogeneous group of youth and young adults with tics and obsessive-compulsive disorder. *J Child Adolesc Psychopharmacol* **2015**, *25*, 76-85, doi:10.1089/cap.2014.0048.

52. Yaddanapudi, K.; Hornig, M.; Serge, R.; De Miranda, J.; Baghban, A.; Villar, G.; Lipkin, W.I. Passive transfer of streptococcus-induced antibodies reproduces behavioral disturbances in a mouse model of pediatric autoimmune neuropsychiatric disorders associated with streptococcal infection. *Mol Psychiatry* **2010**, *15*, 712-726, doi:10.1038/mp.2009.77.

53. Gill, R.K.; Mahmood, S.; Sodhi, C.P.; Nagpaul, J.P.; Mahmood, A. IgG binding and expression of its receptor in rat intestine during postnatal development. *Indian J Biochem Biophys* **1999**, *36*, 252-257.

54. Kurlander, R.J. The effects of corticosteroids on IgG Fc receptor and complement receptor-mediated interaction of monocytes with red cells. *Clin Immunol Immunopathol* **1981**, *20*, 325-335.

55. Denys, D.; de Vries, F.; Cath, D.; Figee, M.; Vulink, N.; Veltman, D.J.; van der Doef, T.F.; Boellaard, R.; Westenberg, H.; van Balkom, A.; et al. Dopaminergic activity in Tourette syndrome and obsessive-compulsive disorder. *Eur Neuropsychopharmacol* **2013**, *23*, 1423-1431, doi:10.1016/j.euroneuro.2013.05.012.

56. Abi-Jaoude, E.; Segura, B.; Obeso, I.; Cho, S.S.; Houle, S.; Lang, A.E.; Rusjan, P.; Sandor, P.; Strafella, A.P. Similar striatal D2/D3 dopamine receptor availability in adults with Tourette syndrome compared with healthy controls: A [(11) C]-(+)-PHNO and [(11) C]raclopride positron emission tomography imaging study. *Hum Brain Mapp* **2015**, *36*, 2592-2601, doi:10.1002/hbm.22793.

57. Hershey, T.; Black, K.J.; Hartlein, J.M.; Barch, D.M.; Braver, T.S.; Carl, J.L.; Perlmutter, J.S. Cognitive-pharmacologic functional magnetic resonance imaging in tourette syndrome: a pilot study. *Biol Psychiatry* **2004**, *55*, 916-925, doi:10.1016/j.biopsych.2004.01.003.

58. Nomura, Y.; Segawa, M. Neurology of Tourette's syndrome (TS) TS as a developmental dopamine disorder: a hypothesis. *Brain Dev* **2003**, *25 Suppl 1*, S37-42.

59. Black, K.J.; Mink, J.W. Response to levodopa challenge in Tourette syndrome. *Mov Disord* **2000**, *15*, 1194-1198, doi:10.1002/1531-8257(200011)15:6<1194::aid-mds1019>3.0.co;2-h.

60. Piazza, P.V.; Barrot, M.; Rouge-Pont, F.; Marinelli, M.; Maccari, S.; Abrous, D.N.; Simon, H.; Le Moal, M. Suppression of glucocorticoid secretion and antipsychotic drugs have similar effects on the mesolimbic dopaminergic transmission. *Proc Natl Acad Sci U S A* **1996**, *93*, 15445-15450.

61. Grey, C.L.; Chang, J.P. Differential modulation of ghrelin-induced GH and LH release by PACAP and dopamine in goldfish pituitary cells. *Gen Comp Endocrinol* **2013**, *191*, 215-224, doi:10.1016/j.ygcen.2013.06.020.

62. Igal, R.A.; Wang, S.; Gonzalez-Baro, M.; Coleman, R.A. Mitochondrial glycerol phosphate acyltransferase directs the incorporation of exogenous fatty acids into triacylglycerol. *J Biol Chem* **2001**, *276*, 42205-42212, doi:10.1074/jbc.M103386200.

63. Agargun, M.Y.; Dulger, H.; Inci, R.; Kara, H.; Ozer, O.A.; Sekeroglu, M.R.; Besiroglu, L. Serum lipid concentrations in obsessive-compulsive disorder patients with and without panic attacks. *Can J Psychiatry* **2004**, *49*, 776-778, doi:10.1177/070674370404901109.

64. Albert, U.; Aguglia, A.; Chiarle, A.; Bogetto, F.; Maina, G. Metabolic syndrome and obsessive-compulsive disorder: a naturalistic Italian study. *Gen Hosp Psychiatry* **2013**, *35*, 154-159, doi:10.1016/j.genhosppsych.2012.10.004.

65. Fagman, J.B.; Wilhelmson, A.S.; Motta, B.M.; Pirazzi, C.; Alexanderson, C.; De Gendt, K.; Verhoeven, G.; Holmang, A.; Anesten, F.; Jansson, J.O.; et al. The androgen receptor confers protection against diet-induced atherosclerosis, obesity, and dyslipidemia in female mice. *Faseb j* **2015**, *29*, 1540-1550, doi:10.1096/fj.14-259234.

66. McMurray, R.W.; Ndebele, K.; Hardy, K.J.; Jenkins, J.K. 17-beta-estradiol suppresses IL-2 and IL-2 receptor. *Cytokine* **2001**, *14*, 324-333, doi:10.1006/cyto.2001.0900.

67. Mortensen, R.; Nissen, T.N.; Blauenfeldt, T.; Christensen, J.P.; Andersen, P.; Dietrich, J. Adaptive Immunity against Streptococcus pyogenes in Adults Involves Increased IFN-gamma and IgG3 Responses Compared with Children. *J Immunol* **2015**, *195*, 1657-1664, doi:10.4049/jimmunol.1500804.

68. Karanth, S.; McCann, S.M. Anterior pituitary hormone control by interleukin 2. *Proc Natl Acad Sci U S A* **1991**, *88*, 2961-2965.

69. Karanth, S.; Marubayashi, U.; McCann, S.M. Influence of dopamine on the altered release of prolactin, luteinizing hormone, and follicle-stimulating hormone induced by interleukin-2 in vitro. *Neuroendocrinology* **1992**, *56*, 871-880.

70. Morer, A.; Chae, W.; Henegariu, O.; Bothwell, A.L.; Leckman, J.F.; Kawikova, I. Elevated expression of MCP-1, IL-2 and PTPR-N in basal ganglia of Tourette syndrome cases. *Brain Behav Immun* **2010**, *24*, 1069-1073, doi:10.1016/j.bbi.2010.02.007.

71. Bos-Veneman, N.G.; Bijzet, J.; Limburg, P.C.; Minderaa, R.B.; Kallenberg, C.G.; Hoekstra, P.J. Cytokines and soluble adhesion molecules in children and adolescents with a tic disorder. *Prog Neuropsychopharmacol Biol Psychiatry* **2010**, *34*, 1390-1395, doi:10.1016/j.pnpbp.2010.06.028.

72. Rao, N.P.; Venkatasubramanian, G.; Ravi, V.; Kalmady, S.; Cherian, A.; Yc, J.R. Plasma cytokine abnormalities in drug-naive, comorbidity-free obsessive-compulsive disorder. *Psychiatry Res* **2015**, *229*, 949-952, doi:10.1016/j.psychres.2015.07.009.

73. Hanisch, U.K.; Rowe, W.; Sharma, S.; Meaney, M.J.; Quirion, R. Hypothalamic-pituitary-adrenal activity during chronic central administration of interleukin-2. *Endocrinology* **1994**, *135*, 2465-2472, doi:10.1210/endo.135.6.7988433.

74. Wolf, W.A.; Martin, J.L.; Kartje, G.L.; Farrer, R.G. Evidence for fibroblast growth factor-2 as a mediator of amphetamine-enhanced motor improvement following stroke. *PLoS One* **2014**, *9*, e108031, doi:10.1371/journal.pone.0108031.

75. Chaturvedi, K.; Sarkar, D.K. Involvement of protein kinase C-dependent mitogen-activated protein kinase p44/42 signaling pathway for cross-talk between estradiol and transforming growth factor-beta3 in increasing basic fibroblast growth factor in folliculostellate cells. *Endocrinology* **2004**, *145*, 706-715, doi:10.1210/en.2003-1063.

76. Mocchetti, I.; Spiga, G.; Hayes, V.Y.; Isackson, P.J.; Colangelo, A. Glucocorticoids differentially increase nerve growth factor and basic fibroblast growth factor expression in the rat brain. *J Neurosci* **1996**, *16*, 2141-2148.

77. Magnaghi, V.; Riva, M.A.; Cavarretta, I.; Martini, L.; Melcangi, R.C. Corticosteroids regulate the gene expression of FGF-1 and FGF-2 in cultured rat astrocytes. *J Mol Neurosci* **2000**, *15*, 11-18, doi:10.1385/jmn:15:1:11.

78. Molteni, R.; Fumagalli, F.; Magnaghi, V.; Roceri, M.; Gennarelli, M.; Racagni, G.; Melcangi, R.C.; Riva, M.A. Modulation of fibroblast growth factor-2 by stress and corticosteroids: from developmental events to adult brain plasticity. *Brain Res Brain Res Rev* **2001**, *37*, 249-258.

79. Hansson, A.C.; Sommer, W.; Rimondini, R.; Andbjer, B.; Stromberg, I.; Fuxe, K. c-fos reduces corticosterone-mediated effects on neurotrophic factor expression in the rat hippocampal CA1 region. *J Neurosci* **2003**, *23*, 6013-6022.

80. Morash, B.; Johnstone, J.; Leopold, C.; Li, A.; Murphy, P.; Ur, E.; Wilkinson, M. The regulation of leptin gene expression in the C6 glioblastoma cell line. *Mol Cell Endocrinol* **2000**, *165*, 97-105.

81. Misso, M.L.; Murata, Y.; Boon, W.C.; Jones, M.E.; Britt, K.L.; Simpson, E.R. Cellular and molecular characterization of the adipose phenotype of the aromatase-deficient mouse. *Endocrinology* **2003**, *144*, 1474-1480, doi:10.1210/en.2002-221123.

82. Penza, M.; Montani, C.; Romani, A.; Vignolini, P.; Pampaloni, B.; Tanini, A.; Brandi, M.L.; Alonso-Magdalena, P.; Nadal, A.; Ottobrini, L.; et al. Genistein affects adipose tissue deposition in a dose-dependent and gender-specific manner. *Endocrinology* **2006**, *147*, 5740-5751, doi:10.1210/en.2006-0365.

83. Schwartz, M.W.; Woods, S.C.; Porte, D., Jr.; Seeley, R.J.; Baskin, D.G. Central nervous system control of food intake. *Nature* **2000**, *404*, 661-671, doi:10.1038/35007534.

84. Lord, G.M.; Matarese, G.; Howard, J.K.; Baker, R.J.; Bloom, S.R.; Lechler, R.I. Leptin modulates the T-cell immune response and reverses starvation-induced immunosuppression. *Nature* **1998**, *394*, 897-901, doi:10.1038/29795.

85. Lawrence, T.; Bebien, M.; Liu, G.Y.; Nizet, V.; Karin, M. IKKalpha limits macrophage NF-kappaB activation and contributes to the resolution of inflammation. *Nature* **2005**, *434*, 1138-1143, doi:10.1038/nature03491.

86. Hsu, L.C.; Enzler, T.; Seita, J.; Timmer, A.M.; Lee, C.Y.; Lai, T.Y.; Yu, G.Y.; Lai, L.C.; Temkin, V.; Sinzig, U.; et al. IL-1beta-driven neutrophilia preserves antibacterial defense in the absence of the kinase IKKbeta. *Nat Immunol* **2011**, *12*, 144-150, doi:10.1038/ni.1976.

87. Krabbe, G.; Minami, S.S.; Etchegaray, J.I.; Taneja, P.; Djukic, B.; Davalos, D.; Le, D.; Lo, I.; Zhan, L.; Reichert, M.C.; et al. Microglial NFkappaB-TNFalpha hyperactivation induces obsessive-compulsive behavior in mouse models of progranulin-deficient frontotemporal dementia. *Proc Natl Acad Sci U S A* **2017**, *114*, 5029-5034, doi:10.1073/pnas.1700477114.

88. Simoncini, T.; Maffei, S.; Basta, G.; Barsacchi, G.; Genazzani, A.R.; Liao, J.K.; De Caterina, R. Estrogens and glucocorticoids inhibit endothelial vascular cell adhesion molecule-1 expression by different transcriptional mechanisms. *Circ Res* **2000**, *87*, 19-25.

89. Ren, H.; Schmalstieg, A.; van Oers, N.S.; Gaynor, R.B. I-kappa B kinases alpha and beta have distinct roles in regulating murine T cell function. *J Immunol* **2002**, *168*, 3721-3731.

90. Vandermoere, F.; El Yazidi-Belkoura, I.; Adriaenssens, E.; Lemoine, J.; Hondermarck, H. The antiapoptotic effect of fibroblast growth factor-2 is mediated through nuclear factor-kappaB activation induced via interaction between Akt and IkappaB kinase-beta in breast cancer cells. *Oncogene* **2005**, *24*, 5482-5491, doi:10.1038/sj.onc.1208713.

91. Lam, Q.L.; Zheng, B.J.; Jin, D.Y.; Cao, X.; Lu, L. Leptin induces CD40 expression through the activation of Akt in murine dendritic cells. *J Biol Chem* **2007**, *282*, 27587-27597, doi:10.1074/jbc.M704579200.

92. Tsatsaronis, J.A.; Walker, M.J.; Sanderson-Smith, M.L. Host responses to group a streptococcus: cell death and inflammation. *PLoS Pathog* **2014**, *10*, e1004266, doi:10.1371/journal.ppat.1004266.

93. Horst, S.A.; Linner, A.; Beineke, A.; Lehne, S.; Holtje, C.; Hecht, A.; Norrby-Teglund, A.; Medina, E.; Goldmann, O. Prognostic value and therapeutic potential of TREM-1 in Streptococcus pyogenes-induced sepsis. *J Innate Immun* **2013**, *5*, 581-590, doi:10.1159/000348283.

94. Murakami, Y.; Akahoshi, T.; Aoki, N.; Toyomoto, M.; Miyasaka, N.; Kohsaka, H. Intervention of an inflammation amplifier, triggering receptor expressed on myeloid cells 1, for treatment of autoimmune arthritis. *Arthritis Rheum* **2009**, *60*, 1615-1623, doi:10.1002/art.24554.

95. Zhong, J.; Huang, W.; Deng, Q.; Wu, M.; Jiang, H.; Lin, X.; Sun, Y.; Huang, X.; Yuan, J. Inhibition of TREM-1 and Dectin-1 Alleviates the Severity of Fungal Keratitis by Modulating Innate Immune Responses. *PLoS One* **2016**, *11*, e0150114, doi:10.1371/journal.pone.0150114.

96. Lin, C.H.; Hsieh, S.C.; Keng, L.T.; Lee, H.S.; Chang, H.T.; Liao, W.Y.; Ho, C.C.; Yu, C.J. Prospective Evaluation of Procalcitonin, Soluble Triggering Receptor Expressed on Myeloid Cells-1 and C-Reactive Protein in Febrile Patients with Autoimmune Diseases. *PLoS One* **2016**, *11*, e0153938, doi:10.1371/journal.pone.0153938.

2

CHAPTER 3

RILUZOLE ATTENUATES L-DOPA-INDUCED ABNORMAL INVOLUNTARY MOVEMENTS THROUGH DECREASING CREB1 ACTIVITY: INSIGHTS FROM A RAT MODEL

ABSTRACT

Chronic administration of L-DOPA, the first-line treatment of dystonic symptoms in childhood or in Parkinson's disease, often leads to the development of abnormal involuntary movements (AIMs), which represent an important clinical problem. Although it is known that Riluzole attenuates L-DOPA-induced AIMs, the molecular mechanisms underlying this effect are not understood. Therefore, we studied the behavior and performed RNA sequencing of the striatum in three groups of rats that all received a unilateral lesion with 6-hydroxy-dopamine in their medial forebrain bundle, followed by the administration of saline, L-DOPA, or L-DOPA combined with Riluzole. First, we provide evidence that Riluzole attenuates AIMs in this rat model. Subsequently, analysis of the transcriptomics data revealed that Riluzole is predicted to reduce the activity of CREB1, a transcription factor that regulates the expression of multiple proteins that interact in a molecular landscape involved in apoptosis. Although this mechanism underlying the beneficial effect of Riluzole on AIMs needs to be confirmed, it provides clues towards novel or existing compounds for the treatment of AIMs that modulate the activity of CREB1 and, hence, its downstream targets.

INTRODUCTION

Chronic administration of the dopamine precursor L-DOPA – the first-line treatment of dystonic symptoms manifesting in childhood or in Parkinson's disease (PD) [1] – often leads to the development of so-called abnormal involuntary movements (AIMs). In humans, L-DOPA-induced AIMs are referred to as L-DOPA-induced dyskinesia (LID) [2], which represents an important clinical problem as approximately 90% of PD patients develop LID within 10 years of starting L-DOPA treatment. As a result, the prescription of L-DOPA to PD patients is often delayed to minimize the risk of developing LID [3].

The pathogenic mechanisms underlying AIMs and clinical LID are still largely unclear. Literature evidence indicates that chronic L-DOPA administration affects multiple neurotransmitter systems [4-6], but mainly the dopaminergic system, i.e., L-DOPA activates striatal Dopamine 1 receptors (D1Rs), resulting in the overstimulation of the 'direct' nigrostriatal pathway [7,8]. In turn, this hypersensitivity of D1Rs in striatal neurons triggers a number of downstream signaling cascades involving – among others – cyclic AMP (cAMP)-activated protein kinase A (PKA) [9,10], the phosphatase inhibitor DARPP-32 [10,11], and the ERK1 and ERK2 (ERK1/2) kinases [12,13] that are subsequently implicated in the development of LID through modulating gene expression and function [14,15]. In this respect, previous transcriptomic and methylation studies in rodent models indeed indicate that AIMs/LID are associated with aberrant gene expression through transcription factors, such as CREB1, proteins from the AP-1 complex [9,16] (such as FOSB) [17], and GADD45 family proteins [17].

Recently, Riluzole has been suggested as a candidate drug to treat AIMs/LID. Indeed, several studies on rodent models have provided evidence for the efficacy of Riluzole in the management of AIMs [2,18,19]. As for human studies, Riluzole showed anti-dyskinetic effects without affecting the anti-parkinsonian action of L-DOPA in a small pilot study [20], but it was ineffective in another clinical trial [21]. Riluzole essentially has anti-glutamatergic properties – including effects on glutamate release, uptake and receptor signaling [22-25], and it protects against glutamate-induced activation of kinases such as ERK1/2 [26]. More specifically, although Riluzole has properties resembling those of a competitive NMDA receptor antagonist, its effects on reducing glutamatergic neurotransmission are more indirect [27]. Indeed, the anti-glutamatergic effects of Riluzole could result from a reduction of glutamate release from synapses through an inhibition of voltage-gated sodium channels [28], a reduction in the postsynaptic calcium influx mediated by P/Q-type calcium channels [29], a reduction in glutamine import into synapses (with glutamine being a precursor for the releasable glutamate pool) [30], or through interfering with the size of the readily releasable glutamate pool [31]. Further, animal model studies suggest that Riluzole is not selective

for glutamate but also reduces the release of acetylcholine, dopamine, and, to a lesser extent, serotonin through mechanisms independent of glutamate receptors [32]. However, a detailed understanding of the molecular mechanism(s) underlying the protective effect of Riluzole on AIMs/LID is essentially lacking.

In this study, we aimed to elucidate the molecular mechanisms underlying the beneficial effect of Riluzole on AIMs. Therefore, we studied the behavior and performed RNA sequencing of the striatum, followed by gene expression analysis and comparison in three groups of rats. All rats received a unilateral lesion with 6-hydroxy-dopamine (6-OHDA) in their medial forebrain bundle (MFB) – resulting in striatal dopaminergic hypersensitivity – after which they were administered saline, L-DOPA (which constitutes a rat model of AIMs), or L-DOPA combined with Riluzole. We found that Riluzole attenuates L-DOPA-induced AIMs in the rat model. In addition, further analysis indicated that Riluzole is predicted to reduce the activity of the transcription factor CREB1, the key hub in a landscape of interacting proteins that are involved in regulating neuronal apoptosis.

MATERIALS AND METHODS
Animals and ethical approvals
Juvenile male Wistar rats (RjHan:WI,) were used in this study. Rats were obtained from our provider (Janvier, Le Genest-St Isle, France) at the age of 14 days together with their mothers. In total, 5 juvenile rats and a mother were housed together with free access to food and water, under a 12h light and dark cycle in temperature and humidity-controlled rooms. All animals were habituated to their housing conditions for one week. Animal housing and experiments were approved by the appropriate institutional governmental agency (Regierungspräsidium Tübingen, Germany) and performed in an AAALAC (Association for Assessment and Accreditation of Laboratory Animal Care International) -accredited facility, following the European Convention for Animal Care and Use of Laboratory Animals.

Stereotaxic surgery
After 1 week of habituation at post-natal day (PND) 21 (n = 48), the rats were separated from their mothers and underwent stereotaxic surgery with 6-hydroxydopamine hydrobromide (6-OHDA). Further details are provided in the Supplementary Methods.

Animal Treatment
Two weeks after stereotaxic surgery, the rats were randomly allocated to 4 groups (n = 12 animals per group) associated to different pharmacological treatments, at the

RILUZOLE ATTENUATES L-DOPA-INDUCED ABNORMAL INVOLUNTARY MOVEMENTS
THROUGH DECREASING CREB1 ACTIVITY: INSIGHTS FROM A RAT MODEL

3

same conditions: the first group was chronically administered (6 times in 2 weeks, intra-peritoneally (*i.p.*)) with a solution of L-DOPA methyl ester hydrochloride and benserazide (Sigma-Aldrich Chemie GmbH, Germany) in saline (6/15 mg/kg, *i.p*). The second group (control) was administered with saline. The third group was chronically administered (6 times in 2 weeks) with Riluzole (Sigma-Aldrich Chemie GmbH, Germany) dissolved in 1% tween (6 mg/kg *i.p*) and L-DOPA/Benserazide (6/15 mg/kg, *i.p*). The fourth (6-OHDA-lesioned) group followed the same procedure as group 1 and was used to verify the presence of the lesion by quantification of dopamine (DA) levels in striatal tissue using high-performance liquid chromatography (HPLC) coupled to electrochemical detection (ECD).

Phenotype scoring

Four weeks after surgery (PND 49), rats were administered their treatment and were individually observed for 1 min every 20 min. Abnormal Involuntary Movements (AIMs) of the limb, mouth and body axis were assessed according to the widely used AIMs rating scale [33]. Briefly, each type of movement was scored on a scale from 0 to 4 (0 = absent; 1 = occasional; 2 = frequent; 3 = continuous but interrupted by sensory distraction; 4 = continuous, severe, not interrupted by sensory distraction). The sum of the independent scores of each body part per time point gave the total AIMs score.

Animal sacrifice and sample extraction

At PND 53, rats were sacrificed 2 h after the administration of a final treatment. Rats were anesthetized for 60 s in 5% isoflurane and quickly decapitated by guillotine. Following brain removal, lesioned and unlesioned striata were extracted, snapped-frozen in liquid nitrogen and stored at -80°C. A schema of the experimental procedure is outlined in Figure 1.

Striatal DA determination through HPLC

DA levels in 12 6-OHDA-lesioned striata compared to their contralateral controls were quantified using HPLC coupled to ECD. Further details are provided in the Supplementary Methods.

Behavioral testing: Statistical analysis

Time-course data were analyzed for statistical significance using two-way analysis of variance (ANOVA) followed by Tukey's multiple comparison test. Dopaminergic HPLC quantification in lesioned versus unlesioned striata was analyzed using a Wilcoxon matched-pairs signed-ranked test.

Experimental Set-up
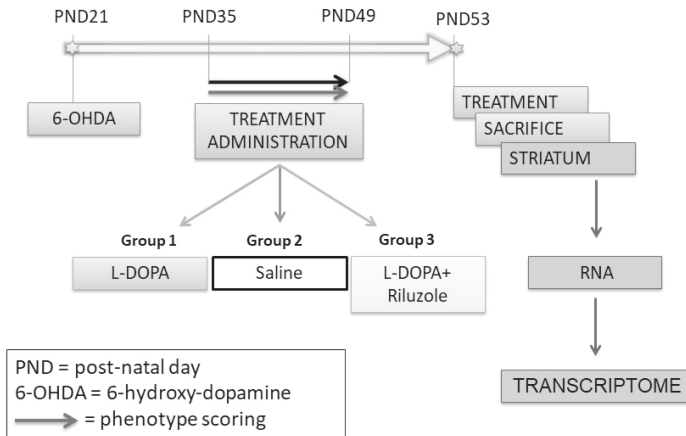
FIGURE 1. Schematic diagram of the protocol employed including the time course of the experiment and the different assays that were used.

RNA sequencing and data analysis

Total RNA was extracted from striatum tissue from 8 animals from each group using the QiagenAllPrep Kit (Qiagen, Hamburg, Germany), according to the manufacturer's instructions. RNA was further quantified using the NanoDrop 1000 Spectrophotometer and Bioanalyzer 2100 (Agilent). Samples with RIN value above 8.0 were used for transcriptome analysis. The sequencing library preparation was done using 200 ng of total RNA input with the TrueSeq RNA Sample Prep Kit v3-Set B (RS-122-2002, Illumina Inc, San Diego, CA) producing a 275bp fragment including adapters in average size. In the final step before sequencing, 12 individual libraries were normalized and pooled together using the adapter indices supplied by the manufacturer. Pooled libraries were clustered on the cBot Instrument from Illumina using the TruSeq SR Cluster Kit v3 – cBot – HS (GD-401-3001, Illumina Inc, San Diego, CA) and sequencing was then performed as 78 bp, single reads and 7 bases index read on an Illumina HiSeq3000 instrument using the TruSeq SBS Kit HS- v3 (50-cycle) (FC-401-3002, Illumina Inc, San Diego, CA). Reads were aligned to the rat genome using the STAR Aligner v2.5.2a [34] with corresponding Ensembl 84 reference genome (http://www.ensembl.org). Sequenced read quality was checked with FastQC v0.11.2 (http://www.bioinformatics.babraham.ac.uk/projects/fastqc/) and alignment quality metrics were calculated using RNASeQC v1.18 [35]. Following read alignment, duplication rates of the RNA sequencing samples were computed with bamUtil v1.0.11 to mark duplicate reads and

the dupRadar v1.4 Bioconductor R package for assessment [36]. Gene expression profiles were quantified using Cufflinks software version 2.2.1 [37] and the feature counts software package [38]. Transcripts with at least 10 reads in 8 samples were retained and further used to identify differentially expressed genes between the following three experimental groups: Saline, L-DOPA and L-DOPA + Riluzole. Statistical analyses were performed using R (www.r-project.org) and the Bioconductor package ([39], www.bioconductor.org) limma-voom [40]. The Benjamini-Hochberg's method was used to correct for multiple testing, and only protein-coding genes with adjusted P-value <0.01, independent of magnitude of change, were considered as differentially expressed and used in the subsequent analyses. The Venn diagram of the final sets of significantly differentially expressed genes for the two comparisons was built with Venny [41]. To assess the effect of Riluzole on L-DOPA-regulated genes, we also looked at the overlap between the genes regulated by L-DOPA (L-DOPA vs. Saline, comparison 1) and the genes regulated by Riluzole in the L-DOPA model (L-DOPA + Riluzole vs. L-DOPA, comparison 2). To quantify this overlap, we used the hypergeometric distribution test [42]:

$$p(x \mid n, M, N) = \frac{\binom{M}{x}\binom{N-M}{n-x}}{\binom{N}{n}}$$

This test calculates the chance of observing exactly x overlapping genes from a total of n differentially expressed genes by Riluzole in the L-DOPA model, with a total of M genes that were differentially expressed by L-DOPA and a total of N genes detected with RNAseq. The total number of unique genes detected with RNAseq (N) consists of genes detected in both comparisons, irrespective of their FC or expression P-value. For all comparisons, only protein-coding genes were considered. To determine the correlation between the fold changes for the overlapping genes in the two comparisons, we created a scatter plot and calculated the Spearman correlation coefficient using the ggscatter function in R package ggpubr.

Upstream regulator and gene enrichment analyses

Using Ingenuity Pathway Analysis (IPA; Qiagen Inc.), we performed upstream regulator and gene enrichment analyses. Based on the differentially expressed genes, IPA generates a list of 'upstream regulators', i.e., proteins or compounds that are able to explain observed gene expression changes in the input dataset. For each upstream regulator, IPA calculates a P-value of overlap (measuring the statistical significance of the overlap between the dataset genes and all genes that are regulated by the upstream regulator) and a z-score (reflecting

the inhibition or activation of the upstream regulator-dependent effects on target gene expression). We selected the major upstream regulator with the best z-score and P-value of overlap for the two comparisons – i.e., L-DOPA vs. Saline and L-DOPA + Riluzole vs. L-DOPA – and used the target genes of this upstream regulator for further analyses. In the gene enrichment analysis, IPA assigns genes and their corresponding mRNAs/proteins to functional (sub)-categories, i.e., 'canonical pathways' and 'biofunctions', with the latter including 'diseases and disorders' and 'molecular and cellular functions'.

Molecular landscape building

Following the upstream regulator and enrichment analyses, we searched the literature for the functions and interactions of all proteins encoded by the target genes of the major upstream regulator and expressed in the opposite direction in the two comparisons, i.e., L-DOPA vs. Saline and L-DOPA + Riluzole vs. L-DOPA. First, we used the UniProt Knowledge Base ([43], http://www.uniprot.org) to gather basic information on the functions of all target genes and their encoded proteins. Subsequently and starting with the interactions reported by IPA, we used PubMed (http://www.ncbi.nlm.nih.gov/pubmed) to search for all functional, experimental evidence-based interactions between the proteins. Based on all gathered information, we generated a protein interaction landscape. The figure depicting this landscape was made using the drawing program Serif DrawPlus version 4.0 (www.serif.com).

qPCR validation of selected CREB1 targets

To provide an additional validation of the RNA sequencing data, we performed qPCR to assess and compare the mRNA expression levels of 10 randomly chosen CREB1 targets in each of the samples of the groups investigated in this study (Saline, L-DOPA, L-DOPA + Riluzole). RNA from the same samples used for the RNA sequencing was reverse-transcribed to cDNA using the RT^2 First-Strand Kit (Qiagen, Cat. number 330404) according to the manufacturer's instructions. Three-step qPCR (95°C for 10min, followed by 40 two-step cycles at 95°C for 15s and 60°C for 30s, and the generation of melting curves from 70 to 95 °C; Rotor-Gene Q 1000, Qiagen) was performed using RT^2 SYBR Green ROX™ qPCR Mastermix (Qiagen, Cat. number 330521) and RT^2 qPCR primer Assays provided by Qiagen The housekeeping genes *Bcap29* and *Cdkn1b* were used as reference for normalization of gene expression, and a Student's t-test was used to assess statistical significance. The full list of primers is specified in Supplementary Table 1.

RESULTS

Assessment of striatal DA depletion by assaying its content

To confirm the degree of dopaminergic denervation in the unilateral 6-OHDA-lesioned rats, total (intracellular and extracellular) dopamine (DA) tissue content in the ipsilateral (lesioned) and contralateral (control) striatum relative to the lesion was assayed by HPLC coupled to ECD. 6-OHDA lesion induced a marked decrease (76 %) in DA concentration in the ipsilateral striatum compared with the contralateral side (Supplementary Figure 1).

Behavioral effects: induction of AIMs by L-DOPA in 6-OHDA-lesioned rats and their mitigation by Riluzole

Intra-MFB 6-OHDA lesion plus 2 weeks of chronic L-DOPA exposure induced strong abnormal involuntary movements (p<0.001), while 6-OHDA-lesioned rats given saline showed no abnormal motor phenotype. Chronic treatment with Riluzole together with L-DOPA was associated with fewer AIMs than L-DOPA alone (p<0.001), as shown in Figure 2.

RNA sequencing data analysis and upstream regulator/gene enrichment analyses

Transcriptomic analysis was performed on the mRNA from the RNA samples isolated from the (lesioned) striatum of Saline-, L-DOPA-, and L-DOPA + Riluzole-treated rats 2 h after the administration of a final injection. This allowed examination of the striatal mRNA gene expression profiles (and assessment of the counteracting effect of Riluzole) at the peak of L-DOPA effectiveness. The statistically significant differences in gene expression levels in striatum of L-DOPA- vs. Saline-treated rats (comparison 1) and in L-DOPA + Riluzole- vs. L-DOPA-treated rats (comparison 2) are shown in Supplementary Data file 1.

Among the differentially expressed genes, 667 were differentially expressed only in comparison 1 and 1200 genes were differentially expressed only in comparison 2. Further, 465 genes were overlapping in that they were differentially expressed in both comparisons (Supplementary Figure 2), and all of these genes were differentially expressed in the opposite direction in the two comparisons (i.e., genes that were upregulated by chronic L-DOPA treatment were downregulated by Riluzole co-administration, and vice versa). The significance of the overlap in differentially expressed genes was calculated by using the hypergeometric distribution test, which showed that the overlap is much greater than would be expected based on random gene selection (P-value = 1.01E-142).
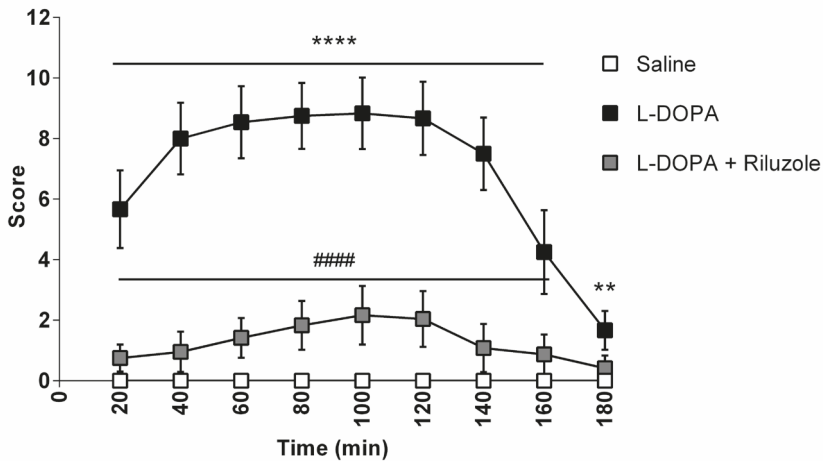
FIGURE 2. Induction of AIMs by L-DOPA in 6-OHDA-lesioned rats and their mitigation by Riluzole. Data shown as mean +/- S.E.M. AIMs scores. Significant differences between the saline and L-DOPA-treated groups are indicated as **p<0.01 and ****p<0.001, and between the L-DOPA and L-DOPA + Riluzole-treated groups as ####p<0.001.

As indicated in Supplementary Table 2, cAMP responsive element binding protein 1 (CREB1) is the top upstream regulator of both the genes that were differentially expressed in comparison 1 and comparison 2, and in these comparisons, CREB1 is predicted to be activated and inhibited, respectively. In addition, CREB1 is the top upstream regulator of the 465 overlapping differentially expressed genes (see previous texts) and there is a highly significant, negative correlation (r= - 0.91, P-value = 2.2E-16) between the fold changes for these genes – including the 58 direct CREB1 target genes – in the two comparisons (Supplementary Figure 3).

Furthermore, gene enrichment analysis (Supplementary Table 3) revealed that the three sets of differentially expressed genes are significantly enriched for a number of 'diseases and disorders' categories, including 'epileptic seizure' (enriched in all three gene sets), as well as 'disorder of basal ganglia' and 'neuromuscular disease' (enriched in the genes from comparison 1). In addition, the gene sets are enriched for multiple 'molecular and cellular functions' categories, such as 'cell death/apoptosis' and 'expression/transcription of RNA' (enriched in all three gene sets) as well as 'development of neurons' (enriched in the genes from comparison 2).

Molecular landscape of CREB1 targets

Subsequently, we further investigated the CREB1-mediated molecular mechanisms implicated in the counteractive effect of Riluzole on L-DOPA-induced changes in gene

expression. Therefore, the set of 58 CREB1 target genes that were regulated in the opposite direction by L-DOPA and Riluzole (Table 1) was studied in more detail and enrichment analysis of these 58 overlapping genes showed that 'epileptic seizure' and 'apoptosis' are the most significantly enriched 'diseases and disorders' and 'molecular and cellular functions' categories, respectively (Supplementary Table 4).

TABLE 1. CREB1 target genes that were significantly differentially expressed in comparisons L-DOPA vs. Saline and L-DOPA + Riluzole vs. L-DOPA with the corresponding fold changes (FDR corrected P-value <0.01). The genes in bold encode proteins that are included in our molecular landscape (Figure 3).

CREB1 target gene	Description	L-DOPA vs. Saline	L-DOPA + Riluzole vs. L-DOPA
Arc	Activity regulated cytoskeleton-associated protein	6.41	-2.99
Atf3	Activating transcription factor 3	10.98	-6.06
Bag3	BCL2-associated athanogene 3	1.80	-1.73
Ccnd3	Cyclin D3	1.22	-1.31
Cdc37	Cell division cycle 37	1.27	-1.28
Cdk19	Cyclin-dependent kinase 19	-1.22	1.18
Cdkn1a	Cyclin-dependent kinase inhibitor 1A	4.09	-2.57
Crem	cAMP-responsive element modulator	1.73	-1.52
Crh	Corticotropin-releasing hormone	6.32	-4.62
Csrnp1	Cysteine and serine-rich nuclear protein 1	3.06	-1.88
Dusp14	Dual specificity phosphatase 14	4.15	-2.44
Egr4	Early growth response 4	10.01	-4.16
Ehd4	EH domain containing 4	1.30	-1.30
Fgf13	Fibroblast growth factor 13	-1.29	1.26
Fos	Fos proto-oncogene, AP-1 transcription factor subunit	12.99	-4.94
Fosb	FosB proto-oncogene, AP-1 transcription factor subunit	17.17	-4.96
Frmd6	FERM domain containing 6	2.16	-1.59
Gaa	Glucosidase alpha, acid	1.46	-1.34
Gadd45b	Growth arrest and DNA damage-inducible beta	3.43	-1.76
Gadd45g	Growth arrest and DNA damage-inducible gamma	4.59	-2.92
Gpr3	G protein-coupled receptor 3	8.19	-3.95
Hspa5	Heat-shock protein family A (Hsp70) member 5	1.64	-1.41
Id1	Inhibitor of DNA binding 1, HLH protein	1.44	-1.57
Igsf9b	Immunoglobulin superfamily member 9B	1.93	-1.63
Inhba	Inhibin beta A subunit	5.76	-3.41

CREB1 target gene	Description	L-DOPA vs. Saline	L-DOPA + Riluzole vs. L-DOPA
Irs2	Insulin receptor substrate 2	6.01	-3.00
Jun	Jun proto-oncogene, AP-1 transcription factor subunit	2.45	-1.70
Junb	JunB proto-oncogene, AP-1 transcription factor subunit	7.83	-3.28
Klf4	Kruppel like factor 4	2.00	-1.60
Lmo1	LIM domain only 1	1.25	-1.23
Midn	Midnolin	2.52	-2.34
Ndufv1	NADH:ubiquinone oxidoreductase core subunit V1	1.19	-1.21
Nfil3	Nuclear factor, interleukin 3 regulated	2.08	-1.51
Npas4	Neuronal PAS domain protein 4	5.50	-5.07
Nptx2	Neuronal pentraxin 2	4.96	-2.70
Npy	Neuropeptide Y	1.72	-2.23
Nr4a1	Nuclear receptor subfamily 4 group A member 1	4.27	-2.15
Nr4a3	Nuclear receptor subfamily 4 group A member 3	10.26	-4.16
Nrgn	Neurogranin	1.56	-1.36
Pdxk	Pyridoxal kinase	1.93	-1.69
Pdyn	Prodynorphin	2.50	-1.75
Per1	Period circadian clock 1	2.18	-1.87
Pim3	Pim-3 proto-oncogene, serine/threonine kinase	1.41	-1.39
Plat	Plasminogen activator, tissue type	1.47	-1.48
Ptgs2	Prostaglandin-endoperoxide synthase 2	5.15	-3.08
Pvr	Poliovirus receptor	2.84	-2.34
Rem2	RRAD and GEM-like GTPase 2	5.42	-2.82
Rheb	Ras homolog enriched in brain	1.49	-1.18
Scg2	Secretogranin II	2.90	-1.69
Sema7a	Semaphorin 7A (John Milton Hagen blood group)	1.30	-1.27
Sertad1	SERTA domain containing 1	2.83	-1.74
Sh3kbp1	SH3 domain containing kinase binding protein 1	-1.15	1.13
Sik1	Salt-inducible kinase 1	3.10	-2.08
Slc32a1	Solute carrier family 32 member 1	1.79	-1.52
Srxn1	Sulfiredoxin 1	6.08	-3.28
Stat3	Signal transducer and activator of transcription 3	1.13	-1.13
Tac1	Tachykinin precursor 1	2,82	-1,92
Vegfa	Vascular endothelial growth factor A	1,33	-1,30

The proteins encoded by 43 of the 58 CREB1 target genes could be placed into a molecular landscape (Figure 3). In the supplementary results (Supplementary Materials), all the protein interactions in this landscape are described in great detail. That being said, we here give a succinct description of the main processes and signaling cascades in the landscape. Importantly, as the main signaling 'hub' in the landscape, CREB1 is a transcription factor that regulates the expression of many target genes involved in neuronal processes such as neuronal survival, differentiation, and development. Further, there are three main landscape cascades in the nucleus. First, the AP-1 transcription factor complex – consisting of JUN, FOS, JUNB and FOSB – binds and interacts with CREB1 and is regulated by and regulates the expression of a number of other landscape proteins, e.g., ATF3 and CREM. In addition, a complex of two functionally related transcription factors – NR4A1 and NR4A3, which regulate neuronal survival downstream of CREB1 – interacts with the AP-1 complex and is regulated by extracellular molecules that are involved in (dopaminergic) apoptosis,
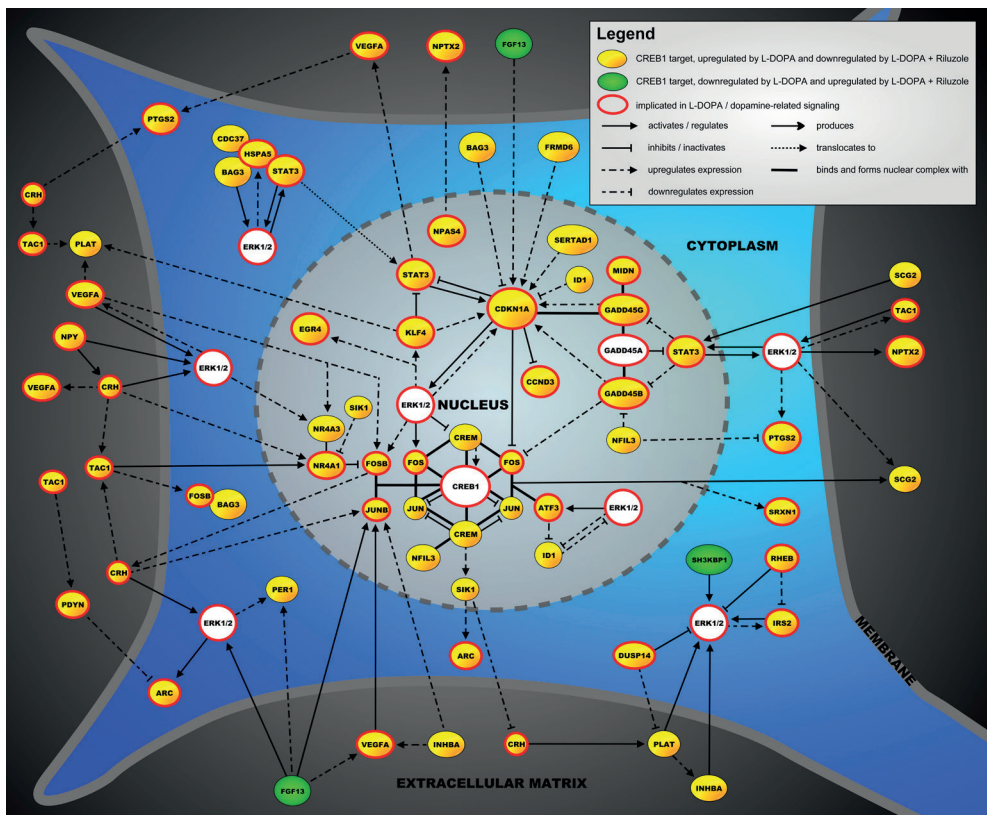
FIGURE 3. The molecular landscape is located in a neuron and shows the functional interactions between proteins encoded by 43 of the 58 CREB1 target genes regulated in the opposite direction by L-DOPA and after Riluzole co-administration in our AIMs model.

such as CRH, TAC1 and VEGFA. The third important signaling cascade in the nucleus centers around the transcription factors of the GADD45 family that regulate the neuronal stress response and apoptosis and interact with other transcription factors like CCND3 and CDKN1A. Further, most other landscape proteins interact with two proteins/protein complexes that regulate neuronal apoptosis and can be found both in the nucleus and cytoplasm, i.e., ERK1/2 and the adaptor protein STAT3. The signaling cascades dependent on ERK1/2 and STAT3 are in turn modulated by a number of extracellular proteins – e.g., FGF13, PLAT and SCG2 – and cytoplasmic regulators – e.g., DUSP14, HSPA5 and IRS2 – with prominent roles in neuronal function and survival.

qPCR validation of selected CREB1 targets

To provide an additional validation of the RNA sequencing data, we performed qPCR to assess and compare the mRNA expression levels of 10 selected CREB1 targets. In Supplementary Figure 4, the expression differences are shown for both comparisons (L-DOPA vs. Saline and L-DOPA + Riluzole vs. L-DOPA). As we were able to validate 8 of the 10 tested mRNA expression differences and the two other differences were not statistically significant but still in the right direction, we submit that the RNA sequencing data in general and the expression data for the CREB1 targets in particular indeed reflect true expression changes.

DISCUSSION

In the current study, we ascertained that 6-OHDA-lesioned rats treated with L-DOPA demonstrate clear AIMS and this is counteracted by chronic exposure to Riluzole, a drug that has already been shown to have some effect on attenuating AIMS in previous studies. Our experiments revealed that Riluzole induces mRNA expression changes in the rat striatum that are tightly linked to the occurrence of L-DOPA-induced AIMs.

Our findings point towards the regulation of apoptosis as a key molecular mechanism underlying both the effect of chronic L-DOPA administration – with the accompanying AIMs – and the 'rebalancing' effect of Riluzole, leading to a reduction of AIMs. In general terms, the landscape that we built based on the CREB1 targets that were expressed in the opposite direction in the AIMs model and after Riluzole administration suggests that chronic administration of L-DOPA tilts the neuronal survival/apoptosis balance towards increased survival (and hence less apoptosis). Conversely, Riluzole administration leads to a reversal of this balance towards less survival and more apoptosis. Indeed, most of the landscape genes encode proteins that have anti-apoptotic properties, and these genes are upregulated after chronic L-DOPA administration, an effect that is counteracted by Riluzole. Mechanistically,

3

as derived from the upstream regulator analysis, the effect of Riluzole is mediated through decreasing the activation of CREB1, i.e., CREB1 (and hence the regulation of its downstream targets) is predicted to be activated upon exposure to L-DOPA and inhibited after adding Riluzole. CREB1 acts as a functional 'go-between' between cytoplasmic kinase/enzyme signaling cascades and nuclear regulation of gene expression. More specifically, CREB1 is known to be activated through phosphorylation by kinases such as ERK1/2 [44] and protein kinase C (PKC) [45] (see subsequent texts), which in turn leads to reduced neuronal apoptosis through the upregulation of anti-apoptotic gene expression by activated CREB1 [46]. In addition, L-DOPA administration to 6-OHDA-lesioned rats was found to markedly increase CREB1 phosphorylation in striatal neurons [47,48] and, interestingly, a very recent study showed that Riluzole reduces neuronal CREB1 phosphorylation [49].

As for how Riluzole would decrease CREB1 activity, there are some clues from the literature. Taken together with our results, these literature findings have led us to propose a putative molecular mechanism – shown in Figure 4 – through which Riluzole could decrease CREB1 activity, modulate apoptosis and ultimately reduce AIMs. First, and as pointed out previously, Riluzole mainly exerts anti-glutamatergic effects which, through a number of mechanisms [27-31], lead to reduced glutamatergic neurotransmission. When activated by glutamate, postsynaptic NMDA receptors activate ERK1/2, kinases with an important role in our landscape that subsequently phosphorylate – and hence activate – CREB1 [44]. These data imply that through its anti-glutamatergic effects, Riluzole would decrease CREB1 activity by reducing NMDA receptor-induced ERK1/2 signaling. Second, Riluzole is a potent intracellular inhibitor of PKC [50], a kinase that positively regulates NMDA receptor function [51] and phosphorylates/activates CREB1, either directly or through activating ERK1/2 [45]. Although not shown in Figure 4, a recent paper reported that Riluzole also reduces presynaptic glutamatergic vesicle recycling and, hence, the size of the readily releaseable glutamate pool through inhibiting PKC [31]. Further, it is interesting that glutamate-induced activation of CREB1 is (partially) blocked by inhibiting ERK1/2 with U0126 [52], a compound that, as opposed to CREB1, is predicted to be inhibited after exposure to L-DOPA and activated by adding Riluzole (see Supplementary Table 2).

Although our study yielded interesting findings, it has some limitations. First, while chronic L-DOPA administration is thought to be the main contributor to the AIMs phenotype through its effect on striatal projection neurons – i.e., through promoting dopamine receptor hypersensitivity in these neurons – lesioning with 6-OHDA affects dopaminergic as well as noradrenergic neurons. As such, a contribution of 6-OHDA-induced noradrenergic denervation to the AIMs phenotype cannot be excluded. In addition, although our results indicate that the effect of Riluzole on reducing AIMs is mediated through lowering CREB1

activity, further studies are needed to confirm that Riluzole (in)directly decreases CREB1 activity through reducing its phosphorylation. In this respect, it is interesting to note that the literature provides some corroborating evidence that phosphorylation-dependent CREB1 activation is indeed an important contributing factor to the development of AIMs.
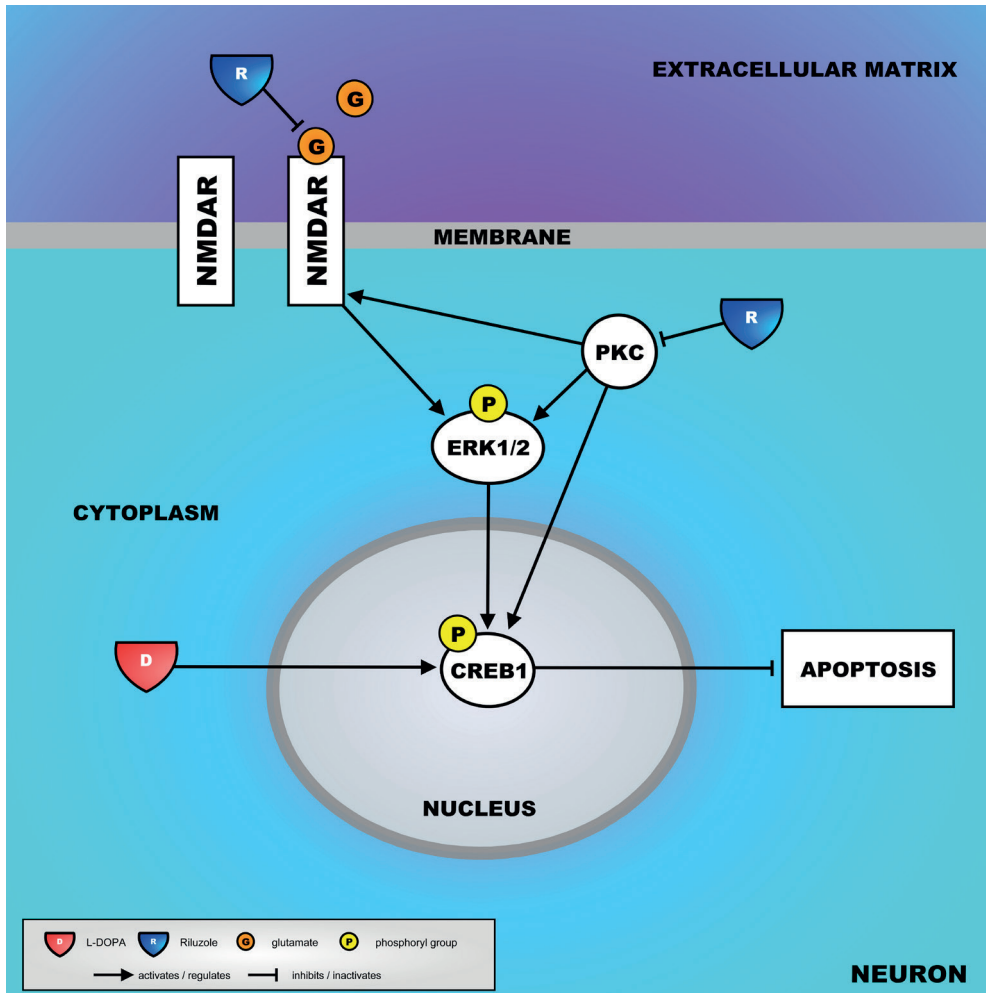
FIGURE 4. Putative mechanisms of how Riluzole could counteract CREB1-mediated gene expression by decreasing the activity of CREB1. Firstly, through a number of mechanisms, Riluzole reduces glutamatergic neurotransmission, which includes less glutamate binding to postsynaptic NMDA glutamate receptors. As a result, NMDA-mediated ERK1/2 signaling and the subsequent activation of CREB1 are also reduced. Secondly, Riluzole could inhibit PKC, a kinase that positively regulates NMDA receptors and activates CREB1 (directly or through activating ERK1/2), leading to a reduced CREB1 activity. The key players in this mechanism – L-DOPA, NMDA glutamate receptors, the kinases ERK1/2 and PKC, and CREB1 itself – are shown.

For example, psychostimulants such as amphetamines and cocaine, and other drugs such as the antipsychotic aripiprazole – that are all known to induce AIMs [53-55] – promote phosphorylation-dependent CREB1 activation in (striatal) neurons [56-58]. Therefore, in addition to confirming the effect of Riluzole, future studies could test other (novel or existing) drugs for their positive effect on AIMs (and LID) through decreasing CREB1 activity.

In conclusion, we have demonstrated that Riluzole attenuates AIMs in 6-OHDA-lesioned rats that were chronically treated with L-DOPA. In addition, RNA sequencing analysis revealed that Riluzole reverses the expression direction of genes regulating mainly pro-apoptotic processes, downstream of activated CREB1. This molecular mechanism underlying the beneficial effect of Riluzole needs to be confirmed in future studies and can be leveraged to design AIMs/LID treatment studies using novel and/or existing compounds.

Author contributions

Conceived and designed the experiments: LP, JW, EN, BH, GP; Performed the experiments: LP, JW, EN, TH; Analyzed the data: LP, JW, EN, TH, GP; Wrote the paper: LP, JW, EN, JG, BH, GP; Reviewed and approved the final version of the manuscript: All authors

Acknowledgements

Conflicts of interest

Boehringer Ingelheim Pharma GmbH& Co. provided support in the form of salary for authors BH and TH, but it did not have any additional role in the study design, data collection and analysis, decision to publish, or preparation of the manuscript.

REFERENCES

1. Maas, R.; Wassenberg, T.; Lin, J.P.; van de Warrenburg, B.P.C.; Willemsen, M. l-Dopa in dystonia: A modern perspective. *Neurology* **2017**, *88*, 1865-1871, doi:10.1212/wnl.0000000000003897.

2. Dekundy, A.; Lundblad, M.; Danysz, W.; Cenci, M.A. Modulation of L-DOPA-induced abnormal involuntary movements by clinically tested compounds: further validation of the rat dyskinesia model. *Behavioural brain research* **2007**, *179*, 76-89, doi:10.1016/j.bbr.2007.01.013.

3. Ahlskog, J.E.; Muenter, M.D. Frequency of levodopa-related dyskinesias and motor fluctuations as estimated from the cumulative literature. *Movement disorders : official journal of the Movement Disorder Society* **2001**, *16*, 448-458.

4. Huot, P.; Johnston, T.H.; Koprich, J.B.; Fox, S.H.; Brotchie, J.M. The pharmacology of L-DOPA-induced dyskinesia in Parkinson's disease. *Pharmacological reviews* **2013**, *65*, 171-222, doi:10.1124/pr.111.005678.

5. Ahmed, I.; Bose, S.K.; Pavese, N.; Ramlackhansingh, A.; Turkheimer, F.; Hotton, G.; Hammers, A.; Brooks, D.J. Glutamate NMDA receptor dysregulation in Parkinson's disease with dyskinesias. *Brain : a journal of neurology* **2011**, *134*, 979-986, doi:10.1093/brain/awr028.

6. Chase, T.N.; Oh, J.D. Striatal mechanisms and pathogenesis of parkinsonian signs and motor complications. *Annals of neurology* **2000**, *47*, S122-129; discussion S129-130.

7. Bordet, R.; Ridray, S.; Schwartz, J.C.; Sokoloff, P. Involvement of the direct striatonigral pathway in levodopa-induced sensitization in 6-hydroxydopamine-lesioned rats. *The European journal of neuroscience* **2000**, *12*, 2117-2123.

8. Solis, O.; Garcia-Montes, J.R.; Gonzalez-Granillo, A.; Xu, M.; Moratalla, R. Dopamine D3 Receptor Modulates l-DOPA-Induced Dyskinesia by Targeting D1 Receptor-Mediated Striatal Signaling. *Cerebral cortex (New York, N.Y. : 1991)* **2017**, *27*, 435-446, doi:10.1093/cercor/bhv231.

9. Charbonnier-Beaupel, F.; Malerbi, M.; Alcacer, C.; Tahiri, K.; Carpentier, W.; Wang, C.; During, M.; Xu, D.; Worley, P.F.; Girault, J.A.; et al. Gene expression analyses identify Narp contribution in the development of L-DOPA-induced dyskinesia. *The Journal of neuroscience : the official journal of the Society for Neuroscience* **2015**, *35*, 96-111, doi:10.1523/jneurosci.5231-13.2015.

10. Santini, E.; Feyder, M.; Gangarossa, G.; Bateup, H.S.; Greengard, P.; Fisone, G. Dopamine- and cAMP-regulated phosphoprotein of 32-kDa (DARPP-32)-dependent activation of extracellular signal-regulated kinase (ERK) and mammalian target of rapamycin complex 1 (mTORC1) signaling in experimental parkinsonism. *The Journal of biological chemistry* **2012**, *287*, 27806-27812, doi:10.1074/jbc.M112.388413.

11. Song, L.; Zhang, Z.; Hu, R.; Cheng, J.; Li, L.; Fan, Q.; Wu, N.; Gan, J.; Zhou, M.; Liu, Z. Targeting the D1-N-methyl-D-aspartate receptor complex reduces L-dopa-induced dyskinesia in 6-hydroxydopamine-lesioned Parkinson's rats. *Drug design, development and therapy* **2016**, *10*, 547-555, doi:10.2147/dddt.s93487.

12. Pavon, N.; Martin, A.B.; Mendialdua, A.; Moratalla, R. ERK phosphorylation and FosB expression are associated with L-DOPA-induced dyskinesia in hemiparkinsonian mice. *Biological psychiatry* **2006**, *59*, 64-74, doi:10.1016/j.biopsych.2005.05.044.

13. Cerovic, M.; Bagetta, V.; Pendolino, V.; Ghiglieri, V.; Fasano, S.; Morella, I.; Hardingham, N.; Heuer, A.; Papale, A.; Marchisella, F.; et al. Derangement of Ras-guanine nucleotide-releasing factor 1 (Ras-GRF1) and extracellular signal-regulated kinase (ERK) dependent striatal plasticity in L-DOPA-induced dyskinesia. *Biological psychiatry* **2015**, *77*, 106-115, doi:10.1016/j.biopsych.2014.04.002.

14. Gerfen, C.R.; Miyachi, S.; Paletzki, R.; Brown, P. D1 dopamine receptor supersensitivity in the dopamine-depleted striatum results from a switch in the regulation of ERK1/2/MAP kinase. *The Journal of neuroscience : the official journal of the Society for Neuroscience* **2002**, *22*, 5042-5054.

15. Westin, J.E.; Vercammen, L.; Strome, E.M.; Konradi, C.; Cenci, M.A. Spatiotemporal pattern of striatal ERK1/2 phosphorylation in a rat model of L-DOPA-induced dyskinesia and the role of dopamine D1 receptors. *Biological psychiatry* **2007**, *62*, 800-810, doi:10.1016/j.biopsych.2006.11.032.

16. Heiman, M.; Heilbut, A.; Francardo, V.; Kulicke, R.; Fenster, R.J.; Kolaczyk, E.D.; Mesirov, J.P.; Surmeier, D.J.; Cenci, M.A.; Greengard, P. Molecular adaptations of striatal spiny projection neurons during levodopa-induced dyskinesia. *Proceedings of the National Academy of Sciences of the United States of America* **2014**, *111*, 4578-4583, doi:10.1073/pnas.1401819111.

17. Figge, D.A.; Eskow Jaunarajs, K.L.; Standaert, D.G. Dynamic DNA Methylation Regulates Levodopa-Induced Dyskinesia. *The Journal of neuroscience : the official journal of the Society for Neuroscience* **2016**, *36*, 6514-6524, doi:10.1523/jneurosci.0683-16.2016.

18. Lundblad, M.; Usiello, A.; Carta, M.; Hakansson, K.; Fisone, G.; Cenci, M.A. Pharmacological validation of a mouse model of l-DOPA-induced dyskinesia. *Experimental neurology* **2005**, *194*, 66-75, doi:10.1016/j.expneurol.2005.02.002.

19. Marin, C.; Jimenez, A.; Bonastre, M.; Chase, T.N.; Tolosa, E. Non-NMDA receptor-mediated mechanisms are involved in levodopa-induced motor response alterations in Parkinsonian rats. *Synapse (New York, N.Y.)* **2000**, *36*, 267-274, doi:10.1002/(sici)1098-2396(20000615)36:4<267::aid-syn3>3.0.co;2-y.

20. Merims, D.; Ziv, I.; Djaldetti, R.; Melamed, E. Riluzole for levodopa-induced dyskinesias in advanced Parkinson's disease. *Lancet (London, England)* **1999**, *353*, 1764-1765, doi:10.1016/s0140-6736(99)00120-8.

21. Bara-Jimenez, W.; Dimitrova, T.D.; Sherzai, A.; Aksu, M.; Chase, T.N. Glutamate release inhibition ineffective in levodopa-induced motor complications. *Movement disorders : official journal of the Movement Disorder Society* **2006**, *21*, 1380-1383, doi:10.1002/mds.20976.

22. Albo, F.; Pieri, M.; Zona, C. Modulation of AMPA receptors in spinal motor neurons by the neuroprotective agent riluzole. *Journal of neuroscience research* **2004**, *78*, 200-207, doi:10.1002/jnr.20244.

23. De Sarro, G.; Siniscalchi, A.; Ferreri, G.; Gallelli, L.; De Sarro, A. NMDA and AMPA/kainate receptors are involved in the anticonvulsant activity of riluzole in DBA/2 mice. *European journal of pharmacology* **2000**, *408*, 25-34.

24. Fumagalli, E.; Funicello, M.; Rauen, T.; Gobbi, M.; Mennini, T. Riluzole enhances the activity of glutamate transporters GLAST, GLT1 and EAAC1. *European journal of pharmacology* **2008**, *578*, 171-176, doi:10.1016/j.ejphar.2007.10.023.

25. Wang, S.J.; Wang, K.Y.; Wang, W.C. Mechanisms underlying the riluzole inhibition of glutamate release from rat cerebral cortex nerve terminals (synaptosomes). *Neuroscience* **2004**, *125*, 191-201, doi:10.1016/j.neuroscience.2004.01.019.

26. Stevenson, A.; Yates, D.M.; Manser, C.; De Vos, K.J.; Vagnoni, A.; Leigh, P.N.; McLoughlin, D.M.; Miller, C.C. Riluzole protects against glutamate-induced slowing of neurofilament axonal transport. *Neuroscience letters* **2009**, *454*, 161-164, doi:10.1016/j.neulet.2009.02.061.

27. Kretschmer, B.D.; Kratzer, U.; Schmidt, W.J. Riluzole, a glutamate release inhibitor, and motor behavior. *Naunyn-Schmiedeberg's archives of pharmacology* **1998**, *358*, 181-190.

28. Urbani, A.; Belluzzi, O. Riluzole inhibits the persistent sodium current in mammalian CNS neurons. *The European journal of neuroscience* **2000**, *12*, 3567-3574.

29. Kim, J.E.; Kim, D.S.; Kwak, S.E.; Choi, H.C.; Song, H.K.; Choi, S.Y.; Kwon, O.S.; Kim, Y.I.; Kang, T.C. Anti-glutamatergic effect of riluzole: comparison with valproic acid. *Neuroscience* **2007**, *147*, 136-145, doi:10.1016/j.neuroscience.2007.04.018.

30. Erickson, J.D. Functional identification of activity-regulated, high-affinity glutamine transport in hippocampal neurons inhibited by riluzole. *Journal of neurochemistry* **2017**, *142*, 29-40, doi:10.1111/jnc.14046.

31. Lazarevic, V.; Yang, Y.; Ivanova, D.; Fejtova, A.; Svenningsson, P. Riluzole attenuates the efficacy of glutamatergic transmission by interfering with the size of the readily releasable neurotransmitter pool. *Neuropharmacology* **2018**, *143*, 38-48, doi:10.1016/j.neuropharm.2018.09.021.

32. Jehle, T.; Bauer, J.; Blauth, E.; Hummel, A.; Darstein, M.; Freiman, T.M.; Feuerstein, T.J. Effects of riluzole on electrically evoked neurotransmitter release. *British journal of pharmacology* **2000**, *130*, 1227-1234, doi:10.1038/sj.bjp.0703424.

33. Winkler, C.; Kirik, D.; Bjorklund, A.; Cenci, M.A. L-DOPA-induced dyskinesia in the intrastriatal 6-hydroxydopamine model of parkinson's disease: relation to motor and cellular parameters of nigrostriatal function. *Neurobiology of disease* **2002**, *10*, 165-186.

34. Dobin, A.; Davis, C.A.; Schlesinger, F.; Drenkow, J.; Zaleski, C.; Jha, S.; Batut, P.; Chaisson, M.; Gingeras, T.R. STAR: ultrafast universal RNA-seq aligner. *Bioinformatics (Oxford, England)* **2013**, *29*, 15-21, doi:10.1093/bioinformatics/bts635.

35. DeLuca, D.S.; Levin, J.Z.; Sivachenko, A.; Fennell, T.; Nazaire, M.D.; Williams, C.; Reich, M.; Winckler, W.; Getz, G. RNA-SeQC: RNA-seq metrics for quality control and process optimization. *Bioinformatics (Oxford, England)* **2012**, *28*, 1530-1532, doi:10.1093/bioinformatics/bts196.

36. Sayols, S.; Scherzinger, D.; Klein, H. dupRadar: a Bioconductor package for the assessment of PCR artifacts in RNA-Seq data. *BMC bioinformatics* **2016**, *17*, 428, doi:10.1186/s12859-016-1276-2.

37. Trapnell, C.; Hendrickson, D.G.; Sauvageau, M.; Goff, L.; Rinn, J.L.; Pachter, L. Differential analysis of gene regulation at transcript resolution with RNA-seq. *Nature biotechnology* **2013**, *31*, 46-53, doi:10.1038/nbt.2450.

38. Liao, Y.; Smyth, G.K.; Shi, W. featureCounts: an efficient general purpose program for assigning sequence reads to genomic features. *Bioinformatics (Oxford, England)* **2014**, *30*, 923-930, doi:10.1093/bioinformatics/btt656.

39. Huber, W.; Carey, V.J.; Gentleman, R.; Anders, S.; Carlson, M.; Carvalho, B.S.; Bravo, H.C.; Davis, S.; Gatto, L.; Girke, T.; et al. Orchestrating high-throughput genomic analysis with Bioconductor. *Nature Methods* **2015**, *12*, 115, doi:10.1038/nmeth.3252.

40. Law, C.W.; Chen, Y.; Shi, W.; Smyth, G.K. voom: precision weights unlock linear model analysis tools for RNA-seq read counts. *Genome Biology* **2014**, *15*, R29, doi:10.1186/gb-2014-15-2-r29.

41. Oliveros, J. VENNY. An interactive tool for comparing lists with Venn diagrams. *BioinfoGP, CNB-CSIC*, doi:citeulike-article-id:6994833.

42. Wu, W.S.; Li, W.H. Systematic identification of yeast cell cycle transcription factors using multiple data sources. *BMC bioinformatics* **2008**, *9*, 522, doi:10.1186/1471-2105-9-522.

43. The UniProt Consortium. UniProt: the universal protein knowledgebase. *Nucleic Acids Research* **2017**, *45*, D158-D169, doi:10.1093/nar/gkw1099.

44. Marini, A.M.; Jiang, H.; Pan, H.; Wu, X.; Lipsky, R.H. Hormesis: a promising strategy to sustain endogenous neuronal survival pathways against neurodegenerative disorders. *Ageing Res Rev* **2008**, *7*, 21-33, doi:10.1016/j.arr.2007.07.003.

45. Mao, L.M.; Tang, Q.; Wang, J.Q. Protein kinase C-regulated cAMP response element-binding protein phosphorylation in cultured rat striatal neurons. *Brain Res Bull* **2007**, *72*, 302-308, doi:10.1016/j.brainresbull.2007.01.009.

46. Mantamadiotis, T.; Lemberger, T.; Bleckmann, S.C.; Kern, H.; Kretz, O.; Martin Villalba, A.; Tronche, F.; Kellendonk, C.; Gau, D.; Kapfhammer, J.; et al. Disruption of CREB function in brain leads to neurodegeneration. *Nature genetics* **2002**, *31*, 47-54, doi:10.1038/ng882.

47. Cole, D.G.; Kobierski, L.A.; Konradi, C.; Hyman, S.E. 6-Hydroxydopamine lesions of rat substantia nigra up-regulate dopamine-induced phosphorylation of the cAMP-response element-binding protein in striatal neurons. *Proceedings of the National Academy of Sciences of the United States of America* **1994**, *91*, 9631-9635.

48. Oh, J.D.; Chartisathian, K.; Ahmed, S.M.; Chase, T.N. Cyclic AMP responsive element binding protein phosphorylation and persistent expression of levodopa-induced response alterations in unilateral nigrostriatal 6-OHDA lesioned rats. *Journal of neuroscience research* **2003**, *72*, 768-780, doi:10.1002/jnr.10629.

49. Akagi, K.; Yamada, M.; Saitoh, A.; Oka, J.I.; Yamada, M. Post-reexposure administration of riluzole attenuates the reconsolidation of conditioned fear memory in rats. *Neuropharmacology* **2018**, *131*, 1-10, doi:10.1016/j.neuropharm.2017.12.009.

50. Noh, K.M.; Hwang, J.Y.; Shin, H.C.; Koh, J.Y. A novel neuroprotective mechanism of riluzole: direct inhibition of protein kinase C. *Neurobiology of disease* **2000**, *7*, 375-383, doi:10.1006/nbdi.2000.0297.

51. Lamanauskas, N.; Nistri, A. Riluzole blocks persistent Na+ and Ca2+ currents and modulates release of glutamate via presynaptic NMDA receptors on neonatal rat hypoglossal motoneurons in vitro. *The European journal of neuroscience* **2008**, *27*, 2501-2514, doi:10.1111/j.1460-9568.2008.06211.x.

52. Perkinton, M.S.; Ip, J.K.; Wood, G.L.; Crossthwaite, A.J.; Williams, R.J. Phosphatidylinositol 3-kinase is a central mediator of NMDA receptor signalling to MAP kinase (Erk1/2), Akt/PKB and CREB in striatal neurones. *Journal of neurochemistry* **2002**, *80*, 239-254.

53. Lane, E.L.; Brundin, P.; Cenci, M.A. Amphetamine-induced abnormal movements occur independently of both transplant- and host-derived serotonin innervation following neural grafting in a rat model of Parkinson's disease. *Neurobiology of disease* **2009**, *35*, 42-51, doi:10.1016/j.nbd.2009.03.014.

54. Jesic, M.P.; Jesic, A.; Filipovic, J.B.; Zivanovic, O. Extrapyramidal syndromes caused by antipsychotics. *Medicinski pregled* **2012**, *65*, 521-526.

55. Maat, A.; Fouwels, A.; de Haan, L. Cocaine is a major risk factor for antipsychotic induced akathisia, parkinsonism and dyskinesia. *Psychopharmacology bulletin* **2008**, *41*, 5-10.

56. Kreibich, A.S.; Briand, L.; Cleck, J.N.; Ecke, L.; Rice, K.C.; Blendy, J.A. Stress-induced potentiation of cocaine reward: a role for CRF R1 and CREB. *Neuropsychopharmacology : official publication of the American College of Neuropsychopharmacology* **2009**, *34*, 2609-2617, doi:10.1038/npp.2009.91.

57. Madsen, H.B.; Navaratnarajah, S.; Farrugia, J.; Djouma, E.; Ehrlich, M.; Mantamadiotis, T.; Van Deursen, J.; Lawrence, A.J. CREB1 and CREB-binding protein in striatal medium spiny neurons regulate behavioural responses to psychostimulants. *Psychopharmacology (Berl)* **2012**, *219*, 699-713, doi:10.1007/s00213-011-2406-1.

58. Pan, B.; Huang, X.F.; Deng, C. Chronic administration of aripiprazole activates GSK3beta-dependent signalling pathways, and up-regulates GABAA receptor expression and CREB1 activity in rats. *Scientific reports* **2016**, *6*, 30040, doi:10.1038/srep30040.

3

SUPPLEMENTARY MATERIALS

Supplementary Data file 1 can be accessed via the publication online: https://doi.org/10.1007/s12035-018-1433-x or through: http://gofile.me/5Nxbd/IvkZFnkGE.

Supplementary Methods

Stereotaxic surgery

After 1 week of habituation at post-natal day (PND) 21 (n=48), rats were separated from their mothers and were stereotaxically injected with a 4.4 µg/µl solution of 6-hydroxydopamine hydrobromide (6-OHDA, Sigma-Aldrich, Germany) in 0.02% ascorbate solution (4µl of injected volume at a speed of 0.3 µL/min) into the left medial forebrain bundle (MFB) according to the following coordinates calculated (in cm) from bregma: Anterior Posterior= -0.41, Medial Lateral=+0.15, Dorsal Ventral= -0.75. After injection, the needle was left in place for 3 additional minutes and then retracted. Surgical anesthesia was induced with 4.5% isoflurane in N_2O/O_2 (70: 30) and reduced to a minimum of 1.2-1.5% isoflurane to ensure anesthesia maintenance. Analgesia was provided with Meloxicam (1mg/kg SC in 2mg/ml injection volume, Boehringer Ingelheim Vetmedica GmbH, Germany) 20 minutes before the surgical procedure took place and at its end. After recovery, rats were housed in groups of 5 siblings to prevent isolation.

Striatal DA determination through HPLC

DA levels in 12 6-OHDA-lesioned striata compared to their contralateral controls were quantified using HPLC coupled to ECD. Frozen samples were homogenized by sonication in a solution of 0.4 N perchloric acid and centrifuged for 20 min at 4 °C. Supernatants were filtered and used for DA quantification. The HPLC system was composed of an HPLC P680 ISO isocratic pump system and an automated ASI-100 sample injector (Dionex, Dreieich, Germany). The electrochemical detector was set at the potential of +650 mV using a glassy carbon electrode and an Ag/AgCl reference electrode (Antec VT-03, Zoeterwoude, Netherlands). A reversed-phase column (100 x 2.1 mm i.d. with pre-column 10 x 2.1 mm i.d., filled with ODS-AQ, 120 Å, 3 µm, YMC Europe GmbH, Dinslaken, Germany) was used for chromatographic separation. The mobile phase consisted of 1.7 mM of 1-octanesulfonic acid sodium salt, 1.0 mM Na2EDTA x 2 H2O, 8.0 mMNaCl, 100.0 mM NaH2PO4 x 2 H2O, adjusted to pH 3.80 with H3PO4, filtered through a 0.22 µm filter (Merck Millipore, Darmstadt, Germany), mixed up with 9.3 % acetonitrile, and delivered with a flow rate of 0.4 ml/min. Aliquots of 10uL were injected by an autosampler with a cooling module temperature of 4°C (ASI-100, Thermo Scientific Dionex, Dreieich, Germany). DA was quantified through the comparison with an external five-point standard calibration. Chromeleon™ 7.1 software (Thermo Scientific Dionex, Dreieich, Germany) was used for data acquisition and calculation.

Supplementary Results

Description of the molecular landscape

As described in the Methods section, we built a molecular landscape located in a neuron that is based on a subset of genes/mRNAs that were differentially expressed between three groups of rats and are all downstream expression targets of CREB1 (cAMP response element binding protein 1). All these genes are listed in Supplementary Data file 1 and in the description below; the proteins encoded by these genes are indicated in bold. Moreover, the evidence linking a number of these genes/proteins to L-DOPA signaling is presented.

Signaling in the molecular landscape originates in the nucleus and is centered around CREB1. As main signaling 'hub' in the landscape, CREB1 is an important transcription factor that regulates the expression of a large number of target genes involved in many neuronal processes, including neuronal survival, differentiation and development. L-DOPA has been found to directly activate the transcriptional function of CREB1 in striatal neurons [1,2]. Another important member of the CREB transcription factor family is **CREM** [3] which binds [4] and is involved in regulating the expression of CREB1 [5]. The CREB1-**CREM** complex also binds and interacts with **FOS** and **JUN** [6]. **FOS** and **JUN** bind each other as well as **FOSB** and **JUNB**. **FOS**, **JUN**, **FOSB** and **JUNB** are part of the AP-1 complex of transcription factors that interacts with CREB1 [7-11] and is known to play a role in apoptosis of (neuronal) cells in response to stress, DNA damaging agents and a general lack of 'survival signals' [12]. Further, CREB1 and **CREM** inhibit the transcriptional activity of **JUN** [6]. In addition, **FOS** and **JUN** interact with **ATF3** [13] and **CREM** interacts with the transcription factor **NFIL3** [14] (see below). **JUN** regulates neuronal differentiation and cell survival. More specifically, **JUN** protects against apoptosis in differentiated PC12 cells that are often used as a model of neuronal differentiation [15]. Interestingly, increased expression levels of **Fos** were reported in rodents that had been injected with 6-hydroxy-dopamine (6-OHDA) [16,17] and subsequently treated with L-DOPA [18-20]. L-DOPA administration also produces a long-lasting increase in the expression levels of **FosB** but not **JunB** [21]. In keeping with these finding, **JunB** was shown to protect against the death of nigral neurons [22].

Furthermore, the extracellular signal-regulated kinases 1 and 2 (ERK1/2) – that can function in both the cytoplasm and nucleus – activate both CREB1 and **CREM** (not shown) [23,24]. In addition, ERK1/2 are involved in increasing the expression of **FOSB** [25] and activate **FOS** [26,27] and **ATF3** [28]. ERK1/2 were originally identified as kinases that regulate neuronal survival and neuroprotection but subsequently, it was found that ERK1/2 also play a critical role in secondary damage mechanisms implicated in a number of neurodegenerative diseases, stroke, CNS injury, and autoimmune diseases of the CNS [29-34]. In addition, a number of studies reported that activation of ERK1/2 in the dopamine-depleted striatum is

induced by L-DOPA administration [35-39]. **ATF3** and ERK1/2 are involved in decreasing the expression of **ID1** [40,41], an anti-apoptotic transcription factor [42], while **ID1** decreases the expression of ERK1/2 [43]. Further, under normal circumstances, **ATF3** is expressed at low levels in both neurons and glia cells but its expression is upregulated in response to injury or stressful stimuli, after which it positively regulates the survival of these cells [44]. In line with our findings, a chromatin immunoprecipitation (ChIP) study also showed that in 6-OHDA-lesioned striata of mice, the expression of **Atf3** as well as the transcription factors **Klf4** and **Npas4** (see below) was upregulated after acute L-DOPA administration [45].

Moreover, **NR4A1** and **NR4A3** belong to the NR4A orphan nuclear receptor family of transcription factors that is rapidly and strongly upregulated after stressful insults to the CNS. NR4A transcription factors are essential for neuronal survival downstream of CREB(1) signaling and may be suitable targets for intervention in neurodegenerative disease [46].

In the MPTP mouse model of PD, **Nr4a1** activation protects dopaminergic neurons [47]. In addition, *Nr4a1* knockout mice display higher locomotor activity, a greater sensitivity to dopamine [48] and increased L-DOPA-induced rotational behavior [49]. Further, **Nr4a1** expression was increased in the caudate nucleus and putamen upon L-DOPA treatment in MPTP monkeys (that are a non-human primate model of PD) [50]. Lastly, *NR4A1* expression was found to be decreased in the blood of PD patients [51]. All these findings are in line with our results showing an overexpression of **NR4A1**. Within the landscape, **NR4A1** binds and forms a functional complex with **NR4A3** [52], **NR4A1** decreases the activity of **FOSB** [53] and the kinase **SIK1** – which can be found in both the nucleus and cytoplasm and is upregulated by **CREM** [54] – reduces **NR4A1** expression [55]. In addition, **TAC1** – an extracellular, potently anti-apoptotic protein [56] that was also found to be increased in a primate model of L-DOPA induced dyskinesia [57] – activates **NR4A1** [58] and upregulates the expression of **FOSB** [59], which apart from the nucleus can also be found in the cytoplasm, were it forms a functional complex with **BAG3**, a co-chaperone protein that regulates neuronal apoptosis and autophagy [60,61]. Interestingly, **Bag3**-mediated autophagy is also involved in the clearance of aggregated proteins associated with age-related neurodegenerative disorders [62-64]. Lastly, corticotropin-releasing hormone (**CRH**) – which functions as a neurotransmitter in the central nervous system (CNS) [65] and regulates neuronal apoptosis [66] as well as dopaminergic neuron function [67] – increases the expression of **JUNB** [68], while **FOSB** increases the expression of **CRH** [69]. Further, **CRH** upregulates the expression of **NR4A1** [70], **TAC1** [71] and the growth factor (see below) **VEGFA** [72] and it activates ERK1/2 [73]. In turn, ERK1/2 upregulates **NR4A3** [74].

Another signaling cascade in the landscape centers around **CDKN1A**, a transcription factor that is also known as p21 (WAF1/CIP1) and is involved in 6-OHDA-induced

dopaminergic cell death [75]. **CDKN1A** inhibits **FOS** and **JUN** [76] while it activates ERK1/2 [77]. **KLF4** and ERK1/2 are involved in upregulating **CDKN1A** expression [77,78], while ERK1/2 also increases the expression of **KLF4** [79]. Further, the growth factor **FGF13** (see below), the transcription factor **SERTAD1** and the cytoplasmic protein **FRMD6** all increase the expression of **CDKN1A** [80-82], whereas **ID1** and **BAG3** decrease its expression [83,84]. **CDKN1A** also inhibits **CCND3** [85], a nuclear regulator of the cell cycle that was found to be significantly increased during 6-OHDA-induced apoptosis of dopaminergic neurons, which is interesting given that loss of cell cycle control has been suggested to lead to death of dopaminergic neurons observed in Parkinson's disease (PD) [86]. Moreover, **GADD45G** – a member of the GADD45 family of nuclear proteins that have an important role in regulating the neuronal stress response and apoptosis [87] – binds, interacts with, and increases the expression of **CDKN1A** [88] and also binds/interacts with **MIDN** [89], a nuclear protein encoded by a gene that has been strongly linked to Parkinson's disease [90,91]. **GADD45G**, **GADD45A** and **GADD45B** – which also upregulates **CDKN1A** expression [92] – bind and form a functional complex [93]. Interestingly, knockout of *Gadd45b* in the L-DOPA-induced dyskinesia (LID)-rodent model results in an increased expression of **Fos** and **FosB** [94], which implies that **GADD45B** downregulates the expression of **FOS** and **FOSB** (not shown). Another study on LID showed that the expression of **Gadd45b** and **Gadd45g** is increased in the lesioned side of the striatum after L-DOPA administration [95]. **Gadd45a** is also involved in 6-OHDA-induced brain toxicity in rats [96]. **NFIL3 –** a transcription factor that plays a neuroprotective role in neurons and constitutes a potential therapeutic target for neurodegeneration [97] – also downregulates the expression of **GADD45B** [98].

Multiple landscape proteins interact with **STAT3**, a protein that can function in both the cytoplasm and nucleus. **STAT3**-dependent signaling plays an important role in counteracting 6-OHDA-induced neuronal cell death by promoting compensatory neuronal proliferation [99]. In the nucleus, **STAT3** is involved in downregulating the expression of **GADD45B** and **GADD45G** [100,101], while it is inhibited by **GADD45A** [102] and **KLF4** [103]. Further, **STAT3** activates **CDKN1A** [104], whereas **CDKN1A** inhibits **STAT3** [105]. In the cytoplasm, **STAT3** forms a functional complex with **HSPA5**, which in turn binds and interacts with **CDC37** and **BAG3** [106,107]. **HSPA5** and **CDC37** are regulators of normal protein homeostasis and the unfolded protein response under physiological stimulation [108-110]. Moreover, it has been reported that increased levels of **Hspa5** protein protect against dopaminergic neurodegeneration in a rat model of PD [111]. ERK1/2 also upregulates **HSPA5** expression [112] while **BAG3** inhibits ERK1/2 function [113]. In addition, **STAT3** and ERK1/2 activate each other [114,115]. **STAT3** is involved in upregulating the expression of **VEGFA** [116] (see below), while the extracellular, neuroendocrine protein **secretogranin-2 (SCG2)** activates

STAT3 [114]. **SCG2** is the precursor of secretoneurin (SN) (not shown), which modulates neurotransmission and inflammatory responses and is involved in neuronal differentiation [117]. Moreover, it was shown that SN induces expression of anti-apoptotic proteins through **STAT3**-dependent signaling [114]. ERK1/2 regulates the expression of **SCG2** [118] and its activity is regulated by the **FOS-JUN**-complex [117]. This complex also upregulates **SRXN1** [119], a cytoplasmic enzyme that protects against oxidative stress-induced damage of dopaminergic neurons [120,121].

There are a number of other signaling cascades in the landscape involving **ERK1/2**. First, **TAC1** (see above) activates ERK1/2 [122], while ERK1/2 is involved in upregulating the expression of both **TAC1** [123] and **PTGS2** [124], a cytoplasmic enzyme that produces prostaglandin, and is upregulated through signaling involving the extracellular proteins **CRH** [125] and **VEGFA** [126] (see above) and downregulated by **NFIL3** (see above) [127]. Furthermore, ERK1/2 regulates the activity of **NPTX2** [128,129], an extracellular protein that is upregulated by **NPAS4** [130]. **NPTX2** is important in neuronal development, neuronal migration, synapse formation, and neurite outgrowth [131,132]. In addition, **Nptx2** was found to be extremely upregulated (>800%) in the substantia nigra of PD patients [131] and it was reported that **Nptx2** expression increases upon L-DOPA administration while LID severity is reduced in *Nptx2* knockout mice [129]. Further, ERK1/2 activity is regulated by the cytoplasmic adaptor protein **SH3KBP1** and by **IRS2** [133], a cytoplasmic insulin-signaling related protein that is also upregulated downstream of ERK1/2 [123]. **IRS2** is implicated in apoptosis and in the regulation of the dopaminergic cell morphology [134], and 6-OHDA injection leads to degradation of **Irs2** [135]. Moreover, the GTP-binding protein **RHEB** inhibits ERK1/2 [136] and decreases the expression of **IRS2** [137]. **RHEB** regulates neuronal plasticity and differentiation in response to injury and stress, and it was shown to preserve and restore nigrostriatal dopaminergic axonal projections in a PD mouse model [138-140]. Interestingly, when it is overexpressed, **Rheb** is able to switch its function and hence become an apoptotic enhancer. ERK1/2 also upregulates the expression of **EGR4**, a transcription factor that is increased by L-DOPA [129]. Another negative regulator of ERK1/2 function is the phosphatase **DUSP14** [141,142] and as such, it negatively regulates ERK signaling in dopamine-depleted striatal neurons during LID [143,144]. **DUSP14** is also involved in downregulating the expression of **PLAT** [145], an extracellular enzyme with roles in neuronal migration and plasticity [146]. In vitro and ex vivo studies also suggest that **Plat** has pro-survival/anti-apoptotic effects on both neurons and oligodendrocytes [147]. **PLAT** increases the expression of the cytokine **INHBA** [148], and both **PLAT** and **INHBA** activate **ERK1/2** [149,150]. In addition, **INHBA** increases the expression of **JUNB** [151] and **VEGFA** [150], a growth factor that itself activates **JUNB** [152] and ERK1/2 [153], and is upregulated

downstream of ERK1/2 [154] and **FGF13** [155], a growth factor that also activates **JUNB** [8]. **VEGFA** has a key role in vascular and neuronal pattering in the developing central nervous system (CNS) [156] and **VEGFA** administration to 6-OHDA- lesioned rats lead to a significant increase in neuronal number [157]. Further, **VEGFA** increases the expression of **FOSB** [158] and **NR4A3** [159] (see above), while **VEGFA**, **TAC1** and **KLF4** all upregulate **PLAT** expression [160-162]. **CRH** activates **PLAT** [163] and is activated by **NPY**, an extracellular hormone that is abundant in the CNS where it negatively and positively regulates apoptosis and autophagy, respectively [164,165], and that activates ERK1/2 [166]. **NPY** expression is also increased in the striatum of PD patients where it acts as a neuroprotective agent [167]. Further, **CRH** expression is downregulated by the kinase **SIK1** [168] (see above) that also upregulates the expression of **ARC**, a brain-specific protein with a role in long-term synaptic plasticity and apoptosis [169,170] that was upregulated in the striatal neurons of a rat LID-model [171,172]. In addition, **ARC** is activated by ERK1/2 [173] and downregulated by **PDYN** [174], a neuropeptide hormone that is upregulated by **TAC1** [59] and has anti-apoptotic effects [175]. Increased expression of **Pdyn** was also observed in the striatum of a rodent LID model [176-178]. Lastly, ERK1/2 upregulates the expression of **PER1** [179], a circadian clock protein that shuttles between the nucleus and cytoplasm and is upregulated by **FGF13** [180], and – in the nucleus – inhibited by **NFIL3** [3] (not shown). **FGF13** is widely expressed in the developing brain and it has a key role in establishing neuronal circuits in the cerebral cortex as well as neuronal polarization [181]. Furthermore, **FGF13** activates ERK1/2 [182].
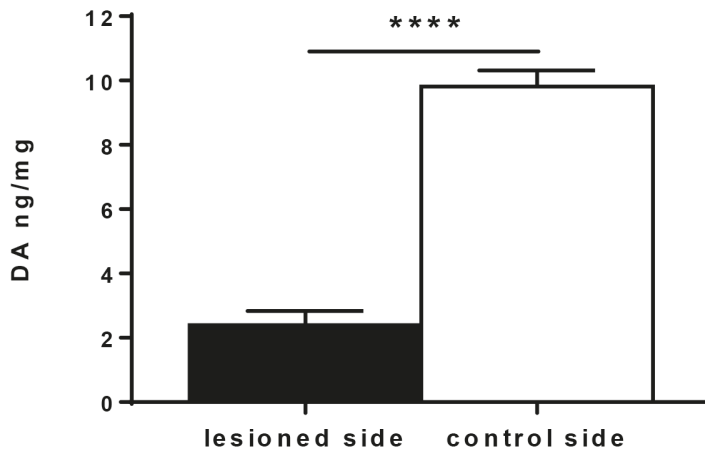
SUPPLEMENTARY FIGURE 1. Effect of unilateral 6-OHDA lesion in the MFB and chronic L-DOPA treatment on rat striatal tissue DA levels measured in the same animals (n= 12). Data is shown as mean +/- S.E.M with **** denoting $p < 0.001$.
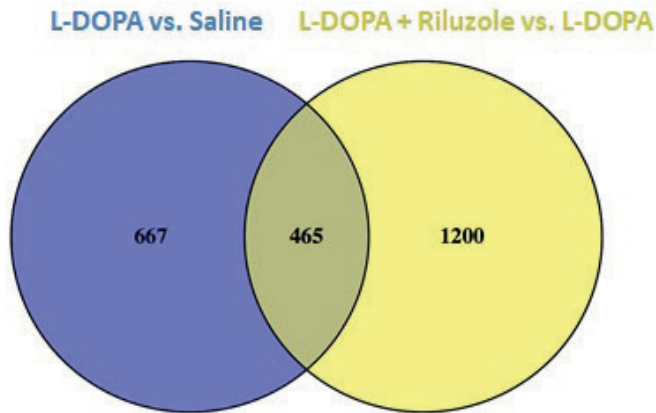
SUPPLEMENTARY FIGURE 2. Venn diagram of unique and overlapping significantly differentially expressed genes (FDR corrected p-value <0.01) in comparisons L-DOPA vs. Saline and L-DOPA + Riluzole vs. L-DOPA. All of these genes were differentially expressed in the opposite direction in the two comparisons. Using the hypergeometric test, we determined that this overlap in differentially expressed genes is highly significant (hypergeometric p-value = 1.01E-142).
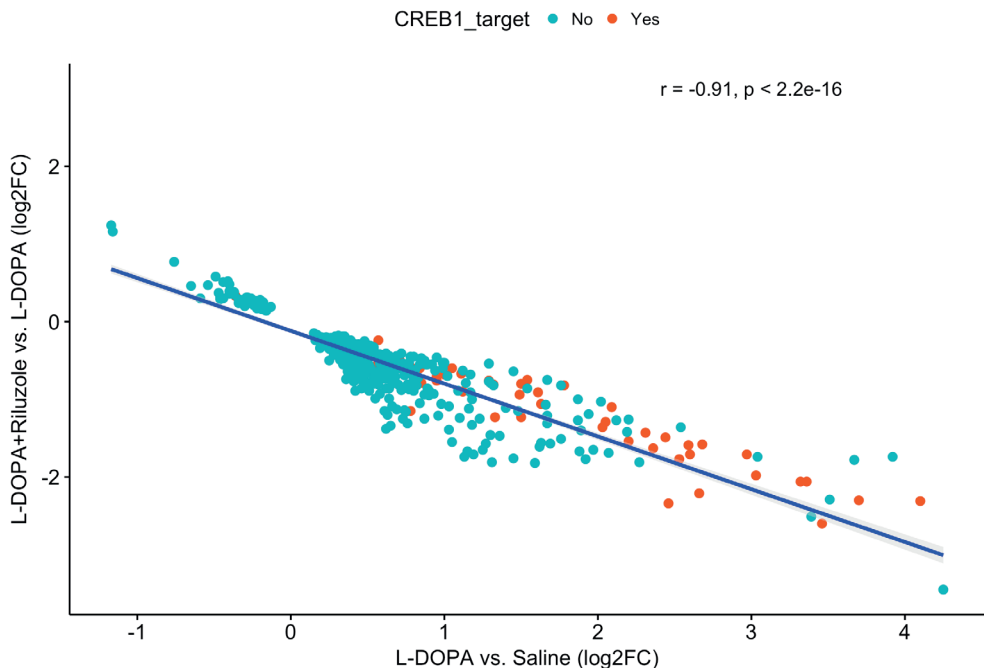
SUPPLEMENTARY FIGURE 3. Scatter plot representing the correlation of $\log_2$ fold changes ($\log_2$FC) observed for overlapping differentially expressed genes – including 58 direct CREB1 target genes – in both comparisons.
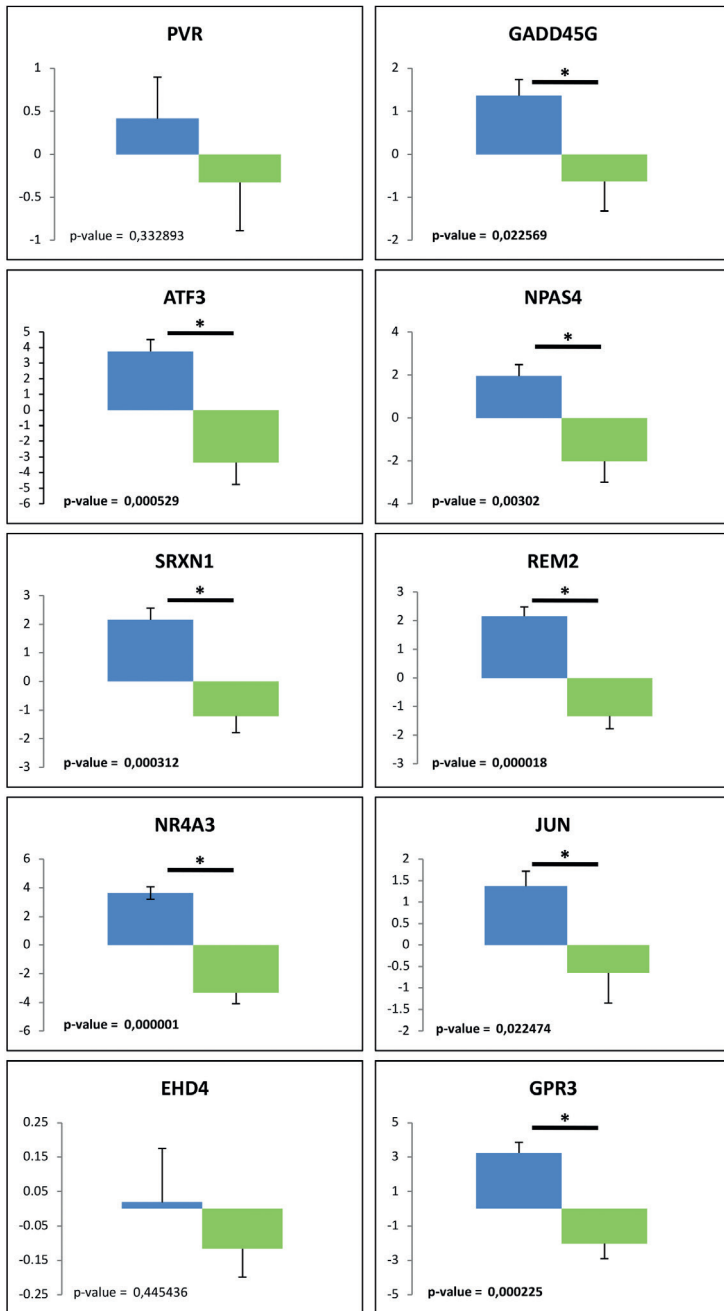
SUPPLEMENTARY FIGURE 4. qPCR validation of 10 selected CREB1 targets. The housekeeping genes *Bcap29* and *Cdkn1b* were used as reference for normalization of gene expression, and a Student's t-test was used to assess statistical significance. Values are shown as $\log_2$FC (Mean + SEM) with blue and green bars representing L-DOPA vs. Saline and L-DOPA + Riluzole vs. L-DOPA, respectively.

SUPPLEMENTARY TABLE 1. List of primers used for qPCR validation

RT² qPCR Primer Assay (Qiagen)		
Gene Symbol	Catalog number	RefSeq Accession
Jun	PPR53221A	NM_021835.3
Npas4	PPR52619A	NM_153626.1
Gpr3	PPR52464A	NM_153727.1
Nr4a3	PPR51343E	NM_017352.1
Srxn1	PPR50360B	NM_00147858.3
Gadd45g	PPR46380A	NM_001077640.1
Pvr	PPR44991A	NM_017076.2
Atf3	PPR44403B	NM_012912.2
Rem2	PPR06549B	NM_022685
Ehd4	PPR43831A	NM_139324
Housekeeping genes		
Gene Symbol	Forward Primer	Reverse Primer
Bcap29	AGAAGGCTTCCGATGCCCT	TGCTCTTTCAGGAGTCGGTCA
Cdkn1b	CAGACGTAAACAGCTCCGAATT	CTCAGTGCTTATACAGGATGTC

SUPPLEMENTARY TABLE 2. Top 10 upstream regulators of significantly differentially expressed genes in comparisons L-DOPA vs. Saline and L-DOPA + Riluzole vs. L-DOPA (FDR corrected p-value <0.01) revealed by Upstream Regulator Analysis performed in IPA.

Upstream Regulator	Type	Activation z-score	P-value of overlap	# Target genes
L-DOPA vs. Saline				
CREB1	transcription regulator	7,52	8,53E-31	102
Forskolin	chemical toxicant	6,06	5,56E-23	100
Cocaine	chemical drug	5,58	1,02E-19	48
PDGF BB	Complex	5,22	1,74E-19	61
beta-estradiol	chemical - endogenous mammalian	4,05	2,01E-19	178
U0126	chemical - kinase inhibitor	-5,07	7,54E-19	76
CREM	transcription regulator	4,19	7,25E-18	39
dalfampridine	chemical drug	4,58	2,66E-17	21
TGFB1	growth factor	3,82	1,10E-16	166
bicuculline	chemical - endogenous non-mammalian	4,48	7,07E-15	21
L-DOPA + Riluzole vs. L-DOPA				
CREB1	transcription regulator	-6,53	1,21E-11	87
F2	Peptidase	-6,33	8,46E-09	48
TP53	transcription regulator	-2,80	2,41E-08	167
CREM	transcription regulator	-2,73	3,16E-08	32
2-amino-5-phosphonovaleric acid	chemical - other	3,20	3,57E-08	31
PDGF BB	Complex	-5,31	6,20E-08	52
Forskolin	chemical toxicant	-5,48	1,26E-07	87
HIF1A	transcription regulator	-4,27	2,98E-07	58
CD40LG	Cytokine	-2,50	3,17E-07	57
U0126	chemical - kinase inhibitor	4,82	4,30E-07	67
Overlapping genes (fold change for Riluzole + L-DOPA vs. L-DOPA)				
CREB1	transcription regulator	-6,19	1,17E-24	58
Forskolin	chemical toxicant	-5,88	5,08E-22	60
Cocaine	chemical drug	-4,32	1,71E-15	28
CREM	transcription regulator	-3,00	5,60E-15	24
dalfampridine	chemical drug	-3,74	2,92E-14	14
PDGF BB	complex	-4,98	3,68E-14	33
U0126	chemical - kinase inhibitor	4,57	4,27E-13	39
kainic acid	chemical toxicant	-4,33	7,23E-13	22
bicuculline	chemical - endogenous non-mammalian	-3,65	8,91E-13	14
IL1B	cytokine	-3,60	1,59E-12	54

3

SUPPLEMENTARY TABLE 3. Gene enrichment analysis of significantly differentially expressed genes (FDR corrected p-value <0.01) in comparisons L-DOPA vs. Saline and L-DOPA + Riluzole vs. L-DOPA.

Diseases and Disorders			Molecular and Cellular Functions		
Category	P-value of overlap	# Genes	Category	P-value of overlap	# Genes
L-DOPA vs. Saline					
Cancer	9,65E-27	979	Cell death	6,63E-17	387
Epileptic seizure	4,95E-26	60	Morphology of cells	4,95E-14	257
Disorder of basal ganglia	1,83E-18	134	Expression of RNA	5,15E-11	241
Neuromuscular disease	3,52E-16	142	Differentiation of connective tissue cells	2,05E-09	96
Huntington's Disease	1,38E-13	96	Organization of cytoplasm	2,68E-09	182
Proliferation of tumor cells	6,68E-08	71	Cell cycle progression	3,94E-09	135
Hereditary optic atrophy	1,04E-06	11	Cell proliferation of fibroblasts	5,28E-09	60
Abnormal morphology of cardiovascular system	1,08E-06	73	Cell movement	1,23E-08	243
Abnormal morphology of skin	4,05E-05	36	Metabolism of protein	2,62E-08	124
Inflammation of joint	9,70E-05	115	Transport of molecule	6,12E-06	177
L-DOPA + Riluzole vs. L-DOPA					
Cancer	5,86E-38	1403	Transcription of RNA	2,15E-19	310
Liver lesion	9,54E-10	605	Morphology of cells	1,11E-15	349
Growth failure	1,30E-09	112	Organization of cytoplasm	1,92E-14	263
Epileptic seizure	1,10E-08	44	Differentiation of connective tissue cells	8,70E-12	131
Infection of cells	7,22E-07	127	Cell death	1,92E-11	494
Abnormal morphology of cardiovascular system	7,76E-07	95	Development of neurons	1,13E-09	144
Proliferation of tumor cells	1,46E-05	83	Cell movement	1,50E-09	333
Pancreatic mass	2,92E-05	335	Cell cycle progression	5,30E-07	168
Autosomal dominant disease	3,67E-04	126	Protein kinase cascade	2,93E-05	69
Phagocytosis of tumor cell lines	5,67E-04	19	Metabolism of protein	1,66E-04	145
Overlapping genes					
Epileptic seizure	2,00E-21	38	Transcription of RNA	8,48E-15	117
Cancer	1,06E-11	400	Apoptosis	1,62E-11	146
Proliferation of tumor cells	2,16E-08	41	Differentiation of connective tissue cells	2,37E-11	57
Necrosis of muscle	3,52E-05	28	Binding of DNA	5,71E-11	51
Abnormal morphology of embryonic tissue	6,35E-05	36	Morphology of cells	1,99E-09	118

SUPPLEMENTARY TABLE 3. Continued

Diseases and Disorders			Molecular and Cellular Functions		
Category	P-value of overlap	# Genes	Category	P-value of overlap	# Genes
Cell death of liver cells	1,65E-04	19	Colony formation	2,19E-09	47
Necrosis of kidney	4,28E-04	26	Cell movement	3,54E-07	114
Inflammation of organ	4,72E-04	67	Formation of filaments	8,37E-07	34
Inflammation of joint	1,93E-03	52	Lymphocyte homeostasis	8,75E-06	40
Abnormal morphology of skin	5,77E-03	16	Synthesis of protein	1,41E-04	32

3

SUPPLEMENTARY TABLE 4. Top 10 'Diseases and Disorders' and 'Molecular and Cellular Functions' categories revealed by gene enrichment analysis in IPA based on 58 overlapping target genes of CREB1. The genes in bold encode proteins that are included in our molecular landscape (Figure 3).

Diseases and Disorders		
Functions and Annotations	BH p-value	Genes
epileptic seizure	2,98E-28	*Arc*, *Atf3*, *Bag3*, *Cdkn1a*, *Crem*, *Egr4*, *Fos*, *Fosb*, *Gadd45b*, *Gadd45g*, *Inhba*, *Jun*, *Junb*, *Nfil3*, *Nptx2*, *Nr4a1*, *Nr4a3*, *Pdyn*, Pim3, *Ptgs2*, *Scg2*, *Sertad1*, *Tac1*
proliferation of tumor cells	1,67E-10	*Atf3*, *Ccnd3*, *Cdkn1a*, *Crem*, *Fos*, *Hspa5*, *Id1*, *Inhba*, *Jun*, *Nr4a1*, Pim3, *Plat*, *Ptgs2*, *Rheb*, *Stat3*, *Tac1*, *Vegfa*
weight gain	9,67E-08	*Cdkn1a*, *Crh*, *Fos*, *Id1*, *Inhba*, *Junb*, *Npy*, *Nr4a1*, *Ptgs2*, Slc32a1, *Stat3*, *Vegfa*
hypertrophy of heart	1,34E-07	*Atf3*, *Cdkn1a*, *Crem*, Gaa, *Inhba*, *Jun*, *Klf4*, *Nr4a3*, *Plat*, *Ptgs2*, *Rheb*, *Stat3*
inflammation of organ	1,34E-07	*Atf3*, *Cdkn1a*, *Crh*, *Dusp14*, Gaa, *Gadd45b*, *Gadd45g*, *Hspa5*, *Id1*, *Jun*, *Junb*, *Klf4*, *Nfil3*, *Npy*, *Nr4a1*, *Pdyn*, *Per1*, *Plat*, *Ptgs2*, *Stat3*, *Tac1*, *Vegfa*
T-cell lymphoproliferative disorder	1,37E-06	*Ccnd3*, *Cdkn1a*, *Crem*, *Gadd45b*, *Id1*, *Irs2*, *Jun*, *Lmo1*, *Nr4a3*, *Per1*, *Sertad1*, *Stat3*, *Vegfa*
Polyarthritis	1,93E-06	*Fos*, *Fosb*, *Gadd45b*, *Nr4a1*, *Nr4a3*, *Plat*, *Ptgs2*, *Stat3*
disorder of basal ganglia	4,78E-06	*Crem*, *Egr4*, *Fgf13*, *Fos*, *Fosb*, *Hspa5*, *Jun*, *Junb*, *Npy*, *Nr4a1*, *Nrgn*, *Ptgs2*, *Scg2*, Slc32a1, *Tac1*
degranulation of mast cells	6,53E-06	*Atf3*, *Crh*, *Fos*, *Junb*, *Nr4a3*, *Plat*, *Tac1*
glucose metabolism disorder	8,85E-06	*Atf3*, *Bag3*, *Cdkn1a*, *Crem*, *Crh*, *Fos*, *Gaa*, *Hspa5*, *Id1*, *Irs2*, *Jun*, *Klf4*, *Npy*, *Nr4a1*, *Nr4a3*, *Pdyn*, *Ptgs2*, *Stat3*, *Vegfa*
Molecular and Cellular Functions		
Functions and Annotations	BH p-value	Molecules
Apoptosis	3,48E-17	*Arc*, *Atf3*, *Bag3*, *Ccnd3*, *Cdc37*, Cdk19, *Cdkn1a*, *Crem*, *Crh*, Csrnp1, *Egr4*, Ehd4, *Fos*, *Fosb*, *Gadd45b*, *Gadd45g*, *Hspa5*, *Id1*, *Inhba*, *Irs2*, *Jun*, *Junb*, *Klf4*, *Nfil3*, *Npas4*, *Nptx2*, *Nr4a1*, *Nr4a3*, Pdxk, *Pdyn*, *Per1*, *Pim3*, *Plat*, *Ptgs2*, Rem2, *Rheb*, Sema7a, *Sh3kbp1*, *Sik1*, *Srxn1*, *Stat3*, *Tac1*, *Vegfa*
cell cycle progression	1,03E-13	*Atf3*, *Ccnd3*, *Cdc37*, Cdk19, *Cdkn1a*, *Crh*, *Fos*, *Frmd6*, *Gadd45b*, *Gadd45g*, *Id1*, *Inhba*, *Irs2*, *Jun*, *Junb*, *Klf4*, *Nr4a1*, *Nr4a3*, *Per1*, Pim3, *Ptgs2*, Rem2, *Sertad1*, *Sik1*, *Stat3*, *Tac1*, *Vegfa*
colony formation of tumor cell lines	2,56E-11	*Atf3*, *Bag3*, *Cdkn1a*, *Fos*, *Frmd6*, *Gadd45b*, *Gadd45g*, *Id1*, *Jun*, *Klf4*, *Nr4a1*, *Ptgs2*, *Sertad1*, *Stat3*, *Vegfa*
proliferation of lymphocytes	4,14E-11	*Ccnd3*, *Cdkn1a*, *Crh*, *Dusp14*, *Fos*, *Gadd45b*, *Hspa5*, *Inhba*, *Irs2*, *Jun*, *Junb*, *Klf4*, *Lmo1*, *Nfil3*, *Npy*, Pim3, *Ptgs2*, *Sh3kbp1*, *Stat3*, *Tac1*, *Vegfa*
transactivation of RNA	8,18E-10	*Ccnd3*, *Crem*, *Fgf13*, *Fos*, *Fosb*, *Gadd45g*, *Id1*, *Inhba*, *Jun*, *Junb*, *Klf4*, *Nr4a1*, *Nr4a3*, *Per1*, *Ptgs2*, *Sh3kbp1*, *Stat3*

SUPPLEMENTARY TABLE 4. Continued

cellular homeostasis	2,6E-09	*Bag3*, *Cdkn1a*, *Crh*, *Fos*, *Gaa*, *Gadd45b*, *Gadd45g*, *Gpr3*, *Hspa5*, *Id1*, *Inhba*, *Irs2*, *Jun*, *Junb*, *Klf4*, *Lmo1*, *Nfil3*, *Npy*, *Nr4a1*, *Ptgs2*, *Rheb*, *Sh3kbp1*, *Sik1*, *Srxn1*, *Stat3*, *Tac1*, *Vegfa*
morphology of cells	1,94E-08	*Atf3*, *Ccnd3*, *Cdkn1a*, *Crem*, *Crh*, *Egr4*, *Ehd4*, *Fgf13*, *Fos*, *Gaa*, *Gpr3*, *Id1*, *Inhba*, *Irs2*, *Jun*, *Junb*, *Klf4*, *Nfil3*, *Npas4*, *Npy*, *Nr4a1*, *Nr4a3*, *Pim3*, *Plat*, *Ptgs2*, *Rheb*, *Stat3*, *Tac1*, *Vegfa*
degeneration of cells	2,93E-08	*Atf3*, *Crem*, *Jun*, *Nfil3*, *Npas4*, *Nr4a3*, *Pdyn*, *Pim3*, *Plat*, *Ptgs2*, *Rheb*, *Stat3*, *Vegfa*
synthesis of DNA	2,93E-08	*Atf3*, *Cdkn1a*, *Crem*, *Fos*, *Id1*, *Inhba*, *Irs2*, *Jun*, *Nr4a1*, *Nr4a3*, *Ptgs2*, *Stat3*, *Tac1*, *Vegfa*
incorporation of thymidine	4,39E-08	*Atf3*, *Cdkn1a*, *Crem*, *Inhba*, *Jun*, *Ptgs2*, *Stat3*, *Vegfa*

3

REFERENCES

1. Kashihara, K.; Ishihara, T.; Akiyama, K.; Kuroda, S.; Morimasa, T.; Shomori, T. Levodopa induces AP-1 and CREB DNA-binding activities in the rat striatum. *Psychiatry and clinical neurosciences* **1995**, *49*, 291-294.

2. Sivam, S.P.; Pugazhenthi, S.; Pugazhenthi, V.; Brown, H. L-DOPA-induced activation of striatal p38MAPK and CREB in neonatal dopaminergic denervated rat: relevance to self-injurious behavior. *Journal of neuroscience research* **2008**, *86*, 339-349, doi:10.1002/jnr.21504.

3. The UniProt Consortium. UniProt: the universal protein knowledgebase. *Nucleic Acids Research* **2017**, *45*, D158-D169, doi:10.1093/nar/gkw1099.

4. Powell, J.D.; Lerner, C.G.; Ewoldt, G.R.; Schwartz, R.H. The -180 site of the IL-2 promoter is the target of CREB/CREM binding in T cell anergy. *Journal of immunology (Baltimore, Md. : 1950)* **1999**, *163*, 6631-6639.

5. Walker, W.H.; Daniel, P.B.; Habener, J.F. Inducible cAMP early repressor ICER down-regulation of CREB gene expression in Sertoli cells. *Molecular and cellular endocrinology* **1998**, *143*, 167-178.

6. Masquilier, D.; Sassone-Corsi, P. Transcriptional cross-talk: nuclear factors CREM and CREB bind to AP-1 sites and inhibit activation by Jun. *The Journal of biological chemistry* **1992**, *267*, 22460-22466.

7. Zerial, M.; Toschi, L.; Ryseck, R.P.; Schuermann, M.; Muller, R.; Bravo, R. The product of a novel growth factor activated gene, fos B, interacts with JUN proteins enhancing their DNA binding activity. *The EMBO journal* **1989**, *8*, 805-813.

8. Herdegen, T.; Leah, J.D. Inducible and constitutive transcription factors in the mammalian nervous system: control of gene expression by Jun, Fos and Krox, and CREB/ATF proteins. *Brain research. Brain research reviews* **1998**, *28*, 370-490.

9. Tullai, J.W.; Chen, J.; Schaffer, M.E.; Kamenetsky, E.; Kasif, S.; Cooper, G.M. Glycogen synthase kinase-3 represses cyclic AMP response element-binding protein (CREB)-targeted immediate early genes in quiescent cells. *The Journal of biological chemistry* **2007**, *282*, 9482-9491, doi:10.1074/jbc.M700067200.

10. Jin, G.; Howe, P.H. Transforming growth factor beta regulates clusterin gene expression via modulation of transcription factor c-Fos. *European journal of biochemistry* **1999**, *263*, 534-542.

11. Rosenberger, S.F.; Finch, J.S.; Gupta, A.; Bowden, G.T. Extracellular signal-regulated kinase 1/2-mediated phosphorylation of JunD and FosB is required for okadaic acid-induced activator protein 1 activation. *The Journal of biological chemistry* **1999**, *274*, 1124-1130.

12. Kaminska, B.; Pyrzynska, B.; Ciechomska, I.; Wisniewska, M. Modulation of the composition of AP-1 complex and its impact on transcriptional activity. *Acta neurobiologiae experimentalis* **2000**, *60*, 395-402.

13. Allan, A.L.; Albanese, C.; Pestell, R.G.; LaMarre, J. Activating transcription factor 3 induces DNA synthesis and expression of cyclin D1 in hepatocytes. *The Journal of biological chemistry* **2001**, *276*, 27272-27280, doi:10.1074/jbc.M103196200.

14. MacGillavry, H.D.; Stam, F.J.; Sassen, M.M.; Kegel, L.; Hendriks, W.T.; Verhaagen, J.; Smit, A.B.; van Kesteren, R.E. NFIL3 and cAMP response element-binding protein form a transcriptional feedforward loop that controls neuronal regeneration-associated gene expression. *The Journal of neuroscience : the official journal of the Society for Neuroscience* **2009**, *29*, 15542-15550, doi:10.1523/jneurosci.3938-09.2009.

15. Leppa, S.; Eriksson, M.; Saffrich, R.; Ansorge, W.; Bohmann, D. Complex functions of AP-1 transcription factors in differentiation and survival of PC12 cells. *Molecular and cellular biology* **2001**, *21*, 4369-4378, doi:10.1128/mcb.21.13.4369-4378.2001.

3

16. Heise, C.E.; Reyes, S.; Mitrofanis, J. Sensory (nociceptive) stimulation evokes Fos expression in the subthalamus of hemiparkinsonian rats. *Neurological research* **2008**, *30*, 277-284, doi:10.1179/016164107x235455.

17. Reyes, S.; Mitrofanis, J. Patterns of FOS expression in the spinal cord and periaqueductal grey matter of 6OHDA-lesioned rats. *The International journal of neuroscience* **2008**, *118*, 1053-1079, doi:10.1080/00207450701239210.

18. Robertson, G.S.; Herrera, D.G.; Dragunow, M.; Robertson, H.A. L-dopa activates c-fos in the striatum ipsilateral to a 6-hydroxydopamine lesion of the substantia nigra. *European journal of pharmacology* **1989**, *159*, 99-100.

19. Cole, D.G.; Growdon, J.H.; DiFiglia, M. Levodopa induction of Fos immunoreactivity in rat brain following partial and complete lesions of the substantia nigra. *Experimental neurology* **1993**, *120*, 223-232, doi:10.1006/exnr.1993.1057.

20. Morelli, M.; Cozzolino, A.; Pinna, A.; Fenu, S.; Carta, A.; Di Chiara, G. L-dopa stimulates c-fos expression in dopamine denervated striatum by combined activation of D-1 and D-2 receptors. *Brain research* **1993**, *623*, 334-336.

21. Cenci, M.A.; Tranberg, A.; Andersson, M.; Hilbertson, A. Changes in the regional and compartmental distribution of FosB- and JunB-like immunoreactivity induced in the dopamine-denervated rat striatum by acute or chronic L-dopa treatment. *Neuroscience* **1999**, *94*, 515-527.

22. Winter, C.; Weiss, C.; Martin-Villalba, A.; Zimmermann, M.; Schenkel, J. JunB and Bcl-2 overexpression results in protection against cell death of nigral neurons following axotomy. *Brain research. Molecular brain research* **2002**, *104*, 194-202.

23. Yehia, G.; Schlotter, F.; Razavi, R.; Alessandrini, A.; Molina, C.A. Mitogen-activated protein kinase phosphorylates and targets inducible cAMP early repressor to ubiquitin-mediated destruction. *The Journal of biological chemistry* **2001**, *276*, 35272-35279, doi:10.1074/jbc.M105404200.

24. He, Z.; Jiang, J.; Kokkinaki, M.; Golestaneh, N.; Hofmann, M.C.; Dym, M. Gdnf upregulates c-Fos transcription via the Ras/Erk1/2 pathway to promote mouse spermatogonial stem cell proliferation. *Stem cells (Dayton, Ohio)* **2008**, *26*, 266-278, doi:10.1634/stemcells.2007-0436.

25. Byun, H.J.; Hong, I.K.; Kim, E.; Jin, Y.J.; Jeoung, D.I.; Hahn, J.H.; Kim, Y.M.; Park, S.H.; Lee, H. A splice variant of CD99 increases motility and MMP-9 expression of human breast cancer cells through the AKT-, ERK-, and JNK-dependent AP-1 activation signaling pathways. *The Journal of biological chemistry* **2006**, *281*, 34833-34847, doi:10.1074/jbc.M605483200.

26. Lutay, N.; Hakansson, G.; Alaridah, N.; Hallgren, O.; Westergren-Thorsson, G.; Godaly, G. Mycobacteria bypass mucosal NF-kB signalling to induce an epithelial anti-inflammatory IL-22 and IL-10 response. *PloS one* **2014**, *9*, e86466, doi:10.1371/journal.pone.0086466.

27. Nowakowski, L.; Kulik-Rechberger, B.; Wrobel, A.; Rechberger, T. [Overactive bladder--a new insight into the pathogenesis of its idiopathic form]. *Ginekologia polska* **2012**, *83*, 844-848.

28. Bottone, F.G., Jr.; Moon, Y.; Alston-Mills, B.; Eling, T.E. Transcriptional regulation of activating transcription factor 3 involves the early growth response-1 gene. *The Journal of pharmacology and experimental therapeutics* **2005**, *315*, 668-677, doi:10.1124/jpet.105.089607.

29. Colucci-D'Amato, L.; Perrone-Capano, C.; di Porzio, U. Chronic activation of ERK and neurodegenerative diseases. *BioEssays : news and reviews in molecular, cellular and developmental biology* **2003**, *25*, 1085-1095, doi:10.1002/bies.10355.

30. Cheung, E.C.; Slack, R.S. Emerging role for ERK as a key regulator of neuronal apoptosis. *Science's STKE : signal transduction knowledge environment* **2004**, *2004*, Pe45, doi:10.1126/stke.2512004pe45.

31. Subramaniam, S.; Unsicker, K. Extracellular signal-regulated kinase as an inducer of non-apoptotic neuronal death. *Neuroscience* **2006**, *138*, 1055-1065, doi:10.1016/j.neuroscience.2005.12.013.

32. Zhuang, S.; Schnellmann, R.G. A death-promoting role for extracellular signal-regulated kinase. *The Journal of pharmacology and experimental therapeutics* **2006**, *319*, 991-997, doi:10.1124/jpet.106.107367.

33. Mebratu, Y.; Tesfaigzi, Y. How ERK1/2 activation controls cell proliferation and cell death: Is subcellular localization the answer? *Cell cycle (Georgetown, Tex.)* **2009**, *8*, 1168-1175, doi:10.4161/cc.8.8.8147.

34. Subramaniam, S.; Unsicker, K. ERK and cell death: ERK1/2 in neuronal death. *The FEBS journal* **2010**, *277*, 22-29, doi:10.1111/j.1742-4658.2009.07367.x.

35. Pavon, N.; Martin, A.B.; Mendialdua, A.; Moratalla, R. ERK phosphorylation and FosB expression are associated with L-DOPA-induced dyskinesia in hemiparkinsonian mice. *Biological psychiatry* **2006**, *59*, 64-74, doi:10.1016/j.biopsych.2005.05.044.

36. Westin, J.E.; Vercammen, L.; Strome, E.M.; Konradi, C.; Cenci, M.A. Spatiotemporal pattern of striatal ERK1/2 phosphorylation in a rat model of L-DOPA-induced dyskinesia and the role of dopamine D1 receptors. *Biological psychiatry* **2007**, *62*, 800-810, doi:10.1016/j.biopsych.2006.11.032.

37. Fiorentini, C.; Savoia, P.; Savoldi, D.; Barbon, A.; Missale, C. Persistent activation of the D1R/Shp-2/Erk1/2 pathway in l-DOPA-induced dyskinesia in the 6-hydroxy-dopamine rat model of Parkinson's disease. *Neurobiology of disease* **2013**, *54*, 339-348, doi:10.1016/j.nbd.2013.01.005.

38. Song, L.; Yang, X.; Ma, Y.; Wu, N.; Liu, Z. The CB1 cannabinoid receptor agonist reduces L-DOPA-induced motor fluctuation and ERK1/2 phosphorylation in 6-OHDA-lesioned rats. *Drug design, development and therapy* **2014**, *8*, 2173-2179, doi:10.2147/dddt.s60944.

39. Park, K.H.; Shin, K.S.; Zhao, T.T.; Park, H.J.; Lee, K.E.; Lee, M.K. L-DOPA modulates cell viability through the ERK-c-Jun system in PC12 and dopaminergic neuronal cells. *Neuropharmacology* **2016**, *101*, 87-97, doi:10.1016/j.neuropharm.2015.09.006.

40. Zigler, M.; Villares, G.J.; Dobroff, A.S.; Wang, H.; Huang, L.; Braeuer, R.R.; Kamiya, T.; Melnikova, V.O.; Song, R.; Friedman, R.; et al. Expression of Id-1 is regulated by MCAM/MUC18: a missing link in melanoma progression. *Cancer research* **2011**, *71*, 3494-3504, doi:10.1158/0008-5472.can-10-3555.

41. Yang, J.; Davies, R.J.; Southwood, M.; Long, L.; Yang, X.; Sobolewski, A.; Upton, P.D.; Trembath, R.C.; Morrell, N.W. Mutations in bone morphogenetic protein type II receptor cause dysregulation of Id gene expression in pulmonary artery smooth muscle cells: implications for familial pulmonary arterial hypertension. *Circulation research* **2008**, *102*, 1212-1221, doi:10.1161/circresaha.108.173567.

42. Zhang, X.; Ling, M.T.; Wong, Y.C.; Wang, X. Evidence of a novel antiapoptotic factor: role of inhibitor of differentiation or DNA binding (Id-1) in anticancer drug-induced apoptosis. *Cancer science* **2007**, *98*, 308-314, doi:10.1111/j.1349-7006.2007.00400.x.

43. Manrique, I.; Nguewa, P.; Bleau, A.M.; Nistal-Villan, E.; Lopez, I.; Villalba, M.; Gil-Bazo, I.; Calvo, A. The inhibitor of differentiation isoform Id1b, generated by alternative splicing, maintains cell quiescence and confers self-renewal and cancer stem cell-like properties. *Cancer letters* **2015**, *356*, 899-909, doi:10.1016/j.canlet.2014.10.035.

44. Campbell, G.; Hutchins, K.; Winterbottom, J.; Grenningloh, G.; Lieberman, A.R.; Anderson, P.N. Upregulation of activating transcription factor 3 (ATF3) by intrinsic CNS neurons regenerating axons into peripheral nerve grafts. *Experimental neurology* **2005**, *192*, 340-347, doi:10.1016/j.expneurol.2004.11.026.

3

45. Sodersten, E.; Feyder, M.; Lerdrup, M.; Gomes, A.L.; Kryh, H.; Spigolon, G.; Caboche, J.; Fisone, G.; Hansen, K. Dopamine signaling leads to loss of Polycomb repression and aberrant gene activation in experimental parkinsonism. *PLoS genetics* **2014**, *10*, e1004574, doi:10.1371/journal.pgen.1004574.

46. Volakakis, N.; Kadkhodaei, B.; Joodmardi, E.; Wallis, K.; Panman, L.; Silvaggi, J.; Spiegelman, B.M.; Perlmann, T. NR4A orphan nuclear receptors as mediators of CREB-dependent neuroprotection. *Proceedings of the National Academy of Sciences of the United States of America* **2010**, *107*, 12317-12322, doi:10.1073/pnas.1007088107.

47. Liu, T.Y.; Yang, X.Y.; Zheng, L.T.; Wang, G.H.; Zhen, X.C. Activation of Nur77 in microglia attenuates proinflammatory mediators production and protects dopaminergic neurons from inflammation-induced cell death. *Journal of neurochemistry* **2017**, *140*, 589-604, doi:10.1111/jnc.13907.

48. Gilbert, F.; Morissette, M.; St-Hilaire, M.; Paquet, B.; Rouillard, C.; Di Paolo, T.; Levesque, D. Nur77 gene knockout alters dopamine neuron biochemical activity and dopamine turnover. *Biological psychiatry* **2006**, *60*, 538-547, doi:10.1016/j.biopsych.2006.04.023.

49. St-Hilaire, M.; Bourhis, E.; Levesque, D.; Rouillard, C. Impaired behavioural and molecular adaptations to dopamine denervation and repeated L-DOPA treatment in Nur77-knockout mice. *The European journal of neuroscience* **2006**, *24*, 795-805, doi:10.1111/j.1460-9568.2006.04954.x.

50. Mahmoudi, S.; Samadi, P.; Gilbert, F.; Ouattara, B.; Morissette, M.; Gregoire, L.; Rouillard, C.; Di Paolo, T.; Levesque, D. Nur77 mRNA levels and L-Dopa-induced dyskinesias in MPTP monkeys treated with docosahexaenoic acid. *Neurobiology of disease* **2009**, *36*, 213-222, doi:10.1016/j.nbd.2009.07.017.

51. Montarolo, F.; Perga, S.; Martire, S.; Navone, D.N.; Marchet, A.; Leotta, D.; Bertolotto, A. Altered NR4A Subfamily Gene Expression Level in Peripheral Blood of Parkinson's and Alzheimer's Disease Patients. *Neurotoxicity research* **2016**, *30*, 338-344, doi:10.1007/s12640-016-9626-4.

52. Pearen, M.A.; Muscat, G.E. Minireview: Nuclear hormone receptor 4A signaling: implications for metabolic disease. *Molecular endocrinology (Baltimore, Md.)* **2010**, *24*, 1891-1903, doi:10.1210/me.2010-0015.

53. Mount, M.P.; Zhang, Y.; Amini, M.; Callaghan, S.; Kulczycki, J.; Mao, Z.; Slack, R.S.; Anisman, H.; Park, D.S. Perturbation of transcription factor Nur77 expression mediated by myocyte enhancer factor 2D (MEF2D) regulates dopaminergic neuron loss in response to 1-methyl-4-phenyl-1,2,3,6-tetrahydropyridine (MPTP). *The Journal of biological chemistry* **2013**, *288*, 14362-14371, doi:10.1074/jbc.M112.439216.

54. Lemberger, T.; Parkitna, J.R.; Chai, M.; Schutz, G.; Engblom, D. CREB has a context-dependent role in activity-regulated transcription and maintains neuronal cholesterol homeostasis. *FASEB journal : official publication of the Federation of American Societies for Experimental Biology* **2008**, *22*, 2872-2879, doi:10.1096/fj.08-107888.

55. Proschel, C.; Hansen, J.N.; Ali, A.; Tuttle, E.; Lacagnina, M.; Buscaglia, G.; Halterman, M.W.; Paciorkowski, A.R. Epilepsy-causing sequence variations in SIK1 disrupt synaptic activity response gene expression and affect neuronal morphology. *European journal of human genetics : EJHG* **2017**, *25*, 216-221, doi:10.1038/ejhg.2016.145.

56. Severini, C.; Improta, G.; Falconieri-Erspamer, G.; Salvadori, S.; Erspamer, V. The tachykinin peptide family. *Pharmacological reviews* **2002**, *54*, 285-322.

57. Bourdenx, M.; Nilsson, A.; Wadensten, H.; Falth, M.; Li, Q.; Crossman, A.R.; Andren, P.E.; Bezard, E. Abnormal structure-specific peptide transmission and processing in a primate model of Parkinson's disease and l-DOPA-induced dyskinesia. *Neurobiology of disease* **2014**, *62*, 307-312, doi:10.1016/j.nbd.2013.10.016.

58. Castro-Obregon, S.; Rao, R.V.; del Rio, G.; Chen, S.F.; Poksay, K.S.; Rabizadeh, S.; Vesce, S.; Zhang, X.K.; Swanson, R.A.; Bredesen, D.E. Alternative, nonapoptotic programmed cell death: mediation by arrestin 2, ERK2, and Nur77. *The Journal of biological chemistry* **2004**, *279*, 17543-17553, doi:10.1074/jbc.M312363200.

59. Saban, M.R.; Nguyen, N.B.; Hammond, T.G.; Saban, R. Gene expression profiling of mouse bladder inflammatory responses to LPS, substance P, and antigen-stimulation. *The American journal of pathology* **2002**, *160*, 2095-2110, doi:10.1016/s0002-9440(10)61159-5.

60. Rosati, A.; Graziano, V.; De Laurenzi, V.; Pascale, M.; Turco, M.C. BAG3: a multifaceted protein that regulates major cell pathways. *Cell death & disease* **2011**, *2*, e141, doi:10.1038/cddis.2011.24.

61. Santoro, A.; Nicolin, V.; Florenzano, F.; Rosati, A.; Capunzo, M.; Nori, S.L. BAG3 is involved in neuronal differentiation and migration. *Cell and tissue research* **2017**, *368*, 249-258, doi:10.1007/s00441-017-2570-7.

62. Lei, Z.; Brizzee, C.; Johnson, G.V. BAG3 facilitates the clearance of endogenous tau in primary neurons. *Neurobiology of aging* **2015**, *36*, 241-248, doi:10.1016/j.neurobiolaging.2014.08.012.

63. Bruno, A.P.; Cefaliello, C.; D'Auria, R.; Crispino, M.; Rosati, A.; Giuditta, A.; Nori, S.L. BAG3 mRNA is present in synaptosomal polysomes of rat brain. *Cell cycle (Georgetown, Tex.)* **2014**, *13*, 1357, doi:10.4161/cc.28655.

64. Gamerdinger, M.; Hajieva, P.; Kaya, A.M.; Wolfrum, U.; Hartl, F.U.; Behl, C. Protein quality control during aging involves recruitment of the macroautophagy pathway by BAG3. *The EMBO journal* **2009**, *28*, 889-901, doi:10.1038/emboj.2009.29.

65. Heinrichs, S.C.; Koob, G.F. Corticotropin-releasing factor in brain: a role in activation, arousal, and affect regulation. *The Journal of pharmacology and experimental therapeutics* **2004**, *311*, 427-440, doi:10.1124/jpet.103.052092.

66. Koutmani, Y.; Politis, P.K.; Elkouris, M.; Agrogiannis, G.; Kemerli, M.; Patsouris, E.; Remboutsika, E.; Karalis, K.P. Corticotropin-releasing hormone exerts direct effects on neuronal progenitor cells: implications for neuroprotection. *Molecular psychiatry* **2013**, *18*, 300-307, doi:10.1038/mp.2012.198.

67. Pan, J.T.; Lookingland, K.J.; Moore, K.E. Differential Effects of Corticotropin-Releasing Hormone on Central Dopaminergic and Noradrenergic Neurons. *Journal of biomedical science* **1995**, *2*, 50-56.

68. Bousquet, C.; Zatelli, M.C.; Melmed, S. Direct regulation of pituitary proopiomelanocortin by STAT3 provides a novel mechanism for immuno-neuroendocrine interfacing. *The Journal of clinical investigation* **2000**, *106*, 1417-1425, doi:10.1172/jci11182.

69. Kageyama, K.; Itoi, K.; Iwasaki, Y.; Niioka, K.; Watanuki, Y.; Yamagata, S.; Nakada, Y.; Das, G.; Suda, T.; Daimon, M. Stimulation of corticotropin-releasing factor gene expression by FosB in rat hypothalamic 4B cells. *Peptides* **2014**, *51*, 59-64, doi:10.1016/j.peptides.2013.11.004.

70. Parkes, D.; Rivest, S.; Lee, S.; Rivier, C.; Vale, W. Corticotropin-releasing factor activates c-fos, NGFI-B, and corticotropin-releasing factor gene expression within the paraventricular nucleus of the rat hypothalamus. *Molecular endocrinology (Baltimore, Md.)* **1993**, *7*, 1357-1367, doi:10.1210/mend.7.10.8264665.

71. Asadi, S.; Alysandratos, K.D.; Angelidou, A.; Miniati, A.; Sismanopoulos, N.; Vasiadi, M.; Zhang, B.; Kalogeromitros, D.; Theoharides, T.C. Substance P (SP) induces expression of functional corticotropin-releasing hormone receptor-1 (CRHR-1) in human mast cells. *The Journal of investigative dermatology* **2012**, *132*, 324-329, doi:10.1038/jid.2011.334.

3

72. Rhee, S.H.; Ma, E.L.; Lee, Y.; Tache, Y.; Pothoulakis, C.; Im, E. Corticotropin Releasing Hormone and Urocortin 3 Stimulate Vascular Endothelial Growth Factor Expression through the cAMP/CREB Pathway. *The Journal of biological chemistry* **2015**, *290*, 26194-26203, doi:10.1074/jbc.M115.678979.

73. Bonfiglio, J.J.; Inda, C.; Senin, S.; Maccarrone, G.; Refojo, D.; Giacomini, D.; Turck, C.W.; Holsboer, F.; Arzt, E.; Silberstein, S. B-Raf and CRHR1 internalization mediate biphasic ERK1/2 activation by CRH in hippocampal HT22 Cells. *Molecular endocrinology (Baltimore, Md.)* **2013**, *27*, 491-510, doi:10.1210/me.2012-1359.

74. Rius, J.; Martinez-Gonzalez, J.; Crespo, J.; Badimon, L. Involvement of neuron-derived orphan receptor-1 (NOR-1) in LDL-induced mitogenic stimulus in vascular smooth muscle cells: role of CREB. *Arteriosclerosis, thrombosis, and vascular biology* **2004**, *24*, 697-702, doi:10.1161/01.ATV.0000121570.00515.dc.

75. Rodriguez-Blanco, J.; Martin, V.; Herrera, F.; Garcia-Santos, G.; Antolin, I.; Rodriguez, C. Intracellular signaling pathways involved in post-mitotic dopaminergic PC12 cell death induced by 6-hydroxydopamine. *Journal of neurochemistry* **2008**, *107*, 127-140, doi:10.1111/j.1471-4159.2008.05588.x.

76. Perlman, H.; Bradley, K.; Liu, H.; Cole, S.; Shamiyeh, E.; Smith, R.C.; Walsh, K.; Fiore, S.; Koch, A.E.; Firestein, G.S.; et al. IL-6 and matrix metalloproteinase-1 are regulated by the cyclin-dependent kinase inhibitor p21 in synovial fibroblasts. *Journal of immunology (Baltimore, Md. : 1950)* **2003**, *170*, 838-845.

77. Lee, S.J.; Cho, S.C.; Lee, E.J.; Kim, S.; Lee, S.B.; Lim, J.H.; Choi, Y.H.; Kim, W.J.; Moon, S.K. Interleukin-20 promotes migration of bladder cancer cells through extracellular signal-regulated kinase (ERK)-mediated MMP-9 protein expression leading to nuclear factor (NF-kappaB) activation by inducing the up-regulation of p21(WAF1) protein expression. *The Journal of biological chemistry* **2013**, *288*, 5539-5552, doi:10.1074/jbc.M112.410233.

78. Bottazzi, M.E.; Zhu, X.; Bohmer, R.M.; Assoian, R.K. Regulation of p21(cip1) expression by growth factors and the extracellular matrix reveals a role for transient ERK activity in G1 phase. *The Journal of cell biology* **1999**, *146*, 1255-1264.

79. Riverso, M.; Montagnani, V.; Stecca, B. KLF4 is regulated by RAS/RAF/MEK/ERK signaling through E2F1 and promotes melanoma cell growth. *Oncogene* **2017**, *36*, 3322-3333, doi:10.1038/onc.2016.481.

80. Johnson, M.R.; Valentine, C.; Basilico, C.; Mansukhani, A. FGF signaling activates STAT1 and p21 and inhibits the estrogen response and proliferation of MCF-7 cells. *Oncogene* **1998**, *16*, 2647-2656, doi:10.1038/sj.onc.1201789.

81. Sugimoto, M.; Martin, N.; Wilks, D.P.; Tamai, K.; Huot, T.J.; Pantoja, C.; Okumura, K.; Serrano, M.; Hara, E. Activation of cyclin D1-kinase in murine fibroblasts lacking both p21(Cip1) and p27(Kip1). *Oncogene* **2002**, *21*, 8067-8074, doi:10.1038/sj.onc.1206019.

82. Visser-Grieve, S.; Hao, Y.; Yang, X. Human homolog of Drosophila expanded, hEx, functions as a putative tumor suppressor in human cancer cell lines independently of the Hippo pathway. *Oncogene* **2012**, *31*, 1189-1195, doi:10.1038/onc.2011.318.

83. Nickoloff, B.J.; Chaturvedi, V.; Bacon, P.; Qin, J.Z.; Denning, M.F.; Diaz, M.O. Id-1 delays senescence but does not immortalize keratinocytes. *The Journal of biological chemistry* **2000**, *275*, 27501-27504, doi:10.1074/jbc.C000311200.

84. Falco, A.; Festa, M.; Basile, A.; Rosati, A.; Pascale, M.; Florenzano, F.; Nori, S.L.; Nicolin, V.; Di Benedetto, M.; Vecchione, M.L.; et al. BAG3 controls angiogenesis through regulation of ERK phosphorylation. *Oncogene* **2012**, *31*, 5153-5161, doi:10.1038/onc.2012.17.

85. He, G.; Siddik, Z.H.; Huang, Z.; Wang, R.; Koomen, J.; Kobayashi, R.; Khokhar, A.R.; Kuang, J. Induction of p21 by p53 following DNA damage inhibits both Cdk4 and Cdk2 activities. *Oncogene* **2005**, *24*, 2929-2943, doi:10.1038/sj.onc.1208474.

86. Copani, A.; Uberti, D.; Sortino, M.A.; Bruno, V.; Nicoletti, F.; Memo, M. Activation of cell-cycle-associated proteins in neuronal death: a mandatory or dispensable path? *Trends in neurosciences* **2001**, *24*, 25-31.

87. Sultan, F.A.; Sweatt, J.D. The role of the Gadd45 family in the nervous system: a focus on neurodevelopment, neuronal injury, and cognitive neuroepigenetics. *Advances in experimental medicine and biology* **2013**, *793*, 81-119, doi:10.1007/978-1-4614-8289-5_6.

88. Azam, N.; Vairapandi, M.; Zhang, W.; Hoffman, B.; Liebermann, D.A. Interaction of CR6 (GADD45gamma) with proliferating cell nuclear antigen impedes negative growth control. *The Journal of biological chemistry* **2001**, *276*, 2766-2774, doi:10.1074/jbc.M005626200.

89. Vinayagam, A.; Stelzl, U.; Foulle, R.; Plassmann, S.; Zenkner, M.; Timm, J.; Assmus, H.E.; Andrade-Navarro, M.A.; Wanker, E.E. A directed protein interaction network for investigating intracellular signal transduction. *Science signaling* **2011**, *4*, rs8, doi:10.1126/scisignal.2001699.

90. Obara, Y.; Imai, T.; Sato, H.; Takeda, Y.; Kato, T.; Ishii, K. Midnolin is a novel regulator of parkin expression and is associated with Parkinson's Disease. *Scientific reports* **2017**, *7*, 5885, doi:10.1038/s41598-017-05456-0.

91. Obara, Y.; Ishii, K. Transcriptome Analysis Reveals That Midnolin Regulates mRNA Expression Levels of Multiple Parkinson's Disease Causative Genes. *Biological & pharmaceutical bulletin* **2018**, *41*, 20-23, doi:10.1248/bpb.b17-00663.

92. Fan, W.; Richter, G.; Cereseto, A.; Beadling, C.; Smith, K.A. Cytokine response gene 6 induces p21 and regulates both cell growth and arrest. *Oncogene* **1999**, *18*, 6573-6582, doi:10.1038/sj.onc.1203054.

93. Kovalsky, O.; Lung, F.D.; Roller, P.P.; Fornace, A.J., Jr. Oligomerization of human Gadd45a protein. *The Journal of biological chemistry* **2001**, *276*, 39330-39339, doi:10.1074/jbc.M105115200.

94. Park, H.Y.; Ryu, Y.K.; Kim, Y.H.; Park, T.S.; Go, J.; Hwang, J.H.; Choi, D.H.; Rhee, M.; Lee, C.H.; Kim, K.S. Gadd45beta ameliorates L-DOPA-induced dyskinesia in a Parkinson's disease mouse model. *Neurobiology of disease* **2016**, *89*, 169-179, doi:10.1016/j.nbd.2016.02.013.

95. Figge, D.A.; Eskow Jaunarajs, K.L.; Standaert, D.G. Dynamic DNA Methylation Regulates Levodopa-Induced Dyskinesia. *The Journal of neuroscience : the official journal of the Society for Neuroscience* **2016**, *36*, 6514-6524, doi:10.1523/jneurosci.0683-16.2016.

96. Kanaan, N.M.; Collier, T.J.; Cole-Strauss, A.; Grabinski, T.; Mattingly, Z.R.; Winn, M.E.; Steece-Collier, K.; Sortwell, C.E.; Manfredsson, F.P.; Lipton, J.W. The longitudinal transcriptomic response of the substantia nigra to intrastriatal 6-hydroxydopamine reveals significant upregulation of regeneration-associated genes. *PloS one* **2015**, *10*, e0127768, doi:10.1371/journal.pone.0127768.

97. Tamai, S.; Imaizumi, K.; Kurabayashi, N.; Nguyen, M.D.; Abe, T.; Inoue, M.; Fukada, Y.; Sanada, K. Neuroprotective role of the basic leucine zipper transcription factor NFIL3 in models of amyotrophic lateral sclerosis. *The Journal of biological chemistry* **2014**, *289*, 1629-1638, doi:10.1074/jbc.M113.524389.

98. Keniry, M.; Pires, M.M.; Mense, S.; Lefebvre, C.; Gan, B.; Justiano, K.; Lau, Y.K.; Hopkins, B.; Hodakoski, C.; Koujak, S.; et al. Survival factor NFIL3 restricts FOXO-induced gene expression in cancer. *Genes & development* **2013**, *27*, 916-927, doi:10.1101/gad.214049.113.

99. Wang, L.; Xu, S.; Xu, X.; Chan, P. (-)-Epigallocatechin-3-Gallate protects SH-SY5Y cells against 6-OHDA-induced cell death through STAT3 activation. *Journal of Alzheimer's disease : JAD* **2009**, *17*, 295-304, doi:10.3233/jad-2009-1048.

100. Kim, J.H.; Qu, A.; Reddy, J.K.; Gao, B.; Gonzalez, F.J. Hepatic oxidative stress activates the Gadd45b gene by way of degradation of the transcriptional repressor STAT3. *Hepatology (Baltimore, Md.)* **2014**, *59*, 695-704, doi:10.1002/hep.26683.

101. Scuto, A.; Kirschbaum, M.; Buettner, R.; Kujawski, M.; Cermak, J.M.; Atadja, P.; Jove, R. SIRT1 activation enhances HDAC inhibition-mediated upregulation of GADD45G by repressing the binding of NF-kappaB/STAT3 complex to its promoter in malignant lymphoid cells. *Cell death & disease* **2013**, *4*, e635, doi:10.1038/cddis.2013.159.

102. Yang, F.; Zhang, W.; Li, D.; Zhan, Q. Gadd45a suppresses tumor angiogenesis via inhibition of the mTOR/STAT3 protein pathway. *The Journal of biological chemistry* **2013**, *288*, 6552-6560, doi:10.1074/jbc.M112.418335.

103. Lim, T.H.; Hu, L.; Yang, C.; He, C.; Lee, H.K. Membrane assisted micro-solid phase extraction of pharmaceuticals with amino and urea-grafted silica gel. *Journal of chromatography. A* **2013**, *1316*, 8-14, doi:10.1016/j.chroma.2013.09.034.

104. Hirano, T.; Ishihara, K.; Hibi, M. Roles of STAT3 in mediating the cell growth, differentiation and survival signals relayed through the IL-6 family of cytokine receptors. *Oncogene* **2000**, *19*, 2548-2556, doi:10.1038/sj.onc.1203551.

105. Coqueret, O.; Gascan, H. Functional interaction of STAT3 transcription factor with the cell cycle inhibitor p21WAF1/CIP1/SDI1. *The Journal of biological chemistry* **2000**, *275*, 18794-18800, doi:10.1074/jbc.M001601200.

106. Li, J.; Bennett, K.; Stukalov, A.; Fang, B.; Zhang, G.; Yoshida, T.; Okamoto, I.; Kim, J.Y.; Song, L.; Bai, Y.; et al. Perturbation of the mutated EGFR interactome identifies vulnerabilities and resistance mechanisms. *Molecular systems biology* **2013**, *9*, 705, doi:10.1038/msb.2013.61.

107. Kong, D.H.; Zhang, Q.; Meng, X.; Zong, Z.H.; Li, C.; Liu, B.Q.; Guan, Y.; Wang, H.Q. BAG3 sensitizes cancer cells exposed to DNA damaging agents via direct interaction with GRP78. *Biochimica et biophysica acta* **2013**, *1833*, 3245-3253, doi:10.1016/j.bbamcr.2013.09.013.

108. Ota, A.; Wang, Y. Cdc37/Hsp90 protein-mediated regulation of IRE1alpha protein activity in endoplasmic reticulum stress response and insulin synthesis in INS-1 cells. *The Journal of biological chemistry* **2012**, *287*, 6266-6274, doi:10.1074/jbc.M111.331264.

109. Malhotra, J.D.; Kaufman, R.J. The endoplasmic reticulum and the unfolded protein response. *Seminars in cell & developmental biology* **2007**, *18*, 716-731, doi:10.1016/j.semcdb.2007.09.003.

110. Bertolotti, A.; Zhang, Y.; Hendershot, L.M.; Harding, H.P.; Ron, D. Dynamic interaction of BiP and ER stress transducers in the unfolded-protein response. *Nature cell biology* **2000**, *2*, 326-332, doi:10.1038/35014014.

111. Salganik, M.; Sergeyev, V.G.; Shinde, V.; Meyers, C.A.; Gorbatyuk, M.S.; Lin, J.H.; Zolotukhin, S.; Gorbatyuk, O.S. The loss of glucose-regulated protein 78 (GRP78) during normal aging or from siRNA knockdown augments human alpha-synuclein (alpha-syn) toxicity to rat nigral neurons. *Neurobiology of aging* **2015**, *36*, 2213-2223, doi:10.1016/j.neurobiolaging.2015.02.018.

112. Vollmer, S.; Haan, C.; Behrmann, I. Oncostatin M up-regulates the ER chaperone Grp78/BiP in liver cells. *Biochemical pharmacology* **2010**, *80*, 2066-2073, doi:10.1016/j.bcp.2010.07.015.

113. Oliveira, F.O., Jr.; Alves, C.R.; Souza-Silva, F.; Calvet, C.M.; Cortes, L.M.; Gonzalez, M.S.; Toma, L.; Boucas, R.I.; Nader, H.B.; Pereira, M.C. Trypanosoma cruzi heparin-binding proteins mediate the adherence of epimastigotes to the midgut epithelial cells of Rhodnius prolixus. *Parasitology* **2012**, *139*, 735-743, doi:10.1017/s0031182011002344.

114. Shyu, W.C.; Lin, S.Z.; Chiang, M.F.; Chen, D.C.; Su, C.Y.; Wang, H.J.; Liu, R.S.; Tsai, C.H.; Li, H. Secretoneurin promotes neuroprotection and neuronal plasticity via the Jak2/Stat3 pathway in murine models of stroke. *The Journal of clinical investigation* **2008**, *118*, 133-148, doi:10.1172/jci32723.

115. Turkson, J.; Bowman, T.; Adnane, J.; Zhang, Y.; Djeu, J.Y.; Sekharam, M.; Frank, D.A.; Holzman, L.B.; Wu, J.; Sebti, S.; et al. Requirement for Ras/Rac1-mediated p38 and c-Jun N-terminal kinase signaling in Stat3 transcriptional activity induced by the Src oncoprotein. *Molecular and cellular biology* **1999**, *19*, 7519-7528.

116. Xu, Q.; Briggs, J.; Park, S.; Niu, G.; Kortylewski, M.; Zhang, S.; Gritsko, T.; Turkson, J.; Kay, H.; Semenza, G.L.; et al. Targeting Stat3 blocks both HIF-1 and VEGF expression induced by multiple oncogenic growth signaling pathways. *Oncogene* **2005**, *24*, 5552-5560, doi:10.1038/sj.onc.1208719.

117. Li, L.; Hung, A.C.; Porter, A.G. Secretogranin II: a key AP-1-regulated protein that mediates neuronal differentiation and protection from nitric oxide-induced apoptosis of neuroblastoma cells. *Cell death and differentiation* **2008**, *15*, 879-888, doi:10.1038/cdd.2008.8.

118. Iwase, K.; Ishihara, A.; Yoshimura, S.; Andoh, Y.; Kato, M.; Seki, N.; Matsumoto, E.; Hiwasa, T.; Muller, D.; Fukunaga, K.; et al. The secretogranin II gene is a signal integrator of glutamate and dopamine inputs. *Journal of neurochemistry* **2014**, *128*, 233-245, doi:10.1111/jnc.12467.

119. Glauser, D.A.; Brun, T.; Gauthier, B.R.; Schlegel, W. Transcriptional response of pancreatic beta cells to metabolic stimulation: large scale identification of immediate-early and secondary response genes. *BMC molecular biology* **2007**, *8*, 54, doi:10.1186/1471-2199-8-54.

120. Soriano, F.X.; Leveille, F.; Papadia, S.; Higgins, L.G.; Varley, J.; Baxter, P.; Hayes, J.D.; Hardingham, G.E. Induction of sulfiredoxin expression and reduction of peroxiredoxin hyperoxidation by the neuroprotective Nrf2 activator 3H-1,2-dithiole-3-thione. *Journal of neurochemistry* **2008**, *107*, 533-543, doi:10.1111/j.1471-4159.2008.05648.x.

121. Sunico, C.R.; Sultan, A.; Nakamura, T.; Dolatabadi, N.; Parker, J.; Shan, B.; Han, X.; Yates, J.R., 3rd; Masliah, E.; Ambasudhan, R.; et al. Role of sulfiredoxin as a peroxiredoxin-2 denitrosylase in human iPSC-derived dopaminergic neurons. *Proceedings of the National Academy of Sciences of the United States of America* **2016**, *113*, E7564-e7571, doi:10.1073/pnas.1608784113.

122. Koon, H.W.; Zhao, D.; Na, X.; Moyer, M.P.; Pothoulakis, C. Metalloproteinases and transforming growth factor-alpha mediate substance P-induced mitogen-activated protein kinase activation and proliferation in human colonocytes. *The Journal of biological chemistry* **2004**, *279*, 45519-45527, doi:10.1074/jbc.M408523200.

123. Fan, H.Y.; Liu, Z.; Johnson, P.F.; Richards, J.S. CCAAT/enhancer-binding proteins (C/EBP)-alpha and -beta are essential for ovulation, luteinization, and the expression of key target genes. *Molecular endocrinology (Baltimore, Md.)* **2011**, *25*, 253-268, doi:10.1210/me.2010-0318.

124. Adderley, S.R.; Fitzgerald, D.J. Oxidative damage of cardiomyocytes is limited by extracellular regulated kinases 1/2-mediated induction of cyclooxygenase-2. *The Journal of biological chemistry* **1999**, *274*, 5038-5046.

125. Yamaguchi, N.; Ogawa, S.; Okada, S. Cyclooxygenase and nitric oxide synthase in the presympathetic neurons in the paraventricular hypothalamic nucleus are involved in restraint stress-induced sympathetic activation in rats. *Neuroscience* **2010**, *170*, 773-781, doi:10.1016/j.neuroscience.2010.07.051.

126. Deng, W.G.; Saunders, M.; Gilroy, D.; He, X.Z.; Yeh, H.; Zhu, Y.; Shtivelband, M.I.; Ruan, K.H.; Wu, K.K. Purification and characterization of a cyclooxygenase-2 and angiogenesis suppressing factor produced by human fibroblasts. *FASEB journal : official publication of the Federation of American Societies for Experimental Biology* **2002**, *16*, 1286-1288, doi:10.1096/fj.01-0844fje.

127. Ozkurt, I.C.; Tetradis, S. Parathyroid hormone-induced E4BP4/NFIL3 down-regulates transcription in osteoblasts. *The Journal of biological chemistry* **2003**, *278*, 26803-26809, doi:10.1074/jbc.M212652200.

3

128. Ludwig, A.; Uvarov, P.; Pellegrino, C.; Thomas-Crusells, J.; Schuchmann, S.; Saarma, M.; Airaksinen, M.S.; Rivera, C. Neurturin evokes MAPK-dependent upregulation of Egr4 and KCC2 in developing neurons. *Neural plasticity* **2011**, *2011*, 1-8, doi:10.1155/2011/641248.

129. Charbonnier-Beaupel, F.; Malerbi, M.; Alcacer, C.; Tahiri, K.; Carpentier, W.; Wang, C.; During, M.; Xu, D.; Worley, P.F.; Girault, J.A.; et al. Gene expression analyses identify Narp contribution in the development of L-DOPA-induced dyskinesia. *The Journal of neuroscience : the official journal of the Society for Neuroscience* **2015**, *35*, 96-111, doi:10.1523/jneurosci.5231-13.2015.

130. Spiegel, I.; Mardinly, A.R.; Gabel, H.W.; Bazinet, J.E.; Couch, C.H.; Tzeng, C.P.; Harmin, D.A.; Greenberg, M.E. Npas4 regulates excitatory-inhibitory balance within neural circuits through cell-type-specific gene programs. *Cell* **2014**, *157*, 1216-1229, doi:10.1016/j.cell.2014.03.058.

131. Moran, L.B.; Hickey, L.; Michael, G.J.; Derkacs, M.; Christian, L.M.; Kalaitzakis, M.E.; Pearce, R.K.; Graeber, M.B. Neuronal pentraxin II is highly upregulated in Parkinson's disease and a novel component of Lewy bodies. *Acta neuropathologica* **2008**, *115*, 471-478, doi:10.1007/s00401-007-0309-3.

132. Bjartmar, L.; Huberman, A.D.; Ullian, E.M.; Renteria, R.C.; Liu, X.; Xu, W.; Prezioso, J.; Susman, M.W.; Stellwagen, D.; Stokes, C.C.; et al. Neuronal pentraxins mediate synaptic refinement in the developing visual system. *The Journal of neuroscience : the official journal of the Society for Neuroscience* **2006**, *26*, 6269-6281, doi:10.1523/jneurosci.4212-05.2006.

133. Rui, L.; Fisher, T.L.; Thomas, J.; White, M.F. Regulation of insulin/insulin-like growth factor-1 signaling by proteasome-mediated degradation of insulin receptor substrate-2. *The Journal of biological chemistry* **2001**, *276*, 40362-40367, doi:10.1074/jbc.M105332200.

134. Russo, S.J.; Bolanos, C.A.; Theobald, D.E.; DeCarolis, N.A.; Renthal, W.; Kumar, A.; Winstanley, C.A.; Renthal, N.E.; Wiley, M.D.; Self, D.W.; et al. IRS2-Akt pathway in midbrain dopamine neurons regulates behavioral and cellular responses to opiates. *Nature neuroscience* **2007**, *10*, 93-99, doi:10.1038/nn1812.

135. Morris, J.K.; Zhang, H.; Gupte, A.A.; Bomhoff, G.L.; Stanford, J.A.; Geiger, P.C. Measures of striatal insulin resistance in a 6-hydroxydopamine model of Parkinson's disease. *Brain research* **2008**, *1240*, 185-195, doi:10.1016/j.brainres.2008.08.089.

136. Karbowniczek, M.; Cash, T.; Cheung, M.; Robertson, G.P.; Astrinidis, A.; Henske, E.P. Regulation of B-Raf kinase activity by tuberin and Rheb is mammalian target of rapamycin (mTOR)-independent. *The Journal of biological chemistry* **2004**, *279*, 29930-29937, doi:10.1074/jbc.M402591200.

137. Shah, O.J.; Wang, Z.; Hunter, T. Inappropriate activation of the TSC/Rheb/mTOR/S6K cassette induces IRS1/2 depletion, insulin resistance, and cell survival deficiencies. *Current biology : CB* **2004**, *14*, 1650-1656, doi:10.1016/j.cub.2004.08.026.

138. Kim, S.R.; Kareva, T.; Yarygina, O.; Kholodilov, N.; Burke, R.E. AAV transduction of dopamine neurons with constitutively active Rheb protects from neurodegeneration and mediates axon regrowth. *Molecular therapy : the journal of the American Society of Gene Therapy* **2012**, *20*, 275-286, doi:10.1038/mt.2011.213.

139. Kim, S.R.; Chen, X.; Oo, T.F.; Kareva, T.; Yarygina, O.; Wang, C.; During, M.; Kholodilov, N.; Burke, R.E. Dopaminergic pathway reconstruction by Akt/Rheb-induced axon regeneration. *Annals of neurology* **2011**, *70*, 110-120, doi:10.1002/ana.22383.

140. Jeon, M.T.; Kim, S.R. Roles of Rheb(S16H) in substantia nigra pars compacta dopaminergic neurons in vivo. *Biomedical reports* **2015**, *3*, 137-140, doi:10.3892/br.2014.397.

141. Yang, C.Y.; Li, J.P.; Chiu, L.L.; Lan, J.L.; Chen, D.Y.; Chuang, H.C.; Huang, C.Y.; Tan, T.H. Dual-specificity phosphatase 14 (DUSP14/MKP6) negatively regulates TCR signaling by inhibiting TAB1 activation. *Journal of immunology (Baltimore, Md. : 1950)* **2014**, *192*, 1547-1557, doi:10.4049/jimmunol.1300989.

142. Huang, C.Y.; Tan, T.H. DUSPs, to MAP kinases and beyond. *Cell & bioscience* **2012**, *2*, 24, doi:10.1186/2045-3701-2-24.

143. Heiman, M.; Heilbut, A.; Francardo, V.; Kulicke, R.; Fenster, R.J.; Kolaczyk, E.D.; Mesirov, J.P.; Surmeier, D.J.; Cenci, M.A.; Greengard, P. Molecular adaptations of striatal spiny projection neurons during levodopa-induced dyskinesia. *Proceedings of the National Academy of Sciences of the United States of America* **2014**, *111*, 4578-4583, doi:10.1073/pnas.1401819111.

144. Gerfen, C.R.; Miyachi, S.; Paletzki, R.; Brown, P. D1 dopamine receptor supersensitivity in the dopamine-depleted striatum results from a switch in the regulation of ERK1/2/MAP kinase. *The Journal of neuroscience : the official journal of the Society for Neuroscience* **2002**, *22*, 5042-5054.

145. Chevrier, N.; Mertins, P.; Artyomov, M.N.; Shalek, A.K.; Iannacone, M.; Ciaccio, M.F.; Gat-Viks, I.; Tonti, E.; DeGrace, M.M.; Clauser, K.R.; et al. Systematic discovery of TLR signaling components delineates viral-sensing circuits. *Cell* **2011**, *147*, 853-867, doi:10.1016/j.cell.2011.10.022.

146. Centonze, D.; Napolitano, M.; Saulle, E.; Gubellini, P.; Picconi, B.; Martorana, A.; Pisani, A.; Gulino, A.; Bernardi, G.; Calabresi, P. Tissue plasminogen activator is required for corticostriatal long-term potentiation. *The European journal of neuroscience* **2002**, *16*, 713-721.

147. Hebert, M.; Lesept, F.; Vivien, D.; Macrez, R. The story of an exceptional serine protease, tissue-type plasminogen activator (tPA). *Revue neurologique* **2016**, *172*, 186-197, doi:10.1016/j.neurol.2015.10.002.

148. Shav-Tal, Y.; Zipori, D. The role of activin a in regulation of hemopoiesis. *Stem cells (Dayton, Ohio)* **2002**, *20*, 493-500, doi:10.1634/stemcells.20-6-493.

149. Mantuano, E.; Lam, M.S.; Gonias, S.L. LRP1 assembles unique co-receptor systems to initiate cell signaling in response to tissue-type plasminogen activator and myelin-associated glycoprotein. *The Journal of biological chemistry* **2013**, *288*, 34009-34018, doi:10.1074/jbc.M113.509133.

150. Poulaki, V.; Mitsiades, N.; Kruse, F.E.; Radetzky, S.; Iliaki, E.; Kirchhof, B.; Joussen, A.M. Activin a in the regulation of corneal neovascularization and vascular endothelial growth factor expression. *The American journal of pathology* **2004**, *164*, 1293-1302, doi:10.1016/s0002-9440(10)63216-6.

151. Hashimoto, M.; Gaddy-Kurten, D.; Vale, W. Protooncogene junB as a target for activin actions. *Endocrinology* **1993**, *133*, 1934-1940, doi:10.1210/endo.133.5.8404639.

152. Seko, Y.; Takahashi, N.; Tobe, K.; Ueki, K.; Kadowaki, T.; Yazaki, Y. Vascular endothelial growth factor (VEGF) activates Raf-1, mitogen-activated protein (MAP) kinases, and S6 kinase (p90rsk) in cultured rat cardiac myocytes. *Journal of cellular physiology* **1998**, *175*, 239-246, doi:10.1002/(sici)1097-4652(199806)175:3<239::aid-jcp1>3.0.co;2-p.

153. Kuba, K.; Matsumoto, K.; Date, K.; Shimura, H.; Tanaka, M.; Nakamura, T. HGF/NK4, a four-kringle antagonist of hepatocyte growth factor, is an angiogenesis inhibitor that suppresses tumor growth and metastasis in mice. *Cancer research* **2000**, *60*, 6737-6743.

154. Liu, Y.; Mueller, B.M. Protease-activated receptor-2 regulates vascular endothelial growth factor expression in MDA-MB-231 cells via MAPK pathways. *Biochemical and biophysical research communications* **2006**, *344*, 1263-1270, doi:10.1016/j.bbrc.2006.04.005.

155. Seghezzi, G.; Patel, S.; Ren, C.J.; Gualandris, A.; Pintucci, G.; Robbins, E.S.; Shapiro, R.L.; Galloway, A.C.; Rifkin, D.B.; Mignatti, P. Fibroblast growth factor-2 (FGF-2) induces vascular endothelial growth factor (VEGF) expression in the endothelial cells of forming capillaries: an autocrine mechanism contributing to angiogenesis. *The Journal of cell biology* **1998**, *141*, 1659-1673.

156. Goldin, L.R.; Martinez, M.M. The detection of linkage and heterogeneity in nuclear families when unaffected individuals are considered unknown. *Progress in clinical and biological research* **1989**, *329*, 195-200.

3

157. Herran, E.; Requejo, C.; Ruiz-Ortega, J.A.; Aristieta, A.; Igartua, M.; Bengoetxea, H.; Ugedo, L.; Pedraz, J.L.; Lafuente, J.V.; Hernandez, R.M. Increased antiparkinson efficacy of the combined administration of VEGF- and GDNF-loaded nanospheres in a partial lesion model of Parkinson's disease. *International journal of nanomedicine* **2014**, *9*, 2677-2687, doi:10.2147/ijn.s61940.

158. Holmes, D.I.; Zachary, I. Placental growth factor induces FosB and c-Fos gene expression via Flt-1 receptors. *FEBS letters* **2004**, *557*, 93-98.

159. Rius, J.; Martinez-Gonzalez, J.; Crespo, J.; Badimon, L. NOR-1 is involved in VEGF-induced endothelial cell growth. *Atherosclerosis* **2006**, *184*, 276-282, doi:10.1016/j.atherosclerosis.2005.04.008.

160. Barua, R.S.; Ambrose, J.A.; Saha, D.C.; Eales-Reynolds, L.J. Smoking is associated with altered endothelial-derived fibrinolytic and antithrombotic factors: an in vitro demonstration. *Circulation* **2002**, *106*, 905-908.

161. Huber, D.; Cramer, E.M.; Kaufmann, J.E.; Meda, P.; Masse, J.M.; Kruithof, E.K.; Vischer, U.M. Tissue-type plasminogen activator (t-PA) is stored in Weibel-Palade bodies in human endothelial cells both in vitro and in vivo. *Blood* **2002**, *99*, 3637-3645.

162. Ohnesorge, N.; Viemann, D.; Schmidt, N.; Czymai, T.; Spiering, D.; Schmolke, M.; Ludwig, S.; Roth, J.; Goebeler, M.; Schmidt, M. Erk5 activation elicits a vasoprotective endothelial phenotype via induction of Kruppel-like factor 4 (KLF4). *The Journal of biological chemistry* **2010**, *285*, 26199-26210, doi:10.1074/jbc.M110.103127.

163. Matys, T.; Pawlak, R.; Matys, E.; Pavlides, C.; McEwen, B.S.; Strickland, S. Tissue plasminogen activator promotes the effects of corticotropin-releasing factor on the amygdala and anxiety-like behavior. *Proceedings of the National Academy of Sciences of the United States of America* **2004**, *101*, 16345-16350, doi:10.1073/pnas.0407355101.

164. Santos-Carvalho, A.; Elvas, F.; Alvaro, A.R.; Ambrosio, A.F.; Cavadas, C. Neuropeptide Y receptors activation protects rat retinal neural cells against necrotic and apoptotic cell death induced by glutamate. *Cell death & disease* **2013**, *4*, e636, doi:10.1038/cddis.2013.160.

165. Ferreira-Marques, M.; Aveleira, C.A.; Carmo-Silva, S.; Botelho, M.; Pereira de Almeida, L.; Cavadas, C. Caloric restriction stimulates autophagy in rat cortical neurons through neuropeptide Y and ghrelin receptors activation. *Aging* **2016**, *8*, 1470-1484, doi:10.18632/aging.100996.

166. Hansel, D.E.; Eipper, B.A.; Ronnett, G.V. Neuropeptide Y functions as a neuroproliferative factor. *Nature* **2001**, *410*, 940-944, doi:10.1038/35073601.

167. Decressac, M.; Pain, S.; Chabeauti, P.Y.; Frangeul, L.; Thiriet, N.; Herzog, H.; Vergote, J.; Chalon, S.; Jaber, M.; Gaillard, A. Neuroprotection by neuropeptide Y in cell and animal models of Parkinson's disease. *Neurobiology of aging* **2012**, *33*, 2125-2137, doi:10.1016/j.neurobiolaging.2011.06.018.

168. Liu, Y.; Poon, V.; Sanchez-Watts, G.; Watts, A.G.; Takemori, H.; Aguilera, G. Salt-inducible kinase is involved in the regulation of corticotropin-releasing hormone transcription in hypothalamic neurons in rats. *Endocrinology* **2012**, *153*, 223-233, doi:10.1210/en.2011-1404.

169. Irie, Y.; Yamagata, K.; Gan, Y.; Miyamoto, K.; Do, E.; Kuo, C.H.; Taira, E.; Miki, N. Molecular cloning and characterization of Amida, a novel protein which interacts with a neuron-specific immediate early gene product arc, contains novel nuclear localization signals, and causes cell death in cultured cells. *The Journal of biological chemistry* **2000**, *275*, 2647-2653.

170. Myrum, C.; Baumann, A.; Bustad, H.J.; Flydal, M.I.; Mariaule, V.; Alvira, S.; Cuellar, J.; Haavik, J.; Soule, J.; Valpuesta, J.M.; et al. Arc is a flexible modular protein capable of reversible self-oligomerization. *The Biochemical journal* **2015**, *468*, 145-158, doi:10.1042/bj20141446.

171. Sgambato-Faure, V.; Buggia, V.; Gilbert, F.; Levesque, D.; Benabid, A.L.; Berger, F. Coordinated and spatial upregulation of arc in striatonigral neurons correlates with L-dopa-induced behavioral sensitization in dyskinetic rats. *Journal of neuropathology and experimental neurology* **2005**, *64*, 936-947.

172. Garcia, P.C.; Real, C.C.; Britto, L.R. The Impact of Short and Long-Term Exercise on the Expression of Arc and AMPARs During Evolution of the 6-Hydroxy-Dopamine Animal Model of Parkinson's Disease. *Journal of molecular neuroscience : MN* **2017**, *61*, 542-552, doi:10.1007/s12031-017-0896-y.

173. Nikolaienko, O.; Eriksen, M.S.; Patil, S.; Bito, H.; Bramham, C.R. Stimulus-evoked ERK-dependent phosphorylation of activity-regulated cytoskeleton-associated protein (Arc) regulates its neuronal subcellular localization. *Neuroscience* **2017**, *360*, 68-80, doi:10.1016/j.neuroscience.2017.07.026.

174. Menard, C.; Tse, Y.C.; Cavanagh, C.; Chabot, J.G.; Herzog, H.; Schwarzer, C.; Wong, T.P.; Quirion, R. Knockdown of prodynorphin gene prevents cognitive decline, reduces anxiety, and rescues loss of group 1 metabotropic glutamate receptor function in aging. *The Journal of neuroscience : the official journal of the Society for Neuroscience* **2013**, *33*, 12792-12804, doi:10.1523/jneurosci.0290-13.2013.

175. Wang, Y.; Ju, W.; Liu, L.; Fam, S.; D'Souza, S.; Taghibiglou, C.; Salter, M.; Wang, Y.T. alpha-Amino-3-hydroxy-5-methylisoxazole-4-propionic acid subtype glutamate receptor (AMPAR) endocytosis is essential for N-methyl-D-aspartate-induced neuronal apoptosis. *The Journal of biological chemistry* **2004**, *279*, 41267-41270, doi:10.1074/jbc.C400199200.

176. Cenci, M.A.; Lee, C.S.; Bjorklund, A. L-DOPA-induced dyskinesia in the rat is associated with striatal overexpression of prodynorphin- and glutamic acid decarboxylase mRNA. *The European journal of neuroscience* **1998**, *10*, 2694-2706.

177. Hanrieder, J.; Ljungdahl, A.; Falth, M.; Mammo, S.E.; Bergquist, J.; Andersson, M. L-DOPA-induced dyskinesia is associated with regional increase of striatal dynorphin peptides as elucidated by imaging mass spectrometry. *Molecular & cellular proteomics : MCP* **2011**, *10*, M111.009308, doi:10.1074/mcp.M111.009308.

178. Chen, Z.; Guan, Q.; Cao, X.; Xu, Y.; Wang, L.; Sun, S. Effect of antisense FosB and CREB on the expression of prodynorphin gene in rats with levodopa-induced dyskinesias. *Journal of Huazhong University of Science and Technology. Medical sciences = Hua zhong ke ji da xue xue bao. Yi xue Ying De wen ban = Huazhong keji daxue xuebao. Yixue Yingdewen ban* **2006**, *26*, 542-544.

179. Morioka, N.; Sugimoto, T.; Sato, K.; Okazaki, S.; Saeki, M.; Hisaoka-Nakashima, K.; Nakata, Y. The induction of Per1 expression by the combined treatment with glutamate, 5-hydroxytryptamine and dopamine initiates a ripple effect on Bmal1 and Cry1 mRNA expression via the ERK signaling pathway in cultured rat spinal astrocytes. *Neurochemistry international* **2015**, *90*, 9-19, doi:10.1016/j.neuint.2015.06.013.

180. Balsalobre, A.; Marcacci, L.; Schibler, U. Multiple signaling pathways elicit circadian gene expression in cultured Rat-1 fibroblasts. *Current biology : CB* **2000**, *10*, 1291-1294.

181. Wu, Q.F.; Yang, L.; Li, S.; Wang, Q.; Yuan, X.B.; Gao, X.; Bao, L.; Zhang, X. Fibroblast growth factor 13 is a microtubule-stabilizing protein regulating neuronal polarization and migration. *Cell* **2012**, *149*, 1549-1564, doi:10.1016/j.cell.2012.04.046.

182. Lu, H.; Shi, X.; Wu, G.; Zhu, J.; Song, C.; Zhang, Q.; Yang, G. FGF13 regulates proliferation and differentiation of skeletal muscle by down-regulating Spry1. *Cell proliferation* **2015**, *48*, 550-560, doi:10.1111/cpr.12200.

3
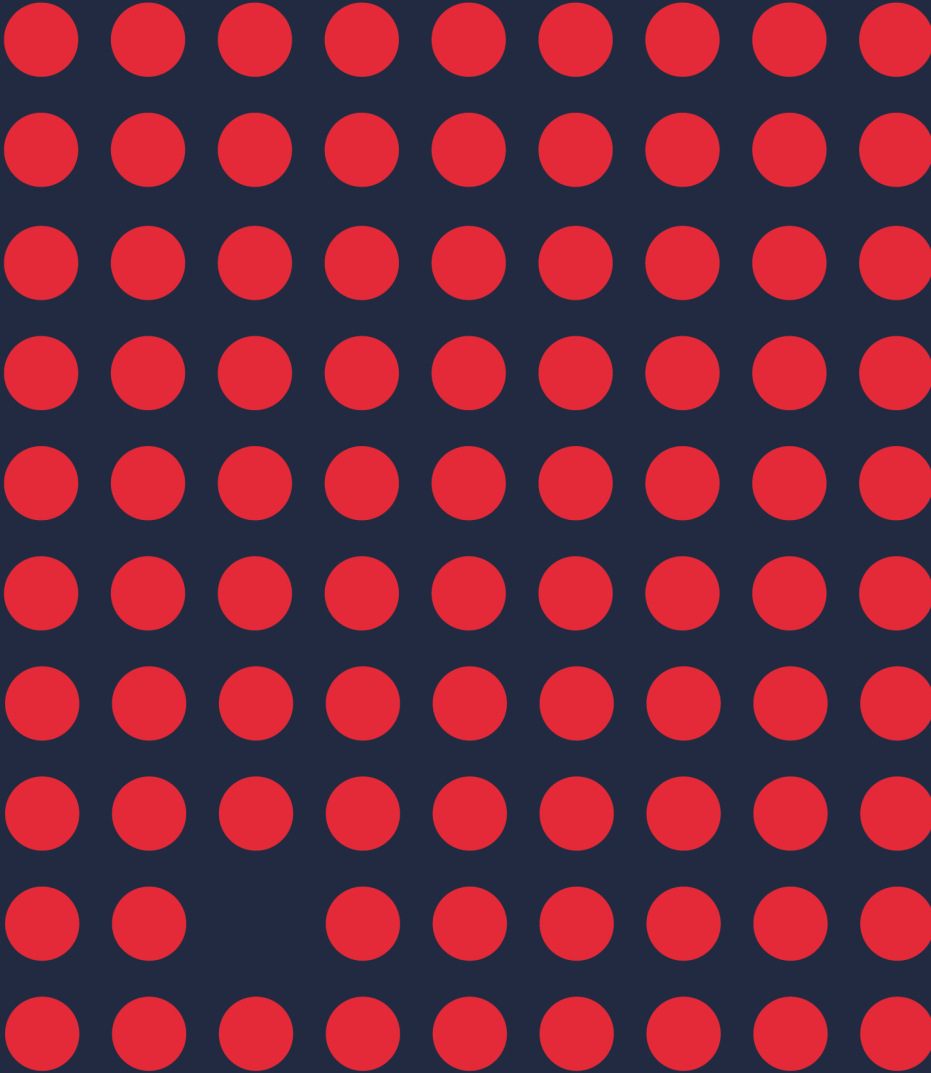
MOLECULAR LANDSCAPE OF TOURETTE'S DISORDER

ABSTRACT

Tourette's disorder (TD) is a highly heritable childhood-onset neurodevelopmental disorder and is caused by a complex interplay of multiple genetic and environmental factors. Yet, the molecular mechanisms underlying the disorder remain largely elusive. In this study, we used the available omics data to compile a list of TD candidate genes, and we subsequently conducted tissue/cell type specificity and functional enrichment analyses of this list. Using genomic data, we also investigated genetic sharing between TD and blood and cerebrospinal fluid (CSF) metabolite levels. Lastly, we built a molecular landscape of TD through integrating the results from these analyses with an extensive literature search to identify the interactions between the TD candidate genes/proteins and metabolites. We found evidence for an enriched expression of the TD candidate genes in four brain regions and the pituitary. The functional enrichment analyses implicated two pathways ('cAMP-mediated signaling' and 'Endocannabinoid Neuronal Synapse Pathway') and multiple biological functions related to brain development and synaptic transmission in TD etiology. Further, we found genetic sharing between TD and the blood and CSF levels of 39 metabolites. The landscape of TD not only provides insights into the (altered) molecular processes that underlie the disease but, through the identification of potential drug targets (such as FLT3, NAALAD2, CX3CL1-CX3CR1, OPRM1, and HRH2), it also yields clues for developing novel TD treatments.

INTRODUCTION

Tourette's disorder (TD) is a childhood-onset neurodevelopmental disorder characterized by multiple motor and vocal tics lasting more than one year. Tics are generally preceded by premonitory urges, peak in severity between the ages of 10 and 12, fluctuate over time, and, in most cases, show improvement by late adolescence or early adulthood. TD affects approximately 1% of the general population, is more prevalent in males and is often associated with other neuropsychiatric comorbidities, including attention-deficit/hyperactivity disorder (ADHD), obsessive-compulsive disorder (OCD), autism spectrum disorders (ASDs), anxiety, and depression [1,2]. TD is a highly familial and heritable disorder [3]. Furthermore, TD is thought to be a complex disease resulting from interactions between multiple genetic and environmental risk factors, although the etiology and pathogenesis of TD have not yet been (fully) elucidated. Genetic studies have suggested that both common genetic variants with small effects and rare variants with larger effects contribute to TD risk, although small sample sizes have hindered the discovery of genome-wide significant signals. Various biological effects of the genes (and their encoded proteins) that have been associated with TD, including alterations in the histaminergic pathway, synaptic transmission, cell adhesion and mitochondrial function, highlight the complexity of the disorder [4,5]. Moreover, environmental factors, such as pre-, peri- and postnatal events, psychological stress and infections, could not only contribute to gene-environment interactions but also affect the development, course, and severity of TD symptoms [6,7]. Neurobiologically, TD appears to involve abnormalities in the development, structure and function of cortico-striato-thalamo-cortical (CSTC) circuits associated with motor and behavioral control and with impaired signaling of multiple modulatory neurotransmitters, especially dopamine [8].

As for treating TD, current therapies – including psychoeducation, behavioral interventions and medication, such as atypical antipsychotics – may partly ameliorate symptoms. However, inadequate control of tics and the occurrence of adverse side effects hinder the treatment of TD. Therefore, novel strategies are required to enhance our understanding of the molecular basis of this disorder, which could in turn provide clues for the development of (more) effective treatments. Previous studies have shown that drug candidates are more likely to pass clinical trials and be approved for patients if they target genes linked to human disease [9,10], highlighting the importance of human genetics in drug target identification. In addition, considering that well-powered studies of candidate gene hypotheses for other complex traits, e.g., schizophrenia [11,12], showed that previously reported positive findings were highly likely to be false positives, we decided to focus on omics data sets.

More specifically, we applied and extended the approach that we used before to build so-called 'molecular landscapes' of complex neuropsychiatric diseases, including ADHD

4

[13], ASDs [14], OCD [15], and Parkinson's disease (PD) [16]. In short, we first compiled a comprehensive list of candidate genes that are associated with TD through one or more types of omics data. These data primarily included genomic data (different types of common and rare genetic variants) and were corroborated by epigenomic data (DNA methylation) and transcriptomic data (differential gene/mRNA expression in blood and brain). To identify the molecular mechanisms that are affected in TD, we then performed tissue/cell type specificity and functional enrichment analyses of the TD candidate genes. As biofluid levels of many metabolites represent 'intermediate phenotypes' (that link genetic or environmental risk factors to a disease) and the variation in these metabolite levels is at least in part attributable to genetic factors [17-19], we also used genomic data to investigate the extent and direction of genetic overlap between TD and the levels of a large number of blood and cerebrospinal fluid (CSF) metabolites. Subsequently, we applied additional selection criteria – that reflected the amount of independent omics evidence – to the list of TD candidate genes, resulting in 'prioritized' TD candidate genes and candidate genes for which less omics evidence implicating them in TD etiology was available. Lastly, we built a molecular landscape of TD through integrating the results from the tissue/cell type and functional enrichment analyses with an elaborate literature search for interactions between the proteins encoded by the TD candidate genes and the metabolites implicated through the genetic overlap analyses and other metabolome/microbiome studies. The resulting TD landscape provides insights into the (altered) molecular processes that underlie the disease as well as potential drug targets that could be further developed into treatments.

RESULTS
Input omics datasets and candidate genes

Based on the literature search and our analyses of the TD GWAS data, we compiled a list of TD candidate genes from the single-omics studies of TD (i.e., genomics, transcriptomics, epigenomics, metabolomics, microbiomics). We provide the characteristics of the included studies in Table S1 and below, we briefly describe the included studies.

Based on the type of omics evidence they provide, we classified the studies as guiding (genomics studies), corroborating (epigenomics and transcriptomics studies) and additional (metabolomics and microbiome) studies. For the genomics data, we compiled a list of TD candidate genes from studies of rare genetic variants/events – (i) eight chromosomal rearrangements studies [20-27] (the main list includes 15 genes and the extended list consists of 23 genes), (ii) fifteen single nucleotide variation (SNV) studies [23,28-41] (the main list includes 134 genes and the extended list consists of 846 genes), and (iii) eleven

copy number variations (CNV) studies [33,40,42-50] (the main list includes 52 genes, and the extended list consists of 956 genes) – and studies of common genetic variants (of single nucleotide polymorphisms or SNPs), i.e., genome-wide association studies (GWASs). The GWAS-derived genes include the results from our own, unpublished analyses of the summary statistics data from the TD GWAS by Yu et al. [51], i.e., 113 genes from the MAGMA analysis, 224 genes from the FUMA analysis, and 143 genes from the TWAS analysis. In addition, the GWAS-derived candidate genes include published results of (other) studies using TD GWASs, including cross-disorder studies and annotation of the GWAS by Yu et al. from the GWAS Catalog [52-56], as well as the preliminary MAGMA results from the newest TD GWAS (available as a preprint on medRxiv at the time of analysis) [57].

Corroborating evidence for the genomic-studies-derived genes was assembled from two epigenome-wide association studies (EWASs) that investigated DNA methylation in the peripheral blood of TD patients versus controls [58,59] (the main list includes 71 genes and the extended list consists of 8 genes), and transcriptomic studies in the brain (postmortem, in the striatum of medicated TD patients vs controls) [60] (957 genes) and blood (medicated [61,62] and unmedicated [63,64] TD patients versus control). We could not find any published proteomic studies of TD.

As for additional evidence, we included findings from three studies that investigated metabolomic changes in the plasma of TD patients [65], serum of PANS patients [66], and urine in a case study of PANDAS-associated tics [67], and from microbiome studies in children with tic disorder [68] and in PANS/PANDAS patients with tics [69]. These results were used as supportive evidence for the metabolites linked to TD through the PRS-based analyses (see below).

We combined the lists of genes implicated through the abovementioned genomic, epigenomic and transcriptomic studies along with their functional annotations into one table (Table S2). In total, we compiled a list of 872 TD candidate genes implicated in TD through the genomic studies (guiding evidence), and this list was subsequently used in tissue and cell specificity and functional enrichment analyses.

Tissue and cell type specificity

We performed specificity analyses to identify the tissues and cell types with enhanced expression of TD-associated genes. We separately analyzed the genes associated with TD based on all types of genomic data and on the postmortem brain transcriptomic data to identify tissues and cell types that contribute to the development of TD and that are particularly affected by lifelong TD, respectively.

Genomic data

In the Tissue Specific Expression Analysis (TSEA), we found that genes preferentially expressed in two out of the 25 human tissues tested were significantly enriched (pSI < 0.05, FDR *p*-value < 0.05, see Materials and Methods) within the 872 TD candidate genes: the brain as a whole (FDR *p*-value =9.17E-09, 148 genes) and the pituitary (FDR *p*-value =1.30E-05, 114 genes; of note, 74 genes were enriched in both the brain and pituitary). We also observed strong expression enrichment in the brain and, to a lesser extent, the pituitary at the more stringent pSI cutoff of 0.01 (brain: FDR *p*-value = 2.73E-05, 81 genes; pituitary: FDR *p*-value = 0.013, 46 genes), which indicated an expression enrichment of specific TD candidate genes in the brain (and pituitary) (File S1).

In the analysis of human spatiotemporal brain gene expression data (6 brain regions across 10 developmental periods), we found that TD gene expression was enriched in seven spatiotemporal coordinates, involving 4 brain regions during specific developmental periods: (I) cerebellum: early fetal period (FDR *p*-value = 0.028, 53 genes); (II) cortex: early mid-fetal period(FDR *p*-value = 0.004, 51 genes), neonatal period/early infancy (FDR *p*-value = 0.005, 33 genes), adolescence (FDR *p*-value = 0.014, 34 genes), young adulthood (FDR *p*-value = 5.021E-04, 48 genes); (III) striatum: early mid-fetal period (FDR *p*-value = 0.043, 36 genes); (IV) thalamus: neonatal period/early infancy (FDR *p*-value = 0.021, 46 genes). We also observed a trend-significant enrichment of the late mid-fetal period in the cortex (FDR *p*-value = 0.052, 36 genes) and mid-late childhood in the cerebellum (FDR *p*-value = 0.079, 53 genes) (File S2).

Taking into account the substantial cellular heterogeneity in brain tissue, we then used single-cell data from adult mice to identify individual candidate cell populations that are likely to be affected in TD. In the Cell Specific Expression Analysis (CSEA), we observed a trend-significant enrichment of two cell populations: Drd2+ medium spiny neurons (MSNs) of the striatum (33 genes) and layer 6 corticothalamic neurons (Ntsr+, 21 genes), although these results did not pass our threshold for significance (FDR *p*-value = 0.160 for both cell types) (File S3).

Brain transcriptomic data

Alterations of gene expression from a complex mix of cells, such as those from brain tissue, may represent changes in the (relative) cellular composition of the tissue [70]. To this end, we also applied the CSEA method to the transcriptomic data from the postmortem striatum of TD patients [60] to infer the cellular fingerprint of a lifelong disease. Among the striatal cell types assessed by CSEA, genes downregulated in TD striatum were overrepresented in the expression profiles of cholinergic interneurons (FDR *p*-value < 0.05 across all pSI thresholds)

and, to a lesser extent, Drd1+ MSNs (FDR p-value = 0.06), indicating a loss and/or reduced function of these cell types. Of note, the enrichment of cholinergic interneurons was also significant for the basal forebrain, which is consistent with their restricted distribution in the central nervous system (CNS), i.e., with these cell types being concentrated in these particular brain regions (the basal forebrain, caudate and putamen) [71]. Furthermore, genes downregulated in the TD striatum were also enriched for genes that are highly expressed in cortical cells, i.e., layer 6 corticothalamic neurons (Ntsr+ neurons), layer 5 pyramidal neurons projecting to the thalamus, spinal cord and striatum (Glt25d2 neurons), and cortical neurons that express the prepronociceptin gene (Pnoc+ neurons) (File S4). The analysis of the WGCNA module that was enriched for downregulated genes further confirmed an overabundance of genes that are highly expressed in interneurons, and it provided evidence for an involvement of Drd2+ MSNs (FDR p-value < 0.05 across all pSI thresholds) (File S5). Lastly, the analysis of upregulated genes revealed an overrepresentation of immunity-related cell types (in the cortex) and glial cells (in the cerebellum and cortex) (File S6), while the WGCNA module analysis yielded a specific enrichment of immune cells (File S7).

Functional enrichment analyses

We used Ingenuity Pathway Analysis (IPA) to identify canonical pathways, diseases/ biological functions and upstream regulators that are enriched within the 872 TD candidate genes. We provide the full results of all analyses performed with IPA in Table S3, while below, we describe the most significant findings (i.e., with FDR p-value < 0.05).

The canonical pathway analysis in IPA identified two signaling pathways that were significantly enriched within the 872 genes: 'cAMP-mediated signaling' and 'Endocannabinoid Neuronal Synapse Pathway' (Table 1). Three genes – *ADCY2, MAPK3,* and *PRKAR2A* – were implicated in both pathways, suggested a (partial) shared underlying biology.

TABLE 1. Canonical Pathways enriched within the TD candidate genes.

Canonical Pathway	FDR p-value	Ratio	Dataset genes in the pathway
cAMP-mediated signaling	1.95E-02	22/235	*ADCY2, AKAP9, CAMK1D, CRHR1, DRD2, DUSP6, FFAR3, FPR1, FPR2, GRK4, HRH2, MAPK3, MPPE1, OPRD1, OPRK1, OPRM1, PALM2AKAP2, PDE4A, PDE6B, PDE9A, PRKAR2A, RGS12*
Endocannabinoid Neuronal Synapse Pathway	2.19E-02	16/149	*ADCY2, CACNA1D, CACNA1I, CACNA1S, CACNA2D3, DAGLA, DNAH1, DNAH10, DNAH3, GNB1L, GRIN2A, MAPK3, PLCH1, PRKAG1, PRKAR2A, RIMS1*

In the diseases and biofunctions analysis, IPA identified significant enrichment of 71 functional annotations contained within two functional categories: Molecular and Cellular Functions and Physiological System Development and Function (Table 2). Most of the enriched functions are linked to the development and function of the nervous system and include many overlapping genes (Table S3-b). The Diseases and Disorders category was highly enriched for cancer-related diseases (Table S3-b). This result is partly driven by the inclusion in IPA of findings from the COSMIC and ClinVar projects, which identified many associations between genes and various cancers, and genes involved in normal biological processes are impacted when these functions are dysregulated by cancer. After filtering the results to exclude cancer, we found a significant association (FDR p-value < 0.05) with 119 disease annotations falling into several higher-level categories, including 'Neurological Disease' (54 annotations), 'Psychological Disorders' (30), 'Developmental Disorder' (19), 'Hereditary Disorder' (17), 'Cardiovascular Disease' (9), 'Skeletal and Muscular Disorders' (9), 'Gastrointestinal Disease' (7), 'Infectious Disease' (5), and 'Inflammatory Disease' (4).

TABLE 2. Biological functions enriched within TD candidate genes.

Molecular and Cellular Functions			Physiological System Development and Function		
Functional annotation	FDR p-value	Genes	Functional annotation	FDR p-value	Genes
Cell movement of neurons	5.73E-09	40	Cognition	8.33E-12	72
Development of neurons*	2.00E-08	92	Learning	4.23E-09	62
Neuritogenesis*	2.03E-08	48	Morphology of nervous system	9.54E-09	107
Migration of neurons*	2.11E-08	38	Development of head	1.32E-08	108
Development of neural cells*	2.90E-08	95	Morphogenesis of nervous tissue	1.95E-08	76
Neurotransmission*	7.57E-08	54	Development of body axis	2.66E-08	112
Organization of cytoplasm	2.01E-07	148	Morphology of brain	2.94E-08	66
Organization of cytoskeleton	4.55E-07	136	Morphology of central nervous system	4.82E-08	70
Microtubule dynamics	6.08E-07	121	Organismal death	5.02E-08	220
Formation of cellular protrusions	9.93E-07	38	Development of central nervous system	1.29E-06	73
Migration of neural cells	2.02E-06	40	Formation of brain	1.54E-06	60
Quantity of neurotransmitter	5.87E-06	27	Abnormal morphology of brain	1.38E-05	50
Transport of molecule	6.29E-06	141	Spatial learning	1.44E-05	28
Synaptic transmission*	2.07E-05	41	Emotional behavior	2.01E-05	38
Cell movement of brain cells	3.39E-05	18	Conditioning	2.17E-05	30
Axonogenesis*	3.68E-05	37	Abnormal morphwology of nervous system	2.23E-05	81

TABLE 2. Continued

Molecular and Cellular Functions			Physiological System Development and Function		
Functional annotation	FDR *p*-value	Genes	Functional annotation	FDR *p*-value	Genes
Branching of cells	4.59E-05	75	Morphology of head	2.26E-05	101
Action potential of cells*	4.61E-05	23	Morphology of nervous tissue	2.44E-05	72
Proliferation of neural cells*	5.92E-05	70	Abnormal morphology of central nervous system	2.46E-05	53
Length of cells	6.46E-05	31	Prepulse inhibition	2.68E-05	17
Morphology of neurons*	7.13E-05	38	Quantity of neurons	3.93E-05	51
Sprouting	1.06E-04	99	Vocalization	4.81E-05	12
Proliferation of neuronal cells*	1.11E-04	56	Vertical rearing	9.39E-05	16
Length of neurons*	1.83E-04	47	Movement of rodents	1.35E-04	26
Shape change of neurites	2.85E-04	20	Social exploration	2.34E-04	12
Abnormal quantity of neurotransmitter	3.28E-04	9	Social behavior	2.61E-04	18
Branching of neurons*	3.36E-04	18	Exploratory behavior	2.65E-04	16
Length of neurites*	3.52E-04	16	Abnormal morphology of body cavity	3.43E-04	126
Migration of brain cells	3.80E-04	15	Nest building behavior	4.37E-04	8
Branching of neurites*	4.15E-04	65	Abnormal morphology of head	4.81E-04	86
Organization of cells	5.56E-04	22	Locomotion	5.03E-04	39
Quantity of monoamines	5.90E-04	24	Morphology of body cavity	6.05E-04	139
Quantity of catecholamine	5.95E-04	20	Development of body trunk	6.47E-04	104
Action potential of neurons*	7.23E-04	19	Quantity of cells	7.26E-04	157
Uptake of dopamine	8.48E-04	7	Self-abusive behavior	7.51E-04	4
			Passive avoidance learning	9.72E-04	9

Table 2 presents the enriched biological functions, the FDR *p*-value of overlap and number of genes involved in each function. * Functional annotations that are shared between the two main functional categories but are reported only once.

In the upstream regulator analysis, none of the identified upstream regulators remained significant after correction for multiple testing (Table S3-c). That being said, the top regulators at a suggestive *p*-value threshold (uncorrected *p*-value <0.01) include – among 'Drugs and Chemicals' – molybdenum disulfide (chemical reagent), topotecan (chemical drug), GnRH analog (biologic drug), lipoxin LXA4 (endogenous chemical), and – among 'Genes, RNAs and Proteins' – NEDD4 (enzyme), OPRM1 (G-protein coupled receptor), ANGPT2 (growth factor), CLCA2 (ion channel), and TEAD4 (transcription regulator).

Shared genetic etiology analyses with levels of blood and cerebrospinal fluid metabolites

Polygenic risk score (PRS)-based analyses

We conducted PRS-based analyses to investigate the presence and extent of genetic overlap between TD and metabolite concentrations in blood and/or CSF. After Bonferroni correction for the number of tests performed, we identified significant associations between TD and the levels of 37 blood metabolites (out of the 993 blood metabolites tested) and 2 CSF metabolites (out of the 338 CSF metabolites tested). The results for these metabolites are presented in Table 3, along with the superpathway and pathway annotations (where applicable). Genetic variants associated with TD explained up to 2.08% of the genetically determined variation in the levels of the 37 significant blood metabolites, and up to 9.90% of the variation in the levels of the two significant CSF metabolites. The complete results of the PRS-based analyses for the blood and CSF metabolites are provided in Table S4a-b.

SNP effect concordance analysis (SECA)

Through performing SECA for the significantly associated metabolites from the PRS-based analyses, we found a significant genetic concordance between TD and the levels of all 39 metabolites (Table 3). Among these, 24 blood metabolites showed positive concordance, indicating that genetic variants associated with TD also convey genetic risk to increased blood levels of these metabolites. The remaining 13 blood metabolites – including indoxyl sulfate, homocitrulline, pyridoxate, myo-inositol, triacylglycerols – and the two CSF metabolites – N-acetyl-aspartyl-glutamate (NAAG) and butyrate – showed negative concordance with TD, implying that genetic variants associated with TD also convey genetic risk to decreased blood/CSF levels of these metabolites.

TABLE 3. Results from the PRS-based and SECA analyses for the levels of 37 blood and 2 CSF metabolites that show evidence for genetic sharing with TD at a Bonferroni corrected p-value <0.05.

Metabolite	Super-pathway	Pathway	P_T	p-value	R^2	N SNPs	Concordance p-value	Concordance with TD	GWAS	N GWAS	Biofluid
Betaine[a]	Amino acid	Glycine, Serine, and Threonine Metabolism	0.5	4.05E-07	1.34%	160355	9.99E-04	+	Rhee	1802	P
Indoxyl sulfate[a]	Amino acid	Tryptophan Metabolism	0.5	7.08E-06	1.29%	160350	9.99E-04	-	Rhee	1455	P
Homocitrulline	Amino acid	Urea cycle; Arginine and Proline Metabolism	0.5	4.41E-06	0.50%	135356	9.99E-04	-	Shin	3950	P, S
Valine[a]	Amino acid	Valine, leucine, and isoleucine metabolism	0.4	4.44E-06	0.30%	130625	9.99E-04	+	Draaisma	6538	S
Pyridoxate[a]	Cofactors and vitamins	Vitamin B6 Metabolism	0.05	4.91E-06	1.34%	25642	9.99E-04	-	Rhee	1453	P
Tumor necrosis factor-beta	Cytokine	NA	0.3	3.75E-06	1.28%	148461	9.99E-04	+	Ahola-Olli	1559	P, S
Phosphatidylcholine diacyl c38:4	Lipid	Glycerophospholipids	0.4	1.54E-08	0.41%	130941	9.99E-04	+	Draaisma	7474	S
Phosphatidylcholine 32:1[a]	Lipid	Glycerophospholipids	0.5	2.94E-07	1.38%	160355	9.99E-04	-	Rhee	1797	P
Phosphatidylcholine 38:5[a]	Lipid	Glycerophospholipids	0.5	3.19E-07	1.37%	160355	9.99E-04	+	Rhee	1797	P
1-arachidonoylglycerophosphoethanolamine*	Lipid	Glycerophospholipids	0.4	3.47E-07	0.33%	115933	9.99E-04	+	Shin	7350	P, S
1-stearoylglycerophosphoethanolamine	Lipid	Glycerophospholipids	0.05	1.50E-06	0.31%	22467	9.99E-04	+	Shin	6929	P, S
Phosphatidylcholine diacyl c38:6	Lipid	Glycerophospholipids	0.5	6.30E-06	0.25%	153336	9.99E-04	+	Draaisma	7475	S
1-arachidonoylglycerophosphocholine*	Lipid	Glycerophospholipids	0.3	6.35E-06	0.27%	93688	9.99E-04	+	Shin	7063	P, S
Phosphatidylcholine diacyl c36:4	Lipid	Glycerophospholipids	0.4	6.58E-06	0.25%	130937	9.99E-04	+	Draaisma	7476	S
Myo-inositol	Lipid	Inositol Metabolism	0.5	8.25E-10	0.49%	135380	9.99E-04	-	Shin	7354	P, S

TABLE 3. Continued

Metabolite	Super-pathway	Pathway	P_T	p-value	R^2	N SNPs	Concordance p-value	Concordance with TD	GWAS	N GWAS	Biofluid
Total lipids in very small VLDL	Lipid	Lipid ratios	0.4	1.73E-06	0.11%	390060	9.99E-04	+	Shin	2859	P, S
Concentration of very small VLDL particles	Lipid	Lipid ratios	0.2	3.27E-06	0.11%	223305	9.99E-04	+	Kettunen	19,273	P, S
Phospholipids in very small VLDL	Lipid	Lipid ratios	0.4	3.37E-06	0.11%	390017	9.99E-04	+	Kettunen	19,273	P, S
Sum SM	Lipid	Lipid ratios	0.3	4.21E-06	1.10%	109794	9.99E-04	+	Rhee	1797	P
Ratio total PC: total LPC	Lipid	Lipid ratios	0.3	5.96E-06	1.06%	109794	9.99E-04	-	Rhee	1797	P
Stearate (18:0)	Lipid	Long Chain Fatty Acid	0.2	3.46E-08	0.39%	68520	9.99E-04	+	Shin	7355	P, S
X-12442−5,8-tetradecadienoate	Lipid	Long Chain Fatty Acid	0.1	8.00E-07	0.31%	39528	9.99E-04	+	Shin	7334	P, S
Palmitate (16:0)	Lipid	Long Chain Fatty Acid	0.3	2.73E-06	0.28%	93694	9.99E-04	+	Shin	7352	P, S
Laurate (12:0)	Lipid	Medium Chain Fatty Acid	0.1	3.77E-07	0.33%	39530	9.99E-04	+	Shin	7346	P, S
Linoleate (18:2n6)[a]	Lipid	Polyunsaturated Fatty Acid (n3 and n6)	0.2	4.67E-08	0.39%	68518	9.99E-04	+	Shin	7333	P, S
Arachidonate (20:4n6)	Lipid	Polyunsaturated Fatty Acid (n3 and n6)	0.5	1.09E-07	0.36%	135383	9.99E-04	+	Shin	7367	P, S
Linolenate [alpha or gamma; (18:3n3 or 6)]	Lipid	Polyunsaturated Fatty Acid (n3 and n6)	0.2	1.38E-06	0.30%	68524	9.99E-04	+	Shin	7338	P, S
Dihomo-linoleate (20:2n6)	Lipid	Polyunsaturated Fatty Acid (n3 and n6)	0.3	6.47E-06	0.26%	93696	9.99E-04	+	Shin	7353	P, S
Sphingomyelin 18:1[a]	Lipid	Sphingolipid Metabolism	0.4	3.87E-10	2.08%	136596	9.99E-04	+	Rhee	1797	P
Sphingomyelin 18:0[a]	Lipid	Sphingolipid Metabolism	0.3	4.64E-07	1.33%	109794	9.99E-04	+	Rhee	1797	P
Triacylglycerol 50:2	Lipid	Triacylglycerol	0.5	2.52E-06	1.15%	160355	9.99E-04	-	Rhee	1797	P
Triacylglycerol 48:0	Lipid	Triacylglycerol	0.5	5.66E-06	1.07%	160355	9.99E-04	-	Rhee	1797	P

TABLE 3. Continued

Metabolite	Super-pathway	Pathway	P_T	p-value	R^2	N SNPs	Concordance p-value	Concordance with TD	GWAS	N GWAS	Biofluid
Triacylglycerol 48:1	Lipid	Triacylglycerol	0.5	7.18E-06	1.04%	160355	9.99E-04	-	Rhee	1797	P
X-11381	Unknown	Unknown	0.1	1.06E-06	0.31%	39527	9.99E-04	-	Shin	7308	P, S
X-04494	Unknown	Unknown	0.4	1.21E-06	0.47%	115916	9.99E-04	-	Shin	4689	P, S
X-12116	Unknown	Unknown	0.5	2.21E-06	0.73%	135350	9.99E-04	-	Shin	2859	P, S
X-09706	Unknown	Unknown	0.5	3.32E-06	0.28%	135378	9.99E-04	-	Shin	7256	P, S
N-acetyl-aspartyl-glutamate (NAAG)	Amino acid	Glutamate Metabolism	0.5	1.80E-08	9.90%	277618	9.99E-04	-	Panyard	291	CSF
Butyrate (4:0)	Lipid	Short Chain Fatty Acid	0.5	2.29E-06	6.97%	277618	9.99E-04	-	Panyard	291	CSF

Note: Superpathway and pathway annotations are given for metabolites with known chemical identity. Metabolites were classified as 'Unknown' if their chemical identity was not yet determined at the time of analysis. Abbreviations: P_T – the most predictive SNP p-value threshold in the base sample (TD); R^2 – the variance explained in the target sample (metabolite levels); N SNPs – the number of SNPs; Concordance p-value – all concordance analyses yielded significant results (i.e., Bonferroni-corrected p-value < 0.05/39 tests=1.28E-03); Concordance with TD – direction of effect estimated in SECA: '+' positive association, '-' negative association; GWAS – source of the target sample phenotypes (metabolite traits) GWAS data – Ahola-Olli [72], Draaisma [73], Kettunen [74], Panyard [75], Rhee [76], Shin [19]; N GWAS – sample size of the target sample phenotypes (metabolite traits); * – indicates metabolites for which identities were inferred based on their fragmentation spectrum and other biochemical evidence; [a] metabolite was also measured in different datasets, but the results did not pass the Bonferroni corrected p-value threshold; PC – phosphatidylcholine; LPC – lysophosphatidylcholine; VLDL – very low-density lipoproteins; SM – sphingomyelin; NA – not available; P – plasma; S – serum; CSF – cerebrospinal fluid.

Molecular landscape of TD

Through the approach described in the Materials and Methods and by integrating the results from the tissue/cell type specificity and functional enrichment analyses with the literature search for interactions between the proteins encoded by the 872 TD candidate genes and the metabolites implicated through the PRS-based analyses, we built a molecular landscape of TD (Figure 1). The landscape is located in the synapse, where presynaptic and postsynaptic neurons interact with astrocytes, microglial cells and the extracellular matrix (ECM), together forming a structure referred to in the literature as the pentapartite synapse [77,78]. For building the landscape, we focused on the 239 proteins encoded by the prioritized TD candidate genes (see Materials and Methods) – that are dark blue in Figure 1 – and their interactions. In addition, if they interacted with at least one of the dark blue proteins, we added some of the remaining proteins encoded by the remaining TD candidate genes for which there was less omics evidence available (see Materials and Methods) – and these proteins are light blue in Figure 1. In total, this amounted to 197 (unique) dark blue proteins and 276 (unique) light blue proteins that are shown in the landscape. The landscape also includes 42 yellow proteins/molecules that have been implicated in TD through transcriptomics/metabolomics data and/or other functional evidence. Lastly, the 11 blood and 2 CSF metabolites of which the levels were found to show significant genetic overlap with TD are indicated in orange and grey, respectively. All interactions between the landscape proteins/molecules can be found – with their corresponding literature references – in Table S5, but below, we have provided a description of the main processes in the landscape, with the key implicated proteins/molecules/metabolites in bold and by part of the neuronal cells where these processes/cascades are mainly taking place.

Description of the TD landscape

Presynaptic and postsynaptic neurons

Extracellular matrix (ECM)

Synapses are enwrapped by a layer of extracellular matrix (ECM), which is important for (shaping and maintaining) synaptic morphology and function. The ECM of the brain consists of non-fibrous proteins such as glycoproteins, matricellular proteins (such as periostin and tenascins), enzymes that regulate ECM deposition and degradation, and fibrous/structural proteins (such as collagens and laminins) [79]. The ECM proteins can modulate the activity or bioavailability of extracellular signaling molecules, such as growth factors, cytokines, chemokines, and extracellular enzymes, and/or bind directly to cell surface receptors to regulate cellular functions. ECM components are synthesized intracellularly in glia and neurons and secreted into the ECM, where they aggregate with the existing matrix, fill the

synaptic cleft, and interact with cell surface receptors. Furthermore, the ECM is also involved in the exchange of nutrients and metabolites between the CNS and systemic circulation [80].

FIGURE 1. Molecular landscape of TD. In this landscape, the interactions between the key proteins/molecules/metabolites implicated in TD in pre- and postsynaptic neurons, astrocytes and/or microglial cells are shown. In Table S5, all interactions between the landscape proteins/molecules/metabolites are provided. In File S8, we provide a pdf version of Figure 1 that will allow interested readers to look up proteins and molecules in the landscape through using the search function. In addition, a larger version of Figure 1 is provided as a fold-out page at the end of this thesis.

First, **THBS1**, an adhesive glycoprotein that is downregulated by **indoxyl sulfate (IS)**, binds and interacts with multiple other landscape proteins, both in the ECM and membrane. Another ECM glycoprotein involved in – among other functions – cell adhesion is **FN1**, and this protein is upregulated by palmitic acid and (also) has very many interactions with other landscape proteins in ECM and membrane. In addition, **POSTN** (**periostin**) is an ECM protein that plays a role in cell adhesion and ECM remodeling by regulating the expression of landscape proteins

– including **FN1** – and interacting with membrane proteins. The tenascin **TNN** is involved in neurite outgrowth through binding the **ITGA4-ITGB1-complex** in the membrane (of microglial cells). Moreover, enzymes that regulate ECM function are the peptidase **DPP4** that (also) binds **FN1**, the protease **HTRA3** that cleaves **FN1**, and **LOLX1**, an oxidase that catalyzes the formation of crosslinks in collagen and elastin fibers. In addition, **RELN** (**reelin**) is a serine protease that regulates many functions, e.g., neuronal adhesion, neuronal migration, neurite outgrowth and synaptic plasticity. **RELN** expression is regulated by the transcription factors **NPAS3** and **TBR1** as well as the membrane receptor **FFAR3** (see below), while **butyric acid** decreases its acetylation and demethylation. Moreover, **RELN** degrades **FN1** and binds/signals through the membrane protein **LRP8** (in astrocytes). Fibrous/structural landscape proteins include several collagen proteins (**COL4A2**, **COL5A1**, **COL6A3**, and **COL8A1**) that regulate synaptogenesis and neuronal cell adhesion, and the laminin **LAMA5**.

Other ECM landscape proteins include the vasoactive peptide **ADM** (that downregulates **FN1**), lipid transport-regulating **APOM** (that downregulates **FN1** and is downregulated by **palmitic acid**), **GCG** (which is a precursor that can be cleaved into multiple peptides, one of which downregulates **FN1**), **CLCA2** (a chloride channel accessory protein that regulates the expression of **CDKNA1** and **FN1**), **CX3CL1** (a membrane protein that is cleaved by the neuronal membrane enzyme **ADAM10** into a soluble form that is a ligand for both **CX3CR1** and the **ITGA4-ITGB1-complex** in the membrane of microglial cells), the interleukins **IL17A** and **IL31**, **LTBP1** – a key regulator of transforming growth factor beta proteins such as **TGFB1** and **TGFB3** – and **NOTCH2NLA**, a component of the NOTCH signaling pathway that regulates neuronal differentiation and can also be located in the cytoplasm. Other ECM proteins with a role in regulating neuronal differentiation and function are **NXPH1** (that binds and interacts with **NRXN1** in the presynaptic membrane), the protease inhibitor **SERPINE2** (that, among other interactions, downregulates the expression of the cytokine **TNFB**), the nerve growth factor **VGF** (that, e.g., regulates **CHGB**, a neuroendocrine secretory granule protein), and members of the WNT protein family (**WNT1**, **WNT3**, **WNT5A**, and **WNT10B**) that modulate many processes such as neuronal differentiation and migration, dendrite development, synaptogenesis, adult neurogenesis, and neural plasticity (summarized in [81]).

Cell membrane

Neuronal cell membrane proteins connect extracellular and intracellular signaling cascades and largely determine a neuronal cell's capacity to communicate and interact with its environment. Different types of cell membrane proteins can be discerned, including enzymes, receptors, ion channels, transporters, cell adhesion-regulating proteins, and other membrane proteins [82].

First, a number of landscape proteins are membrane-located enzymes, such as **DPEP2** (involved in the metabolism of **arachidonic acid**), **FKBP11** (that regulates protein folding), **MARK3** (involved in the phosphorylation of **MAPT**), and **NAALAD2**, an enzyme that is expressed in neuronal and astrocytic membranes and regulates **glutamate** synthesis, see below. In addition, **DAGLA** is a membrane-located enzyme that is involved in the metabolism of **arachidonic acid** and **stearic acid**. **DAGLA** also complexes with the presynaptic transporter **SLC6A4** (see below) and with the postsynaptic density scaffolding protein **HOMER2**. Furthermore, like the related protein **ZDHHC8** in the Golgi membrane (see below), the membrane-located enzyme **ZDHCC17** transfers **palmitic acid** onto target proteins, and it also complexes with **TNFB** and other landscape proteins, including the membrane proteins **LMBR1L** and **TMEM100B**.

As for receptors, different functional classes are located in the (neuronal) cell membrane. In this respect, several landscape proteins are G protein-coupled receptors (GPCRs). GPCRs are highly expressed throughout the brain and regulate synaptic transmission and plasticity [83]. After being bound and activated by their ligands, GPCRs regulate downstream signaling through stimulatory G-proteins – **CRHR1**, the receptor for the hormone **CRH** and in this way a major regulator of the hypothalamic-pituitary-adrenal (HPA) cascade, and **HRH2**, a receptor of histamine that interacts with the TD-linked enzyme **histidine decarboxylase** (**HDC**) (see below) and regulates **arachidonic acid** production – and inhibitory G proteins. Examples of the latter type of GPCRs include **CX3CR1** (a membrane receptor that is highly expressed in microglial cells and that is activated and involved in regulating the immune response through binding its ligand **CX3CL1**, which itself also signals through the membrane **ITGA4-ITGB1-complex**) and **DRD2**, a **dopamine** receptor that interacts with, regulates, or is regulated by multiple landscape proteins. Other membrane GPCRs that signal through inhibitory G-proteins are **FFAR3** (that is activated by **butyrate** and downregulates the expression of landscape proteins like **RELN** and the potassium channel (see below) **KCNH5**), as well as **FPR1**, **FPR2** and **FPR3**, chemokine receptors that form a functional complex, regulate inflammation, and are regulated by the extracellular proteins **ANXA1** and arachidonic acid metabolite LXA4 and by intracellular **BHLE40** and **COP1**. Further, opioid receptors representing the μ, δ, and κ families – encoded by the **OPRM1**, **OPRD1** and **OPRK1** genes, respectively – interact with each other (with **OPRM1** signaling through both stimulatory and inhibitory G-proteins) and multiple landscape proteins in the cell membrane (**CD302**, **DRD2**, **EGFR**, **SLC6A4**), extracellular space (**ADM**, **FN1**) and cytoplasm (**CKB**, **CRKL**, **HSP90AA1**, **NCL**, **PI4KA**, **TLN2**). Lastly, the **PROK2-PROKR2 complex** induces the production of gonadotropin-releasing hormone (GnRH), which has been linked to TD (see below). Other non-GPCR landscape membrane receptors include the kinase receptors **EGFR**

– that interacts with many landscape proteins, including being inhibited by the cytoplasmic protein **ERRFI1** – and **FLT3** that, when bound/activated by the cytokine **FLT3LG**, regulates the phosphorylation of **MAPK3** and **MAPT**. Moreover, **FLT3** regulates the expression of nuclear **EXCC6**, cytoplasmic **PIM1**, and lysosomal **MPO**, and is degraded by **RNF115**. Other membrane receptors in the landscape include **IL17RB** – which forms a functional complex with IL17RA that has **IL17A** as its ligand – and **PLA2R1**, a receptor of phospholipase A2 (not shown) that upregulates the expression of the mitochondrial enzyme **MGST1** (see below). Further, **PTPRU** is a (pre) synaptic phosphatase receptor involved in the development and maintenance of dopaminergic neurons [84], while **NOTCH1** is a (pre)synaptic membrane receptor that interacts with multiple landscape proteins and, upon ligand activation, the notch intracellular domain (**NOTCH1-ID**) is released into the cytoplasm and subsequently the nucleus, where it functions as a transcription factor through, e.g., interacting with **RERE** (see below). Moreover, a number of landscape proteins are (subunits of) neurotransmitter receptors that, when activated through neurotransmitter binding, function as ligand-gated ion channels (see below): the **acetylcholine** receptor subunits **CHRNA7** and **CHRNB4**, the **GABA** (**γ-aminobutyric acid**) receptor subunits **GABRA2**, **GABRB3** and **GABRG1**, and the NMDA **glutamate** receptor subunits **GRIN1**, **GRIN2A**, **GRIN2B** and **GRIN3A**. Lastly, **SELE** (**selectin-E**) is a (pre-or post)synaptic membrane receptor that is involved in immunoadhesion and that is (also) highly expressed in brain vascular endothelial cells. **SELE** binds its membrane-located ligand extracellular **SELPLG** – which leads to its dephosphorylation – and its expression is regulated by intracellular **ENO1**, **ESR1**, **indoxyl sulfate**, **MAPK3K4**, **MAPK3**, **MRTFA** and **RCAN1**, membrane-located **NOTCH1**, and secreted, extracellular **SERPINE2**.

In addition, several membrane-located ion channels operate in the landscape. A first group of ion channels are the neurotransmitter receptors that, upon activation, function as ligand-gated ion channels (see above). Secondly, the landscape contains multiple (subunits of) voltage-gated ion channels that mediate the transport of (univalent and divalent) ions into neuronal cells, including the calcium channel subunit **CACNA1D**, the chloride channel subunit **CLCN2** (which is activated by **arachidonic acid**), the sodium channel subunit **SCN5A**, and the potassium channel subunits **HCN1**, **HCN4**, **KCNH3, KCNH5**, **KCNJ11** and astrocytic **KCNK1**, with the latter also being regulated by the cytoplasmic enzyme **SENP1** (see below).

Members of the ATP-binding cassette (ABC) family of transporters – **ABCA7** and **ABCG8** (which itself forms a functional complex with extracellular **APOM** (see above)) – play a role in lipid homeostasis. In addition, **ABCC1** mediates the export of organic anions and many drugs from the cytoplasm. In astrocytes, the expression of **ABCG8** is regulated by **NR1H2**, whereas **ABCC1** forms a complex with the multifunctional membrane protein **LMBR1L** (see below). Other landscape transporters belong to the solute carrier family of proteins, including the

(post)synaptic sodium/bicarbonate cotransporter **SLC4A10** that regulates intracellular pH, **SLC6A2** – a presynaptic amine transporter that inhibits both **DRD2** and **SLC6A4** – and the presynaptic serotonin transporter **SLC6A4** that interacts with many landscape proteins and terminates the action of serotonin in the synaptic cleft by transporting serotonin (back) into presynaptic neurons. In addition, **SLC23A1** transports **vitamin C** into presynaptic neurons, **SCL26A2** transports sulfate into these neurons (not shown), and **SLC30A9** as well as **SLC39A12** transport **zinc** into postsynaptic neurons and astrocytes, respectively.

Several membrane proteins in the landscape also have an important role in regulating cell adhesion, i.e., **CD47** – which is bound and activated by **THBS1** and forms a complex with the (microglial) **ITGA4-ITGB1-complex** – and **CD276** that form a presynaptic complex, and **CD302** that forms a presynaptic complex with **OPRM1**. Further, **CNTN6** – which complexes with **NOTCH1**, leading to the release of **NOTCH1-ID** to the nucleus (not shown) – and **CNTNAP2** – of which the expression is regulated by the transcription factor **FOXP2** – are proteins of the contactin family that regulate (pre)synaptic cell adhesion. In addition, **CDHR1** is a cell adhesion protein of which the expression is upregulated by **CX3CL1**, while presynaptic **NRCAM** and the postsynaptic protocadherins **PCDH7**, **PCDH12** and **PCDH17** – which also interact with each other – are cell adhesion proteins that are involved in the establishment and maintenance of specific neuronal connections in the brain. Lastly, the teneurin proteins **TENM2** – that binds the **ADGRL1** receptor – and **TENM4** – that complexes with extracellular **OLFM1** (see below) – also regulate neuronal cell adhesion and connectivity.

Lastly, a number of 'other' membrane proteins act in the landscape. First, presynaptic neuroligins like **NLGN3** and **NLGN4X** regulate synapse function and synaptic signal transmission through forming a synapse-spanning functional complex with postsynaptic neurexins such as **NRXN1**. In the same way, presynaptic **EFNA5** and postsynaptic **EPHB2** can form a synapse-spanning complex that modulates synaptic function. Moreover, the membrane protein **RIMBP2** regulates (pre)synaptic transmission through interacting with the membrane-located scaffold protein **RIMS1** and the calcium channel **CACNA1D**. **AGRN** (**agrin**) is a transmembrane protein that is large enough to span the synaptic cleft and act across it [85,86] (not shown) and forms multiple functional complexes with other intra- and extracellular landscape proteins. Another membrane protein that interacts with many other landscape proteins is **LMBR1L**. In addition, the membrane protein **KIDINS220** is a key regulator of synaptic plasticity through binding and interacting with extracellular **FN1** and **OLFM1**, as well as cytoplasmic **GAK** (see below). In turn, **OLFM1** – which also binds **TENM4** (see above) – inhibits complex formation between the inner cell membrane-associated protein **RTN4R** and the transmembrane protein **LINGO1**, with the **RTN4R**-**LINGO1-complex** being a key regulator of axonal growth.

Cytoskeleton

The cytoskeleton has three components, i.e., actin filaments, intermediate filaments, and microtubules (MTs), and a large number of landscape proteins regulate the function of these components and interact with each other as well as cytoplasmic, nuclear, and membrane-located proteins. In CNS cells, the cytoskeleton is crucial for cell shape and physiology, and it also forms specialized structures such as growth cones – that are responsible for axon elongation and guidance during development – dendritic spines and synapses – that form the structural basis for nerve cell communication and higher order processes such as learning and memory – and membrane specializations critical for the initiation and propagation of nerve impulses.

Firstly, actin filaments play an important role in neuronal development, including regulating growth cone dynamics (**ACTR3**), remodeling of dendritic spines (**ABI2**, **DBN1**), and migration of neuronal precursors [87] (**ABI2**, **DBN1**). In addition, certain landscape proteins link the cytoskeleton to the cell membrane (**ANK3**, **EPB41**), while other – at least to some extent cytoskeletal – proteins regulate actin filament organization (**KLHL5**, **LIMCH1**, **MPRIP**, **PDLIM7**), actin-based transport (myosins including **MYO10**, **MYO19**), and cell adhesion (**CTNNA3**, **LIMCH1**, **PKP4**, **TLN2**, **TRIP6**).

Secondly, intermediate filaments (or neurofilaments) are important for organelle positioning, transport, and function [88], and **PRPH** is an important protein in neurofilaments.

Lastly, the crosstalk between actin filaments and MTs is important for regulating cytoskeleton-associated processes such as cell migration, cell division, cell polarity and cell (neuronal) shape. More specifically, MTs are composed of tubulin dimers – different combinations of **TUBA1A**, **TUBA1B** and/or **TUBA1C** – and serve as routes for intracellular transport and structural support for dendrites and axons. In addition, MTs contribute to the development, maintenance, and plasticity of synapses, including roles in (pre)synaptic vesicle (re)cycling, mitochondrial arrangement, and interactions with receptors in the neuronal membrane [89]. In addition, the centrosome is the main MT-organizing centre and is the main site of microtubule nucleation and anchoring involved in many processes, particularly during cell division, cell migration and differentiation. In this respect, the landscape contains several proteins that are involved in centrosome function: **CEP85L**, **CEP128**, **CENJP**, **HAUS3**, **MPHOSPH9**, **PCM1**, and **WDR62**. Furthermore, the landscape contains a large number of MT-associated motor proteins that move along MTs and regulate intracellular protein trafficking and transports: proteins from the **DNAH-complex** (**DNAH1**, **DNAH3**, **DNAH5**, **DNAH7**, **DNAH10** (not shown), and **DNAH11**), **DYNC2H1** and **DYNC2I1** (involved in retrograde transport), **KIF26B** and **KLC1** (that specifically regulate organelle transport along MTs).

Lastly, landscape proteins regulate the function/stability/organization of MTs, including **ABGL4**, **CAPN6**, **CCDC66**, **MAPT**, **MTUS2**, **NCKAP5L**, and **NINL**.

Cytoplasm

The cytoplasm has many functions in (neuronal) cells, including regulating signal transduction between the cell membrane and the nucleus and/or cellular organelles/other cell parts, producing molecules/metabolites involved in many signaling cascades (e.g., glycolysis, gluconeogenesis, protein biosynthesis) and storing or transporting these molecules/metabolites from their production site to other parts of the cell, post-translational modifications of synthesized proteins, and cell cycle regulation.

First, a number of landscape proteins are located in the cytoplasm but mainly regulate cytoskeletal processes. These proteins include **RHOA** and its activators **ARHGAP26**, **DLC1**, **KALRN**, **NGEF** and **TRIO**. In addition, cytoplasmic **FARP2**, **GCA**, **TJP1** and **TROAP** regulate cell adhesion through interacting with the cytoskeleton.

Moreover, a large number of cytoplasmic landscape proteins are enzymes, including **DGKQ** (involved in lipid metabolism), **ENO1** (involved in glycolysis) and **POFUT1** – that form a complex, with **POFUT1** also regulating, through fucosylation, membrane-located **NOTCH1** and transmembrane **AGRN** – **MDH1** (involved in the TCA cycle) and **PFKM** (involved in glycolysis and inhibited by **citrate**). Other cytoplasmic landscape enzymes are involved in regulating the metabolism of phosphatidylinositol (PI), with (changes in) PI (metabolites) having been linked to normal human brain development and aging as well as organizing the cell membrane [90] [91], i.e., **IMPA1** (important enzyme for maintaining intracellular levels of the PI metabolite **myo-inositol** (**MI**) that mediates brain signaling in response to hormones, neurotransmitters and growth factors [92]), **OSBPL2**, **PI4KA**, **PIKFYVE** and **PLCH1**. Further, two (partially) cytoplasmic landscape enzymes – **AHCY** and **COMT** – are involved in the metabolism of S-adenosylmethionine (SAM) – the methyl donor for most methylation reactions in cells, including histone and DNA methylation in the nucleus – that for its synthesis requires **betaine**, which itself is synthesized in the mitochondria (see below). In addition, **PRMT1** – which is activated by **FAM98B** – is involved in (arginine) methylation of multiple proteins and histones. Moreover, cAMP – that is produced by **ADCY2** – is degraded by **PDE4A**, an enzyme that binds and interacts with **PRKAR2A**, a kinase that is regulated by cAMP. Further, **SULT4A1** is involved in the metabolism of multiple neurotransmitters. Lastly, **HDC** – an enzyme that is upregulated by **TNFB** – interacts with the histamine receptor **HRH2** (see above) and converts **histidine** to histamine using pyridoxal 5'-phosphate (**PLP**, the active form of vitamin B6) as cofactor, while **WWOX** is an oxidoreductase enzyme that interacts with multiple landscape proteins in the cytoplasm and nucleus where it functions as an adaptor protein and transcriptional repressor, respectively.

Multiple cytoplasmic proteins also regulate (mainly presynaptic) vesicle transport/trafficking (**CLTC1**, **NSF**, **VPS13A**), recycling (**GAK** and **STON2** (highly expressed in astrocytes) and exocytosis (**DYSF** , **PREPL**, **SNAP29**). **DYSF** is a cell membrane and cytoplasmic protein that uses calcium as a cofactor and regulates the expression of both extracellular **FN1** and cytoplasmic **ACTR3**.

Further, a large number of cytoplasmic landscape proteins regulate post-translational modifications of proteins, i.e., ubiquitination and SUMOylation. Both these modifications are reversible processes that regulate protein localization and activity. Ubiquitination marks proteins for proteasome-dependent degradation, while sumoylation is not used to tag proteins for degradation but modifies proteins involved in many cellular processes including gene expression, chromatin structure, signal transduction, DNA damage response and cell cycle progression. Molecular chaperone proteins like **BAG5** and **HSP90AA1** – that has very many interactions in the landscape, such as forming a complex with the adaptor protein **ST13** – play an important role in maintaining a protein's native folding and function, which protects against the buildup of misfolded proteins [93]. When misfolded proteins interact with chaperones (which cannot be refolded), they can be shuttled for ubiquitin-dependent proteasome degradation.

As for ubiquitination-related proteins, the landscape contains both ubiquitin-conjugating enzymes – including **UBE2J1** and **BIRC6**, an anti-apoptotic protein that has **CASP8** (which itself is a protease with multiple interactions in the landscape) and **DIABLO** as its ubiquitination targets – and many E3 ubiquitin ligases, i.e., **ASB3** (which degrades **TNFRSF1B**) and **ASB8**, the complex of **COP1**, **COPS9**, **DCAF1** (which degrades **ESR1**) and **RBX1**, **DCAF12**, **FBXL17** (which degrades **PRMT1**), **RNF115** (which degrades **EGFR** and **FLT3**), **RNF4** and **RNF41**. After having been ubiquitinated, proteins are degraded by the 26S proteasome complex, of which the landscape proteins **ADRM1**, **PSMD7, PSMD14** are subunits. In addition, **PSME4** is an associated component of the proteasome that promotes ubiquitin-independent degradation and binds with **PSMD14** and **FBXL17**. Ubiquitination is counterbalanced by the action of deubiquitinating enzymes (DUBs) that remove ubiquitin from target proteins, such as **UCHL1** and **USP4**. Lastly, **DESI1**, **PIAS3**, **PIAS4**, **SENP1**, and **SENP6** are proteins that can operate in the cytoplasm and – mainly – the nucleus and that regulate the SUMOylation of proteins.

The landscape also contains several RNA-binding proteins (RBPs) that function both in the cytoplasm and nucleus and regulate various aspects of mRNA metabolism, including mRNA processing, stability, transport and translation and thus affect neurodevelopment, synapse homeostasis, and the neuronal cytoskeleton [94]: **EDC4**, **MARF1**, **MEX3B**, and **PAN3** – that all form a complex – **IGF2BP1**, **NCL**, **PIWIL1 –** which binds and stabilizes the mRNA of **DHX57** – **MAPT**, **RBMS1** (that complexes with **MEX3B**), **RBFOX1**, **SPATS2**, **TNRC6A**, and

YTHDF2.

In addition, the landscape contains many cytoplasmic kinases that are involved in specific signaling cascades, including **MAPK3** – a kinase that regulates and interacts with many other landscape proteins – and the NF-kappa-B (NFKB) kinase complex that interacts with the landscape proteins/kinases **LRRC14**, **TANK** – that downregulates **TNFB** expression – **TBR1**, **TNIP2**, **TRAF3**, and **TRIP6**. Other kinases in the landscape include **CRKL** (a kinase that interacts with multiple other landscape proteins, including increasing the expression of **HDC** and **TNFB** as well as activating **MAPK3**), **GRK4** (which inhibits **MAPK3**), and the cAMP-dependent **PRKAR2A**. In addition to kinases, a number of phosphatases operate in the landscape, such as **DUSP6**, **PPP1R3A**, **PPP1R3B** and **PPP2R2B**.

Further, multiple cytoplasmic landscape proteins – some of which can also be located in the nucleus – regulate the cell cycle. In this respect, **CDKN1A**, a protein with many interactions in the landscape, is an important regulator of cell cycle progression (and other landscape processes). **PIM1** phosphorylates **CDKN1A**, which results in the relocation of **CDKN1A** to the cytoplasm and enhanced **CDKN1A** stability, while the nuclear/cytoplasmic protein **FHIT** – that also complexes with **ENO1** – upregulates **CDKN1A** expression. Other cytoplasmic landscape proteins involved in cell cycle regulation are the kinases **GAK**, **PKN2** and **STK38**, and **TOB2**.

Lastly, four 'miscellaneous' landscape proteins can be located in the cytoplasm and – to some extent – in the nucleus and have (very) many interactions with other landscape proteins, i.e., **CASP8**, **EP300**, **ESR1** and **RICTOR**. First, **CASP8** is a key regulator of apoptosis, and its activity/expression is regulated by **arachidonic acid**, **butyric acid**, **citrate**, **GABA**, **glutamate**, and **palmitic acid**. Further, **CASP8** activity is regulated by – among other proteins – cytoplasmic **DIABLO** and nuclear **IP6K2** (an enzyme involved in phosphatidylinositol metabolism, see above). In addition, **EP300** functions as an acetyltransferase for proteins such as **ESR1**, **ETS1**, **GABPB1**, **PHF5A** and **TADA3** (in the nucleus), and **MAPK3**, **MAPT**, **PRMT1** (in the cytoplasm). Upon binding its ligand, the female sex hormone **estradiol**, **ESR1** can either function as a cytoplasmic adapter protein or as a nuclear transcription factor. The nuclear translocation – and hence transcriptional activation/activity – of **ESR1** activity/activation is regulated by **MACROD1** and the **WWC1**-**DLC1**-**complex**. **RICTOR** is part of the mammalian target of rapamycin (mTOR) complex 2 (mTORC2), a multiprotein complex critical for cell growth and metabolism. **RICTOR** forms a functional complex with multiple landscape proteins and regulates the expression of membrane-located **DRD2**, cytoplasmic **PSMD7** and **PSME4**, and mitochondrial **NDUFA4**.

Organelles
Multiple interacting landscape proteins are involved in regulating mitochondrial functioning in both pre-and postsynaptic neurons.

Specifically, several TD landscape proteins are mitochondrial matrix proteins that regulate mitochondrial translation, including translation factors (**GUF1**, **LRPPRC**, **GFM2**, **MTIF3**, **MTRFR**), mt-tRNA synthetase (**NARS2**), 39S subunit proteins of mitochondrial ribosome (**MRPL3** and **MRPL40**) and rRNA methyltransferase **MRM1**. Mitochondrial translation is essential for maintaining the cellular energetic balance through the synthesis of proteins involved in the oxidative phosphorylation (OXPHOS). This is required for adenosine triphosphate (ATP) production and the folding of the mitochondrial cristae. Therefore, impaired mitochondrial translation results in diminished ATP production and consequent cellular energy deficit [95], as well as impaired maintenance of mitochondrial DNA (mtDNA) [96].

Several mitochondrial proteins are involved in importing and sorting other proteins (**IMMP2L**, **XPNPEP3**, **DNAJC15**). Specifically, **IMMP2L** and **DNAJC15** – located in the mitochondrial inner membrane – are involved in the processing and activation of **DIABLO**, which is subsequently released into the cytosol, where it can initiate apoptosis through activating caspases (such as **CASP8**). Other landscape proteins are involved in mitochondrial fusion and cristae formation (**OPA1**) and mitophagy (**PARK7** and **MAP1LC3B**).

Multiple mitochondrial landscape proteins operate in metabolic pathways. These include proteins that regulate the metabolism of: (1) carbohydrates related to the tricarboxylic acid (TCA) cycle, such as the interconversion of **citrate** (**CIT**) to isocitrate via **cis-aconitate** (**CAA**), catalyzed by **ACO2**, the transport of **citrate** by **SLC25A1,** and the conversion of malate to **pyruvate** catalyzed by **ME2**; (2) the urea cycle, in which the **CPS1** enzyme is required to convert ammonia into urea and protect the brain from ammonia toxicity [97]; (3) amino acids, including **NAT8L**, an enzyme that synthesizes N-acetylaspartate (NAA), which is subsequently converted with **glutamate** to form N-acetylaspartyl-glutamate (**NAAG**), in a cytoplasmic reaction catalyzed by **RIMKLA** and **RIMKLB**; (4) choline and **betaine**, with both enzymes catalyzing one step of the two-step process of choline to **betaine** conversion: **CHDH** and **ALDH7A**; and (5) detoxification/control of reactive oxygen species (ROS) levels and glutathione metabolism (**TXNRD2** and **MGST1**).

The neurodevelopment and normal function of synapses also depend on a readily available supply of ATP. In neurons, the majority of ATP is generated in the mitochondria by OXPHOS via the electron transport chain (ETC) and the ATP synthase complex. Multiple landscape proteins are subunits or assembly factors of the ETC, specifically Complex I proteins (**NDUFA13**, **NDUFA6**, **NDUFB1**, **NUBPL**), Complex IV proteins (**NDUFA4**, **PNKD**), and the ATP synthase complex (**ATP5IF1**). Furthermore, creatine kinase B (**CKB**) reversibly catalyses the transfer of phosphate between ATP and creatine (**CR**) for the synthesis of phosphocreatine (**PCR**) in the so-called phosphocreatine shuttle, which acts as an energy buffering system between the mitochondrial sites of ATP production and the cytosolic sites of ATP utilization.

In addition, **MPV17**, an ion channel in the inner mitochondrial membrane, may also be involved in the control of OXPHOS, apart from its role in mitochondrial deoxynucleotide homeostasis and mtDNA maintenance. Similarly, **POLG** that encodes the catalytic subunit of DNA polymerase γ, is responsible for mtDNA replication and maintenance.

Lastly, **MICU3** is a brain-specific enhancer of mitochondrial calcium uptake that forms a heterodimer with **MICU1**.

The endoplasmic reticulum (ER) is a large, dynamic organelle that has multiple roles in the cell. First, the ER has an important role in lipid biosynthesis and metabolism, e.g., enzymes such as **CEPT1** (involved in phospholipid metabolism), **CERS5** and **SGPP2** (involved in sphingolipid metabolism), and **DHDDS** and **NUS1** (involved in lipid metabolism in general). In addition, ER-located enzymes in the landscape are involved in protein modification, including fucosylation (**POFUT1**) and palmitoylation (**ZDHHC11**, which catalyzes the addition of **palmitic acid** onto various proteins thus affecting their localization and function). Further, landscape ER proteins regulate intracellular protein transport: **LMAN2**, **MPPE1**, **PIGW**, **SORT1**, and **VAMP7**. Other landscape proteins are involved in ubiquitin-dependent degradation of misfolded ER proteins: chaperone proteins **DNAJC18** and **DNAJC22**, **GABARAPL2**, **SEL1L**, **SELENOK**, **TMBIM6**, **TMEM33**, and **UBE2J1**. Lastly, **TMBIM6** also functions as a calcium transporter that modulates ER calcium homeostasis.

The Golgi apparatus (GA) is the main site of protein modification, which includes transferring chondroitin sulfate (CS), the most abundant type of proteoglycan expressed in CNS acting as a barrier molecule affecting axonal growth, neuronal cell migration and plasticity [98] (**CSGALNACT2**), and transferring **palmitic acid** onto **DRD2** (**ZDHHC8**), which is important for **DRD2** relocating to the neuronal membrane [99]. In addition, the GA is involved in regulating protein trafficking (**AP3B2**, **DOP1B**, **MPPE1**, **SORT1**, and **VAMP7**) and **zinc** transport (**SLC30A6**).

The peroxisomes are multifunctional organelles that contribute to fatty acid/lipid metabolism (**ACAA1** and **SLC27A2**) and metabolite/cofactor transport (**SLC25A17**, which is inhibited by **pyridoxal 5'-phosphate**). In addition, two landscape proteins are involved in peroxisome biogenesis and proliferation, i.e., **PEX2** and **PEX11B**.

The lysosomes constitute the major proteolytic compartment and contain multiple landscape proteins, i.e., **KLHL22**, **LAPTM5** and **VPS13A**, that are involved in the degradation of target proteins such as **DEPDC5** and **NPRL2**. In addition, the peroxidase **MPO** is activated by **arginine**, inhibited by **butyric acid**, forms a functional complex in the extracellular space with **FN1**, and is involved in oxidative stress and lysosomal damage.

In presynaptic neurons, several landscape proteins regulate the function of endosomes (EN), including membrane trafficking, degradation of proteins such as **EFGR**, and protein transport to lysosomes or cytoplasmic vesicles (CVs) (**ARL8B**, **DNAJC13**, **PIKFYVE**, and

ZFYVE28). In turn, CVs mediate autophagy and protein transport to and from the plasma membrane and between organelles, and landscape proteins are specifically involved in CV-linked autophagy (**GABARAPL2**, **MAP1LC3B**, **TBC1D5**), CV trafficking, exocytosis (of proteins like **PAM**, an enzyme that catalyzes the conversion of inactive to active (secreted) neuropeptides) and/or recycling (**ASTN2**, **CLTCL1**, **PTPRN2**, **SORT1**, **VAMP7**).

Nucleus

In the nucleus of pre-and postsynaptic neurons, four groups of proteins can be discerned. The first group of proteins are part and/or regulate the function of the nuclear pore complex (NPC) that mediates nucleocytoplasmic transport, genome organization and gene expression [100]: **GLE1**, **NUP85**, **NUTF2**, **RANBP1**, **RANGAP1**, **TOR1A, TNIK**, and **WDR62**. The second group of proteins regulate rRNA processing and ribosome synthesis, including **BMS1**, **DGCR8**, **NOP14**, and **TCOF1**. The third group of landscape proteins in the nucleus are functionally involved in transcriptional regulation as well as DNA and histone modifications. In this respect, the landscape contains a large number of transcription factors, such as **BBX**, **CDX2**, **GABPB1**, **GTF2H1**, **GTF2IRD1**, **HOXB4**, **JUND**, **MYT1L** and **POU3F2** (which both have a key role in neuronal differentiation), **NR4A2** (which is highly expressed in dopaminergic neurons and e.g., upregulates **DRD2** expression), **PHF3**, **TEAD2**, **TERF2IP**, **USF2**, and the zinc finger proteins **ZNF536**, **ZNF664**, **ZNF837**, and **ZNHIT3**. In addition, some of the landscape transcription factors are specifically known to activate gene transcription, e.g., **ETS1** – which is activated by **TCF20**, itself a transcriptional activator – **GTF2A1**, **MRTFA**, and **POU4F2**. Other transcription factors specifically repress gene transcription, including **AEBP1**, **ATN1**, **BHLHE40**, **FOXP1** – which is specific to dopaminergic neurons, regulates the expression of landscape proteins like **CDKNA1** and **CNTN6**, and is regulated by **EP300** – **POU4F2**, **RERE** – which functionally interacts the intracellular, nuclear domain of **NOTCH1** (**NOTCH1-ID**) – **RUNX1T1** – which interacts with **ATN1**, **ETS1** and the histone-modifying enzyme (see below) **EP300** – and **TBR1**. Further, the landscape contains a few other proteins that regulate the transcriptional process itself, i.e., the subunits of the DNA-dependent RNA polymerases II (**POLR2I**) and III (**POLR3C**, **POLR3H**), and **XRN2**. Moreover, as transcription proceeds, transcripts are (differently) capped, spliced, and polyadenylated so they can be efficiently exported across the nuclear envelope to the cytoplasm for translation of mRNA to protein. Landscape proteins that are involved in this pre-mRNA processing include **FIP1L1** (involved in polyadenylation), **LRPPRC** (which, in addition to its role in the mitochondria (see above), regulates nuclear mRNA export), and multiple proteins that regulate pre-mRNA splicing, as part of splicing complexes: **ESS2**, **GEMIN6**, **SF3A2**, **SNU13**, three splicing factors of the SRSF protein family – **SRSF3** (also involved in nuclear mRNA export), **SRSF4** and **SRSF7** – and **SUGP1**. In addition, **WDR61** – a nuclear protein that

has multiple interactions with other landscape proteins – and **PHF5A** bind each other and are a part of the PAF1C complex that regulates transcription elongation and chromatin structure (see below) [101], with **PHF5A** also being involved in pre-mRNA splicing.

Multiple landscape proteins are implicated in chromatin remodeling, i.e., post-translational modifications (PTMs) of DNA, histones and non-histone targets, including acetylation, methylation and sumoylation, which in turn affects gene transcription [102]. The PTMs are performed by multi-protein complexes that are recruited to act at specific regions of chromatin, and landscape proteins that are members of these complexes include **ACTR8**, **INO80D** and **MCRS1** (that bind and are part of the INO80 complex), **BCL11A** and **BCL7A** (subunits of BAF complex), **BRPF3**, **KANSL1**, **KAT14** and **TADA3** (that bind and are part of the ATAC complex, with **TADA3** also activating **CDKN1A** and being regulated by **EP300**), **MORF4L2**, and **L3MBTL2** and **PHC3** (that are part of the polycomb repressor complex, which keeps genes in a non-transcribed state). As for specific PTMs, the aforementioned and other landscape proteins are involved in DNA/histone acetylation (**BRPF3**, **EP300** – that also acts on non-histone targets, including **ETS1**, **GABPB1** and **PRMT1** – **KANSL1**, **KAT14**, **MCRS1**, **MORF4L2**, **PHF14**, and **TADA3**), methylation (six histone methyltransferases – **ASHL1**, **KMT5A**, **KMT2C**, **KMT2D**, **NSD1** and **NSD3** – and one histone demethylase, **KDM5B**), and (de)sumoylation (**PIAS4** – which mediates the sumoylation of e.g., **PARK7** – and **SENP6**).

Lastly, the fourth group of nuclear landscape proteins are involved in DNA damage repair: **ERCC5** (involved in repairing UV-induced DNA damage), **GTF2H1** (a transcription factor (see above) that also repairs damaged DNA), **IHO1** (which repairs double-strand DNA breaks), **MAU2** and **NIPBL** – which are part of the cohesin complex that repairs DNA damage – **RPA2** (which binds and stabilizes ssDNA) and **XRCC6**, a protein that repairs DNA damage and has very many interactions with other landscape proteins.

Microglial cells and astrocytes

Microglial cells

Microglial cells play diverse roles in brain development and adult brain function, including the regulation of synaptic plasticity and pruning. They also serve as brain macrophages and are important for the brain immune response, as they are primary sources of immune response factors such as cytokines that in turn can modulate synaptic plasticity [103]. The membrane receptors/proteins (**CD47, CX3CR1** (which is a microglia-specific receptor), **ITGA4**, **ITGB1**) and extracellular cytokines (**CX3CL1**) and other molecules (**FN1** and **TNN**) that are expressed in and regulate the function of microglial cells have already been described above in the part about pre-and postsynaptic neurons.

Astrocytes

Astrocytes and their projections envelop pre- and postsynaptic neurons and closely approach the synaptic cleft, representing key components of the synapse that are active mediators of synaptic function [104,105]. In addition, astrocytes are important for maintaining the blood-brain barrier (BBB) and brain cholesterol metabolism [106]. A number of protein interactions that (also) occur in astrocytes have already been described above in the part about pre-and postsynaptic neurons. Below, we have added proteins and their interactions that are – to some extent – specific to astrocytes.

NR1H2 (also known as Liver X receptor beta, LXRβ) is a transcription factor that is mainly expressed in astrocytes and other glial cells [107] and that has an important role in regulating brain cholesterol metabolism and dopaminergic neuronal function. In the landscape, **NR1H2** downregulates the expression of both **TSHR** and **DIO2**. **TSHR** is a GPCR that signals through stimulatory G-proteins and forms a functional complex with **FN1** but that also regulates thyroid hormone synthesis through binding and being activated by its ligand, thyroid stimulating hormone (**TSH**). In addition, **DIO2** is an ER membrane-located enzyme that the conversion of thyroxine or **T4** (the inactive form of thyroid hormone) to triiodothyronine or **T3** (the active form of thyroid hormone). **T3** generated by **DIO2** is then transported out of astrocytes and into neurons by the membrane transporter **SLC16A2**. Furthermore, **DIO2** is degraded by the ER membrane-located ubiquitination protein **UBE2J1**, it forms a complex with cytoplasmic **RBX1**, and it is involved in downregulating the expression of the transcription factor **NR4A2**. **NR1H2** also regulates the expression of the membrane cholesterol/lipid transporter **ABCG8**. Lastly, histamine (see above) is transported in and out of astrocytes (and presynaptic neurons) by the membrane transporters **SLC22A3** and **SLC29A3**, while in astrocytes, it is also methylated and hence inactivated by the **HNMT** enzyme.

Below, we will provide six examples of key landscape proteins that are interesting putative (novel) drug targets for TD – i.e., FLT3, NAALAD2, CXC3R1 and CXC3L1, OPRM1, and HRH2 – and we discuss why and how these targets can be linked to four aspects of target specificity (i.e., regional, temporal, molecular and modulatory specificity).

DISCUSSION

In this paper, we have compiled, analyzed and integrated different types of omics data into a molecular landscape of TD. Below, we will discuss the main findings from our analyses and provide examples of putative drug targets derived from the landscape that could be modulated with a beneficial effect on TD.

First, we tested the (general) hypothesis that the expression of genes for a specific disease will be relatively enhanced in tissue and cell types that are vulnerable to this disease. We found that TD candidate gene expression is enhanced in the brain and pituitary, two tissues that were shown to be rich in neural cells [108]. Our subsequent spatiotemporal analysis of brain tissue revealed that especially the cerebellum, cortex, striatum, and thalamus across various developmental periods may be involved in TD etiology. These results are consistent with previous reports of alterations in anatomical and functional circuits involving the cortex, striatum and thalamus (see above) as well as the cerebellum being key contributors to the pathogenesis of TD [109,110]. Furthermore, our analyses of mouse data showed enriched expression of TD candidate genes in two cell types in particular, i.e., Drd2+ MSNs and layer 6 corticothalamic neurons. In keeping with their potential involvement in TD, these two cell types are also enriched among genes that were found to be downregulated in the postmortem striatum of TD patients, which further suggests that TD onset and progression may be particularly related to deficits in the function or presence of these cells. Drd2+ medium spiny neurons (MSNs) are inhibitory/GABAergic neurons (MSNs) that express the dopamine D2 receptor and, together with Drd1+ MSNs, they constitute approximately 95% of the neurons in the striatum, the main input structure of the basal ganglia. Drd2+ MSN neurons act as crucial regulators of striatal output via the 'indirect' pathway and so alter striatal mediated 'action'. Further, these MSNs receive convergent excitatory inputs from the cortical and thalamic areas and further project to the output nuclei of the basal ganglia circuit [111]. In addition, Drd2+ MSNs have been shown to be crucial in habit formation in mice [112,113]. This is particularly interesting because both from a cognitive-behavioral and neuroscientific perspective, tics – the hallmark of TD – can be viewed as habits that have been formed over time and that are associated with premonitory sensations and can, at least partially, be controlled [114-118]. As a result, habit reversal training (HRT) is currently among the first-line behavioral interventions aimed at reducing tics [119,120]. Further, rodent studies have shown that Drd2 expression changes during development, with increased expression across early postnatal life and peak Drd2 expression by early adolescence, followed by decreased expression in adulthood (reviewed in [121]). In accordance, the dopaminergic excitability of Drd2+ MSNs also decreases during the juvenile period [122] and in humans, a similar peak of dopaminergic innervation of the striatum was observed in preadolescence, with a subsequent decrease during adulthood [123]. In addition, postmortem studies have shown an increased DRD2 density in the frontal cortex and striatum of TD patients [124,125] while it was also demonstrated in monozygotic twins that differences in DRD2 binding influence TD severity [126]. Based on all these findings, it seems that drugs aimed at reducing DRD2 activity during the critical

time window associated with TD (i.e., childhood to (early) adolescence) would be beneficial and indeed, DRD2 antagonists are currently still the standard pharmacological treatment of TD/tics [127]. The downregulated genes in postmortem TD striatum were also enriched for genes that are highly specific to cholinergic neurons, in line with the observed reduction of cholinergic (ChAT+) interneurons in postmortem immunohistochemical studies of TD patient striatum [60,128]. Interestingly, habit formation (see above) is (also) modulated by striatal cholinergic interneurons [129,130], and these neurons are also important for synchronizing the activity of (Drd2+) MSNs that suppresses or ends a movement bout [131]. In addition, pharmacotherapy with cholinergic drugs has been observed to modulate motor tics [132]. Lastly, we found that the upregulated genes in postmortem TD striatum are highly expressed in glial and immune cells, which may imply that inflammation-mediated mechanisms (also) contribute to TD, but this enrichment was not found through our analysis of the genetic data. Taken together, our tissue and cell type specificity analyses suggest that TD is not confined to a single brain region and that there are potentially multiple cellular routes to TD.

Our analyses of the TD candidate genes revealed two significantly enriched pathways: 'cAMP-mediated signaling' and 'Endocannabinoid Neuronal Synapse Pathway'. In Figure S1 and Figure S2, we provide a graphical representation of the two pathways at the cellular level in which the proteins encoded by TD candidate genes and the metabolites implicated through the PRS-based analyses are indicated in purple. First, cAMP (3'-5'-cyclic adenosine monophosphate) is an important second messenger molecule that is used for intracellular signal transduction. cAMP is produced from ATP by adenylate cyclases (such as the landscape protein ADCY2) that themselves are activated through stimulatory GPCRs (including the landscape proteins CRHR1, HRH2, OPRM1, and TSHR) or inhibited through inhibitory GPCRs (landscape proteins DRD2 – the dopamine receptor that interacts with many landscape proteins and is also enriched in TD-linked Drd2+ neurons, see above – FPR1, FPR2, FFAR3, OPRD1, OPRK1, OPRM1). Furthermore, cAMP is degraded by phosphodiesterase enzymes [133], such as the landscape protein PDE4A and it regulates synaptic function through activating protein kinase A (PKA) (of which the landscape protein PRKAR2A is a regulatory subunit) [134]. All these findings suggest that abnormalities in cAMP signaling could be a central functional theme in TD etiology. In this respect, studies of postmortem brains from TD patients have revealed reduced concentrations of cAMP in the cerebral cortex and putamen [135,136]. Conversely, increased cortical and striatal levels of cAMP and associated reduced levels of phosphodiesterase activity have been associated with stereotypic, tic-like behavior of deer mice [137]. Changes in cAMP levels and activity in dopaminergic neurons during development may also underlie tic-like symptoms in ADHD, a disorder that is highly comorbid with TD [138]. Lastly and interestingly, some drugs that target cAMP-mediated

signaling are already in use to treat TD or in the clinical trial phase, e.g., the DRD2 modulator aripiprazole, the DRD2 antagonist risperidone and the opioid receptor antagonist naloxone (see below), further implying that cAMP signaling is altered in TD.

The second pathway that is enriched within the TD candidate genes points towards an involvement of (altered) endocannabinoid signaling in TD etiology. The endocannabinoid system (ECS) comprises two cannabinoid receptors – CNR1 and CNR2 – their ligands, the endocannabinoids, and the enzymes regulating endocannabinoid synthesis and degradation. CNR1 is highly expressed in the CNS, while CNR2 is mainly expressed in immune cells and activated microglia, with some expression also detected in the CNS. Further, endocannabinoids are endogenous lipid-signaling molecules that are produced in the cell membrane from phospholipid precursors and act as messengers that modulate pre-and postsynaptic functions [139,140] in multiple brain regions. The two best characterized endocannabinoids are arachidonoyl ethanolamide (AEA or anandamide) and 2-arachidonoylglycerol (2-AG). Interestingly, endocannabinoids are also derivatives of arachidonic acid (AA) and our PRS-based analyses implicated genetic sharing between TD and increased AA blood levels (see below). Previous studies have also suggested altered ECS signaling in the pathophysiology of TD. In this respect, studies have yielded inconclusive results regarding genetic variation in CNR1 being associated with TD [141,142] but significantly increased CSF levels of several endocannabinoids as well as AA were reported in TD patients compared with controls [143]. In addition, the enriched 'Endocannabinoid Neuronal Synapse Pathway' contains the key landscape protein DAGLA, an enzyme that can be located in the pre-and postsynaptic membrane (see above) and that produces 2-AG in an autocrine fashion [144]. Moreover, *Dagla* KO zebrafish show stereotypical movements and deficits in motion perception [145]. Interestingly, several enzymes in the enriched endocannabinoid-related pathway (shown in Figure S2) are also encoded by genes that are not TD candidate genes – and that are therefore not in the landscape – but of which the expression is differentially regulated in the blood of TD patients. Specifically, FAAH – an enzyme that hydrolyzes AEA to AA – was upregulated in the blood of TD patients aged 5-9 [62]. In addition, ABHD6 – an enzyme that hydrolyzes 2-AG to AA – was upregulated in the blood of TD patients aged 13-16, and ABHD6 expression was positively correlated with symptom severity in adult TD patients [62,63]. AEA can also be produced through the hydrolysis of N-acyl-phosphatidylethanolamines (NAPEs) by the enzyme NAPEPLD – that was downregulated in the blood of TD patients aged 5-9 [62] – or by the combined action of the enzymes ABHD4 (downregulated in the blood of TD patients aged 13-16) and GDE1 (of which the expression in blood was negatively correlated with TD severity) [62,63]. Furthermore, inhibition of FAAH and MGLL (an enzyme that degrades 2-AG to AA) resulted in

increased levels of AEA and 2-AG, respectively, which – in mice – disrupted habit formation [146,147] that has been hypothesized to also be underlying TD (see above). In addition, when bound and activated by endocannabinoids, CNR1 can act as an inhibitory GPCR that suppresses cAMP production and subsequent PKA activation [148,149]. This constitutes a link between the endocannabinoid pathway and the cAMP pathway discussed above, with the landscape proteins ADCY2 and PRKAR2A also being involved in both enriched pathways. Moreover, when CNR1 and DRD2 are co-expressed, co-stimulation with agonists of these two receptors led to an increase in cAMP production in striatal neurons, while when applied separately, CNR1 or DRD2 agonists inhibited cAMP production [150], which suggests a link between endocannabinoid, cAMP and dopaminergic signaling. Lastly, cannabinoid receptors are also a prime target of the exogenous cannabinoid D9-tetrahydrocannabinol (THC), the psychotropic component of cannabis. In this respect, a putatively beneficial role of cannabis in TD treatment comes from anecdotal evidence of patients reporting improvement in their tics after using cannabis [151] as well as some case studies and clinical trials (summarized in [152,153]). That being said, as most of these studies provide only low level of evidence for a beneficial effect, the European and American authorities currently only recommend cannabis use for (adult) treatment-resistant TD cases in which established therapy did not alleviate symptoms [154-156]. In addition, developmental observations suggest that endocannabinoid receptor expression increases only gradually in the postnatal period, which (partially) explains the observed insensitivity to the psychoactive effects of cannabis in young people. Therefore, it was hypothesized that children may respond positively to medicinal applications of cannabis without undesirable central effects [157]. However, only three single case reports are currently available to suggest that a medicinal form of cannabis would be effective and safe for treating severe tics in minors with TD [158-160].

In addition to the pathway analysis, we conducted further analyses for biological functions that are enriched within the TD candidate genes. Most of the enriched functions are related to processes such as development, migration and proliferation of neurons/brain cells (leading to neuronal circuitry development), synaptic function, and neurotransmission. In this respect, previous studies have reported altered synaptic plasticity in TD patients compared to controls (in the cortex and brain stem) [161-163]. In addition, a recent study assessed the enrichment of multiple gene sets using individual-level genotype data and identified three genome-wide significant gene sets that are implicated in TD, i.e., ligand-gated ion channel signaling, lymphocytic signaling, and cell adhesion and trans-synaptic signaling [5].

Apart from the analyses of which we discussed the results above, we performed PRS-based analyses to determine the presence, extent, and direction of genetic overlap between

TD and blood or CSF metabolite levels. Below, we will discuss the main findings from these analyses. As a general comment, we would like to point out that although different levels of metabolites in the blood (plasma or serum) may not directly reflect changes in the brain, they reflect alterations in metabolic pathways in the body and may therefore be associated indirectly with the development of TD. In addition, many metabolites can cross the BBB – via transporters or diffusion – and changes in the blood levels of these metabolites likely lead to more direct changes in the brain and vice versa.

First, we found genetic sharing between TD and higher blood levels of betaine. Betaine (also known as trimetylglycine) is an amino acid that is taken up into the body through the diet or can be synthesized in the mitochondria from choline in a two-step process catalysed by landscape proteins CHDH and ALDH7A. Betaine acts as an important cellular osmolyte and a methyl donor for the conversion of homocysteine to methionine – and hence increases methionine levels [164] – as part of the methionine cycle [165]. This cycle produces S-adenosylmethionine (SAM) and S-adenosylhomocysteine (SAH), key modulators of cellular methylation and hence epigenetic regulators [166,167]. Interestingly, MAT2A and MAT2B, two enzymes from the methionine cycle – that converts methionine to SAM – were found to be upregulated in the blood of TD patients aged 13-16 [62], while the landscape proteins PRMT1 and AHCY catalyse the subsequent conversion of SAM to SAH and SAH to homocysteine, respectively. In addition, the blood expression of PRMT1 is correlated with TD severity [63]. Further, methionine was shown to induce stereotypy and prepulse inhibition deficits in mice [168] and to increase amphetamine-induced stereotyped behaviors in rats [169]. Higher homocysteine serum and plasma concentrations were also found in patients with primary dystonia compared to controls [170,171]. All these findings provide further support to an involvement of homocysteine/methionine metabolism in TD, in which alterations in homocysteine/methionine levels would lead to changes in methylation of downstream substrates, including histones and result in altered gene expression [166,167].

We also identified a shared genetic etiology between TD and decreased blood levels of pyridoxate, the primary catabolic product of vitamin B6. Blood levels of pyridoxate are strongly correlated with blood levels of its precursor pyridoxal 5'-phosphate (PLP), the active form of vitamin B6. Therefore, pyridoxate has been suggested as a possible complementary and short-term marker of vitamin B6 status [172]. In this respect, previous studies have shown that supplementation of vitamin B6 in combination with other molecules such as magnesium [173,174] was safe and effective in alleviating symptoms of TD in children and adolescents. Furthermore, enzymes involved in the metabolism of pyridoxate and PLP were found to be differentially expressed in TD patients: ALPL – that catalyzes the dephosphorylation of PLP to pyridoxal (the transportable form of vitamin B6) – was

upregulated in the postmortem striatum of TD patients [60], while PDXK – that catalyzes the conversion of vitamin B6 precursors to their phosphorylated counterparts, including PLP – and PHOSPHO2 – that dephosphorylates PLP – were downregulated in the blood of children with TD [62]. Moreover, the blood expression of AOX1 – that converts PLP to pyridoxate – was positively correlated with TD severity [63]. Interestingly, magnesium – that is a cofactor of many landscape proteins – is (also) a cofactor for most of these enzymes. Lastly and importantly, vitamin B6 (PLP) acts as a cofactor in various enzymatic reactions, including the conversion of histidine to histamine by the important landscape protein HDC.

Furthermore, we found genetic sharing between TD and increased blood levels of Tumor necrosis factor-beta (TNFB), a cytokine that is produced by lymphocytes. In the landscape, TNFB interacts with several proteins, and it induces downstream signaling by binding to heterodimeric TNFRSF1A and TNFRSF1B [175]. TNFRSF1A and TNFRSF1B expression is upregulated in the striatum of TD patients [60] and the blood expression of TNFSRF1B is negatively correlated with TD symptom severity [63]. In addition, a mutation in *TNFRSF1A* has been linked to persistent tics [176]. A direct involvement of TNFB in the pathogenesis of TD has not been studied but some evidence for its (putative) role in TD comes from studies on autoimmune disorders. First, TNFB regulates the formation of tertiary lymphoid-like structures [177,178], such as the murine nasal-associated lymphoid tissue (NALT) [179] that is analogous to the human tonsils/adenoids [180]. Group A streptococcal (GAS) bacteria that are present in both mouse NALT and human tonsils [181] are crucial in the pathophysiology of PANDAS, an autoimmune disease that presents itself as a combination of tics and OCD-like symptoms [182]. In addition, streptococcal superantigens – that are involved in PANDAS [183] – directly stimulate the secretion of TNFB [184]. Further, TNFB is crucial for protecting against Toxoplasma bacterial infection in the CNS [185], which is interesting because a possible role of Toxoplasma infection in the pathogenesis of TD and tic disorder has been reported [186,187].

Furthermore, we identified genetic overlap between TD and decreased blood levels of myo-inositol (MI). MI is a metabolite of the second messenger phosphatidylinositol (PI) [188], and PI and its metabolites regulate normal human brain development and aging as well as the organization of the cell membrane [90,91]. In addition, MI (derivatives) play crucial roles in various processes, such as signal transduction, osmoregulation, membrane biogenesis and trafficking, cytoskeletal organization, gene expression, DNA repair, energy metabolism and autophagy, and they have been implicated in multiple disorders [189]. In line with our findings, a brain MRS study in TD reported reduced MI levels in the left frontal cortex [190]. The levels of intracellular MI are dependent on de novo synthesis, conversion of MI derivatives, uptake from the extracellular fluid and/or degradation. In this respect,

a role for altered MI signaling in TD is also implicated by the fact that some key enzymes involved in the synthesis of MI were found to be differentially expressed in the brain and/ or blood of TD patients: HK2 (increased in the postmortem striatum of TD patients [60], ISYNA1 (an enzyme that catalyses the rate-limiting step in MI synthesis and of which the expression was downregulated in the blood of TD patients aged 5-9 and 13-16 [62]) and the landscape protein IMPA1 (upregulated in the blood of TD patients aged 10-12 [62]). Moreover, *Impa1* KO mice showed TD-like behaviors, including increased motor activity in the open field and forced-swim tests, hyperactivity, and stereotypy in the home cage [191]. Four landscape proteins involved in the conversion of MI derivatives were also differentially expressed: PLCH1 (downregulated in TD striatum [60]), PI4KA (downregulated in the blood of TD patients aged 5-9 [62]), PIKFYVE (upregulated in blood of TD patients aged 13-16 [62]) and IP6K2 (alternatively spliced in the blood of TD patients and blood expression is negatively correlated with TD severity [63,64]. Further, the expression of the MI transporter SLC5A11 was dysregulated in the blood of TD patients (upregulated and downregulated in TD patients aged 5-9 and 13-16, respectively [62]). Lastly, MI is catabolized in the kidneys by the enzyme MIOX, and blood expression of MIOX was found to be upregulated in TD patients aged 5-9 [62].

Our PRS-based analyses also revealed genetic sharing between TD and increased or decreased blood levels of multiple types of lipids, including glycerophospholipids, sphingolipids, triacylglycerols, fatty acids, myo-inositol (see above) and lipid ratios. As for fatty acids (FA), these are utilized as energy source, signaling molecules and structural components of membranes [192], and depending on their chemical structure and chain length, they are classified as saturated, monounsaturated, or polyunsaturated (PUFA). In this respect, we found genetic sharing between TD and increased blood levels of saturated, long chain FA, such as stearate (stearic acid) and palmitate (palmitic acid), as well as (long chain) PUFA. These PUFA are divided into omega-6 FA – including the essential PUFA linoleate (linoleic acid, LA) that is a precursor of gamma-linolenate (gamma-linolenic acid) and arachidonate (arachidonic acid, AA, see above) – and omega-3 FA, such as the essential PUFA alpha-linolenate (alpha-linolenic acid). Palmitic acid (PA) is the most common saturated FA found in the human body and can be provided through the diet or be synthesized endogenously from other FA – such as palmitoylethanolamide (PAE) that is increased in the CSF of TD patients [143] and that is converted to PA by FAAH, an enzyme that is also involved in AA synthesis (see above) – carbohydrates and amino acids. PA represents 20–30% of total FA in membrane phospholipids and adipose triacylglycerols [193] and it has multiple functions – reflected by the multiple landscape proteins of which it regulates the expression or activity – including palmitoylation, a posttranslational modification of proteins

that involves the attachment of PA to specific cysteines, which increases the hydrophobicity of cytoplasmic proteins and hence increases their affinity for cytosolic membrane surfaces. Further, AA is the biologically active omega-6 FA and represents about 20% of the neuronal FA. AA is converted to various eicosanoids that are important mediators of inflammation – with both pro- and anti-inflammatory activities – and is involved in regulating synaptic transmission [194]. More specifically, AA is released from membrane phospholipids through phospholipase enzymes. Subsequently, AA can be metabolized by three different groups of enzymes, i.e., cyclooxygenases, lipoxygenases and cytochrome P450 enzymes that generate numerous biologically active mediators, many of which are potential preventive and therapeutic targets for various diseases [195]. In this respect, it is interesting that the cyclooxygenase PTGS1 and the lipoxygenases ALOX5, ALOX5AP and ALOX15B were all found to be upregulated in the postmortem striatum of TD patients [60]. Moreover, and as already discussed above, AA is a precursor for endocannabinoids and therefore, it has an important role in regulating both endocannabinoid and cAMP signaling, the two pathways that were significantly enriched in the TD candidate genes (see above). Linked to this, the extracellular and anti-inflammatory [196] metabolite LXA4 – which is synthesized from AA through sequential actions of lipoxygenases – mostly exerts its effects through GPCRs such as the landscape protein FPR2 and CNR1. As for its effect on CNR1, LXA4 was found to act as an allosteric modulator of CNR1, thereby enhancing its affinity for AEA and ultimately decreasing cAMP production [197], which may make LXA4 a potential TD treatment that could be used instead of the cannabinoids themselves (see above). Lastly, omega-3 and omega-6 FA compete with each other in their effects on downstream signaling [198]. In keeping with this, omega-3 FA can decrease the bodily levels of omega-6 FA through being ingested via the diet (e.g., from fish oil) and they have important anti-inflammatory properties, e.g., through inhibiting NFKB signaling [199]. Therefore, it follows that omega-3 FA would constitute a putative adjunctive treatment of TD and indeed, a randomized, double-blind, placebo-controlled trial in children indicated that omega-3 FA supplementation may be beneficial in the reduction of tic-related impairment for some children and adolescents with TD, but not for tics per se [200].

In addition to blood metabolites, we found genetic sharing between TD and the CSF levels of two metabolites: NAAG and butyrate. As for NAAG, we will discuss this metabolite and its links with TD in detail below. Butyrate (or butyric acid, BA) is a short chain fatty acid naturally produced by bacterial fermentation of undigested carbohydrates, such as dietary fiber in the gut. Interestingly, different levels of BA-producing bacterial groups [201-203] – including Roseburia [68], Faecalibacteriumin [204] and Bacteroidia [205] – were found in the microbiome of TD/tic disorder patients compared to controls, suggesting that rebalancing

of gut microbiota could be a promising biological therapy for TD [206]. BA then travels from the gut through the systemic circulation and reaches the brain, where it crosses the BBB via monocarboxylated transporters of the SCL16 family [207], including SLC16A3, SLC16A4 and SLC16A7 that were found to be differentially expressed in the blood or postmortem brain tissue of TD patients [60,62]. In the brain, BA can act as a regulator of the immune response through its anti-inflammatory actions in microglia [208], an epigenetic regulator that increases gene expression through inhibiting histone deacetylation [209,210] and/or as an endogenous ligand for a subset of GPCRs, including the landscape protein FFAR3 and – not shown in the landscape – FFAR2 (upregulated in postmortem TD brain) [60] and HCAR2 (of which the blood expression is negatively correlated with TD severity) [63]. BA also modulates the expression/activity of many (other) landscape proteins. In the extracellular matrix, BA decreases the expression of COL4A2, COL5A1, COL6A3, IL17A, TNFAIP2, it increases the expression of ANXA1 and WNT5, and it regulates the acetylation and methylation of RELN. In the cytoplasm, BA increases the activity of HDC – leading to increased histamine synthesis, see below – and CASP8, while it also increases the expression of CDKN1A and GAK. Further, BA decreases the expression of cytoplasmic ESR1, NCL and PRKAR2A, and it increases the release of DIABLO from mitochondria. In addition, BA activates cAMP-PKA signaling – although independently from GCPR-mediated signaling) [211] – and there is a positive association between BA and endocannabinoids in human subjects (enrolled in a 6-week exercise intervention) [212], indicating that BA regulates both pathways that were enriched in our data. Lastly, previous studies have suggested a beneficial role of BA in treatment of neuropsychiatric conditions, such as ASDs [213,214], Huntington's disease (HD) and PD, where it exerts neuroprotective effects, supports mitochondrial function, and decreases behavioral abnormalities [215-218] through inhibiting histone deacetylation [217,219]. Further, BA was shown to positively affect memory-related synaptic plasticity [220] and omega-3 FA (see above) were shown to restore the normal levels of BA-producing bacteria [221]. All these findings suggest that approaches aimed at increasing (CNS) butyrate levels – e.g., through changing the gut microbiome or having an omega-3 FA-rich diet – may be considered as (adjunctive) treatments for TD.

Based on all our data and analyses, we built an integrated molecular landscape of TD that contains interactions between more than 500 proteins, metabolites and other molecules, and above, we have already described the main landscape processes. Before providing more details about specific putative drug targets that we identified in the landscape and as a more general comment, we would like to note that multiple landscape proteins – spanning different subcellular locations – are involved in protein degradation. These include (proteins constituting) the ubiquitin-proteasome system in the cytoplasm,

ER proteins involved in ubiquitin-dependent degradation of misfolded ER proteins, CV-mediated autophagy, and molecular chaperones, and all these proteins regulate the removal and recycling of misfolded proteins and damaged organelles. Further, impairment of these processes and accumulation of protein aggregates and faulty organelles can lead to the generation of oxidative stress, inflammation, and cell death [222], which in turn affects synapse formation, maturation, and plasticity [223]. In addition, based on the four aspects of target specificity described in the Materials and Methods, we identified a number of putative drug targets in the TD landscape, and we will describe six of these targets in more detail below.

First, FLT3 is a membrane-located receptor tyrosine kinase that regulates inflammation and other immunity-related functions [224]. *FLT3* is the most significantly associated gene in the largest GWAS of TD published to date [51]. FLT3 shows regional specificity for TD, as it is highly expressed in the brain and in our TWAS, we found TD-associated eQTLs with a positive effect on *FLT3* expression in multiple brain regions (top finding for the cortex; Z-score= 4.66 and *p*-value = 3.24E-06). In keeping with this, a recent study also found the most significant TD-associated TWAS signal for the cortex and, more specifically, the dorsolateral prefrontal cortex [225]. In the same study, the authors reported an increased expression of FLT3 in lymphoblastoid cell lines derived from TD patients compared to controls [225]. As for its temporal specificity for TD, FLT3 is highly expressed in two brain regions for which we have found spatiotemporal enrichment of TD candidate gene expression (see above), i.e., in the cerebellum (in the neonatal period and infancy, early and middle-late childhood, adolescence, and young adulthood) and in the thalamus (in adolescence and young adulthood). Moreover, FLT3 has considerable molecular specificity for TD as it interacts with multiple other landscape proteins. For example, upon binding its ligand, the cytokine FLT3LG – which has been linked to TD as well, as FLT3LG blood expression is positively correlated with TD symptom severity [63] – regulates the phosphorylation of MAPK3 and MAPT, two highly interactive landscape proteins, while it also regulates the expression of cytoplasmic PIM1 and nuclear EXCC6, two proteins that (also) interact with many other landscape proteins. Lastly, FLT3 (putatively) has modulatory specificity for TD because, and as mentioned above, TD-associated eQTLs upregulate *FLT3* expression in multiple brain regions, which suggests that inhibition of FLT3 (function) could have a beneficial effect on TD symptoms. In this respect, it is interesting that inhibitors of FLT3 have been approved for various cancers and have been trialed with positive effect for multiple T-cell mediated autoimmune diseases [224] that are genetically and/or clinically overlapping/comorbid with TD [226-228]. Moreover, FLT3 inhibitors have been found to have a therapeutic effect in (human) cell and mouse models of Rett syndrome, a genetically determined neurodevelopmental disorder

[229], and to alleviate peripheral neuropathic pain in mice [230]. The above being said, additional *in silico*, *in vitro* and *in vivo* studies are needed to further determine if and how FLT3-based treatments for TD could be developed.

Another promising drug target from the landscape is NAALAD2, an enzyme that is expressed in neuronal and astrocytic membranes and that converts N-acetyl-aspartyl-glutamate (NAAG) to N-acetylaspartate (NAA, which is synthesized by the mitochondrial landscape enzyme NAT8L) and glutamate. Conversely, NAAG is formed from NAA and glutamate by the cytoplasmic landscape enzymes RIMKLA and RIMKLB. As for its regional and temporal specificity for TD, NAALAD2 is highly expressed in the pituitary, neurons and astrocytes [231] and it is highly expressed in the striatum during young adulthood [232], respectively. Further, NAALAD2 has molecular specificity for TD because it works on two important, TD-linked neurotransmitters: NAAG and glutamate. NAAG is one of the only CSF markers for which we found genetic sharing with TD and it is thought to function as a neurotransmitter in both the CNS and peripheral nervous system, with its lowest expression being in the pituitary [233], a finding that is in line with NAALAD2 expression being the highest in this brain region (see above). In a magnetic resonance spectroscopy (MRS) study, patients with TD also had reduced levels of NAA in the left putamen and bilateral frontal cortex [190]. In addition, the main excitatory neurotransmitter glutamate – that is converted from NAAG by NAALAD2 – interacts with multiple landscape proteins. Furthermore, a number of MRS studies have investigated the involvement of (brain) glutamate in TD, but this has yielded inconsistent results [234-236]. Lastly, it seems that NAALAD2 also has (putative) modulatory specificity for TD. In addition to genetic sharing (see above), we found a negative genetic concordance between TD and CSF levels of NAAG, indicating that genetic variants associated with TD are also associated with decreased NAAG CSF levels. In turn, this suggests that (brain) NAALAD2 – which uses NAAG to 'produce' glutamate – should be inhibited to treat TD. Furthermore, transcriptomic profiling has shown decreased RIMKLB levels and increased NAT8L levels in the blood of TD patients aged 5 to 9 [62], as well as alternative splicing of *RIMKLA* in the blood of adult TD patients [64]. All these findings suggest that in addition to inhibiting NAALAD2, a treatment to reduce TD symptoms may be to activate/increase NAAG synthesis. However, there are currently no known treatments that increase NAAG synthesis. Interestingly, inhibiting FLT3 (see above) also prevents glutamate-induced toxicity [237] – that could be the result of increased NAALAD2 expression/activity – which constitutes a functional link between NAALAD2 and FLT3. Moreover, NAALAD2 inhibitors – that elevate synaptic NAAG levels [238] – were found to reduce stereotypical movements in different mouse models (of schizophrenia) [239,240], which further highlights the suitability of NAALAD2 as a novel TD target and the need to conduct further experiments to develop it into an effective TD treatment.

Two other interacting putative drug targets from the landscape are the membrane receptor CX3CR1 and its ligand, the chemokine CX3CL1. CX3CR1 is highly expressed in the microglial cell membrane. In addition, the CX3CR1-CX3CL1-complex plays a key role in regulating brain inflammation [241] as well as synaptic pruning and connectivity [242-244], while CX3CL1 is also located in the neuronal cell membrane where it can be cleaved into a soluble chemokine by the membrane-located landscape enzyme ADAM10 [245,246]. As for their regional specificity for TD, the expression of CX3CR1 was found to be upregulated in the (postmortem) striatum of TD patients (FC=1.78) [60] and increased CX3CL1 blood expression is correlated with increased TD symptom severity [63]. Both proteins also show temporal specificity for TD. CX3CR1 expression is upregulated in the blood of TD patients aged 10-12 years (FC=1.18) [62] and in mouse striatum, Cx3cr1 shows a temporal expression pattern corresponding to developmental stages that could be linked to TD occurrence and resolution (i.e., first upregulation, then downregulation) [247]. In addition, CX3CL1 is highly expressed in the striatum (in the neonatal period, early infancy and early childhood), cortex (neonatal period, early infancy, early childhood and adolescence) and the thalamus (neonatal period and early infancy), while mouse Cxc3l1 also shows the same temporal expression pattern in the striatum than Cx3cr1 does [247]. Moreover, CX3CR1 and CX3CL1 have molecular specificity for TD, and this not only through forming a functional complex with each other but also through additional effects of CXC3L1 on multiple other landscape proteins – that were not all drawn in the landscape but can be found in Table S5 – e.g., as a ligand of the ITGA4-ITGB1-complex and through upregulating the expression of extracellular POSTN and membrane-located CDHR1. Lastly, there is some evidence that the CX3CR1-CX3CL1-complex could be modulated with a beneficial effect on TD. However, both an inhibition and activation of this complex have been found to have a neuroprotective effect, depending on whether the intervention was done in the developing or adult brain [248]. For instance, neutralizing antibodies against (brain) CX3CR1 ameliorated exogenous CX3CL1-induced PD-like behaviors in an adult rat model [249], while another study in a mouse model of PD revealed the neuroprotective capacity of CX3CL1 that resides solely upon the soluble form but not the membrane-located form of CX3CL1 [250]. Moreover, in a mouse model of Rett syndrome, it was shown that the presence of CX3CR1 is detrimental to the neurodevelopmental trajectory and (partial) ablation of *CX3CR1* attenuated disease severity [251]. For these reasons, further studies are needed to further determine if and how CX3CR1/CX3CL1-based treatments for TD could be developed.

Further, the TD landscape contains three presynaptic membrane-located opioid receptors – OPRM1, OPRK1 and OPRD1 – of which we think that especially OPRM1 fits all aspects of drug target specificity for TD. OPRM1 is an opioid receptor of the μ family that

mediates downstream signaling through binding both endogenous opioids (such as endorphin and endomorphin) and synthetic opioids (such as morphine, heroin, fentanyl and methadone) [252,253]. OPRM1 shows regional specificity for TD, as OPRM1 is highly expressed in the brain but its expression is specifically downregulated in the (postmortem) striatum of TD patients (FC= -1.43) [60]. OPRM1 also has temporal specificity for TD as it is highly expressed in the thalamus (in the early fetal period, early-mid fetal period, neonatal-early infancy period, adolescence and young adulthood) and the cerebellum (late fetal period and late infancy). Moreover, OPRM1 has considerable molecular specificity for TD as it interacts with multiple other landscape proteins, including the opioid receptors of the δ and κ families OPRD1 and OPRK1. In addition, OPRM1, OPRD1 and OPRK1 are involved in cAMP-mediated signaling (one of the two enriched pathways within the TD candidate genes), while OPRM1 is also a (putative) upstream regulator of multiple landscape genes (see above). As for the – putative – modulatory specificity of OPRM1, it should first be noted that abnormalities of the opioid system have been found in TD previously [254,255]. In this respect, previous reports have shown that pharmacological manipulation of the endogenous opioid system has a beneficial effect on TD (symptoms). Specifically, several case reports [256-258] and a randomized, double-blind, placebo-controlled study [259] have suggested that TD symptom reduction may be achieved with an opioid receptor antagonist such as naloxone or naltrexone that both have a high binding affinity for OPRM1 [260]. In addition, some studies have indicated dose-dependent effects of naloxone in patients with TD, with low doses causing a decrease in tics while higher doses cause increased tics [261,262]. Conversely, case reports have also shown that the full OPRM1 agonist methadone and the partial OPRM1 agonist buprenorphine are successful in alleviating symptoms of TD [263,264]. Furthermore, impaired OPRM1 function has been suggested to lead to decreased release of gonadotropin-releasing hormone (GnRH) [265] that is produced by the PROK2-PROKR2 complex in the landscape. In turn, this leads to a reduced secretion of the gonadotrophins LH and FSH that have been found to be especially lower in the plasma of male TD patients, and this associated with the onset of puberty [266]. Given the above, further studies are required to assess which opioid receptor agonists and/or antagonists could be used to treat TD and when these drugs would need to be administered to have the best effect and least side effects.

The last putative drug target from the landscape that we would like to discuss in some detail is HRH2, a (neuronal) membrane receptor of histamine. Firstly, HRH2 shows regional specificity for TD, as it is highly expressed in both excitatory and inhibitory neurons [267], and its expression in blood has been found to be negatively correlated with symptom severity in TD symptoms [63]. As for its temporal specificity, HRH2 expression is upregulated in the blood of TD patients aged 10-12 (FC=1.12) [62] and in mouse striatum, Hrh2 shows a

temporal expression pattern corresponding to developmental stages that could be linked to TD occurrence and resolution (i.e., first upregulation, then downregulation) [247]. In addition, HRH2 is highly expressed in the striatum (in the neonatal period, early infancy, early childhood and adolescence) and cortex (neonatal period, early infancy, early childhood, adolescence and early adulthood). Moreover, HRH2 has molecular specificity for TD, as it binds and interacts with HDC, the cytoplasmic enzyme that has been linked to TD by strong genetic evidence [28,268,269] and the results from our analyses (Table S2) and that converts histidine to the HRH2 ligand histamine. In addition, HRH2 regulates the production of arachidonic acid, one of the top metabolites emerging from the PRS-based analyses (see above) and it upregulates the expression of IL17A, a cytokine that itself has several interactions in the landscape and of which the blood levels were found to be increased in TD patients [270,271]. Further, HDC uses PLP as its cofactor to synthesize histamine from histidine, with both PLP and histidine being implicated in TD through our analyses (see above). Histamine (see above) is also transported in and out of astrocytes and presynaptic neurons by the landscape transporters SLC22A3 and SLC29A3, while in astrocytes, it is also methylated and hence inactivated by the HNMT enzyme [272]. The blood expression of HNMT was also found to be upregulated is TD patients aged 13-16 (FC=1.70), while that of SLC22A3 was downregulated in TD patients aged 10-13 (FC=-1.10) and positively correlated with TD severity [62,63], further suggesting a dysregulation of histamine metabolism in TD. Specifically, and linked to the putative modulatory specificity of HRH2, low brain concentrations of its ligand histamine have been reported in the *Hdc* knockout (KO) mouse model of TD, and histamine repletion ameliorated tic-like stereotypical movements in these animals [273]. In addition, histamine bound to HRH2 has been shown to have a neuroprotective effect by alleviating the NMDA glutamate receptor-induced excitotoxicity via cAMP signaling [274]. Moreover, the histamine precursor histidine was shown to promote astrocyte migration and provide neuroprotection through HRH2 [275]. Histidine and HNMT inhibitors also ameliorated methamphetamine-induced stereotyped behavior and behavioral sensitization in rodent models, while HDC inhibitors and HRH2 antagonists enhanced this behavior [276-282]. As histamine does not cross the BBB [283], a potential strategy to increase the brain levels of histamine – that could then bind and signal through HRH2 – would be to provide additional histidine through the diet. Histidine is transported across the BBB by SLC3A2 and SLC7A5 that form heterodimers [284] and are both upregulated in TD postmortem striatum [60]. This being said, further studies are needed to assess the effects of histidine supplementation and/or administering agonists of HRH2 other than histamine (that pass the BBB) on TD symptoms.

Our study should be viewed in the context of a number of strengths and limitations. Particular strengths are that, to our knowledge, we have analyzed all available omics data for TD for the

first time and integrated the results from these analyses with an extensive literature search for interactions between the TD-linked genes/proteins and metabolites into a molecular landscape of the disease. In turn, this TD landscape not only provides insights into the altered molecular processes that underlie the disease but also, and importantly, it enabled the identification of biologically meaningful drug target leads for further studies. An important limitation of the study was that because of the lack of omics data for specific TD symptoms, we decided to use a 'broad' definition of the TD phenotype, and because of this, we could not derive any insights about the molecular mechanisms underlying these specific symptoms from our results. Moreover, a number of omics studies of which we used the data were limited in sample size and therefore likely underpowered for a meaningful statistical analysis of the individual study results. However, we tried to address this by prioritizing those genes/proteins for building the landscape that have been implicated in TD through one type of genomic evidence and at least one other type of genomics or other omics evidence (i.e., the 'dark blue' genes/proteins). Another limitation is that the PRS-based analyses that we conducted only consider the joint effect of (very) many common genetic variants associated with TD, but further studies are needed to elucidate whether and to what extent rare genetic variants (also) contribute to metabolite levels. In addition, more advanced methods would need to be applied to dissect the 'broad' PRS-based signal containing hundreds of thousands of SNPs into genetic loci and even individual genes. Furthermore, the PRS-based approach only represents a starting point for identifying genetically determined levels of blood or CSF biomarkers, and further studies using for example Mendelian Randomization and metabolomics could help identify any causal or pleiotropic effects of specific metabolites on TD, and vice versa [285]. Lastly, both the protein-protein interaction databases that we used and the extensive literature search that we conducted for building the landscape are – by default – incomplete and more interactions may become known and be experimentally validated in the future. Therefore, additional studies are required to follow up on and validate/corroborate the main findings and leads from our landscape. For example, future in vivo and interventional studies could be done that modulate metabolites and/or interactions between genes/proteins and metabolites through existing medications or dietary changes, and that may provide new ways to lessen the burden of TD.

MATERIALS AND METHODS

Literature search and selection of omics data sets

We searched public databases (i.e., PubMed and Europe PMC [286], which include peer-reviewed articles and preprints, GWAS Catalog [52]) for human 'omics' studies in subjects with Tourette's disorder (TD) or tic disorders, as well as pediatric acute onset neuropsychiatric syndrome (PANS) including pediatric autoimmune neuropsychiatric disorders associated

with streptococcal infection (PANDAS), which have been proposed as etiological subtypes of TD [287]. The 'omics' notion refers to system-wide data derived from high throughput assays measuring simultaneously all or nearly all molecules of the same type at the various level of cellular functions. These comprise: (I) genomics – the study of sequence level DNA variation associated with the disorder that can be identified through linkage analysis in family-based studies and through association studies in family and population-based data, including (a) common single nucleotide sequence variation (base changes/substitutions/insertions/ deletion), referred to as single nucleotide polymorphisms (SNPs), found at frequencies greater than 1% in a population and investigated in genome-wide association studies (GWASs)), (b) rare single nucleotide variants (SNVs), usually exceedingly rare or unique to an individual, investigated in next-generation sequencing (NGS) studies, most often focused on protein-coding regions of the genome, known as exome sequencing), (c) rare structural variation, including copy number variation (CNV), referring collectively to differences that are at least 50 bp in length between two individual genomes; (d) chromosomal aberrations; (II) epigenomics – the study of non-sequence level DNA modifications (changes that are heritable and do not entail a change in DNA sequence [288]), including: DNA methylation, histone modifications, chromatin modelling; (III) transcriptomics – the study of RNA transcript abundance and expression using microarrays or RNA-sequencing (RNA-seq), including protein-coding messenger RNA (mRNA) and two types of noncoding RNA with regulatory roles: long noncoding RNA (lncRNA) and microRNA (miRNA), with the latter also recognized as a type of epigenetic machinery; (IV) proteomics – the study of protein abundance and expression using antibody-based arrays and mass spectrometry (MS); (V) metabolomics – the study of low molecular weight compounds (metabolites) using techniques such as liquid chromatography- mass spectrometry (LC-MS) or nuclear magnetic resonance spectroscopy (NMR); (VI) microbiomics - the study of fecal microbiota as a proxy for microbiota of the gastrointestinal tract (gut microbiota). Microbiome studies were included if they reported bioactive microbiota-derived metabolites related to the alternations in the microbial composition, as microbial metabolites could affect brain activity in the microbiota–gut–brain bidirectional communication [289]. We conducted this literature search for eligible data up to December 1, 2021; otherwise-eligible studies published after this date were not included in our analyses. Also, reference lists from reviews were used for reference checking. Studies were excluded if (i) the study was published in a language other than English, (ii) molecules assayed or analyzed were limited to those in candidate genes/molecules, (iii) data was not accessible. Findings considered significant in the primary publication by the study authors, using their experimental design and thresholds, are included in our main lists, while subthreshold findings are listed in the extended lists.

Analyses of TD GWAS summary statistics

We obtained the summary statistics of the largest TD GWAS meta-analysis of 14,307 individuals from the PGC website (https://www.med.unc.edu/pgc/). Prior to further analyses, we applied filters to the summary statistics, as implemented in the munge sumstats.py script (version 1.0.1), available within the LD score regression package (ldsc) [290]; https://github.com/bulik/ldsc): a) imputation quality INFO score above 0.9; b) sample MAF above 1%; c) remove indels and structural variants; d) remove strand-ambiguous SNPs; e) remove SNPs whose alleles do not match the alleles in 1000 Genomes.

To better understand the mechanism by which variations at GWAS loci influence susceptibility to TD, we used different methods to dissect GWAS loci and identify TD-relevant genes. We focused on strategies aiming to prioritize genes rather than variants to arrive at more interpretable results.

Genome-wide gene-based analysis in MAGMA

We used Multi-marker Analysis of GenoMic Annotation (MAGMA), v1.09 [291], to perform gene-based analysis of the TD GWAS meta-analysis summary statistics. MAGMA combines multiple variants that are mapped to a gene, while adjusting for the linkage disequilibrium (LD) between those variants and tests the joint association of all variants in the gene with the phenotype. This approach reduces the number of tests that need to be performed and enables the identification of effects consisting of multiple weaker associations that would be missed in the individual variant analysis. Specifically, for each of 19,427 protein-coding genes included in the NCBI 37.3 database, we considered all single nucleotide polymorphisms (SNPs) located in the gene body (0kb) and 100kb windows on both sides. Then, using an updated SNP-wise Mean model, we combined the resulting SNP p-values into a gene test statistic (the sum over squared SNP Z-statistics) and computed the corresponding gene p-value. We used the 1000 Genome Project Phase 3 European population as reference data to account for the LD-induced covariance of SNP p-values. For further analyses, we considered genes with the p-value < 1.0E-03, a less stringent cut-off to enable retrieval of suggestive associations. Previous studies have shown that SNPs in (the vicinity of) a gene with sub-threshold p-values as high as 1.00E-04 are likely to carry a significant biological signal affecting gene expression and function and may reach significance in later higher-powered studies [292,293].

SNP functional annotation and gene mapping in FUMA

SNP functional annotation

We used FUMA online platform (v1.3.6b, [294], http://fuma.ctglab.nl/) for identification of genomic risk loci and functional annotation of SNPs from the TD GWAS meta-analysis

summary statistics. We first identified independent significant SNPs with a *p*-value < 1.0E-05 and are independent of each other at r^2<0.6. These SNPs were further represented by lead SNPs, which are a subset of the independent significant SNPs in approximate linkage equilibrium with each other at r^2<0.1 (based on LD information calculated from 1000 genomes). We then defined associated genomic loci by merging any physically overlapping lead SNPs (linkage disequilibrium (LD) blocks<250kb apart). We selected all candidate SNPs in associated genomic loci that were in LD (r^2>0.6) with one of the independent significant SNPs, had a *p*-value < 0.05 and minor allele frequency (MAF)>0.0001, for functional annotation. Functional consequences for these SNPs were obtained by matching SNPs' chromosomes, base-pair positions, and reference and alternate alleles to databases containing known functional annotations, including ANNOVAR categories [295], Combined Annotation Dependent Depletion (CADD) scores [296], RegulomeDB scores [297], and chromatin states [298,299]. ANNOVAR categories identify the SNP's genic position (e.g., intron, exon, intergenic) and associated function. CADD scores predict how deleterious the effect of a SNP is likely to be for a protein structure/function, with higher scores referring to higher deleteriousness. A CADD score above 12.37 is the threshold to be potentially pathogenic [296]. The RegulomeDB score is a categorical score based on information from expression quantitative trait loci (eQTLs) and chromatin marks, ranging from 1 to 7, with lower scores indicating a higher probability of having a regulatory function.

Gene mapping

Subsequently, we used FUMA to map functionally annotated SNPs to genes by combining three mapping strategies: positional, eQTL and 3D chromatin interaction mappings. For positional mapping, SNPs were mapped to known protein-coding genes in the human reference assembly (GRCh37/hg19) based on the physical distance of 10kb windows on both sides. For eQTL and chromatin interaction mappings, we performed analyses (1) across all available tissue/cell types – enabling full extracting of possible candidate genes and (2) within brain – to prioritize brain-specific candidate genes by eQTLs and chromatin interactions. Specifically, for brain-specific eQTL mapping, we used only brain-related eQTL data available within FUMA: eQTL Catalogue [300]: BrainSeq (DLPFC) [301] and Schwartzentruber_2018 (Sensory neurons) [302], PsychENCODE (PFC, TC, CB) [303], xQTL (DLPFC) [304], The CommonMind Consortium (CMC) (DLPFC) [305], BRAINEAC (10 brain regions) (http://www. braineac.org/), GTExv8 Brain (13 brain regions). We used a false discovery rate (FDR) *p*-value of 0.05 to define significant eQTL associations. FUMA annotates those significant eQTLs with candidate SNPs and those SNPs are mapped to the gene whose expression is potentially affected by the SNPs. In brain-specific chromatin interaction mapping, we identified

significant chromatin loops (FDR *p*-value < 1.0E-06) using built-in chromatin interaction data from: the dorsolateral prefrontal cortex and hippocampus [306], adult and fetal cortex [307], prefrontal cortex from PsychENCODE [303], FANTOM5 [308]. In FUMA, the candidate SNPs are required to be overlapped with one end of the loop and transcription start sites (TSS) of genes (500bp up- and 250bp downstream from the TSS) with the other end of the loop to be mapped. Since HiC is designed to measure the physical interactions of two genomic regions, not all significant loops necessarily contain functional interactions. We further limited chromatin interaction mapping to those where SNPs overlap with enhancer regions and gene TSSs overlap with promoter regions predicted by Roadmap consortium (http://egg2.wustl.edu/roadmap/data/byDataType/dnase/). In brain-specific analyses, we used only E053-E082 brain [299] for those annotations. For all analyses, we also performed additional filtering of SNPs based on functional annotations (CADD and RegulomeDB), as it affects gene prioritization (setting a CADD score threshold will cause FUMA to use only highly deleterious SNPs or filtering SNPs by RegulomeDB score prioritizes SNPs which are likely to affect regulatory elements per one of the mapping strategies).

Transcriptome-wide association study

Under the assumption that the effect of genetic variation on a phenotype is mediated by gene expression, we performed a transcriptome-wide association study (TWAS) to integrate TD GWAS meta-analysis summary statistics and cis-eQTL signals and prioritize candidate risk genes for TD. TWAS was implemented in FUSION [309] using the FUSION. assoc.test.R script with default settings over all autosomal chromosomes. Pre-computed SNP-expression weights from all tissue reference samples from GTEx Consortium (GTEx v7) were obtained from the FUSION website (http://gusevlab.org/projects/fusion/). We applied this recommended agnostic approach to scan all tissues models to improve our ability to detect relevant regulatory mechanisms that mediate the phenotypic association [310]. To discover genes whose expression is regulated by the same variants that underlie GWAS hits, we performed colocalization analysis using the interface to the coloc R package [311] available in FUSION for all genes below TWAS *p*-value threshold of 5E-04 (Fusion.assoc_ test.R --coloc_P flag). This Bayesian approach evaluates the posterior probability (PP) that genetic associations within a locus for two outcomes are driven by a shared causal variant. It enables the distinction between associations driven by horizontal pleiotropy (1 causal SNP affecting both gene expression and phenotype; posterior probability PP4) and linkage (2 causal SNPs in LD affecting gene expression and phenotype separately; posterior probability PP3). Significant features were considered as colocalized based on their low PP3 (<0.2) used as a less stringent threshold for evidence of non-independent association signal, as applied

previously [312]. Of note, while TWAS tests for association between gene expression and a phenotype, it accounts only for genetically predicted expression (common cis eQTLs) and constitutes only a small fraction of total expression that also includes environmental and technical components [313].

Shared genetic etiology analyses with levels of blood and cerebrospinal fluid metabolites

Polygenic risk score (PRS)-based analyses

Polygenic risk score (PRS) is used to summarize the aggregated risk from common variants across the genome, and it is a valuable tool for comparing the shared genetic basis of different traits. To test for genetic sharing between TD and levels of blood metabolites, cytokines and metals, as well as levels of CSF metabolites, we performed polygenic risk score (PRS)-based analyses in PRSice (v1.25) [314] using the summary-summary statistic based approach. As 'base phenotype', we used TD GWAS meta-analysis summary statistics. As 'target phenotypes', we used publicly available GWAS summary statistics for a total of 993 blood (serum and/or plasma) traits reported in six separate studies, including 941 metabolites [19,73,74,76], 41 cytokines [72] and 11 metals [315], as well as 338 CSF metabolic traits [75]. First, we performed clumping in PLINK (v1.90) [316] to remove SNPs in linkage disequilibrium (LD, based on $R^2>0.25$ within 500kb window) with the SNP with the smallest p-value in the base phenotype and generate sets of independent SNPs. Subsequently, we calculate PRS in PRSice using clumped SNPs whose p-value in the base phenotype were below seven broad p-value thresholds (P_T) (0.001, 0.05, 0.1, 0.2, 0.3, 0.4, and 0.5) to select the one that maximized the variance explained (R^2) for the base phenotype in the target phenotypes. PRS are estimated as a sum of risk alleles across SNPs with GWAS p-values below a given p-value threshold, weighted by the effect sizes estimated by the GWAS. Finally, we performed regression to test the association between the PRS and target phenotypes, i.e., the extent to which combined SNPs from each of the seven P_T-linked PRS for TD predict each of the target phenotypes (993 blood and 338 CSF metabolic traits' levels). To account for the large number of tests, we applied Bonferroni correction and set p-value thresholds of 7.19E-06 (0.05/(993 tests x 7 P_{Ts})) and 2.11E-05 (0.05/(338 tests x 7 P_{Ts})) to designate statistically significant results for blood and CSF metabolic traits, respectively. We also calculated Benjamini-Hochberg adjusted (FDR) p-value and set a less stringent cut-off of FDR p-value < 0.01 to retrieve suggestive associations [317].

SNP effect concordance analyses (SECA)

For the statistically significant findings from the PRS-based analyses, we performed SNP Effect Concordance analysis (SECA) [318] to test for the genetic concordance (i.e., the same

SNP effect directions across both traits) between TD and blood/CSF metabolite levels. We applied Bonferroni-correction to account for the number of tests performed in SECA and to designate statistically significant results.

Integration, annotation, and prioritization of omics studies results

Integration of omics studies results

We unified gene symbols and Entrez Gene identifiers (Entrez ID) across different genomic, transcriptomic and epigenomic datasets using 'HGNChelper' [319,320] and 'org.Hs.eg.db' [321] R packages. The 'HGNChelper' package identifies known aliases and outdated gene symbols based on the HUGO Gene Nomenclature Committee (HGNC) database [322], as well as common mislabeling introduced by spreadsheets, and provides corrections where possible. We used the most current available maps of aliases for correcting gene symbols. The 'org.Hs.eg.db' annotation package extracts Entrez Gene identifiers for gene symbols using data provided by Entrez Gene ftp://ftp.ncbi.nlm.nih.gov/gene/DATA (date stamp from the source: 2021-Sep-13). Gene lists were merged into a master table by unified Entrez ID and gene symbol. Genes for which Entrez ID was not identified were not included in our subsequent analyses. All analyzes were conducted in R [323].

We unified metabolite names across different studies using information from the Human Metabolome Database (HMDB) [324]. Some metabolites were classified as 'Unknown', indicating that their chemical identity was not yet determined at the time of analysis. Metabolites were assigned to metabolic groups – superpathways (amino acids, carbohydrates, cofactors and vitamins, energy, lipids, nucleotides, peptides, and xenobiotic metabolism) and pathways, based on the description in the Kyoto Encyclopedia of Genes and Genomes database (KEGG) [325]. Given that some metabolites are differently preserved in blood plasma and serum, and that platforms may differ in extraction protocols, we examined all metabolites included in the original studies and have not selected the largest sample available for a particular metabolite.

Gene-level annotation of omics studies results

We annotated genes with a set of molecular features that would facilitate building of the molecular landscape and provide a rationale to further prioritize genes for therapeutic targeting. Specifically, we used information contained in the UniProt Knowledgebase (UniProtKb) [326] (http://www.uniprot.org/) to extract functional and subcellular localization annotations for genes/proteins. We used Human Protein Atlas (HPA) version 21.0 [267] (http://v21. proteinatlas.org) to obtain data on tissue and cell expression of RNA/protein, as well as their subcellular location. Genes were considered to be expressed in the brain if they were detected on at least RNA level in the mammalian brain (integrated data from human, pig and mouse).

In HPA, protein expression is based on immunohistochemical data. Each subcellular location is given one of the four reliability scores (Enhanced, Supported, Approved, or Uncertain) based on available protein/RNA/gene characterization data from both HPA and the UniProtKB/Swiss-Prot database. Furthermore, we extracted information on the potential functional importance of a gene/protein, such as essentiality and druggability. A gene is considered essential when it's indispensable for the reproductive success of an organism thus loss of its function compromises the viability or fitness of the organism. In humans, essentiality is estimated based on loss-of-function (LoF) mutation intolerance, either from population exome sequencing (in vivo) data – statistical estimates of unexpected mutational depletion identifies genes presumed to be subjected to functional constraints [327]; or (2) CRISPR-based in vitro perturbation experiments – systematic testing of gene silencing effects on human cell cultures identifies genes that affect cell viability or optimal fitness upon perturbation. To this end, we used human gene essentiality estimations based on different measures of tolerance to LoF mutations provided by Bartha et al., 2018 [328] (extracted from Supplementary information S2). Estimates include the following scores based on the Exome Aggregation Consortium (ExAC) sample of 60 706 human exomes [327]: residual variation intolerance score (RVIS) [329], Evo-Tol [330], missense Z-score [331], LoFtool [332], probability of haploinsufficiency (Phi) [333], probability of loss-of-function intolerance (pLI) [327] and selection coefficient against heterozygous loss-of-function (shet) [334]. Scores based on cell culture perturbation-based experiments include data from KBM7, Raji, Jiyoye, HCT116 and K562 cell lines [335]; the KBM7 cell line [336], and RPE1, GBM514, HeLa and DLD1 cell lines [337]. Furthermore, we used information on gene druggability that could give scope for drug repurposing or redesign. The druggable genome can be defined as the genes/gene products known or predicted to interact with drugs, ideally with a therapeutic benefit to the patient. To prioritize druggable genes, we used the list of 4479 genes defined by Finan et al. as the 'druggable genome' ([338], provided in table S1). Genes reported by Finan et al. are divided into 3 Tiers corresponding to their position in the drug development pipeline: Tier 1 contains genes encoding targets of approved or clinical trial drugs, Tier 2 genes encoding targets with high sequence similarity to Tier 1 proteins or targeted by small drug-like molecules, and Tier 3 contains genes encoding secreted and extracellular proteins, genes encoding proteins with more distant similarity to Tier 1 targets, and genes belonging to the main druggable gene families not already included in Tier 1 and Tier 2 (GPCRs, nuclear hormone receptors, ion channels, kinases, and phosphodiesterases).

Prioritization of omics studies results

Since the DNA sequence remains unaltered throughout life and is not influenced by environment or development (apart from somatic mutations), genetic variants associated

with the disorder are thought to contribute to/precede, and not be a consequence of, disease development. Moreover, previous studies have shown that drug candidates are more likely to pass clinical trials and be approved for patients if they target genes linked to human disease [9,10], highlighting the importance of human genetics in target identification and drug discovery. Given the above, we prioritized the results of genomics studies of TD and used them as an anchor point for further analyses exploring molecular mechanisms implicated in TD etiology and modeling interactions of other omics data. Specifically, we complied the primary list of TD candidate genes for enrichment analyses (referred to as 'TD candidate genes' throughout the text), which included genes reported as primary significant findings (main lists) from: GWAS-based analyses (MAGMA, FUMA, TWAS, cross-disorder), preliminary MAGMA of the newest TD GWAS, rare single nucleotide variants (SNVs), copy number variations (CNVs), chromosomal aberrations, as well as genes reported as subthreshold findings (included in the extended lists) – only if they were reported in at least two separate studies. We classified studies based on assigned evidence level as: guiding (genomics studies), corroborating (epigenomic and transcriptomic studies) and additional (metabolomics, microbiome). Of note, given the paucity of data, we decided to not consider evidence about the (putative) regulations of mRNAs/proteins by miRNAs.

Tissue and cell type specificity analyses

To test the assumption that genes associated with disease are more likely to be highly expressed in the tissues and cells afflicted by the disease, we performed tissue and cell type specificity analyses.

We used the Tissue Specific Expression Analysis (TSEA, v1.0: Updated 03/03/14) [339] and the Cell Specific Expression Analysis (CSEA) [340,341] web tools to test whether genes preferentially expressed in any given tissue or cell type were enriched in the set of 872 TD genes. For the TSEA, we used the gene expression data for 25 broad human tissue types derived from the Genotype-Tissue Expression (GTEx) project [342] and human brain region- and time-specific gene expression RNA seq data obtained from the BrainSpan Atlas [343]. For the CSEA, we used the mouse cell type-specific gene expression profiling experiments that were conducted on a single platform, most using published translating ribosome affinity purification (TRAP) data, as described in [341]. TRAP method estimates a rate of protein synthesis and is a better predictor of actual protein levels than measurements of mRNA levels [344]. The specificity of expression was represented as a specificity index probability (pSI) statistic at thresholds 0.05 to 0.0001, with a smaller value indicating higher specificity. For details on pSI score calculation, we refer to the original publication [339]. We considered genes with pSI statistics smaller than 0.05 as significantly enriched in the tissue or cell type.

The overlap between TD genes and the genes enriched in each tissue or cell type was estimated using Fisher's exact test followed by false discovery rate (FDR) correction with Benjamini–Hochberg method. The significance threshold was defined as FDR P < 0.05.

We additionally applied CSEA to the results of differential expression analysis of postmortem transcriptome data from the striatum of TD patients [60] to investigate which cell types are particularly affected by the lifelong TD. These analyses were performed separately for down-and up-regulated genes from combined analysis of caudate and putamen, as well as for the top modules from the weighted gene co-expression network analysis (WGCNA) that were most significantly enriched for down- and up-regulated genes. Such joint analyses can further improve the power to detect cellular composition alterations from transcriptomic data [70].

Functional enrichment analyses

We used Ingenuity Pathway Analysis (IPA) software (QIAGEN, Hilden, Germany) to identify canonical pathways, diseases and functions, and upstream regulators that were enriched in the set of 872 TD candidate genes. The significance of the association between our dataset and the given pathway, disease/function, and upstream regulator was measured using the right-tailed Fisher's Exact Test, followed by false discovery rate (FDR) calculation using the Benjamini-Hochberg method to correct for multiple-testing. A threshold of FDR p-value < 0.05 ($-\log$ (FDR p-value) > 1.3) was used to designate statistically significant findings, while results with unadjusted p-value < 0.01 are reported as suggestive associations. For statistical calculations, all genes associated with pathways, functions, and regulators in the Ingenuity Knowledge Base (IKB) were used as the reference set.

Canonical pathways are well-characterized metabolic and cell signaling cascades derived from the literature and public and third-party databases compiled in the IKB. For canonical pathways, apart from the p-value of overlap, a ratio indicating the strength of the association is also provided (the number of genes from the dataset that map to the pathway divided by the total number of genes that map to the canonical pathway). Pathways with high ratios and low p-values may be the most likely candidates for an explanation of the observed phenotype.

In the diseases and functions analysis, IPA identifies diseases and biological processes associated with the dataset based on the prior knowledge of expected causal effects between genes/proteins and the diseases/functions contained in the IKB. We report results organized in the three main categories: 'Diseases and Disorders', 'Molecular and Cellular Functions', and 'Physiological System Development and Function', along with the FDR p-value of overlap and (number of) molecules associated with each function.

Upstream regulator analysis identifies 'upstream regulators' – molecules that may control the expression of target genes in our dataset, based on the expected causal effects derived from the literature. We report upstream regulators classified into two main groups: 'Drugs and Chemicals' and 'Genes, RNAs and Proteins'.

Molecular landscape of TD

First, we filtered the TD candidate genes (see above) based on the number of lines of supporting evidence, prioritizing genes that (a) are present in at least two independent main genetic lists (studies/analyses) or where a genetic finding had corroborating evidence in epigenetic or transcriptomic studies (requiring evidence from two independent blood studies or one brain study), (b) genes that are expressed in brain (tissues) based on the data in HPA, and (c) genes that are protein-coding. This step resulted in the list of TD 'prioritized' candidate genes and their encoded proteins that we focused on for building the landscape, with the remaining genes/proteins from the candidate list – for which less omics evidence was available – only being used in a second stage (see below).

Second, we filtered the metabolites linked to TD through the PRS-based analyses and/or (other metabolome/microbiome studies), based on the strength of the supporting (genetic) evidence. We included HMDB-annotated metabolites implicated through PRS-based analyses with (a) a Bonferroni-adjusted p-value < 0.05, (b) an FDR p-value < 0.01, if they were also implicated through other metabolome/microbiome studies, or (c) an FDR p-value < 0.05, if they were replicated in PRS-based analyses and implicated through metabolome/microbiome studies. We also included metabolites linked through PRS-based analyses (FDR p-value < 0.05) or metabolome/microbiome studies if they could be directly linked to a TD-associated protein through a functional or metabolic interaction (e.g., the TD-associated protein is a transporter or receptor for the metabolite).

Subsequently, to build the actual molecular landscape of TD, we applied an approach that was used previously for other neuropsychiatric diseases [16,345]. The UniProt Protein Knowledge Base (http://www.uniprot.org) [326] was used to gather basic information on the function(s) and subcellular localization(s) of all the landscape candidate genes/proteins. We also used PubMed (http://www.ncbi.nlm.nih.gov) to identify the functional, experimental evidence-based interactions between the landscape candidate proteins. This included assembling protein-protein interactions (PPIs) and protein-metabolite interactions data from several literature-curated resources that contain high-quality interactions with experimental evidence. These included primary and secondary databases, such as the Ingenuity Knowledge Base available in IPA, OmniPath [346], The Human Reference Interactome (HuRI) [347] (http://www.interactome-atlas.org), High-quality INTeractomes

(HINT) [348] (http://hint.yulab.org/), and The Integrated Interactions Database (IID) [349] (http://iid.ophid.utoronto.ca). These protein-protein interaction resources differ in the number and types of relationships they capture, e.g., physical binary interactions, enzymatic reactions, or functional relationships, and taken together, the resources provide good coverage of the protein interactome. From this interactome data, we then selected the interactions between the proteins encoded by the prioritized TD candidate genes (see above) as well as – and in a second stage – between proteins encoded by prioritized TD candidate genes and proteins encoded by other genes from the list of candidate genes for which less omics evidence was available, proteins/genes implicated in TD through transcriptomics data and/or other functional evidence, as well as the metabolites emerging from our PRS-based analyses.

Furthermore, we annotated interacting proteins with their contextual information, including cell expression from HPA and subcellular localization from UniProtKb. Biological processes carried out by interacting proteins are separated in the cellular and subcellular space, which helps their precise regulation [350]. Therefore, we (also) curated assembled interactome data to retain interactions that are biologically likely to occur in a given (sub) cellular location. For example, if in a binary interaction both proteins did not share the same localization or at least one compartment in multiple localized proteins, the interaction was ruled out as likely not occurring, an approach that has been used before [351]. Furthermore, all self-interactions were removed and not considered for the landscape. In addition, we determined the most likely cell type for each interaction based on the expression profiles contained in the HPA and the results of our cell type specificity analyses.

Lastly, we used the program Serif DrawPlus version 4.0 (www.serif.com, Nottingham, UK) to draw the figure depicting the molecular landscape of TD. We tried to avoid repetitive drawing of a protein or protein-protein interactions as much as possible. If multiple locations of a protein-protein interaction were possible, functional interaction and/or expression data or other protein-protein interactions were used to identify the (most) appropriate location.

Selection of putative drug targets from the built molecular landscape of TD

After building the molecular landscape, we selected some putative drug targets based on four broad aspects of target specificity. First, a good drug target should be highly expressed in the (brain) tissues and cell types that are affected in the disease [352,353] (in this case TD) – and preferably differentially expressed in comparison with healthy controls – constituting the regional specificity of the target. To evaluate this aspect of target specificity, we analysed the available postmortem brain data, although the differential expression of

the genes/proteins in these data may cause TD or represent a consequence of TD (including compensatory mechanisms). Linked to the regional specificity, putative drug targets should also be temporally associated with the onset and/or progression of TD. To assess this temporal specificity, we again looked at the available data, including transcriptional data during striatal development [247] – which correspond to different stages of brain development and function that in turn could be linked to TD symptom occurrence, peak and resolution – and temporal gene expression data in (normal) brain tissue [343] and the blood of TD patients [62]. A third aspect of an ideal drug target for TD – that is linked to the molecular landscape – is its molecular specificity, i.e., whether it is involved in (multiple) biological processes and protein interactions in the landscape. Lastly, a suitable drug target needs to have sufficient modulatory specificity, in that it should be inherently druggable [338] and modulating the target in a certain direction – e.g., because disease-associated variants are eQTLs that (up-or down) regulate the expression of the target [354], which is especially the case for essential genes that are relatively depleted for eQTLs [355] – has a (putative) beneficial aspect on TD (symptoms).

CONCLUSIONS

In conclusion, through integrating the results from multiple analyses of TD-linked genes derived from different types of omics data with an extensive literature search, we built a molecular landscape of TD. This landscape provides insights into the altered subcellular, molecular, and metabolic pathways and processes that are underlying the disease, including cAMP signaling, endocannabinoid signaling, multiple metabolic pathways – e.g., involving polyunsaturated fatty acids such as arachidonic acid, butyrate, NAAG, and myo-inositol – and synaptic functioning. Importantly, the landscape also yields clues towards potential drug targets (FLT3, NAALAD2, CX3CL1-CX3CR1, OPRM1, and HRH2) that can be further developed into TD treatments.

Author Contributions

Conceptualization, J.W. and G.P.; Methodology, J.W., W.D.W., G.P.; Investigation, J.W., W.D.W., G.P.; Data curation, J.W.; Writing—original draft preparation, J.W., G.P.; Writing—review and editing, J.W., W.D.W., J.K.B, J.C.G. G.P.; Visualization, J.W., W.D.W., G.P.; Supervision, G.P.; Funding acquisition, J.K.B., J.C.G., G.P. All authors have read and agreed to the published version of the manuscript.

Funding

Conflicts of Interest

G.P. is director and J.W. as well as W.D.W. are employees of Drug Target ID, Ltd., but their activities at this company do not constitute competing interests with regard to this paper. In the past 3 years, J.K.B. has been a consultant to / member of advisory board of / and/or speaker for Takeda, Roche, Medice, Angelini, Janssen, Boehringer-Ingelheim, and Servier. He is not an employee of any of these companies, and not a stock shareholder of any of these companies. He has no other financial or material support, including expert testimony, patents, royalties. J.C.G. does not report any conflicts of interest. In addition, the funders had no role in the design of the study, in the collection, analyses, or interpretation of data, in the writing of the manuscript, or in the decision to publish the results.

REFERENCES

1. Robertson, M.M.; Eapen, V.; Singer, H.S.; Martino, D.; Scharf, J.M.; Paschou, P.; Roessner, V.; Woods, D.W.; Hariz, M.; Mathews, C.A.; et al. Gilles de la Tourette syndrome. *Nat Rev Dis Primers* **2017**, *3*, 16097, doi:10.1038/nrdp.2016.97.

2. Martino, D.; Ganos, C.; Pringsheim, T.M. Chapter Fifty-Three - Tourette Syndrome and Chronic Tic Disorders: The Clinical Spectrum Beyond Tics. In *International Review of Neurobiology*, Chaudhuri, K.R., Titova, N., Eds.; Academic Press: 2017; Volume 134, pp. 1461-1490.

3. Mataix-Cols, D.; Isomura, K.; Pérez-Vigil, A.; Chang, Z.; Rück, C.; Larsson, K.J.; Leckman, J.F.; Serlachius, E.; Larsson, H.; Lichtenstein, P. Familial Risks of Tourette Syndrome and Chronic Tic Disorders. A Population-Based Cohort Study. *JAMA Psychiatry* **2015**, *72*, 787-793, doi:10.1001/jamapsychiatry.2015.0627.

4. Sun, N.; Tischfield, J.A.; King, R.A.; Heiman, G.A. Functional Evaluations of Genes Disrupted in Patients with Tourette's Disorder. *Front Psychiatry* **2016**, *7*, 11, doi:10.3389/fpsyt.2016.00011.

5. Tsetsos, F.; Yu, D.; Sul, J.H.; Huang, A.Y.; Illmann, C.; Osiecki, L.; Darrow, S.M.; Hirschtritt, M.E.; Greenberg, E.; Muller-Vahl, K.R.; et al. Synaptic processes and immune-related pathways implicated in Tourette syndrome. *Transl Psychiatry* **2021**, *11*, 56, doi:10.1038/s41398-020-01082-z.

6. Mathews, C.A.; Scharf, J.M.; Miller, L.L.; Macdonald-Wallis, C.; Lawlor, D.A.; Ben-Shlomo, Y. Association between pre- and perinatal exposures and Tourette syndrome or chronic tic disorder in the ALSPAC cohort. *Br J Psychiatry* **2014**, *204*, 40-45, doi:10.1192/bjp.bp.112.125468.

7. Tagwerker Gloor, F.; Walitza, S. Tic Disorders and Tourette Syndrome: Current Concepts of Etiology and Treatment in Children and Adolescents. *Neuropediatrics* **2016**, *47*, 84-96, doi:10.1055/s-0035-1570492.

8. Harris, K.; Singer, H.S. Tic disorders: neural circuits, neurochemistry, and neuroimmunology. *J Child Neurol* **2006**, *21*, 678-689, doi:10.1177/08830738060210080901.

9. King, E.A.; Davis, J.W.; Degner, J.F. Are drug targets with genetic support twice as likely to be approved? Revised estimates of the impact of genetic support for drug mechanisms on the probability of drug approval. *PLoS Genet* **2019**, *15*, e1008489, doi:10.1371/journal.pgen.1008489.

10. Nelson, M.R.; Tipney, H.; Painter, J.L.; Shen, J.; Nicoletti, P.; Shen, Y.; Floratos, A.; Sham, P.C.; Li, M.J.; Wang, J.; et al. The support of human genetic evidence for approved drug indications. *Nat Genet* **2015**, *47*, 856-860, doi:10.1038/ng.3314.

11. Johnson, E.C.; Border, R.; Melroy-Greif, W.E.; de Leeuw, C.A.; Ehringer, M.A.; Keller, M.C. No Evidence That Schizophrenia Candidate Genes Are More Associated With Schizophrenia Than Noncandidate Genes. *Biol Psychiatry* **2017**, *82*, 702-708, doi:10.1016/j.biopsych.2017.06.033.

12. Farrell, M.S.; Werge, T.; Sklar, P.; Owen, M.J.; Ophoff, R.A.; O'Donovan, M.C.; Corvin, A.; Cichon, S.; Sullivan, P.F. Evaluating historical candidate genes for schizophrenia. *Mol Psychiatry* **2015**, *20*, 555-562, doi:10.1038/mp.2015.16.

13. Poelmans, G.; Pauls, D.L.; Buitelaar, J.K.; Franke, B. Integrated genome-wide association study findings: identification of a neurodevelopmental network for attention deficit hyperactivity disorder. *Am J Psychiatry* **2011**, *168*, 365-377, doi:10.1176/appi.ajp.2010.10070948.

14. Poelmans, G.; Franke, B.; Pauls, D.L.; Glennon, J.C.; Buitelaar, J.K. AKAPs integrate genetic findings for autism spectrum disorders. *Transl Psychiatry* **2013**, *3*, e270, doi:10.1038/tp.2013.48.

15. van de Vondervoort, I.; Poelmans, G.; Aschrafi, A.; Pauls, D.L.; Buitelaar, J.K.; Glennon, J.C.; Franke, B. An integrated molecular landscape implicates the regulation of dendritic spine formation through insulin-related signalling in obsessive-compulsive disorder. *J Psychiatry Neurosci* **2016**, *41*, 280-285, doi:10.1503/jpn.140327.

4

16. Klemann, C.; Martens, G.J.M.; Sharma, M.; Martens, M.B.; Isacson, O.; Gasser, T.; Visser, J.E.; Poelmans, G. Integrated molecular landscape of Parkinson's disease. *NPJ Parkinsons Dis* **2017**, *3*, 14, doi:10.1038/s41531-017-0015-3.

17. Ramautar, R.; Berger, R.; van der Greef, J.; Hankemeier, T. Human metabolomics: strategies to understand biology. *Curr Opin Chem Biol* **2013**, *17*, 841-846, doi:10.1016/j.cbpa.2013.06.015.

18. Hagenbeek, F.A.; Pool, R.; van Dongen, J.; Draisma, H.H.M.; Jan Hottenga, J.; Willemsen, G.; Abdellaoui, A.; Fedko, I.O.; den Braber, A.; Visser, P.J.; et al. Heritability estimates for 361 blood metabolites across 40 genome-wide association studies. *Nature Communications* **2020**, *11*, 39, doi:10.1038/s41467-019-13770-6.

19. Shin, S.Y.; Fauman, E.B.; Petersen, A.K.; Krumsiek, J.; Santos, R.; Huang, J.; Arnold, M.; Erte, I.; Forgetta, V.; Yang, T.P.; et al. An atlas of genetic influences on human blood metabolites. *Nat Genet* **2014**, *46*, 543-550, doi:10.1038/ng.2982.

20. Matsumoto, N.; David, D.E.; Johnson, E.W.; Konecki, D.; Burmester, J.K.; Ledbetter, D.H.; Weber, J.L. Breakpoint sequences of an 1;8 translocation in a family with Gilles de la Tourette syndrome. *Eur J Hum Genet* **2000**, *8*, 875-883, doi:10.1038/sj.ejhg.5200549.

21. Petek, E.; Windpassinger, C.; Vincent, J.B.; Cheung, J.; Boright, A.P.; Scherer, S.W.; Kroisel, P.M.; Wagner, K. Disruption of a novel gene (IMMP2L) by a breakpoint in 7q31 associated with Tourette syndrome. *Am J Hum Genet* **2001**, *68*, 848-858, doi:10.1086/319523.

22. Verkerk, A.J.; Mathews, C.A.; Joosse, M.; Eussen, B.H.; Heutink, P.; Oostra, B.A.; Tourette Syndrome Association International Consortium for, G. CNTNAP2 is disrupted in a family with Gilles de la Tourette syndrome and obsessive compulsive disorder. *Genomics* **2003**, *82*, 1-9, doi:10.1016/s0888-7543(03)00097-1.

23. Abelson, J.F.; Kwan, K.Y.; O'Roak, B.J.; Baek, D.Y.; Stillman, A.A.; Morgan, T.M.; Mathews, C.A.; Pauls, D.L.; Rasin, M.R.; Gunel, M.; et al. Sequence variants in SLITRK1 are associated with Tourette's syndrome. *Science* **2005**, *310*, 317-320, doi:10.1126/science.1116502.

24. Breedveld, G.J.; Fabbrini, G.; Oostra, B.A.; Berardelli, A.; Bonifati, V. Tourette disorder spectrum maps to chromosome 14q31.1 in an Italian kindred. *Neurogenetics* **2010**, *11*, 417-423, doi:10.1007/s10048-010-0244-7.

25. Patel, C.; Cooper-Charles, L.; McMullan, D.J.; Walker, J.M.; Davison, V.; Morton, J. Translocation breakpoint at 7q31 associated with tics: further evidence for IMMP2L as a candidate gene for Tourette syndrome. *Eur J Hum Genet* **2011**, *19*, 634-639, doi:10.1038/ejhg.2010.238.

26. Hooper, S.D.; Johansson, A.C.; Tellgren-Roth, C.; Stattin, E.L.; Dahl, N.; Cavelier, L.; Feuk, L. Genome-wide sequencing for the identification of rearrangements associated with Tourette syndrome and obsessive-compulsive disorder. *BMC Med Genet* **2012**, *13*, 123, doi:10.1186/1471-2350-13-123.

27. Bertelsen, B.; Melchior, L.; Jensen, L.R.; Groth, C.; Nazaryan, L.; Debes, N.M.; Skov, L.; Xie, G.; Sun, W.; Brondum-Nielsen, K.; et al. A t(3;9)(q25.1;q34.3) translocation leading to OLFM1 fusion transcripts in Gilles de la Tourette syndrome, OCD and ADHD. *Psychiatry Res* **2015**, *225*, 268-275, doi:10.1016/j.psychres.2014.12.028.

28. Ercan-Sencicek, A.G.; Stillman, A.A.; Ghosh, A.K.; Bilguvar, K.; O'Roak, B.J.; Mason, C.E.; Abbott, T.; Gupta, A.; King, R.A.; Pauls, D.L.; et al. L-histidine decarboxylase and Tourette's syndrome. *N Engl J Med* **2010**, *362*, 1901-1908, doi:10.1056/NEJMoa0907006.

29. Sundaram, S.K.; Huq, A.M.; Sun, Z.; Yu, W.; Bennett, L.; Wilson, B.J.; Behen, M.E.; Chugani, H.T. Exome sequencing of a pedigree with Tourette syndrome or chronic tic disorder. *Ann Neurol* **2011**, *69*, 901-904, doi:10.1002/ana.22398.

30. Eriguchi, Y.; Kuwabara, H.; Inai, A.; Kawakubo, Y.; Nishimura, F.; Kakiuchi, C.; Tochigi, M.; Ohashi, J.; Aoki, N.; Kato, K.; et al. Identification of candidate genes involved in the etiology of sporadic Tourette syndrome by exome sequencing. *Am J Med Genet B Neuropsychiatr Genet* **2017**, *174*, 712-723, doi:10.1002/ajmg.b.32559.

31. Willsey, A.J.; Fernandez, T.V.; Yu, D.; King, R.A.; Dietrich, A.; Xing, J.; Sanders, S.J.; Mandell, J.D.; Huang, A.Y.; Richer, P.; et al. De Novo Coding Variants Are Strongly Associated with Tourette Disorder. *Neuron* **2017**, *94*, 486-499 e489, doi:10.1016/j.neuron.2017.04.024.

32. Sun, N.; Nasello, C.; Deng, L.; Wang, N.; Zhang, Y.; Xu, Z.; Song, Z.; Kwan, K.; King, R.A.; Pang, Z.P.; et al. The PNKD gene is associated with Tourette Disorder or Tic disorder in a multiplex family. *Mol Psychiatry* **2018**, *23*, 1487-1495, doi:10.1038/mp.2017.179.

33. Wang, S.; Mandell, J.D.; Kumar, Y.; Sun, N.; Morris, M.T.; Arbelaez, J.; Nasello, C.; Dong, S.; Duhn, C.; Zhao, X.; et al. De Novo Sequence and Copy Number Variants Are Strongly Associated with Tourette Disorder and Implicate Cell Polarity in Pathogenesis. *Cell Rep* **2018**, *24*, 3441-3454 e3412, doi:10.1016/j.celrep.2018.08.082.

34. Carias, K.V.; Wevrick, R. Clinical and genetic analysis of children with a dual diagnosis of Tourette syndrome and autism spectrum disorder. *J Psychiatr Res* **2019**, *111*, 145-153, doi:10.1016/j.jpsychires.2019.01.023.

35. Depienne, C.; Ciura, S.; Trouillard, O.; Bouteiller, D.; Leitao, E.; Nava, C.; Keren, B.; Marie, Y.; Guegan, J.; Forlani, S.; et al. Association of Rare Genetic Variants in Opioid Receptors with Tourette Syndrome. *Tremor Other Hyperkinet Mov (N Y)* **2019**, *9*, doi:10.7916/tohm.v0.693.

36. Vadgama, N.; Pittman, A.; Simpson, M.; Nirmalananthan, N.; Murray, R.; Yoshikawa, T.; De Rijk, P.; Rees, E.; Kirov, G.; Hughes, D.; et al. De novo single-nucleotide and copy number variation in discordant monozygotic twins reveals disease-related genes. *Eur J Hum Genet* **2019**, *27*, 1121-1133, doi:10.1038/s41431-019-0376-7.

37. Liu, S.; Tian, M.; He, F.; Li, J.; Xie, H.; Liu, W.; Zhang, Y.; Zhang, R.; Yi, M.; Che, F.; et al. Mutations in ASH1L confer susceptibility to Tourette syndrome. *Mol Psychiatry* **2020**, *25*, 476-490, doi:10.1038/s41380-019-0560-8.

38. Yuan, A.; Wang, Z.; Xu, W.; Ding, Q.; Zhao, Y.; Han, J.; Sun, J. A Rare Novel CLCN2 Variation and Risk of Gilles de la Tourette Syndrome: Whole-Exome Sequencing in a Multiplex Family and a Follow-Up Study in a Chinese Population. *Front Psychiatry* **2020**, *11*, 543911, doi:10.3389/fpsyt.2020.543911.

39. Zhao, X.; Wang, S.; Hao, J.; Zhu, P.; Zhang, X.; Wu, M. A Whole-Exome Sequencing Study of Tourette Disorder in a Chinese Population. *DNA Cell Biol* **2020**, *39*, 63-68, doi:10.1089/dna.2019.4746.

40. Cao, X.; Zhang, Y.; Abdulkadir, M.; Deng, L.; Fernandez, T.V.; Garcia-Delgar, B.; Hagstrom, J.; Hoekstra, P.J.; King, R.A.; Koesterich, J.; et al. Whole-exome sequencing identifies genes associated with Tourette's disorder in multiplex families. *Mol Psychiatry* **2021**, *26*, 6937-6951, doi:10.1038/s41380-021-01094-1.

41. Halvorsen, M.; Szatkiewicz, J.; Mudgal, P.; Yu, D.; Psychiatric Genomics Consortium, T.S.O.C.D.W.G.; Nordsletten, A.E.; Mataix-Cols, D.; Mathews, C.A.; Scharf, J.M.; Mattheisen, M.; et al. Elevated common variant genetic risk for tourette syndrome in a densely-affected pedigree. *Mol Psychiatry* **2021**, doi:10.1038/s41380-021-01277-w.

42. Lawson-Yuen, A.; Saldivar, J.S.; Sommer, S.; Picker, J. Familial deletion within NLGN4 associated with autism and Tourette syndrome. *Eur J Hum Genet* **2008**, *16*, 614-618, doi:10.1038/sj.ejhg.5202006.

43. Sundaram, S.K.; Huq, A.M.; Wilson, B.J.; Chugani, H.T. Tourette syndrome is associated with recurrent exonic copy number variants. *Neurology* **2010**, *74*, 1583-1590, doi:10.1212/WNL.0b013e3181e0f147.

44. Fernandez, T.V.; Sanders, S.J.; Yurkiewicz, I.R.; Ercan-Sencicek, A.G.; Kim, Y.S.; Fishman, D.O.; Raubeson, M.J.; Song, Y.; Yasuno, K.; Ho, W.S.; et al. Rare copy number variants in tourette syndrome disrupt genes in histaminergic pathways and overlap with autism. *Biol Psychiatry* **2012**, *71*, 392-402, doi:10.1016/j.biopsych.2011.09.034.

45. Melchior, L.; Bertelsen, B.; Debes, N.M.; Groth, C.; Skov, L.; Mikkelsen, J.D.; Brøndum-Nielsen, K.; Tümer, Z. Microduplication of 15q13.3 and Xq21.31 in a family with Tourette syndrome and comorbidities. *Am J Med Genet B Neuropsychiatr Genet* **2013**, *162b*, 825-831, doi:10.1002/ajmg.b.32186.

46. Nag, A.; Bochukova, E.G.; Kremeyer, B.; Campbell, D.D.; Muller, H.; Valencia-Duarte, A.V.; Cardona, J.; Rivas, I.C.; Mesa, S.C.; Cuartas, M.; et al. CNV analysis in Tourette syndrome implicates large genomic rearrangements in COL8A1 and NRXN1. *PLoS One* **2013**, *8*, e59061, doi:10.1371/journal.pone.0059061.

47. McGrath, L.M.; Yu, D.; Marshall, C.; Davis, L.K.; Thiruvahindrapuram, B.; Li, B.; Cappi, C.; Gerber, G.; Wolf, A.; Schroeder, F.A.; et al. Copy number variation in obsessive-compulsive disorder and tourette syndrome: a cross-disorder study. *J Am Acad Child Adolesc Psychiatry* **2014**, *53*, 910-919, doi:10.1016/j.jaac.2014.04.022.

48. Prontera, P.; Napolioni, V.; Ottaviani, V.; Rogaia, D.; Fusco, C.; Augello, B.; Serino, D.; Parisi, V.; Bernardini, L.; Merla, G.; et al. DPP6 gene disruption in a family with Gilles de la Tourette syndrome. *Neurogenetics* **2014**, *15*, 237-242, doi:10.1007/s10048-014-0418-9.

49. Huang, A.Y.; Yu, D.; Davis, L.K.; Sul, J.H.; Tsetsos, F.; Ramensky, V.; Zelaya, I.; Ramos, E.M.; Osiecki, L.; Chen, J.A.; et al. Rare Copy Number Variants in NRXN1 and CNTN6 Increase Risk for Tourette Syndrome. *Neuron* **2017**, *94*, 1101-1111 e1107, doi:10.1016/j.neuron.2017.06.010.

50. Maccarini, S.; Cipani, A.; Bertini, V.; Skripac, J.; Salvi, A.; Borsani, G.; Marchina, E. Inherited duplication of the pseudoautosomal region Xq28 in a subject with Gilles de la Tourette syndrome and intellectual disability: a case report. *Mol Cytogenet* **2020**, *13*, 23, doi:10.1186/s13039-020-00493-3.

51. Yu, D.; Sul, J.H.; Tsetsos, F.; Nawaz, M.S.; Huang, A.Y.; Zelaya, I.; Illmann, C.; Osiecki, L.; Darrow, S.M.; Hirschtritt, M.E.; et al. Interrogating the Genetic Determinants of Tourette's Syndrome and Other Tic Disorders Through Genome-Wide Association Studies. *Am J Psychiatry* **2019**, *176*, 217-227, doi:10.1176/appi.ajp.2018.18070857.

52. Buniello, A.; MacArthur, J.A.L.; Cerezo, M.; Harris, L.W.; Hayhurst, J.; Malangone, C.; McMahon, A.; Morales, J.; Mountjoy, E.; Sollis, E.; et al. The NHGRI-EBI GWAS Catalog of published genome-wide association studies, targeted arrays and summary statistics 2019. *Nucleic Acids Res* **2019**, *47*, D1005-d1012, doi:10.1093/nar/gky1120.

53. Cross-Disorder Group of the Psychiatric Genomics Consortium. Genomic Relationships, Novel Loci, and Pleiotropic Mechanisms across Eight Psychiatric Disorders. *Cell* **2019**, *179*, 1469-1482 e1411, doi:10.1016/j.cell.2019.11.020.

54. Reay, W.R.; Cairns, M.J. Pairwise common variant meta-analyses of schizophrenia with other psychiatric disorders reveals shared and distinct gene and gene-set associations. *Transl Psychiatry* **2020**, *10*, 134, doi:10.1038/s41398-020-0817-7.

55. Peyrot, W.J.; Price, A.L. Identifying loci with different allele frequencies among cases of eight psychiatric disorders using CC-GWAS. *Nat Genet* **2021**, *53*, 445-454, doi:10.1038/s41588-021-00787-1.

56. Yang, Z.; Wu, H.; Lee, P.H.; Tsetsos, F.; Davis, L.K.; Yu, D.; Lee, S.H.; Dalsgaard, S.; Haavik, J.; Barta, C.; et al. Investigating Shared Genetic Basis Across Tourette Syndrome and Comorbid Neurodevelopmental Disorders Along the Impulsivity-Compulsivity Spectrum. *Biol Psychiatry* **2021**, *90*, 317-327, doi:10.1016/j.biopsych.2020.12.028.

57. Tsetsos, F.; Topaloudi, A.; Jain, P.; Yang, Z.; Yu, D.; Kolovos, P.; Tumer, Z.; Rizzo, R.; Hartmann, A.; Depienne, C.; et al. Genome-wide Association Study identifies two novel loci for Gilles de la Tourette Syndrome. *medRxiv* **2021**, 2021.2012.2011.21267560, doi:10.1101/2021.12.11.21267560.

58. Zilhão, N.R.; Padmanabhuni, S.S.; Pagliaroli, L.; Barta, C.; Smit, D.J.; Cath, D.; Nivard, M.G.; Baselmans, B.M.; van Dongen, J.; Paschou, P.; et al. Epigenome-Wide Association Study of Tic Disorders. *Twin Res Hum Genet* **2015**, *18*, 699-709, doi:10.1017/thg.2015.72.

59. Hildonen, M.; Levy, A.M.; Hansen, C.S.; Bybjerg-Grauholm, J.; Skytthe, A.; Debes, N.M.; Tan, Q.; Tümer, Z. EWAS of Monozygotic Twins Implicate a Role of mTOR Pathway in Pathogenesis of Tic Spectrum Disorder. *Genes (Basel)* **2021**, *12*, doi:10.3390/genes12101510.

60. Lennington, J.B.; Coppola, G.; Kataoka-Sasaki, Y.; Fernandez, T.V.; Palejev, D.; Li, Y.; Huttner, A.; Pletikos, M.; Sestan, N.; Leckman, J.F.; et al. Transcriptome Analysis of the Human Striatum in Tourette Syndrome. *Biol Psychiatry* **2016**, *79*, 372-382, doi:10.1016/j.biopsych.2014.07.018.

61. Lit, L.; Gilbert, D.L.; Walker, W.; Sharp, F.R. A subgroup of Tourette's patients overexpress specific natural killer cell genes in blood: a preliminary report. *Am J Med Genet B Neuropsychiatr Genet* **2007**, *144B*, 958-963, doi:10.1002/ajmg.b.30550.

62. Lit, L.; Enstrom, A.; Sharp, F.R.; Gilbert, D.L. Age-related gene expression in Tourette syndrome. *J Psychiatr Res* **2009**, *43*, 319-330, doi:10.1016/j.jpsychires.2008.03.012.

63. Tian, Y.; Gunther, J.R.; Liao, I.H.; Liu, D.; Ander, B.P.; Stamova, B.S.; Lit, L.; Jickling, G.C.; Xu, H.; Zhan, X.; et al. GABA- and acetylcholine-related gene expression in blood correlate with tic severity and microarray evidence for alternative splicing in Tourette syndrome: a pilot study. *Brain Res* **2011**, *1381*, 228-236, doi:10.1016/j.brainres.2011.01.026.

64. Tian, Y.; Liao, I.H.; Zhan, X.; Gunther, J.R.; Ander, B.P.; Liu, D.; Lit, L.; Jickling, G.C.; Corbett, B.A.; Bos-Veneman, N.G.; et al. Exon expression and alternatively spliced genes in Tourette Syndrome. *Am J Med Genet B Neuropsychiatr Genet* **2011**, *156B*, 72-78, doi:10.1002/ajmg.b.31140.

65. Xi, L.; Zhou, F.; Sha, H.; Zhu, W.; Hu, X.; Ruan, J.; Huang, Y.; Zhang, Y.; Long, H. Potential Plasma Metabolic Biomarkers of Tourette Syndrome Discovery Based on Integrated Non-Targeted and Targeted Metabolomics Screening. *Research Square* **2020**, doi:10.21203/rs.3.rs-126790/v1.

66. Murgia, F.; Gagliano, A.; Tanca, M.G.; Or-Geva, N.; Hendren, A.; Carucci, S.; Pintor, M.; Cera, F.; Cossu, F.; Sotgiu, S.; et al. Metabolomic Characterization of Pediatric Acute-Onset Neuropsychiatric Syndrome (PANS). *Frontiers in Neuroscience* **2021**, *15*, doi:10.3389/fnins.2021.645267.

67. Piras, C.; Pintus, R.; Pruna, D.; Dessì, A.; Atzori, L.; Fanos, V. Pediatric Acute-onset Neuropsychiatric Syndrome and <i>Mycoplasma Pneumoniae</i> Infection: A Case Report Analysis with a Metabolomics Approach. *Current Pediatric Reviews* **2020**, *16*, 183-193, doi: http://dx.doi.org/10.2174/1573396315666191022102925.

68. Xi, W.; Gao, X.; Zhao, H.; Luo, X.; Li, J.; Tan, X.; Wang, L.; Zhao, J.B.; Wang, J.; Yang, G.; et al. Depicting the composition of gut microbiota in children with tic disorders: an exploratory study. *J Child Psychol Psychiatry* **2021**, doi:10.1111/jcpp.13409.

69. Quagliariello, A.; Del Chierico, F.; Russo, A.; Reddel, S.; Conte, G.; Lopetuso, L.R.; Ianiro, G.; Dallapiccola, B.; Cardona, F.; Gasbarrini, A.; et al. Gut Microbiota Profiling and Gut–Brain Crosstalk in Children Affected by Pediatric Acute-Onset Neuropsychiatric Syndrome and Pediatric Autoimmune Neuropsychiatric Disorders Associated With Streptococcal Infections. *Frontiers in Microbiology* **2018**, *9*, doi:10.3389/fmicb.2018.00675.

70. Xu, X.; Nehorai, A.; Dougherty, J. Cell Type Specific Analysis of Human Brain Transcriptome Data to Predict Alterations in Cellular Composition. *Syst Biomed (Austin)* **2013**, *1*, 151-160, doi:10.4161/sysb.25630.

71. Vanderah, T.W.; Gould, D.J. Organization of the Brainstem. In *Nolte's The Human Brain*, Eighth Edition ed.; Elsevier: 2021; pp. 258-284.

72. Ahola-Olli, A.V.; Würtz, P.; Havulinna, A.S.; Aalto, K.; Pitkänen, N.; Lehtimäki, T.; Kähönen, M.; Lyytikäinen, L.P.; Raitoharju, E.; Seppälä, I.; et al. Genome-wide Association Study Identifies 27 Loci Influencing Concentrations of Circulating Cytokines and Growth Factors. *Am J Hum Genet* **2017**, *100*, 40-50, doi:10.1016/j.ajhg.2016.11.007.

73. Draisma, H.H.M.; Pool, R.; Kobl, M.; Jansen, R.; Petersen, A.-K.; Vaarhorst, A.A.M.; Yet, I.; Haller, T.; Demirkan, A.; Esko, T.; et al. Genome-wide association study identifies novel genetic variants contributing to variation in blood metabolite levels. *Nature Communications* **2015**, *6*, 7208, doi:10.1038/ncomms8208.

74. Kettunen, J.; Demirkan, A.; Würtz, P.; Draisma, H.H.; Haller, T.; Rawal, R.; Vaarhorst, A.; Kangas, A.J.; Lyytikäinen, L.P.; Pirinen, M.; et al. Genome-wide study for circulating metabolites identifies 62 loci and reveals novel systemic effects of LPA. *Nat Commun* **2016**, *7*, 11122, doi:10.1038/ncomms11122.

75. Panyard, D.J.; Kim, K.M.; Darst, B.F.; Deming, Y.K.; Zhong, X.; Wu, Y.; Kang, H.; Carlsson, C.M.; Johnson, S.C.; Asthana, S.; et al. Cerebrospinal fluid metabolomics identifies 19 brain-related phenotype associations. *Commun Biol* **2021**, *4*, 63, doi:10.1038/s42003-020-01583-z.

76. Rhee, E.P.; Ho, J.E.; Chen, M.H.; Shen, D.; Cheng, S.; Larson, M.G.; Ghorbani, A.; Shi, X.; Helenius, I.T.; O'Donnell, C.J.; et al. A genome-wide association study of the human metabolome in a community-based cohort. *Cell Metab* **2013**, *18*, 130-143, doi:10.1016/j.cmet.2013.06.013.

77. Aramideh, J.A.; Vidal-Itriago, A.; Morsch, M.; Graeber, M.B. Cytokine Signalling at the Microglial Penta-Partite Synapse. *Int J Mol Sci* **2021**, *22*, doi:10.3390/ijms222413186.

78. Ferrer-Ferrer, M.; Dityatev, A. Shaping Synapses by the Neural Extracellular Matrix. *Front Neuroanat* **2018**, *12*, 40, doi:10.3389/fnana.2018.00040.

79. Krishnaswamy, V.R.; Benbenishty, A.; Blinder, P.; Sagi, I. Demystifying the extracellular matrix and its proteolytic remodeling in the brain: structural and functional insights. *Cell Mol Life Sci* **2019**, *76*, 3229-3248, doi:10.1007/s00018-019-03182-6.

80. De Luca, C.; Colangelo, A.M.; Virtuoso, A.; Alberghina, L.; Papa, M. Neurons, Glia, Extracellular Matrix and Neurovascular Unit: A Systems Biology Approach to the Complexity of Synaptic Plasticity in Health and Disease. *International Journal of Molecular Sciences* **2020**, *21*, 1539.

81. Mulligan, K.A.; Cheyette, B.N. Neurodevelopmental Perspectives on Wnt Signaling in Psychiatry. *Mol Neuropsychiatry* **2017**, *2*, 219-246, doi:10.1159/000453266.

82. Almén, M.S.; Nordström, K.J.; Fredriksson, R.; Schiöth, H.B. Mapping the human membrane proteome: a majority of the human membrane proteins can be classified according to function and evolutionary origin. *BMC Biol* **2009**, *7*, 50, doi:10.1186/1741-7007-7-50.

83. Gerber, K.J.; Squires, K.E.; Hepler, J.R. Roles for Regulator of G Protein Signaling Proteins in Synaptic Signaling and Plasticity. *Mol Pharmacol* **2016**, *89*, 273-286, doi:10.1124/mol.115.102210.

84. Liu, J.; Yang, L.; Li, H.; Cai, Y.; Feng, J.; Hu, Z. Conditional ablation of protein tyrosine phosphatase receptor U in midbrain dopaminergic neurons results in reduced neuronal size. *J Chem Neuroanat* **2022**, *124*, 102135, doi:10.1016/j.jchemneu.2022.102135.

85. Daniels, M.P. The role of agrin in synaptic development, plasticity and signaling in the central nervous system. *Neurochem Int* **2012**, *61*, 848-853, doi:10.1016/j.neuint.2012.02.028.

86. Hilgenberg, L.G.; Su, H.; Gu, H.; O'Dowd, D.K.; Smith, M.A. Alpha3Na+/K+-ATPase is a neuronal receptor for agrin. *Cell* **2006**, *125*, 359-369, doi:10.1016/j.cell.2006.01.052.

87. Xie, X.; Mahmood, S.R.; Gjorgjieva, T.; Percipalle, P. Emerging roles of cytoskeletal proteins in regulating gene expression and genome organization during differentiation. *Nucleus* **2020**, *11*, 53-65, doi:10.1080/19491034.2020.1742066.

88. Herrmann, H.; Strelkov, S.V.; Burkhard, P.; Aebi, U. Intermediate filaments: primary determinants of cell architecture and plasticity. *J Clin Invest* **2009**, *119*, 1772-1783, doi:10.1172/jci38214.

89. Parato, J.; Bartolini, F. The microtubule cytoskeleton at the synapse. *Neurosci Lett* **2021**, *753*, 135850, doi:10.1016/j.neulet.2021.135850.

90. Rapoport, S.I.; Primiani, C.T.; Chen, C.T.; Ahn, K.; Ryan, V.H. Coordinated Expression of Phosphoinositide Metabolic Genes during Development and Aging of Human Dorsolateral Prefrontal Cortex. *PLoS One* **2015**, *10*, e0132675, doi:10.1371/journal.pone.0132675.

91. Posor, Y.; Jang, W.; Haucke, V. Phosphoinositides as membrane organizers. *Nature Reviews Molecular Cell Biology* **2022**, doi:10.1038/s41580-022-00490-x.

92. Parthasarathy, L.K.; Ratnam, L.; Seelan, S.; Tobias, C.; Casanova, M.F.; Parthasarathy, R.N. Mammalian Inositol 3-phosphate Synthase: Its Role in the Biosynthesis of Brain Inositol and its Clinical Use as a Psychoactive Agent. In *Biology of Inositols and Phosphoinositides: Subcellular Biochemistry*, Majumder, A.L., Biswas, B.B., Eds.; Springer US: Boston, MA, 2006; pp. 293-314.

93. Gupta, M.K.; Randhawa, P.K.; Masternak, M.M. Role of BAG5 in Protein Quality Control: Double-Edged Sword? *Front Aging* **2022**, *3*, 844168, doi:10.3389/fragi.2022.844168.

94. Prashad, S.; Gopal, P.P. RNA-binding proteins in neurological development and disease. *RNA Biol* **2021**, *18*, 972-987, doi:10.1080/15476286.2020.1809186.

95. Aibara, S.; Singh, V.; Modelska, A.; Amunts, A. Structural basis of mitochondrial translation. *eLife* **2020**, *9*, e58362, doi:10.7554/eLife.58362.

96. O'Leary, N.A.; Wright, M.W.; Brister, J.R.; Ciufo, S.; Haddad, D.; McVeigh, R.; Rajput, B.; Robbertse, B.; Smith-White, B.; Ako-Adjei, D.; et al. Reference sequence (RefSeq) database at NCBI: current status, taxonomic expansion, and functional annotation. *Nucleic Acids Res* **2016**, *44*, D733-745, doi:10.1093/nar/gkv1189.

97. Nguyen, N.D.; Wang, D. Multiview learning for understanding functional multiomics. *PLoS Comput Biol* **2020**, *16*, e1007677, doi:10.1371/journal.pcbi.1007677.

98. Carulli, D.; Laabs, T.; Geller, H.M.; Fawcett, J.W. Chondroitin sulfate proteoglycans in neural development and regeneration. *Curr Opin Neurobiol* **2005**, *15*, 116-120, doi:10.1016/j.conb.2005.01.014.

99. Ebersole, B.; Petko, J.; Woll, M.; Murakami, S.; Sokolina, K.; Wong, V.; Stagljar, I.; Lüscher, B.; Levenson, R. Effect of C-Terminal S-Palmitoylation on D2 Dopamine Receptor Trafficking and Stability. *PLoS One* **2015**, *10*, e0140661, doi:10.1371/journal.pone.0140661.

100. Beck, M.; Hurt, E. The nuclear pore complex: understanding its function through structural insight. *Nat Rev Mol Cell Biol* **2017**, *18*, 73-89, doi:10.1038/nrm.2016.147.

101. Francette, A.M.; Tripplehorn, S.A.; Arndt, K.M. The Paf1 Complex: A Keystone of Nuclear Regulation Operating at the Interface of Transcription and Chromatin. *J Mol Biol* **2021**, *433*, 166979, doi:10.1016/j.jmb.2021.166979.

102. Sheikh, B.N.; Guhathakurta, S.; Akhtar, A. The non-specific lethal (NSL) complex at the crossroads of transcriptional control and cellular homeostasis. *EMBO Rep* **2019**, *20*, e47630, doi:10.15252/embr.201847630.

103. Colonna, M.; Butovsky, O. Microglia Function in the Central Nervous System During Health and Neurodegeneration. *Annu Rev Immunol* **2017**, *35*, 441-468, doi:10.1146/annurev-immunol-051116-052358.

4

104. Allen, N.J.; Barres, B.A. Glia — more than just brain glue. *Nature* **2009**, *457*, 675-677, doi:10.1038/457675a.

105. Eroglu, C.; Barres, B.A. Regulation of synaptic connectivity by glia. *Nature* **2010**, *468*, 223-231, doi:10.1038/nature09612.

106. Mauch, D.H.; Nägler, K.; Schumacher, S.; Göritz, C.; Müller, E.C.; Otto, A.; Pfrieger, F.W. CNS synaptogenesis promoted by glia-derived cholesterol. *Science* **2001**, *294*, 1354-1357, doi:10.1126/science.294.5545.1354.

107. Dai, Y.B.; Tan, X.J.; Wu, W.F.; Warner, M.; Gustafsson, J. Liver X receptor β protects dopaminergic neurons in a mouse model of Parkinson disease. *Proc Natl Acad Sci U S A* **2012**, *109*, 13112-13117, doi:10.1073/pnas.1210833109.

108. Breschi, A.; Muñoz-Aguirre, M.; Wucher, V.; Davis, C.A.; Garrido-Martín, D.; Djebali, S.; Gillis, J.; Pervouchine, D.D.; Vlasova, A.; Dobin, A.; et al. A limited set of transcriptional programs define major cell types. *Genome research* **2020**, *30*, 1047-1059, doi:10.1101/gr.263186.120.

109. Caligiore, D.; Mannella, F.; Arbib, M.A.; Baldassarre, G. Dysfunctions of the basal ganglia-cerebellar-thalamo-cortical system produce motor tics in Tourette syndrome. *PLOS Computational Biology* **2017**, *13*, e1005395, doi:10.1371/journal.pcbi.1005395.

110. Wan, X.; Zhang, S.; Wang, W.; Su, X.; Li, J.; Yang, X.; Tan, Q.; Yue, Q.; Gong, Q. Gray matter abnormalities in Tourette Syndrome: a meta-analysis of voxel-based morphometry studies. *Transl Psychiatry* **2021**, *11*, 287, doi:10.1038/s41398-021-01394-8.

111. Kreitzer, A.C. Physiology and pharmacology of striatal neurons. *Annu Rev Neurosci* **2009**, *32*, 127-147, doi:10.1146/annurev.neuro.051508.135422.

112. Smith, A.C.W.; Jonkman, S.; Difeliceantonio, A.G.; O'Connor, R.M.; Ghoshal, S.; Romano, M.F.; Everitt, B.J.; Kenny, P.J. Opposing roles for striatonigral and striatopallidal neurons in dorsolateral striatum in consolidating new instrumental actions. *Nature Communications* **2021**, *12*, 5121, doi:10.1038/s41467-021-25460-3.

113. Sun, Z.; Wu, M.; Ren, W. Striatal D2: Where habits and newly learned actions meet. *Learn Behav* **2022**, doi:10.3758/s13420-022-00526-4.

114. Leckman, J.F.; Riddle, M.A. Tourette's Syndrome: When Habit-Forming Systems Form Habits of Their Own? *Neuron* **2000**, *28*, 349-354, doi:10.1016/S0896-6273(00)00114-8.

115. Maia, T.V.; Conceicao, V.A. The Roles of Phasic and Tonic Dopamine in Tic Learning and Expression. *Biol Psychiatry* **2017**, *82*, 401-412, doi:10.1016/j.biopsych.2017.05.025.

116. Delorme, C.; Salvador, A.; Valabrègue, R.; Roze, E.; Palminteri, S.; Vidailhet, M.; de Wit, S.; Robbins, T.; Hartmann, A.; Worbe, Y. Enhanced habit formation in Gilles de la Tourette syndrome. *Brain* **2015**, *139*, 605-615, doi:10.1093/brain/awv307.

117. Shephard, E.; Groom, M.J.; Jackson, G.M. Implicit sequence learning in young people with Tourette syndrome with and without co-occurring attention-deficit/hyperactivity disorder. *Journal of Neuropsychology* **2019**, *13*, 529-549, doi:https://doi.org/10.1111/jnp.12167.

118. Beste, C.; Münchau, A. Tics and Tourette syndrome - surplus of actions rather than disorder? *Movement Disorders* **2018**, *33*, 238-242, doi:https://doi.org/10.1002/mds.27244.

119. Fründt, O.; Woods, D.; Ganos, C. Behavioral therapy for Tourette syndrome and chronic tic disorders. *Neurology: Clinical Practice* **2017**, *7*, 148, doi:10.1212/CPJ.0000000000000348.

120. Petruo, V.; Bodmer, B.; Bluschke, A.; Münchau, A.; Roessner, V.; Beste, C. Comprehensive Behavioral Intervention for Tics reduces perception-action binding during inhibitory control in Gilles de la Tourette syndrome. *Scientific Reports* **2020**, *10*, 1174, doi:10.1038/s41598-020-58269-z.

121. Reynolds, L.M.; Flores, C. Mesocorticolimbic Dopamine Pathways Across Adolescence: Diversity in Development. *Front Neural Circuits* **2021**, *15*, 735625, doi:10.3389/fncir.2021.735625.

122. Lieberman, O.J.; McGuirt, A.F.; Mosharov, E.V.; Pigulevskiy, I.; Hobson, B.D.; Choi, S.; Frier, M.D.; Santini, E.; Borgkvist, A.; Sulzer, D. Dopamine Triggers the Maturation of Striatal Spiny Projection Neuron Excitability during a Critical Period. *Neuron* **2018**, *99*, 540-554.e544, doi: https://doi.org/10.1016/j.neuron.2018.06.044.

123. Haycock, J.W.; Becker, L.; Ang, L.; Furukawa, Y.; Hornykiewicz, O.; Kish, S.J. Marked disparity between age-related changes in dopamine and other presynaptic dopaminergic markers in human striatum. *J Neurochem* **2003**, *87*, 574-585, doi:10.1046/j.1471-4159.2003.02017.x.

124. Minzer, K.; Lee, O.; Hong, J.J.; Singer, H.S. Increased prefrontal D2 protein in Tourette syndrome: a postmortem analysis of frontal cortex and striatum. *Journal of the Neurological Sciences* **2004**, *219*, 55-61, doi:https://doi.org/10.1016/j.jns.2003.12.006.

125. Yoon, D.Y.; Gause, C.D.; Leckman, J.F.; Singer, H.S. Frontal dopaminergic abnormality in Tourette syndrome: A postmortem analysis. *Journal of the Neurological Sciences* **2007**, *255*, 50-56, doi:https://doi.org/10.1016/j.jns.2007.01.069.

126. Wolf, S.S.; Jones, D.W.; Knable, M.B.; Gorey, J.G.; Lee, K.S.; Hyde, T.M.; Coppola, R.; Weinberger, D.R. Tourette syndrome: prediction of phenotypic variation in monozygotic twins by caudate nucleus D2 receptor binding. *Science* **1996**, *273*, 1225-1227, doi:10.1126/science.273.5279.1225.

127. Singer, H.S. Treatment of tics and tourette syndrome. *Curr Treat Options Neurol* **2010**, *12*, 539-561, doi:10.1007/s11940-010-0095-4.

128. Kataoka, Y.; Kalanithi, P.S.; Grantz, H.; Schwartz, M.L.; Saper, C.; Leckman, J.F.; Vaccarino, F.M. Decreased number of parvalbumin and cholinergic interneurons in the striatum of individuals with Tourette syndrome. *J Comp Neurol* **2010**, *518*, 277-291, doi:10.1002/cne.22206.

129. Favier, M.; Janickova, H.; Justo, D.; Kljakic, O.; Runtz, L.; Natsheh, J.Y.; Pascoal, T.A.; Germann, J.; Gallino, D.; Kang, J.I.; et al. Cholinergic dysfunction in the dorsal striatum promotes habit formation and maladaptive eating. *J Clin Invest* **2020**, *130*, 6616-6630, doi:10.1172/jci138532.

130. Aoki, S.; Liu, A.W.; Akamine, Y.; Zucca, A.; Zucca, S.; Wickens, J.R. Cholinergic interneurons in the rat striatum modulate substitution of habits. *European Journal of Neuroscience* **2018**, *47*, 1194-1205, doi:https://doi.org/10.1111/ejn.13820.

131. Gritton, H.J.; Howe, W.M.; Romano, M.F.; DiFeliceantonio, A.G.; Kramer, M.A.; Saligrama, V.; Bucklin, M.E.; Zemel, D.; Han, X. Unique contributions of parvalbumin and cholinergic interneurons in organizing striatal networks during movement. *Nat Neurosci* **2019**, *22*, 586-597, doi:10.1038/s41593-019-0341-3.

132. Quik, M.; Boyd, J.T.; Bordia, T.; Perez, X. Potential Therapeutic Application for Nicotinic Receptor Drugs in Movement Disorders. *Nicotine Tob Res* **2019**, *21*, 357-369, doi:10.1093/ntr/nty063.

133. Schramm, M.; Selinger, Z. Message transmission: receptor controlled adenylate cyclase system. *Science* **1984**, *225*, 1350-1356, doi:10.1126/science.6147897.

134. Taskén, K.; Skålhegg, B.S.; Taskén, K.A.; Solberg, R.; Knutsen, H.K.; Levy, F.O.; Sandberg, M.; Orstavik, S.; Larsen, T.; Johansen, A.K.; et al. Structure, function, and regulation of human cAMP-dependent protein kinases. *Adv Second Messenger Phosphoprotein Res* **1997**, *31*, 191-204, doi:10.1016/s1040-7952(97)80019-5.

135. Singer, H.S.; Hahn, I.H.; Krowiak, E.; Nelson, E.; Moran, T. Tourette's syndrome: a neurochemical analysis of postmortem cortical brain tissue. *Ann Neurol* **1990**, *27*, 443-446, doi:10.1002/ana.410270415.

136. Singer, H.S.; Hahn, I.H.; Moran, T.H. Abnormal dopamine uptake sites in postmortem striatum from patients with Tourette's syndrome. *Ann Neurol* **1991**, *30*, 558-562, doi:10.1002/ana.410300408.

4

137. Korff, S.; Stein, D.J.; Harvey, B.H. Cortico-striatal cyclic AMP-phosphodiesterase-4 signalling and stereotypy in the deer mouse: Attenuation after chronic fluoxetine treatment. *Pharmacology Biochemistry and Behavior* **2009**, *92*, 514-520, doi:https://doi.org/10.1016/j.pbb.2009.01.025.

138. Andersen, S.L. Changes in the second messenger cyclic AMP during development may underlie motoric symptoms in attention deficit/hyperactivity disorder (ADHD). *Behavioural Brain Research* **2002**, *130*, 197-201, doi: https://doi.org/10.1016/S0166-4328(01)00417-X.

139. Vendel, E.; de Lange, E.C. Functions of the CB1 and CB 2 receptors in neuroprotection at the level of the blood-brain barrier. *Neuromolecular Med* **2014**, *16*, 620-642, doi:10.1007/s12017-014-8314-x.

140. Castillo, P.E.; Younts, T.J.; Chávez, A.E.; Hashimotodani, Y. Endocannabinoid signaling and synaptic function. *Neuron* **2012**, *76*, 70-81, doi:10.1016/j.neuron.2012.09.020.

141. Szejko, N.; Fichna, J.P.; Safranow, K.; Dziuba, T.; Żekanowski, C.; Janik, P. Association of a Variant of CNR1 Gene Encoding Cannabinoid Receptor 1 With Gilles de la Tourette Syndrome. *Front Genet* **2020**, *11*, 125, doi:10.3389/fgene.2020.00125.

142. Gadzicki, D.; Müller-Vahl, K.R.; Heller, D.; Ossege, S.; Nöthen, M.M.; Hebebrand, J.; Stuhrmann, M. Tourette syndrome is not caused by mutations in the central cannabinoid receptor (CNR1) gene. *Am J Med Genet B Neuropsychiatr Genet* **2004**, *127b*, 97-103, doi:10.1002/ajmg.b.20159.

143. Müller-Vahl, K.R.; Bindila, L.; Lutz, B.; Musshoff, F.; Skripuletz, T.; Baumgaertel, C.; Sühs, K.W. Cerebrospinal fluid endocannabinoid levels in Gilles de la Tourette syndrome. *Neuropsychopharmacology* **2020**, *45*, 1323-1329, doi:10.1038/s41386-020-0671-6.

144. Watson, S.; Chambers, D.; Hobbs, C.; Doherty, P.; Graham, A. The endocannabinoid receptor, CB1, is required for normal axonal growth and fasciculation. *Mol Cell Neurosci* **2008**, *38*, 89-97, doi:10.1016/j.mcn.2008.02.001.

145. Martella, A.; Sepe, R.M.; Silvestri, C.; Zang, J.; Fasano, G.; Carnevali, O.; De Girolamo, P.; Neuhauss, S.C.; Sordino, P.; Di Marzo, V. Important role of endocannabinoid signaling in the development of functional vision and locomotion in zebrafish. *Faseb j* **2016**, *30*, 4275-4288, doi:10.1096/fj.201600602R.

146. Gianessi, C.A.; Groman, S.M.; Taylor, J.R. The effects of fatty acid amide hydrolase inhibition and monoacylglycerol lipase inhibition on habit formation in mice. *Eur J Neurosci* **2022**, *55*, 922-938, doi:10.1111/ejn.15129.

147. Hilário, M.R.; Clouse, E.; Yin, H.H.; Costa, R.M. Endocannabinoid signaling is critical for habit formation. *Front Integr Neurosci* **2007**, *1*, 6, doi:10.3389/neuro.07.006.2007.

148. Wade, M.R.; Tzavara, E.T.; Nomikos, G.G. Cannabinoids reduce cAMP levels in the striatum of freely moving rats: an in vivo microdialysis study. *Brain Res* **2004**, *1005*, 117-123, doi:10.1016/j.brainres.2004.01.039.

149. Pacheco, M.; Childers, S.R.; Arnold, R.; Casiano, F.; Ward, S.J. Aminoalkylindoles: actions on specific G-protein-linked receptors. *J Pharmacol Exp Ther* **1991**, *257*, 170-183.

150. Glass, M.; Felder, C.C. Concurrent stimulation of cannabinoid CB1 and dopamine D2 receptors augments cAMP accumulation in striatal neurons: evidence for a Gs linkage to the CB1 receptor. *J Neurosci* **1997**, *17*, 5327-5333, doi:10.1523/jneurosci.17-14-05327.1997.

151. Sandyk, R.; Awerbuch, G. Marijuana and Tourette's syndrome. *J Clin Psychopharmacol* **1988**, *8*, 444-445, doi:10.1097/00004714-198812000-00021.

152. Artukoglu, B.B.; Bloch, M.H. The Potential of Cannabinoid-Based Treatments in Tourette Syndrome. *CNS Drugs* **2019**, *33*, 417-430, doi:10.1007/s40263-019-00627-1.

153. Szejko, N.; Saramak, K.; Lombroso, A.; Müller-Vahl, K. Cannabis-based medicine in treatment of patients with Gilles de la Tourette syndrome. *Neurol Neurochir Pol* **2022**, *56*, 28-38, doi:10.5603/PJNNS.a2021.0081.

154. Müller-Vahl, K.R.; Szejko, N.; Verdellen, C.; Roessner, V.; Hoekstra, P.J.; Hartmann, A.; Cath, D.C. European clinical guidelines for Tourette syndrome and other tic disorders: summary statement. *Eur Child Adolesc Psychiatry* **2022**, *31*, 377-382, doi:10.1007/s00787-021-01832-4.

155. Pringsheim, T.; Okun, M.S.; Müller-Vahl, K.; Martino, D.; Jankovic, J.; Cavanna, A.E.; Woods, D.W.; Robinson, M.; Jarvie, E.; Roessner, V.; et al. Practice guideline recommendations summary: Treatment of tics in people with Tourette syndrome and chronic tic disorders. *Neurology* **2019**, *92*, 896-906, doi:10.1212/wnl.0000000000007466.

156. Roessner, V.; Eichele, H.; Stern, J.S.; Skov, L.; Rizzo, R.; Debes, N.M.; Nagy, P.; Cavanna, A.E.; Termine, C.; Ganos, C.; et al. European clinical guidelines for Tourette syndrome and other tic disorders-version 2.0. Part III: pharmacological treatment. *Eur Child Adolesc Psychiatry* **2022**, *31*, 425-441, doi:10.1007/s00787-021-01899-z.

157. Fride, E. The endocannabinoid-CB receptor system: Importance for development and in pediatric disease. *Neuro Endocrinol Lett* **2004**, *25*, 24-30.

158. Hasan, A.; Rothenberger, A.; Münchau, A.; Wobrock, T.; Falkai, P.; Roessner, V. Oral delta 9-tetrahydrocannabinol improved refractory Gilles de la Tourette syndrome in an adolescent by increasing intracortical inhibition: a case report. *J Clin Psychopharmacol* **2010**, *30*, 190-192, doi:10.1097/JCP.0b013e3181d236ec.

159. Szejko, N.; Jakubovski, E.; Fremer, C.; Kunert, K.; Mueller-Vahl, K. Delta-9-tetrahydrocannabinol for the treatment of a child with Tourette syndrome - case report. *European Journal of Medical Case Reports* **2018**, *2*, 39-41, doi:10.24911/ejmcr/2/11.

160. Szejko, N.; Jakubovski, E.; Fremer, C.; Müller-Vahl, K.R. Vaporized Cannabis Is Effective and Well-Tolerated in an Adolescent with Tourette Syndrome. *Medical Cannabis and Cannabinoids* **2019**, *2*, 60-64, doi:10.1159/000496355.

161. Wu, S.W.; Gilbert, D.L. Altered neurophysiologic response to intermittent theta burst stimulation in Tourette syndrome. *Brain Stimul* **2012**, *5*, 315-319, doi:10.1016/j.brs.2011.04.001.

162. Suppa, A.; Belvisi, D.; Bologna, M.; Marsili, L.; Berardelli, I.; Moretti, G.; Pasquini, M.; Fabbrini, G.; Berardelli, A. Abnormal cortical and brain stem plasticity in Gilles de la Tourette syndrome. *Mov Disord* **2011**, *26*, 1703-1710, doi:10.1002/mds.23706.

163. Brandt, V.C.; Niessen, E.; Ganos, C.; Kahl, U.; Bäumer, T.; Münchau, A. Altered synaptic plasticity in Tourette's syndrome and its relationship to motor skill learning. *PLoS One* **2014**, *9*, e98417, doi:10.1371/journal.pone.0098417.

164. Wilcken, D.E.; Wilcken, B.; Dudman, N.P.; Tyrrell, P.A. Homocystinuria--the effects of betaine in the treatment of patients not responsive to pyridoxine. *N Engl J Med* **1983**, *309*, 448-453, doi:10.1056/nejm198308253090802.

165. McKeever, M.P.; Weir, D.G.; Molloy, A.; Scott, J.M. Betaine-homocysteine methyltransferase: organ distribution in man, pig and rat and subcellular distribution in the rat. *Clin Sci (Lond)* **1991**, *81*, 551-556, doi:10.1042/cs0810551.

166. Mentch, S.J.; Mehrmohamadi, M.; Huang, L.; Liu, X.; Gupta, D.; Mattocks, D.; Gómez Padilla, P.; Ables, G.; Bamman, M.M.; Thalacker-Mercer, A.E.; et al. Histone Methylation Dynamics and Gene Regulation Occur through the Sensing of One-Carbon Metabolism. *Cell Metab* **2015**, *22*, 861-873, doi:10.1016/j.cmet.2015.08.024.

167. Chen, N.C.; Yang, F.; Capecci, L.M.; Gu, Z.; Schafer, A.I.; Durante, W.; Yang, X.F.; Wang, H. Regulation of homocysteine metabolism and methylation in human and mouse tissues. *Faseb j* **2010**, *24*, 2804-2817, doi:10.1096/fj.09-143651.

168. Wang, L.; Alachkar, A.; Sanathara, N.; Belluzzi, J.D.; Wang, Z.; Civelli, O. A Methionine-Induced Animal Model of Schizophrenia: Face and Predictive Validity. *Int J Neuropsychopharmacol* **2015**, *18*, doi:10.1093/ijnp/pyv054.

4

169. Taylor, M. Dietary modification of amphetamine stereotyped behaviour: The action of tryptophan, methionine, and lysine. *Psychopharmacology* **1979**, *61*, 81-83, doi:10.1007/BF00426815.

170. Muller, U.J.; Frick, B.; Winkler, C.; Fuchs, D.; Wenning, G.K.; Poewe, W.; Mueller, J. Homocysteine and serum markers of immune activation in primary dystonia. *Mov Disord* **2005**, *20*, 1663-1667, doi:10.1002/mds.20667.

171. Müller, T.; Woitalla, D.; Hunsdiek, A.; Kuhn, W. Elevated plasma levels of homocysteine in dystonia. *Acta Neurol Scand* **2000**, *101*, 388-390, doi:10.1034/j.1600-0404.2000.90339.x.

172. Ueland, P.M.; Ulvik, A.; Rios-Avila, L.; Midttun, Ø.; Gregory, J.F. Direct and Functional Biomarkers of Vitamin B6 Status. *Annu Rev Nutr* **2015**, *35*, 33-70, doi:10.1146/annurev-nutr-071714-034330.

173. Garcia-Lopez, R.; Perea-Milla, E.; Garcia, C.R.; Rivas-Ruiz, F.; Romero-Gonzalez, J.; Moreno, J.L.; Faus, V.; Aguas Gdel, C.; Diaz, J.C. New therapeutic approach to Tourette Syndrome in children based on a randomized placebo-controlled double-blind phase IV study of the effectiveness and safety of magnesium and vitamin B6. *Trials* **2009**, *10*, 16, doi:10.1186/1745-6215-10-16.

174. García-López, R.; Romero-González, J.; Perea-Milla, E.; Ruiz-García, C.; Rivas-Ruiz, F.; de Las Mulas Béjar, M. [An open study evaluating the efficacy and security of magnesium and vitamin B(6) as a treatment of Tourette syndrome in children]. *Med Clin (Barc)* **2008**, *131*, 689-691, doi:10.1157/13129113.

175. Mauri, D.N.; Ebner, R.; Montgomery, R.I.; Kochel, K.D.; Cheung, T.C.; Yu, G.L.; Ruben, S.; Murphy, M.; Eisenberg, R.J.; Cohen, G.H.; et al. LIGHT, a new member of the TNF superfamily, and lymphotoxin alpha are ligands for herpesvirus entry mediator. *Immunity* **1998**, *8*, 21-30, doi:10.1016/s1074-7613(00)80455-0.

176. Garcia-Delgar, B.; Morer, A.; Luber, M.J.; Coffey, B.J. Obsessive-Compulsive Disorder, Tics, and Autoinflammatory Diseases: Beyond PANDAS. *J Child Adolesc Psychopharmacol* **2016**, *26*, 847-850, doi:10.1089/cap.2016.29118.bjc.

177. Kratz, A.; Campos-Neto, A.; Hanson, M.S.; Ruddle, N.H. Chronic inflammation caused by lymphotoxin is lymphoid neogenesis. *J Exp Med* **1996**, *183*, 1461-1472, doi:10.1084/jem.183.4.1461.

178. Gommerman, J.L.; Browning, J.L. Lymphotoxin/LIGHT, lymphoid microenvironments and autoimmune disease. *Nature Reviews Immunology* **2003**, *3*, 642-655, doi:10.1038/nri1151.

179. Ying, X.; Chan, K.; Shenoy, P.; Hill, M.; Ruddle, N.H. Lymphotoxin plays a crucial role in the development and function of nasal-associated lymphoid tissue through regulation of chemokines and peripheral node addressin. *Am J Pathol* **2005**, *166*, 135-146, doi:10.1016/s0002-9440(10)62239-0.

180. Park, H.S.; Francis, K.P.; Yu, J.; Cleary, P.P. Membranous cells in nasal-associated lymphoid tissue: a portal of entry for the respiratory mucosal pathogen group A streptococcus. *J Immunol* **2003**, *171*, 2532-2537, doi:10.4049/jimmunol.171.5.2532.

181. Dileepan, T.; Smith, E.D.; Knowland, D.; Hsu, M.; Platt, M.; Bittner-Eddy, P.; Cohen, B.; Southern, P.; Latimer, E.; Harley, E.; et al. Group A Streptococcus intranasal infection promotes CNS infiltration by streptococcal-specific Th17 cells. *J Clin Invest* **2016**, *126*, 303-317, doi:10.1172/jci80792.

182. Hutanu, A.; Reddy, L.N.; Mathew, J.; Avanthika, C.; Jhaveri, S.; Tummala, N. Pediatric Autoimmune Neuropsychiatric Disorders Associated With Group A Streptococci: Etiopathology and Diagnostic Challenges. *Cureus* **2022**, *14*, e27729, doi:10.7759/cureus.27729.

183. Kim, S.W.; Grant, J.E.; Kim, S.I.; Swanson, T.A.; Bernstein, G.A.; Jaszcz, W.B.; Williams, K.A.; Schlievert, P.M. A possible association of recurrent streptococcal infections and acute onset of obsessive-compulsive disorder. *J Neuropsychiatry Clin Neurosci* **2004**, *16*, 252-260, doi:10.1176/jnp.16.3.252.

184. Spaulding, A.R.; Salgado-Pabón, W.; Kohler, P.L.; Horswill, A.R.; Leung, D.Y.; Schlievert, P.M. Staphylococcal and streptococcal superantigen exotoxins. *Clinical microbiology reviews* **2013**, *26*, 422-447.

185. Schlüter, D.; Kwok, L.Y.; Lütjen, S.; Soltek, S.; Hoffmann, S.; Körner, H.; Deckert, M. Both lymphotoxin-alpha and TNF are crucial for control of Toxoplasma gondii in the central nervous system. *J Immunol* **2003**, *170*, 6172-6182, doi:10.4049/jimmunol.170.12.6172.

186. Krause, D.; Matz, J.; Weidinger, E.; Wagner, J.; Wildenauer, A.; Obermeier, M.; Riedel, M.; Müller, N. Association between intracellular infectious agents and Tourette's syndrome. *Eur Arch Psychiatry Clin Neurosci* **2010**, *260*, 359-363, doi:10.1007/s00406-009-0084-3.

187. Akaltun, İ.; Kara, T.; Sertan Kara, S.; Ayaydın, H. Seroprevalance Anti-Toxoplasma gondii antibodies in children and adolescents with tourette syndrome/chronic motor or vocal tic disorder: A case-control study. *Psychiatry Res* **2018**, *263*, 154-157, doi:10.1016/j.psychres.2018.03.020.

188. Croze, M.L.; Soulage, C.O. Potential role and therapeutic interests of myo-inositol in metabolic diseases. *Biochimie* **2013**, *95*, 1811-1827, doi:10.1016/j.biochi.2013.05.011.

189. Fisher, S.K.; Novak, J.E.; Agranoff, B.W. Inositol and higher inositol phosphates in neural tissues: homeostasis, metabolism and functional significance. *Journal of Neurochemistry* **2002**, *82*, 736-754, doi:https://doi.org/10.1046/j.1471-4159.2002.01041.x.

190. Devito, T.J.; Drost, D.J.; Pavlosky, W.; Neufeld, R.W.J.; Rajakumar, N.; McKinlay, B.D.; Williamson, P.C.; Nicolson, R.O.B. Brain Magnetic Resonance Spectroscopy in Tourette's Disorder. *Journal of the American Academy of Child & Adolescent Psychiatry* **2005**, *44*, 1301-1308, doi:10.1097/01. chi.0000181046.52078.f4.

191. Cryns, K.; Shamir, A.; Van Acker, N.; Levi, I.; Daneels, G.; Goris, I.; Bouwknecht, J.A.; Andries, L.; Kass, S.; Agam, G.; et al. IMPA1 is essential for embryonic development and lithium-like pilocarpine sensitivity. *Neuropsychopharmacology* **2008**, *33*, 674-684, doi:10.1038/sj.npp.1301431.

192. Lauritzen, L.; Hansen, H.S.; Jørgensen, M.H.; Michaelsen, K.F. The essentiality of long chain n-3 fatty acids in relation to development and function of the brain and retina. *Prog Lipid Res* **2001**, *40*, 1-94, doi:10.1016/s0163-7827(00)00017-5.

193. Carta, G.; Murru, E.; Banni, S.; Manca, C. Palmitic Acid: Physiological Role, Metabolism and Nutritional Implications. *Front Physiol* **2017**, *8*, 902, doi:10.3389/fphys.2017.00902.

194. Nishizaki, T.; Nomura, T.; Matsuoka, T.; Tsujishita, Y. Arachidonic acid as a messenger for the expression of long-term potentiation. *Biochemical and biophysical research communications* **1999**, *254*, 446-449.

195. Wang, B.; Wu, L.; Chen, J.; Dong, L.; Chen, C.; Wen, Z.; Hu, J.; Fleming, I.; Wang, D.W. Metabolism pathways of arachidonic acids: mechanisms and potential therapeutic targets. *Signal Transduction and Targeted Therapy* **2021**, *6*, 94, doi:10.1038/s41392-020-00443-w.

196. Zhu, J.; Li, L.; Ding, J.; Huang, J.; Shao, A.; Tang, B. The Role of Formyl Peptide Receptors in Neurological Diseases via Regulating Inflammation. *Front Cell Neurosci* **2021**, *15*, 753832, doi:10.3389/fncel.2021.753832.

197. Pamplona, F.A.; Ferreira, J.; Menezes de Lima, O., Jr.; Duarte, F.S.; Bento, A.F.; Forner, S.; Villarinho, J.G.; Bellocchio, L.; Wotjak, C.T.; Lerner, R.; et al. Anti-inflammatory lipoxin A4 is an endogenous allosteric enhancer of CB1 cannabinoid receptor. *Proc Natl Acad Sci U S A* **2012**, *109*, 21134-21139, doi:10.1073/pnas.1202906109.

198. Lands, W.E.; Libelt, B.; Morris, A.; Kramer, N.C.; Prewitt, T.E.; Bowen, P.; Schmeisser, D.; Davidson, M.H.; Burns, J.H. Maintenance of lower proportions of (n - 6) eicosanoid precursors in phospholipids of human plasma in response to added dietary (n - 3) fatty acids. *Biochim Biophys Acta* **1992**, *1180*, 147-162, doi:10.1016/0925-4439(92)90063-s.

4

199. Rudkowska, I.; Paradis, A.M.; Thifault, E.; Julien, P.; Tchernof, A.; Couture, P.; Lemieux, S.; Barbier, O.; Vohl, M.C. Transcriptomic and metabolomic signatures of an n-3 polyunsaturated fatty acids supplementation in a normolipidemic/normocholesterolemic Caucasian population. *J Nutr Biochem* **2013**, *24*, 54-61, doi:10.1016/j.jnutbio.2012.01.016.

200. Gabbay, V.; Babb, J.S.; Klein, R.G.; Panzer, A.M.; Katz, Y.; Alonso, C.M.; Petkova, E.; Wang, J.; Coffey, B.J. A double-blind, placebo-controlled trial of ω-3 fatty acids in Tourette's disorder. *Pediatrics* **2012**, *129*, e1493-1500, doi:10.1542/peds.2011-3384.

201. Louis, P.; Flint, H.J. Diversity, metabolism and microbial ecology of butyrate-producing bacteria from the human large intestine. *FEMS Microbiol Lett* **2009**, *294*, 1-8, doi:10.1111/j.1574-6968.2009.01514.x.

202. Louis, P.; Flint, H.J. Formation of propionate and butyrate by the human colonic microbiota. *Environmental Microbiology* **2017**, *19*, 29-41, doi: https://doi.org/10.1111/1462-2920.13589.

203. Flint, H.J.; Scott, K.P.; Duncan, S.H.; Louis, P.; Forano, E. Microbial degradation of complex carbohydrates in the gut. *Gut Microbes* **2012**, *3*, 289-306, doi:10.4161/gmic.19897.

204. Wang, Y.; Xu, H.; Jing, M.; Hu, X.; Wang, J.; Hua, Y. Gut Microbiome Composition Abnormalities Determined Using High-Throughput Sequencing in Children With Tic Disorder. *Front Pediatr* **2022**, *10*, 831944, doi:10.3389/fped.2022.831944.

205. Ni, J.-J.; Xu, Q.; Yan, S.-S.; Han, B.-X.; Zhang, H.; Wei, X.-T.; Feng, G.-J.; Zhao, M.; Pei, Y.-F.; Zhang, L. Gut Microbiota and Psychiatric Disorders: A Two-Sample Mendelian Randomization Study. *Frontiers in microbiology* **2021**, *12*, 737197, doi:10.3389/fmicb.2021.737197.

206. Zhao, H.; Shi, Y.; Luo, X.; Peng, L.; Yang, Y.; Zou, L. The Effect of Fecal Microbiota Transplantation on a Child with Tourette Syndrome. *Case reports in medicine* **2017**, *2017*, 6165239, doi:10.1155/2017/6165239.

207. Vijay, N.; Morris, M.E. Role of monocarboxylate transporters in drug delivery to the brain. *Curr Pharm Des* **2014**, *20*, 1487-1498, doi:10.2174/13816128113199990462.

208. Huuskonen, J.; Suuronen, T.; Nuutinen, T.; Kyrylenko, S.; Salminen, A. Regulation of microglial inflammatory response by sodium butyrate and short-chain fatty acids. *Br J Pharmacol* **2004**, *141*, 874-880, doi:10.1038/sj.bjp.0705682.

209. Candido, E.P.M.; Reeves, R.; Davie, J.R. Sodium butyrate inhibits histone deacetylation in cultured cells. *Cell* **1978**, *14*, 105-113, doi:https://doi.org/10.1016/0092-8674(78)90305-7.

210. Zhang, J.; Zhong, Q. Histone deacetylase inhibitors and cell death. *Cell Mol Life Sci* **2014**, *71*, 3885-3901, doi:10.1007/s00018-014-1656-6.

211. Wang, A.; Si, H.; Liu, D.; Jiang, H. Butyrate activates the cAMP-protein kinase A-cAMP response element-binding protein signaling pathway in Caco-2 cells. *J Nutr* **2012**, *142*, 1-6, doi:10.3945/jn.111.148155.

212. Vijay, A.; Kouraki, A.; Gohir, S.; Turnbull, J.; Kelly, A.; Chapman, V.; Barrett, D.A.; Bulsiewicz, W.J.; Valdes, A.M. The anti-inflammatory effect of bacterial short chain fatty acids is partially mediated by endocannabinoids. *Gut Microbes* **2021**, *13*, 1997559, doi:10.1080/19490976.2021.1997559.

213. Rose, S.; Bennuri, S.C.; Davis, J.E.; Wynne, R.; Slattery, J.C.; Tippett, M.; Delhey, L.; Melnyk, S.; Kahler, S.G.; MacFabe, D.F.; et al. Butyrate enhances mitochondrial function during oxidative stress in cell lines from boys with autism. *Transl Psychiatry* **2018**, *8*, 42, doi:10.1038/s41398-017-0089-z.

214. Kratsman, N.; Getselter, D.; Elliott, E. Sodium butyrate attenuates social behavior deficits and modifies the transcription of inhibitory/excitatory genes in the frontal cortex of an autism model. *Neuropharmacology* **2016**, *102*, 136-145, doi:10.1016/j.neuropharm.2015.11.003.

215. Beal, M.F.; Ferrante, R.J. Experimental therapeutics in transgenic mouse models of Huntington's disease. *Nat Rev Neurosci* **2004**, *5*, 373-384, doi:10.1038/nrn1386.

216. Naia, L.; Cunha-Oliveira, T.; Rodrigues, J.; Rosenstock, T.R.; Oliveira, A.; Ribeiro, M.; Carmo, C.; Oliveira-Sousa, S.I.; Duarte, A.I.; Hayden, M.R.; et al. Histone Deacetylase Inhibitors Protect Against Pyruvate Dehydrogenase Dysfunction in Huntington's Disease. *J Neurosci* **2017**, *37*, 2776-2794, doi:10.1523/jneurosci.2006-14.2016.

217. St Laurent, R.; O'Brien, L.M.; Ahmad, S.T. Sodium butyrate improves locomotor impairment and early mortality in a rotenone-induced Drosophila model of Parkinson's disease. *Neuroscience* **2013**, *246*, 382-390, doi:10.1016/j.neuroscience.2013.04.037.

218. Langley, B.; Gensert, J.M.; Beal, M.F.; Ratan, R.R. Remodeling chromatin and stress resistance in the central nervous system: histone deacetylase inhibitors as novel and broadly effective neuroprotective agents. *Curr Drug Targets CNS Neurol Disord* **2005**, *4*, 41-50, doi:10.2174/1568007053005091.

219. Sharma, S.; Taliyan, R.; Singh, S. Beneficial effects of sodium butyrate in 6-OHDA induced neurotoxicity and behavioral abnormalities: Modulation of histone deacetylase activity. *Behav Brain Res* **2015**, *291*, 306-314, doi:10.1016/j.bbr.2015.05.052.

220. Fischer, A.; Sananbenesi, F.; Wang, X.; Dobbin, M.; Tsai, L.H. Recovery of learning and memory is associated with chromatin remodelling. *Nature* **2007**, *447*, 178-182, doi:10.1038/nature05772.

221. Watson, H.; Mitra, S.; Croden, F.C.; Taylor, M.; Wood, H.M.; Perry, S.L.; Spencer, J.A.; Quirke, P.; Toogood, G.J.; Lawton, C.L.; et al. A randomised trial of the effect of omega-3 polyunsaturated fatty acid supplements on the human intestinal microbiota. *Gut* **2018**, *67*, 1974-1983, doi:10.1136/gutjnl-2017-314968.

222. Li, H.; Dong, J.; Cai, M.; Xu, Z.; Cheng, X.D.; Qin, J.J. Protein degradation technology: a strategic paradigm shift in drug discovery. *J Hematol Oncol* **2021**, *14*, 138, doi:10.1186/s13045-021-01146-7.

223. Jarome, T.J.; Helmstetter, F.J. The ubiquitin-proteasome system as a critical regulator of synaptic plasticity and long-term memory formation. *Neurobiol Learn Mem* **2013**, *105*, 107-116, doi:10.1016/j.nlm.2013.03.009.

224. Whartenby, K.A.; Small, D.; Calabresi, P.A. FLT3 inhibitors for the treatment of autoimmune disease. *Expert Opin Investig Drugs* **2008**, *17*, 1685-1692, doi:10.1517/13543784.17.11.1685.

225. Liao, C.; Vuokila, V.; Catoire, H.; Akçimen, F.; Ross, J.P.; Bourassa, C.V.; Dion, P.A.; Meijer, I.A.; Rouleau, G.A. Transcriptome-wide association study reveals increased neuronal FLT3 expression is associated with Tourette's syndrome. *Commun Biol* **2022**, *5*, 289, doi:10.1038/s42003-022-03231-0.

226. Mataix-Cols, D.; Frans, E.; Pérez-Vigil, A.; Kuja-Halkola, R.; Gromark, C.; Isomura, K.; Fernández de la Cruz, L.; Serlachius, E.; Leckman, J.F.; Crowley, J.J.; et al. A total-population multigenerational family clustering study of autoimmune diseases in obsessive-compulsive disorder and Tourette's/chronic tic disorders. *Mol Psychiatry* **2018**, *23*, 1652-1658, doi:10.1038/mp.2017.215.

227. Fernández de la Cruz, L.; Mataix-Cols, D. General health and mortality in Tourette syndrome and chronic tic disorder: A mini-review. *Neuroscience & Biobehavioral Reviews* **2020**, *119*, 514-520, doi:https://doi.org/10.1016/j.neubiorev.2020.11.005.

228. Tylee, D.S.; Sun, J.; Hess, J.L.; Tahir, M.A.; Sharma, E.; Malik, R.; Worrall, B.B.; Levine, A.J.; Martinson, J.J.; Nejentsev, S.; et al. Genetic correlations among psychiatric and immune-related phenotypes based on genome-wide association data. *Am J Med Genet B Neuropsychiatr Genet* **2018**, *177*, 641-657, doi:10.1002/ajmg.b.32652.

4

229. Tang, X.; Drotar, J.; Li, K.; Clairmont, C.D.; Brumm, A.S.; Sullins, A.J.; Wu, H.; Liu, X.S.; Wang, J.; Gray, N.S.; et al. Pharmacological enhancement of <i>KCC2</i> gene expression exerts therapeutic effects on human Rett syndrome neurons and <i>Mecp2</i> mutant mice. *Science Translational Medicine* **2019**, *11*, eaau0164, doi:doi:10.1126/scitranslmed.aau0164.

230. Rivat, C.; Sar, C.; Mechaly, I.; Leyris, J.P.; Diouloufet, L.; Sonrier, C.; Philipson, Y.; Lucas, O.; Mallié, S.; Jouvenel, A.; et al. Inhibition of neuronal FLT3 receptor tyrosine kinase alleviates peripheral neuropathic pain in mice. *Nat Commun* **2018**, *9*, 1042, doi:10.1038/s41467-018-03496-2.

231. Bzdega, T.; Crowe, S.L.; Ramadan, E.R.; Sciarretta, K.H.; Olszewski, R.T.; Ojeifo, O.A.; Rafalski, V.A.; Wroblewska, B.; Neale, J.H. The cloning and characterization of a second brain enzyme with NAAG peptidase activity. *J Neurochem* **2004**, *89*, 627-635, doi:10.1111/j.1471-4159.2004.02361.x.

232. General Principles and a Phenomenology-Based Approach to Movement Disorders and Inherited Metabolic Disorders. In *Movement Disorders and Inherited Metabolic Disorders: Recognition, Understanding, Improving Outcomes*, Ebrahimi-Fakhari, D., Pearl, P.L., Eds.; Cambridge University Press: Cambridge, 2020; pp. 1-170.

233. Morland, C.; Nordengen, K. N-Acetyl-Aspartyl-Glutamate in Brain Health and Disease. *Int J Mol Sci* **2022**, *23*, doi:10.3390/ijms23031268.

234. Kanaan, A.S.; Gerasch, S.; García-García, I.; Lampe, L.; Pampel, A.; Anwander, A.; Near, J.; Möller, H.E.; Müller-Vahl, K. Pathological glutamatergic neurotransmission in Gilles de la Tourette syndrome. *Brain* **2017**, *140*, 218-234, doi:10.1093/brain/aww285.

235. Naaijen, J.; Forde, N.J.; Lythgoe, D.J.; Akkermans, S.E.; Openneer, T.J.; Dietrich, A.; Zwiers, M.P.; Hoekstra, P.J.; Buitelaar, J.K. Fronto-striatal glutamate in children with Tourette's disorder and attention-deficit/hyperactivity disorder. *Neuroimage Clin* **2017**, *13*, 16-23, doi:10.1016/j.nicl.2016.11.013.

236. Mahone, E.M.; Puts, N.A.; Edden, R.A.E.; Ryan, M.; Singer, H.S. GABA and glutamate in children with Tourette syndrome: A (1)H MR spectroscopy study at 7T. *Psychiatry Res Neuroimaging* **2018**, *273*, 46-53, doi:10.1016/j.pscychresns.2017.12.005.

237. Kang, Y.; Tiziani, S.; Park, G.; Kaul, M.; Paternostro, G. Cellular protection using Flt3 and PI3Kα inhibitors demonstrates multiple mechanisms of oxidative glutamate toxicity. *Nat Commun* **2014**, *5*, 3672, doi:10.1038/ncomms4672.

238. Zhong, C.; Zhao, X.; Van, K.C.; Bzdega, T.; Smyth, A.; Zhou, J.; Kozikowski, A.P.; Jiang, J.; O'Connor, W.T.; Berman, R.F.; et al. NAAG peptidase inhibitor increases dialysate NAAG and reduces glutamate, aspartate and GABA levels in the dorsal hippocampus following fluid percussion injury in the rat. *J Neurochem* **2006**, *97*, 1015-1025, doi:10.1111/j.1471-4159.2006.03786.x.

239. Olszewski, R.T.; Bukhari, N.; Zhou, J.; Kozikowski, A.P.; Wroblewski, J.T.; Shamimi-Noori, S.; Wroblewska, B.; Bzdega, T.; Vicini, S.; Barton, F.B.; et al. NAAG peptidase inhibition reduces locomotor activity and some stereotypes in the PCP model of schizophrenia via group II mGluR. *J Neurochem* **2004**, *89*, 876-885, doi:10.1111/j.1471-4159.2004.02358.x.

240. Olszewski, R.T.; Wegorzewska, M.M.; Monteiro, A.C.; Krolikowski, K.A.; Zhou, J.; Kozikowski, A.P.; Long, K.; Mastropaolo, J.; Deutsch, S.I.; Neale, J.H. Phencyclidine and dizocilpine induced behaviors reduced by N-acetylaspartylglutamate peptidase inhibition via metabotropic glutamate receptors. *Biol Psychiatry* **2008**, *63*, 86-91, doi:10.1016/j.biopsych.2007.04.016.

241. Pawelec, P.; Ziemka-Nalecz, M.; Sypecka, J.; Zalewska, T. The Impact of the CX3CL1/CX3CR1 Axis in Neurological Disorders. *Cells* **2020**, *9*, doi:10.3390/cells9102277.

242. Limatola, C.; Ransohoff, R.M. Modulating neurotoxicity through CX3CL1/CX3CR1 signaling. *Front Cell Neurosci* **2014**, *8*, 229, doi:10.3389/fncel.2014.00229.

243. Zhan, Y.; Paolicelli, R.C.; Sforazzini, F.; Weinhard, L.; Bolasco, G.; Pagani, F.; Vyssotski, A.L.; Bifone, A.; Gozzi, A.; Ragozzino, D.; et al. Deficient neuron-microglia signaling results in impaired functional brain connectivity and social behavior. *Nat Neurosci* **2014**, *17*, 400-406, doi:10.1038/nn.3641.

244. Gunner, G.; Cheadle, L.; Johnson, K.M.; Ayata, P.; Badimon, A.; Mondo, E.; Nagy, M.A.; Liu, L.; Bemiller, S.M.; Kim, K.W.; et al. Sensory lesioning induces microglial synapse elimination via ADAM10 and fractalkine signaling. *Nat Neurosci* **2019**, *22*, 1075-1088, doi:10.1038/s41593-019-0419-y.

245. Garton, K.J.; Gough, P.J.; Blobel, C.P.; Murphy, G.; Greaves, D.R.; Dempsey, P.J.; Raines, E.W. Tumor necrosis factor-alpha-converting enzyme (ADAM17) mediates the cleavage and shedding of fractalkine (CX3CL1). *J Biol Chem* **2001**, *276*, 37993-38001, doi:10.1074/jbc.M106434200.

246. Hundhausen, C.; Misztela, D.; Berkhout, T.A.; Broadway, N.; Saftig, P.; Reiss, K.; Hartmann, D.; Fahrenholz, F.; Postina, R.; Matthews, V.; et al. The disintegrin-like metalloproteinase ADAM10 is involved in constitutive cleavage of CX3CL1 (fractalkine) and regulates CX3CL1-mediated cell-cell adhesion. *Blood* **2003**, *102*, 1186-1195, doi:10.1182/blood-2002-12-3775.

247. Yang, L.; Su, Z.; Wang, Z.; Li, Z.; Shang, Z.; Du, H.; Liu, G.; Qi, D.; Yang, Z.; Xu, Z.; et al. Transcriptional profiling reveals the transcription factor networks regulating the survival of striatal neurons. *Cell Death Dis* **2021**, *12*, 262, doi:10.1038/s41419-021-03552-8.

248. Sheridan, G.K.; Murphy, K.J. Neuron-glia crosstalk in health and disease: fractalkine and CX3CR1 take centre stage. *Open Biol* **2013**, *3*, 130181, doi:10.1098/rsob.130181.

249. Shan, S.; Hong-Min, T.; Yi, F.; Jun-Peng, G.; Yue, F.; Yan-Hong, T.; Yun-Ke, Y.; Wen-Wei, L.; Xiang-Yu, W.; Jun, M.; et al. New evidences for fractalkine/CX3CL1 involved in substantia nigral microglial activation and behavioral changes in a rat model of Parkinson's disease. *Neurobiol Aging* **2011**, *32*, 443-458, doi:10.1016/j.neurobiolaging.2009.03.004.

250. Morganti, J.M.; Nash, K.R.; Grimmig, B.A.; Ranjit, S.; Small, B.; Bickford, P.C.; Gemma, C. The soluble isoform of CX3CL1 is necessary for neuroprotection in a mouse model of Parkinson's disease. *J Neurosci* **2012**, *32*, 14592-14601, doi:10.1523/jneurosci.0539-12.2012.

251. Horiuchi, M.; Smith, L.; Maezawa, I.; Jin, L.W. CX(3)CR1 ablation ameliorates motor and respiratory dysfunctions and improves survival of a Rett syndrome mouse model. *Brain Behav Immun* **2017**, *60*, 106-116, doi:10.1016/j.bbi.2016.02.014.

252. Wang, J.B.; Johnson, P.S.; Persico, A.M.; Hawkins, A.L.; Griffin, C.A.; Uhl, G.R. Human mu opiate receptor. cDNA and genomic clones, pharmacologic characterization and chromosomal assignment. *FEBS Lett* **1994**, *338*, 217-222, doi:10.1016/0014-5793(94)80368-4.

253. Law, P.Y.; Wong, Y.H.; Loh, H.H. Molecular mechanisms and regulation of opioid receptor signaling. *Annu Rev Pharmacol Toxicol* **2000**, *40*, 389-430, doi:10.1146/annurev.pharmtox.40.1.389.

254. Haber, S.N.; Kowall, N.W.; Vonsattel, J.P.; Bird, E.D.; Richardson, E.P., Jr. Gilles de la Tourette's syndrome. A postmortem neuropathological and immunohistochemical study. *J Neurol Sci* **1986**, *75*, 225-241, doi:10.1016/0022-510x(86)90097-3.

255. Leckman, J.F.; Riddle, M.A.; Berrettini, W.H.; Anderson, G.M.; Hardin, M.; Chappell, P.; Bissette, G.; Nemeroff, C.B.; Goodman, W.K.; Cohen, D.J. Elevated CSF dynorphin A [1-8] in Tourette's syndrome. *Life Sci* **1988**, *43*, 2015-2023, doi:10.1016/0024-3205(88)90575-9.

256. Sandyk, R. The effects of naloxone in Tourette's syndrome. *Ann Neurol* **1985**, *18*, 367-368, doi:10.1002/ana.410180322.

257. Sandyk, R. Naloxone withdrawal exacerbates Tourette syndrome. *J Clin Psychopharmacol* **1986**, *6*, 58-59, doi:10.1097/00004714-198602000-00029.

258. Sandyk, R. Naloxone abolishes obsessive-compulsive behavior in Tourette's syndrome. *Int J Neurosci* **1987**, *35*, 93-94, doi:10.3109/00207458708987115.

259. Kurlan, R.; Majumdar, L.; Deeley, C.; Mudholkar, G.S.; Plumb, S.; Como, P.G. A controlled trial of propoxyphene and naltrexone in patients with Tourette's syndrome. *Ann Neurol* **1991**, *30*, 19-23, doi:10.1002/ana.410300105.

260. Emmerson, P.J.; Liu, M.R.; Woods, J.H.; Medzihradsky, F. Binding affinity and selectivity of opioids at mu, delta and kappa receptors in monkey brain membranes. *J Pharmacol Exp Ther* **1994**, *271*, 1630-1637.

261. Chappell, P.B.; Leckman, J.F.; Riddle, M.A.; Anderson, G.M.; Listwack, S.J.; Ort, S.I.; Hardin, M.T.; Scahill, L.D.; Cohen, D.J. Neuroendocrine and behavioral effects of naloxone in Tourette syndrome. *Adv Neurol* **1992**, *58*, 253-262.

262. van Wattum, P.J.; Chappell, P.B.; Zelterman, D.; Scahill, L.D.; Leckman, J.F. Patterns of response to acute naloxone infusion in Tourette's syndrome. *Mov Disord* **2000**, *15*, 1252-1254, doi:10.1002/1531-8257(200011)15:6<1252::aid-mds1030>3.0.co;2-i.

263. Meuldijk, R.; Colon, E.J. Methadone treatment of Tourette's disorder. *Am J Psychiatry* **1992**, *149*, 139-140, doi:10.1176/ajp.149.1.139b.

264. Sarajlija, M.; Raketic, D.; Nesic, N. Heroin Addiction in Serbian Patients With Tourette Syndrome. *J Psychiatr Pract* **2018**, *24*, 424-427, doi:10.1097/pra.0000000000000341.

265. Sandyk, R.; Bamford, C.R. Opioid modulation of gonadotrophin release in Tourette's syndrome. *Int J Neurosci* **1988**, *39*, 233-234, doi:10.3109/00207458808985709.

266. Grossman, A.; Moult, P.J.; Cunnah, D.; Besser, M. Different opioid mechanisms are involved in the modulation of ACTH and gonadotrophin release in man. *Neuroendocrinology* **1986**, *42*, 357-360, doi:10.1159/000124463.

267. Uhlen, M.; Fagerberg, L.; Hallstrom, B.M.; Lindskog, C.; Oksvold, P.; Mardinoglu, A.; Sivertsson, A.; Kampf, C.; Sjostedt, E.; Asplund, A.; et al. Proteomics. Tissue-based map of the human proteome. *Science* **2015**, *347*, 1260419, doi:10.1126/science.1260419.

268. Karagiannidis, I.; Dehning, S.; Sandor, P.; Tarnok, Z.; Rizzo, R.; Wolanczyk, T.; Madruga-Garrido, M.; Hebebrand, J.; Nöthen, M.M.; Lehmkuhl, G.; et al. Support of the histaminergic hypothesis in Tourette syndrome: association of the histamine decarboxylase gene in a large sample of families. *J Med Genet* **2013**, *50*, 760-764, doi:10.1136/jmedgenet-2013-101637.

269. Alexander, J.; Potamianou, H.; Xing, J.; Deng, L.; Karagiannidis, I.; Tsetsos, F.; Drineas, P.; Tarnok, Z.; Rizzo, R.; Wolanczyk, T.; et al. Targeted Re-Sequencing Approach of Candidate Genes Implicates Rare Potentially Functional Variants in Tourette Syndrome Etiology. *Front Neurosci* **2016**, *10*, 428, doi:10.3389/fnins.2016.00428.

270. Cheng, Y.-h.; Zheng, Y.; He, F.; Yang, J.-h.; Li, W.-b.; Wang, M.-l.; Cui, D.-y.; Chen, Y. Detection of Autoantibodies and Increased Concentrations of Interleukins in Plasma from Patients with Tourette's Syndrome. *Journal of Molecular Neuroscience* **2012**, *48*, 219-224, doi:10.1007/s12031-012-9811-8.

271. Yeon, S.-m.; Lee, J.H.; Kang, D.; Bae, H.; Lee, K.Y.; Jin, S.; Kim, J.R.; Jung, Y.W.; Park, T.W. A cytokine study of pediatric Tourette's disorder without obsessive compulsive disorder. *Psychiatry Research* **2017**, *247*, 90-96, doi:https://doi.org/10.1016/j.psychres.2016.11.005.

272. Yoshikawa, T.; Naganuma, F.; Iida, T.; Nakamura, T.; Harada, R.; Mohsen, A.S.; Kasajima, A.; Sasano, H.; Yanai, K. Molecular mechanism of histamine clearance by primary human astrocytes. *Glia* **2013**, *61*, 905-916, doi:10.1002/glia.22484.

273. Baldan, L.C.; Williams, K.A.; Gallezot, J.D.; Pogorelov, V.; Rapanelli, M.; Crowley, M.; Anderson, G.M.; Loring, E.; Gorczyca, R.; Billingslea, E.; et al. Histidine decarboxylase deficiency causes tourette syndrome: parallel findings in humans and mice. *Neuron* **2014**, *81*, 77-90, doi:10.1016/j.neuron.2013.10.052.

274. Dai, H.; Zhang, Z.; Zhu, Y.; Shen, Y.; Hu, W.; Huang, Y.; Luo, J.; Timmerman, H.; Leurs, R.; Chen, Z. Histamine protects against NMDA-induced necrosis in cultured cortical neurons through H2 receptor/cyclic AMP/protein kinase A and H3 receptor/GABA release pathways. *Journal of Neurochemistry* **2006**, *96*, 1390-1400, doi: https://doi.org/10.1111/j.1471-4159.2005.03633.x.

275. Liao, R.-j.; Jiang, L.; Wang, R.-r.; Zhao, H.-w.; Chen, Y.; Li, Y.; Wang, L.; Jie, L.-Y.; Zhou, Y.-d.; Zhang, X.-n.; et al. Histidine provides long-term neuroprotection after cerebral ischemia through promoting astrocyte migration. *Scientific Reports* **2015**, *5*, 15356, doi:10.1038/srep15356.

276. Ito, C.; Onodera, K.; Watanabe, T.; Sato, M. Effects of histamine agents on methamphetamine-induced stereotyped behavior and behavioral sensitization in rats. *Psychopharmacology (Berl)* **1997**, *130*, 362-367, doi:10.1007/s002130050251.

277. Joshi, V.V.; Balsara, J.J.; Jadhav, J.H.; Chandorkar, A.G. Effect of L-histidine and chlorcyclizine on apomorphine-induced climbing behaviour and methamphetamine stereotypy in mice. *Eur J Pharmacol* **1981**, *69*, 499-502, doi:10.1016/0014-2999(81)90456-8.

278. Itoh, Y.; Nishibori, M.; Oishi, R.; Saeki, K. Neuronal histamine inhibits methamphetamine-induced locomotor hyperactivity in mice. *Neurosci Lett* **1984**, *48*, 305-309, doi:10.1016/0304-3940(84)90055-7.

279. Clapham, J.; Kilpatrick, G.J. Thioperamide, the selective histamine H3 receptor antagonist, attenuates stimulant-induced locomotor activity in the mouse. *Eur J Pharmacol* **1994**, *259*, 107-114, doi:10.1016/0014-2999(94)90498-7.

280. Kitanaka, J.; Kitanaka, N.; Tatsuta, T.; Morita, Y.; Takemura, M. Blockade of brain histamine metabolism alters methamphetamine-induced expression pattern of stereotypy in mice via histamine H1 receptors. *Neuroscience* **2007**, *147*, 765-777, doi:10.1016/j.neuroscience.2007.05.006.

281. Kitanaka, J.; Kitanaka, N.; Hall, F.S.; Uhl, G.R.; Tatsuta, T.; Morita, Y.; Tanaka, K.; Nishiyama, N.; Takemura, M. Histamine H3 receptor agonists decrease hypothalamic histamine levels and increase stereotypical biting in mice challenged with methamphetamine. *Neurochem Res* **2011**, *36*, 1824-1833, doi:10.1007/s11064-011-0500-8.

282. Kitanaka, N.; Hall, F.S.; Kobori, S.; Kushihara, S.; Oyama, H.; Sasaoka, Y.; Takechi, M.; Tanaka, K.I.; Tomita, K.; Igarashi, K.; et al. Metoprine, a histamine N-methyltransferase inhibitor, attenuates methamphetamine-induced hyperlocomotion via activation of histaminergic neurotransmission in mice. *Pharmacol Biochem Behav* **2021**, *209*, 173257, doi:10.1016/j.pbb.2021.173257.

283. Moro, J.; Tomé, D.; Schmidely, P.; Demersay, T.C.; Azzout-Marniche, D. Histidine: A Systematic Review on Metabolism and Physiological Effects in Human and Different Animal Species. *Nutrients* **2020**, *12*, doi:10.3390/nu12051414.

284. Yamakami, J.; Sakurai, E.; Sakurada, T.; Maeda, K.; Hikichi, N. Stereoselective blood-brain barrier transport of histidine in rats. *Brain Res* **1998**, *812*, 105-112, doi:10.1016/s0006-8993(98)00958-5.

285. Paternoster, L.; Tilling, K.; Davey Smith, G. Genetic epidemiology and Mendelian randomization for informing disease therapeutics: Conceptual and methodological challenges. *PLoS Genet* **2017**, *13*, e1006944, doi:10.1371/journal.pgen.1006944.

4

286. Ferguson, C.; Araújo, D.; Faulk, L.; Gou, Y.; Hamelers, A.; Huang, Z.; Ide-Smith, M.; Levchenko, M.; Marinos, N.; Nambiar, R.; et al. Europe PMC in 2020. *Nucleic acids research* **2021**, *49*, D1507-D1514, doi:10.1093/nar/gkaa994.

287. Morer, A.; Lázaro, L.; Sabater, L.; Massana, J.; Castro, J.; Graus, F. Antineuronal antibodies in a group of children with obsessive-compulsive disorder and Tourette syndrome. *J Psychiatr Res* **2008**, *42*, 64-68, doi:10.1016/j.jpsychires.2006.09.010.

288. Dupont, C.; Armant, D.R.; Brenner, C.A. Epigenetics: definition, mechanisms and clinical perspective. *Semin Reprod Med* **2009**, *27*, 351-357, doi:10.1055/s-0029-1237423.

289. Sharon, G.; Sampson, T.R.; Geschwind, D.H.; Mazmanian, S.K. The Central Nervous System and the Gut Microbiome. *Cell* **2016**, *167*, 915-932, doi:10.1016/j.cell.2016.10.027.

290. Bulik-Sullivan, B.K.; Loh, P.R.; Finucane, H.K.; Ripke, S.; Yang, J.; Patterson, N.; Daly, M.J.; Price, A.L.; Neale, B.M. LD Score regression distinguishes confounding from polygenicity in genome-wide association studies. *Nat Genet* **2015**, *47*, 291-295, doi:10.1038/ng.3211.

291. de Leeuw, C.A.; Mooij, J.M.; Heskes, T.; Posthuma, D. MAGMA: generalized gene-set analysis of GWAS data. *PLoS computational biology* **2015**, *11*, e1004219, doi:10.1371/journal.pcbi.1004219.

292. Wang, X.; Tucker, N.R.; Rizki, G.; Mills, R.; Krijger, P.H.; de Wit, E.; Subramanian, V.; Bartell, E.; Nguyen, X.X.; Ye, J.; et al. Discovery and validation of sub-threshold genome-wide association study loci using epigenomic signatures. *Elife* **2016**, *5*, doi:10.7554/eLife.10557.

293. Hammond, R.K.; Pahl, M.C.; Su, C.; Cousminer, D.L.; Leonard, M.E.; Lu, S.; Doege, C.A.; Wagley, Y.; Hodge, K.M.; Lasconi, C.; et al. Biological constraints on GWAS SNPs at suggestive significance thresholds reveal additional BMI loci. *Elife* **2021**, *10*, doi:10.7554/eLife.62206.

294. Watanabe, K.; Taskesen, E.; van Bochoven, A.; Posthuma, D. Functional mapping and annotation of genetic associations with FUMA. *Nat Commun* **2017**, *8*, 1826, doi:10.1038/s41467-017-01261-5.

295. Wang, K.; Li, M.; Hakonarson, H. ANNOVAR: functional annotation of genetic variants from high-throughput sequencing data. *Nucleic Acids Res* **2010**, *38*, e164, doi:10.1093/nar/gkq603.

296. Kircher, M.; Witten, D.M.; Jain, P.; O'Roak, B.J.; Cooper, G.M.; Shendure, J. A general framework for estimating the relative pathogenicity of human genetic variants. *Nat Genet* **2014**, *46*, 310-315, doi:10.1038/ng.2892.

297. Boyle, A.P.; Hong, E.L.; Hariharan, M.; Cheng, Y.; Schaub, M.A.; Kasowski, M.; Karczewski, K.J.; Park, J.; Hitz, B.C.; Weng, S.; et al. Annotation of functional variation in personal genomes using RegulomeDB. *Genome Res* **2012**, *22*, 1790-1797, doi:10.1101/gr.137323.112.

298. Ernst, J.; Kellis, M. ChromHMM: automating chromatin-state discovery and characterization. *Nat Methods* **2012**, *9*, 215-216, doi:10.1038/nmeth.1906.

299. Kundaje, A.; Meuleman, W.; Ernst, J.; Bilenky, M.; Yen, A.; Heravi-Moussavi, A.; Kheradpour, P.; Zhang, Z.; Wang, J.; Ziller, M.J.; et al. Integrative analysis of 111 reference human epigenomes. *Nature* **2015**, *518*, 317-330, doi:10.1038/nature14248.

300. Kerimov, N.; Hayhurst, J.D.; Peikova, K.; Manning, J.R.; Walter, P.; Kolberg, L.; Samoviča, M.; Sakthivel, M.P.; Kuzmin, I.; Trevanion, S.J.; et al. eQTL Catalogue: a compendium of uniformly processed human gene expression and splicing QTLs. *bioRxiv* **2021**, 2020.2001.2029.924266, doi:10.1101/2020.01.29.924266.

301. Jaffe, A.E.; Straub, R.E.; Shin, J.H.; Tao, R.; Gao, Y.; Collado-Torres, L.; Kam-Thong, T.; Xi, H.S.; Quan, J.; Chen, Q.; et al. Developmental and genetic regulation of the human cortex transcriptome illuminate schizophrenia pathogenesis. *Nat Neurosci* **2018**, *21*, 1117-1125, doi:10.1038/s41593-018-0197-y.

302. Schwartzentruber, J.; Foskolou, S.; Kilpinen, H.; Rodrigues, J.; Alasoo, K.; Knights, A.J.; Patel, M.; Goncalves, A.; Ferreira, R.; Benn, C.L.; et al. Molecular and functional variation in iPSC-derived sensory neurons. *Nat Genet* **2018**, *50*, 54-61, doi:10.1038/s41588-017-0005-8.

303. Wang, D.; Liu, S.; Warrell, J.; Won, H.; Shi, X.; Navarro, F.C.P.; Clarke, D.; Gu, M.; Emani, P.; Yang, Y.T.; et al. Comprehensive functional genomic resource and integrative model for the human brain. *Science* **2018**, *362*, eaat8464, doi:10.1126/science.aat8464.

304. Ng, B.; White, C.C.; Klein, H.U.; Sieberts, S.K.; McCabe, C.; Patrick, E.; Xu, J.; Yu, L.; Gaiteri, C.; Bennett, D.A.; et al. An xQTL map integrates the genetic architecture of the human brain's transcriptome and epigenome. *Nat Neurosci* **2017**, *20*, 1418-1426, doi:10.1038/nn.4632.

305. Fromer, M.; Roussos, P.; Sieberts, S.K.; Johnson, J.S.; Kavanagh, D.H.; Perumal, T.M.; Ruderfer, D.M.; Oh, E.C.; Topol, A.; Shah, H.R.; et al. Gene expression elucidates functional impact of polygenic risk for schizophrenia. *Nat Neurosci* **2016**, *19*, 1442-1453, doi:10.1038/nn.4399.

306. Schmitt, A.D.; Hu, M.; Jung, I.; Xu, Z.; Qiu, Y.; Tan, C.L.; Li, Y.; Lin, S.; Lin, Y.; Barr, C.L.; et al. A Compendium of Chromatin Contact Maps Reveals Spatially Active Regions in the Human Genome. *Cell Rep* **2016**, *17*, 2042-2059, doi:10.1016/j.celrep.2016.10.061.

307. Giusti-Rodríguez, P.; Lu, L.; Yang, Y.; Crowley, C.A.; Liu, X.; Juric, I.; Martin, J.S.; Abnousi, A.; Allred, S.C.; Ancalade, N.; et al. Using three-dimensional regulatory chromatin interactions from adult and fetal cortex to interpret genetic results for psychiatric disorders and cognitive traits. *bioRxiv* **2019**, 406330, doi:10.1101/406330.

308. Andersson, R.; Gebhard, C.; Miguel-Escalada, I.; Hoof, I.; Bornholdt, J.; Boyd, M.; Chen, Y.; Zhao, X.; Schmidl, C.; Suzuki, T.; et al. An atlas of active enhancers across human cell types and tissues. *Nature* **2014**, *507*, 455-461, doi:10.1038/nature12787.

309. Gusev, A.; Ko, A.; Shi, H.; Bhatia, G.; Chung, W.; Penninx, B.W.; Jansen, R.; de Geus, E.J.; Boomsma, D.I.; Wright, F.A.; et al. Integrative approaches for large-scale transcriptome-wide association studies. *Nat Genet* **2016**, *48*, 245-252, doi:10.1038/ng.3506.

310. Barbeira, A.N.; Dickinson, S.P.; Bonazzola, R.; Zheng, J.; Wheeler, H.E.; Torres, J.M.; Torstenson, E.S.; Shah, K.P.; Garcia, T.; Edwards, T.L.; et al. Exploring the phenotypic consequences of tissue specific gene expression variation inferred from GWAS summary statistics. *Nat Commun* **2018**, *9*, 1825, doi:10.1038/s41467-018-03621-1.

311. Giambartolomei, C.; Vukcevic, D.; Schadt, E.E.; Franke, L.; Hingorani, A.D.; Wallace, C.; Plagnol, V. Bayesian test for colocalisation between pairs of genetic association studies using summary statistics. *PLoS Genet* **2014**, *10*, e1004383, doi:10.1371/journal.pgen.1004383.

312. Gusev, A.; Lawrenson, K.; Lin, X.; Lyra, P.C., Jr.; Kar, S.; Vavra, K.C.; Segato, F.; Fonseca, M.A.S.; Lee, J.M.; Pejovic, T.; et al. A transcriptome-wide association study of high-grade serous epithelial ovarian cancer identifies new susceptibility genes and splice variants. *Nat Genet* **2019**, *51*, 815-823, doi:10.1038/s41588-019-0395-x.

313. Wainberg, M.; Sinnott-Armstrong, N.; Mancuso, N.; Barbeira, A.N.; Knowles, D.A.; Golan, D.; Ermel, R.; Ruusalepp, A.; Quertermous, T.; Hao, K.; et al. Opportunities and challenges for transcriptome-wide association studies. *Nat Genet* **2019**, *51*, 592-599, doi:10.1038/s41588-019-0385-z.

314. Euesden, J.; Lewis, C.M.; O'Reilly, P.F. PRSice: Polygenic Risk Score software. *Bioinformatics* **2015**, *31*, 1466-1468, doi:10.1093/bioinformatics/btu848.

315. Ng, E.; Lind, P.M.; Lindgren, C.; Ingelsson, E.; Mahajan, A.; Morris, A.; Lind, L. Genome-wide association study of toxic metals and trace elements reveals novel associations. *Hum Mol Genet* **2015**, *24*, 4739-4745, doi:10.1093/hmg/ddv190.

4

316. Purcell, S.; Neale, B.; Todd-Brown, K.; Thomas, L.; Ferreira, M.A.; Bender, D.; Maller, J.; Sklar, P.; de Bakker, P.I.; Daly, M.J.; et al. PLINK: a tool set for whole-genome association and population-based linkage analyses. *Am J Hum Genet* **2007**, *81*, 559-575, doi:10.1086/519795.

317. Benjamini, Y.; Hochberg, Y. Controlling the False Discovery Rate: A Practical and Powerful Approach to Multiple Testing. *Journal of the Royal Statistical Society. Series B (Methodological)* **1995**, *57*, 289-300.

318. Nyholt, D.R. SECA: SNP effect concordance analysis using genome-wide association summary results. *Bioinformatics* **2014**, *30*, 2086-2088, doi:10.1093/bioinformatics/btu171.

319. Oh, S.; Abdelnabi, J.; Al-Dulaimi, R.; Aggarwal, A.; Ramos, M.; Davis, S.; Riester, M.; Waldron, L. HGNChelper: identification and correction of invalid gene symbols for human and mouse. *F1000Res* **2020**, *9*, 1493, doi:10.12688/f1000research.28033.1.

320. Waldron, L.; Riester, M. *HGNChelper: Identify and Correct Invalid HGNC Human Gene Symbols and MGI Mouse Gene Symbols*, R package version 0.8.1.; 2019.

321. Carlson, M. *org.Hs.eg.db: Genome wide annotation for Human*, R package version 3.12.0; 2020.

322. Tweedie, S.; Braschi, B.; Gray, K.; Jones, T.E.M.; Seal, R.L.; Yates, B.; Bruford, E.A. Genenames.org: the HGNC and VGNC resources in 2021. *Nucleic Acids Res* **2021**, *49*, D939-D946, doi:10.1093/nar/gkaa980.

323. R Core Team *R: A language and environment for statistical computing*, R Foundation for Statistical Computing: Vienna, Austria, 2020.

324. Wishart, D.S.; Guo, A.; Oler, E.; Wang, F.; Anjum, A.; Peters, H.; Dizon, R.; Sayeeda, Z.; Tian, S.; Lee, B.L.; et al. HMDB 5.0: the Human Metabolome Database for 2022. *Nucleic Acids Res* **2022**, *50*, D622-d631, doi:10.1093/nar/gkab1062.

325. Kanehisa, M.; Goto, S.; Sato, Y.; Furumichi, M.; Tanabe, M. KEGG for integration and interpretation of large-scale molecular data sets. *Nucleic Acids Res* **2012**, *40*, D109-114, doi:10.1093/nar/gkr988.

326. UniProt, C. UniProt: the universal protein knowledgebase in 2021. *Nucleic Acids Res* **2021**, *49*, D480-D489, doi:10.1093/nar/gkaa1100.

327. Lek, M.; Karczewski, K.J.; Minikel, E.V.; Samocha, K.E.; Banks, E.; Fennell, T.; O'Donnell-Luria, A.H.; Ware, J.S.; Hill, A.J.; Cummings, B.B.; et al. Analysis of protein-coding genetic variation in 60,706 humans. *Nature* **2016**, *536*, 285-291, doi:10.1038/nature19057.

328. Bartha, I.; di Iulio, J.; Venter, J.C.; Telenti, A. Human gene essentiality. *Nat Rev Genet* **2018**, *19*, 51-62, doi:10.1038/nrg.2017.75.

329. Petrovski, S.; Wang, Q.; Heinzen, E.L.; Allen, A.S.; Goldstein, D.B. Genic intolerance to functional variation and the interpretation of personal genomes. *PLoS Genet* **2013**, *9*, e1003709, doi:10.1371/journal.pgen.1003709.

330. Rackham, O.J.; Shihab, H.A.; Johnson, M.R.; Petretto, E. EvoTol: a protein-sequence based evolutionary intolerance framework for disease-gene prioritization. *Nucleic Acids Res* **2015**, *43*, e33, doi:10.1093/nar/gku1322.

331. Samocha, K.E.; Robinson, E.B.; Sanders, S.J.; Stevens, C.; Sabo, A.; McGrath, L.M.; Kosmicki, J.A.; Rehnström, K.; Mallick, S.; Kirby, A.; et al. A framework for the interpretation of de novo mutation in human disease. *Nat Genet* **2014**, *46*, 944-950, doi:10.1038/ng.3050.

332. Fadista, J.; Oskolkov, N.; Hansson, O.; Groop, L. LoFtool: a gene intolerance score based on loss-of-function variants in 60 706 individuals. *Bioinformatics* **2017**, *33*, 471-474, doi:10.1093/bioinformatics/btv602.

333. Bartha, I.; Rausell, A.; McLaren, P.J.; Mohammadi, P.; Tardaguila, M.; Chaturvedi, N.; Fellay, J.; Telenti, A. The Characteristics of Heterozygous Protein Truncating Variants in the Human Genome. *PLoS Comput Biol* **2015**, *11*, e1004647, doi:10.1371/journal.pcbi.1004647.

334. Cassa, C.A.; Weghorn, D.; Balick, D.J.; Jordan, D.M.; Nusinow, D.; Samocha, K.E.; O'Donnell-Luria, A.; MacArthur, D.G.; Daly, M.J.; Beier, D.R.; et al. Estimating the selective effects of heterozygous protein-truncating variants from human exome data. *Nat Genet* **2017**, *49*, 806-810, doi:10.1038/ng.3831.

335. Wang, T.; Wei, J.J.; Sabatini, D.M.; Lander, E.S. Genetic screens in human cells using the CRISPR-Cas9 system. *Science* **2014**, *343*, 80-84, doi:10.1126/science.1246981.

336. Blomen, V.A.; Májek, P.; Jae, L.T.; Bigenzahn, J.W.; Nieuwenhuis, J.; Staring, J.; Sacco, R.; van Diemen, F.R.; Olk, N.; Stukalov, A.; et al. Gene essentiality and synthetic lethality in haploid human cells. *Science* **2015**, *350*, 1092-1096, doi:10.1126/science.aac7557.

337. Hart, T.; Chandrashekhar, M.; Aregger, M.; Steinhart, Z.; Brown, K.R.; MacLeod, G.; Mis, M.; Zimmermann, M.; Fradet-Turcotte, A.; Sun, S.; et al. High-Resolution CRISPR Screens Reveal Fitness Genes and Genotype-Specific Cancer Liabilities. *Cell* **2015**, *163*, 1515-1526, doi:10.1016/j.cell.2015.11.015.

338. Finan, C.; Gaulton, A.; Kruger, F.A.; Lumbers, R.T.; Shah, T.; Engmann, J.; Galver, L.; Kelley, R.; Karlsson, A.; Santos, R.; et al. The druggable genome and support for target identification and validation in drug development. *Sci Transl Med* **2017**, *9*, doi:10.1126/scitranslmed.aag1166.

339. Wells, A.; Kopp, N.; Xu, X.; O'Brien, D.R.; Yang, W.; Nehorai, A.; Adair-Kirk, T.L.; Kopan, R.; Dougherty, J.D. The anatomical distribution of genetic associations. *Nucleic Acids Res* **2015**, *43*, 10804-10820, doi:10.1093/nar/gkv1262.

340. Dougherty, J.D.; Schmidt, E.F.; Nakajima, M.; Heintz, N. Analytical approaches to RNA profiling data for the identification of genes enriched in specific cells. *Nucleic Acids Res* **2010**, *38*, 4218-4230, doi:10.1093/nar/gkq130.

341. Xu, X.; Wells, A.B.; O'Brien, D.R.; Nehorai, A.; Dougherty, J.D. Cell type-specific expression analysis to identify putative cellular mechanisms for neurogenetic disorders. *J Neurosci* **2014**, *34*, 1420-1431, doi:10.1523/jneurosci.4488-13.2014.

342. The Genotype-Tissue Expression (GTEx) project. *Nat Genet* **2013**, *45*, 580-585, doi:10.1038/ng.2653.

343. Miller, J.A.; Ding, S.L.; Sunkin, S.M.; Smith, K.A.; Ng, L.; Szafer, A.; Ebbert, A.; Riley, Z.L.; Royall, J.J.; Aiona, K.; et al. Transcriptional landscape of the prenatal human brain. *Nature* **2014**, *508*, 199-206, doi:10.1038/nature13185.

344. Ingolia, N.T.; Ghaemmaghami, S.; Newman, J.R.; Weissman, J.S. Genome-wide analysis in vivo of translation with nucleotide resolution using ribosome profiling. *Science* **2009**, *324*, 218-223, doi:10.1126/science.1168978.

345. Klemann, C.; Visser, J.E.; Van Den Bosch, L.; Martens, G.J.M.; Poelmans, G. Integrated molecular landscape of amyotrophic lateral sclerosis provides insights into disease etiology. *Brain Pathol* **2018**, *28*, 203-211, doi:10.1111/bpa.12485.

346. Türei, D.; Korcsmáros, T.; Saez-Rodriguez, J. OmniPath: guidelines and gateway for literature-curated signaling pathway resources. *Nat Methods* **2016**, *13*, 966-967, doi:10.1038/nmeth.4077.

347. Luck, K.; Kim, D.K.; Lambourne, L.; Spirohn, K.; Begg, B.E.; Bian, W.; Brignall, R.; Cafarelli, T.; Campos-Laborie, F.J.; Charloteaux, B.; et al. A reference map of the human binary protein interactome. *Nature* **2020**, *580*, 402-408, doi:10.1038/s41586-020-2188-x.

4

348. Das, J.; Yu, H. HINT: High-quality protein interactomes and their applications in understanding human disease. *BMC Systems Biology* **2012**, *6*, 92, doi:10.1186/1752-0509-6-92.

349. Kotlyar, M.; Pastrello, C.; Ahmed, Z.; Chee, J.; Varyova, Z.; Jurisica, I. IID 2021: towards context-specific protein interaction analyses by increased coverage, enhanced annotation and enrichment analysis. *Nucleic Acids Res* **2022**, *50*, D640-d647, doi:10.1093/nar/gkab1034.

350. Veres, D.V.; Gyurkó, D.M.; Thaler, B.; Szalay, K.Z.; Fazekas, D.; Korcsmáros, T.; Csermely, P. ComPPI: a cellular compartment-specific database for protein-protein interaction network analysis. *Nucleic Acids Res* **2015**, *43*, D485-493, doi:10.1093/nar/gku1007.

351. Rachlin, J.; Cohen, D.D.; Cantor, C.; Kasif, S. Biological context networks: a mosaic view of the interactome. *Mol Syst Biol* **2006**, *2*, 66, doi:10.1038/msb4100103.

352. Rouillard, A.D.; Hurle, M.R.; Agarwal, P. Systematic interrogation of diverse Omic data reveals interpretable, robust, and generalizable transcriptomic features of clinically successful therapeutic targets. *PLoS Comput Biol* **2018**, *14*, e1006142, doi:10.1371/journal.pcbi.1006142.

353. Ryaboshapkina, M.; Hammar, M. Tissue-specific genes as an underutilized resource in drug discovery. *Sci Rep* **2019**, *9*, 7233, doi:10.1038/s41598-019-43829-9.

354. Plenge, R.M.; Scolnick, E.M.; Altshuler, D. Validating therapeutic targets through human genetics. *Nat Rev Drug Discov* **2013**, *12*, 581-594, doi:10.1038/nrd4051.

355. Glassberg, E.C.; Gao, Z.; Harpak, A.; Lan, X.; Pritchard, J.K. Evidence for Weak Selective Constraint on Human Gene Expression. *Genetics* **2019**, *211*, 757-772, doi:10.1534/genetics.118.301833.

SUPPLEMENTARY MATERIALS

Supplementary information (File S1-S8 and Table S1-S5) can be accessed via the publication online: https://www.mdpi.com/article/10.3390/ijms24021428/s1 or through: http://gofile.me/5Nxbd/IvkZFnkGE

4
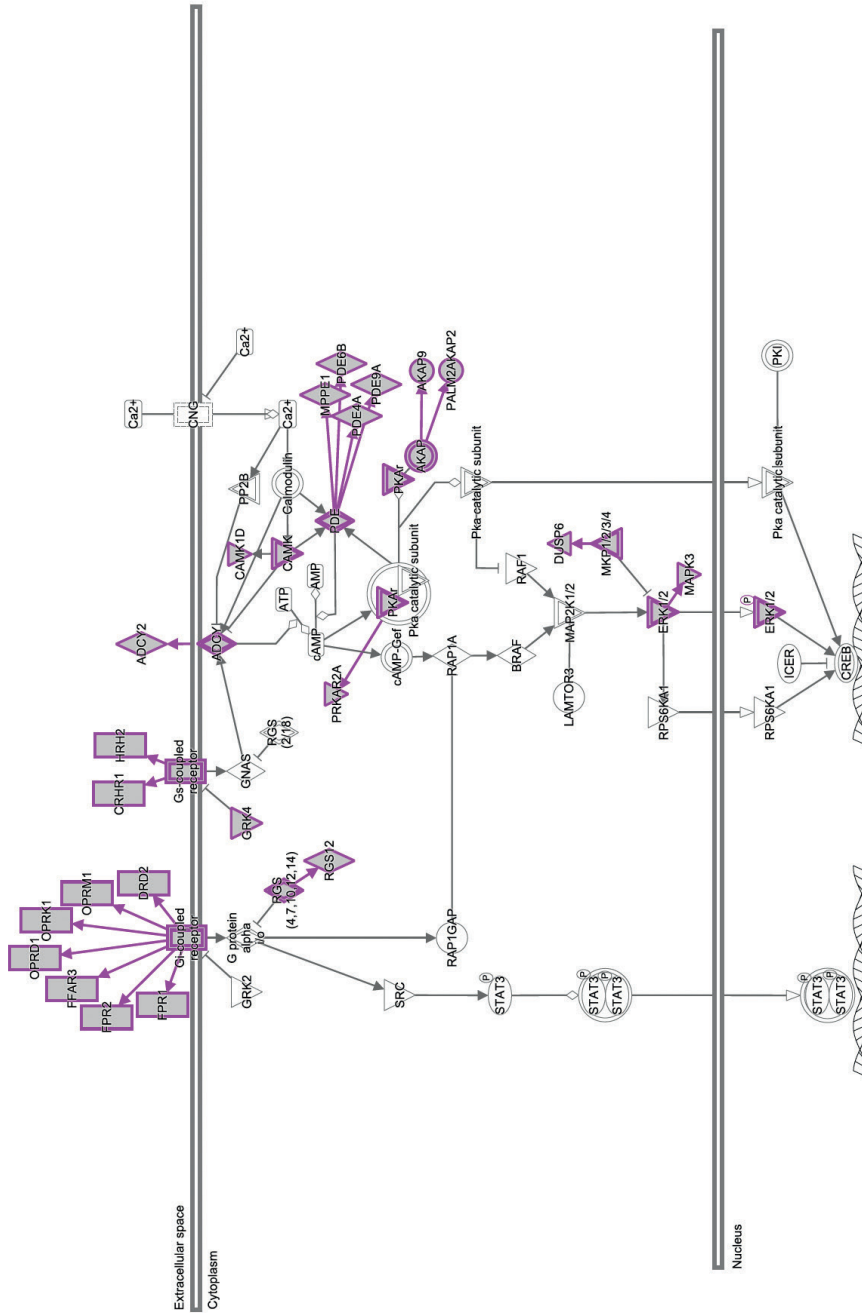
FIGURE S1. cAMP-mediated Signaling Pathway identified by IPA. The diagram represents the cAMP-mediated Signaling Pathway at the cellular level. Molecules are represented as nodes, and the biological relationship between two nodes is represented as an edge (line). Molecules highlighted with pink-outline and gray color represent genes/proteins/protein complexes which members appear in the set of 872 TD candidate genes. Abbreviations: P – phosphorylation.
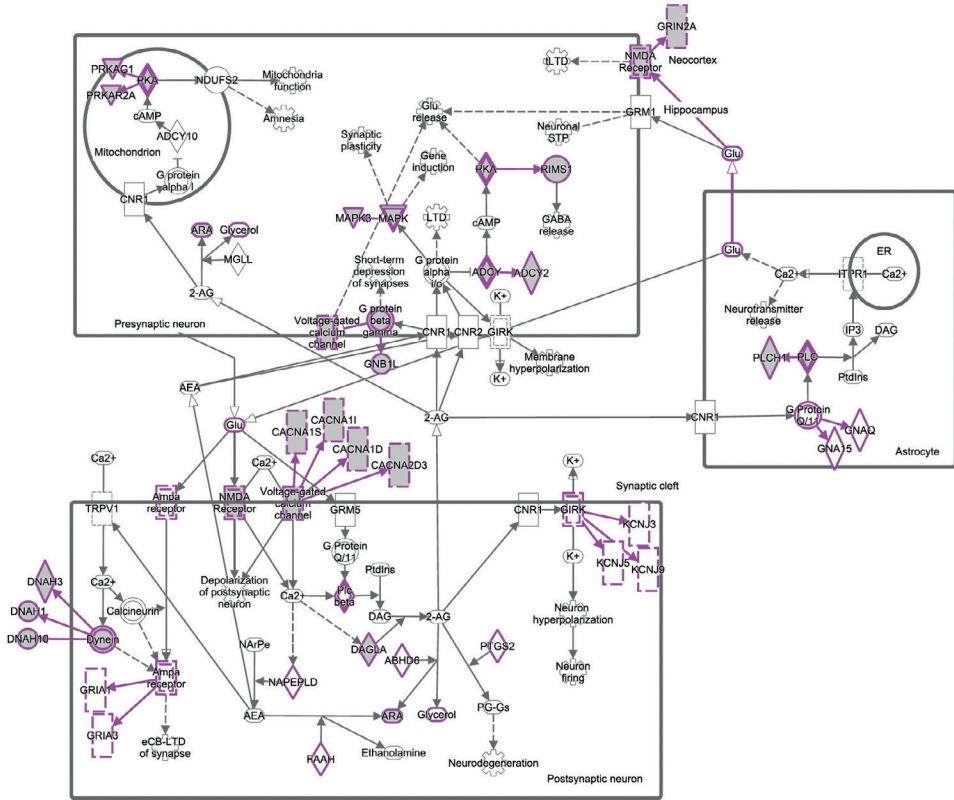
FIGURE S2. Endocannabinoid Neuronal Synapse Pathway identified by IPA. The diagram represents the Endocannabinoid Neuronal Synapse Pathway at the cellular level. Molecules are represented as nodes, and the biological relationship between two nodes is represented as an edge (line). Molecules highlighted with pink-outline and gray color represent genes/proteins/protein complexes which members appear in the set of 872 TD candidate genes and metabolites which showed shared genetic etiology with TD in the PRS-based analyses at Bonferroni adjusted *p*-value < 0.05. Pink outlined molecules without a color indicate metabolites which showed shared genetic etiology with TD at FDR *p*-value < 0.01 or genes that were differentially expressed in the blood or brain tissue of TD patients. Double-bordered molecules represent groups or complexes. Pink arrows indicate members of a complex that are present in the set of 872 TD candidate genes. Abbreviations: ARA – arachidonic acid; 2-AG – 2-arachidonoylglycerol; AEA – anandamine; NArPe –Narachidonylphosphatidylethanolamine; cAMP – cyclic AMP; Glu – glutamate, DAG – diacylglycerol; LTD – Long-term synaptic depression; tLTD – Timing-dependent long-term depression; eCB-LTD of synapse – Endocannabinoid-dependent long-term depression of synapse; Neuronal STP – short-term potentiation of neurons; PtdIns – phosphatidylinositol

CHAPTER 5

SHARED GENETIC ETIOLOGY BETWEEN OBSESSIVE-COMPULSIVE DISORDER, OBSESSIVE-COMPULSIVE SYMPTOMS IN THE POPULATION, AND INSULIN SIGNALING

ABSTRACT

Obsessive-compulsive symptoms (OCS) in the population have been linked to obsessive-compulsive disorder (OCD) in genetic and epidemiological studies. Insulin signaling has been implicated in OCD. We extend previous work by assessing genetic overlap between OCD, population-based OCS, and central nervous system (CNS) and peripheral insulin signaling. We conducted genome-wide association studies (GWASs) in the population-based Philadelphia Neurodevelopmental Cohort (PNC, 650 children and adolescents) of the total OCS score and six OCS factors from an exploratory factor analysis of 22 questions. Subsequently, we performed polygenic risk score (PRS)-based analysis to assess shared genetic etiologies between clinical OCD (using GWAS data from the Psychiatric Genomics Consortium), the total OCS score and OCS factors. We then performed gene-set analyses with a set of OCD-linked genes centered around CNS insulin-regulated synaptic function and PRS-based analyses for five peripheral insulin signaling-related traits. For validation purposes, we explored data from the independent Spit for Science population cohort (5047 children and adolescents). In the PNC, we found a significant shared genetic etiology between OCD and 'guilty taboo thoughts'. In the Spit for Science cohort, we additionally observed genetic sharing between 'symmetry/counting/ordering' and 'contamination/cleaning'. The CNS insulin-linked gene-set also associated with 'symmetry/counting/ordering' in the PNC. Further, we identified genetic sharing between peripheral insulin signaling-related traits: type 2 diabetes with 'aggressive taboo thoughts', and levels of fasting insulin and 2 h glucose with OCD. In conclusion, OCD, OCS in the population and insulin-related traits share genetic risk factors, indicating a common etiological mechanism underlying somatic and psychiatric disorders.

INTRODUCTION

Obsessive-compulsive disorder (OCD) is a heterogeneous psychiatric condition characterized by persistent, intrusive thoughts and urges (obsessions) and repetitive, intentional behaviors (compulsions) [1]. OCD affects 2-3% of the world's population [2,3]. OCD is moderately heritable, with approximately 40% of the phenotypic variance explained by genetic factors, and a higher genetic heritability has been reported in childhood onset OCD [4-6]. The genetic architecture of OCD is complex, with multiple genetic variants of small effect size contributing to its etiology. This has hampered the identification and replication of genetic susceptibility factors. A meta-analysis of hypothesis-driven candidate gene association studies has implicated serotoninergic and catecholaminergic genes in OCD, while studies focusing on glutamatergic and neurotrophic genes have shown inconsistent results [7]. Neither of the two independent genome-wide association studies (GWASs) of OCD [8,9] nor a subsequent meta-analysis (2688 cases and 7037 controls) [10] – including children, adolescents and adults – yielded genome-wide significant findings, likely due to lack of power. However, the meta-analysis demonstrated that the polygenic signal from either sample predicted OCD status in the other sample, indicating the polygenic nature of the disorder [10].

The diagnosis of OCD is based solely on clinical symptoms, and no genetic or biological markers are available with sufficient specificity and accuracy to be clinically actionable [11]. However, factor analyses of OCD symptoms have consistently identified specific OCD symptom clusters or dimensions, with the most reliable including contamination/cleaning, doubt/checking, symmetry/ordering, and unacceptable/taboo thoughts [11-14].

Obsessive-compulsive symptoms (OCS) are also present in the general population [15-17]. Indeed, 21 to 38 % of individuals in the population endorse obsessions and/or compulsions, although only a small minority (2-3 %) meet the DSM-5 criteria for a clinical OCD diagnosis [18,19]. OCS are also heritable, with their heritability ranging from 30 to 77% [20,21]. In addition to contributing to overall OCS, genetic factors contribute to specific OCS dimensions, including contamination/cleaning [22-24] and checking/ordering [24,25]. Genetic overlap between clinical OCD and OCS in the population is suggested by the fact that polygenic risk scores (PRS) based on OCD GWAS data significantly predict OCS in two population-based samples of 6931 and 3982 individuals, respectively [20,26]. Moreover, a very recent analysis found that compulsive symptoms in the general population overlap with the genetic liability for clinical OCD [27] and incorporating compulsive symptom GWAS data in a meta-analysis with OCD GWAS data yielded new findings in gene-based and gene enrichment analyses. Therefore, genetic studies of OCS in the general population could aid in the identification of susceptibility loci for clinical OCD and provide insight in specific symptom domains affected by individual genetic risk factors.

5

In a study aiming to identify molecular mechanisms underlying OCD, we earlier performed integration of the top-ranked results from the existing GWASs with genes implicated in OCD through other evidence. This resulted in a 'molecular landscape' that suggested the involvement of genes regulating postsynaptic dendritic spine formation and function through central nervous system (CNS) insulin-dependent signaling [28]. Support for a role of dysregulated insulin signaling in OCD and OCS comes from studies showing increased OCS in men with type 1 diabetes [29] and from a study indicating that OCD patients have a higher risk of developing type 2 diabetes (T2D) [30]. Furthermore, OCS were found to be positively correlated with blood levels of glycosylated hemoglobin (HbA1c), a diagnostic measure of T2D [31], and OCD patients had markedly higher levels of fasting glucose (a characteristic of T2D) [32].

In this paper, we aimed to assess the presence and extent of genetic overlap between OCD, OCS in the population, and insulin signaling, using the largest available data sets. Specifically, we parsed phenotypic heterogeneity using an exploratory factor analysis of OCS measured in a population cohort of children and adolescents. Subsequently, using PRS-based analyses, we investigated the presence of shared genetic etiologies between OCD and the total and factorized OCS. We then assessed genetic sharing between OCD, OCS, and insulin-related traits. In addition to assessing shared genetic etiologies, we tested for potential overlapping biology using gene-set analyses. Lastly, we extended our findings in an independent population cohort of children and adolescents.

MATERIALS AND METHODS

Sample, phenotypic, and genetic data

We studied OCS in the Philadelphia Neurodevelopmental Cohort (PNC) [33-37], which includes 8719 children and adolescents aged 8-21 years with neurobehavioral phenotypes and genome-wide genotyping data. Participants in the PNC provided written consent for genomic studies when they presented to the Children's Hospital of Philadelphia health care network. OCS were assessed with GO-ASSESS, a computerized version of the Kiddie-Schedule for Affective Disorders and Schizophrenia (K-SADs) [38]. For the current study, we selected 22 GO-ASSESS questions that corresponded to the diagnostic criteria for OCD (Supplementary Table 1). Participants were included if they answered the questions related to obsessions and/or compulsions. If those questions were all answered 'no', we allowed the questions on the consequences of obsessions and compulsions to be left blank, as no consequences are expected if no symptoms are present. The scores for each of the questions (0 for 'no' and 1 for 'yes') were then summed to create a total OCS score (range 0-22). Genome-wide genotyping in the PNC cohort was performed in waves using six different genotyping platforms (details in Supplementary Methods). As a primary aim of our study was to assess the genetic overlap

between OCD and OCS in the population, we only used phenotypic and genetic data from those PNC participants who answered positively on at least one of the questions related to the presence of obsessions and/or compulsions. This resulted in a final sample of 650 individuals for the subsequent factor and genome-wide association analyses.

Factor analysis

First, using SPSS 23 (SPSS Technologies, Armonk, NY, USA), we determined the internal consistency (Cronbach's α) of the 22 questions that constitute the total OCS scores in the 650 PNC participants. We then conducted a factor analysis of the scores on the 22 questions using Promax rotation to determine the number of factors that, when combined, explains the largest portion of the observed variance in the total OCS score. Specifically, we considered scree plots, eigenvalues >1 and the cumulative variance explained when selecting the number of factors and assigned questions to factors based on the highest absolute loading value.

Genome-wide association analyses

Quality control filtering was applied to the genetic data to remove non-European individuals, single nucleotide polymorphisms (SNPs) with low minor allele frequency (MAF) (<0.05), poor genotype call rate (<95%), and deviations from Hardy-Weinberg equilibrium ($P < 1 \times 10^{-6}$) (details in the Supplementary Methods). The imputation protocol used MaCH [39] for haplotype phasing and minimac [40] for imputation. Imputed SNPs with low imputation quality score ($r^2 < 0.8$) and low MAF (<0.05) were removed. If the total OCS score or the scores for the OCS factors fell within the limits of a normal distribution (i.e., a skewness and kurtosis between -1 and 1), we used a continuous trait design for the genome-wide association analysis. Otherwise, we used a pseudo case-control design, in which all individuals with a score of 0 for a factor were defined as 'controls' and compared against the 'pseudo cases', i.e., all individuals with a score of 1 or more for that factor. GWASs were carried out with mach2qtl [39] using the total OCS score and the scores for those factors that showed sufficient variation as phenotypes, with age, gender, and the four principal components from MDS included as covariates. GWASs were performed separately for each genotyping platform and combined in an inverse-variance-weighted meta-analysis using METAL [41], accounting for genomic inflation.

Shared genetic etiology analyses

OCD and OCS

First, we determined the level of shared genetic etiology between diagnosed OCD and OCS in the population. For this, we used the summary statistics from the meta-analysis of the two published GWASs of OCD [10] (data provided through the Psychiatric Genomics Consortium (PGC) for 2688

OCD cases and 7037 controls) as the 'base' sample for polygenic risk score (PRS)-based analyses in PRSice [42]. The summary statistics from the GWASs of the different OCS in the PNC were used as the 'target' samples for the PRS-based analyses. For details see Supplementary Methods.

OCD, OCS and peripheral insulin signaling-related traits

To determine the level of genetic sharing between five peripheral insulin signaling-related traits and OCD as well as OCS, we conducted PRS-based analyses in PRSice [42], as described above. As base samples, we used summary statistics data from GWASs of the following peripheral insulin signaling-related traits: type 2 diabetes (T2D) and the blood levels of four T2D markers: HbA1c, fasting insulin, fasting glucose and glucose 2 hours after an oral glucose challenge (2hGlu) (details in Supplementary Methods). As target samples of the PRS-based analyses, we used the summary statistics from the OCD GWAS meta-analysis and the GWASs of the total OCS score and the scores for the OCS factors in the PNC. Multiple comparisons correction for all tests performed (i.e., for the tests assessing genetic sharing between OCD and OCS and the tests assessing genetic sharing between the five insulin-related traits and OCD as well as OCS) was done using the Benjamini-Hochberg false discovery rate (FDR) method. With this method, we aggregated the calculated p-values of the shared genetic etiology analyses [43,44], which is similar to the approaches used in earlier studies working with multiple phenotypes and PRSice [45,46].

Gene-set analyses

We first compiled a set of genes encoding proteins from our molecular landscape of OCD [28] (see above). In this paper by van de Vondervoort et al., the OCD landscape was built based on proteins that have been implicated in the disease through different types of genetic evidence. Firstly, proteins were included if their corresponding genes have been implicated in OCD through SNPs from the published GWASs that are associated at $P < 1.00E-04$ and are located within the gene and/or 100 kb of flanking downstream and upstream sequences. In addition, genes/proteins were included that have been implicated in other ways in OCD etiology. After critical evaluation of the literature, only genes/proteins that have received support through findings from (genetic) animal studies, gene mutations, and/or two or more independent candidate gene association studies (or at least nominal significance in meta-analysis) and/or mRNA/protein expression studies, were included. Our selection resulted in a set of 51 autosomal genes for subsequent analyses. Using the GWAS results of the total OCS score and the scores for the OCS factors, competitive gene-set analyses were then performed using the Multimarker Analysis of GenoMic Annotation (MAGMA) software [47], see Supplementary Methods. P-values were considered significant if they exceeded a Bonferroni-corrected threshold accounting for the number of phenotypes tested ($P < 0.05/7$

tests (total OCS score and six OCS factors) = 7.14E-03). For significant gene-set associations, we looked at the individual gene-wide P-values and applied Bonferroni correction (P < 0.05/51 genes in the gene-set = 9.80E-4).

Validation analyses in an independent population sample

In order to validate and possibly expand our findings, we performed PRS-based and gene-set analyses using data from GWASs of OCS in an independent population sample: the 'Spit for Science' project, which includes 16718 children and adolescents aged 6-17 years recruited from a local science museum [48]. OCS were measured using the Toronto Obsessive-Compulsive Scale (TOCS), a validated 21-item parent-or self-report questionnaire [15]. TOCS items are scored from -3 (far less often than others of the same age) to +3 (far more often than others of the same age). We first assessed which TOCS questions could be grouped into OCS factors similar to those calculated based on the PNC data. Only two OCS factors (being 'symmetry/counting/ordering' and 'contamination/cleaning') were similar and therefore could be used for validation purposes, see Supplementary Table 2. Genome-wide genotyping data for 5047 individuals of Caucasian descent entered the 'continuous trait' GWAS analysis for each factor. A description of genotyping, quality control and imputation can be found elsewhere [49] and GWAS details in the Supplementary Methods. Using summary statistics of the GWASs of the two TOCS OCS factors, we examined the shared genetic etiology between OCD and the TOCS OCS factors, and between the five peripheral insulin signaling-related traits and the TOCS OCS factors. As described above for the PNC data, multiple comparisons correction was done using the FDR method for all tests performed in the Spit for Science cohort. Gene-set analyses between the set of 51 genes from the OCD landscape and the two TOCS OCS factors were also performed.

RESULTS

Factor analysis

The internal consistency between the scores on the 22 OCS questions from the PNC was satisfactory (Cronbach's α=0.69). Supplementary Figure 1A shows the total score distribution (mean=6.4, s.d.=3.35). Factor analysis revealed an eight factors solution as the best-fitting model, explaining 58.6% of the variance in the total score. We named these eight OCS factors 'impairment', 'symmetry/counting/ordering', 'contamination/cleaning', 'aggressive taboo thoughts', 'repetition', 'guilty taboo thoughts', 'distress', and 'religious taboo thoughts' (Table 1; factor score distributions in Supplementary Figure 1B).

TABLE 1. Item content of and loadings on the eight factors that constitute the best fitting model to explain the variance in the total score of the 22 items from the questionnaire of obsessive-compulsive symptoms that was completed by 650 participants from the PNC cohort. Taken together, the eight factors explain 58.6% of the variance in the total score of OCD symptoms in the general population from the questionnaire.

Factor 1 *Impairment*	(14.63% of the variance in the total score explained)
Items	Factor loadings
OCD024 Did these thoughts and behaviors prevent you from doing things you normally would do?	0.537
OCD025 Did having these thoughts or behaviors bother you a lot?	0.717
OCD032 You told me (insert endorsed thoughts/behaviors). How much did having these thoughts/behaviors upset or bother you? How much did you ever feel upset or disappointed with yourself because of your thoughts/behaviors?	0.741
OCD033 How much did the thoughts/behaviors you have told me about cause problems for you at home, at school/work, or with your family or friends?	0.716
OCD034 Did you stay home from school/work because of your behaviors/thoughts?	0.339
Factor 2 *Symmetry/counting/ordering*	(10.58% of the variance in the total score explained)
Items	Factor loadings
OCD007 Have you ever been bothered by thoughts that don't make sense to you, that come over and over again and won't go away, such as need for symmetry/exactness?	0.682
OCD012 Have you ever had to do something over and over again – that would have made you feel really nervous if you couldn't do it, like: counting?	0.588
OCD013 Have you ever had to do something over and over again – that would have made you feel really nervous if you couldn't do it, like: checking (for example, doors, locks, ovens)?	0.545
OCD016 Have you ever had to do something over and over again – that would have made you feel really nervous if you couldn't do it, like: ordering or arranging things?	0.776
OCD017 Have you ever had to do something over and over again – that would have made you feel really nervous if you couldn't do it, like: doing things over and over again at bedtime, like arranging the pillows, sheets, or other things?	0.513
Factor 3 *Contamination/cleaning*	(7.54% of the variance in the total score explained)
Items	Factor loadings
OCD003 Have you ever been bothered by thoughts that don't make sense to you, that come over and over again and won't go away, such as thoughts about contamination/germs/illness?	0.871
OCD011 Have you ever had to do something over and over again - that would have made you feel really nervous if you couldn't do it, like: cleaning or washing (for example, your hands, house)?	0.757

TABLE 1. Continued

Factor 4 *Aggressive taboo thoughts*	(6.02% of the variance in the total score explained)
Items	Factor loadings
OCD001 Have you ever been bothered by thoughts that don't make sense to you, that come over and over again and won't go away, such as concern with harming others/self?	0.503
OCD002 Have you ever been bothered by thoughts that don't make sense to you, that come over and over again and won't go away, such as pictures of violent things?	0.845
OCD006 Have you ever been bothered by thoughts that don't make sense to you, that come over and over again and won't go away, such as forbidden/bad thoughts?	0.578
Factor 5 *Repetition*	(5.56% of the variance in the total score explained)
Items	Factor loadings
OCD014 Have you ever had to do something over and over again – that would have made you feel really nervous if you couldn't do it, like: getting dressed over and over again?	0.782
OCD015 Have you ever had to do something over and over again – that would have made you feel really nervous if you couldn't do it, like: going in and out a door over and over again?	0.662
Factor 6 *Guilty taboo thoughts*	(5.04% of the variance in the total score explained)
Items	Factor loadings
OCD004 Have you ever been bothered by thoughts that don't make sense to you, that come over and over again and won't go away, such as fear that you would do something/say something bad without intending to?	0.758
OCD005 Have you ever been bothered by thoughts that don't make sense to you, that come over and over again and won't go away, such as feelings that bad things that happened were your fault?	0.722
Factor 7 *Distress*	(4.68% of the variance in the total score explained)
Items	Factor loadings
OCD009 Did these thoughts continue to bother you no matter how hard you tried to get rid of them or ignore them?	0.770
OCD010 Did you try not to think about (thoughts), try to keep them out of your head, or try to push the thoughts away?	0.552
Factor 8 *Religious taboo thoughts*	(4.56% of the variance in the total score explained)
Items	Factor loadings
OCD008 Have you ever been bothered by thoughts that don't make sense to you, that come over and over again and won't go away, such as religious thoughts?	0.722

Genome-wide association analyses

Based on the distributions of the scores, we used a continuous trait design for the GWASs of the total OCS score and the factors 'impairment', 'symmetry/counting/ordering', and 'distress'. A pseudo case-control design was used for the factors 'contamination/cleaning' and 'aggressive taboo thoughts', and 'guilty taboo thoughts'. The distribution of the scores on the OCS factors 'repetition' and 'religious taboo thoughts' showed too little variation to be taken forward (Supplementary Figure 1B). Because of the lack of power – with only 650 individuals per GWAS – we do not report individual GWAS results, but we have used the GWAS results for PRS-based analyses.

Shared genetic etiology analyses
OCD and OCS

We found statistically significant evidence for a shared genetic etiology between diagnosed OCD and the population-based OCS factor 'guilty taboo thoughts' ($R2 = 2.28\%$; $P = 2.52E-03$) (Supplementary Figure 2 and Table 2).

OCD, OCS, and peripheral insulin signaling-related traits

We found statistically significant evidence for a shared genetic etiology between T2D and 'aggressive taboo thoughts' ($R^2 = 1.86\%$; $P = 5.95E-03$) (Supplementary Figure 3A and Table 3). Fasting insulin levels showed genetic sharing with OCD ($R^2 = 0.26\%$; $P = 7.67E-05$) and for HbA1c and fasting glucose levels, we did not find evidence of genetic sharing. Lastly, we observed genetic sharing between 2 h glucose levels and OCD ($R^2 = 0.14\%$; $P = 4.75E-03$) (Supplementary Figure 3B-E and Table 3).

TABLE 2. PRS-based results for shared genetic etiology between OCD and the total OCS score as well as the scores for six OCS factors

	P_T	P-value	R^2	nSNPs
Total OCS score	0.05	4.72E-01	0.04%	26653
Impairment	0.2	2.61E-01	0.51%	81294
Symmetry/counting/ordering	0.001	3.53E-01	0.23%	1007
Contamination/cleaning	0.2	1.12E-01	0.85%	81294
Aggressive taboo thoughts	0.4	2.28E-01	0.46%	135230
Guilty taboo thoughts	**0.3**	**2.52E-03**	**2.28%**	**110197**
Distress	0.1	4.05E-01	0.13%	47020

Shown in this table are the best SNP P-value thresholds (P_T) for the PRSice analyses between OCD – ('base' sample) – and the total OCS score and six OCS factors – ('target' samples), their Benjamini-Hochberg adjusted P-values (P-value) for shared genetic etiology, the variance explained in the target sample phenotypes (R^2), and the number of SNPs (nSNPs). Significant findings are indicated in bold.

TABLE 3. PRS-based results for shared genetic etiology between five peripheral insulin-signaling-related traits and OCD and OCS

'base' sample	'target' sample	P_T	P-value	R2	nSNPs
Type 2 Diabetes	OCD	0.1	2.80E-01	0.03%	138256
	Total OCS score	0.2	3.36E-01	0.28%	83578
	Impairment	0.3	4.10E-01	0.11%	114988
	Symmetry/counting/ordering	0.3	2.56E-01	0.53%	114988
	Contamination/cleaning	0.5	3.53E-01	0.24%	158182
	Aggressive taboo thoughts	**0.2**	**5.95E-03**	**1.86%**	**83578**
	Guilty taboo thoughts	0.5	1.89E-01	0.68%	158182
	Distress	0.3	4.72E-01	0.02%	114988
HbA1c	OCD	0.001	4.15E-01	0.01%	1152
	Total OCS score	0.2	7.64E-02	1.00%	64945
	Impairment	0.2	2.28E-01	0.58%	64945
	Symmetry/counting/ordering	0.05	4.10E-01	0.11%	21040
	Contamination/cleaning	0.001	3.21E-01	0.33%	1030
	Aggressive taboo thoughts	0.05	7.99E-02	0.97%	21040
	Guilty taboo thoughts	0.1	4.03E-01	0.15%	37363
	Distress	0.05	4.07E-01	0.13%	21040
Fasting Insulin	**OCD**	**0.2**	**7.67E-05**	**0.26%**	**12557**
	Total OCS score	0.1	3.74E-01	0.19%	6564
	Impairment	0.001	4.10E-01	0.11%	328
	Symmetry/counting/ordering	0.4	4.72E-01	0.04%	18227
	Contamination/cleaning	0.1	4.47E-01	0.07%	6564
	Aggressive taboo thoughts	0.4	4.66E-01	0.06%	18227
	Guilty taboo thoughts	0.001	2.61E-01	0.52%	328
	Distress	0.1	2.80E-01	0.43%	6564
Fasting Glucose	OCD	0.4	3.53E-01	0.02%	21586
	Total OCS score	0.3	4.16E-01	0.10%	14814
	Impairment	0.1	4.10E-01	0.12%	6861
	Symmetry/counting/ordering	0.001	2.80E-01	0.39%	481
	Contamination/cleaning	0.001	2.28E-01	0.58%	481
	Aggressive taboo thoughts	0.5	2.71E-01	0.49%	21798
	Guilty taboo thoughts	0.1	3.21E-01	0.33%	6861
	Distress	0.05	3.53E-01	0.23%	4271
2h Glucose	**OCD**	**0.5**	**4.75E-03**	**0.14%**	**24148**
	Total OCS score	0.1	4.72E-01	0.02%	5202
	Impairment	0.2	3.53E-01	0.22%	9362
	Symmetry/counting/ordering	0.4	4.10E-01	0.11%	16970
	Contamination/cleaning	0.05	2.71E-01	0.49%	2962
	Aggressive taboo thoughts	0.001	2.28E-01	0.59%	186
	Guilty taboo thoughts	0.001	9.74E-02	0.90%	186
	Distress	0.2	3.53E-01	0.25%	9362

Shown in this table are the best SNP P-value thresholds (P_T) for the PRSice analyses between five peripheral insulin signaling-related traits – ('base' samples), and OCD as well as OCS factors – ('target' sample)s, their Benjamini-Hochberg adjusted P-values (P-value), the variance explained (R^2) in the target sample phenotypes, and the number of SNPs (nSNPs). Significant findings are indicated in bold.

Gene-set analyses

MAGMA-based gene-set analysis for the CNS insulin signaling genes extracted from our earlier-defined OCD landscape containing 33329 SNPs (effective number of SNPs after adjusting for LD structure=2189) revealed a significant association with 'symmetry/counting/ordering' (P=4.08E-03) (Supplementary Table 3). Within the significant gene-set, none of the individual genes showed gene-wide association (Supplementary Table 4). No significant associations were found with the total OCS score or the five other OCS factors.

Validation analyses in an independent population sample

Two OCS factors were similar between the PNC and Spit for Science cohort, i.e., 'symmetry/counting/ordering' and 'contamination/cleaning' (Supplementary Table 2 and Supplementary Figure 4A-B). Using summary statistics of the GWASs of these two factors, we found that diagnosed OCD shows genetic sharing with 'symmetry/counting/ordering$_{TOCS}$' (R^2 = 0.49%; FDR-adjusted P = 2.42E-05) and 'contamination/cleaning$_{TOCS}$' (R^2 = 0.23%; FDR-adjusted P = 4.07E-03).

We also observed a shared genetic etiology between T2D and 'contamination/cleaning$_{TOCS}$' (R^2 = 0.28%; FDR-adjusted P = 1.59E-03) (Supplementary Table 5 and Supplementary Figure 5A-C). Gene-set analysis for the OCD landscape genes in the two OCS$_{TOCS}$ factors revealed no significant associations.

All results from the PRS-based analyses are summarized in Table 4.

TABLE 4. Summary of results from PRS-based analyses

'Target 'sample	'Base' sample					
	OCD	Type 2 Diabetes	HbA1c	Fasting Insulin	Fasting Glucose	2h Glucose
PNC						
Total OCS score	4.72E-01	3.36E-01	7.64E-02	3.74E-01	4.16E-01	4.72E-01
	0.04%	0.28%	1.00%	0.19%	0.10%	0.02%
Impairment	2.61E-01	4.10E-01	2.28E-01	4.10E-01	4.10E-01	3.53E-01
	0.51%	0.11%	0.58%	0.11%	0.12%	0.22%
Symmetry/counting/ordering	3.53E-01	2.56E-01	4.10E-01	4.72E-01	2.80E-01	4.10E-01
	0.23%	0.53%	0.11%	0.04%	0.39%	0.11%
Contamination/cleaning	1.12E-01	3.53E-01	3.21E-01	4.47E-01	2.28E-01	2.71E-01
	0.85%	0.24%	0.33%	0.07%	0.58%	0.49%
Aggressive taboo thoughts	2.28E-01	**5.95E-03**	7.99E-02	4.66E-01	2.71E-01	2.28E-01
	0.46%	**1.86%**	0.97%	0.06%	0.49%	0.59%
Guilty taboo thoughts	**2.52E-03**	1.89E-0.1	4.03E-01	2.61E-01	3.21E-01	9.74E-02
	2.28%	0.68%	0.15%	0.52%	0.33%	0.90%
Distress	4.05E-01	4.72E-01	4.07E-01	2.80E-01	3.53E-01	3.53E-01
	0.13%	0.02%	0.13%	0.43%	0.23%	0.25%

TABLE 1. Continued

'Target 'sample	'Base' sample					
	OCD	Type 2 Diabetes	HbA1c	Fasting Insulin	Fasting Glucose	2h Glucose
PGC						
OCD	-	2.80E-01	4.15E-01	**7.67E-05**	3.53E-01	**4.75E-03**
	-	0.03%	0.01%	**0.26%**	0.02%	**0.14%**
Spit for Science						
Symmetry/counting/ordering$_{TOCS}$	**2.42E-05**	3.39E-01	2.71E-01	3.71E-01	2.47E-01	4.45E-01
	0.49%	0.03%	0.04%	0.02%	0.04%	0.01%
Contamination/cleaning$_{TOCS}$	**4.07E-03**	**1.59E-03**	1.68E-01	4.37E-01	4.36E-01	3.76E-01
	0.23%	**0.28%**	0.05%	0.01%	0.01%	0.02%

Shown in this table are the Benjamini-Hochberg adjusted P-values at the best SNP P-value thresholds along with the variance explained for each of the 'base' and 'target' sample pairs from PRS analyses in PRSice. Significant findings are indicated in bold. Abbreviations: PNC – Philadelphia Neurodevelopmental Cohort, PGC – Psychiatric Genomics Consortium, TOCS – Toronto Obsessive-Compulsive Scale

DISCUSSION

In this study, we extended previous work by assessing genetic etiologies between OCD, OCS in the population, and CNS and peripheral insulin signaling. While previous studies [20,26] have yielded a shared genetic etiology between OCD and the total population-based OCS score, our analyses using phenotypic and genetic data of 650 children and adolescents from the population (PNC cohort) found genetic sharing between OCD and the OCS factor 'guilty taboo thoughts'. In the larger Spit for Science cohort (n=5047), we expanded our results by showing genetic sharing between OCD and 'symmetry/counting/ordering' as well as 'contamination/cleaning'. Our findings are in keeping with the literature suggesting (at least partial) genetic overlap between OCD and population-based OCS [20,22-24,27]. Since OCD is genetically correlated with other psychiatric disorders (e.g., Anorexia Nervosa, Major Depressive Disorder, and Tourette Syndrome [50]), future studies investigating OCS as (a) shared trait(s) between disorders could help address underlying biological mechanisms of comorbidity.

OCD and OCS have been linked to altered CNS and peripheral insulin signaling. When testing for potential overlapping biology, we found significant association between a set of 51 autosomal OCD genes centered around CNS insulin-regulated synaptic function and 'symmetry/counting/ordering'. As for peripheral insulin signaling, we found genetic sharing between T2D and – based on the PNC data – 'aggressive taboo thoughts', and – in the Spit for Science cohort – between T2D and 'contamination/cleaning'. For two out of the four T2D blood markers (blood levels of fasting insulin and 2hGlu), we also identified a shared genetic etiology

with OCD. These findings provide support for 'dysregulated' peripheral insulin signaling as a biological process contributing to both OCD and population-based OCS. Further evidence for a role of (altered) peripheral insulin signaling in OCD etiology is suggested by the fact that selective serotonin reuptake inhibitors (SSRIs), the first-line pharmacological treatment for OCD, positively affect diabetic parameters when used to treat depressive symptoms in T2D (i.e., decreasing HbA1c levels and insulin requirement, and increasing insulin sensitivity) [51]. Interestingly, SSRIs are particularly effective for treating harm-related obsessions, which are a part of 'aggressive taboo thoughts' [52]. This is in line with our finding of genetic sharing between T2D and 'aggressive taboo thoughts'. In addition, a recent study demonstrated that bilateral deep brain stimulation (DBS), a safe and effective treatment option for pharmaco-resistant OCD, not only reduced OCD symptoms but also decreased fasting insulin levels in the blood of both OCD patients with T2D and non-diabetic OCD patients [53]. Moreover, insulin in the CNS – either entering from the periphery by crossing the blood brain barrier [54] or synthesized in the CNS [55] – has important non-metabolic functions, including modulating synaptic plasticity [56] and learning and memory [57,58].

Although it is not clear yet what the relative contributions are of dysregulated peripheral and CNS insulin signaling to OCD and OCS, we recently demonstrated that compulsivity observed in Tallyho (TH) mice, a rodent model of T2D, is potentially linked to disturbances in insulin signaling. TH mice both displayed compulsive behavior and increased glucose levels in their dorsomedial striatum, which could be due to decreased action of peripheral and/or CNS insulin, and the glucose levels correlated with compulsivity [59].

The current results should be viewed in light of some strengths and limitations. A strength is that we used quantitative symptom scores collected through questionnaires in the general population, which has enabled us to generate OCS phenotypes that we could then perform GWASs on. Using samples selected from the community may also reduce selection bias, which can occur when patient samples are analysed (e.g., individuals suffering from several comorbid disorders are more likely to present for clinical care) [60]. A limitation of the current study is the small sample size of the GWASs and limited power to discover new single genetic variant associations. However, this sample size was large enough to provide proof of concept for genetic sharing between OCD, OCS in the population, and insulin signaling. A second limitation we faced was that the questions in the discovery and validation cohorts were not exactly the same, which may partly explain the lack of validation. Another limitation may be that the proportions of the variance in the target phenotypes being explained by the base phenotypes are quite small. However, these 'variances explained' are in fact similar to or higher than those found in similar analyses, e.g., the PRS derived from a GWAS of OCD explained (only) 0.20% of the variance in OCS in a

population sample [20]. Moreover, as the variance explained is dependent on the size of the 'base sample' for the generation of the PRS [61], the observed variances explained with the still relatively small meta-GWAS of OCD as base sample may be underestimated.

In conclusion, we identified a shared genetic etiology between OCD, OCS in the population, and both CNS and peripheral insulin signaling. Our results imply that altered insulin signaling is not only relevant for somatic disorders but is also involved in the etiology of psychiatric disorders and related symptoms in the population, especially OCD and OCS. Further studies are needed to disentangle the contributions of peripheral and CNS insulin production and signaling to these disorders and symptoms.

Code availability

Code used to perform the analyses is available upon request.

5

Acknowledgements

Conflicts of interest

J.M.S. has received honoraria from Abide Therapeutics regarding treatments for OCD and related disorders. In the past 3 years, J.K.B. has been a consultant to / member of advisory board of / and/or speaker for Shire, Roche, Medice, and Servier. He is not an employee of any of these companies, and not a stock shareholder of any of these companies. He has no other financial or material support, including expert testimony, patents, royalties. BF has received educational speaking fees from Medice and Shire. G.P. is director of Drug Target ID (DTID) Ltd. The remaining authors declare that they have no conflict of interest.

REFERENCES

1. Association, A.P. Diagnostic and Statistican Manual of Mental Disorders. Fifth Edition. *Arlington, VA: American Psychiatric Publishing* **2013**.

2. Weissman, M.M.; Bland, R.C.; Canino, G.J.; Greenwald, S.; Hwu, H.G.; Lee, C.K.; Newman, S.C.; Oakley-Browne, M.A.; Rubio-Stipec, M.; Wickramaratne, P.J.; et al. The cross national epidemiology of obsessive compulsive disorder. The Cross National Collaborative Group. *The Journal of clinical psychiatry* **1994**, *55 Suppl*, 5-10.

3. Ruscio, A.M.; Stein, D.J.; Chiu, W.T.; Kessler, R.C. The epidemiology of obsessive-compulsive disorder in the National Comorbidity Survey Replication. *Mol Psychiatry* **2010**, *15*, 53-63, doi:10.1038/mp.2008.94.

4. Taylor, S. Etiology of obsessions and compulsions: a meta-analysis and narrative review of twin studies. *Clin Psychol Rev* **2011**, *31*, 1361-1372, doi:10.1016/j.cpr.2011.09.008.

5. van Grootheest, D.S.; Cath, D.; Hottenga, J.J.; Beekman, A.T.; Boomsma, D.I. Genetic factors underlie stability of obsessive-compulsive symptoms. *Twin research and human genetics : the official journal of the International Society for Twin Studies* **2009**, *12*, 411-419, doi:10.1375/twin.12.5.411.

6. van Grootheest, D.S.; Cath, D.C.; Beekman, A.T.; Boomsma, D.I. Twin studies on obsessive-compulsive disorder: a review. *Twin Res Hum Genet* **2005**, *8*, 450-458, doi:10.1375/183242705774310060.

7. Taylor, S. Molecular genetics of obsessive-compulsive disorder: a comprehensive meta-analysis of genetic association studies. *Mol Psychiatry* **2013**, *18*, 799-805, doi:10.1038/mp.2012.76.

8. Mattheisen, M.; Samuels, J.F.; Wang, Y.; Greenberg, B.D.; Fyer, A.J.; McCracken, J.T.; Geller, D.A.; Murphy, D.L.; Knowles, J.A.; Grados, M.A.; et al. Genome-wide association study in obsessive-compulsive disorder: results from the OCGAS. *Mol Psychiatry* **2015**, *20*, 337-344, doi:10.1038/mp.2014.43.

9. Stewart, S.E.; Yu, D.; Scharf, J.M.; Neale, B.M.; Fagerness, J.A.; Mathews, C.A.; Arnold, P.D.; Evans, P.D.; Gamazon, E.R.; Davis, L.K.; et al. Genome-wide association study of obsessive-compulsive disorder. *Molecular psychiatry* **2013**, *18*, 788-798, doi:10.1038/mp.2012.85.

10. International Obsessive Compulsive Disorder Foundation Genetics, C.; Studies, O.C.D.C.G.A. Revealing the complex genetic architecture of obsessive-compulsive disorder using meta-analysis. *Mol Psychiatry* **2018**, *23*, 1181-1188, doi:10.1038/mp.2017.154.

11. Calamari, J.E.; Wiegartz, P.S.; Riemann, B.C.; Cohen, R.J.; Greer, A.; Jacobi, D.M.; Jahn, S.C.; Carmin, C. Obsessive-compulsive disorder subtypes: an attempted replication and extension of a symptom-based taxonomy. *Behaviour research and therapy* **2004**, *42*, 647-670, doi:10.1016/S0005-7967(03)00173-6.

12. Mataix-Cols, D.; Rauch, S.L.; Manzo, P.A.; Jenike, M.A.; Baer, L. Use of factor-analyzed symptom dimensions to predict outcome with serotonin reuptake inhibitors and placebo in the treatment of obsessive-compulsive disorder. *The American journal of psychiatry* **1999**, *156*, 1409-1416, doi:10.1176/ajp.156.9.1409.

13. Summerfeldt, L.J.; Richter, M.A.; Antony, M.M.; Swinson, R.P. Symptom structure in obsessive-compulsive disorder: a confirmatory factor-analytic study. *Behaviour research and therapy* **1999**, *37*, 297-311, doi:10.1016/s0005-7967(98)00134-x.

14. Leckman, J.F.; Grice, D.E.; Boardman, J.; Zhang, H.; Vitale, A.; Bondi, C.; Alsobrook, J.; Peterson, B.S.; Cohen, D.J.; Rasmussen, S.A.; et al. Symptoms of obsessive-compulsive disorder. *Am J Psychiatry* **1997**, *154*, 911-917, doi:10.1176/ajp.154.7.911.

15. Park, L.S.; Burton, C.L.; Dupuis, A.; Shan, J.; Storch, E.A.; Crosbie, J.; Schachar, R.J.; Arnold, P.D. The Toronto Obsessive-Compulsive Scale: Psychometrics of a Dimensional Measure of Obsessive-Compulsive Traits. *Journal of the American Academy of Child and Adolescent Psychiatry* **2016**, *55*, 310-318 e314, doi:10.1016/j.jaac.2016.01.008.

16. Alvarenga, P.G.; Cesar, R.C.; Leckman, J.F.; Moriyama, T.S.; Torres, A.R.; Bloch, M.H.; Coughlin, C.G.; Hoexter, M.Q.; Manfro, G.G.; Polanczyk, G.V.; et al. Obsessive-compulsive symptom dimensions in a population-based, cross-sectional sample of school-aged children. *J Psychiatr Res* **2015**, *62*, 108-114, doi:10.1016/j.jpsychires.2015.01.018.

17. Fullana, M.A.; Mataix-Cols, D.; Caspi, A.; Harrington, H.; Grisham, J.R.; Moffitt, T.E.; Poulton, R. Obsessions and compulsions in the community: prevalence, interference, help-seeking, developmental stability, and co-occurring psychiatric conditions. *Am J Psychiatry* **2009**, *166*, 329-336, doi:10.1176/appi.ajp.2008.08071006.

18. Fullana, M.A.; Vilagut, G.; Rojas-Farreras, S.; Mataix-Cols, D.; de Graaf, R.; Demyttenaere, K.; Haro, J.M.; de Girolamo, G.; Lepine, J.P.; Matschinger, H.; et al. Obsessive-compulsive symptom dimensions in the general population: results from an epidemiological study in six European countries. *Journal of affective disorders* **2010**, *124*, 291-299, doi:10.1016/j.jad.2009.11.020.

19. Barzilay, R.; Patrick, A.; Calkins, M.E.; Moore, T.M.; Wolf, D.H.; Benton, T.D.; Leckman, J.F.; Gur, R.C.; Gur, R.E. Obsessive-Compulsive Symptomatology in Community Youth: Typical Development or a Red Flag for Psychopathology? *Journal of the American Academy of Child and Adolescent Psychiatry* **2019**, *58*, 277-286 e274, doi:10.1016/j.jaac.2018.06.038.

20. den Braber, A.; Zilhao, N.R.; Fedko, I.O.; Hottenga, J.J.; Pool, R.; Smit, D.J.; Cath, D.C.; Boomsma, D.I. Obsessive-compulsive symptoms in a large population-based twin-family sample are predicted by clinically based polygenic scores and by genome-wide SNPs. *Translational psychiatry* **2016**, *6*, e731, doi:10.1038/tp.2015.223.

21. Mathews, C.A.; Delucchi, K.; Cath, D.C.; Willemsen, G.; Boomsma, D.I. Partitioning the etiology of hoarding and obsessive-compulsive symptoms. *Psychol Med* **2014**, *44*, 2867-2876, doi:10.1017/s0033291714000269.

22. Chacon, P.; Rosario-Campos, M.C.; Pauls, D.L.; Hounie, A.G.; Curi, M.; Akkerman, F.; Shimabokuro, F.H.; de Mathis, M.A.; Lopes, A.C.; Hasler, G.; et al. Obsessive-compulsive symptoms in sibling pairs concordant for obsessive-compulsive disorder. *Am J Med Genet B Neuropsychiatr Genet* **2007**, *144b*, 551-555, doi:10.1002/ajmg.b.30457.

23. Brakoulias, V.; Starcevic, V.; Martin, A.; Berle, D.; Milicevic, D.; Viswasam, K. The familiality of specific symptoms of obsessive-compulsive disorder. *Psychiatry research* **2016**, *239*, 315-319, doi:10.1016/j.psychres.2016.03.047.

24. Burton, C.L.; Park, L.S.; Corfield, E.C.; Forget-Dubois, N.; Dupuis, A.; Sinopoli, V.M.; Shan, J.; Goodale, T.; Shaheen, S.M.; Crosbie, J.; et al. Heritability of obsessive-compulsive trait dimensions in youth from the general population. *Translational psychiatry* **2018**, *8*, 191, doi:10.1038/s41398-018-0249-9.

25. Kohlrausch, F.B.; Giori, I.G.; Melo-Felippe, F.B.; Vieira-Fonseca, T.; Velarde, L.G.; de Salles Andrade, J.B.; Fontenelle, L.F. Association of GRIN2B gene polymorphism and Obsessive Compulsive disorder and symptom dimensions: A pilot study. *Psychiatry research* **2016**, *243*, 152-155, doi:10.1016/j.psychres.2016.06.027.

26. Taylor, M.J.; Martin, J.; Lu, Y.; Brikell, I.; Lundstrom, S.; Larsson, H.; Lichtenstein, P. Association of Genetic Risk Factors for Psychiatric Disorders and Traits of These Disorders in a Swedish Population Twin Sample. *JAMA psychiatry* **2019**, *76*, 280-289, doi:10.1001/jamapsychiatry.2018.3652.

27.	Smit, D.J.A.; Cath, D.; Zilhao, N.R.; Ip, H.F.; Denys, D.; den Braber, A.; de Geus, E.J.C.; Verweij, K.J.H.; Hottenga, J.J.; Boomsma, D.I. Genetic meta-analysis of obsessive-compulsive disorder and self-report compulsive symptoms. *American journal of medical genetics. Part B, Neuropsychiatric genetics : the official publication of the International Society of Psychiatric Genetics* **2019**, 785311, doi:10.1002/ajmg.b.32777.

28.	van de Vondervoort, I.; Poelmans, G.; Aschrafi, A.; Pauls, D.L.; Buitelaar, J.K.; Glennon, J.C.; Franke, B. An integrated molecular landscape implicates the regulation of dendritic spine formation through insulin-related signalling in obsessive-compulsive disorder. *Journal of psychiatry & neuroscience : JPN* **2016**, *41*, 280-285, doi:10.1503/jpn.140327.

29.	Winocour, P.H.; Main, C.J.; Medlicott, G.; Anderson, D.C. A psychometric evaluation of adult patients with type 1 (insulin-dependent) diabetes mellitus: prevalence of psychological dysfunction and relationship to demographic variables, metabolic control and complications. *Diabetes Res* **1990**, *14*, 171-176.

30.	Isomura, K.; Brander, G.; Chang, Z.; Kuja-Halkola, R.; Rück, C.; Hellner, C.; Lichtenstein, P.; Larsson, H.; Mataix-Cols, D.; Fernández de la Cruz, L. Metabolic and Cardiovascular Complications in Obsessive-Compulsive Disorder: A Total Population, Sibling Comparison Study With Long-Term Follow-up. *Biol Psychiatry* **2018**, *84*, 324-331, doi:10.1016/j.biopsych.2017.12.003.

31.	Kontoangelos, K.; Raptis, A.E.; Papageorgiou, C.C.; Papadimitriou, G.N.; Rabavilas, A.D.; Dimitriadis, G.; Raptis, S.A. The association of the metabolic profile in diabetes mellitus type 2 patients with obsessive-compulsive symptomatology and depressive symptomatology: new insights. *International journal of psychiatry in clinical practice* **2013**, *17*, 48-55, doi:10.3109/13651501.2012.697563.

32.	Albert, U.; Aguglia, A.; Chiarle, A.; Bogetto, F.; Maina, G. Metabolic syndrome and obsessive-compulsive disorder: a naturalistic Italian study. *General hospital psychiatry* **2013**, *35*, 154-159, doi:10.1016/j.genhosppsych.2012.10.004.

33.	Satterthwaite, T.D.; Elliott, M.A.; Ruparel, K.; Loughead, J.; Prabhakaran, K.; Calkins, M.E.; Hopson, R.; Jackson, C.; Keefe, J.; Riley, M.; et al. Neuroimaging of the Philadelphia neurodevelopmental cohort. *NeuroImage* **2014**, *86*, 544-553, doi:10.1016/j.neuroimage.2013.07.064.

34.	Calkins, M.E.; Merikangas, K.R.; Moore, T.M.; Burstein, M.; Behr, M.A.; Satterthwaite, T.D.; Ruparel, K.; Wolf, D.H.; Roalf, D.R.; Mentch, F.D.; et al. The Philadelphia Neurodevelopmental Cohort: constructing a deep phenotyping collaborative. *Journal of child psychology and psychiatry, and allied disciplines* **2015**, *56*, 1356-1369, doi:10.1111/jcpp.12416.

35.	Gur, R.C.; Calkins, M.E.; Satterthwaite, T.D.; Ruparel, K.; Bilker, W.B.; Moore, T.M.; Savitt, A.P.; Hakonarson, H.; Gur, R.E. Neurocognitive growth charting in psychosis spectrum youths. *JAMA psychiatry* **2014**, *71*, 366-374, doi:10.1001/jamapsychiatry.2013.4190.

36.	Calkins, M.E.; Moore, T.M.; Merikangas, K.R.; Burstein, M.; Satterthwaite, T.D.; Bilker, W.B.; Ruparel, K.; Chiavacci, R.; Wolf, D.H.; Mentch, F.; et al. The psychosis spectrum in a young U.S. community sample: findings from the Philadelphia Neurodevelopmental Cohort. *World psychiatry : official journal of the World Psychiatric Association (WPA)* **2014**, *13*, 296-305, doi:10.1002/wps.20152.

37.	Satterthwaite, T.D.; Connolly, J.J.; Ruparel, K.; Calkins, M.E.; Jackson, C.; Elliott, M.A.; Roalf, D.R.; Hopson, R.; Prabhakaran, K.; Behr, M.; et al. The Philadelphia Neurodevelopmental Cohort: A publicly available resource for the study of normal and abnormal brain development in youth. *NeuroImage* **2016**, *124*, 1115-1119, doi:10.1016/j.neuroimage.2015.03.056.

38.	Kaufman, J.; Birmaher, B.; Brent, D.; Rao, U.; Flynn, C.; Moreci, P.; Williamson, D.; Ryan, N. Schedule for Affective Disorders and Schizophrenia for School-Age Children-Present and Lifetime Version (K-SADS-PL): initial reliability and validity data. *Journal of the American Academy of Child and Adolescent Psychiatry* **1997**, *36*, 980-988, doi:10.1097/00004583-199707000-00021.

5

39. Li, Y.; Willer, C.J.; Ding, J.; Scheet, P.; Abecasis, G.R. MaCH: using sequence and genotype data to estimate haplotypes and unobserved genotypes. *Genetic epidemiology* **2010**, *34*, 816-834, doi:10.1002/gepi.20533.

40. Howie, B.; Fuchsberger, C.; Stephens, M.; Marchini, J.; Abecasis, G.R. Fast and accurate genotype imputation in genome-wide association studies through pre-phasing. *Nat Genet* **2012**, *44*, 955-959, doi:10.1038/ng.2354.

41. Willer, C.J.; Li, Y.; Abecasis, G.R. METAL: fast and efficient meta-analysis of genomewide association scans. *Bioinformatics (Oxford, England)* **2010**, *26*, 2190-2191, doi:10.1093/bioinformatics/btq340.

42. Euesden, J.; Lewis, C.M.; O'Reilly, P.F. PRSice: Polygenic Risk Score software. *Bioinformatics* **2015**, *31*, 1466-1468, doi:10.1093/bioinformatics/btu848.

43. Benjamini, Y.; Hochberg, Y. Controlling the false discovery rate: a practical and powerful approach to multiple testing. *J R Stat Soc Ser B (Methodological)* **1995**, *57: 289–300*.

44. Glickman, M.E.; Rao, S.R.; Schultz, M.R. False discovery rate control is a recommended alternative to Bonferroni-type adjustments in health studies. *Journal of clinical epidemiology* **2014**, *67*, 850-857, doi:10.1016/j.jclinepi.2014.03.012.

45. Harris, S.E.; Hagenaars, S.P.; Davies, G.; David Hill, W.; Liewald, D.C.M.; Ritchie, S.J.; Marioni, R.E.; Metastroke Consortium, I.C.f.B.P.G.-W.A.S.; International Consortium for Blood Pressure Genome-Wide Association, S.; Aging, C.C.; et al. Molecular genetic contributions to self-rated health. *International journal of epidemiology* **2017**, *46*, 994-1009, doi:10.1093/ije/dyw219.

46. Hagenaars, S.P.; Harris, S.E.; Davies, G.; Hill, W.D.; Liewald, D.C.; Ritchie, S.J.; Marioni, R.E.; Fawns-Ritchie, C.; Cullen, B.; Malik, R.; et al. Shared genetic aetiology between cognitive functions and physical and mental health in UK Biobank (N=112 151) and 24 GWAS consortia. *Molecular psychiatry* **2016**, *21*, 1624-1632, doi:10.1038/mp.2015.225.

47. de Leeuw, C.A.; Mooij, J.M.; Heskes, T.; Posthuma, D. MAGMA: generalized gene-set analysis of GWAS data. *PLoS computational biology* **2015**, *11*, e1004219, doi:10.1371/journal.pcbi.1004219.

48. Crosbie, J.; Arnold, P.; Paterson, A.; Swanson, J.; Dupuis, A.; Li, X.; Shan, J.; Goodale, T.; Tam, C.; Strug, L.J.; et al. Response inhibition and ADHD traits: correlates and heritability in a community sample. *Journal of abnormal child psychology* **2013**, *41*, 497-507, doi:10.1007/s10802-012-9693-9.

49. Burton, C.L.; Wright, L.; Shan, J.; Xiao, B.; Dupuis, A.; Goodale, T.; Shaheen, S.M.; Corfield, E.C.; Arnold, P.D.; Schachar, R.J.; et al. SWAN scale for ADHD trait-based genetic research: a validity and polygenic risk study. *Journal of child psychology and psychiatry, and allied disciplines* **2019**, *60*, 988-997, doi:10.1111/jcpp.13032.

50. Brainstorm, C.; Anttila, V.; Bulik-Sullivan, B.; Finucane, H.K.; Walters, R.K.; Bras, J.; Duncan, L.; Escott-Price, V.; Falcone, G.J.; Gormley, P.; et al. Analysis of shared heritability in common disorders of the brain. *Science (New York, N.Y.)* **2018**, *360*, eaap8757, doi:10.1126/science.aap8757.

51. Janardhan Reddy, Y.C.; Sundar, A.S.; Narayanaswamy, J.C.; Math, S.B. Clinical practice guidelines for Obsessive-Compulsive Disorder. *Indian journal of psychiatry* **2017**, *59*, S74-S90, doi:10.4103/0019-5545.196976.

52. Landeros-Weisenberger, A.; Bloch, M.H.; Kelmendi, B.; Wegner, R.; Nudel, J.; Dombrowski, P.; Pittenger, C.; Krystal, J.H.; Goodman, W.K.; Leckman, J.F.; et al. Dimensional predictors of response to SRI pharmacotherapy in obsessive-compulsive disorder. *Journal of affective disorders* **2010**, *121*, 175-179, doi:10.1016/j.jad.2009.06.010.

53. ter Horst, K.W.; Lammers, N.M.; Trinko, R.; Opland, D.M.; Figee, M.; Ackermans, M.T.; Booij, J.; van den Munckhof, P.; Schuurman, P.R.; Fliers, E.; et al. Striatal dopamine regulates systemic glucose metabolism in humans and mice. *Science translational medicine* **2018**, *10*, eaar3752, doi:10.1126/scitranslmed.aar3752.

54. Margolis, R.U.; Altszuler, N. Insulin in the cerebrospinal fluid. *Nature* **1967**, *215*, 1375-1376, doi:10.1038/2151375a0.

55. Clarke, D.W.; Mudd, L.; Boyd, F.T., Jr.; Fields, M.; Raizada, M.K. Insulin is released from rat brain neuronal cells in culture. *J Neurochem* **1986**, *47*, 831-836, doi:10.1111/j.1471-4159.1986.tb00686.x.

56. Chiu, S.L.; Chen, C.M.; Cline, H.T. Insulin receptor signaling regulates synapse number, dendritic plasticity, and circuit function in vivo. *Neuron* **2008**, *58*, 708-719, doi:10.1016/j.neuron.2008.04.014.

57. Dou, J.T.; Chen, M.; Dufour, F.; Alkon, D.L.; Zhao, W.Q. Insulin receptor signaling in long-term memory consolidation following spatial learning. *Learn Mem* **2005**, *12*, 646-655, doi:10.1101/lm.88005.

58. Zhao, W.; Chen, H.; Xu, H.; Moore, E.; Meiri, N.; Quon, M.J.; Alkon, D.L. Brain insulin receptors and spatial memory. Correlated changes in gene expression, tyrosine phosphorylation, and signaling molecules in the hippocampus of water maze trained rats. *J Biol Chem* **1999**, *274*, 34893-34902, doi:10.1074/jbc.274.49.34893.

59. van de Vondervoort, I.; Amiri, H.; Bruchhage, M.M.K.; Oomen, C.A.; Rustogi, N.; Cooper, J.D.; van Asten, J.J.A.; Heerschap, A.; Bahn, S.; Williams, S.C.R.; et al. Converging evidence points towards a role of insulin signaling in regulating compulsive behavior. *Translational psychiatry* **2019**, *9*, 225, doi:10.1038/s41398-019-0559-6.

60. Gibbs, N.A. Nonclinical populations in research on obsessive-compulsive disorder: A critical review. *Clinical Psychology Review* **1996**, *16*, 729-773, doi:10.1016/S0272-7358(96)00043-8.

61. Dudbridge, F. Power and predictive accuracy of polygenic risk scores. *PLoS genetics* **2013**, *9*, e1003348, doi:10.1371/journal.pgen.1003348.

5

SUPPLEMENTARY MATERIALS

Supplementary Methods

Sample, phenotypic, and genetic data

We studied OCS in the Philadelphia Neurodevelopmental Cohort (PNC) [1-4], which includes 8719 children and adolescents aged 8-21 years with neurobehavioral phenotypes and genome-wide genotyping data. Participants in the PNC provided written consent for genomic studies when they presented to the Children's Hospital of Philadelphia health care network. Notably, participants from Philadelphia Neurodevelopmental Cohort (PNC) were not recruited from psychiatric clinics, and the sample is not enriched for individuals who seek psychiatric help. Genome-wide genotyping in the PNC has been performed in waves using six different genotyping platforms. Genotypes are available through the NIMH Database of Genotypes and Phenotypes (dbGaP), study accession ID phs000607.v1.p1. (https://www.ncbi.nlm.nih.gov/projects/gap/cgi-bin/study.cgi?study_id=phs000607.v1.p1&phv=292&phd=&pha=&pht=3445&phvf=28&phdf=&phaf=&phtf=&dssp=1&consent=&temp=1) [5]. We assessed the phenotypic distributions per platform, and for this study used the two genetic platforms with the largest number of individuals with phenotypic data, HumanOmniExpress-12v1.0 (OmniExpress) and Human610_Quadv1_B (610Quad) (n=1989 and n=1257, respectively). Hence, genome-wide genotyping data were available for 3246 individuals who also completed the 22 OCD questions. Ancestry was addressed by only selecting individuals of self-reported European descent and by using multidimensional scaling (MDS) analysis. Ancestry outliers (i.e., of non-European descent) were excluded based on visual inspection of the first two principal components, leaving 3041 individuals for analyses (n=1860 from 610Quad and n=1181 from OmniExpress). The final sample of 650 individuals for the subsequent factor and genome-wide association analyses included 418 individuals from 610Quad and 232 from OmniExpress.

Shared genetic etiology analyses

Before generating polygenic risk scores with PRSice [6], clumping was performed using PLINK [7] to select independent index SNPs for each linkage disequilibrium (LD) block in the genome. Based on the significance level of the SNPs in the base sample, the index SNPs were selected and form clumps of all other SNPs that are within 500 kb and are in LD (r^2>0.25).

PRSice was then used to generate polygenic risk scores for OCD that are the sum of genome-wide SNPs associated with OCD weighted by their effect sizes estimated from the PGC OCD meta-GWAS and only including SNPs that exceed seven broad P-value thresholds. The seven thresholds that were used are 0.001, 0.05, 0.1, 0.2, 0.3, 0.4, and 0.5. PRSice calculated P-values of shared genetic etiology between the base OCD phenotype and

the target phenotypes (total score of OCS and scores for the OCS factors) for each of the seven P-value thresholds (P_T). Subsequently, the calculated P-values for genetic sharing were aggregated and corrected for multiple comparisons using the false discovery rate (FDR) method [8,9]. To calculate the FDR, we applied the Benjamini-Hochberg method implemented through mne.stats.fdr_correction function in python.

To determine the level of genetic sharing between five peripheral insulin signaling-related traits and OCD as well as OCS, we also conducted PRS-based analyses in PRSice [6]. As base samples, we used summary statistics data from GWASs of the following peripheral insulin signaling-related traits: type 2 diabetes (T2D) (GWAS of 26,676 cases and 132,532 controls) [10] as well as the blood levels of four T2D markers: HbA1c (GWAS of 123,665 general population subjects; increased HbA1c levels are a diagnostic measure of T2D) [11], fasting insulin (GWAS of 108,557 general population subjects; increasing fasting insulin levels lead to insulin resistance, the pathological hallmark of T2D) [12], fasting glucose (GWAS of 133,010 general population subjects; increased fasting glucose levels (hyperglycemia) are a characteristic of T2D) [12], and glucose 2 hours after an oral glucose challenge (2-hour glucose or 2hGlu) (GWAS of 42,854 general population subjects; 2hGlu, a clinical measure of glucose tolerance used in the diagnosis of T2D) [12].

Gene-set analyses

For gene-set analyses, we first compiled a set of all genes encoding proteins within our molecular landscape of OCD that is involved in regulating postsynaptic dendritic spine formation and function through CNS insulin-dependent signaling [13].

This resulted in a set of 52 unique genes but as our genome-wide association analysis only included autosomal SNPs, we had to omit one gene located on the X chromosome (*HTR2C*), leaving a final set of 51 genes for subsequent analysis. Gene-set analysis was then performed using the Multimarker Analysis of GenoMic Annotation (MAGMA) software [14]. We selected all SNPs located within each of the 51 genes (0 kb window) after which all single SNP P-values were transformed into a gene test-statistic by taking the mean of the $\chi2$ statistic among the SNPs in each gene. Gene association tests were performed taking LD between SNPs into account using the 1000 Genomes Project European sample as a reference to estimate the LD between SNPs within the genes (http://ctglab.nl/software/MAGMA/ref_ data/g1000_ceu.zip). Gene-wide P-values were converted to z-values reflecting the strength of the association each gene has with each of the OCS factors. Subsequently, we tested whether the 51 genes in the OCD landscape are jointly associated with the total score of OCS and the scores for the OCS factors. We used an intercept-only linear regression model, including a subvector corresponding to the genes in the gene-set. To test whether the

association was different from the association of the genes outside the gene-set, taking into account the polygenic nature of our traits, the regression model was expanded to include all annotated genes in the genome outside the gene-set. To account for the potentially confounding factors of gene size and gene density, both gene size and gene density as well as their logarithms were included as covariates in the gene-set analysis.

Validation analyses in an independent population sample
To conduct the GWASs of the two OCS factors derived from the Spit for Science data, a linear regression model was used, adjusting for age, sex, respondent (questionnaire filled by parent or child), genotyping platform (Illumina HumanCoreExome-12 (v1-0) bead-chip or the HumanOmni1-Quad (v1.0) bead-chip), and the first 6 principal components from MDS.

The significance between the SNP imputed allele dosage and the response was calculated from a Wald test. Only SNPs with minor allele frequency > 0.01 and imputation quality (allelic R2) > 0.60 were tested.

Supplementary Tables

SUPPLEMENTARY TABLE 1. Customized questionnaire of obsessive-compulsive symptoms in the general population. The 22 questions were from GO-ASSESS, a computerized version of the Kiddie-Schedule for Affective Disorders and Schizophrenia (K-SADs).

Nr	Questions
OCD001	Have you ever been bothered by thoughts that don't make sense to you, that come over and over again and won't go away, such as concern with harming others/self?
OCD002	Have you ever been bothered by thoughts that don't make sense to you, that come over and over again and won't go away, such as pictures of violent things?
OCD003	Have you ever been bothered by thoughts that don't make sense to you, that come over and over again and won't go away, such as thoughts about contamination/germs/illness?
OCD004	Have you ever been bothered by thoughts that don't make sense to you, that come over and over again and won't go away, such as fear that you would do something/say something bad without intending to?
OCD005	Have you ever been bothered by thoughts that don't make sense to you, that come over and over again and won't go away, such as feelings that bad things that happened were your fault?
OCD006	Have you ever been bothered by thoughts that don't make sense to you, that come over and over again and won't go away, such as forbidden/bad thoughts?
OCD007	Have you ever been bothered by thoughts that don't make sense to you, that come over and over again and won't go away, such as need for symmetry/exactness?
OCD008	Have you ever been bothered by thoughts that don't make sense to you, that come over and over again and won't go away, such as religious thoughts?
OCD009	Did these thoughts continue to bother you no matter how hard you tried to get rid of them or ignore them?
OCD010	Did you try not to think about (thoughts), try to keep them out of your head, or try to push the thoughts away?
OCD011	Have you ever had to do something over and over again – that would have made you feel really nervous if you couldn't do it, like: cleaning or washing (for example, your hands, house)?
OCD012	Have you ever had to do something over and over again – that would have made you feel really nervous if you couldn't do it, like: counting?
OCD013	Have you ever had to do something over and over again – that would have made you feel really nervous if you couldn't do it, like: checking (for example, doors, locks, ovens)?
OCD014	Have you ever had to do something over and over again – that would have made you feel really nervous if you couldn't do it, like: getting dressed over and over again?
OCD015	Have you ever had to do something over and over again – that would have made you feel really nervous if you couldn't do it, like: going in and out a door over and over again?
OCD016	Have you ever had to do something over and over again – that would have made you feel really nervous if you couldn't do it, like: ordering or arranging things?
OCD017	Have you ever had to do something over and over again – that would have made you feel really nervous if you couldn't do it, like: doing things over and over again at bedtime, like arranging the pillows, sheets, or other things?

5

SUPPLEMENTARY TABLE 1. Continued

Nr	Questions
OCD024	Did these thoughts and behaviors prevent you from doing things you normally would do?
OCD025	Did having these thoughts or behaviors bother you a lot?
OCD032	You told me (insert endorsed thoughts/behaviors). How much did having these thoughts/behaviors upset or bother you? How much did you ever feel upset or disappointed with yourself because of your thoughts/behaviors?
OCD033	How much did the thoughts/behaviors you have told me about cause problems for you at home, at school/work, or with your family or friends?
OCD034	Did you stay home from school/work because of your behaviors/thoughts?

Note: (1) The answers to questions OCD032 and OCD033 were re-categorized from a 10-point scale into binary responses (i.e., with scores from 0 to 4 converted into a score of 0 for 'no' and scores from 5 to 10 converted into a score of 1 for 'yes') for compatibility with the other 20 questions for which there were only two possible answers ('no' = score of 0,'yes' = score of 1). (2) For the data selection, if the questions related to obsessions (OCD001-OCD008) and/or compulsions (OCD011-OCD17) were completed and all those questions were answered 'no', we allowed the questions on the consequences of obsessions and compulsions (OCD009, OCD010, OCD024, OCD025, OCD032, OCD033, OCD034) to be left blank, as no consequences are expected if no symptoms are present. The scores for each of the questions were then summed to create a total OCS score (range 0-22).

SUPPLEMENTARY TABLE 2. Content of two novel OCS factors that could be compiled from the Toronto Obsessive-Compulsive Scale (TOCS) questions and that are similar in the questions they contain to the two factors ('symmetry/counting/ordering' and 'contamination/cleaning') from the Philadelphia Neurodevelopmental Cohort (PNC) data.

Factor Symmetry/counting/ordering $_{TOCS}$

TOCS items:

'Do Certain': Needs to do certain things (e.g., counting steps)

'Checks': Checks things

'Count': Needs to count objects

'Symmetry': Needs things to be symmetrical

'Interfere': Gets upset when people rearrange things

'Repeat': Repeats actions until just right

'Not Exactly': Worries if something done not exactly right

Factor Contamination/cleaning $_{TOCS}$

TOCS items:

'Dirt': Hates dirt/dirty things

'Germs': Worries about germs

'Wash': Needs to wash hands

'Clean': Worries about being clean

SUPPLEMENTARY TABLE 3. MAGMA-based gene-set analysis for the 51 CNS insulin signaling genes extracted from our earlier-defined OCD landscape. P-values were considered significant if they exceeded a Bonferroni-corrected threshold accounting for the number of phenotypes tested (P < 0.05/7 tests (total OCS score and six OCS factors) = 0.00714).

Trait	P-value
Total OCS score	0.76762
Impairment	0.98503
Symmetry/counting/ordering	**0.00408**
Contamination/cleaning	0.33586
Aggressive taboo thoughts	0.30643
Guilty taboo thoughts	0.16893
Distress	0.32738

SUPPLEMENTARY TABLE 4. Gene-wide association results for 51 unique genes from the OCD landscape and the OCS factors 'symmetry/counting/ordering'

Gene	P-value	Gene	P-value
ADD3	0.2045	LNX1	0.4954
ARHGAP15	0.5126	MEIS2	0.4562
BDNF	0.5325	MTUS2	0.2716
BTBD3	0.0080	NOS1	0.2508
CCNC	0.1823	NSG2	0.9420
CYTIP	0.1470	PDE4D	0.7043
DCC	0.3287	PRDM13	0.4412
DLGAP1	0.6954	RACGAP1	0.7330
DLGAP3	0.0465	REXO1	0.2719
DNAI1	0.5131	SEMA4D	0.1606
DOCK1	0.5564	SERPINH1	0.2660
EBF2	0.4170	SLC1A1	0.1345
EFNA5	0.1995	SLIT3	0.5258
EREG	0.1279	SLITRK5	0.9651
FKBP1A	0.6049	SORBS1	0.1688
GJD2	0.1083	TBP	0.2024
GNRH1	0.1992	TFDP2	0.1525
GRIN2B	0.0217	TMEM252	0.1308
HOXB8	0.3795	TNF	0.7841
HTR1B	0.8224	TRIOBP	0.8752
IGF1	0.0085	TSPAN14	0.2407
IGF1R	0.7069	TXNL1	0.8934
IRS2	0.5154	UBL3	0.0890
ITGA9	0.8512	ZBTB43	0.5905
KCNB2	0.3086	ZFP64	0.5493
KCNQ1	0.8696		

Note: Shown in this table are the gene-wide results from the MAGMA analyses of the 51 genes from the molecular landscape of OCD and the OCS factor 'symmetry/counting/ordering'. None of the individual genes reached the Bonferroni-corrected P-value threshold of significance (P= 0.05/51 = 0.00098).

SUPPLEMENTARY TABLE 5. PRS-based results for shared genetic etiology between OCD and two novel TOCS-based OCS factors and between five peripheral insulin signaling-related traits and two novel TOCS-based OCS factors.

'base' sample	'target' sample	P_T	P-value	R^2	nSNPs
OCD	**Symmetry/counting/ordering** $_{TOCS}$	**0.3**	**2.42E-05**	**0.49%**	**149119**
	Contamination/cleaning $_{TOCS}$	**0.4**	**4.07E-03**	**0.23%**	**185917**
Type 2 Diabetes	Symmetry/counting/ordering $_{TOCS}$	0.1	3.39E-01	0.03%	66870
	Contamination/cleaning $_{TOCS}$	**0.1**	**1.59E-03**	**0.28%**	**67614**
HbA1c	Symmetry/counting/ordering $_{TOCS}$	0.05	2.71E-01	0.04%	20779
	Contamination/cleaning $_{TOCS}$	0.001	1.68E-01	0.05%	1018
Fasting insulin	Symmetry/counting/ordering $_{TOCS}$	0.05	3.71E-01	0.02%	3926
	Contamination/cleaning $_{TOCS}$	0.05	4.37E-01	0.01%	3965
Fasting glucose	Symmetry/counting/ordering $_{TOCS}$	0.001	2.47E-01	0.04%	484
	Contamination/cleaning $_{TOCS}$	0.5	4.36E-01	0.01%	21851
2 h Glucose	Symmetry/counting/ordering $_{TOCS}$	0.05	4.45E-01	0.01%	2924
	Contamination/cleaning $_{TOCS}$	0.2	3.76E-01	0.02%	9344

Shown in this table are the best SNP P-value thresholds (P_T) for the PRSice analyses between OCD and two novel TOCS-based OCS factors and between five peripheral insulin signaling-related traits and two novel TOCS-based OCS factors, their Benjamini and Hochberg adjusted P-values for shared genetic etiology (P-value), the variance explained in the target sample phenotypes (R^2), and the number of SNPs (nSNPs). Significant findings are indicated in bold. Abbreviations: TOCS=Toronto Obsessive-Compulsive Scale

5

Supplementary Figures
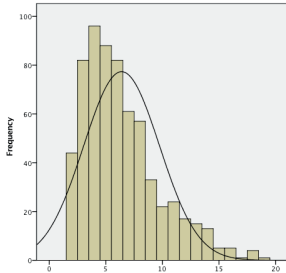
SUPPLEMENTARY FIGURE 1A. Histogram showing the distribution of the total OCS score in 650 children and adolescents aged 8-21 in the Philadelphia Neurodevelopmental Cohort (288 males and 362 females).
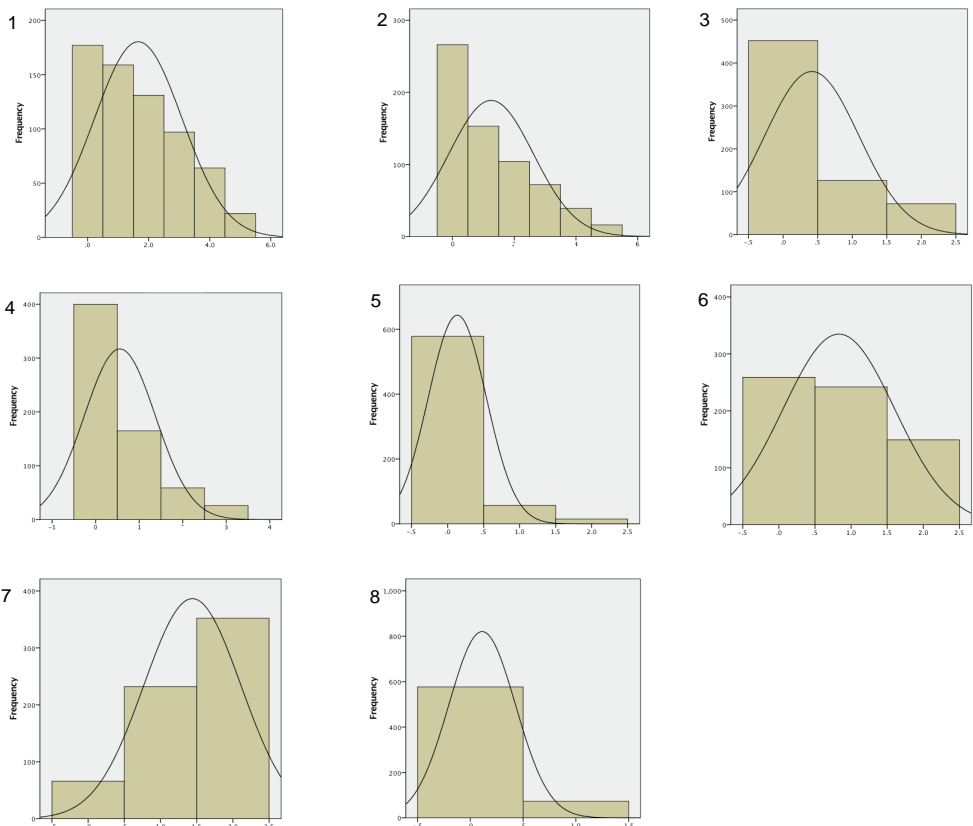

SUPPLEMENTARY FIGURE 1B. Histograms showing the distributions of the scores on eight OCS factors – that add up to the total OCS score – in 650 children and adolescents aged 8-21 in the Philadelphia Neurodevelopmental Cohort (288 males and 362 females): 1 'Impairment', 2 'Symmetry/counting/ordering', 3 'Contamination/cleaning', 4 'Aggressive taboo thoughts', 5 'Repetition', 6 'Guilty taboo thoughts', 7 'Distress', and 8 'Religious taboo thoughts'.
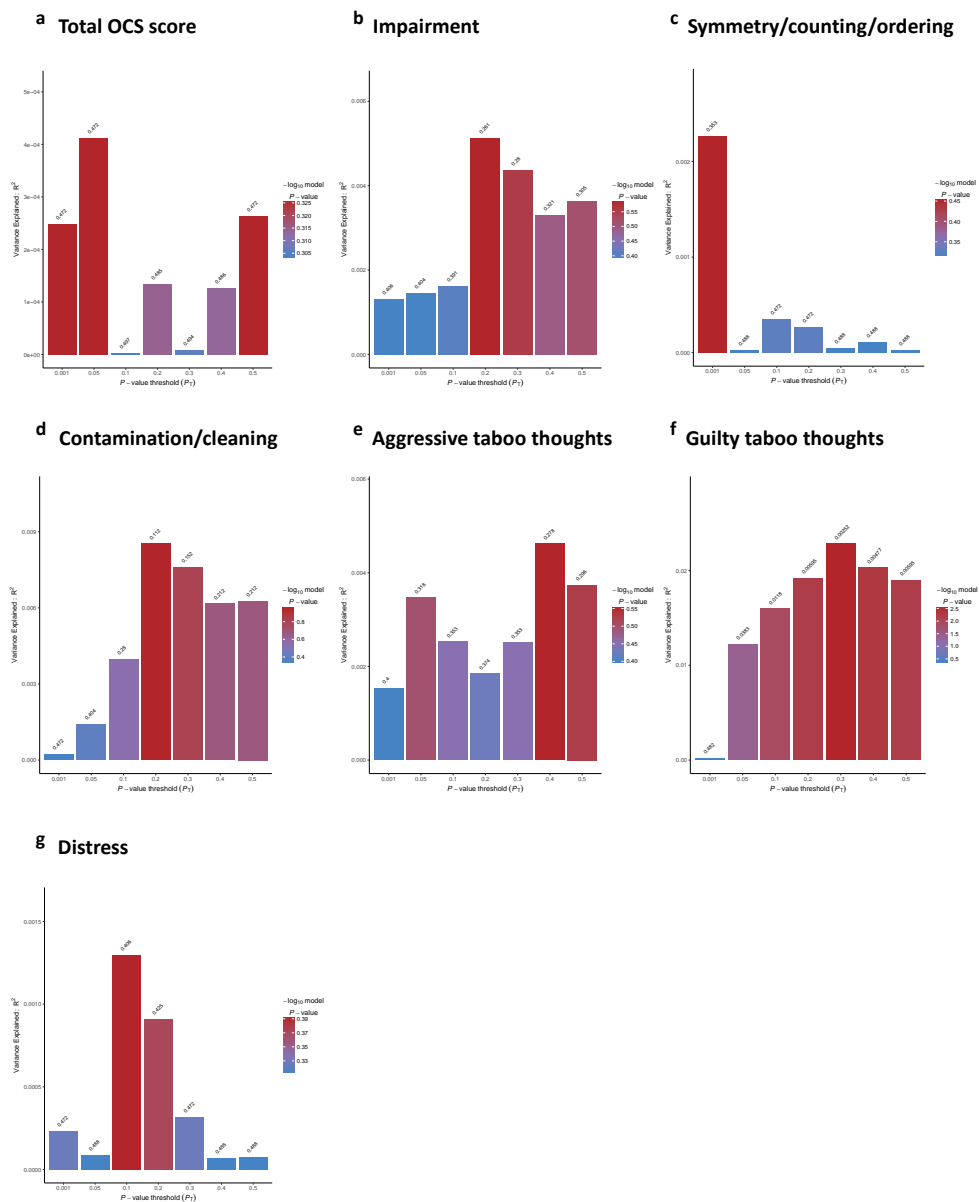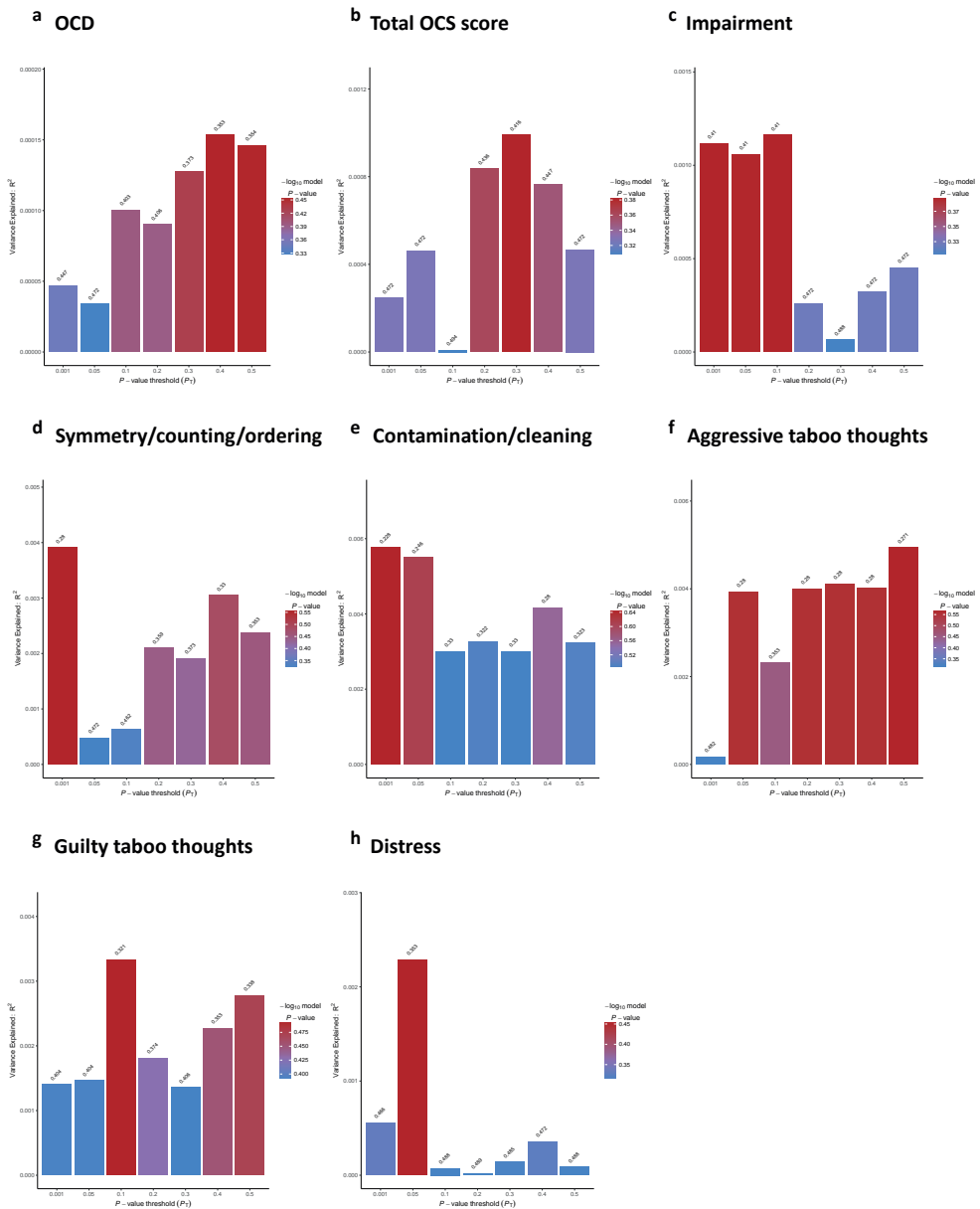
SUPPLEMENTARY FIGURE 2. Bar plots from PRSice showing results at seven broad P-value thresholds (P$_T$) for shared genetic etiology between obsessive-compulsive disorder (OCD) and the total obsessive-compulsive symptom (OCS) score as well as six OCS factors (a–g) (see Materials and Methods). The numbers above the bars indicate the P-values for shared genetic etiology, and these P-values were corrected using the Benjamini-Hochberg false discovery rate method.
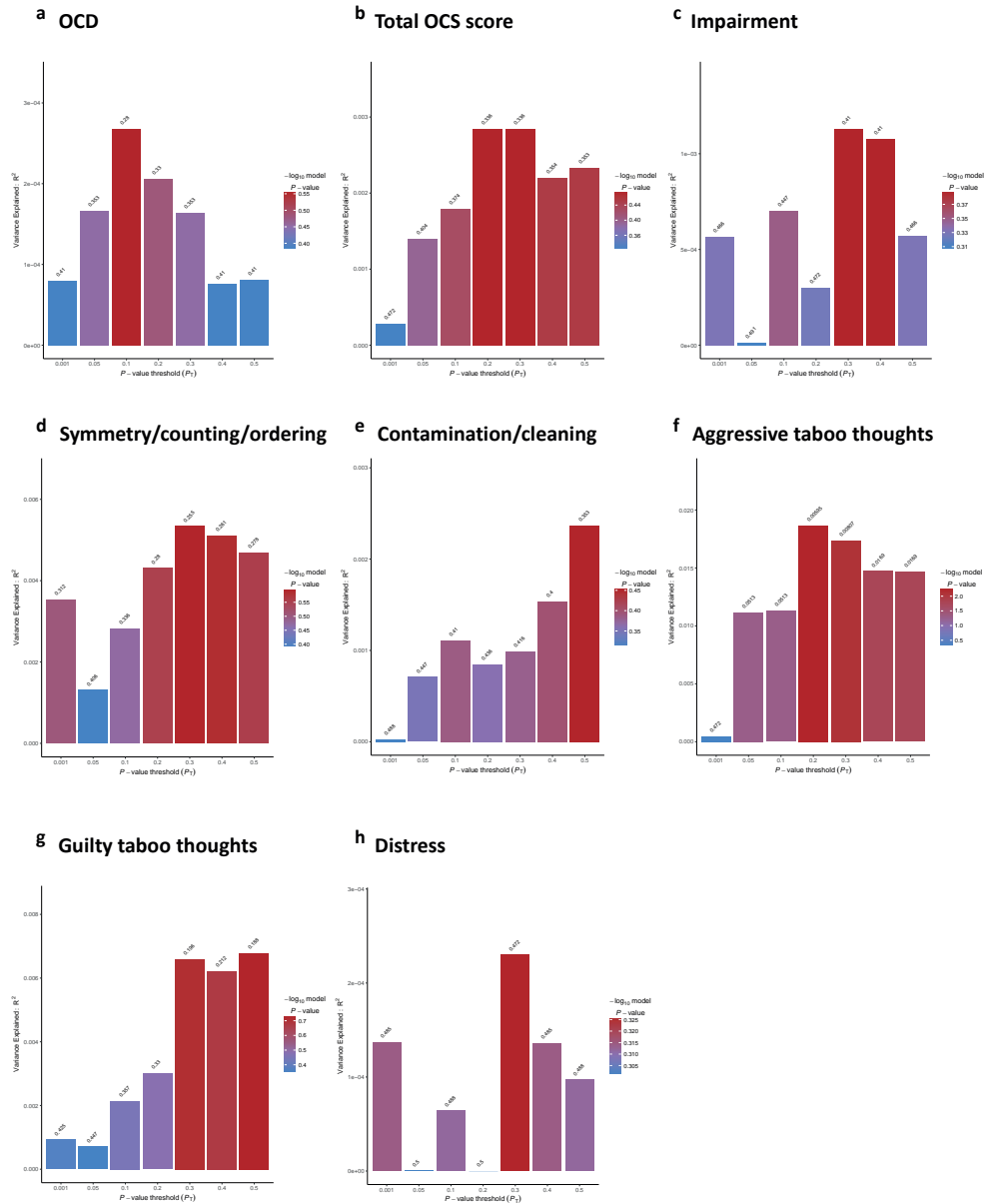
SUPPLEMENTARY FIGURE 3A. Bar plots from PRSice showing results at seven broad P-value thresholds (P_T) for shared genetic etiology between Type 2 Diabetes and obsessive-compulsive disorder (OCD), the total obsessive-compulsive symptom (OCS) score as well as six OCS factors (a–h) (see Materials and Methods). The numbers above the bars indicate the P-values for shared genetic etiology, and these P-values were corrected using the Benjamini-Hochberg false discovery rate method.
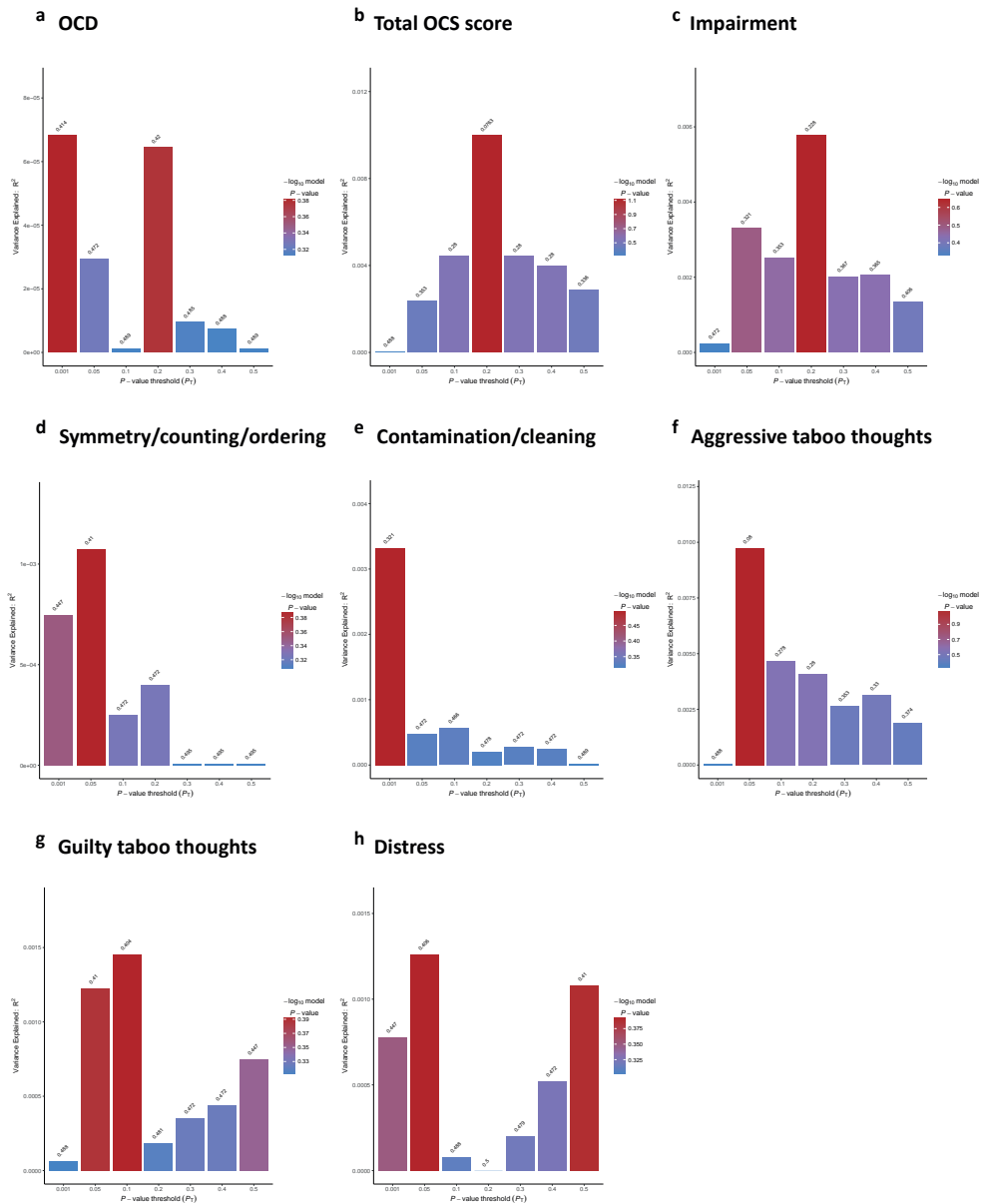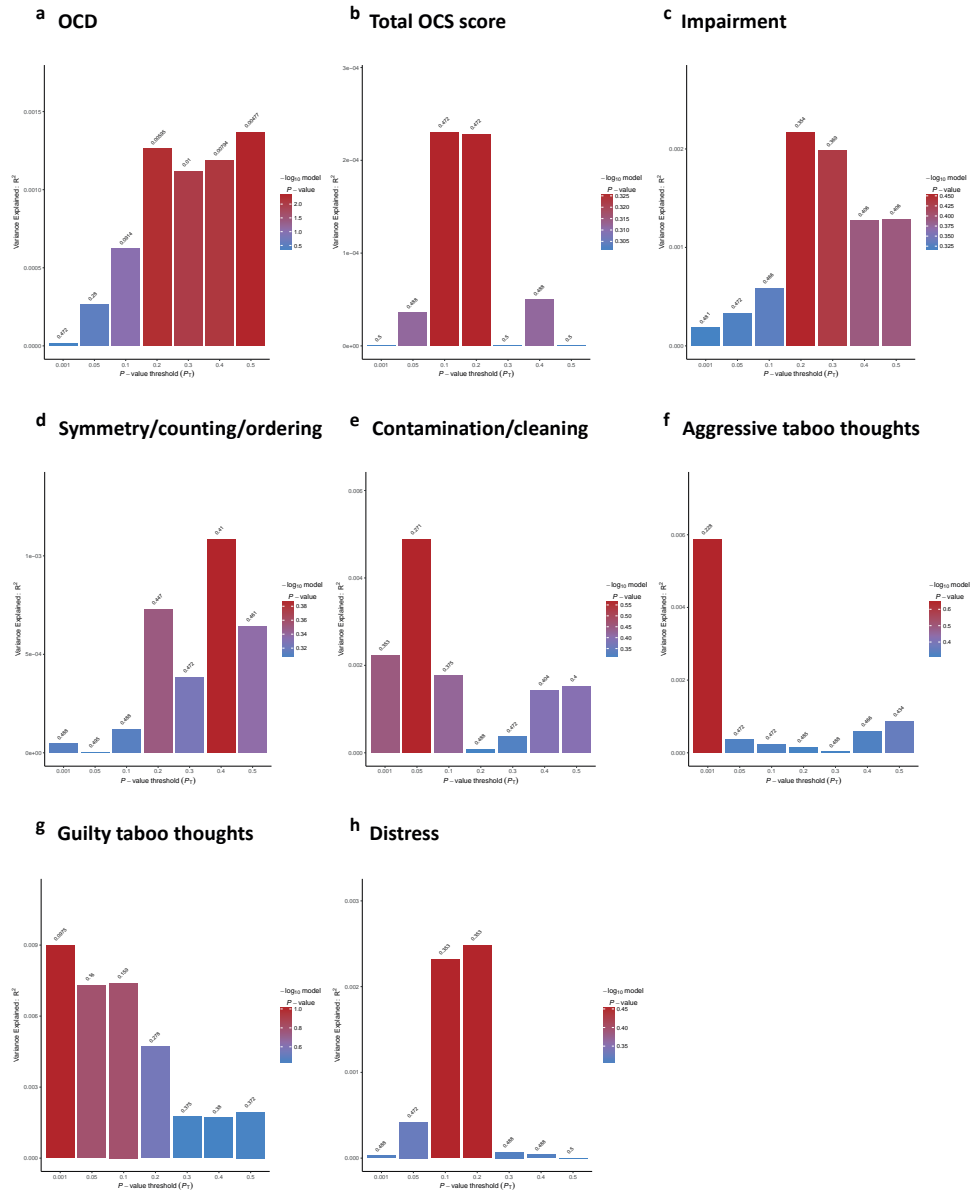
SUPPLEMENTARY FIGURE 3B. Bar plots from PRSice showing results at seven broad P-value thresholds (P_T) for shared genetic etiology between HbA1c blood levels and obsessive-compulsive disorder (OCD), the total obsessive-compulsive symptom (OCS) score as well as six OCS factors (a–h) (see Materials and Methods). The numbers above the bars indicate the P-values for shared genetic etiology, and these P-values were corrected using the Benjamini-Hochberg false discovery rate method.
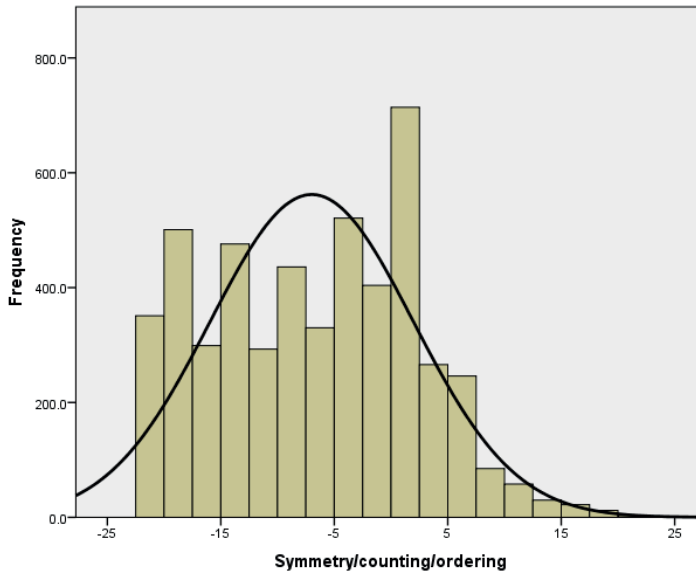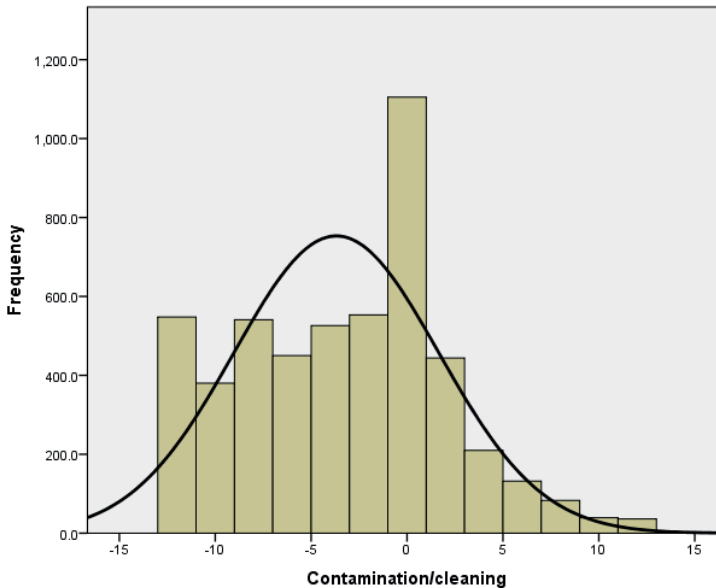
5
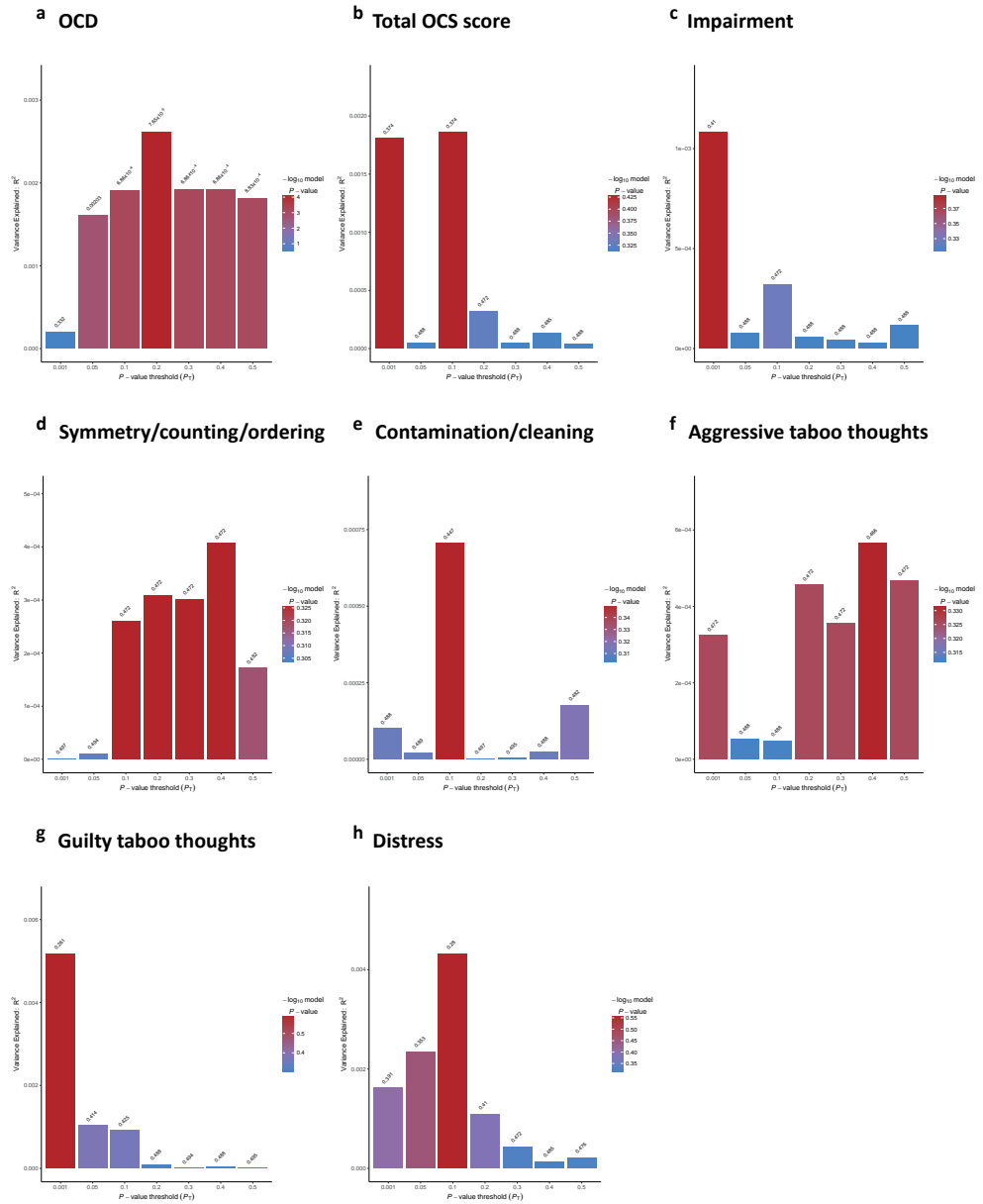
SUPPLEMENTARY FIGURE 3C. Bar plots from PRSice showing results at seven broad P-value thresholds (P_T) for shared genetic etiology between Fasting Insulin and obsessive-compulsive disorder (OCD), the total obsessive-compulsive symptom (OCS) score as well as six OCS factors (a–h) (see Materials and Methods). The numbers above the bars indicate the P-values for shared genetic etiology, and these P-values were corrected using the Benjamini-Hochberg false discovery rate method.

SUPPLEMENTARY FIGURE 3D. Bar plots from PRSice showing results at seven broad P-value thresholds (P$_T$) for shared genetic etiology between Fasting Glucose and obsessive-compulsive disorder (OCD), the total obsessive-compulsive symptom (OCS) score as well as six OCS factors (a–h) (see Materials and Methods). The numbers above the bars indicate the P-values for shared genetic etiology, and these P-values were corrected using the Benjamini-Hochberg false discovery rate method.

SUPPLEMENTARY FIGURE 3E. Bar plots from PRSice showing results at seven broad P-value thresholds (P_T) for shared genetic etiology between 2 h Glucose and obsessive-compulsive disorder (OCD), the total obsessive-compulsive symptom (OCS) score as well as six OCS factors (a–h) (see Materials and Methods). The numbers above the bars indicate the P-values for shared genetic etiology, and these P-values were corrected using the Benjamini-Hochberg false discovery rate method.

SUPPLEMENTARY FIGURE 4A. Histogram showing the distribution of the 'symmetry/counting/ordering' score in 5047 children and adolescents aged 6-17 in the Spit for Science Cohort.


SUPPLEMENTARY FIGURE 4B. Histogram showing the distribution of the 'contamination/cleaning' score in 5047 children and adolescents aged 6-17 in the Spit for Science Cohort.

a Symmetry/counting/ordering TOCS
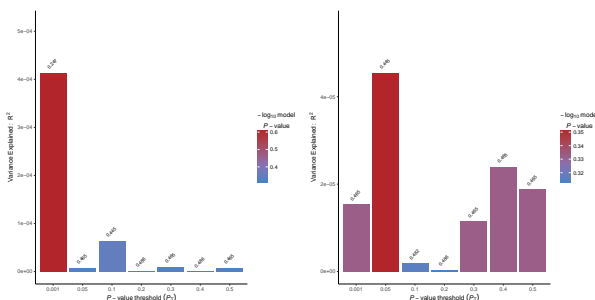
b Contamination/cleaning TOCS
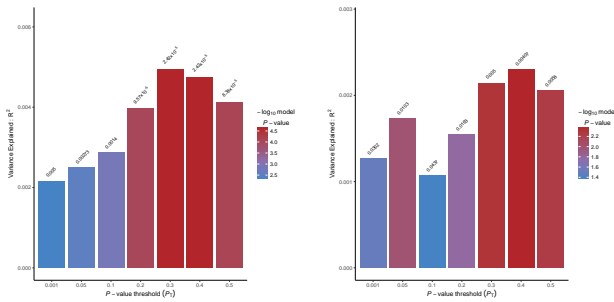
SUPPLEMENTARY FIGURE 5A. Bar plots from PRSice showing results at seven broad P-value thresholds (P_T) for shared genetic etiology between obsessive-compulsive disorder (OCD) and two TOCS OCS factors (see Materials and Methods). The numbers above the bars indicate the P-values for shared genetic etiology, and these P-values were corrected using the Benjamini-Hochberg false discovery rate method.

a Type 2 Diabetes
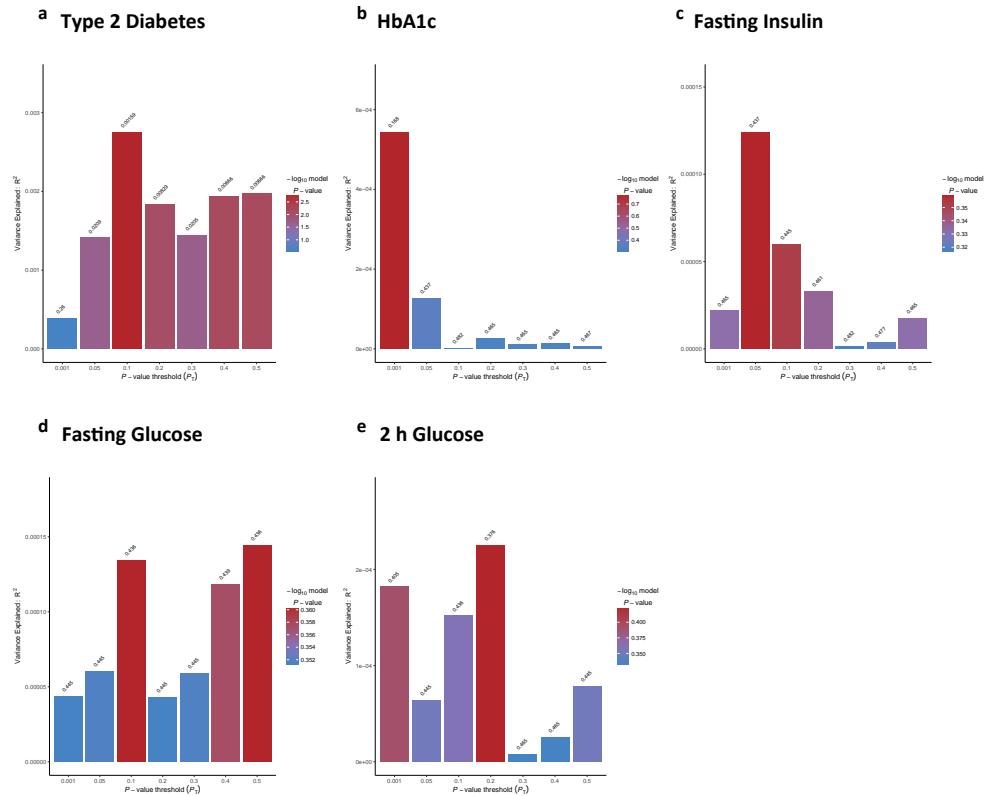
b HbA1c

c Fasting Insulin
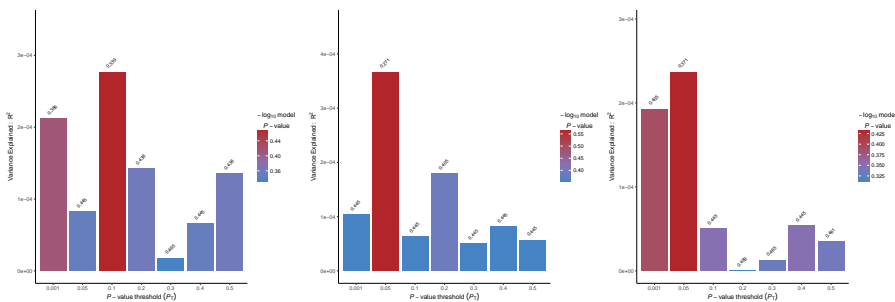
d Fasting Glucose

e 2 h Glucose

SUPPLEMENTARY FIGURE 5B. Bar plots from PRSice showing results at seven broad P-value thresholds (P_T) for shared genetic etiology between five peripheral insulin signaling-related traits (Type 2 Diabetes, HbA1C blood levels and blood levels of fasting insulin, fasting glucose and 2h Glucose) and TOCS factor 'symmetry/counting/ordering' (a–e) (see Materials and Methods). The numbers above

the bars indicate the P-values for shared genetic etiology, and these P-values were corrected using the Benjamini-Hochberg false discovery rate method.

SUPPLEMENTARY FIGURE 5C. Bar plots from PRSice showing results at seven broad P-value thresholds (P_T) for shared genetic etiology between five peripheral insulin signaling-related traits (Type 2 Diabetes, HbA1C blood levels and blood levels of fasting insulin, fasting glucose and 2h Glucose) and TOCS factor 'contamination/cleaning' (a–e) (see Materials and Methods). The numbers above the bars indicate the P-values for shared genetic etiology, and these P-values were corrected using the Benjamini-Hochberg false discovery rate method.

REFERENCES

1. Satterthwaite, T.D.; Connolly, J.J.; Ruparel, K.; Calkins, M.E.; Jackson, C.; Elliott, M.A.; Roalf, D.R.; Ryan Hopsona, K.P.; Behr, M.; Qiu, H.; et al. The Philadelphia Neurodevelopmental Cohort: A publicly available resource for the study of normal and abnormal brain development in youth. *Neuroimage* **2016**, *124*, 1115-1119, doi:10.1016/j.neuroimage.2015.03.056.

2. Calkins, M.E.; Merikangas, K.R.; Moore, T.M.; Burstein, M.; Behr, M.A.; Satterthwaite, T.D.; Ruparel, K.; Wolf, D.H.; Roalf, D.R.; Mentch, F.D.; et al. The Philadelphia Neurodevelopmental Cohort: constructing a deep phenotyping collaborative. *Journal of child psychology and psychiatry, and allied disciplines* **2015**, *56*, 1356-1369, doi:10.1111/jcpp.12416.

3. Satterthwaite, T.D.; Elliott, M.A.; Ruparel, K.; Loughead, J.; Prabhakaran, K.; Calkins, M.E.; Hopson, R.; Jackson, C.; Keefe, J.; Riley, M.; et al. Neuroimaging of the Philadelphia neurodevelopmental cohort. *NeuroImage* **2014**, *86*, 544-553, doi:10.1016/j.neuroimage.2013.07.064.

4. Gur, R.C.; Calkins, M.E.; Satterthwaite, T.D.; Ruparel, K.; Bilker, W.B.; Moore, T.M.; Savitt, A.P.; Hakonarson, H.; Gur, R.E. Neurocognitive growth charting in psychosis spectrum youths. *JAMA Psychiatry* **2014**, *71*, 366-374, doi:10.1001/jamapsychiatry.2013.4190.

5. Glessner, J.T.; Reilly, M.P.; Kim, C.E.; Takahashi, N.; Albano, A.; Hou, C.; Bradfield, J.P.; Zhang, H.; Sleiman, P.M.; Flory, J.H.; et al. Strong synaptic transmission impact by copy number variations in schizophrenia. *Proceedings of the National Academy of Sciences of the United States of America* **2010**, *107*, 10584-10589, doi:10.1073/pnas.1000274107.

6. Euesden, J.; Lewis, C.M.; O'Reilly, P.F. PRSice: Polygenic Risk Score software. *Bioinformatics* **2015**, *31*, 1466-1468, doi:10.1093/bioinformatics/btu848.

7. Purcell, S.; Neale, B.; Todd-Brown, K.; Thomas, L.; Ferreira, M.A.; Bender, D.; Maller, J.; Sklar, P.; de Bakker, P.I.; Daly, M.J.; et al. PLINK: a tool set for whole-genome association and population-based linkage analyses. *Am J Hum Genet* **2007**, *81*, 559-575, doi:10.1086/519795.

8. Benjamini, Y.; Hochberg, Y. Controlling the false discovery rate: a practical and powerful approach to multiple testing. *J R Stat Soc Ser B (Methodological)* **1995**, *57*, 289-300.

9. Glickman, M.E.; Rao, S.R.; Schultz, M.R. False discovery rate control is a recommended alternative to Bonferroni-type adjustments in health studies. *Journal of clinical epidemiology* **2014**, *67*, 850-857, doi:10.1016/j.jclinepi.2014.03.012.

10. Scott, R.A.; Scott, L.J.; Magi, R.; Marullo, L.; Gaulton, K.J.; Kaakinen, M.; Pervjakova, N.; Pers, T.H.; Johnson, A.D.; Eicher, J.D.; et al. An Expanded Genome-Wide Association Study of Type 2 Diabetes in Europeans. *Diabetes* **2017**, *66*, 2888-2902, doi:10.2337/db16-1253.

11. Wheeler, E.; Leong, A.; Liu, C.T.; Hivert, M.F.; Strawbridge, R.J.; Podmore, C.; Li, M.; Yao, J.; Sim, X.; Hong, J.; et al. Impact of common genetic determinants of Hemoglobin A1c on type 2 diabetes risk and diagnosis in ancestrally diverse populations: A transethnic genome-wide meta-analysis. *PLoS Med* **2017**, *14*, e1002383, doi:10.1371/journal.pmed.1002383.

12. Scott, R.A.; Lagou, V.; Welch, R.P.; Wheeler, E.; Montasser, M.E.; Luan, J.; Magi, R.; Strawbridge, R.J.; Rehnberg, E.; Gustafsson, S.; et al. Large-scale association analyses identify new loci influencing glycemic traits and provide insight into the underlying biological pathways. *Nat Genet* **2012**, *44*, 991-1005, doi:10.1038/ng.2385.

13. van de Vondervoort, I.; Poelmans, G.; Aschrafi, A.; Pauls, D.L.; Buitelaar, J.K.; Glennon, J.C.; Franke, B. An integrated molecular landscape implicates the regulation of dendritic spine formation through insulin-related signalling in obsessive-compulsive disorder. *Journal of psychiatry & neuroscience : JPN* **2016**, *41*, 280-285, doi:10.1503/jpn.140327.

14. de Leeuw, C.A.; Mooij, J.M.; Heskes, T.; Posthuma, D. MAGMA: generalized gene-set analysis of GWAS data. *PLoS computational biology* **2015**, *11*, e1004219, doi:10.1371/journal.pcbi.1004219.

5
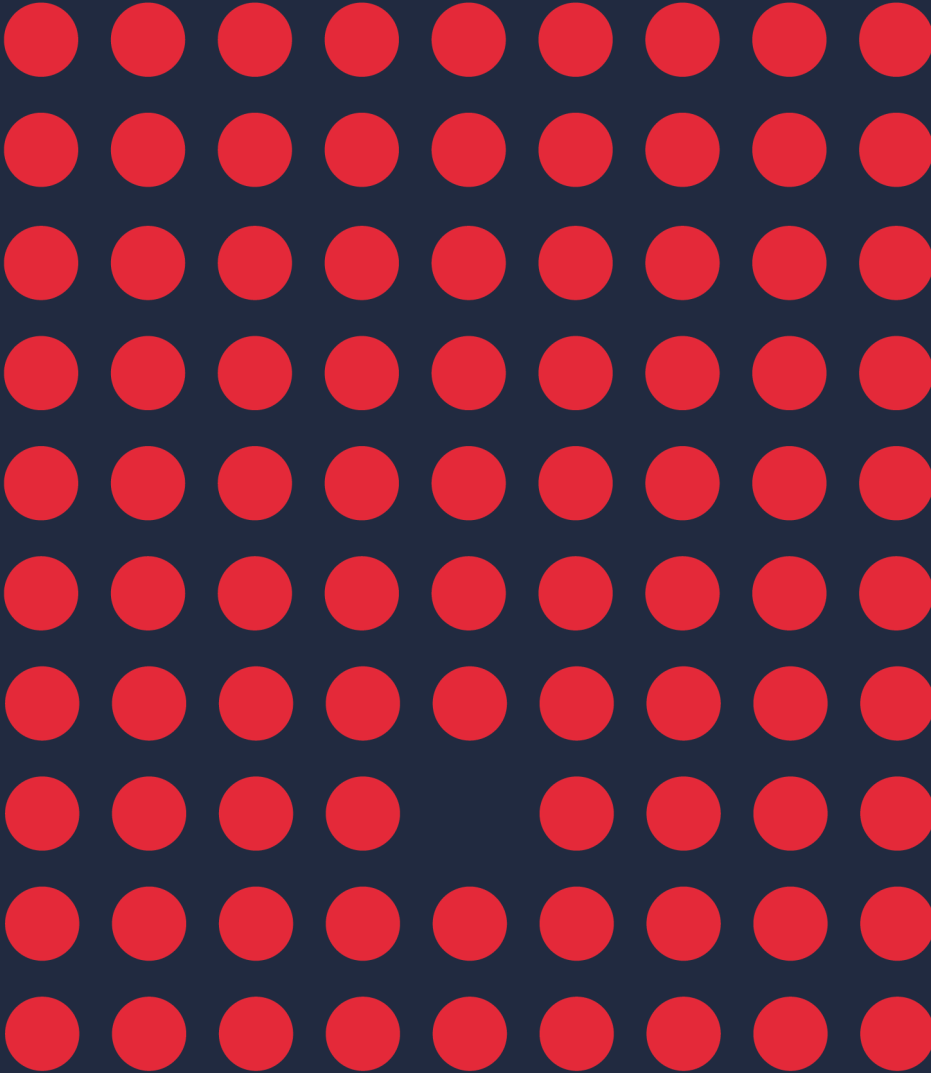
CHAPTER 6

SUMMARY AND GENERAL DISCUSSION

TD and OCD are both phenotypically heterogenous disorders with complex etiologies and they are frequently comorbid. Because the neurobiological and molecular underpinnings of these disorders are poorly understood and current treatments are only partially effective, there has been and continues to be intensive research on the molecular and cellular mechanisms underlying TD/OCD and their therapies, in order to determine the factors that convey risk or resilience. This thesis includes studies based on animal model and human omics data that used an integrated approach – including analyses at the cellular, molecular, and behavioral levels – and were aimed at advancing our knowledge of the altered molecular mechanisms involved in TD and OCD and the identification of putative novel treatment targets. In this final chapter, I will briefly summarize the studies presented in the thesis, and I will integrate and discuss the main findings.

SUMMARY OF THE MAIN FINDINGS FROM THE THESIS

In **Chapter 2**, we investigated whether early life stress modulates the individual susceptibility to PANDAS – Pediatric Autoimmune Neuropsychiatric Disorders Associated with Streptococcus – through a longitudinal study in mice. We observed that injections with Group A Streptococcal (GAS) bacteria induced PANDAS behavioral abnormalities – i.e., TD- and/or OCD-like symptoms – in mice (such as reduced sensorimotor gating and increased perseverative behavior), as well as a reduced reactivity to a serotonergic agonist and increased inflammatory infiltrates in the anterior diencephalon. Neonatal corticosterone (CORT) administration – mimicking chronic stress – mitigated most of the GAS-induced behavioral, immunohistochemical and molecular alterations. These compensatory effects co-occurred with modifications in hypothalamic pituitary adrenal axis (HPA) activity that was reflected in increased circulating glucocorticoids concentrations, as well as increased serum levels of the anti-inflammatory cytokine IL-9 and changes in striatal gene expression. Our analyses of the striatal differential gene expression data highlighted a role of the female sex hormone (beta)-estradiol and other signaling molecules regulated by estradiol (FGF2, IgG, DA, LH, LEP, IL2, IKBKB) as important upstream regulators of molecular mechanisms associated with the phenotypic abnormalities observed in GAS mice and the compensatory role of neonatal CORT. Specifically, GAS exposures inhibited (beta)-estradiol-mediated regulation of gene expression, while neonatal CORT compensated for this effect. These data support the hypothesis that elevations in glucocorticoids may promote central immunomodulatory processes.

TD is also conceptualized as a hyperkinetic movement disorder, or dyskinesia, characterized by excessive and repetitive abnormal involuntary movements (AIMs) or tics [1].

AIMs also often develop after chronic administration of Levodopa, the first-line treatment of dystonic symptoms in childhood or in Parkinson's disease, leading to the development of so-called Levodopa-Induced Dyskinesia (LID). Riluzole has been suggested as a candidate drug to treat AIMs/LID. Therefore, in **Chapter 3**, we investigated the behavioral and molecular effects of Riluzole in a juvenile rat model of LID. We observed that Riluzole attenuated Levodopa-induced AIMs in the rat model. Subsequently, our analysis of differential striatal gene expression data from LID rats revealed that Riluzole is predicted to reduce the activity of CREB1 (cAMP response element binding protein 1). CREB1 is a transcription factor that regulates the expression of multiple interacting proteins involved in regulating neuronal processes, such as neuronal survival/apoptosis, differentiation, and development and that acts as a functional 'go-between' between cytoplasmic kinase/enzyme signaling cascades and nuclear regulation of gene expression.

In **Chapter 4**, we integrated the available human omics data on TD to build a so-called 'molecular landscape' of the disease. More specifically, we compiled a list of TD candidate genes, and we subsequently conducted tissue/cell type specificity and functional enrichment analyses of this list. Using genomic data, we also investigated genetic sharing between TD and blood and cerebrospinal fluid (CSF) metabolite levels. We found that the TD candidate genes show enriched expression in four brain regions (cerebellum, cortex, striatum, and thalamus) across various developmental periods and the pituitary. The functional enrichment analyses implicated two pathways, i.e., 'cAMP-mediated signaling' and 'Endocannabinoid Neuronal Synapse Pathway', as well as multiple biological functions related to brain development and synaptic transmission in TD etiology. Further, we found genetic sharing between TD and the blood and CSF levels of 39 metabolites, including butyrate, NAAG, myo-inositol, the cytokine TNFB and polyunsaturated fatty acids such as arachidonic acid. Lastly, we integrated the different types of omics data to build the molecular landscape of TD that provides insights into the (altered) molecular processes that underlie the disease and that identifies putative novel drug targets (including FLT3, NAALAD2, CX3CL1-CX3CR1, OPRM1, and HRH2) that could be modulated with a beneficial effect on TD.

Epidemiological and genetic studies have shown associations between clinical OCD and obsessive-compulsive symptoms (OCS) in the population. Further, dysregulated insulin signaling in the periphery and central nervous system (CNS) has been implicated in both OCD and OCS. In **Chapter 5**, we built on this previous work by assessing the presence and extent of shared genetic etiology between OCD, OCS in the population, and peripheral and CNS insulin signaling, using the largest available genomic data sets. Our polygenic risk score (PRS)-based analyses revealed genetic overlap between OCD and three OCS, i.e., 'guilty taboo thoughts', 'symmetry/counting/ordering' and 'contamination/cleaning',

assessed across two population cohorts of children and adolescents. As for peripheral insulin signaling, we identified genetic sharing between Type 2 Diabetes and two OCS, i.e., 'aggressive taboo thoughts' and 'contamination/cleaning', and between two insulin-related traits – blood levels of fasting insulin and 2 h glucose – and OCD. Furthermore, a set of OCD genes centered around CNS insulin signaling was associated with 'symmetry/counting/ordering'. Taken together, these findings provide further support for (at least partial) genetic overlap between OCD and population-based OCS, as well as for altered insulin signaling as a common biological process contributing to both OCD and OCS in the population.

DISCUSSION OF THE FINDINGS
Translation of findings from animal models to human disease

A better understanding of the cellular and molecular mechanisms underlying TD and OCD and their therapies is critical for developing more effective treatments. In this respect, animal models have proven invaluable in the study of these mechanisms. In **Chapters 2** and **3**, we used two animal models of TD/OCD-related behaviors and performed transcriptomic profiling of the striatal tissue to investigate the molecular mechanisms associated with disease and altered by the therapeutic interventions (neonatal stress and Riluzole). In this way, we were able to pinpoint a number of upstream regulators that could be driving the observed changes in gene expression.

To assess the similarities between disease-associated molecular processes occurring in animal models and humans – and hence attempt to translate findings from animal models to human disease – I have compared (i) the list of TD candidate genes constructed based on the genomic data on TD and used to build the molecular landscape of TD, as well as the list of differentially expressed genes observed in the brains (striatum) of TD patients (both described in **Chapter 4**) with the differentially expressed genes observed in animal models described in **Chapter 2** and **Chapter 3**, and (ii) the results from functional enrichment analyses performed on these sets of genes that inform on the biological processes involved.

Overall, the two rodent models produced distinct striatal differential gene expression signatures induced by GAS and L-DOPA administration, as well as the modulatory effects of neonatal stress and Riluzole, respectively. I have compared the gene expression signatures present in each of the animal models, focusing on the genes that were shared with the TD candidate genes and the genes that are differentially expressed in the postmortem striatum of TD patients.

As for the PANDAS mice model, the orthologs of 24 TD candidate genes were found to be (also) affected by GAS infection or neonatal CORT administration in GAS mice (Figure 1).

Of the four genes that we found to be differentially expressed upon GAS infection, two genes encode TD landscape proteins: *KM2TD* was upregulated and *CHDH* was downregulated. Among the 20 genes affected by neonatal CORT administration in GAS mice, 12 were also encoding landscape proteins, with *CHGB, ASB8, ADM, CPS1, FKBP11, MACROD1, MAPT* and *PEX11* being upregulated, and *FARP2, KIF26, ME2,* and *RELN* being downregulated. Further, 25 genes were differentially expressed in the TD postmortem striatum, including *TGFB3* that encodes a TD landscape protein. *TGFB3* was upregulated in CORT-GAS mice, suggesting that its increased expression in TD postmortem striatum could be a compensatory effect.
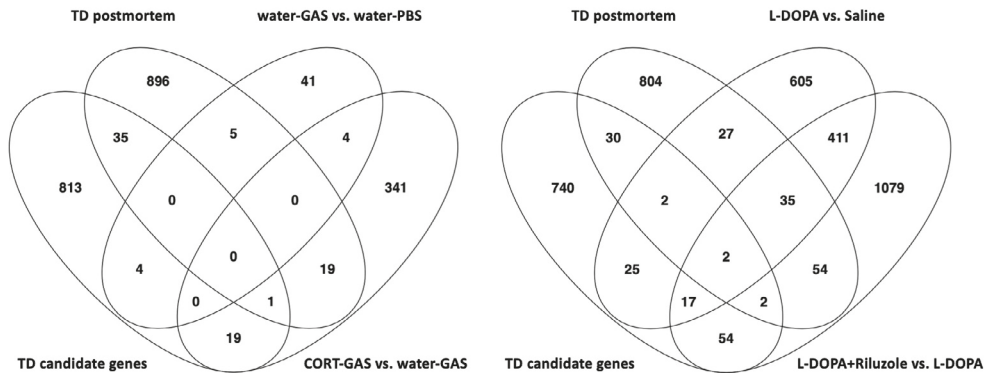

FIGURE 1. Venn diagrams representing the comparisons of gene lists generated and/or analyzed in Chapter 2 (water-GAS vs. water-PBS, CORT-GAS vs. water-GAS), Chapter 3 (L-DOPA vs. Saline, L-DOPA + Riluzole vs. L-DOPA) and Chapter 4 (TD candidate genes, TD postmortem striatum) of this thesis.

As for the LID rat model, when we focus on the (465) genes of which the expression was affected by L-DOPA and restored by Riluzole treatment (**Chapter 3**), the orthologs of 19 genes were also TD candidate genes (Figure 1). Of these, two TD landscape genes (*CDKN1A* and *PIM1*) were also found to be upregulated in TD postmortem brain, and this change in expression was concordant with their expression being upregulated upon L-DOPA and restored (i.e., downregulated again) by Riluzole in the LID rat model. Furthermore, 35 genes were differentially expressed in the (human) TD postmortem brain and after L-DOPA and Riluzole administration in rats (Figure 1). Among them, 25 genes show the same pattern of expression as *CDKN1A* and *PIM1*, i.e., upregulation in TD postmortem striatum and upon L-DOPA administration in the rat model, and downregulation upon Riluzole treatment. This concordant pattern of expression between (human) postmortem TD striatum and rats treated with L-DOPA to induce AIMs suggests that similar biological mechanisms are underlying the disease in humans and animals, while the restoring effect of Riluzole suggests that decreasing gene expression leads to a reduction of TD symptoms. One of the 25 genes that follow the

above-described expression pattern is *CX3CL1*, a gene that encodes one of the key potential novel drug targets emerging from the TD landscape (**Chapter 4**). *KCNE5* – coding for a potassium channel subunit – is another gene of which the expression shows the same pattern, while it is also downregulated by neonatal CORT in GAS mice. Interestingly, the TD landscape protein PIM1 phosphorylates (and hence regulates the activity of) CDKN1A and its expression is regulated by FLT3 [2-4], one of the key potential drug targets for TD from our landscape (**Chapter 4**). In this respect, the abovementioned results from our experiments in the LID rat model – i.e., L-DOPA upregulates the expression of *CDKN1A* and *PIM1* whereas Riluzole reduces the expression of these genes – provide further support for our selection of FLT3 as a novel drug target for TD that should be inhibited to have a beneficial effect on TD symptoms. Further, 10 of the 35 affected genes (including *CRH* that encodes a TD landscape protein) were downregulated in both TD postmortem striatum and upon Riluzole treatment in LID rats and upregulated upon L-DOPA injection (or vice versa). This concordant expression pattern between TD postmortem striatum and from LID-rats treated with Riluzole (and discordant for the L-DOPA effect) could reflect compensatory molecular mechanisms in TD. Furthermore, 27 TD candidate genes were differentially expressed upon L-DOPA treatment but not upon Riluzole and two of these genes (*CHGB* and *VGF*), both encoding proteins in the TD landscape) have also shown decreased expression in TD postmortem brain, which is discordant with the changes after L-DOPA administration. Another 27 genes were differentially expressed in TD postmortem striatum and upon L-DOPA treatment, with both concordant and discordant expression patterns. One of these 27 genes – *SERPINE1* – was also differentially expressed in the PANDAS mice model, and we found that *SERPINE1* expression was downregulated upon CORT treatment of GAS mice. Moreover, 56 TD candidate genes were found to be affected by Riluzole treatment in the LID rat model and not by L-DOPA, of which two genes – *OPRK1* and *DOC3* – were also differentially expressed in TD postmortem striatum. *OPRK1* was downregulated in postmortem TD striatum and upregulated upon Riluzole treatment in the LID rat model, suggesting that increasing its expression would have a beneficial effect on TD. This is especially relevant given that OPRK1 is a landscape protein, and it is one of the opioid receptors that we proposed as a group of putative novel TD drug targets (**Chapter 4**). Lastly, 54 genes were differentially expressed in TD postmortem striatum and after Riluzole treatment (Figure 1). These include three genes – *PROK2, SELPLG* and *TGFB1* – that encode TD landscape proteins of which the expression is increased in the postmortem TD brain and decreased in Riluzole-treated LID rats, implying that lowering the expression of these genes could be beneficial for TD. Overall, the concordance and discordance of expression of individual genes varied between each animal model and their expression profiles in postmortem TD brain. Nevertheless, the examples discussed above provide evidence that the findings from studies

in animals could be translated to (research in) humans and inform about the underlying molecular mechanisms and possible treatments of TD.

Furthermore, some biological processes seem to emerge as important in TD etiology from both the analyses we performed for building the TD landscape and our experiments in the animal models.

As further detailed in **Chapter 4**, the functional gene enrichment analysis of the TD candidate genes for the landscape implicated the 'cAMP-mediated signaling' pathway and the 'Endocannabinoid neuronal synapse pathway' in the disease, as well as several other functional themes linked to nervous system development and functions, e.g., neurogenesis and synaptic transmission. Interestingly, the enrichment analysis of the genes of which the expression was affected by L-DOPA and restored by Riluzole treatment (**Chapter 3**) revealed CREB1 as the main signaling hub regulating the expression of 43 interacting proteins that form a molecular landscape and are involved in processes such as neuronal survival, differentiation, and development. Furthermore, CREB1 – 'cAMP responsive element binding protein 1' is part of the cAMP signaling pathway [1] in which it acts as a phosphorylation-dependent transcription factor that stimulates transcription upon binding to the cAMP response element (CREs) in target genes. More specifically, CREB1 is known to be activated through phosphorylation by kinases – including ERK1 (MAPK3) and ERK2 (MAPK1), protein kinase C (PKC) and protein kinase A (PKA) – which in turn leads to reduced neuronal apoptosis as a result of anti-apoptotic genes being upregulated by activated CREB1 [5-7]. In addition, L-DOPA administration to 6-OHDA-lesioned rats was found to markedly increase CREB1 phosphorylation in striatal neurons while Riluzole reduces neuronal CREB1 phosphorylation [8-10]. Furthermore, another signaling cascade in the landscape of CREB1-regulated proteins centers around CDKN1A, a transcription factor that is involved in 6-OHDA-induced dopaminergic cell death and that is also an important TD landscape protein (see above). Together, these findings across human and animal studies highlight the central role of cAMP signaling in the etiology/pathophysiology and possibly also treatment of TD.

Lastly, we found genetic sharing between TD and decreased CSF levels of butyrate (butyric acid/ BA, see **Chapter 4**) and in this respect, it is interesting that BA as an 'upstream regulator' was also predicted to be activated in GAS mice that have been neonatally exposed to corticosterone (CORT) and that have attenuated GAS-induced behaviors (**Chapter 2**). BA is a short chain fatty acid that is naturally produced by bacterial fermentation of undigested carbohydrates, such as dietary fibers in the gut. Moreover, decreased levels of BA-producing bacteria were not only found in TD patients (**Chapter 4**) but also in children with paediatric acute-onset neuropsychiatric syndrome (PANS), which adds further weight to our findings in the PANDAS mice model. In addition, BA has been shown to modulate cAMP signaling, CDKN1A

6

and ESR1 expression [11-14], and to positively affect memory-related synaptic plasticity [15], further integrating animal and human study findings and providing a stronger rationale for using BA-increasing approaches – e.g., through changing the gut microbiome – as adjunctive treatments for TD [16]. Another molecule that links our findings is beta-estradiol, the active form of the main female sex hormone estrogen. First, as an upstream regulator, beta-estradiol was predicted to be inhibited in GAS mice and activated in GAS mice that have been neonatally exposed to CORT and that have attenuated GAS-induced behaviors (**Chapter 2**). We also found that the estrogen receptor ESR1 is one of the most interactive proteins in the TD landscape, where it acts as a cytoplasmic adapter protein or as a nuclear transcription factor (**Chapter 4**). The nuclear translocation – and hence transcriptional activation – of ESR1 is positively regulated by the TD landscape protein MACROD1 [17] and, interestingly, the expression of *MACROD1* was increased in GAS mice that have been neonatally exposed to CORT (**Chapter 2**).

Molecular similarities and differences between TD and comorbid neuropsychiatric disorders (ASDs, ADHD and OCD)

In **Chapter 4**, we built a molecular landscape of TD, by applying and extending the approach that was used before to build molecular landscapes of related neuropsychiatric disorders, i.e., autism spectrum disorders (ASDs) [5], attention-deficit/hyperactivity disorder (ADHD) [6], and obsessive-compulsive disorder (OCD) [7].
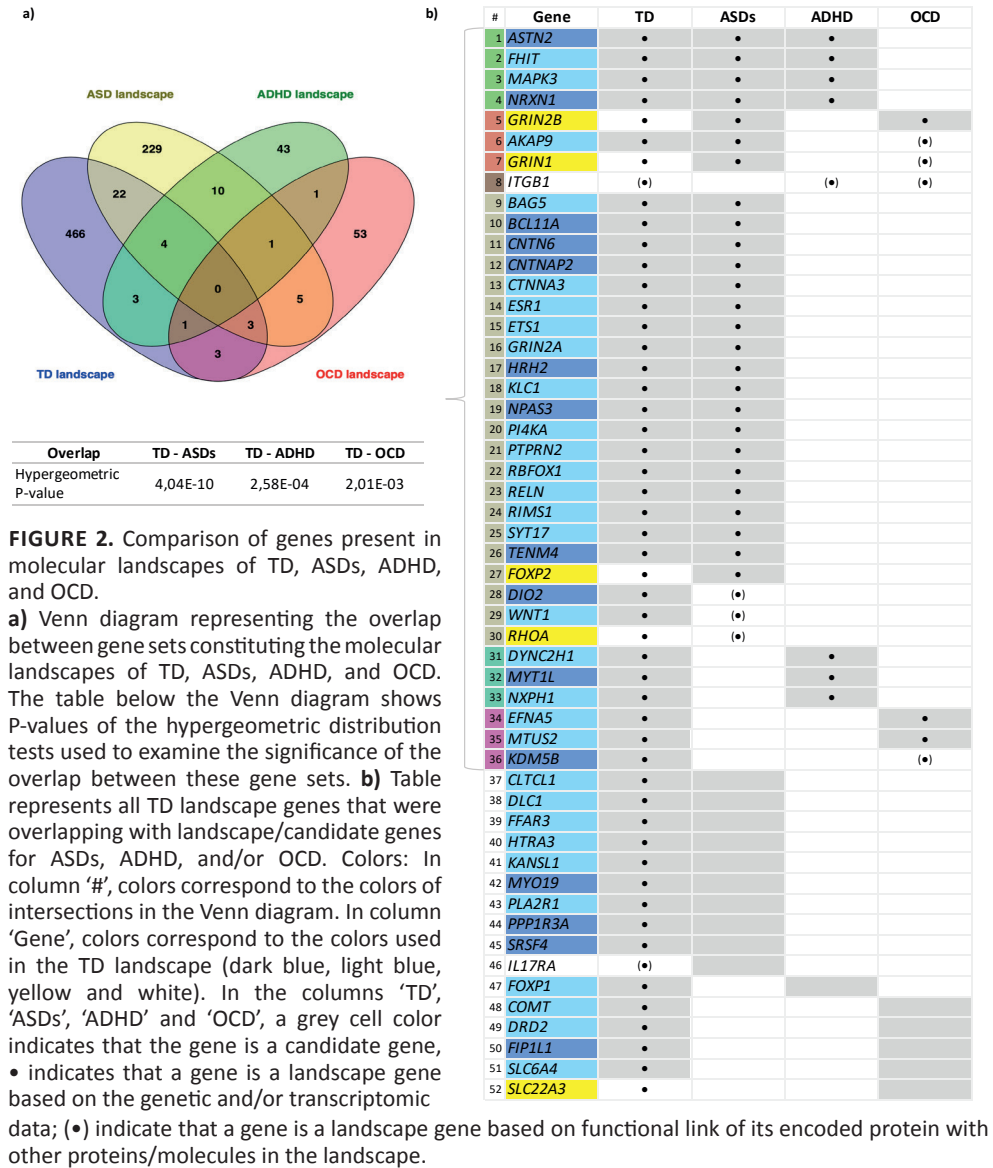
When comparing our findings for TD with findings for the three disorders, we observed that certain genes, biological processes and signaling pathways are common between TD and ASDs, ADHD and/or OCD, whereas other genes/processes/pathways seem to be (more) specific to a disorder. On a gene level, we observe a significant overlap between genes/proteins present in the molecular landscape of TD and the landscapes of all three disorders, with the strongest overlap signal between TD- and ASDs-related genes (hypergeometric P-value = 4.04E-10) (Figure 2a). In total, 36 genes are implicated in TD and at least one other disorder (Figure 2b, rows 1-36), with the largest overlap being for ASD (29 genes), followed by ADHD (8 genes) and OCD (7 genes). Eight genes are shared between TD and two other disorders, i.e., *ASTN2*, *FHIT*, *MAPK3*, *NRXN1* are implicated in TD, ASDs and ADHD, while *AKAP9*, *GRIN1* and *GRIN2B* encode proteins in the landscapes of TD, ASDs and OCD, and ITGB1 functionally interacts with proteins in the landscapes of TD, ADHD and OCD (Figure 2b). Furthermore, sixteen TD landscape genes were also implicated in ASDs, ADHD and/or OCD through genetic evidence, although they could not be directly placed in the landscapes of these disorders at the time they were built (rows 37-52 in Figure 2b).

As for biological processes, genes/proteins interacting in the molecular landscapes of TD, ASDs, ADHD and OCD were all functionally enriched in categories related to neurological

disease and nervous system development and function. The neurobiological processes of neurogenesis – involving neurite outgrowth and formation of dendritic spines – seem to be shared across all four disorders. In addition, the landscape of TD, ASDs and OCD share processes related to neurotransmission and synaptic function/plasticity. In the OCD landscape, this synaptic plasticity was linked more specifically to CNS insulin signaling, while in the ASD landscape, testicular steroidogenesis seemed to be specifically involved. When comparing genes shared between the TD landscape and the landscapes of ASDs, ADHD and OCD in relation to these functional themes, we identified many overlapping genes that are related to neurite outgrowth (and that function in the extracellular matrix, cell membrane, cytoplasm, cytoskeleton and nucleus of developing neurons: *AKAP9, ASTN2, BAG5, BCL11A, CNTN6, CTNNA3, DIO2, DYNC2H1, ESR1, ETS1, FHIT, FOXP2, ITGB1, KLC1, MAPK3* (*ERK1*), *MTUS2, MYT1L, NPAS3, NRXN1, NXPH1, RELN, RHOA, TENM4* (*ODZ4*), *WNT1*), and synaptic function and neurotransmission (*AKAP9, CNTNAP2, GRIN1, GRIN2A, GRIN2B, PI4KA, NRXN1, PTPRN2, RHOA, RIMS1, RBFOX1* (*A2BP1*), *SYT17*).

Several of the shared genes were directly linked to one disorder via genetic data and indirectly i.e., through their functional link with other molecules interacting in the landscape – to another disorder (*AKAP9, GRIN1, GRIN2B, DIO2, WNT1, RHOA, KDM5B (JARID1B)*), while ITGB1 was <u>only</u> implicated in TD, ADHD, and OCD through its functional interactions with other landscape proteins.

In addition to the overlap at the level of individual genes and biological processes, we observed sharing between some important molecular cascades within the landscapes. Signaling downstream of the presynaptic membrane protein NRXN1 is shared between the TD, ASD and ADHD landscapes, where it is involved in synaptic function as well as neurite outgrowth. In addition, MAPK3 (mitogen-activated protein kinase 3, also known as ERK1)-dependent signaling is implicated in TD, ASDs and ADHD, where MAPK3 acts as a regulator of synaptic plasticity and interacts with multiple landscape proteins, including FLT3, one of our proposed novel drug targets for TD. MAPK3 is also involved in the two pathways that we found to be enriched within the TD candidate genes, i.e., 'Endocannabinoid Neuronal Synapse Pathway' and 'cAMP-mediated signaling' (**Chapter 4**). cAMP signaling is also important in the ASD and ADHD landscapes, while this pathway was regulated by the drugs that are used to treat ADHD symptoms – i.e., stimulants regulate the expression of CREB5 [18,19] – and TD-like behavior in our rat model (i.e., Riluzole decreases the activity of CREB1, see above (**Chapter 3**). This further highlights the importance of this pathway in the etiology of comorbid neuropsychiatric disorders and in the molecular mechanisms underlying the beneficial effect of treatments for these disorders.

6

a)

Overlap	TD - ASDs	TD - ADHD	TD - OCD
Hypergeometric P-value	4,04E-10	2,58E-04	2,01E-03

b)

#	Gene	TD	ASDs	ADHD	OCD
1	ASTN2	•	•	•	
2	FHIT	•	•	•	
3	MAPK3	•	•	•	
4	NRXN1	•	•	•	
5	GRIN2B	•	•		•
6	AKAP9	•	•		(•)
7	GRIN1	•	•		(•)
8	ITGB1	(•)		(•)	(•)
9	BAG5	•	•		
10	BCL11A	•	•		
11	CNTN6	•	•		
12	CNTNAP2	•	•		
13	CTNNA3	•	•		
14	ESR1	•	•		
15	ETS1	•	•		
16	GRIN2A	•	•		
17	HRH2	•	•		
18	KLC1	•	•		
19	NPAS3	•	•		
20	PI4KA	•	•		
21	PTPRN2	•	•		
22	RBFOX1	•	•		
23	RELN	•	•		
24	RIMS1	•	•		
25	SYT17	•	•		
26	TENM4	•	•		
27	FOXP2	•	•		
28	DIO2	•	(•)		
29	WNT1	•	(•)		
30	RHOA	•	(•)		
31	DYNC2H1	•		•	
32	MYT1L	•		•	
33	NXPH1	•		•	
34	EFNA5	•			•
35	MTUS2	•			•
36	KDM5B	•			(•)
37	CLTCL1	•			
38	DLC1	•			
39	FFAR3	•			
40	HTRA3	•			
41	KANSL1	•			
42	MYO19	•			
43	PLA2R1	•			
44	PPP1R3A	•			
45	SRSF4	•			
46	IL17RA	(•)			
47	FOXP1	•			
48	COMT	•			
49	DRD2	•			
50	FIP1L1	•			
51	SLC6A4	•			
52	SLC22A3	•			

FIGURE 2. Comparison of genes present in molecular landscapes of TD, ASDs, ADHD, and OCD.

a) Venn diagram representing the overlap between gene sets constituting the molecular landscapes of TD, ASDs, ADHD, and OCD. The table below the Venn diagram shows P-values of the hypergeometric distribution tests used to examine the significance of the overlap between these gene sets. **b)** Table represents all TD landscape genes that were overlapping with landscape/candidate genes for ASDs, ADHD, and/or OCD. Colors: In column '#', colors correspond to the colors of intersections in the Venn diagram. In column 'Gene', colors correspond to the colors used in the TD landscape (dark blue, light blue, yellow and white). In the columns 'TD', 'ASDs', 'ADHD' and 'OCD', a grey cell color indicates that the gene is a candidate gene, • indicates that a gene is a landscape gene based on the genetic and/or transcriptomic data; (•) indicate that a gene is a landscape gene based on functional link of its encoded protein with other proteins/molecules in the landscape.

Another shared signaling cascade centers around estradiol-activated ESR1, a highly interactive molecule in the TD and ASDs landscapes and an important regulator of molecular processes described in our PANDAS mice model (see above, **Chapter 2**). When comparing the OCD and TD landscapes, CNS insulin signaling does not seem to be (directly) present in the TD landscape, although the two genes that we found to be shared between TD, ASDs,

and OCD – *GRIN1* and *GRIN2B* – encode components of the NMDA receptor for glutamate that plays a key role in regulating insulin-dependent dendritic spine formation, which in turn affects synaptic plasticity [20]. Interestingly, the rat ortholog of *GRIN1* also showed increased expression after L-DOPA administration in our LID model (**Chapter 3**). Further, the AKAP family of proteins – that bind and recruit PKA to its substrates – integrates signaling cascades in the ASD landscape. AKAP9, one of these proteins, also operates in the TD and OCD landscapes, where it is involved in regulating neurite outgrowth and synaptic function/maintenance, including through modulation of GRIN1 [21,22]. In addition, through its effect on PKA, AKAP9 is an important regulator of cAMP signaling [23], the process that emerged from both our animal and human studies (see above). Another interesting example is *ASTN2*, a gene that for astrotactin-2, a membrane protein that is involved in calcium-dependent cell-cell adhesion and glial-guided neuronal migration during brain development [8]. ASTN2 was implicated in the ASD and ADHD landscapes via common genetic variants, while studies that were published after publication of the ASD, ADHD and OCD landscapes have also reported CNVs affecting *ASTN2* or both *ASTN2* and *TRIM32* – a small gene that is located within an intron of *ASTN2*, that is transcribed from the opposite strand and that encodes a protein involved in ubiquitin-protease degradation [21] – in boys presenting with ADHD, ASDs [12] and OCD [13]. Subsequent CNV screening of the *ASTN2/TRIM32* locus confirmed its enrichment among individuals with ASDs, ADHD and OCD, and this especially in males but not in females [14]. These findings could help explain (a part of) the molecular basis for the skewed sex ratios observed in the TD, ASDs and ADHD. Furthermore, *TRIM32* knockout mice were reported to exhibit ASD-like behaviors and hyperexcitability, which was accompanied by decreased numbers of cortical GABAergic interneurons [22] and pyramidal neurons, subsequently resulting in an imbalance of excitatory and inhibitory neurotransmission and an impaired synaptic plasticity [23,24]. We also found increased expression of *TRIM32* after Riluzole treatment our LID model (**Chapter 3**).

Lastly, we would like to note that for building the landscapes of the four neuropsychiatric disorders, there were considerable differences in the amount of available genetic (and other) data, the used analytic methods, and the criteria that were used for including genes/proteins in each of the landscapes. Therefore, it is possible and likely that genes that seemed to be specific for a disorder at the time the landscape was built will turn out to be pleiotropic based on studies published after the landscape studies themselves were published. Furthermore, the (relative) clinical specificity of each disorder could be partially explained by different and (relatively) disorder-specific functional consequences of disturbed biological processes – such as neurite outgrowth and synaptic function –

linked to differences in the spatiotemporal expression pattern of the genes involved, and, importantly, the modulatory effect of the environment. In this respect, the tissue and cell specificity analyses that we performed for the TD landscape implicated rather specific brain regions, time points and neuronal subtypes in the etiology of the disease. Although similar analyses have not been performed for the ASD, ADHD and OCD landscapes and based on the literature, it seems that relatively specific alterations in anatomical and functional circuits involving different brain regions and neuronal subtypes have been implicated in each of these disorders.

Genetic sharing between OCD/TD, OCS and insulin signaling

Etiological – and hence also genetic – similarities and differences between TD and OCD can be further evaluated by examining their symptom dimensions, each of which may contribute independently and differently to the clinical diagnoses of TD and OCD.

In **Chapter 5**, we report shared genetic etiologies between OCD and certain obsessive-compulsive symptoms (OCS), i.e., 'guilty taboo thoughts', 'symmetry/counting/ordering', and 'contamination/cleaning'. These findings are in keeping with the literature suggesting at least partial genetic overlap between OCD and population OCS [24-28]. Further, OCD has been linked to altered CNS insulin signaling (i.e., through the OCD landscape) [29] and in **Chapter 5**, we also found genetic sharing between peripheral insulin-related phenotypes (i.e., Type 2 Diabetes (T2D), plasma levels of glucose 2 h after an oral glucose challenge (2hG), and plasma levels of fasting insulin (FI)) and OCD/OCS. Since TD and OCD are clinically and genetically correlated (see above) [30-32], investigating which OCS and insulin-related traits are genetically shared between TD and OCD could help to identify the molecular mechanisms underlying their comorbidity and may also be useful in identifying drug targets to treat symptoms that are shared across both diagnoses. To this end, we estimated the presence and extent of genetic overlap between TD and OCS, as well as with peripheral insulin-related traits, applying the approach that we used in **Chapter 5** (i.e., polygenic risk score (PRS)-based analyses), and the results of these analyses are shown in Table 1. We found a shared genetic etiology between TD and four OCS factors, of which three also show genetic sharing with OCD – 'guilty taboo thoughts', 'symmetry/counting/ordering', and 'contamination/cleaning' - while for 'aggressive taboo thoughts', we only found genetic overlap with TD (and not with OCD). The 'symmetry/counting/ordering' factor was the most significant finding from the analyses in the PNC cohort and was replicated in the independent 'Spit for Science' cohort. These findings of genetic overlap between TD and OCS are in line with previous comparative and factor-analytic studies between TD and OCD,

where especially aggressive obsessions and symmetry-related behavior were found to be associated with tic-related OCD (i.e., OCD with comorbid tics) and TD [33-42]. In addition, our findings are in keeping with previous genetic studies in clinical samples [41,42], implying that the overlap between the disorders at the behavioral level can be (partially) explained by shared genetics.

As for the peripheral insulin traits, all five traits were significant at least once in the results of the PRS-based analyses for TD and OCD, with one – 2hG – being shared with both TD and OCD (Table 1). Fasting insulin seemed to be specifically overlapping genetically with OCD, while T2D, (plasma levels of) HbA1C and (plasma levels of) fasting glucose specifically showed genetic sharing with TD. Interestingly, antipsychotics use in TD patients has also been associated with adverse effects on glucose regulation, such as increased fasting glucose levels [43]. Moreover, T2D showed genetic overlap with TD and 'aggressive taboo thoughts', the OCS for which we only found genetic sharing with TD (and not OCD). In this respect, TD patients have also been shown to have an increased risk of developing T2D, which was higher in males compared to females and in TD patients with comorbid ADHD [44]. 'Aggressive taboo thoughts' were also phenotypically and genetically associated with a comorbid diagnosis of ADHD in TD patients [42]. In addition, ADHD was reported to be more prevalent in children with diabetes compared to healthy controls [45], and T2D has been associated with both ADHD [46,47] and OCD [47,48]. Further, a recent study investigated the genetic overlap between a large number of neuropsychiatric disorders and peripheral insulin-related traits – using GWAS data for larger samples and different methods – and found a negative genetic correlation between OCD and T2D, while the results for the other four insulin-related traits were not significant [49]. In addition, none of the insulin-related traits showed a significant genetic correlation with TD, while T2D and FG were positively correlated with ADHD. Lastly and interestingly, there is evidence of altered cAMP signaling – the key process linking all our studies – (also) playing in role in insulin metabolism [50] and T2D [51]. Taken together, the findings from the literature and our analyses indicate that there is a highly complex pattern of genetic relationships between TD, OCD/OCS and insulin traits – potentially involving cAMP signaling – that needs to be further investigated in order to draw any meaningful conclusions about how these relationships may be important clinically.

6

TABLE 1. Summary of the results from PRS-based analyses estimating shared genetic etiology between TD/OCD and OCS and peripheral insulin-related traits.

'Target 'sample	'Base' sample						
	TD	OCD	T2D	HbA1c	FI	FG	2hG
PNC							
Total OCS score	8.38E-02	4.72E-01	3.36E-01	7.64E-02	3.74E-01	4.16E-01	4.72E-01
	0.46%	0.04%	0.28%	1.00%	0.19%	0.10%	0.02%
Impairment	8.42E-02	2.61E-01	4.10E-01	2.28E-01	4.10E-01	4.10E-01	3.53E-01
	0.46%	0.51%	0.11%	0.58%	0.11%	0.12%	0.22%
Symmetry/counting/ordering	**6.86E-06**	3.53E-01	2.56E-01	4.10E-01	4.72E-01	2.80E-01	4.10E-01
	3.62%	0.23%	0.53%	0.11%	0.04%	0.39%	0.11%
Contamination/cleaning	**1.72E-03**	1.12E-01	3.53E-01	3.21E-01	4.47E-01	2.28E-01	2.71E-01
	1.87%	0.85%	0.24%	0.33%	0.07%	0.58%	0.49%
Aggressive taboo thoughts	**8.23E-03**	2.28E-01	**5.95E-03**	7.99E-02	4.66E-01	2.71E-01	2.28E-01
	1.31%	0.46%	**1.86%**	0.97%	0.06%	0.49%	0.59%
Guilty taboo thoughts	**1.89E-02**	**2.52E-03**	1.89E-0.1	4.03E-01	2.61E-01	3.21E-01	9.74E-02
	0.97%	**2.28%**	0.68%	0.15%	0.52%	0.33%	0.90%
Distress	2.04E-01	4.05E-01	4.72E-01	4.07E-01	2.80E-01	3.53E-01	3.53E-01
	0.19%	0.13%	0.02%	0.13%	0.43%	0.23%	0.25%
Spit for Science							
Symmetry/counting/ordering$_{TOCS}$	**4.33E-02**	**2.42E-05**	3.39E-01	2.71E-01	3.71E-01	2.47E-01	4.45E-01
	0.09%	**0.49%**	0.03%	0.04%	0.02%	0.04%	0.01%
Contamination/cleaning$_{TOCS}$	2.42E-01	**4.07E-03**	**1.59E-03**	1.68E-01	4.37E-01	4.36E-01	3.76E-01
	0.02%	**0.23%**	**0.28%**	0.05%	0.01%	0.01%	0.02%
PGC							
TD	-	-	**6.86E-11**	**1.12E-02**	7.09E-02	**2.61E-03**	4.07E-02
	-	-	**0.35%**	**0.06%**	0.02%	**0.08%**	0.03%
OCD	-	-	2.80E-01	4.15E-01	**7.67E-05**	3.53E-01	**4.75E-03**
	-	-	0.03%	0.01%	**0.26%**	0.02%	**0.14%**

Shown in this table are the Benjamini-Hochberg adjusted P-values at the best SNP P-value thresholds along with the variance explained for each of the 'base' and 'target' sample pairs from PRS-based analyses. Significant findings are indicated in bold. PNC Philadelphia Neurodevelopmental Cohort, PGC Psychiatric Genomics Consortium, TOCS Toronto Obsessive-Compulsive Scale, TD Tourette's disorder, OCD obsessive-compulsive disorder, T2D Type 2 Diabetes, HbA1c glycated hemoglobin, FI fasting insulin, FG fasting glucose, 2hG 2-h glucose.

Suggestions for future research

In this thesis, we used animal models and human omics data to elucidate the altered, shared and unique molecular mechanisms underlying TD and OCD. First, we examined the effects of Riluzole and neonatal stress on the molecular mechanisms implicated in TD- and OCD-like behaviors in a rat and mouse model, respectively. The rodent models that we used focused exclusively on gene expression in the striatum and did not include other brain regions that have been implicated in the neurobiology of TD and OCD. Moreover, only genome-wide human expression data for the striatum were available at the time of our analyses. Therefore, future studies in other (animal and human) brain structures and at the level of specific cell types are needed to extend our knowledge on the molecular processes related to TD and OCD development and enable the elucidation of brain region-specific mechanisms. Furthermore, the extensive data integration in our molecular landscape of TD allowed us to suggest a number of potential novel drug targets. In this respect, future studies – including both TD-focused and basic science studies – could further validate, complement and/or update the findings from the TD landscape to better understand the molecular mechanisms involved. In addition, targeted animal/cell model and interventional studies could be conducted to assess the (putatively) beneficial effect of (existing) medications and/or dietary changes in modulating the selected drug targets and their interactions with metabolites. Furthermore, the omics data that we used to build the landscape is representative for a broad and heterogenous TD phenotype, with the majority of TD patients also having comorbid conditions. As we found through the comparisons of the molecular landscapes of TD, ASDs, ADHD, and OCD, there is a substantial overlap at the level of individual genes as well as biological processes between these disorders. That being said, the complex nature of these disorders and their clinical/genetic overlap requires further longitudinal studies in large, well-characterized samples (including clinical phenotypes, environmental exposures, laboratory measures, treatment patterns, and genetic data) that will be instrumental to determine more homogenous samples – potentially also genetically more homogeneous patients – that are not necessarily confined to individual disorders. In line with this, alternative subphenotypes defined through symptom-level factor and latent class analyses – e.g., [41,42] – could help to uncover common clinical factors that cut across diagnostic categories. In addition, classes of individuals with varying combinations of TD and comorbid OCD/ASDs/ADHD could be further exploited in genetic analyses. Moreover, longitudinal studies are required to further evaluate if the clustering patterns detected in cross-sectional studies truly reflect etiological heterogeneity and/or different stages of disease progression or other temporal variation (such as differences in the levels of metabolomic biomarkers). This would all help us in better understanding the involved risk (genetic and environmental)

factors contributing to disease risk and progression for a given individual at a given point of time, and for developing the tools (e.g., biomarkers) and interventions that allow for a more targeted response. In this respect, the spatiotemporal patterns of gene expression seem to be of key importance, as disease mechanisms are not only represented by (alterations in) specific genes/proteins and biological pathways but also, and more importantly, by their impact across specific cell/tissue types and across the life course. Further, through limitations in the available data on gene isoforms, the analyses in this thesis were restricted to the gene level, and future studies at the isoform level could provide more insights into specific gene regulation patterns. For instance, different expression ratios of the long and short isoforms of ASTN2 – a gene that encodes a protein shared by the TD, ASD and ADHD landscapes (see above) – with age suggest that these isoforms may play different roles during brain development [14]. In addition, given the gender differences in the prevalence of (subtypes of) TD, OCD and their comorbid disorders, e.g., a further functional dissection of the influences gender has on ASTN2 isoforms during brain development may inform on new treatment strategies. Lastly, in this thesis we investigated shared genetic etiology through PRS-based analyses. These types of analyses provide a starting point for further studies using different methods that could dissect the 'broad' PRS-based signal containing hundreds of thousands of SNPs into smaller genetic loci and even individual genes and/ or identify causal or pleiotropic effects of specific traits on TD/OCD, and vice versa [52]. In addition, as the PRS-based analyses only consider the joint effect of (very) many common genetic variants associated with TD/OCD and related traits, further studies are needed to elucidate whether and to what extent rare genetic variants (also) contribute to this effect.

REFERENCES

1. Sanger, T.D.; Chen, D.; Fehlings, D.L.; Hallett, M.; Lang, A.E.; Mink, J.W.; Singer, H.S.; Alter, K.; Ben-Pazi, H.; Butler, E.E.; et al. Definition and classification of hyperkinetic movements in childhood. *Mov Disord* **2010**, *25*, 1538-1549, doi:10.1002/mds.23088.

2. Wang, Z.; Bhattacharya, N.; Mixter, P.F.; Wei, W.; Sedivy, J.; Magnuson, N.S. Phosphorylation of the cell cycle inhibitor p21Cip1/WAF1 by Pim-1 kinase. *Biochim Biophys Acta* **2002**, *1593*, 45-55, doi:10.1016/s0167-4889(02)00347-6.

3. Zhang, Y.; Wang, Z.; Magnuson, N.S. Pim-1 kinase-dependent phosphorylation of p21Cip1/WAF1 regulates its stability and cellular localization in H1299 cells. *Mol Cancer Res* **2007**, *5*, 909-922, doi:10.1158/1541-7786.Mcr-06-0388.

4. Li, L.; Piloto, O.; Kim, K.T.; Ye, Z.; Nguyen, H.B.; Yu, X.; Levis, M.; Cheng, L.; Small, D. FLT3/ITD expression increases expansion, survival and entry into cell cycle of human haematopoietic stem/progenitor cells. *Br J Haematol* **2007**, *137*, 64-75, doi:10.1111/j.1365-2141.2007.06525.x.

5. Marini, A.M.; Jiang, H.; Pan, H.; Wu, X.; Lipsky, R.H. Hormesis: a promising strategy to sustain endogenous neuronal survival pathways against neurodegenerative disorders. *Ageing Res Rev* **2008**, *7*, 21-33, doi:10.1016/j.arr.2007.07.003.

6. Mao, L.M.; Tang, Q.; Wang, J.Q. Protein kinase C-regulated cAMP response element-binding protein phosphorylation in cultured rat striatal neurons. *Brain Res Bull* **2007**, *72*, 302-308, doi:10.1016/j.brainresbull.2007.01.009.

7. Mantamadiotis, T.; Lemberger, T.; Bleckmann, S.C.; Kern, H.; Kretz, O.; Villalba, A.M.; Tronche, F.; Kellendonk, C.; Gau, D.; Kapfhammer, J. Disruption of CREB function in brain leads to neurodegeneration. *Nature genetics* **2002**, *31*, 47-54.

8. Cole, D.G.; Kobierski, L.A.; Konradi, C.; Hyman, S.E. 6-Hydroxydopamine lesions of rat substantia nigra up-regulate dopamine-induced phosphorylation of the cAMP-response element-binding protein in striatal neurons. *Proceedings of the National Academy of Sciences* **1994**, *91*, 9631-9635.

9. Oh, J.D.; Chartisathian, K.; Ahmed, S.M.; Chase, T.N. Cyclic AMP responsive element binding protein phosphorylation and persistent expression of levodopa-induced response alterations in unilateral nigrostriatal 6-OHDA lesioned rats. *Journal of neuroscience research* **2003**, *72*, 768-780.

10. Akagi, K.; Yamada, M.; Saitoh, A.; Oka, J.-I.; Yamada, M. Post-reexposure administration of riluzole attenuates the reconsolidation of conditioned fear memory in rats. *Neuropharmacology* **2018**, *131*, 1-10.

11. Wang, A.; Si, H.; Liu, D.; Jiang, H. Butyrate activates the cAMP-protein kinase A-cAMP response element-binding protein signaling pathway in Caco-2 cells. *J Nutr* **2012**, *142*, 1-6, doi:10.3945/jn.111.148155.

12. Wilson, A.J.; Byun, D.S.; Popova, N.; Murray, L.B.; L'Italien, K.; Sowa, Y.; Arango, D.; Velcich, A.; Augenlicht, L.H.; Mariadason, J.M. Histone deacetylase 3 (HDAC3) and other class I HDACs regulate colon cell maturation and p21 expression and are deregulated in human colon cancer. *J Biol Chem* **2006**, *281*, 13548-13558, doi:10.1074/jbc.M510023200.

13. Langley, B.; Gensert, J.M.; Beal, M.F.; Ratan, R.R. Remodeling chromatin and stress resistance in the central nervous system: histone deacetylase inhibitors as novel and broadly effective neuroprotective agents. *Curr Drug Targets CNS Neurol Disord* **2005**, *4*, 41-50, doi:10.2174/1568007053005091.

14. Rocha, W.; Sanchez, R.; Deschênes, J.; Auger, A.; Hébert, E.; White, J.H.; Mader, S. Opposite effects of histone deacetylase inhibitors on glucocorticoid and estrogen signaling in human endometrial Ishikawa cells. *Mol Pharmacol* **2005**, *68*, 1852-1862, doi:10.1124/mol.105.014514.

6

15. Fischer, A.; Sananbenesi, F.; Wang, X.; Dobbin, M.; Tsai, L.H. Recovery of learning and memory is associated with chromatin remodelling. *Nature* **2007**, *447*, 178-182, doi:10.1038/nature05772.

16. Zhao, H.; Shi, Y.; Luo, X.; Peng, L.; Yang, Y.; Zou, L. The Effect of Fecal Microbiota Transplantation on a Child with Tourette Syndrome. *Case reports in medicine* **2017**, *2017*, 6165239, doi:10.1155/2017/6165239.

17. Han, W.D.; Zhao, Y.L.; Meng, Y.G.; Zang, L.; Wu, Z.Q.; Li, Q.; Si, Y.L.; Huang, K.; Ba, J.M.; Morinaga, H.; et al. Estrogenically regulated LRP16 interacts with estrogen receptor alpha and enhances the receptor's transcriptional activity. *Endocr Relat Cancer* **2007**, *14*, 741-753, doi:10.1677/erc-06-0082.

18. Andersen, S.L.; Arvanitogiannis, A.; Pliakas, A.M.; LeBlanc, C.; Carlezon, W.A., Jr. Altered responsiveness to cocaine in rats exposed to methylphenidate during development. *Nat Neurosci* **2002**, *5*, 13-14, doi:10.1038/nn777.

19. Jones, D.C.; Kuhar, M.J. Cocaine-amphetamine-regulated transcript expression in the rat nucleus accumbens is regulated by adenylyl cyclase and the cyclic adenosine 5'-monophosphate/protein kinase a second messenger system. *J Pharmacol Exp Ther* **2006**, *317*, 454-461, doi:10.1124/jpet.105.096123.

20. Ryan, T.J.; Kopanitsa, M.V.; Indersmitten, T.; Nithiananantharajah, J.; Afinowi, N.O.; Pettit, C.; Stanford, L.E.; Sprengel, R.; Saksida, L.M.; Bussey, T.J.; et al. Evolution of GluN2A/B cytoplasmic domains diversified vertebrate synaptic plasticity and behavior. *Nat Neurosci* **2013**, *16*, 25-32, doi:10.1038/nn.3277.

21. Sheng, M.; Pak, D.T. Ligand-gated ion channel interactions with cytoskeletal and signaling proteins. *Annu Rev Physiol* **2000**, *62*, 755-778, doi:10.1146/annurev.physiol.62.1.755.

22. Husi, H.; Ward, M.A.; Choudhary, J.S.; Blackstock, W.P.; Grant, S.G. Proteomic analysis of NMDA receptor-adhesion protein signaling complexes. *Nat Neurosci* **2000**, *3*, 661-669, doi:10.1038/76615.

23. Tang, T.S.; Bezprozvanny, I. Dopamine receptor-mediated Ca(2+) signaling in striatal medium spiny neurons. *J Biol Chem* **2004**, *279*, 42082-42094, doi:10.1074/jbc.M407389200.

24. Den Braber, A.; Zilhão, N.; Fedko, I.; Hottenga, J.; Pool, R.; Smit, D.; Cath, D.; Boomsma, D. Obsessive–compulsive symptoms in a large population-based twin-family sample are predicted by clinically based polygenic scores and by genome-wide SNPs. *Translational psychiatry* **2016**, *6*, e731-e731.

25. Chacon, P.; Rosario-Campos, M.C.; Pauls, D.L.; Hounie, A.G.; Curi, M.; Akkerman, F.; Shimabokuro, F.H.; de Mathis, M.A.; Lopes, A.C.; Hasler, G. Obsessive–compulsive symptoms in sibling pairs concordant for obsessive–compulsive disorder. *American Journal of Medical Genetics Part B: Neuropsychiatric Genetics* **2007**, *144*, 551-555.

26. Brakoulias, V.; Starcevic, V.; Martin, A.; Berle, D.; Milicevic, D.; Viswasam, K. The familiality of specific symptoms of obsessive-compulsive disorder. *Psychiatry research* **2016**, *239*, 315-319.

27. Burton, C.L.; Park, L.S.; Corfield, E.C.; Forget-Dubois, N.; Dupuis, A.; Sinopoli, V.M.; Shan, J.; Goodale, T.; Shaheen, S.-M.; Crosbie, J. Heritability of obsessive–compulsive trait dimensions in youth from the general population. *Translational psychiatry* **2018**, *8*, 1-10.

28. Smit, D.J.A.; Cath, D.; Zilhão, N.R.; Ip, H.F.; Denys, D.; den Braber, A.; de Geus, E.J.C.; Verweij, K.J.H.; Hottenga, J.-J.; Boomsma, D.I. Genetic meta-analysis of obsessive-compulsive disorder and self-report compulsive symptoms. *American Journal of Medical Genetics Part B: Neuropsychiatric Genetics* **2020**, *183*, 208-216, doi:https://doi.org/10.1002/ajmg.b.32777.

29. van de Vondervoort, I.; Poelmans, G.; Aschrafi, A.; Pauls, D.L.; Buitelaar, J.K.; Glennon, J.C.; Franke, B. An integrated molecular landscape implicates the regulation of dendritic spine formation through insulin-related signalling in obsessive-compulsive disorder. *J Psychiatry Neurosci* **2016**, *41*, 280-285, doi:10.1503/jpn.140327.

30. Brainstorm, C.; Anttila, V.; Bulik-Sullivan, B.; Finucane, H.K.; Walters, R.K.; Bras, J.; Duncan, L.; Escott-Price, V.; Falcone, G.J.; Gormley, P.; et al. Analysis of shared heritability in common disorders of the brain. *Science* **2018**, *360*, doi:10.1126/science.aap8757.

31. Hirschtritt, M.E.; Lee, P.C.; Pauls, D.L.; Dion, Y.; Grados, M.A.; Illmann, C.; King, R.A.; Sandor, P.; McMahon, W.M.; Lyon, G.J.; et al. Lifetime prevalence, age of risk, and genetic relationships of comorbid psychiatric disorders in Tourette syndrome. *JAMA Psychiatry* **2015**, *72*, 325-333, doi:10.1001/jamapsychiatry.2014.2650.

32. Cross-Disorder Group of the Psychiatric Genomics Consortium. Electronic address, p.m.h.e.; Cross-Disorder Group of the Psychiatric Genomics, C. Genomic Relationships, Novel Loci, and Pleiotropic Mechanisms across Eight Psychiatric Disorders. *Cell* **2019**, *179*, 1469-1482 e1411, doi:10.1016/j.cell.2019.11.020.

33. George, M.S.; Trimble, M.R.; Ring, H.A.; Sallee, F.R.; Robertson, M.M. Obsessions in obsessive-compulsive disorder with and without Gilles de la Tourette's syndrome. *Am J Psychiatry* **1993**, *150*, 93-97, doi:10.1176/ajp.150.1.93.

34. de Groot, C.M.; Bornstein, R.A.; Janus, M.-D.; Mavissakalian, M.R. Patterns of obsessive compulsive symptoms in tourette subjects are independent of severity. *Anxiety* **1994**, *1*, 268-274, doi:https://doi.org/10.1002/anxi.3070010604.

35. Petter, T.; Richter, M.A.; Sandor, P. Clinical features distinguishing patients with Tourette's syndrome and obsessive-compulsive disorder from patients with obsessive-compulsive disorder without tics. *J Clin Psychiatry* **1998**, *59*, 456-459, doi:10.4088/jcp.v59n0903.

36. Cath, D.C.; Spinhoven, P.; Hoogduin, C.A.; Landman, A.D.; van Woerkom, T.C.; van de Wetering, B.J.; Roos, R.A.; Rooijmans, H.G. Repetitive behaviors in Tourette's syndrome and OCD with and without tics: what are the differences? *Psychiatry Res* **2001**, *101*, 171-185, doi:10.1016/s0165-1781(01)00219-0.

37. Jaisoorya, T.S.; Reddy, Y.C.; Srinath, S.; Thennarasu, K. Obsessive-compulsive disorder with and without tic disorder: a comparative study from India. *CNS Spectr* **2008**, *13*, 705-711, doi:10.1017/s1092852900013791.

38. Huisman-van Dijk, H.M.; Schoot, R.; Rijkeboer, M.M.; Mathews, C.A.; Cath, D.C. The relationship between tics, OC, ADHD and autism symptoms: A cross- disorder symptom analysis in Gilles de la Tourette syndrome patients and family-members. *Psychiatry Res* **2016**, *237*, 138-146, doi:10.1016/j.psychres.2016.01.051.

39. Kloft, L.; Steinel, T.; Kathmann, N. Systematic review of co-occurring OCD and TD: Evidence for a tic-related OCD subtype? *Neuroscience & Biobehavioral Reviews* **2018**, *95*, 280-314, doi:https://doi.org/10.1016/j.neubiorev.2018.09.021.

40. de Vries, F.E.; Cath, D.C.; Hoogendoorn, A.W.; van Oppen, P.; Glas, G.; Veltman, D.J.; van den Heuvel, O.A.; van Balkom, A.J. Tic-related versus tic-free obsessive-compulsive disorder: clinical picture and 2-year natural course. *The Journal of Clinical Psychiatry* **2016**, *77*, 12464.

41. Darrow, S.M.; Hirschtritt, M.E.; Davis, L.K.; Illmann, C.; Osiecki, L.; Grados, M.; Sandor, P.; Dion, Y.; King, R.; Pauls, D.; et al. Identification of Two Heritable Cross-Disorder Endophenotypes for Tourette Syndrome. *Am J Psychiatry* **2017**, *174*, 387-396, doi:10.1176/appi.ajp.2016.16020240.

42. Hirschtritt, M.E.; Darrow, S.M.; Illmann, C.; Osiecki, L.; Grados, M.; Sandor, P.; Dion, Y.; King, R.A.; Pauls, D.; Budman, C.L.; et al. Genetic and phenotypic overlap of specific obsessive-compulsive and attention-deficit/hyperactive subtypes with Tourette syndrome. *Psychol Med* **2018**, *48*, 279-293, doi:10.1017/s0033291717001672.

43. Rizzo, R.; Eddy, C.M.; Calí, P.; Gulisano, M.; Cavanna, A.E. Metabolic effects of aripiprazole and pimozide in children with Tourette syndrome. *Pediatr Neurol* **2012**, *47*, 419-422, doi:10.1016/j.pediatrneurol.2012.08.015.

6

44. Brander, G.; Isomura, K.; Chang, Z.; Kuja-Halkola, R.; Almqvist, C.; Larsson, H.; Mataix-Cols, D.; Fernández de la Cruz, L. Association of Tourette Syndrome and Chronic Tic Disorder With Metabolic and Cardiovascular Disorders. *JAMA Neurol* **2019**, *76*, 454-461, doi:10.1001/jamaneurol.2018.4279.

45. Zahed, G.; Shakiba, M.; Seifi, K. The Prevalence of Psychological Disorders among Children with Diabetes Aged 5-12 Years Old Referred to the Endocrinology Clinic of Mofid Hospital, Tehran, Iran in 2014-2015. *Iran J Child Neurol* **2018**, *12*, 101-112.

46. Chen, Q.; Hartman, C.A.; Haavik, J.; Harro, J.; Klungsøyr, K.; Hegvik, T.A.; Wanders, R.; Ottosen, C.; Dalsgaard, S.; Faraone, S.V.; et al. Common psychiatric and metabolic comorbidity of adult attention-deficit/hyperactivity disorder: A population-based cross-sectional study. *PLoS One* **2018**, *13*, e0204516, doi:10.1371/journal.pone.0204516.

47. Wimberley, T.; Horsdal, H.T.; Brikell, I.; Laursen, T.M.; Astrup, A.; Fanelli, G.; Bralten, J.; Poelmans, G.; Gils, V.V.; Jansen, W.J.; et al. Temporally ordered associations between type 2 diabetes and brain disorders - a Danish register-based cohort study. *BMC Psychiatry* **2022**, *22*, 573, doi:10.1186/s12888-022-04163-z.

48. Isomura, K.; Brander, G.; Chang, Z.; Kuja-Halkola, R.; Rück, C.; Hellner, C.; Lichtenstein, P.; Larsson, H.; Mataix-Cols, D.; Fernández de la Cruz, L. Metabolic and Cardiovascular Complications in Obsessive-Compulsive Disorder: A Total Population, Sibling Comparison Study With Long-Term Follow-up. *Biol Psychiatry* **2018**, *84*, 324-331, doi:10.1016/j.biopsych.2017.12.003.

49. Fanelli, G.; Franke, B.; De Witte, W.; Ruisch, I.H.; Haavik, J.; van Gils, V.; Jansen, W.J.; Vos, S.J.B.; Lind, L.; Buitelaar, J.K.; et al. Insulinopathies of the brain? Genetic overlap between somatic insulin-related and neuropsychiatric disorders. *Transl Psychiatry* **2022**, *12*, 59, doi:10.1038/s41398-022-01817-0.

50. Tengholm, A.; Gylfe, E. cAMP signalling in insulin and glucagon secretion. *Diabetes Obes Metab* **2017**, *19 Suppl 1*, 42-53, doi:10.1111/dom.12993.

51. Yang, H.; Yang, L. Targeting cAMP/PKA pathway for glycemic control and type 2 diabetes therapy. *J Mol Endocrinol* **2016**, *57*, R93-r108, doi:10.1530/jme-15-0316.

52. Paternoster, L.; Tilling, K.; Davey Smith, G. Genetic epidemiology and Mendelian randomization for informing disease therapeutics: Conceptual and methodological challenges. *PLoS Genet* **2017**, *13*, e1006944, doi:10.1371/journal.pgen.1006944.

6
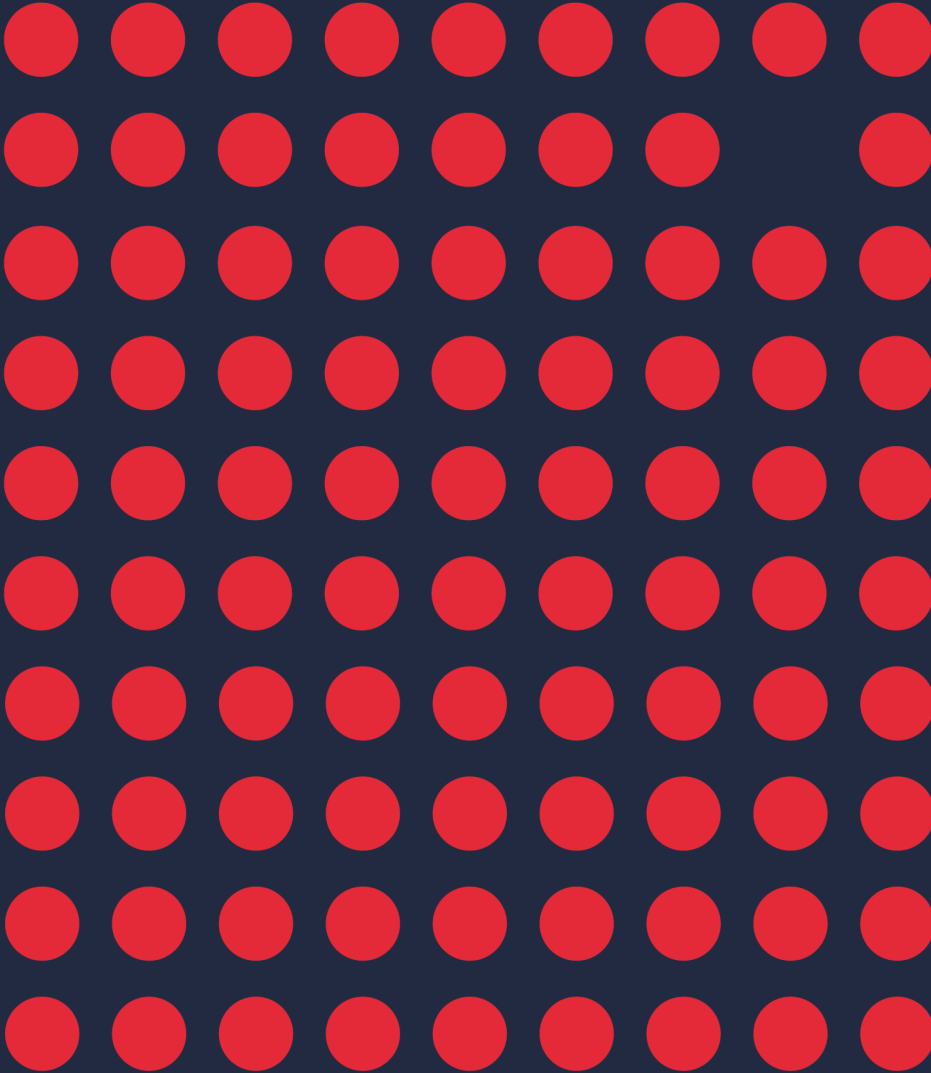
APPENDICES

NEDERLANDSE SAMENVATTING

RESEARCH DATA MANAGEMENT

ACKNOWLEDGEMENTS

CURRICULUM VITAE

PORTFOLIO

PUBLICATIONS

DONDERS GRADUATE SCHOOL
FOR COGNITIVE NEUROSCIENCE

NEDERLANDSE SAMENVATTING

Het syndroom of de stoornis van Gilles de la Tourette – tegenwoordig omschreven als (stoornis van) Tourette – en obessief-compulsieve stoornis (OCS) zijn twee heterogene stoornissen met complexe oorzaken die vaak samen voorkomen. Omdat de neurologische en moleculaire processen die ten grondslag liggen aan deze stoornissen maar gedeeltelijk begrepen zijn, en de huidige behandelingen slechts gedeeltelijk effectief zijn, wordt er nog steeds veel onderzoek gedaan naar de (verstoorde) moleculaire en cellulaire mechanismen die ten grondslag liggen aan Tourette/OCS en hun behandelingen, en dit om risico- en beschermende factoren voor beide stoornissen te identificeren. Dit proefschrift omvat studies op basis van diermodellen en humane 'omics' data die geanalyseerd werden op het cellulaire, moleculaire en gedragsmatige niveau, met als doel het vergroten van onze kennis over de gewijzigde moleculaire mechanismen die betrokken zijn bij Tourette en OCS en het identificeren van mogelijke doelwitten voor nieuwe behandelingen.

In **hoofdstuk 1** is een algemene inleiding over de stoornis van Tourette en OCS gegeven waarin de historische context, klinische en epidemiologische aspecten en de huidige kennis over de genetische risicofactoren voor, en neurobiologische aspecten van, beide stoornissen is beschreven, samen met een overzicht van de gebruikte behandelingen en diermodellen.

In **hoofdstuk 2** hebben we onderzocht of stress in het vroege leven de individuele vatbaarheid voor PANDAS – Pediatric Autoimmune Neuropsychiatric Disorders Associated with Streptococcus – beïnvloedt door middel van een longitudinaal onderzoek bij muizen. We hebben gevonden dat injecties met Groep A Streptokokken (GAS) bacteriën PANDAS-gerelateerd afwijkend gedrag – d.w.z. Tourette- en/of OCS-achtig gedrag – verzoorzaakt in muizen (zoals een verminderde sensomotorische gating en toegenomen volhardend gedrag), evenals een verminderde reactiviteit op een serotonerge agonist en verhoogde inflammatoire infiltraten in het voorste diencephalon (van de hersenen van deze muizen). Neonatale toediening van corticosteron (CORT) – wat chronische stress nabootst – verzachtte de meeste door GAS veroorzaakte gedrags-, immunohistochemische en moleculaire veranderingen. Deze compenserende effecten traden samen op met modificaties in de activiteit van de hypothalamus-hypofyse-bijnieras, wat verder tot uiting kwam in verhoogde glucocorticoïdenconcentraties in het bloed, evenals verhoogde serumspiegels van het ontstekingsremmende cytokine IL-9 en veranderingen in striatale genexpressie. Onze analyses van de striatale differentiële genexpressiegegevens wezen op een rol van het vrouwelijk geslachtshormoon (beta)-oestradiol en andere signaalmoleculen die gereguleerd worden door oestradiol (FGF2, IgG, DA, LH, LEP, IL2, IKBKB) als belangrijke stroomopwaartse regulatoren van moleculaire mechanismen geassocieerd met de fenotypische afwijkingen die worden waargenomen bij GAS-muizen en bij de compenserende rol van neonatale CORT.

Concreet remden GAS-blootstellingen de (beta)-oestradiol-gemedieerde regulatie van genexpressie, terwijl neonatale CORT dit effect compenseerde. Deze gegevens ondersteunen de hypothese dat verhogingen van glucocorticoïden centrale immunomodulerende processen kunnen bevorderen.

De stoornis van Tourette kan ook geconceptualiseerd worden als een hyperkinetische bewegingsstoornis of dyskinesie, gekenmerkt door overmatige en repetitieve abnormale onwillekeurige bewegingen (AIM's) of tics. AIM's ontwikkelen zich ook vaak na chronische toediening van Levodopa, de eerstelijnsbehandeling van dystonische symptomen in de kindertijd of bij de ziekte van Parkinson, wat leidt tot de ontwikkeling van de zogenaamde 'door levodopa geïnduceerde dyskinesie' (LID). Riluzole is voorgesteld als een kandidaat-medicijn voor de behandeling van AIM's/LID. Daarom hebben we in **hoofdstuk 3** de gedrags- en moleculaire effecten van Riluzole onderzocht in een juveniel ratmodel van LID. We hebben waargenomen dat Riluzole de door Levodopa geïnduceerde AIM's in het rattenmodel verzwakt. Vervolgens onthulde onze analyse van differentiële striatale genexpressiegegevens van LID-ratten dat wordt voorspeld dat Riluzol de activiteit van CREB1 (cAMP response element binding protein 1) vermindert. CREB1 is een transcriptiefactor die de expressie reguleert van meerdere op elkaar inwerkende eiwitten die betrokken zijn bij het reguleren van neuronale processen, zoals neuronale overleving/apoptose, differentiatie en ontwikkeling en dat fungeert als een 'go-between' tussen cytoplasmatisch kinase- en enzyme-gerelateerde signaalcascades en de regulatie van genexpressie in de celkern.

In **hoofdstuk 4** hebben we de beschikbare humane omics-gegevens over de stoornis van Tourette geïntegreerd om een zogenaamd 'moleculair landschap' van de ziekte te bouwen. Meer specifiek hebben we een lijst van Tourette-kandidaatgenen samengesteld, en vervolgens hebben we weefsel-/celtypespecificiteit- en functionele verrijkingsanalyses op de genen in deze lijst uitgevoerd. Met behulp van genomische gegevens hebben we ook de genetische overlap tussen Tourette en de niveaus van metabolieten in het bloed en cerebrospinale vloeistof (cerebrospinal fluid, CSF) onderzocht. We ontdekten dat de Tourette-kandidaatgenen een verrijkte expressie vertonen in de hypofyse en gedurende verschillende ontwikkelingsperioden in vier hersengebieden (cerebellum, cortex, striatum en thalamus). De functionele verrijkingsanalyses impliceerden dat twee pathways, namelijk 'cAMP-mediated signaling' en 'Endocannabinoid Neuronal Synapse Pathway', en meerdere biologische functies gerelateerd aan hersenontwikkeling en synaptische transmissie betrokken zijn bij de etiologie van Tourette. Verder vonden we genetische overlap tussen Tourette en de bloed- en CSF-niveaus van 39 metabolieten, waaronder butyraat, NAAG, myo-inositol, het cytokine TNFB en meervoudig onverzadigde vetzuren zoals arachidonzuur. Tenslotte hebben we alle verschillende soorten omics-gegevens geïntegreerd om een

moleculair landschap van Tourette te bouwen. Dit landschap verschaft nieuwe inzichten in de (veranderde) moleculaire processen die ten grondslag liggen aan de ziekte en op basis van het landschap konden ook meerdere eiwitten geïdentificeerd worden die kunnen worden gemoduleerd met een gunstig effect op Tourette en daarom mogelijke doelwitten voor nieuwe medicijnen zijn (inclusief FLT3, NAALAD2, CX3CL1-CX3CR1, OPRM1, en HRH2).

Epidemiologische en genetische studies hebben associaties aangetoond tussen klinische OCS en obsessief-compulsieve symptomen in de algemene bevolking (ocs). Daarnaast is ontregelde insulinesignalering in de periferie en het centrale zenuwstelsel betrokken bij zowel OCS als ocs. In **hoofdstuk 5** bouwden we voort op dit eerdere werk door de aanwezigheid en mate van gedeelde genetische etiologie tussen OCS, ocs in de populatie en insuline signalering in de perifere en het centrale zenuwstelsel te beoordelen, met behulp van de grootste beschikbare genomische datasets. Onze zogenaamde 'polygenic risk score-based analyses' onthulden genetische overlap tussen OCS en drie ocs, nl. 'schuldige taboe-gedachten', 'symmetrie/tellen/ordenen' en 'besmetting/schoonmaken', en dit in twee verschillende populatiecohorten van kinderen en adolescenten. Wat betreft perifere insulinesignalering vonden we genetische overlap tussen diabetes type 2 en twee ocs, 'agressieve taboe-gedachten' en 'besmetting/reiniging', en tussen twee insulinegerelateerde kenmerken – bloedspiegels van nuchtere insuline en 2 uur-glucose – en OCS. Bovendien vonden we een associatie tussen een set van OCS-genen die insulinesignalering in het centrale zenuwstelsel reguleren en 'symmetrie/tellen/ordenen'. Alles bij elkaar genomen bieden onze bevindingen verdere ondersteuning voor het bestaan van (ten minste gedeeltelijke) genetische overlap tussen OCS en ocs in de bevolking, evenals voor veranderde insulinesignalering als een algemeen biologisch proces dat bijdraagt aan zowel OCS als ocs in de bevolking.

Tenslotte vat ik in **hoofdstuk 6** de belangrijkste resultaten van dit proefschrift samen en bediscussieer ze in de bredere context van de bestaande literatuur. Meer specifiek vergelijk ik onze bevindingen uit de studies in de twee diermodellen (**hoofdstuk 2** en **hoofdstuk 3**) met deze uit het Tourette landschap (**hoofdstuk 4**) en bespreek ik hoe de bevindingen uit de diermodellen mogelijk kunnen 'vertaald' worden in bijkomende inzichten mbt de biologische processen die ten grondslag liggen aan de stoornis van Tourette. Daarnaast ben ik nagegaan welke genen en biologische processen overlappen tussen het Tourette landschap en gelijkaardige landschappen voor andere ontwikkelingsstoornissen, nl. autisme spectrum stoornissen (ASS), 'attention-deficit/hyperactivity disorder' (ADHD) en OCS. Ook heb ik de analyses die beschreven zijn in **hoofdstuk 5** nog verder uitgebreid om de aanwezigheid en mate van genetische overlap te bepalen tussen OCS, Tourette en insuline-gerelateerde kenmerken, en geef ik een aantal suggesties voor toekomstig onderzoek.

RESEARCH DATA MANAGEMENT

Part of this thesis is based on the results from animal studies (Chapters 2 and 3). These studies were performed in compliance with the appropriate European, Italian, and German regulations, and approved by the local Animal Welfare Body, as detailed in the respective chapters. Part of this thesis is also based on the results from human studies (Chapter 5) or existing data from published papers (Chapters 4 and 5), and all these studies were conducted in accordance with the principles of the Declaration of Helsinki. Ethical approval was granted by the institutional review boards of all participating centers, as described in the studies, and informed consent was obtained from research participants.

The human phenotypic and genetic data for Chapter 5 was accessed through the NIMH Database of Genotypes and Phenotypes (dbGaP), study accession ID phs000607.v1.p1., based on a Data Use Certification Agreement. Other (human) omics data that were used and analyzed in Chapters 4 and 5 are available through publicly accessible websites and servers, as described in the respective chapters. These data, as well as the experimental and RNA sequencing data that were generated and analyzed in Chapters 2 and 3, are digitally stored on a secure server of Drug Target ID (DTID), Ltd., Nijmegen, The Netherlands, or on the department server of the Department of Human Genetics of the Radboud University Medical Center, Nijmegen, The Netherlands.

Data shown in this thesis were made reusable for future research by adding sufficient documentation (research protocol, descriptive files, and program code and scripts used to provide the results) and by using preferred and sustainable data formats. Data will be stored for 10 years following the termination of each project. The data sets analyzed during this research are available from the corresponding author on reasonable request. Studies presented in Chapters 2 - 5 have been published open access.

A

ACKNOWLEDGEMENTS

CURRICULUM VITAE

Joanna Widomska was born on the 22nd of April 1988, in Kielce, Poland. She studied Biotechnology at the University of Life Sciences in Poznań, Poland, where she obtained her B.Eng. (2011) and M.Sc. (2012) degrees. During her engineering studies, she spent a year as a student within the Erasmus Programme at the Justus-Liebig University, Gießen, Germany. During her M.Sc. studies, she also did an internship on the genetics of drug response in inflammatory bowel disease at the Institute of Human Genetics of the Polish Academy of Sciences, Poznań, under the supervision of Dr. Marzena Skrzypczak-Zielińska. Following up on her M.Sc. work, Joanna joined the pharmacogenomics group led by Prof. Munir Pirmohamed at the Wolfson Centre for Personalised Medicine, University of Liverpool, UK, where she worked as an early-stage researcher within the Marie Curie Initial Training Network (ITN) 'Fighting Drug Failure'. In 2014, she started her Ph.D. research in the Translational Psychiatry group led by Dr. Jeffrey Glennon, and under the supervision of Prof. Jan Buitelaar, Dr. Glennon and Dr. Geert Poelmans, at the Donders Institute for Brain, Cognition and Behaviour, Nijmegen, The Netherlands. Her Ph.D. project was part of the Marie Curie ITN 'TS-EUROTRAIN' that focused on investigating the etiology and pathophysiology of Tourette's disorder (TD) and related disorders, such as obsessive-compulsive disorder (OCD), attention-deficit/hyperactivity disorder (ADHD) and autism spectrum disorders (ASDs). In her Ph.D., Joanna aimed at identifying the molecular mechanisms underlying TD and OCD through animal and human omics studies. During her Ph.D., Joanna also did a secondment at the Center for Human Genetics Research, Massachusetts General Hospital, Harvard Medical School, Boston, USA. In Boston, she received training in the analysis of GWAS and RNA-seq data in the lab of Dr. Jeremiah Scharf and Dr. Michael Talkowski. Since 2017 Joanna has been working at Drug Target ID (DTID), a spin-out of Radboud University specialized in the interpretation of large biological data sets and building molecular landscapes. At DTID, Joanna is currently involved in several research projects with academic and industrial partners.

A

PORTFOLIO

Courses & Workshops	Organizer & Location	Year
Graduate School Introduction Day	Donders Graduate School, Nijmegen	2014
International Workshop on Neurodevelopmental Disorders. Focus on Tourette Syndrome: Human Molecular Genetics	TS-EUROTRAIN consortium, Reykiavik	2014
Allen Brain Atlas Hands-On Training Workshop	Allen Institute for Brain Science, Maastricht University Medical Center	2014
NGS Bioinformatics Workshop 'microRNA Analysis Using High-Throughput Sequencing'	ecSeq Bioinformatics, Leipzig	2014
TS-EUROTRAIN Workshop 'Presentation and Communication'	TS-EUROTRAIN consortium, Hannover	2014
Translational Bioinformatics Workshop	Guy's and St Thomas' NHS Foundation Trust and King's College London	2015
Scientific integrity	Radboudumc, Nijmegen	2015
Achieving your goals and performing more successfully in your PhD	Radboud University, Nijmegen	2015
Refresher course of Statistics	Radboud University, Nijmegen	2015
Neurotransmitters in Tourette Syndrome: From neurobiology to neuroimaging	TS-EUROTRAIN consortium, London	2015
RNA-seq data analysis (5th edition)	BioSB research school and Leiden University Medical Center, Leiden	2015
TS-EUROTRAIN Workshop 'Entrepreneurship, commercialization and management'	TS-EUROTRAIN consortium, Hannover	2015
Bayesian analysis with JASP: A fresh way to do statistics	Donders Graduate School and International Max Planck Research School, Nijmegen	2017
Advanced Conversation	Radboud University, Nijmegen	2017
Career Guidance for International PhDs	Radboud University, Nijmegen	2017
The Art of Presenting Science	Radboud University, Nijmegen	2017
Perfecting your Academic Writing Skills	Radboud University, Nijmegen	2017
Analysis of single cell RNA-seq data	Physalia-courses, Berlin	2018
Graduate School Day	Donders Graduate School, Nijmegen	2018
Multiomics Data Integration Using R	Medical Genetics Center South-West Netherlands, Online	2020

Conferences	Location	Year
Annual Meeting of the European Society for the Study of Tourette Syndrome and International Conference for Tourette Syndrome	Paris	2014
TS-EUROTRAIN: Mid-Term Review Meeting	Alexandroupoli[*]	2014
Donders Discussions	Nijmegen	2014
Dutch Bioinformatics & Systems Biology Conference	Lunteren	2015
I World Congress on Tourette Syndrome and Tic Disorders	London[#]	2015
World Congress of Psychiatric Genetics	Toronto[#]	2015
	Orlando[#]	2017
	Glasgow[#]	2018
	Anaheim[#]	2019
10th European Conference on Tourette Syndrome and Tic Disorders	Seville[*]	2017
International Myotonic Dystrophy Consortium Meeting IDMC-12	Gothenburg[#]	2019
The 6th International Conference on Quantitative Genetics	Online[#]	2020

Seminars & Lectures	Location	Year
Donders theme meetings	Nijmegen	2014-2018
Radboud Research Rounds	Nijmegen	2014-2018
RIMLS Technical Forum	Nijmegen	2014-2015
CHGR Research presentations	Cambridge	2016
Medical and Population Genetics Program Meetings	Boston	2016

* oral presentation, # poster presentation

A

PUBLICATIONS

Articles included in this thesis

Macri, S.*, Spinello, C.*, **Widomska, J.***, Magliozzi, R.*, Poelmans, G., Invernizzi, R.W., Creti, R., Roessner, V., Bartolini, E., Margarit, I., Glennon, J., Laviola, G. (2018). Neonatal corticosterone mitigates autoimmune neuropsychiatric disorders associated with streptococcus in mice. *Scientific Reports*, *8*(1), 10188. DOI:10.1038/s41598-018-28372-3.

Pagliaroli, L.*, **Widomska, J.***, Nespoli, E., Hildebrandt, T., Barta, C., Glennon, J., Hengerer, B., Poelmans, G. (2019). Riluzole Attenuates L-DOPA-Induced Abnormal Involuntary Movements Through Decreasing CREB1 Activity: Insights from a Rat Model. *Molecular Neurobiology*, *56*(7), 5111-5121. DOI:10.1007/s12035-018-1433-x.

Bralten, J.*, **Widomska, J.***, Witte, W., Yu, D., Mathews, C.A., Scharf, J.M., Buitelaar, J., Crosbie, J., Schachar, R., Arnold, P., Lemire, M., Burton, C.L., Franke, B.*, Poelmans, G.* (2020). Shared genetic etiology between obsessive-compulsive disorder, obsessive-compulsive symptoms in the population, and insulin signaling. *Translational Psychiatry, 10*(1), 121. DOI:10.1038/s41398-020-0793-y.

Widomska, J., De Witte, W., Buitelaar, J.K., Glennon, J.C., Poelmans, G. (2023). Molecular Landscape of Tourette's Disorder. *International Journal of Molecular Sciences, 24*(2), 1428. DOI:10.3390/ijms24021428.

Articles not included in this thesis

Forde, N.J.*, Kanaan, A.S.*, **Widomska, J.**, Padmanabhuni, S.S., Nespoli, E., Alexander, J., Rodriguez Arranz, J.I., Fan, S., Houssari, R., Nawaz, M.S., … Paschou, P. (2016). TS-EUROTRAIN: A European-Wide Investigation and Training Network on the Etiology and Pathophysiology of Gilles de la Tourette Syndrome. *Frontiers in Neuroscience, 10*, 384. DOI:10.3389/fnins.2016.00384.

Nieuwenhuis, S., Okkersen, K., **Widomska, J.**, Blom, P., t Hoen, P.A.C., van Engelen, B., Glennon, J.C. (2019). Insulin Signaling as a Key Moderator in Myotonic Dystrophy Type 1. *Frontiers in Neurology, 10*, 1229. DOI:10.3389/fneur.2019.01229.

Nieuwenhuis, S.*, **Widomska, J.***, Blom, P., 't Hoen, P.-B.A.C., van Engelen, B.G.M., Glennon, J.C. (2022). Blood Transcriptome Profiling Links Immunity to Disease Severity in Myotonic Dystrophy Type 1 (DM1). *International Journal of Molecular Sciences, 23*(6). DOI:10.3390/ijms23063081.

Post, W.M., **Widomska, J.**, Grens, H., Coenen, M.J.H., Martens, F.M.J., Janssen, D.A.W., IntHout, J., Poelmans, G., Oosterwijk, E.*, Kluivers, K.B.* (2022). Molecular Processes in Stress Urinary Incontinence: A Systematic Review of Human and Animal Studies. *International Journal of Molecular Sciences, 23*(6). DOI:10.3390/ijms23063401.

van der Linden, R.J., Gerritsen, J.S., Liao, M., **Widomska, J.**, Pearse, R.V., 2nd, White, F.M., Franke, B., Young-Pearse, T.L., Poelmans, G. (2022). RNA-binding protein ELAVL4/HuD ameliorates Alzheimer's disease-related molecular changes in human iPSC-derived neurons. *Progress in Neurobiology*, *217*, 102316. DOI:10.1016/j.pneurobio.2022.102316.

Jain, P., …, The TS-EUROTRAIN Network (including **Widomska, J.**), …, Paschou, P. (2023). Polygenic risk score-based phenome-wide association study identifies novel associations for tourette syndrome. *Translational Psychiatry*, *13*(1), 69. DOI:10.1038/s41398-023-02341-5

Tsetsos, F., …, The TS-EUROTRAIN network (including **Widomska, J.**), …, Paschou, P. (2023). Genome-wide Association Study points to novel locus for Gilles de la Tourette Syndrome. *Biological Psychiatry.* DOI:10.1016/j.biopsych.2023.01.023.

Kluivers, K.B.*, Lince, S.L.*, Ruiz-Zapata, A.M., Post, W.M., Cartwright, R., Kerkhof, M.H., **Widomska, J.**, De Witte, W., Pecanka, J., Kiemeney, L.A., Vermeulen, S.H., Goeman, J.J., Allen-Brady, K., Oosterwijk, E., Poelmans G. (2023). Molecular landscape of pelvic organ prolapse provides insights into disease etiology. *International Journal of Molecular Sciences, 24*(7), 6087. DOI:10.3390/ijms24076087

Post, W.M., **Widomska, J.**, Oosterwijk, E., De Witte, W., Coenen, M.J.H., Janssen, D.A.W., Martens, F., Cartwright, R., Minassian, V.A., Penney, K.L., Thomas, L.F., Skogholt, A.H., Stafne, S.N., Hveem, K., Kluivers, K.B., Poelmans, G. (2023). A molecular landscape of stress urinary incontinence in women suggests an important role of beta-catenin signaling in disease etiology. *Journal of Urology (JU) Open Plus* [In press]

*Equal contribution

A

DONDERS GRADUATE SCHOOL FOR COGNITIVE NEUROSCIENCE

For a successful research Institute, it is vital to train the next generation of young scientists. To achieve this goal, the Donders Institute for Brain, Cognition and Behaviour established the Donders Graduate School for Cognitive Neuroscience (DGCN), which was officially recognised as a national graduate school in 2009. The Graduate School covers training at both Master's and PhD level and provides an excellent educational context fully aligned with the research programme of the Donders Institute.

The school successfully attracts highly talented national and international students in biology, physics, psycholinguistics, psychology, behavioral science, medicine and related disciplines. Selective admission and assessment centers guarantee the enrolment of the best and most motivated students.

The DGCN tracks the career of PhD graduates carefully. More than 50% of PhD alumni show a continuation in academia with postdoc positions at top institutes worldwide, e.g., Stanford University, University of Oxford, University of Cambridge, UCL London, MPI Leipzig, Hanyang University in South Korea, NTNU Norway, University of Illinois, North Western University, Northeastern University in Boston, ETH Zürich, University of Vienna etc.. Positions outside academia spread among the following sectors: specialists in a medical environment, mainly in genetics, geriatrics, psychiatry and neurology. Specialists in a psychological environment, e.g., as specialist in neuropsychology, psychological diagnostics or therapy. Positions in higher education as coordinators or lecturers. A smaller percentage enters business as research consultants, analysts or head of research and development. Fewer graduates stay in a research environment as lab coordinators, technical support or policy advisors. Upcoming possibilities are positions in the IT sector and management position in pharmaceutical industry. In general, the PhDs graduates almost invariably continue with high-quality positions that play an important role in our knowledge economy.

For more information on the DGCN as well as past and upcoming defenses please visit: http://www.ru.nl/donders/graduate-school/phd/
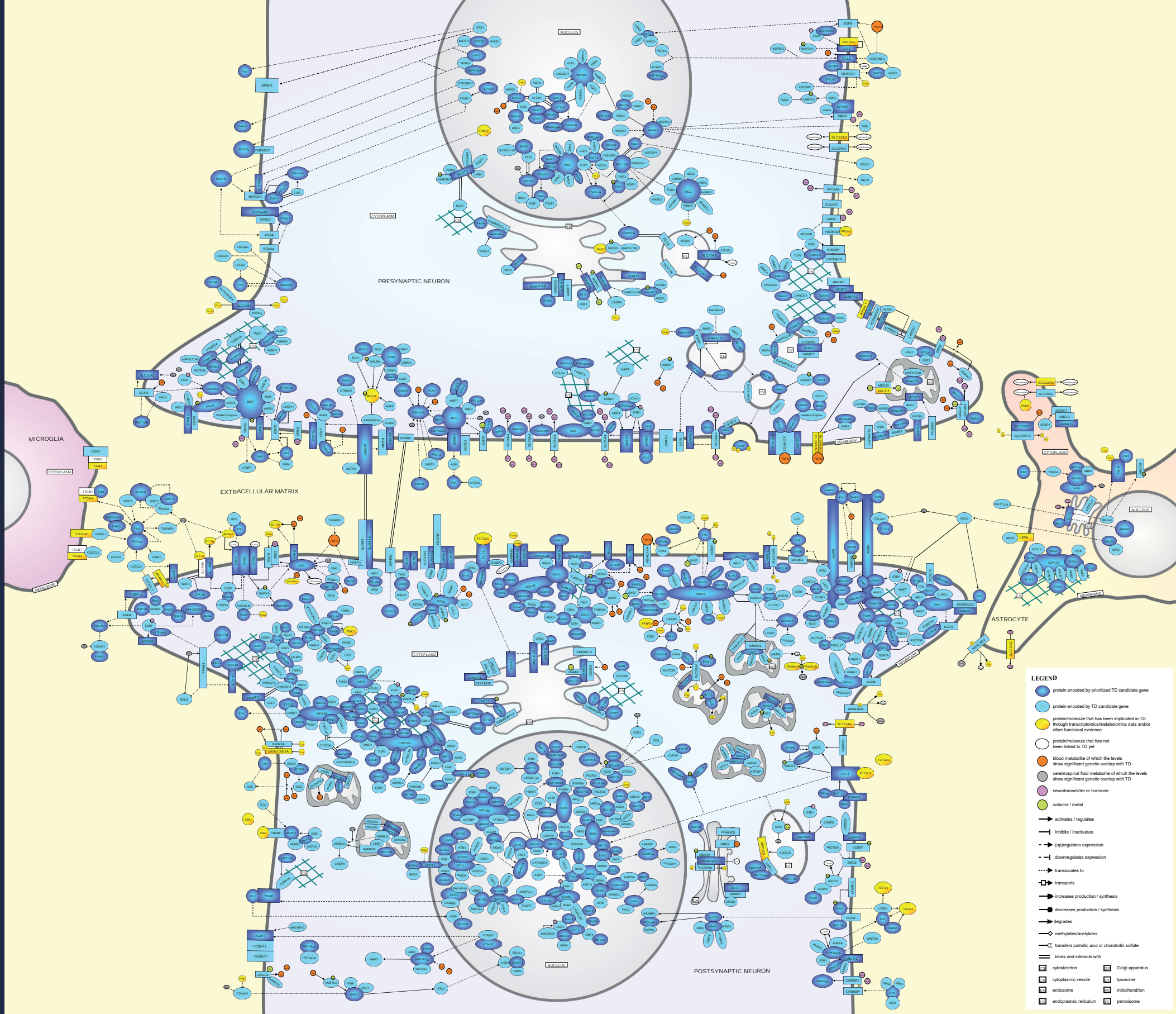
LEGEND

- protein encoded by prioritized TD candidate gene
- protein encoded by TD candidate gene
- protein/molecule that has been implicated in TD through transcriptomics/metabolomics data and/or other functional evidence
- protein/molecule that has not been linked to TD yet
- blood metabolite of which the levels show significant genetic overlap with TD
- cerebrospinal fluid metabolite of which the levels show significant genetic overlap with TD
- neurotransmitter or hormone
- cofactor / metal

→ activates / regulates
⊣ inhibits / inactivates
⇢ (up)regulates expression
⊣- - downregulates expression
⋯▸ translocates to
▭▭ transports
➤ increases production / synthesis
●— decreases production / synthesis
➤ degrades
◇ methylates/acetylates
⫱ transfers palmitic acid or chondrotin sulfate
═ binds and interacts with

- cytoskeleton
- cytoplasmic vesicle
- endosome
- endoplasmic reticulum
- Golgi apparatus
- lysosome
- mitochondrion
- peroxisome

MICROGLIA

PRESYNAPTIC NEURON

EXTRACELLULAR MATRIX

POSTSYNAPTIC NEURON

ASTROCYTE

NUCLEUS

CYTOPLASM

FIGURE 1. Molecular landscape of TD. In this landscape, the interactions between the key proteins/molecules/metabolites implicated in TD in pre- and postsynaptic neurons, astrocytes and/or microglial cells are shown. In Table S5, all interactions between the landscape proteins/molecules/metabolites are provided. In File S8, we provide a pdf version of Figure 1 that will allow interested readers to look up proteins and molecules in the landscape through using the search function.